

Journal of Hymenoptera Research

Content of volume 97, 2024

- 1 **Rearing *Thyridanthrax fenestratus* (Diptera, Bombyliidae) on *Pemphredon fabricii* (Hymenoptera, Crabronidae) prepupae**
Petr Heneberg, Petr Bogusch, Alena Astapenková
- 15 **The first reliable fossil record of the tribe Centistini (Hymenoptera, Braconidae, Euphorinae): a new subgenus and species of braconid wasp in Danish amber**
Sergey A. Belokobylskij, Dmitry V. Vasilenko, Evgeny E. Perkovsky
- 29 **High hymenopteran parasitoid infestation rates in Czech populations of the *Euphydryas aurinia* butterfly inferred using a new molecular marker**
Hana Konvičková, Václav John, Martin Konvička, Michal Rindoš, Jan Hřeček
- 43 **Corrigendum: Ulmer JM, Janšta P, Azar D, Krogmann L (2023) At the dawn of megadiversity – Protoitidae, a new family of Chalcidoidea (Hymenoptera) from Lower Cretaceous Lebanese amber. Journal of Hymenoptera Research 96: 879–924. doi:10.3897/jhr.96.105494**
Jonah M. Ulmer, Petr Janšta, Dany Azar, Lars Krogmann
- 45 **A DNA-barcoding-based approach to quantitatively investigate larval food resources of cavity-nesting wasps from trap nests**
Luisa Timm, Johanna Schaal, Manuela Sann
- 57 **A newly recorded genus *Microdynerus* Thomson, 1874 and a review of its related genus *Leptochilus* de Saussure, 1853 (Hymenoptera, Vespidae, Eumeninae) from China**
Yue Bai, Bin Chen, Ting-Jing Li
- 85 **Erimerinae, a prior name to Microdontomerinae (Hymenoptera, Torymidae) with the description of a new genus and three new species from Iran**
Hossein Lotfalizadeh, Zohreh Mirzaee, Gholamreza Tavakoli-Korghond, Petr Janšta, Jean-Yves Rasplus
- 105 **Description and mitochondrial genome sequencing of a new species of inquiline gall wasp, *Synergus nanlingensis* (Hymenoptera, Cynipidae, Synergini), from China**
Yu-Bo Duan, Yan-Jie Wang, Dao-Hong Zhu, Yang Zeng, Xiu-Dan Wang

- 127 **Annotated checklist of the megachilid bees of Corsica (Hymenoptera, Megachilidae)**
Romain Le Divelec, Alexandre Cornuel-Willermoz, Matthieu Aubert, Adrien Perrard
- 191 **A new species of *Uscanoidea* Girault (Hymenoptera, Trichogrammatidae), an egg parasitoid of *Monalonia dissimulatum* Distant (Hemiptera, Miridae)**
Jean Gamboa, Lucía Pérez-Benavides, Esaú Ospina-Peñuela, Francisco Serna, Gennaro Viggiani
- 207 **Redescription of *Apanteles mimoristae* (Hymenoptera, Braconidae), a parasitoid of the native pyralid cactus moth *Melitara* cf. *nephelepa* in central Mexico**
Renato Villegas-Luján, Robert Plowes, Lawrence E. Gilbert, Julio Cesar Rodríguez, Ricardo Canales-del-Castillo, Gabriel Gallegos-Morales, Martha P. España-Luna, José Fernández-Triana, Sergio R. Sanchez-Peña
- 229 **First discovery of *Plutarchia* (Hymenoptera, Eurytomidae) in Palearctic region, with description of a new species from South Korea**
Duk-Young Park, Seunghwan Lee
- 241 **A new species of the presocial potter wasp genus *Calligaster* de Saussure, 1852 (Hymenoptera, Vespidae, Eumeninae) from Vietnam**
Cuong Quang Nguyen, Hoa Thi Dang, Lien Thi Phuong Nguyen
- 255 **An integrative taxonomic study of north temperate *Cotesia* Cameron (Hymenoptera, Braconidae, Microgastrinae) that form silken cocoon balls, with the description of a new species**
Vladimir Žikić, Milana Mitrović, Saša S. Stanković, José L. Fernández-Triana, Maja Lazarević, Kees van Achterberg, Dawid Marczak, Marijana Ilić Milošević, Mark R. Shaw
- 277 **Discovery of a new *Pseudalomya* Telenga, 1930 (Hymenoptera, Ichneumonidae, Ichneumoninae) species from Taiwan and its implications for the systematic position of this genus**
Hsuan-Pu Chen, Namiki Kikuchi, Shiuh-Feng Shiao
- 297 **Justin Schmidt's originality**
Christopher K. Starr, Robert S. Jacobson, William L. Overal
- 307 **A review of *Trypoxylon* Latreille, 1796 (Hymenoptera, Crabronidae) of Southwest China with descriptions of two new species**
Yan Fu, Nawaz Haider Bashir, Qiang Li, Li Ma
- 349 **A new European species of *Mesocrina* (Hymenoptera, Braconidae, Alysiinae, Alysiini) with notes on the biology and systematics of the genus**
H. Charles J. Godfray, Cornelis van Achterberg
- 363 **Six in one: cryptic species and a new host record for *Olixon* Cameron (Rhopalosomatidae, Hymenoptera) revealed by DNA barcoding**
Allaina L. Armstrong, Jayme E. Sones, Volker Lohrmann, Paul D. N. Hebert, Dan H. Janzen, Winnie Hallwachs, Jeremy D. Blaschke

- 379 **Review of the ant genus *Manica* (Hymenoptera, Formicidae), with a new record of the genus in China and description of a new species**
Yuqing He, Zhilin Chen, Congcong Du
- 399 **Cryptic or underworked? Taxonomic revision of the *Antistrophus rufus* species complex (Cynipoidea, Aulacideini)**
Louis F. Nastasi, John F. Tooker, Charles K. Davis, Cecil N. Smith, Timothy S. Frey, M. J. Hatfield, Tara M. Presnall, Heather M. Hines, Andrew R. Deans
- 441 **Circumscription of the *Ganaspis brasiliensis* (Ihering, 1905) species complex (Hymenoptera, Figitidae), and the description of two new species parasitizing the spotted wing drosophila, *Drosophila sukuzii* Matsumura, 1931 (Diptera, Drosophilidae)**
Jeffrey Sosa-Calvo, Mattias Forsbåge, Matthew L. Buffington
- 471 **Description of one new species of *Agriotypus* Curtis, 1832 (Hymenoptera, Ichneumonidae, Agriotypinae) from South Korea**
Jin-Kyung Choi, Jong-Wook Lee, Kazuhiko Konishi, Kyong-In Suh, Andrew M. R. Bennett
- 491 **A new enigmatic genus of the ichneumonid subfamily Ctenopelmatinae (Hymenoptera, Ichneumonidae) from Thailand**
Avunjikkattu P. Ranjith, Donald L. J. Quicke, Alexey Reshchikov, Buntika A. Butcher
- 505 **Gynandromorph records of *Melissodes trinodis* and *Melissodes communis* (Hymenoptera, Apidae) from North Dakota, USA**
Joshua W. Campbell, C. K. Pei, Karen W. Wright
- 513 **New records of bees (Hymenoptera, Apoidea) from Morocco**
Ablam Sentil, Paolo Rosa, Clément Tourbez, Achik Dorchin, Petr Bogusch, Denis Michez
- 531 **Distribution of the sand wasp *Bicyrtes variegatus* (Oliver, 1789) (Hymenoptera, Crabronidae) in the Galápagos Islands, with notes on its ecology**
Andrea C. Román, Patricio Picón-Rentería, Charlotte E. Causton, Lenyn Betancourt-Cargua, Catherine Frey, Henri W. Herrera
- 541 **Use of a novel nesting material by the spider wasp *Dipogon variegatus* (Hymenoptera, Pompilidae)**
Sergio Alpacete, Gonzalo Sancho, Jordi Bosch
- 545 **The genus *Acercephala* and observations of the life history of *Acercephala hanuuanamu* sp. nov. (Hymenoptera, Cerocephalidae) and its bark beetle host on the island of O'ahu, Hawai'i**
David N. Honsberger, Maya Honsberger, J. Hau'oli Lorenzo-Elarco, Mark G. Wright
- 591 ***Telenomus* Haliday (Hymenoptera, Scelionidae) parasitizing Pentatomidae (Hemiptera) in the Palearctic region**
Francesco Tortorici, Bianca Orrù, Alexander V. Timokhov, Alexandre Bout, Marie-Claude Bon, Luciana Tavella, Elijah J. Talamas

- 621 Integrative characterisation of the Northwestern European species of *Anacharis* Dalman, 1823 (Hymenoptera, Cynipoidea, Figitidae) with the description of three new species**
Jonathan Vogel, Mattias Forshage, Saskia B. Bartsch, Anne Ankermann, Christoph Mayer, Pia von Falkenhausen, Vera Rduch, Björn Müller, Christoph Braun, Hans-Joachim Krammer, Ralph S. Peters
- 699 Phenology of microhymenoptera and their potential threat by insect decline**
Maura Haas-Renninger, Sonia Bigalk, Tobias Frenzel, Raffaele Gamba, Sebastian Görn, Michael Haas, Andreas Haselböck, Thomas Hörren, Martin Sorg, Ingo Wendt, Petr Jansta, Olaf Zimmermann, Johannes L. M. Steidle, Lars Krogmann
- 721 Solitary folded-winged wasps of the genus *Zethus* Fabricius (Vespidae, Zethinae) parasitised by two new species of Strepsiptera on different continents**
Daniel Benda, Hans Pohl, Rolf Beutel, Jakub Straka
- 741 Parasitoid wasps associated with *Antigastra catalaunalis* (Lepidoptera, Crambidae) in Northern Sinaloa, Mexico**
Ramón A. Sarazú-Pillado, Héctor González-Hernández, J. Refugio Lomeli-Flores, Jorge M. Valdez-Carrasco, Edgardo Cortez-Mondaca, Ariel Guzmán-Franco
- 755 Integrative taxonomy of a new species of a bumble bee-mimicking brood parasitic bee, *Tetralonioidella mimetica* (Hymenoptera, Apoidea, Apidae), investigated through phylogenomics**
Michael C. Orr, Douglas Chesters, Paul H. Williams, Thomas J. Wood, Qingsong Zhou, Silas Bossert, Trevor Sless, Natapot Warrit, Pierre Rasmont, Guillaume Ghisbain, Mira Boustani, A'rong Luo, Yuan Feng, Ze-Qing Niu, Chao-Dong Zhu
- 781 Five new species of *Metapolybia* Ducke, 1905, with the description of the male genitalia of seven species of the genus (Hymenoptera, Vespidae, Polistinae)**
Gustavo B. Cortes, Fernando B. Noll, James M. Carpenter, Sergio R. Andena
- 807 Three new species of *Conostigmus* from China and redescription of *Conostigmus ampullaceus* Dessart, 1997 (Hymenoptera, Megaspilidae)**
Xu Wang, Shanshan Cui, Fang Li, Yixin Huang, Huayan Chen
- 825 Diversity and differentiation of the *Chelonus* (*Microchelonus*) species of the Galapagos archipelago (Hymenoptera, Braconidae, Cheloninae)**
Ada L. Sandoval-B, Scott Richard Shaw, Henri W. Herrera, Carlos E. Sarmiento
- 849 The genus *Lasioglossum* Curtis, 1833 (Hymenoptera, Halictidae) in Azerbaijan**
Yulia V. Astafurova, Mahir M. Maharramov, Maxim Yu. Proshchalykin
- 881 An update on the wild bee fauna (Hymenoptera, Apoidea, Anthophila) of Serbia**
Sonja Mudri-Stojnić, Andrijana Andrić, Laura Likov, Ana Grković, Tamara Tot, Ivana Kavgić, Ante Vujić

- 895** **Molecular data support *Bombus sonorus* and *Bombus pensylvanicus* (Hymenoptera, Apidae) as distinct species**
Jessica L. Beckham, Jeff A. Johnson, Russell S. Pfau
- 915** **A new species of *Braunsia* (Hymenoptera, Braconidae, Agathidinae), a natural enemy of *Cydalima perspectalis* (Lepidoptera, Crambidae) from South Korea: species description and notes on its biology**
Soohyun Kim, Jong Bong Choi, Hwal-Su Hwang, Marc Kenis, M. Lukas Seehausen, Ikju Park, Jin-Kyung Choi, Kyeong-Yeoll Lee, Michael J. Sharkey, Ilgoa Kang
- 937** **A new species of *Merismomorpha* Girault, 1913 (Chalcidoidea, Pteromalidae) from the Palaearctic region**
Ekaterina V. Tselikh, Jean-Yves Rasplus, Jaehyeon Lee, Natalie Dale-Skey, Ankita Gupta, Deok-Seo Ku
- 945** **Annotated checklist of family- and genus-group names associated with *Scoliidae* (Hymenoptera, Aculeata)**
Christopher K. Taylor
- 1007** **An annotated checklist of the bees of Washington state**
Chanda S. Bartholomew, Elizabeth A. Murray, Silas Bossert, Joel Gardner, Chris Looney
- 1123** **First detection of *Trissolcus japonicus* (Ashmead) (Hymenoptera, Scelionidae) in southwestern France**
Guillaume Martel, Alexandre Bout, Francesco Tortorici, Rachid Hamidi, Luciana Tavella, Maud Thomas
- 1141** **Five new species of *Passaloecus* Shuckard (Hymenoptera, Crabronidae) from China, with a key to Chinese species**
Jinghong Li, Li Ma, Qiang Li
- 1163** **Checklists of the Ceraphronoidea, Cynipoidea, Evanioidea, Stephanoidea and Trigonalynoidea (Hymenoptera) of Canada, Alaska and Greenland**
Andrew M. R. Bennett, Matthew L. Buffington, Andrew R. Deans, Mattias Forshage, George Melika, István Mikó, David R. Smith
- 1221** **Life history of two new species of *Prorops* (Hymenoptera, Bethyloidea) ectoparasitic on adult *Hypothenemus eruditus* beetles (Curculionidae, Scolytinae) in Hawai'i**
David N. Honsberger, Karl N. Magnacca, J. Hau'oli Lorenzo-Elarco, Mark G. Wright
- 1257** **Discovery of the subfamily *Microleptinae* (Hymenoptera, Ichneumonidae) from India and Thailand with the description of five new species**
Avunjikkattu P. Ranjith, Andrei E. Humala, Dharma Rajan Priyadarsanan, Buntika A. Butcher
- 1285** **Review of *Bicarini* Quicke & Walker and *Chelonogastra* Ashmead (Hymenoptera, Braconidae, Braconinae) in China, with the description of two new species**
Yang Li, Cornelis van Achterberg, Cheng-Jin Yan, Xue-Xin Chen

- 1301** Integrative taxonomic revision of the Nearctic *Perilampus hyalinus* species complex (Hymenoptera, Chalcidoidea, Perilampidae) resolves 100 years of confusion about the host associations of *P. hyalinus* Say
Jeong Jae Yoo, D. Christopher Darling
- 1385** *Telenomus dendrolimi* (Matsumura) (Hymenoptera, Scelionidae) reared from the eggs of *Dendrolimus houi* (Lajonquiere) (Lepidoptera, Lasiocampidae) from China
Hua-Yan Chen, Elijah Talamas, Zachary Labey, Norman F. Johnson, Ci-Ding Lu, Guang-Hong Liang
- 1403** Compatibility of released and adventive populations of *Ganaspis kimorum* Buffington, 2024, (Cynipoidea, Figitidae), parasitoid of the spotted-wing drosophila *Drosophila suzukii* (Matsumura, 1931)
Judith M. Stahl, Fabrizio Lisi, Thaliana Samarin, Xingeng Wang, Elizabeth H. Beers, Kent M. Daane
- 1417** A new species and new records of *Hoplitis* Klug (Hymenoptera, Megachilidae) from Russia
Alexander V. Fateryga, Maxim Yu. Proshchalykin, Evgeny V. Abakumov

Rearing *Thyridanthrax fenestratus* (Diptera, Bombyliidae) on *Pemphredon fabricii* (Hymenoptera, Crabronidae) prepupae

Petr Heneberg¹, Petr Bogusch², Alena Astapenková²

1 Charles University, Third Faculty of Medicine, Prague, Czech Republic **2** University of Hradec Králové, Faculty of Science, Hradec Králové, Czech Republic

Corresponding author: Petr Heneberg (petr.heneberg@lf3.cuni.cz)

Academic editor: Volker Lohrmann | Received 30 July 2023 | Accepted 20 December 2023 | Published 3 January 2024

<https://zoobank.org/0AD9A03D-4926-441E-801F-6C3991F7BAE0>

Citation: Heneberg P, Bogusch P, Astapenková A (2024) Rearing *Thyridanthrax fenestratus* (Diptera, Bombyliidae) on *Pemphredon fabricii* (Hymenoptera, Crabronidae) prepupae. Journal of Hymenoptera Research 97: 1–13. <https://doi.org/10.3897/jhr.97.110282>

Abstract

Thyridanthrax fenestratus (Fallén, 1814) is a bombyliid with poorly understood biology. It was recently shown to locally but frequently parasitize *Pemphredon fabricii* (M. Müller, 1911) (Hymenoptera: Crabronidae), a crabronid wasp that abundantly nests in old *Lipara*-induced galls on the common reed *Phragmites australis* (Cav.) Trin. ex Steud., 1840. The parasitism modes in Bombyliidae and *Thyridanthrax* spp. are not uniform. Here, we report that *Th. fenestratus* switches facultatively between killing the host almost immediately (idiobiont strategy) and killing the host at a later developmental stage (koinobiont strategy). We document the koinobiont parasitoid strategy for a series of *Th. fenestratus* larvae parasitizing *P. fabricii*. We found that a significant portion of *Th. fenestratus* larvae spend winter as young larvae and start feeding on fully developed and defecated prepupae of *P. fabricii* only after the end of cold-induced winter diapause. The time needed for the development of *Th. fenestratus* larvae exceeds several times the time needed for pupation of *P. fabricii* prepupae; the parasitized prepupae, therefore, remain paralyzed until the parasitic larva completes feeding. Fungicides, which alter the pupation of the host larva, seem to have negligible effects on *Th. fenestratus* larvae. The ability to switch between the two parasitism strategies has already been reported for several *Anthrax* spp., though the ability to block the host in the defecated prepupa stage and prevent its pupation following cold-induced diapause is herein reported for the first time.

Keywords

Diptera, eclosion, ectoparasite, idiobiont, koinobiont, parasitoid, pupation

Introduction

Thyridanthrax fenestratus (Fallen, 1814) is a Palearctic species of bee fly (Evenhuis and Greathead 2015). Larval stages are thought to live in the soil (Oldroyd 1969) and be parasitoids of cocoons and predators of eggs of locusts (Acrididae: *Dociostaurus maroccanus* in Spain and Algeria, see Künckel d'Hercule 1893–1905, 1894; Delassus et al. 1929; Del Cañizo 1943; *Arcyptera microptera* in various parts of Russia and at Crimea, see Mokřeckij 1895; Bezrukov 1922; Porčinskij 1894, 1895; *Podisma pedestris* in Russia, see Porčinskij 1894, 1895, and *Schistocerca gregaria* in Algeria, see Sergent 1916) and other grasshoppers (Pamphagidae: *Ocneridia volxemii* in Algeria, see Künckel d'Hercule 1893–1905, 1894). Some butterfly species are probably parasited too (Noctuidae: *Apamea anceps*, see Engel 1932–37; Grigorieva 1958; Zaitsev 1966; Tomaj 1977; Greathead and Evenhuis 1998; Motyčková 2012). Reports from the Netherlands and Britain describe *Th. fenestratus* as parasitizing *Ammophila* spp. larvae (Pontin 1961; Miles and Muggleton 2010; Noordijk et al. 2016; Slikboer et al. 2019). More recently, abundant *Th. fenestratus* larvae in nests of the crabronid wasp *Pemphredon fabricii* were reported (Bogusch et al. 2015, 2018). In contrast, *Th. fenestratus* larvae were rarely reported in nests of the crabronid wasp *Trypoxylon deceptorium* Antropov, 1991 (Bogusch et al. 2015). The larvae are thought to be generalists attacking the nests of various Crabronidae and Sphecidae (Bogusch et al. 2018). For an unclear reason, *Th. fenestratus* host specialization has some local consequences. Although *P. fabricii*, *Tr. deceptorium*, and *Th. fenestratus* distribution ranges overlap in a large part of Europe, the *P. fabricii* and *Tr. deceptorium* nests attacked by *Th. fenestratus* have been reported only in the Pannonian lowland, despite intensive research having been conducted in other regions of occurrence of both these species (e.g., Bohemia, i.e., western part of Czechia) (Bogusch et al. 2018). In Czechia, *Th. fenestratus* adults are active from mid-June until mid-August (Motyčková et al. 2012; Čelechovský et al. 2020). Adults are typically found in sun-exposed forest ecotones, dirt roads (Čelechovský et al. 2020), heathlands (Drake 1991; Lake 2002; Čelechovský et al. 2020), and other dry sandy habitats (Noordijk et al. 2016; Slikboer et al. 2019), where they visit flowers and feed on nectar and pollen.

The bee fly *Th. fenestratus* was abundant in old common reed galls induced by *Lipara lucens* and has been previously reported from the tailing pond of ash and slug from the lignite powerplant near Hodonín (Czechia; 21% of 29 examined *P. fabricii* nests were parasitized) and at a fishpond with sandy bedrock near Sekule (Slovakia; 24% of 89 examined *P. fabricii* nests were parasitized) (Bogusch et al. 2015; Heneberg et al. 2022). They were abundantly present near Hodonín, even though this sampling site was contaminated with arsenic ($40 \mu\text{g g}^{-1}$), copper ($26 \mu\text{g g}^{-1}$), and sulfur ($4616 \mu\text{g g}^{-1}$) (Heneberg et al. 2022). When focusing on *Lipara*-induced common reed galls, *Th. fenestratus* was most abundantly associated with galls 10–14 mm in diameter (also preferred by *P. fabricii*) and present more abundantly in galls on the stems of small or intermediate thickness (also preferred by *P. fabricii*). These stems typically occur in reed beds less stressed by drought or other factors (Astapenková et al. 2017). The larvae of *Th. fenestratus* in galls induced by *L. lucens* frequently suffer from fungal infections (Heneberg et al. 2016).

The mature larva of *Th. fenestratus* was described by Séguy (1932); a drawing of the mature larva was also published by Oldroyd (1969). However, more recently, Bogusch et al. (2015) reported deviations from the original descriptions. Séguy (1932) and Oldroyd (1969) described the larval mandibles of *Th. fenestratus* as bidentate, with lateral hooks, which is in contrast to the findings by Bogusch et al. (2015) and to other larval Bomblyliidae (Oldroyd 1969). Prominent sharp mandibles with three teeth oriented backward were present (Bogusch et al. 2015). Mature larvae reach 4.9 ± 0.8 mm in length. The development and immature larvae of *Th. fenestratus* have been documented by Künckel d'Herculais (1893–1905). There is a report of *Th. fenestratus* rearing from naturally infected *Ammophila pubescens* Curtis, 1836 cocoons (Miles and Muggleton 2010). However, as *A. pubescens* larva spins cocoons, direct observation of their development was impossible. Nevertheless, the above report was the first proof that *Th. fenestratus* allows parasitized larvae to complete their growth, feed on the food supplies provided by the parent wasp, and to spin a cocoon. The cocoon was not intact, and therefore, the authors were uncertain whether the larva was attached to the host larva during the whole time or whether it had eaten some of its host's provisions, bored into the cocoon from below after the cocoon was formed and then only consumed the wasp prepupa or pupa (Miles and Muggleton 2010).

In the present study, we document the development of *Th. fenestratus* on naturally infected *P. fabricii* prepupae under laboratory conditions. The larvae, including host prepupae, were exposed to various field-realistic concentrations of azole fungicides that are commonly used in agriculture (ECDC 2013), namely, difenoconazole, penconazole, and tebuconazole. These azoles have been shown to affect the timing of metamorphosis into adults of the host species (Heneberg and Bogusch 2022), but their effects on *Th. fenestratus* and dipterans, in general, are unknown. Selected other azole fungicides were previously documented to kill dipterans (Kenneke et al. 2009; Saraiva et al. 2018; do Prado et al. 2023). Development was documented, and differences in its timing were tracked.

Materials and methods

To analyze the geographic distribution of the *Th. fenestratus* population parasitizing *P. fabricii*, we considered the data on reed galls induced by *L. lucens*. These consisted of 176 reed beds in Czechia, Poland, Hungary, Slovakia, Austria, Slovenia, and Italy. We included only those reed beds in which the reed galls induced by *L. lucens* were positive for *P. fabricii*. The list of coordinates of examined reed beds that were positive for *P. fabricii* is provided in Suppl. material 1. Numbers of *P. fabricii* obtained by cutting the galls, numbers of *Th. fenestratus* obtained using the same procedure, and the total numbers of galls cut are indicated for sampling sites that were *Th. fenestratus*-positive. We did not show the numbers of *P. fabricii* and *Th. fenestratus* obtained from galls from which the inquiline was allowed to rear but were not cut individually, as *Th. fenestratus* often remain in the galls after rearing in rearing bags, and the detected parasitism intensities would, therefore, be underestimated.

For rearing analysis, we collected prepupae of *P. fabricii* parasitized by *Th. fenestratus* at sampling sites Hajnáčka (48.2126403°N, 19.9546442°E; 20 Jan 2022) and Šíd (48.2660036°N, 19.8795681°E; 21 Jan 2022). Both localities are in the Cerová vrchovina mountains in southern Slovakia. The collected nests were present in ≥ 1 -year-old common reed galls induced by *L. lucens*.

When larvae of *P. fabricii* are 7–20 days old, they stop feeding and line up in the nest one after the other in a row. All of them defecate, shed to become a prepupa, and build a cocoon from their silk on the inner side of the gall, without septa between the larval chambers. Therefore, when collected in January, the reed galls contained defecated fully grown prepupae in cold-induced diapause (Bogusch et al. 2018). The prepupae require only a few days (usually four to six) to pupate and develop synchronously to adults when exposed to the laboratory temperature.

We cut all the collected galls on 22–23 Jan 2022 and kept the excised prepupae at 4 °C until placed in 96-well plates (Brand, Wertheim, Germany) on 25 Feb 2022. We placed the prepupae individually in the wells and allowed them to acclimate to their new environment for 24 h at 23 °C and > 90% humidity. We performed the experiment together with exposure of the nonparasitized prepupae of *P. fabricii* to the same compounds (see the analysis published in Heneberg and Bogusch (2022) for more details). On 26 Feb 2022 (Day 0), we exposed the parasitized prepupae to three triazole formulations, each at a concentration equal to or lower than those recommended by their manufacturers for use in spraying crops to eliminate fungi. The tested compounds were penconazole (Merck, Darmstadt, Germany; batch BCBZ4909, 99.0% purity), difeconazole (Merck; batch BCCD4900, 95.5% purity), and tebuconazole (Merck; batch BCCF9398, 99.1% purity). Before the final dilution, all compounds were first diluted at 50 mg mL⁻¹ in dimethyl sulfoxide (DMSO), and DMSO alone was therefore used as a control. We sprayed the compounds using Potter Precision Laboratory Spray Tower (Burkard Scientific, Uxbridge, UK). The application rate of the applied solutions was constant at 2 $\mu\text{L cm}^{-2}$.

On Days 4 through 48, following the application of triazole fungicides, we checked the treated digger wasps at least every other day for molting, wing development, and mortality (with a break between Days 32 and 42). During the experiment, we kept the digger wasps at 23 °C with >90% humidity. We recorded the time until the full development of wings and mortality.

Results and discussion

We found *Th. fenestratus* to parasitize *P. fabricii* at 15 of the 176 reed beds that were positive for *P. fabricii*. These sites were located mainly in Slovakia (6) and Hungary (4), but several sampling sites were also positive for *Th. fenestratus* in southeastern Czechia (3), eastern Italy (1), and eastern Austria (1). Except for the single sampling site at the border of Italy and Slovenia, all other *Th. fenestratus*-positive *P. fabricii* sampling sites were located in the Pannonian lowland. The restriction of *Th. fenestratus*-positive *P. fabricii* sampling sites to the Pannonian lowland is surprising given that the distribution ranges of

both examined species are much broader and many other sampling sites were located in regions where both species are present (Fig. 1). The *Th. fenestratus* prevalence at *Th. fenestratus*-positive *P. fabricii* sampling sites was $11.6\% \pm 4.1\%$ (mean \pm SE), max 52.9% (reed beds of Neusiedler See near Oggau, Austria), min 0.8% (sampling site Tát, Hungary).

At sampling sites where *P. fabricii* was parasitized by *Th. fenestratus*, two asynchronous populations of this dipteran were present. First, some larvae were overwintering as fully grown; we included one of them in the examined dataset (Fig. 2, P-400-D8). These overwintering larvae were previously found in *P. fabricii* nests at other sampling sites as well (e.g., Hodonín and Sekule mentioned in the Introduction (Bogusch et al. 2015; Heneberg et al. 2022)) and represented the previously described populations parasitizing this host. To date, it is unclear whether *Th. fenestratus* is a true parasitoid or whether it eats part of its host's provisions (Miles and Muggleton 2010). Moreover, as host use in Bombyliidae varies, it was unclear whether these parasitoids act as koinobionts, allowing some further development of infected hosts, or idiobionts, which kill and consume their host in the state in which it is attacked (Yeates and Greathead 2008).

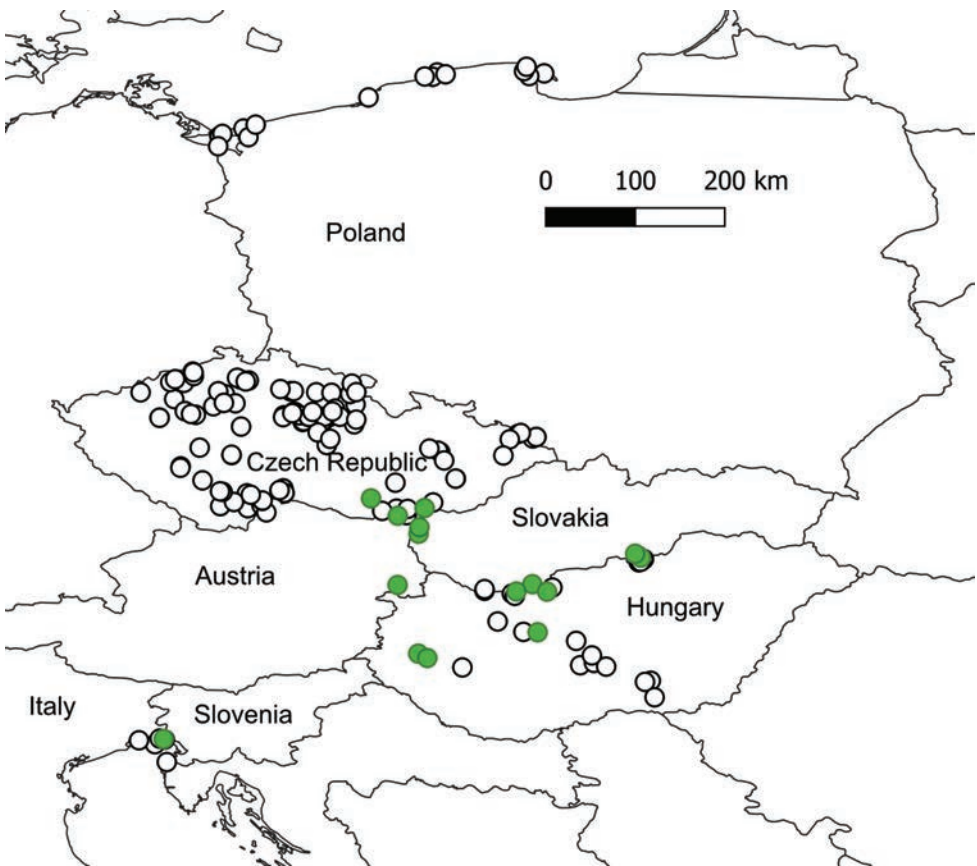


Figure 1. Map of examined sampling sites that were positive for *P. fabricii* (circles). Empty circles indicate sampling sites where only *P. fabricii* was found. Green circles indicate sites where *P. fabricii* was parasitized by *Th. fenestratus*. Source data are available in Suppl. material 1.

A part of the *Th. fenestratus* population, however, adopts a different overwintering strategy. A planidium finds the larva or prepupa of its host and overwinters on the defecated host prepupa. We did not observe the planidium directly, but when we sorted out individual overwintering *P. fabricii* prepupae, tiny attached *Th. fenestratus* larvae were already present on them. The attached larvae induce a block of the development of parasitized prepupae. Under laboratory conditions, the *P. fabricii* prepupae mostly (>80%) developed into pupae four days after removal from cold conditions. Nearly all (>98%) developed into pupae at six days following removal from cold conditions (Heneberg and Bogusch 2022). All the parasitized prepupae remained blocked at this developmental stage – see the illustration figure of one of the analyzed 96-well plates at Day 10 (Fig. 3). The nonparasitized prepupae pupated at the indicated time and metamorphosed to adults at Days 12–14.

We observed the development of 11 individuals spending diapause as first- or second-instar larvae. Seven completed their development successfully, whereas four failed to develop. Two of those that failed to develop had issues with the integrity of their paralyzed prey – the prey changed color and later was overgrown with mold, which also killed the *Th. fenestratus* larvae. In the other two cases, the fully grown larvae failed to pupate, became infected, and died (Fig. 2).

A single host prepupa is sufficient to support the development of a single *Th. fenestratus* larva. The time to pupation was 12 days in the case of the larva that was fully grown at the end of diapause. The seven individuals that grew out only after diapause pupated at Days 18, 20 (3×), 22, 24, and 26 (21.4 ± 1.0 days, median = 20 days) (Fig. 2).

All seven individuals that spent diapause as a first- or second-instar larvae and completed subsequent pupation also succeeded in metamorphosis to adults. Additionally, the single individual observed as overwintering as fully grown succeeded in metamorphosis to adult. It took 20 days for the latter individual to metamorphose from pupa to adult. It took the individuals spending diapause as the first- or second-instar larvae and completed subsequent pupation 20 (2×), 21, 22 (2×), and 24 (2×) days (21.9 ± 0.6 days, median = 22 days) to metamorphose from pupa to adult (Fig. 2). Representative images illustrating critical events in the development of *Th. fenestratus* on overwintering prepupae of *P. fabricii* are shown in Fig. 4.

A long-standing question is whether the larvae of bombyliid flies paralyze and kill the host immediately or at the very late stages of feeding. Adult females lack features that would allow them to paralyze the host. Therefore, it is believed that most bombyliid fly larvae contact the host in the state in which it is consumed (as typical idiobionts) and that the host is not immediately paralyzed or killed (which would be a koinobiont strategy) (Yeates and Greathead 2008). Evidence for other bombyliid species suggests that the host is killed only in the final stages of parasitoid development. However, here, we show clear evidence that parasitic larvae induce a development block of their host prepupae at very early stages, at the latest immediately after diapause. Therefore, while nonparasitized prepupae need only four days to pupate after diapause, the parasitized prepupae never pupate and remain alive and paralyzed for several weeks, which only allows for the complete growth of the parasitic larva until pupation.

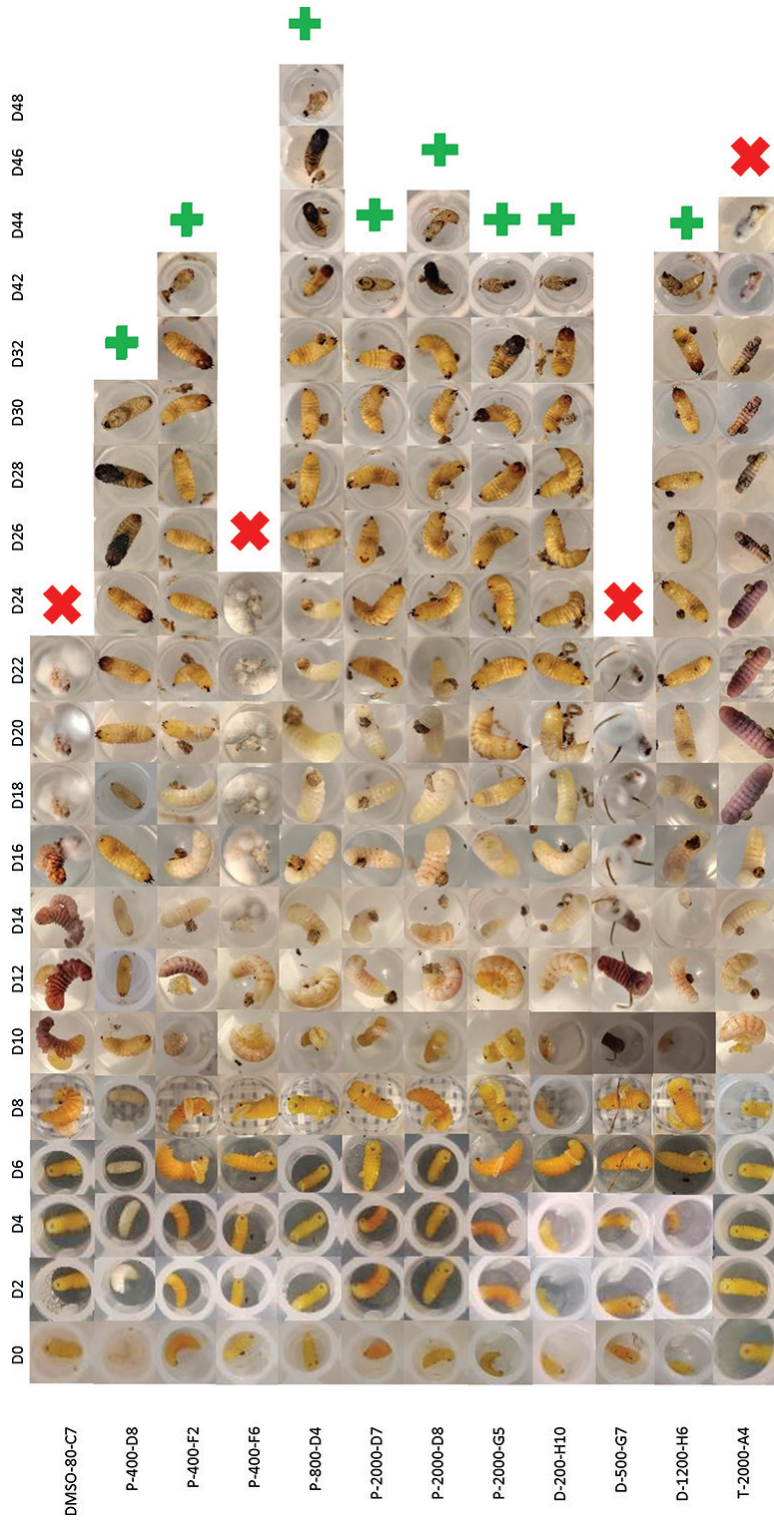


Figure 2. Time-lapse evidence of the development of *Th. fenestratus* under laboratory conditions following cold-induced diapause. The X-axis indicates days elapsed since the termination of cold-induced diapause. Individual lines represent photographs of the same individual. The individual in the second line spent the cold-induced diapause as a fully grown larva; all others spent the winter attached to the defecated prepupa but did not grow before the cold-induced diapause. Letters indicate the treatment (DMSO = control, P = penconazole, D = difeconazole, T = tebuconazole; numbers (200, 400, 500, 800, 1200, 2000) indicate the dilution of the study compounds (for more details, refer to Heneberg and Bogusch 2022); letters with numbers indicate the positions in 96-well plates.

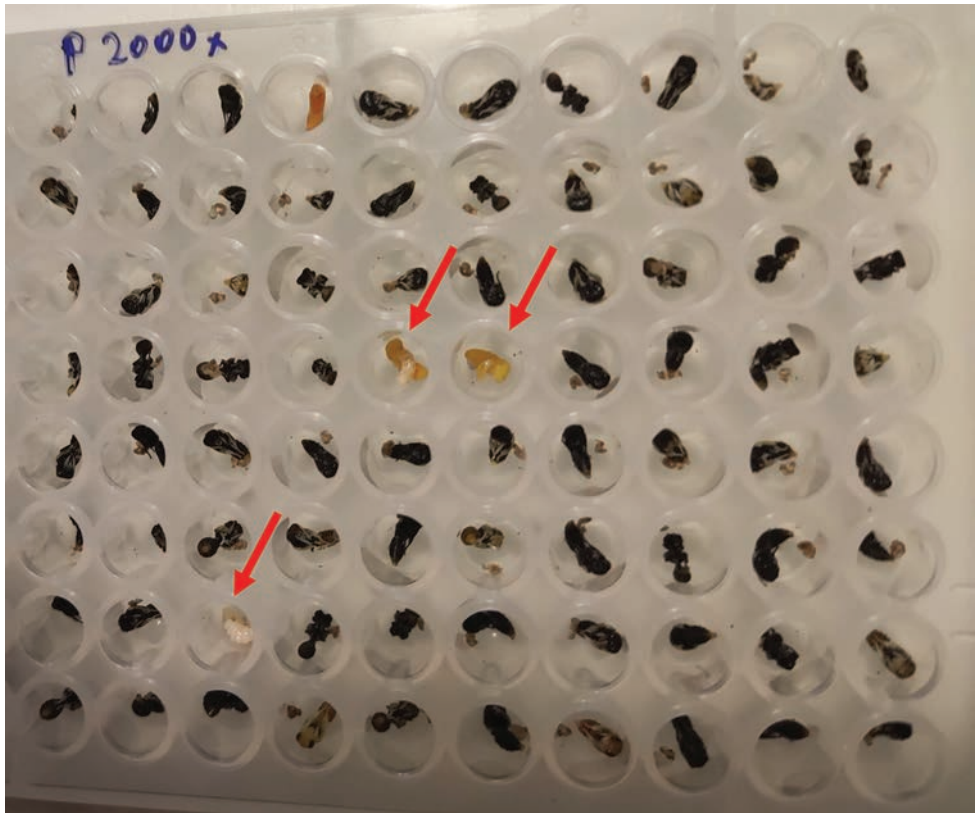


Figure 3. Representative figure of the 96-well plate at D10 with typically developing *P. fabricii* (already pupated, two to four days ahead of the metamorphosis to the adults) treated with penconazole ($50 \mu\text{g mL}^{-1}$) and with prepupae in wells D7, D8, and G5, which are parasitized by *Th. fenestratus*. The parasitized prepupae did not pupate and remained paralyzed and were killed within the ensuing four days.

Correspondingly, reports of some *Anthrax* spp. claim that their larvae may adopt different strategies when parasitizing tiger beetle (Coleoptera: Cicindelidae) larvae. While they parasitized any tiger beetle larval instar, they remained in a second instar for up to nine months, depending on the host stage and time of year. Once the tiger beetle larva constructs a pupal chamber and becomes a prepupa, the *Anthrax* larva begins rapid growth and reaches full size in one or two weeks (Palmer 1982; Shelford 1913). Thus, the larva appears to behave as a koinobiont or idiobiont based on the time of the year and host developmental stage. Given that two stages of *Th. fenestratus* larvae are found in *Lipara*-induced reed galls, this parasitic species appears to employ a similar strategy. Whether the first-instar larva feeds on the aphid provisions remains unclear, as some other bombyliid species are reported to feed on provisions and develop only on the prepupa or pupa (Bohart 1960; Du Merle 1979). Regarding our experiments with *Th. fenestratus*, we removed all *P. fabricii* prepupae from their cocoons before beginning experiments. Thus, the parasitic larvae must have been attached to them during the cold-induced diapause.



Figure 4. Representative figures illustrating critical events in the development of *Th. fenestratus* on overwintering prepupae of *P. fabricii*. In bombyliid flies, the first stage, triungulin, is active and immediately molts after attaching to its host to the second stage (likely D6), which has already attached itself and is not distinctly curved. This stage can overwinter (as does the pupa). Early third instar (likely D8) and late third instar (likely D14) can be diagnosed by their characteristic curvature. D24 and D34 represent pupae.

We exposed *P. fabricii* prepupae with *Th. fenestratus* larvae to three topically applied fungicides before their growth. However, we did not observe any adverse effects of exposure to the indicated fungicides on the bee flies. The larva treated with DMSO (control) died during development because of fungal infection. There were no concentration-dependent differences in the development and survival of the larvae treated with difeconazole and penconazole, including a lack of effects at the highest

concentrations used (Fig. 2). The only unclear result is with regard to the single tebuconazole-treated larva, which died after it completed its growth, just before pupation. However, more larvae treated with the same compound are needed to provide a definitive answer on tebuconazole's effects on this dipteran.

In conclusion, we found that *Th. fenestratus* facultatively switches between killing the host almost immediately (idiobiont strategy) and killing the host at a later developmental stage (koinobiont strategy). We documented the koinobiont parasitoid strategy in detail using a series of *Th. fenestratus* larvae parasitizing their hymenopteran host *P. fabricii*, which nests in *Lipara*-induced reed galls. We found that a significant portion of *Th. fenestratus* larvae overwinter as young larvae and start feeding on fully developed and defecated prepupae of *P. fabricii* only after the end of cold-induced winter diapause. The time needed for the development of *Th. fenestratus* larvae exceeds several times the time needed for pupation of *P. fabricii* prepupae; the parasitized prepupae, therefore, remain paralyzed until the parasitic larva completes feeding.

Acknowledgments

The study was supported by the Czech Science Foundation project 23-07303S and the University of Hradec Králové, Faculty of Science project Specific Research 2101/2022. We thank Wojciech Pulawski and Neal Evenhuis for their helpful and constructive peer-review comments.

References

- Astapenková A, Heneberg P, Bogusch P (2017) Larvae and nests of aculeate Hymenoptera (Hymenoptera: Aculeata) nesting in reed galls induced by *Lipara* spp. (Diptera: Chloropidae) with a review of species recorded. Part II. PLOS ONE 12: e0169592. <https://doi.org/10.1371/journal.pone.0169592>
- Bezrukov YuG (1922) Kratkoe soobščenie o dejatelnosti Omskoj laboratorii Sibirskogo Entomologičeskogo Bjuro za 1919–1922 g.g. Izvestija Sibirskogo Entomologičeskogo Bjuro 1: 26–20. [in Russian]
- Bogusch P, Astapenková A, Heneberg P (2015) Larvae and nests of six aculeate Hymenoptera (Hymenoptera: Aculeata) nesting in reed galls induced by *Lipara* spp. (Diptera: Chloropidae) with a review of species recorded. PLOS ONE 10: e0130802. <https://doi.org/10.1371/journal.pone.0130802>
- Bogusch P, Havelka J, Astapenková A, Heneberg P (2018) New type of progressive provisioning as a characteristic parental behaviour of the crabronid wasp *Pemphredon fabricii* (Hymenoptera Crabronidae). Ethology, Ecology & Evolution 30: 114–127. <https://doi.org/10.1080/03949370.2017.1323801>

- Bohart GE, Stephen WP, Eppley RK (1960) The biology of *Heterostylum robustum* (Diptera: Bombyliidae), a parasite of the alkali bee. *Annals of the Entomological Society of America* 53: 425–435. <https://doi.org/10.1093/aesa/53.3.425>
- Čelechovský A, Čelechovský D, Čelechovský M (2020) Dlouhososky *Exhyalanthrax afer* (Fabricius, 1794) a *Thyridanthrax fenestratus* (Fallén, 1814) – první nálezy v Národním parku Podyjí (Diptera: Bombyliidae). *Thayensia (Znojmo)* 17: 247–250.
- Del Cañizo J (1943) Parasitos de la langosta en España. I. Dípteros bombilidos. Dirección general de Agricultura, Sección de Plagas del Campo y Fitopatología, Servicio de Lucha contra la Langosta (Madrid).
- Delassus M, Pasquier R, Laffond P, Ruff, Lepigre A (1929) La lute contre les sauterelles en Algérie. Gouvernement general de l'Algérie, Direction de l'Agriculture, du Commerce et de la Colonisation (Alger).
- Do Prado CCA, Queiroz LG, da Silva FT, de Paiva TCB (2023) Toxicological effects caused by environmental relevant concentrations of ketoconazole in *Chironomus sancticaroli* (Diptera, Chironomidae) larvae evaluated by oxidative stress biomarkers. *Comparative Biochemistry and Physiology Part C: Toxicology & Pharmacology* 264: 109532. <https://doi.org/10.1016/j.cbpc.2022.109532>
- Drake CM (1991) Provisional atlas of the Larger Brachycera (Diptera) of Britain and Ireland. Biological Records Centre, NERC Institute of Terrestrial Ecology, Monks Wood Experimental Station (Huntingdon).
- Du Merle P (1979) Biologie de la larve planidium de *Villa brunnea* Beck., diptère bombyliide parasite de la processionnaire du pin. 1. Recherche et découverte de l'hôte. *Annales de Zoologie Ecologie Animale* 11: 289–304.
- ECDC (2013) Risk assessment on the impact of environmental usage of triazoles on the development and spread of resistance to medical triazoles in *Aspergillus* species. ECDC (Stockholm).
- Engel EO (1932–1937) 25. Bombyliidae. In: Lindner E (Ed.) *Die Fliegen der Paläarktischen Region*. E. Schweizerbart (Stuttgart), 1–619.
- Evenhuis NL, Greathead DJ (2015) World catalog of bee flies (Diptera: Bombyliidae). Revised September 2015. <http://hbs.bishopmuseum.org/bombcat/bombcat-revised2015.pdf> [cited as 22 July 2023]
- Greathead DJ, Evenhuis NL (1998) Family Bombyliidae. In: Papp L, Darvas B (Eds) *Contributions to a Manual of Palaearctic Diptera (with special reference to flies of economic importance)*. Vol. 2. Nematocera and Lower Brachycera. Science Herald (Budapest), 487–512.
- Grigorieva TG (1958) Zernovye sovki i borba s nimi. Gosudarstvennoe Izdatelstvo sel'skohozjajstvennoj Literatry, Moscow & Leningrad. [in Russian]
- Heneberg P, Bizos J, Čmoková A, Kolařík M, Astapenková A, Bogusch P (2016) Assemblage of filamentous fungi associated with aculeate hymenopteran brood in reed galls. *Journal of Invertebrate Pathology* 113: 95–106. <https://doi.org/10.1016/j.jip.2015.12.007>
- Heneberg P, Bogusch P (2022) Commonly used triazole fungicides accelerate the metamorphosis of digger wasps (Hymenoptera: Spheciformes). *Environmental Science and Pollution Research* 29: 67430–67441. <https://doi.org/10.1007/s11356-022-22684-8>

- Heneberg P, Bogusch P, Astapenková A, Řezáč M (2022) Life in extreme habitats: the number of prepupae per nest of the crabronid wasp *Pemphredon fabricii* is constant even under pressure from high concentrations of toxic elements. *Environmental Science and Pollution Research* 29: 16091–16102. <https://doi.org/10.1007/s11356-021-16881-0>
- Kenneke J, Mazur C, Kellock K, Overmyer J (2009) Mechanistic approach to understanding the toxicity of the azole fungicide triadimefon to a nontarget aquatic insect and implications for exposure assessment. *Environmental Science and Technology* 43: 5507–5513. <https://doi.org/10.1021/es900351w>
- Künckel d'Herculais J (1893–1905) Invasions des acridiens (vulgo sauterelles) en Algérie. Imprimerie administrative et commerciale Girault, A. Franceschi, successeur (Alger).
- Künckel d'Herculais J (1894) Les diptères parasites des acridiens: les Bombyliides. Hypnodie larvaire et metamorphose avec stade d'activité et stade de repos. *Comptes Rendus de l'Académie des Sciences, Paris* 118, 926–929.
- Lake S (2002) The role of livestock grazing in the conservation of lowland heath. PhD Thesis. University of Southampton, Faculty of Science (Southampton).
- Miles S, Muggleton J (2010) The rearing of *Thyridanthrax fenestratus* (Fallen, 1814) (Diptera, Bombyliidae) from a cocoon of *Ammophila pubescens* (Curtis, 1836) (Hymenoptera, Sphecidae). *Dipterists Digest* 17: 45–46.
- Mokržeckij S (1895) O parazitah saranči i kobylok. *Hozjain* 14: 271–272. [in Russian]
- Motyčková V (2012) Dlouhosoky podčeledí Anthracinae a Exoprosopinae v České republice a na Slovensku (Diptera: Bombyliidae). BSc. Thesis. Palacký University in Olomouc, Faculty of Science (Olomouc).
- Noordijk J, Smit JT, Smit J, Vreugdenhil D (2016) De insectengemeenschap van aangelegde steilranden op de heide. *Entomologische Berichten* 76: 48–55.
- Oldroyd H (1969) Diptera Brachycera, Section (a) Tabanoidea and Asiloidea. *Handbooks for the identification of British insects*. Royal Entomological Society (London).
- Palmer MIL (1982) Biology and behavior of two species of *Anthrax* (Diptera: Bombyliidae), parasitoids of the larvae of tiger beetles (Coleoptera: Cicindelidae). *Annals of the Entomological Society of America* 75: 61–70. <https://doi.org/10.1093/aesa/75.1.61>
- Pontin AJ (1961) *Thyridanthrax fenestratus* Fall. (Dipt., Bombyliidae) parasitic on *Ammophila* (Hym., Sphecidae). *Entomologist's Monthly Magazine, London* 96: 26.
- Porčinskij IA (1894) O kobyľkah povreždavših posevy I travy v gubernijah Permskoj, Tobolskoj I Orenburgskoj. Departament Zemledelija (St. Peterburg). [in Russian]
- Porčinskij IA (1895) Les parasites des criquets nuidibles en Russie (Fin). *Eremobia muricata*. Departament Zemledelija (St. Peterburg). [in Russian]
- Saraiva AS, Sarmiento RA, Golovko O, Randak T, Pestana JL, Soares AM (2018) Lethal and sub-lethal effects of cyproconazole on freshwater organisms: a case study with *Chironomus riparius* and *Dugesia tigrina*. *Environmental Science and Pollution Research* 25: 12169–12176. <https://doi.org/10.1007/s11356-017-1180-y>
- Séguy E (1932) Étude sur les diptères parasites ou prédateurs des sauterelles. *Encyclopédie Entomologique, B II, Diptères* 6: 11–40.
- Sergent E (1916) Campagne d'experimentation de la méthode biologique contre les *Schistocerca peregrina* dans la vallée de la Haute Tafna, commune mixte de Sebduou (département

- d'Oran). Existence d'une épizootie autochtone vaccinnante (mai, juin, Juillet 1915). Annales de l'Institut Pasteur, Paris 30: 209–224.
- Shelford VE (1913) The life history of a bee-fly (*Spogostylum anale* Say) parasite of the larva of a tiger beetle (*Cicindela scutellaris* Say var. *lecontei* Hald.). Annals of the Entomological Society of America 6: 213–225. <https://doi.org/10.1093/aesa/6.2.213>
- Slikboer L, Smit JT, Zeegers T (2019) Honingbijen & wilde bestuivers in defensieterreinen. Deel I: Doornspijkse Hei. EIS Kenniscentrum Insecten (Leiden).
- Tomaj V (1977) Československé druhy čeledi Bombyliidae (Diptera). MSc. Thesis. University of J. E Purkyně in Brno, Faculty of Science (Brno).
- Yeates DK, Greathead D (2008) The evolutionary pattern of host use in the Bombyliidae (Diptera): a diverse family of parasitoid flies. Biological Journal of the Linnean Society 60: 149–185. <https://doi.org/10.1111/j.1095-8312.1997.tb01490.x>
- Zaitsev VF (1966) Paraziticheskie mukhi semeistva Bombyliidae (Diptera) v faune Zakavkaz'ya. Izdatel'stvo 'Nauka', Moscow, Leningrad.

Supplementary material I

Coordinates of sampling sites used to generate Fig. 1

Authors: Petr Heneberg, Petr Bogusch, Alena Astapenková

Data type: xlsx

Explanation note: All the listed sampling sites were positive for *P. fabricii*. Numbers of *P. fabricii* obtained by cutting the galls, numbers of *T. fenestratus* obtained using the same procedure, and total numbers of galls cut are indicated for sampling sites that were *T. fenestratus*-positive.

Copyright notice: This dataset is made available under the Open Database License (<http://opendatacommons.org/licenses/odbl/1.0/>). The Open Database License (ODbL) is a license agreement intended to allow users to freely share, modify, and use this Dataset while maintaining this same freedom for others, provided that the original source and author(s) are credited.

Link: <https://doi.org/10.3897/jhr.97.110282.suppl1>

The first reliable fossil record of the tribe Centistini (Hymenoptera, Braconidae, Euphorinae): a new subgenus and species of braconid wasp in Danish amber

Sergey A. Belokobylskij¹, Dmitry V. Vasilenko^{2,3}, Evgeny E. Perkovsky⁴

1 Zoological Institute of the Russian Academy of Sciences, St. Petersburg 199034, Russia **2** A.A. Borissiak Paleontological Institute of the Russian Academy of Sciences, Profsoyuznaya Str. 123, Moscow 117647, Russia **3** Cherepovets State University, Cherepovets 162600, Russia **4** Natural History Museum of Denmark, Universitetsparken 15, Copenhagen 2100, Denmark

Corresponding author: Sergey A. Belokobylskij (doryctes@gmail.com)

Academic editor: J.M. Jasso-Martínez | Received 15 November 2023 | Accepted 2 January 2024 | Published 17 January 2024

<https://zoobank.org/2B4CCF9C-0AC0-458C-89AE-029367F23D16>

Citation: Belokobylskij SA, Vasilenko DV, Perkovsky EE (2024) The first reliable fossil record of the tribe Centistini (Hymenoptera, Braconidae, Euphorinae): a new subgenus and species of braconid wasp in Danish amber. *Journal of Hymenoptera Research* 97: 15–27. <https://doi.org/10.3897/jhr.97.115789>

Abstract

A new subgenus and species of the braconid parasitoid of the tribe Centistini s. l. (Euphorinae), *Centistoides* (*Palaeoides*) *magnioculus* Belokobylskij, **subgen. et sp. nov.**, from late Eocene Danish amber are described and illustrated from one female. This is the first time the tribe of euphorine parasitoids is reliably documented in the fossil record. A key to all genera and subgenera of this suprageneric taxonomic group is compiled. The discussion about position of the genus *Parasyrrhizus* Brues, composition of the tribe Centistini s. l., and the composition of the Danish amber hymenopteran fauna are provided.

Keywords

Asiacentistes, *Centistoides*, description, Eocene, ovipositor, subgenus, venation

Introduction

The extant members of the euphorine tribe Centistini include two genera with a mediocubital vein (M+CU1) of the fore wing that is distinctly desclerotised, namely *Allurus* Foerster, 1863 and *Centistes* Haliday, 1835 (with five subgenera: *Anartionyx*

van Achterberg, 1985, *Ancylocentrus* Foerster, 1863, *Centistes* s. str., *Chaetocentistes* Belokobylskij, 2000, and *Syrrhizus* Foerster, 1863). In addition, two morphologically very similar genera but with a distinctly sclerotised mediocubital vein (M+CU1) of the fore wing, *Asiacentistes* Belokobylskij, 1995 and *Centistoides* van Achterberg, 1992, were also attributed to this tribe (van Achterberg 1992; Belokobylskij 1995; Yu et al. 2016). However, a recent molecular phylogenetic study of Euphorinae genera obtained for *Asiacentistes* (Stigenberg et al. 2015) indicated its isolated phylogenetic position in the tribe as well as in the entire Euphorinae subfamily. Such a conclusion requires additional confirmation based on an analysis of more genes because the numerous morphological features clearly support belonging these genera to the Euphorinae.

The Centistini species are known as imagobionts (Shaw 2004), the endoparasitoids of the adults of beetles mainly from the families Chrysomelidae, Curculionidae (especially Scolytinae), Coccinellidae, Carabidae, etc. (Belokobylskij 1996; Yu et al. 2016). Members of this group of genera have a long, wide and strongly laterally compressed ovipositor mainly hidden inside of the metasoma, making Centistini species one of the most specialised and advanced forms of Euphorinae.

In this paper the first member (female) of the tribe Centistini sensu lato found in the fossil record is described and illustrated from a specimen in Danish amber.

Materials and methods

Priabonian Danish amber of late Eocene age (34–37 Mya) was reviewed by Heie (1967), Larsson (1978), Nadein et al. (2016) and references therein. Larsson (1978) supposed that the amber was redeposited to the Miocene lignites of Jutland from South Swedish Eocene forests.

The braconid specimens were examined with an Olympus SZ51 stereomicroscope. Photographs were obtained using a Leica Z16 APO stereomicroscope equipped with a Leica DFC 450 camera and processed with LAS Core.

The terminology employed for morphological features and sculpture, as well as body measurements, follow Belokobylskij and Maetô (2009). Wing venation nomenclature also follows Belokobylskij and Maetô (2009), with the terminology of van Achterberg (1993) shown in parentheses.

The material used for this study is deposited in the collection of the Natural History Museum of Denmark (NHMD). The holotype inclusion is located in a thin, nearly rectangular piece of amber measuring 8.0 × 6.5 mm.

Systematic part

Class Insecta Linnaeus, 1758

Order Hymenoptera Linnaeus, 1758

Family Braconidae Nees, 1811

Subfamily Euphorinae Foerster, 1863**Tribe Centistini Čapek, 1970****Key to the world genera and subgenera of the tribe Centistini sensu lato**

- 1 Mediocubital vein (M+CU1) of fore wing distinctly sclerotised and pigmented **2**
- Mediocubital vein (M+CU1) of fore wing unsclerotised and transparent **3**
- 2 Malar groove present, but sometimes incomplete. Apical segment of antenna without distal spine. Laterope of first metasomal tergite very shallow and small. Dorsal valve of ovipositor apically with wide and finely aciculate lobe. Ovipositor sheath thick and short (posterior view), very densely setose apically. Hind tibia with distinct small sparse spines at its external side.....
- ***Asiacentistes Belokobylskij, 1995***
- Malar groove and suture absent. Apical segment of antenna with distal spine. Laterope of first metasomal tergite rather deep. Dorsal valve of ovipositor apically without lobe. Ovipositor sheath thin and elongate (posterior view), glabrous or relatively sparsely setose apically. Hind tibia without spines at external sides..... ***Centistoides van Achterberg, 1992***
- 3 Claw splitting apically. Hind coxa with distinct acuminate ventro-posterior projection. Metasomal sternites often medially with double teeth
- ***Allurus Foerster, 1863***
- Claw not splitting apically, simple. Hind coxa always without ventro-posterior projection. Metasomal sternites medially usually without teeth (*Centistes* Haliday, 1835)..... **4**
- 4 First abscissa of medial vein (1-SR+M) of fore wing absent; discoidal (discal) and second radiomedial (submarginal) cells fused. – Notauli always absent.....
- ***Centistes (subgenus Syrrhizus Foerster, 1863)***
- First abscissa of medial vein (1-SR+M) of fore wing present; discoidal (discal) and second radiomedial (submarginal) cells separated..... **5**
- 5 Fore coxa on posterior (inner) side in very dense and short brush-like setae. Ovipositor sheaths thick and widened distally (dorsal and lateral views). Apex of ovipositor narrow and sinuated. Hypopygium and two posterior sternites of metasoma in very dense and short setae
- ***Centistes (subgenus Chaetocentistes Belokobylskij, 2000)***
- Fore coxa on posterior (inner) side without brush-like setae. Ovipositor sheaths rather flat and usually parallel-sided or narrowed distally (dorsal and lateral views). Apex of ovipositor rather wide and straight. Hypopygium and two posterior sternites of metasoma with usual and rather sparse setae..... **6**
- 6 Mesoscutum completely without notauli ***Centistes (subgenus Centistes s. str.)***
- Mesoscutum usually with rather distinct and complete notauli; however, sometimes notauli shallow and weakly visible; rarely notauli mainly absent anteriorly, but mesoscutum always with distinct medioposterior elongate or subround pit..... **7**

- 7 Inner claw of hind leg much larger than claw of fore leg (especially in female), hooked and larger than outer claw. Second abscissa of mediocubital vein (1-M) of hind wing shorter than basal vein (1 r-m). Ovipositor sheath widened submedially..... ***Centistes* (subgenus *Anartionyx* van Achterberg, 1985)**
- Inner claw of hind leg only slightly larger than claw of fore leg, subequal to its inner claw. Second abscissa of mediocubital vein (1-M) of hind wing subequal to basal vein (1 r-m). Ovipositor sheath often with subparallel-sided or evenly narrowed distally..... ***Centistes* (subgenus *Ancyllocentrus* Foerster, 1863)**

Genus *Centistoides* van Achterberg, 1992

Type species. *Centistoides doesburgi* van Achterberg, 1992, by monotypy and original designation.

Notes. This small Madagascan-Neotropical genus includes two extant species, *Centistoides doesburgi* van Achterberg, 1992 from Suriname (van Achterberg 1992) and *C. ophthalmicus* (Granger, 1949) from Madagascar, a species that was only recently transferred to this genus from *Centistes* (Belokobylskij 2018).

The Eastern Palaearctic genus *Asiacentistes* Belokobylskij also has two extant species, *A. alekseevi* (Belokobylskij, 1992) and *A. sinicus* Chen & Belokobylskij, 2001 (Belokobylskij 1995; Chen et al. 2001), and is very similar to *Centistoides*. The differences between these taxa are given in the key above.

Documented here the first reliable fossil member of the tribe Centistini s. l. is found in Danish amber, and it possesses a distinctly sclerotised mediocubital vein (M+CU1) of the fore wing. On the basis of all visible characters of this amber inclusion (for example, malar suture absent, apical antennal segment with distinct distal spine, ovipositor apically without lobe, ovipositor sheath thin and elongate in posterior view, sparsely setose apically) it was placed in the genus *Centistoides*; however, this specimen has some features that necessitated a separate subgenus for it within *Centistoides*.

A short redescription of the genus *Centistoides* and descriptions of the new subgenus as well as the new fossil species are given below.

Diagnosis of the genus. Occipital carina absent dorsally, only developed on lateral and ventral parts of temple, joining hypostomal carina above base of mandible. Ocelli distinctly enlarged. Eye large. Malar suture absent, but sometimes present short malar groove. Mandible strongly twisted apically. Palpi short, maxillary palpus 3–5-segmented, labial palpus 1–2-segmented. Antenna weakly setiform, apical segment of antenna with distinct distal spine. Mesosoma short and high. Notauli completely absent. Prescutellar depression usually entirely smooth or weakly rugulose, without or only with medial carina. Prepectal carina complete. Mesopleuron mainly smooth; precoxal sulcus absent. Metapleural flange absent or very short. Propodeum without or with weak areolation, with incomplete or complete posterior areola. Radial (marginal) cell of fore wing distinctly shortened. Discoidal (discal) cell usually sessile; petiole (1-SR) absent. First abscissa of medial vein (1-SR+M) of fore wing present. Recurrent vein (m-cu) antefurcal.

Mediocubital vein (M+CU1) entirely sclerotized and pigmented. In hind wing, second abscissa of mediocubital vein (1-M) much shorter than first abscissa (M+CU) and shorter than basal vein (r-m). Hind coxa large and subround. Fore femur usually more robust than hind femur. Tarsal claws robust, distinctly curved apically, simple. First metasomal tergite wide and short, almost parallel-sided or weakly narrowed behind spiracles, smooth, without dorsope. Second metasomal tergite smooth; second suture usually absent. Ovipositor strongly compressed, strongly curved and without armament and ventral lobe apically. Ovipositor sheath short, wide, flattened, truncate apically.

***Palaeoides Belokobylskij*, subgen. nov.**

<https://zoobank.org/5942B572-DB42-4325-825B-2892397FEF7D>

Type species. *Centistoides (Palaeoides) magniocolus* sp. nov., by present designation.

Etymology. Named after “Palaeo” (Greek for “ancient”) and part of the generic name *Centistoides* from the tribe Centistini.

Description. Ocelli less distinctly enlarged (Fig. 1D, E). Palpi longer, maxillary palpus more than 3-segmented, perhaps with 5 segments; labial palpus at least 2-segmented (Fig. 1D). Prescutellar depression with five carinae (Fig. 1D). Precoxal sulcus present, but very shallow (Figs 1A, 2C). In fore wing, discoidal (discal) cell petiolate anteriorly, petiole (1-SR) medium length (Fig. 2A, B). Mediocubital vein (M+CU1) entirely distinctly sclerotised and pigmented (Fig. 2A, B). Fore femur not more robust than hind femur (Fig. 2C). Tarsal claws weakly curved apically (Figs 1A, 2A, C). Second metasomal suture present but fine (Fig. 1F). Ovipositor sheath weakly narrowed apically (Fig. 1F).

Diagnosis. The genus *Centistoides* (as well as *Asiacentistes*) characterised by the fore wing mediocubital vein (M+CU1) distinctly sclerotised and pigmented, when such a vein in most Centistini genera is clearly desclerotised and transparent (spectral). Both known *Centistoides* species, *C. doesburgi* van Achterberg, 1992 and *C. ophthalmicus* (Granger, 1949), together with the genus *Asiacentistes*, have a sessile or sessile discoidal (discal) cell in the fore wing (van Achterberg 1992; Belokobylskij 1995, 2018), while in the new subgenus, *Palaeoides* subgen. nov., the discoidal (discal) cell of the fore wing is petiolate.

***Centistoides (Palaeoides) magniocolus* Belokobylskij, sp. nov.**

<https://zoobank.org/40746ECE-38DF-4FA8-BF3D-4AFB6F400376>

Figs 1, 2

Type material. Holotype: female, NHMD # 115540, with labels “Braconidae A.K. Andersen 28-3 /1968” and “Euphorinae ? huge ovipositor”. Danish amber, late Eocene. Syninclusion: female of Chironomidae.

Description. Female. Body length 3.8 mm; fore wing length 3.6 mm.

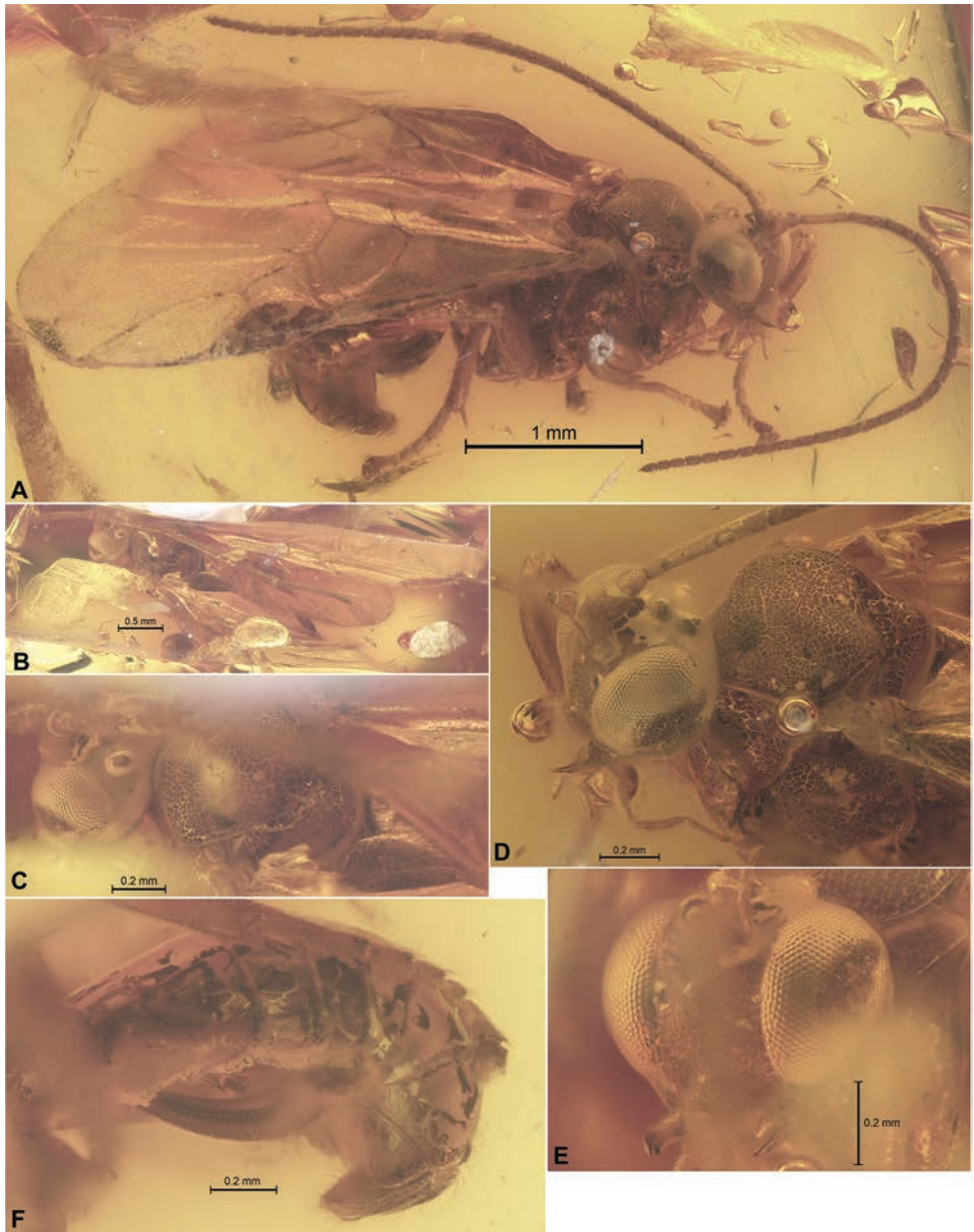


Figure 1. *Centistoides (Palaeooides) magniocolus* sp. nov. (female, holotype, Danish amber, NHMD # 115540) **A** habitus, right dorso-lateral view **B** habitus, dorsal view **C** head and mesosoma, dorsal view **D** head and anterior part of mesosoma, dorso-lateral view **E** head, fronto-lateral view **F** metasoma and ovipositor, lateral view.

Head: Head rather short; occiput distinctly concave. Eye large, glabrous, ~ 1.4 times as high as broad (sublateral view); transverse diameter of eye almost 2.0 times longer than temple (subdorsal view). Ocelli medium-sized, convex, situated almost in

equilateral triangle; POL approximately 0.8 times Od, 2.0 times OOL; Od ~ 2.2 times OOL. Face weakly convex, its width ~ 0.8 times mid-height. Clypeus distinctly convex, its width ~ 2.0 times mid-height, 0.8 times width of face. Malar space ~ 0.15 times height of eye, ~ 0.7 times basal width of mandible. Malar suture absent. Mandible distinctly twisted in apical half, with two apical teeth.

Antenna: Antenna long, almost filiform, 28-segmented, about as long as body. Scape 1.5 times longer than its maximum width, ~ 2.0 times longer than pedicel. First flagellar segment rather wide, 4.5 times longer than its maximum width, 1.2 times longer than second segment. Penultimate segment 1.5 times longer than its maximum width, 0.7 times as long as apical segment. Apical antennal segment with distinct distal spine.

Mesosoma: Mesosoma 1.2 times longer than its maximum height. Neck of prothorax short. Mesoscutum anteriorly distinctly convex and weakly protruding forward, without anterolateral corners. Notauli completely absent. Prescutellar depression (scutellar sulcus) rather short, densely crenulate. Scutellum short and weakly convex. Subalar depression shallow and narrow, smooth. Propodeum strongly curvedly narrowed posteriorly (lateral view).

Wings: Fore wing wide, 2.7 times longer than its maximum width. Pterostigma wide, 3.2 times longer than its width. Radial (marginal) cell distinctly shortened, 3.2 times longer than its maximum width. Metacarp (1-R1) 0.7 times as long as pterostigma. Radial vein (r) arising weakly behind middle of pterostigma. First (r) and second (3-RS+SR1) radial abscissae forming obtuse angle; first abscissa (r) 0.4 times as long as maximum width of pterostigma. Second radial abscissa (3-RS+SR1) evenly curved, almost 9.0 times longer than first abscissa (r), 2.7 times longer than first radiomedial vein (2-RS). Recurrent vein (m-cu) distinctly antefurcal, 2.0 times longer than second abscissa of medial vein (2-SR+M), 0.6 times as long as first radiomedial vein (2-RS), 0.45 times as long as basal vein (1-M). First abscissa of medial vein (1-SR+M) weakly sinuate. Discoidal (discal) cell 1.1 times longer than its maximum width. Nervulus (cu-a) 0.8 times as long as distance (1-CU1) between basal vein (1-M) and nervulus (cu-a). Parallel vein (CU1a) distinctly curved basally. Brachial (subdiscal) cell relatively short and rather wide. Hind wing ~ 4.5 times longer than its maximum width. Submedial (subbasal) cell long and wide; first abscissa of mediocubital vein (M+CU) ~ 4.0 times longer than second abscissa (1-M).

Legs: Fore femur wide, ~ 3.3 times longer than its maximum width. Fore tarsus shortened; tarsal segments mainly short. Hind coxa wide and short, massive, ~ 1.3 times longer than its maximum width. Hind femur ~ 4.0 times longer than its width. Hind tibia distinctly thickened. Hind tarsus shorter than hind tibia. Claw simple.

Metasoma: Metasoma curved down posteriorly, approximately as long as head and mesosoma combined. First metasomal tergite with distinct and complete dorsal carinae, approximately as long as propodeum. Second suture perhaps absent. Subposterior sternite with pair of short ventral teeth. Ovipositor wide, compressed and distinctly curved; dorsal valve of ovipositor apically without lobe. Ovipositor sheath rather thin (ventral view), short and wide, narrowed distally, with short apical tubercle (lateral view), covered by rather long and almost erect setae; sheath 2.2 times longer than its width, ~ 0.7 times as long as first tergite.

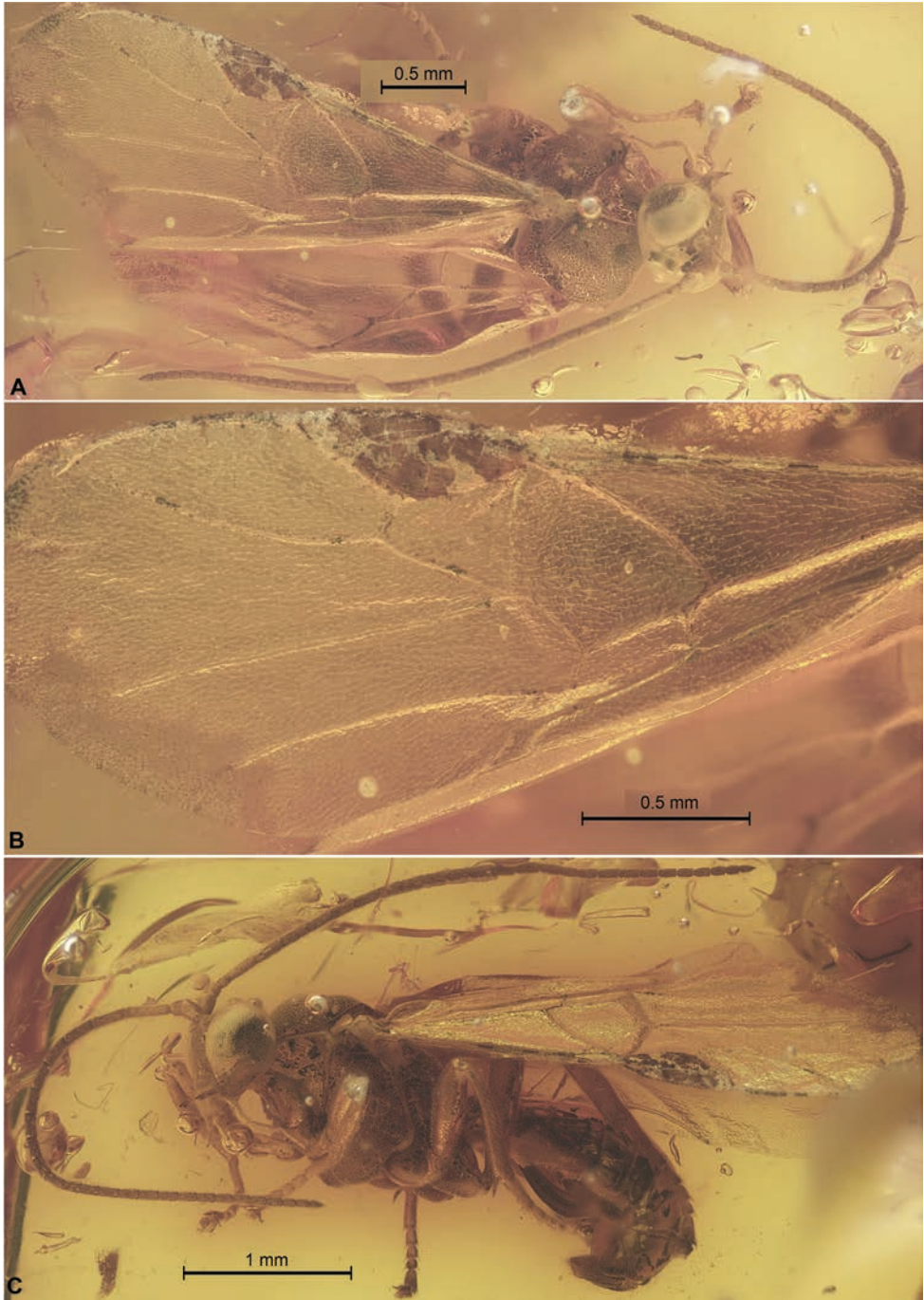


Figure 2. *Centistoides (Palaeoides) magniocolus* sp. nov. (female, holotype, Danish amber, NHMD # 115540) **A** wings, head and mesosoma, dorso-lateral view **B** fore wing **C** habitus, left sublateral view.

Sculpture: Body mainly smooth; sculpture of propodeum not visible, but perhaps with transverse carina.

Colour: Body dark brown to black. Palpi yellow. Antenna mainly black, brown basally. Legs mainly light reddish brown or reddish brown, hind tibia dark. Fore wing hyaline. Pterostigma entirely dark brown.

Male. Unknown.

Etymology. This species is named after Latin “magnus” (large) and “oculus” (eye), because the eyes of the new species are distinctly enlarged.

Comparative diagnosis. The new species differs from the type species of the genus *Centistoides*, *C. doesburgi* van Achterberg, 1992, primarily by subgeneric characters. The differences between all known species of *Centistoides* are shown in the key below.

Key to species of the genus *Centistoides*

- 1 Discoidal (discal) cell of fore wing petiolate anteriorly; first abscissa of medial vein (1-SR+M) arising from basal vein (1-M). Subposterior sternite of metasoma with pair of short ventral teeth. – Prescutellar depression with five transverse carinae. Tarsal claws weakly curved apically. Ovipositor sheath narrowed apically. Fore wing length 3.6 mm. Fossil..... *C. (Palaeoides) magniocus* **sp. nov.**
- Discoidal (discal) cell of fore wing sessile anteriorly; first abscissa of medial vein (1-SR+M) arising from parastigma. Subposterior sternite of metasoma without ventral teeth..... **2**
- 2 First medial abscissa (1-SR+M) of fore wing sinuate; second medial abscissa (2-SR+M) long, 0.6 times as long as recurrent vein. Discoidal (first discal) cell anteriorly narrowly sessile. First transverse anal vein (1a) present. Propodeum with distinct basomedian carina and with areola completely delineated by carinae. Prescutellar depression (scutellar sulcus) sculptured. Ovipositor sheath relatively thick, but flattened on narrow flanges dorsally and apically, rather densely setose apically. Fore wing length 4.7 mm. Afrotropics (Madagascar) *C. (s. str.) ophthalmicus* (**Granger, 1949**)
- First medial abscissa (1-SR+M) of fore wing straight; second medial abscissa (2-SR+M) short, ~ 0.3 times as long as recurrent vein. Discoidal (first discal) cell anteriorly broadly sessile. First transverse anal vein (1a) absent. Propodeum without basomedian carina, with areola incompletely delineated by carinae anteriorly. Prescutellar depression (scutellar sulcus) smooth. Ovipositor sheath entirely flatted, truncate and glabrous apically. Fore wing length 3.0 mm. Neotropics (Suriname) *C. (s. str.) doesburgi* **van Achterberg, 1992**

Discussion

The fossil genus and species presumably from the tribe Centistini, *Parasyrrhizus ludens* Brues, 1933, was described from Baltic amber based on two males in the subfamily

Leiophroninae (= Euphorinae) (Brues 1933). This genus was compared with euphorine genus *Syrrhizus* Foerster, 1863 (now the subgenus of *Centistes* Haliday, 1835) on the basis of the fore wing venation without first abscissa of medial vein (1-SR+M) and respectively fused first radiomedial (submarginal) and discoidal (discal) cells. However, already in the World Catalogue (Shenefelt 1970), *Parasyrrhizus* was transferred to the subfamily Calyptinae (= Brachistinae), though without explanation. Perhaps the reason for this transfer was based on the brachial (subdiscal) cell of the fore wing closed distally by the recurrent vein (CU1b) (according to the figure: Brues 1933: fig. 52), characters never recorded in Euphorinae members. It appears only the discovery of the female of this species with a visible ovipositor (both of its types, males, may have been lost after World War II) will finally resolve its suprageneric membership.

Thus, *Centistoides (Palaeoides) magniocolus* sp. nov. is the first reliable fossil record of Centistini sensu lato found as an inclusion in amber.

It should be noted that in a recent molecular phylogenetic analysis of the subfamily Euphorinae, it was shown that the genus *Asiacentistes* (which is very similar and probably closely related to *Centistoides*) does not belong to the Euphorinae s. str. (Stigenberg et al. 2015), and this genus may be the sister taxon to the clade Cenocoelinae+Euphorinae. On the other side, the members of the tribe Centistini are similar morphologically, especially on the basis of the wing venation, to the representatives of the tribe Brachistini (Brachistinae). However, the brachistine females never had such a peculiar ovipositor as presented in *Asiacentistes* and *Centistoides* together with all other members of the tribe Centistini s. str., namely wide, laterally compressed, curved and mainly hidden inside of the female metasoma. This type of ovipositor, which had been known only in euphorine imagobionts until now, allowed them to effectively penetrate the body of strongly sclerotised hosts through the intersegmental membrane between the sclerites of the abdomen. Such host stages are never used by brachistines, which are known as egg-larval endoparasitoids. Perhaps both of these genera, *Asiacentistes* and *Centistoides*, and the fossil subgenus described here, which differs from other Centistini s. str. by the distinctly sclerotized mediocubital vein (M+CU) of the fore wing, form a separate tribe. However, for confirmation of this suggestion, we would need additional molecular phylogenetic analysis of more genes.

The former braconid subfamily Betylobraconinae (currently Betylobraconini in Rogadinae), represented in the Eocene by the genus *Mesocentrus* Szépliget, 1900 (Butcher et al. 2014), and the ant tribe Leptomymecini (Dlussky et al. 2014), the two hitherto known suprageneric hymenopteran taxa with the oldest records from Danish amber, remain unrecorded from Baltic amber. For comparison, in the far better-studied non-ant hymenopteran fauna of Rovno amber, only two such taxa are known: parasitic wasps subfamily Eucoilinae (Figitidae) (they are very common now, so perhaps they have been overlooked in Baltic amber) as well as an extinct crabronid wasps tribe Protomicroidini (Perkovsky 2018). All six Danish Encyrtidae genera (Chalcidoidea) (Simutnik and Perkovsky 2017, 2018, 2023; Simutnik et al. 2023), three braconid genera (Butcher et al. 2014; Kittel 2018; this paper), three genera of ants and one of Bethyilidae (Perkovsky 2018) remain unknown from Baltic amber. Out of those, two encyrtid (Simutnik et al. 2021; Simutnik et al. 2023) and two ant genera

(Perkovsky 2016), together with the bethylid genus *Sierola* Cameron, 1881 (Ramos et al. 2014), are recorded from Rovno amber. At least Betylobraconini, Leptomyrmecini, *Centistoides*, *Sierola* and an ant genus *Pristomyrmex* Mayr, 1866 (Radchenko and Perkovsky 2021) can be classified as cryophobic taxa (Jenkins Shaw et al. 2023 and references therein). Thus, the discovery of a new subgenus described in the present paper confirms the theory that the fauna of Danish amber (as well as that of Rovno amber, see Kirichenko-Babko and Perkovsky 2023 and references therein) was likely noticeably more thermophilic than Baltic amber fauna (Perkovsky 2016, 2017).

Overall, 45% of Danish amber hymenopteran genera remain unknown from Baltic amber (authors' data) – one and a half times higher than the proportion of known Rovno amber hymenopteran genera not yet discovered in Baltic amber, and even higher than the proportion of non-ant Rovno amber hymenopteran genera unknown from Baltic amber (41%, Belokobylskij et al. 2023). Although the Danish amber hymenopteran fauna is in urgent need of revision, the high level of endemism suggests an independent geographic origin of this fauna.

Acknowledgements

We are very thankful to Prof. Alexandr P. Rasnitsyn (Palaeontological Institute, Moscow, Russia) for his useful consultation and discussion. We are sincerely grateful Madeline V. Pankowski (Rockville, USA) for improving the English of our manuscript. The authors are also very thankful to Prof. Cornelis van Achterberg (Leiden, the Netherlands) and unknown reviewer for their good opinion and useful comments on the first version of the manuscript.

This study was performed as part of the Russian State Research Project No. 122031100272–3 for SAB. EEP was supported by the Scholars at Risk Ukraine (SARU) program, jointly funded by the Villum Foundation, Carlsberg Foundation and Novo Nordisk Foundation, and by the grant “Support and development of the amber collection of the Statens Naturhistoriske Museum” from Dr. Bøje Benzons Støttefond.

References

- Belokobylskij SA (1995) A new genus and ten species of the subfamily Euphorinae (Hymenoptera: Braconidae) from the Russian Far East. *Zoosystematica Rossica* 3(2): 293–312.
- Belokobylskij SA (1996) Parasitism on the beetles (Coleoptera) as important stage in the evolution of braconid wasps (Hymenoptera, Braconidae). Part I. *Entomologicheskoe Obozrenie* 75(3): 660–676. [In Russian]
- Belokobylskij SA (2018) *Notioperilitus* gen. nov., a new braconid genus (Hymenoptera: Braconidae: Euphorinae) from Australia, parasitoid of adult Morabinae (Orthoptera: Eumastacidae), with remarks on the generic placement of two Afrotropical euphorine species. *Zootaxa* 4441(2): 298–310. <https://doi.org/10.11646/zootaxa.4441.2.6>

- Belokobylskij SA, Maetô K (2009) Doryctinae (Hymenoptera, Braconidae) of Japan. Fauna Mundi. Vol. 1. Warszawska Drukarnia Naukowa, Warszawa, 806 pp.
- Belokobylskij SA, Simutnik SA, Vasilenko DV, Perkovsky EE (2023) First record of the parasitoid subfamily Doryctinae (Hymenoptera, Braconidae) in Rovno amber: description of a new genus and species with stigma-like enlargement on the hind wing of the male. Journal of Hymenoptera Research 95: 59–72. <https://doi.org/10.3897/jhr.95.96784>
- Brues CT (1933) The parasitic Hymenoptera of the Baltic amber. Bernstein Forschungen 3: 4–178.
- Butcher BA, Zaldivar-Riverón A, van De Kamp T, dos Santos Rolo T, Baumbach T, Quicke DLJ (2014) Extension of historical range of Betylobraconinae (Hymenoptera: Braconidae) into Palaearctic Region based on a Baltic amber fossil, and description of a new species of *Mesocentrus Szépligetii* from Papua New Guinea. Zootaxa 3860(5): 449–463. <https://doi.org/10.11646/zootaxa.3860.5.4>
- Chen X, Belokobylskij SA, He J-H, Ma Y (2001) The genus *Asiacentistes* Belokobylskij (Hymenoptera: Braconidae) from China. Oriental Insects 35: 167–170. <https://doi.org/10.1080/00305316.2001.10417296>
- Dlussky G, Radchenko A, Dubovikoff D (2014) A new enigmatic ant genus from late Eocene Danish amber and its evolutionary and zoogeographic significance. Acta Palaeontologica Polonica 59(4): 931–939. <http://dx.doi.org/10.4202/app.2012.0028>
- Heie O (1967) Studies on fossil aphids (Homoptera: Aphidoidea). Spolia Zoologica Musei Hauniensis 26: 1–274.
- Jenkins Shaw J, Perkovsky EE, Ślipiński A, Escalona H, Solodovnikov A (2023) An extralimital fossil of the genus *Diagrypnodes* (Coleoptera: Salpingidae: Inoepelinae). Historical Biology. <https://doi.org/10.1080/08912963.2023.2206858>
- Kirichenko-Babko M, Perkovsky EE (2023) The first neotropical Carabidae (Coleoptera) from the Eocene of Ukraine: finding the first Old World ant nest beetle related to *Eohomopterus* in the Rovno amber. Earth and Environmental Science Transactions of the Royal Society of Edinburgh 114(1–2): 115–124. <https://doi.org/10.1017/S1755691023000105>
- Kittel RN (2018) First record of the genus *Phanerotomella* (Hymenoptera: Braconidae) from Baltic amber with the description of a new species. Zootaxa 4482(1): 197–200. <https://doi.org/10.11646/zootaxa.4482.1.11>
- Larsson SG (1978) Baltic amber – a paleobiological study. Klampenborg, Denmark: Scandinavian Science Press, 192 pp. <https://doi.org/10.1163/9789004631243>
- Nadein KS, Perkovsky EE, Moseyko AG (2016) New late Eocene Chrysomelidae (Insecta: Coleoptera) from Baltic, Rovno and Danish ambers. Papers in Palaeontology 2(1): 117–137. <https://doi.org/10.1002/spp2.1034>
- Perkovsky EE (2016) Tropical and Holarctic ants in Late Eocene ambers. Vestnik Zoologii 50(2): 111–122. <https://doi.org/10.1515/vzoo-2016-0014>
- Perkovsky EE (2017) Comparison of biting midges of the Early Eocene Cambay amber (India) and Late Eocene European ambers supports the independent origin of European ambers. Vestnik Zoologii 51(6): 275–284. <https://doi.org/10.1515/vzoo-2017-0033>
- Perkovsky EE (2018) Only a half of species of Hymenoptera in Rovno amber is common with Baltic amber. Vestnik Zoologii 52(5): 353–360. <https://doi.org/10.2478/vzoo-2018-0037>

- Radchenko AG, Perkovsky EE (2021) Wheeler's dilemma revisited: first *Oecophylla-Lasius* syn-inclusion and other ants syninclusions in the Bitterfeld amber (late Eocene). *Invertebrate Zoology* 18(1): 47–65. <https://doi.org/10.15298/invertzool.18.1.05>
- Ramos MS, Perkovsky EE, Rasnitsyn AP, Azevedo CO (2014) Revision of Bethylinae fossils (Hymenoptera: Bethylinae) from Baltic, Rovno and Oise amber, with comments on the Tertiary fauna of the subfamily. *Neues Jahrbuch für Geologie und Paläontologie, Abhandlungen* 271(2): 203–228. <https://doi.org/10.1127/0077-7749/2014/0385>
- Shaw SR (2004) Essay on the evolution of adult-parasitism in the subfamily Euphorinae (Hymenoptera: Braconidae). *Proceedings of the Russian Entomological Society* 75(1): 82–95.
- Shenefelt RD (1970) Braconidae 2. Helconinae, Calyptinae, Mimagathidinae, Triaspininae. *Hymenopterorum Catalogus (nova editio). Pars 5. Dr. W. Junk N.V., 's-Gravenhage*, 177–306.
- Simutnik SA, Perkovsky EE (2017) *Protocopidosoma* gen. nov. (Hymenoptera, Chalcidoidea, Encyrtidae) from the late Eocene Danish amber. *Paleontological Journal* 51(3): 288–290. <https://doi.org/10.1134/S0031030117030108>.
- Simutnik SA, Perkovsky EE (2018) *Dencyrtus* gen. nov. (Hymenoptera, Chalcidoidea, Encyrtidae) from the late Eocene Danish amber. *Paleontological Journal* 52(3): 290–293. <https://doi.org/10.1134/S0031030118030139>.
- Simutnik SA, Perkovsky EE (2023) Description of a new genus and species of Encyrtidae (Hymenoptera: Chalcidoidea) from Danish amber, based on a male specimen featuring an antenna with a distinct anellus. *Zootaxa* 5369(3): 437–445. <https://doi.org/10.11646/zootaxa.5369.3.7>
- Simutnik SA, Pankowski MV, Perkovsky EE (2023) First record of *Archaeocercoides puchkovi* Simutnik, 2022 (Hymenoptera, Chalcidoidea, Encyrtidae) from late Eocene Danish amber. *Palaeoentomology* 6(6): 616–619. <https://doi.org/10.11646/palaeoentomology.6.6.3>
- Simutnik SA, Perkovsky EE, Khomych MR & Vasilenko DV (2021) First record of the *Sulia glaesaria* Simutnik, 2015 (Hymenoptera, Chalcidoidea, Encyrtidae) from Rovno amber. *Journal of Hymenoptera Research* 88: 85–102. <https://doi.org/10.3897/jhr.88.75941>
- Stigenberg J, Boring CA, Ronquist F (2015) Phylogeny of the parasitic wasp subfamily Euphorinae (Braconidae) and evolution of its host preferences. *Systematic Entomology* 40: 570–591. <https://doi.org/10.1111/syen.12122>
- van Achterberg C (1992) *Centistoides* gen. nov. (Hymenoptera: Braconidae: Euphorinae) from Suriname. *Zoologische Mededelingen* 66(23): 345–348.
- van Achterberg C (1993) Illustrated key to the subfamilies of the Braconidae (Hymenoptera: Ichneumonoidea). *Zoologische Verhandlungen* 283: 1–189.
- Yu DS, van Achterberg C, Horstmann K (2016) Taxapad 2016. Ichneumonoidea 2015. Nepean, Ottawa, Ontario. [Database on flash-drive]

High hymenopteran parasitoid infestation rates in Czech populations of the *Euphydryas aurinia* butterfly inferred using a new molecular marker

Hana Konvičková^{1,2}, Václav John^{1,2,3}, Martin Konvička^{1,2}, Michal Rindoš^{1,2}, Jan Hrček^{1,2}

1 Institute of Entomology, Biology Centre CAS, Branisovska 31, CZ-37005 Ceske Budejovice, Czech Republic

2 Faculty of Science, University of South Bohemia, Branisovska 1760, CZ-37005 Ceske Budejovice, Czech Republic

3 Nature Conservation Agency of the Czech Republic, Kaplanova 1931/1, CZ-14800, Praha 11, Czech Republic

Corresponding author: Hana Konvičková (hpatzenhauerova@gmail.com)

Academic editor: Petr Janšta | Received 24 September 2023 | Accepted 8 January 2024 | Published 29 January 2024

<https://zoobank.org/144B6E44-54F0-4BDD-84AA-833A0EC6533A>

Citation: Konvičková H, John V, Konvička M, Rindoš M, Hrček J (2024) High hymenopteran parasitoid infestation rates in Czech populations of the *Euphydryas aurinia* butterfly inferred using a new molecular marker. Journal of Hymenoptera Research 97: 29–42. <https://doi.org/10.3897/jhr.97.113231>

Abstract

We apply a molecular approach to quantify the level of hymenopteran parasitoids infestation in the larvae of the marsh fritillary (*Euphydryas aurinia*), a declining butterfly species, in western Bohemia, Czech Republic, in two subsequent years. We used the novel primer HymR157 in combination with known universal 28SD1F to establish a PCR detection system which amplifies hymenopteran parasitoids, but not the lepidopteran host. In the 14 sampled *E. aurinia* colonies, the infestation rates per individuum were 33.3% and 40.2%; whereas per sampled larval colony, these were on average 38.5% (range 0–100) and 40.1% (0–78). The per-colony infestation rates correlated with the numbers of larval webs censused per colony the year prior to sampling the parasitoids, pointing to a time lag in parasitoid infestation rates. The levels of the hymenopteran parasitoid prevalence are thus relatively high, supporting the importance of parasitoids for the population dynamics of the threatened host. The detection primers we developed can detect a range of hymenopteran parasitoids on other butterfly hosts.

Keywords

butterfly ecology, Braconidae, Lepidoptera, Marsh Fritillary, molecular detection, Nymphalidae, population dynamics

Introduction

Hymenopteran parasitoids are one of the most diverse groups of animals in terrestrial ecosystems and play a key role in the natural regulation of their host populations (La Salle and Gauld 1991; Forbes et al. 2018). The impact of parasitoids on their hosts can vary depending on their ecological specialisation, but in general they are known to cause significant levels of mortality in their hosts (Hawkins 1994). High levels of parasitism may also pose a potential threat to many threatened butterfly species, especially to various specialists in fragmented landscapes (cf. Anton et al. 2007). Species of the genus *Euphydryas* Scudder, 1872 (Nymphalidae: Melitaeini) represent a suitable system for studying host-parasitoid interactions, as egg clutches and webs with gregarious caterpillars can easily be detected in the field (Stamp 1981; Hula et al. 2004; Johansson et al. 2019). Previous studies using rearing have shown that the level of parasitism varied annually and depended mainly on weather conditions, which play a key role in the synchronisation between larval development and the emergence of parasitoids (Porter 1979, 1983).

The Marsh Fritillary, *Euphydryas aurinia* (Rottemburg, 1775) is an EU-protected butterfly, declining in many European countries (van Swaay et al. 2010), including the Czech Republic (Hejda et al. 2017). It belongs to a genetically polymorphic group of closely related taxa, the “*E. aurinia* complex” (cf. Korb et al. 2016), with a wide Palearctic distribution and regional habitat and host plant specificity (e.g., Munguira et al. 1997; Singer et al. 2002; Junker et al. 2010; Korb et al. 2016). In Central and Western Europe, its main habitats are oligotrophic grasslands, and the most frequently used host plant is *Succisa pratensis* Moench (Dipsacaceae) (Warren 1994; Anthes et al. 2003; Konvička et al. 2003; Meister et al. 2015). The butterfly is monovoltine, with flight period in late spring/early summer when the mated females oviposit on leaf rosettes of the host plant. The larvae feed gregariously in silken webs on the plants until overwintering. They enter hibernation with the host plants’ senescence in mid-September and resume feeding solitarily in April. In the Czech Republic, the distribution is restricted to the western part of the country (Fig. 1), where it forms three distinct metapopulation clusters inhabiting ≈90 separate oligotrophic meadow patches interconnected by dispersal (Zimmermann et al. 2011; Junker et al. 2021; Tájek et al. 2023). This system is monitored annually by counting larval nests (cf. Ojanen et al. 2013) and displays remarkable within-site and inter-annual dynamics with booms and bursts (John et al. in rev.).

Like many other insects, *E. aurinia* hosts numerous hymenopteran parasitoids (Wahlberg et al. 2001; Eliasson and Shaw 2003; Stefanescu et al. 2009). The braconids of the genus *Cotesia* (Cameron, 1891), gregarious endoparasitoids of Lepidoptera, can be considered the most important and numerous. Their adult females oviposit into haemolymph of lepidopteran caterpillars; their larvae feed internally, break through the cuticle in the prepupal larval instar, and form silky external cocoons, in which they pupate, and from which the adult wasps hatch (Kester and Barbosa 1991; Pakarinen 2011). It was long believed that the main hymenopteran parasitoid of European Melitaeini butterflies was *Cotesia melitaeorum* (Wilkinson, 1937), remarkable for its plurivoltine development, in which successive wasp broods oviposit on successive caterpillar

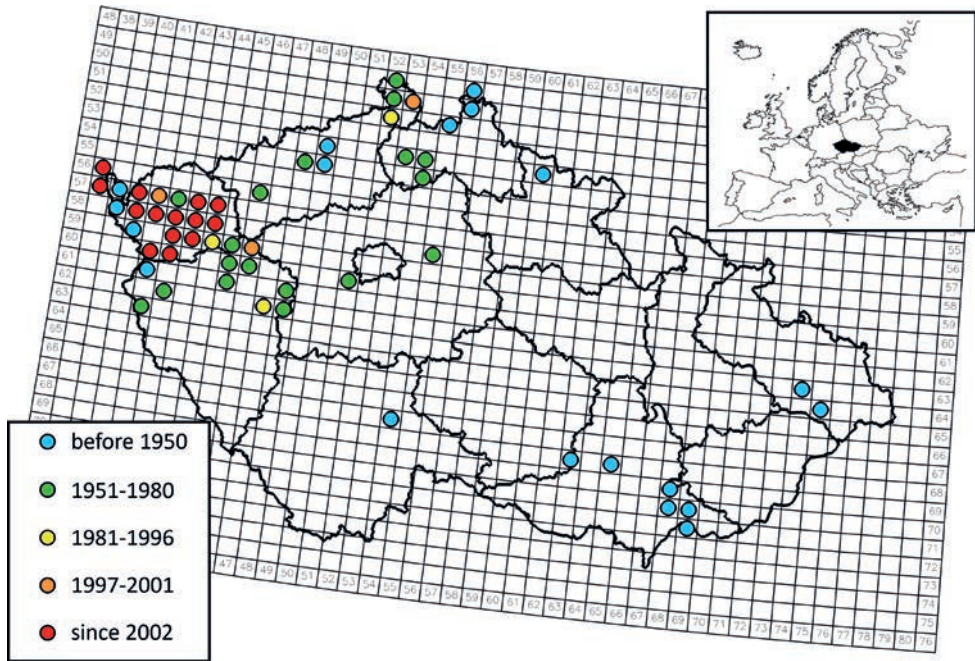


Figure 1. The distribution of *Euphydryas aurinia* in the Czech Republic, historic records included, based on Beneš et al. (2002), with actualisations. The inset in upper right corner shows the position of the country in Europe.

instars (Shaw et al. 2009; Pakarinen 2011). A molecular approach complicated the matter by revealing that *C. melitaeorum* is a complex of several cryptic species (Kankare et al. 2005c; Stefanescu et al. 2009). Regardless, the following hymenopteran parasitoids of *E. aurinia* have been so far reported from the Czech Republic: Braconidae – *Cotesia melitaeorum* (Wilkinson, 1937), *C. tibialis* (Curtis, 1830); Pteromalidae – *Pteromalus puparum* (Linnaeus, 1758); Ichneumonidae – *Ichneumon emancipatus* (Wesmael, 1845), *Ichneumon gracilicornis* (Gravenhorst, 1849) (Shaw et al. 2009; Yu et al. 2012).

Diverse methods were used so far to study the parasitoids of *E. aurinia*, and related butterflies, ranging from field counts of hymenopteran cocoons (Ford and Ford 1930; Porter 1983), captive rearing (Eliasson and Shaw 2003), field experiments with captive-reared material (Stamp 1981) to population genetic studies targeting parasitoid adults (Lei and Hanski 1997; Van Nouhuys and Lei 2004). However, the question pivotal to the butterfly population dynamics and conservation, that of infestation rates relative to population cycle and state of the butterfly colonies, seems to be little explored. This is probably due to the work requirements for rearing both butterflies and parasitoids (cf. Klapwijk and Lewis 2014), combined with destructivity of such methods for field populations. To quantify the parasitism rates in the Czech Republic populations of *E. aurinia*, we developed a molecular method, allowing rapid and low-cost detection of Hymenoptera parasitoids' incidence.

DNA-based methods are increasingly used in studies of parasitoid-hosts interactions (Zhu et al. 2019; Jeffs et al. 2021). The protocols so far developed for Lepidoptera/Hymenoptera systems mainly focused on COI locus, commonly referred as barcode (Folmer et al. 1994; Hebert et al. 2004), with the hope that the solid barcoding databases will assist species' identification (Toro-Delgado et al. 2022). Particularly good results were obtained via a reversal approach when the adult parasitoids were screened for host DNA shortly after their emergence (Rougerie et al. 2011) or in a species-poor natural system (high Arctic: Wirta et al. 2014). However, use of COI-based primers may be unreliable without subsequent sequencing, because deeply phylogenetically conserved bases are few and too far between in COI to place a group specific primer. Therefore, it was necessary to find a novel primer or primer pair which would amplify Hymenoptera but not Lepidoptera in the mixed samples containing the DNA of known lepidopteran host and unidentified hymenopteran parasitoids. We found such a potential primer in the nuclear region encoding the 28S ribosomal DNA. The novel primer, together with a primer published by Larsen (1992), targets part of the 28S gene and aims to amplify only Hymenoptera.

In this paper, we quantify Hymenoptera parasitoids infestation rates in a selection of the Czech Republic populations of *Euphydryas aurinia* and relate the infestation rates to the stage of the butterfly population cycle. Additionally, we document utility of our primers' combination for rapid Hymenoptera infestation assessment in butterflies.

Material and methods

We sampled *E. aurinia* caterpillars in western Bohemia (Fig. 1) in late August and early September. We sampled two caterpillars per larval web (105 webs in total) from 13 sites in 2019 and four per web (90 webs in total) from 9 sites in 2020.

While sampling the caterpillars, we recorded the following: Julian *date*, to account for infestation changes during larval period; *longest* and *shortest dimension* of the larval web (cm); *ward height*, i.e., visually estimated height of surrounding vegetation in 2.5 metre radius circles around each larval web sampled; *host plant density*, expressed as the number of *Succisa* flowerheads in the circle; and *webs density*, expressed as the number of larval webs in the circle.

The material was stored in 96% ethanol, the DNA was extracted using the Tissue Genomic DNA Mini Kit (GenAid Biotech, Taiwan) following the manufacturer's protocol.

We targeted a part of the 28S D1 region. We used primer 28SD1F (GGG-GAGGAAAAGAACTAAC; Larsen et al. 1992) in combination with a new primer HymR157 (TGGCCCCATTCAAGATGG) with a resulting product of 164–167 bp. For the primer design, we assembled a library of target sequences (Hymenoptera parasitoids) and non-target sequences (Lepidoptera) from sequences available in GenBank (primarily PopSet 300390962, Heraty et al. 2011). We aligned the sequences in GENEIOUS PRIME 2020.2.4 (<https://www.geneious.com>) software and used AMPLICON software (Jarman 2003) to identify sections with concentrat-

ed nucleotides that consistently differ between the target and non-target groups. We then manually screened these promising sections and used general rules of thumb to design candidate primers. We aimed for at least three differences between target and non-target groups in the first five positions at the 3' end of the primer for reliable specificity. We then tested the candidate primer in an in-silico PCR in GENEIOUS and optimized melting temperature in the primer pairs by extending or shortening the primers.

Each in vitro PCR reaction contained 6.5 μ l of Combi PPP Mastermix (Top-Bio, Czech Republic), 4.5 μ l of H₂O, 0.5 μ l of both reverse and forward primer, and 1 μ l of DNA template. The cycling conditions of PCR were as follows: 94 °C of initial denaturation (5 mins), 30 cycles at 94 °C denaturation (40 secs), 50 °C annealing (30 secs), and 72 °C elongation (1 min), with the final elongation at 72 °C (5 mins). The presence/absence of PCR products was checked using agarose electrophoresis (1.5% gel, 150V, 30 mins). The samples with a band on the gel were assumed as positive; i.e., individuals infested by parasitoids (Fig. 2).

To test the utility of the primer used, we also carried out control reactions which contained DNA extracted from various adult hymenopteran parasitoids and butterflies (Fig. 2) to assure that we amplified only the potential parasitoids and not the butterfly. Some of the obtained PCR products (n=4) of parasitoids from positive *E. aurinia* samples were sequenced in SEQme (Czech Republic) to confirm hymenopteran origin. We checked the identity of the obtained sequences by using BLAST (nBLAST algorithm) (<https://blast.ncbi.nlm.nih.gov>, Altschul et al. 1990).

Positive results were recalculated to infestation levels per larval web (1/0 factor, infested or not) and per site (% of larvae sampled). To relate the per-web infestation level to larval web properties, we carried out logistic regressions (binomial error distribution; in R 4.2.3, R Core Team 2018) with infestation (1/0) as the dependent variable; and the longest and shortest web ground projections, surrounding vegetation height, *Succisa* density, and number of larval webs as predictors. We used the information theory approach, comparing the fitted regression Akaike information criteria (AIC) with AIC of the null model, $\gamma+1$, and considered models with Δ AIC > \approx 2.0 as fitting the data.

To relate the per site percentual infestation to larval counts at the sites, we used data from annual monitoring of the sites, ongoing since 2001 (Hula et al. 2004). Over this time, larval counts were obtained for roughly $\frac{3}{4}$ of site x year combinations (John et al. in rev., Suppl. material 1).

Results

Out of 210 (year 2019) and 358 (year 2020) *E. aurinia* caterpillars assayed for hymenopteran DNA, we obtained 70 and 144 positive results, respectively; i.e., the total infestation rates were 33.3% and 40.2% per individuum. On a per-site basis, this translates to mean \pm SD / median / range 38.5 \pm 29.89 / 40 / 0–100 per cent in 2019, and 40.1 \pm 26.51 / 50 / 0–77.5 per cent in 2020.

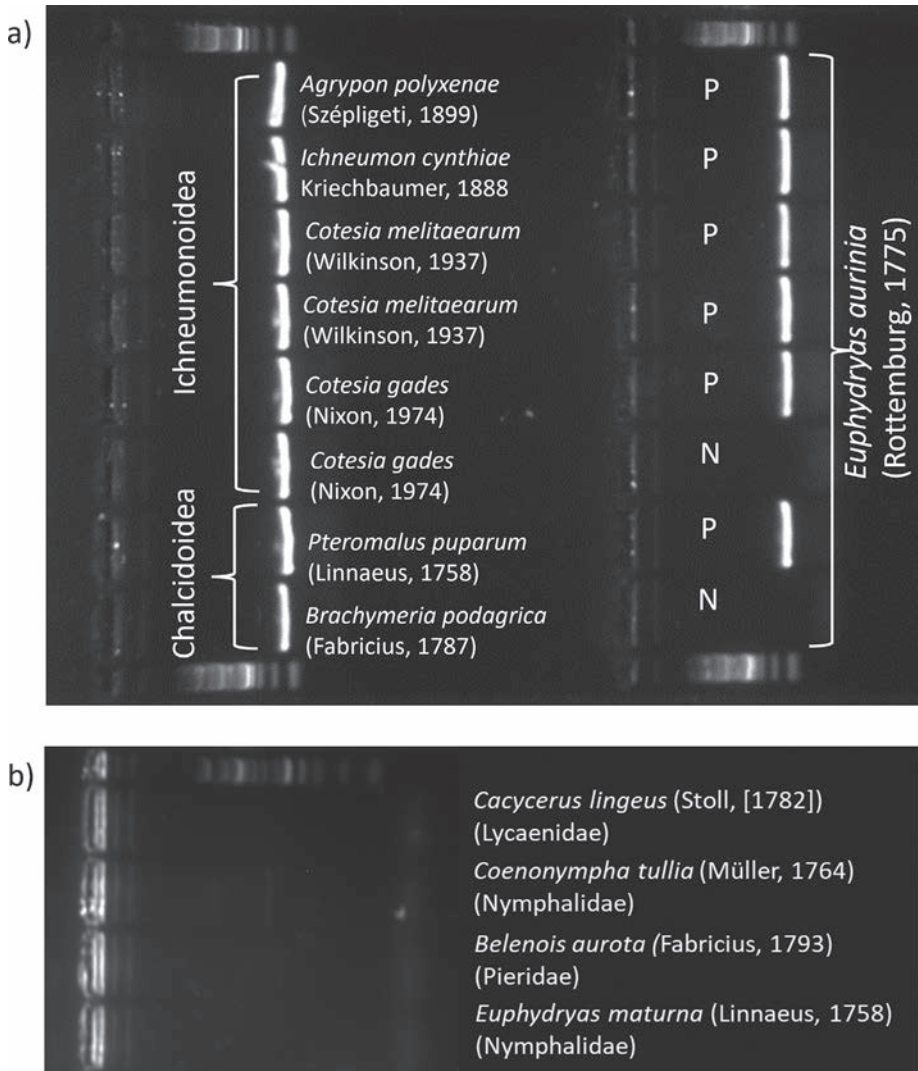


Figure 2. Electrophoresis gels used to assess whether the primers used can discriminate lepidopteran hosts and hymenopteran parasitoids **a** various adult hymenopteran parasitoids (PCRs are positive) and positive (P) and negative (N) samples of *E. aurinia* **b** four species of adult butterflies; PCRs are negative. The adult specimens of Hymenoptera and Lepidoptera were identified by M. Rindoš, M. Konvička, and Z. Faltýnek Fric.

The sequences of the positive samples were 124–126 bp long. The most similar sequences in GenBank according to nblast algorithm are those of *Cotesia glomerata* (Linnaeus, 1758), with the query identity 95.2–96.03%. The next similar sequences did not even reach a match of 93%.

According to the logistic regressions, none of the recorded properties of larval webs were related to infestation of the web (Table 1).

At the level of individual colonies, the infestation rates were highly variable (Fig. 3a). The per-site infestation levels did not correlate with larval web counts from

Table 1. Logistic regressions relating field-measured properties of larval webs to infestation of the sampled larvae.

Model	Predictor mean \pm SD/median/range	Coefficient	Residual deviance	Residual DF	AIC
Null 1^a			223.2	160	225.2
<i>Longest dimension</i>	4.3 \pm 2.68/4/1–13	0.038	222.9	159	226.9
<i>Shortest dimension</i>	7.6 \pm 12.76/12/3–40	-0.001	146.5	159	227.2
Null 2^a			181.1	194	237.7
<i>Julian date</i>	240 \pm 4.3/238/235–248	0.052	178.9	193	239.0
<i>Sward height</i>	42 \pm 23.1/4/5–100	0.010	178.8	193	239.8
<i>Host plant density</i>	76 \pm 49.5/60/5–200	0.004	179.6	193	237.7
<i>Webs density</i>	1.7 \pm 1.98/1/0–9	-0.095	179.6	193	236.9

The fitted single-term models are compared with the null model(s) following the information theory approach. None of the models was significant, as Δ AIC (null – fitted model) were always < 2.0 .

^aWe fitted two null models, because measurements of *E. aurinia* larval webs were not available for 34 webs, which were disintegrated at the time of sampling the caterpillars.

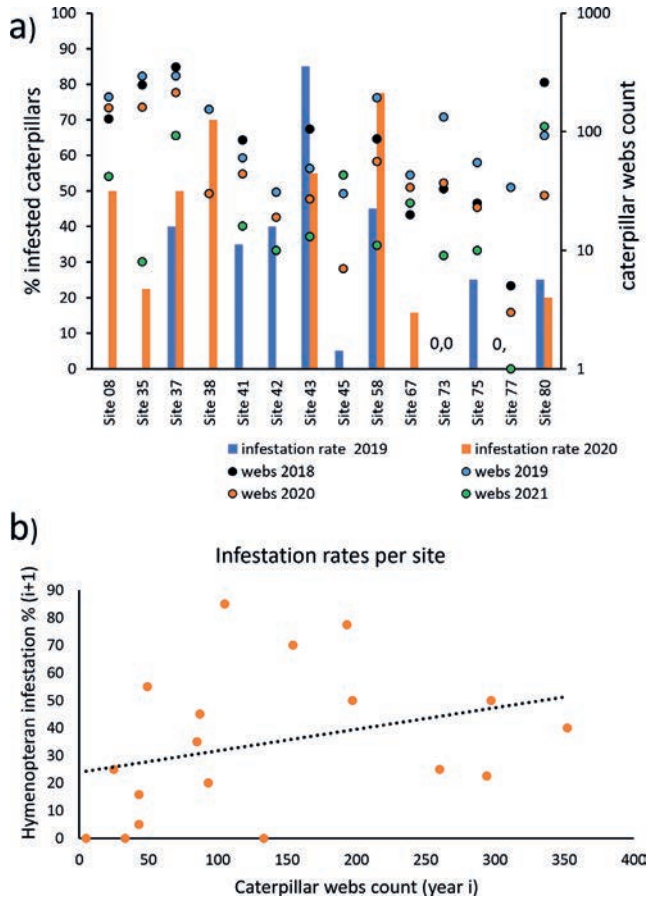


Figure 3. Per-site hymenopteran parasitoids infestation rates in colonies of the butterfly *Euphydryas aurinia* in two consecutive years (2019–20), with information of caterpillar web counts in the respective colonies in 2018–2021 (above), and illustration of the relationship between hymenopteran parasitoids infestation rates and *E. aurinia* caterpillar web counts in the previous year (below).

the same year (Spearman's $r_s = 0.11$, $t_{(17df)} = 0.46$, $p = 0.65$) or with web counts in the subsequent year ($r_s = 0.31$, $t_{(16df)} = 1.32$, $p = 0.21$), but did correlate positively with the larval webs' counts from the previous year (i.e., 2018 web counts for 2019 sampling, and 2019 web counts for 2020 sampling: $r_s = 0.46$, $t_{(16df)} = 2.07$, $p = 0.054$) (Fig. 3b).

Because the absolute values of web counts highly varied among the sites (Fig. 3a), depending, e.g., on the site areas, we also recalculated web counts into percentage fractions of a ten-year (2011–2021) maximum for the given site, and recalculated the correlations, with no significant results (identical year percentage web counts: $r_s = -0.23$, $t_{(17df)} = -0.99$, $p = 0.37$; previous year percentage web counts: $r_s = 0.31$, $t_{(16df)} = 1.31$, $p = 0.21$, subsequent year percentage web counts: $r_s = 0.10$, $t_{(16df)} = 0.40$, $p = 0.69$).

Discussion

The novel combination of primers 28SD1F (Larsen 1992) and HymR157 allowed us labour-efficient detection of high infestation rate in the declining *E. aurinia* butterfly by Hymenoptera parasitoids. Sequencing a selection of the obtained PCR products suggested that some of the parasitoids belong to the genus *Cotesia* Cameron, 1891. This is supported by the fact that other hymenopteran parasitoids known from our region, *Ichneumon* spp. and *Pteromalus* spp., attack pre-pupation larvae and pupae, respectively, whereas we worked with pre-diapause larvae. The gene 28S D1 is currently little represented in nucleotide databases for genus *Cotesia*, which, together with the unsettled taxonomy of *Cotesia* wasps infecting Melitaeinae butterflies (cf. Kankare et al. 2005a, b), precludes specific identification at this moment. This highlights the need to continue building comprehensive reference libraries for species identification. Such libraries are currently well developed for the COI gene, but supplementing it with a marker in another locus could improve discrimination power in some complex cases. Still, our approach allowed quantifying hymenopteran infestation rates in the declining butterfly, revealing that per-colony infestation rate is affected by larval webs density in the previous season.

Although the role of parasitoids on population fluctuations of *E. aurinia*, and related species, had been proposed almost a century ago (Ford and Ford 1930), relatively few authors quantified the natural infestation rates, with widely varying results. Infestation rates of <5% were reported, e.g., for the American congeneric species *E. editha* (Boisduval, 1852) (Singer and Erlich 1979) and *E. chalcona* (Doubleday, 1847) (Lincoln et al. 1982). Similar results were obtained for *E. aurinia* from Sweden, with rates 2.6% (Eliasson and Shaw 2003), and Spain, where the rates were 2.4–5.1% (Stefanescu et al. 2009). The latter study in fact covered a newly recognised species, *E. beckeri* (Lederer, 1853), feeding on *Lonicera* spp. The rates detected by us, 33.3% and 40.2% in two consecutive years, are more comparable to the situations reported for American *E. phaeton* (Drury, 1773) (up to ≈10% in larvae prior to diapause) (Stamp 1981), *E. maturna* (Linnaeus, 1758) in the Czech Republic (69%) (Dolek et

al. 2006) and Sweden (32%) (Eliasson and Shaw 2003). For *E. aurinia*, values higher than ours ($\approx 90\%$) were reported by Ford and Ford (1930) from Britain during peaks of cyclic fluctuation of the butterfly population, whereas Klapwijk and Lewis (2014) reported a high range of infestation rates within individual webs (4–83%) from Britain. This all points to a high variation among sites, seasons, parasitoids' generations, and *Euphydryas* species in hymenopteran infestation rates. In detailed studies of the closely related Melitaeinae model species, *Melitaea cinxia* (Linnaeus, 1758), this variation was attributed to spatial positions of butterfly colonies, competition among parasitoids and hyperparasitism, and annual variation in weather (e.g., Lei and Hanski 1997; Van Nouhuys and Lei 2004). Arguably, some of the reported variation may also be due to the diversity of methods applied by various authors, ranging from field counts of infested caterpillars (Lei and Hanski 1997), through captive rearing (Stamp 1981; Eliasson and Shaw 2003; Klapwijk and Lewis 2014), to molecular methods as used here. Possibly, the molecular detection reveals higher infestation rates than rearing, because some of the infested larvae may die prior to the parasitoid emergence. Causes of this mortality are then interpreted as “unknown” (e.g., in Eliasson and Shaw 2003).

Klapwijk and Lewis (2014) observed that the probability of caterpillar web infestation increased in webs isolated from other *E. aurinia* larval webs. We did not detect any relationship to the webs or surrounding vegetation parameters, but these results may be biased, because – for conservation concerns – we sampled the caterpillars solely from colonies containing a high number of larval webs during the sampling. The mean \pm SD webs' number of sampled colonies were 116 ± 97.3 and 60 ± 66.6 , whereas the numbers across all colonies were 53 ± 57.8 ($n = 44$) and 19 ± 38.0 ($n = 70$) in 2019 and 2020, respectively (John et al. in rev.). Conservation concerns also prevented quantifying the proportion of infestation per larval web, which would require killing all the caterpillars (cf. Klapwijk and Lewis 2014).

It also should be noted that our approach did not distinguish parasitoids from hyperparasitoids; i.e., the insects developing within parasitoids and thus killing them (Nair et al. 2016). A hyperparasitoid, however, can infest only a larva already infested by a parasitoid, and hence hyperparasitoids presence does not affect our findings on hymenopteran infestation rates.

With all the limitations, we found that the infestation rate per site positively correlated with per-site caterpillar webs' numbers of the previous year. This is fully expected if the parasitoids need a rich resource supply (i.e., high host density) to multiply in a butterfly colony, depleting the hosts' numbers in the process (Ford and Ford 1930; Frazer 1954; Porter 1981, 1983). A time delay in parasitoids infestation, and higher likelihood of infestation of larger and more connected host colonies, were found by Lei and Hanski (1997) in the metapopulation system of *M. cinxia* and its parasitoids. Although the inter-annual abundance changes of Melitaeini butterflies' colonies are likely influenced by numerous other factors, including variation in weather (Brunbjerg et al. 2017) or site vegetation management (Johansson et al. 2019; Tájek et al. 2023), natural enemies' pressure certainly plays a significant role.

Conclusions

The DNA-based method detected high hymenopteran parasitoids' infestation rates in colonies of the declining butterfly, *Euphydryas aurinia*. These rates, however, widely varied among the butterfly colonies and between two study years, likely interfering with, and possibly driving, the inter-annual butterfly abundance changes within colonies, as well as the metapopulation dynamics of the butterfly, described in detail by John et al. (in review). Our primer combination seems to be promising for wider use in detecting infestation of butterflies by Hymenoptera parasitoids. In our control tests, it amplified various Hymenoptera but not several butterfly species tested (Fig. 2). However, potential users should first test that the detection works also in their system to avoid false positive and false negative results.

Acknowledgements

Part of the development of the primers took place during the stay of JH in the lab of Graham Stone, University of Edinburgh. The work was funded by the Technology Agency of the Czech Republic (SS01010526). JH was supported by Czech Science Foundation grant no. 20-30690S.

References

- Altschul SE, Gish W, Miller W, Myers EW, Lipman DJ (1990) Basic local alignment search tool. *Journal of Molecular Biology* 215: 403–410. [https://doi.org/10.1016/S0022-2836\(05\)80360-2](https://doi.org/10.1016/S0022-2836(05)80360-2)
- Anthes N, Fartmann T, Hermann G, Kaule G (2003) Combining larval habitat quality and metapopulation structure—the key for successful management of pre-alpine *Euphydryas aurinia* colonies. *Journal of Insect Conservation* 7: 175–185. <https://doi.org/10.1023/A:1027330422958>
- Anton C, Zeisset I, Musche M, Durka W, Boomsma JJ, Settele J (2007) Population structure of a large blue butterfly and its specialist parasitoid in a fragmented landscape. *Molecular Ecology* 16: 3828–3838. <https://doi.org/10.1111/j.1365-294X.2007.03441.x>
- Beneš J, Konvička M, Dvořák J, Fric Z, Havelda Z, Pavličko A, Vrabec V, Weidenhoffer Z [Eds] (2002) Motýli České republiky rozšíření a ochrana I, II. [Butterflies of The Czech Republic: distribution and conservation I, II]. Společnost pro ochranu motýlů, Kolín, 857 pp.
- Brunbjerg AK, Høye TT, Eskildsen A, Nygaard B, Damgaard CF, Ejrnæs R (2017) The collapse of marsh fritillary (*Euphydryas aurinia*) populations associated with declining host plant abundance. *Biological Conservation* 211: 117–124. <https://doi.org/10.1016/j.biocon.2017.05.015>
- Dolek M, Freese-Hager A, Cizek O, Gros P (2006) Mortality of early instars in the highly endangered butterfly *Euphydryas maturna* (Nymphalidae). *Nota Lepidopterologica* 2: 221–224.

- Eliasson CU, Shaw MR (2003) Prolonged life cycles, oviposition sites, foodplants and *Cotesia* parasitoids of Melitaeini butterflies in Sweden. *Oedippus* 21: 1–52.
- Folmer O, Black M, Hoeh W, Lutz R, Vrijenhoek R (1994) DNA primers for amplification of mitochondrial cytochrome c oxidase subunit I from diverse metazoan invertebrates. *Molecular Marine Biology and Biotechnology* 3: 294–299.
- Forbes AA, Bagley RK, Beer MA, Hippee AC, Widmayer HA (2018) Quantifying the unquantifiable: why Hymenoptera, not Coleoptera, is the most speciose animal order. *BMC Ecology* 18: 1–21. <https://doi.org/10.1186/s12898-018-0176-x>
- Ford HD, Ford EB (1930) Fluctuation in numbers and its influence on variation in *Melitaea aurinia* Rott. (Lepidoptera). *Transactions of the Entomological Society of London* 78: 345–351. <https://doi.org/10.1111/j.1365-2311.1930.tb00392.x>
- Frazer FG (1954) High mortality of *Euphydryas aurinia* Rott. (Lep: Nymphalidae) from parasitism by *Apanteles bignellii* Marsh. (Hym: Braconidae). *Entomologists' Monthly Magazine* 90: e253.
- Hawkins BA (1994) *Pattern and Process in Host-Parasitoid Interactions*. Cambridge University Press, Cambridge, [x +] 190 pp. <https://doi.org/10.1017/CBO9780511721885>
- Hebert PDN, Penton EH, Burns JM, Janzen DH, Hallwachs W (2004) Ten species in one: DNA barcoding reveals cryptic species in the neotropical skipper butterfly *Astraptes fulgerator*. *Proceedings of the National Academy of Sciences of the United States of America* 101: 14812–14817. <https://doi.org/10.1073/pnas.0406166101>
- Hejda R, Farkač J, Chobot K (2017) Červený Seznam Ohrožených Druhů České Republiky: Bezobratlí [Red list of invertebrates of the Czech Republic]. *Příroda* 36: 1–611.
- Heraty J, Ronquist F, Carpenter JM, Hawks D, Schulmeister S, Dowling AP, Murray D, Munro J, Wheeler WC, Schiff N, Sharkey M (2011) Evolution of the hymenopteran megaradiation. *Molecular Phylogenetics and Evolution* 60: 73–88. <https://doi.org/10.1016/j.ympev.2011.04.003>
- Hula V, Konvička M, Pavlíčko A, Fric ZF (2004) Marsh Fritillary (*Euphydryas aurinia*) in the Czech Republic: monitoring, metapopulation structure, and conservation of an endangered butterfly. *Entomologica Fennica* 15: 231–241. <https://doi.org/10.33338/ef.84226>
- Jarman SN (2003) Amplicon: software for designing PCR primers on aligned sequences. [Distributed by the author, Australian Antarctic Division, Kingston.] *Bioinformatics* 20(10): 1644–1645. <https://doi.org/10.1093/bioinformatics/bth121>
- Jeffs CT, Terry JCD, Higgie M, Jandová A, Konvičková H, Brown JJ, Lue CH, Schiffer M, O'Brien EK, Bridle J, Hřček J, Lewis OT (2021) Molecular analyses reveal consistent food web structure with elevation in rainforest *Drosophila*-parasitoid communities. *Ecography* 44: 403–413. <https://doi.org/10.1111/ecog.05390>
- Johansson V, Kindvall O, Askling J, Franzén M (2019) Intense grazing of calcareous grasslands has negative consequences for the threatened marsh fritillary butterfly. *Biological Conservation* 239: e108280. <https://doi.org/10.1016/j.biocon.2019.108280>
- John V, Tájek P, Mariňáková Kopečková M, Jiskra P, Zimmermann K, Hula V, Fric ZF, Konvička M (in review) Two decades of monitoring and active conservation of the Marsh fritillary (*Euphydryas aurinia*) in the Czech Republic.
- Junker M, Wagner S, Gros P, Schmitt T (2010) Changing demography and dispersal behaviour: ecological adaptations in an alpine butterfly. *Oecologia* 164: 971–980. <https://doi.org/10.1007/s00442-010-1720-3>

- Junker M, Konvička M, Zimmermann K, Schmitt T (2021) Gene-flow within a butterfly metapopulation: the marsh fritillary *Euphydryas aurinia* in western Bohemia (Czech Republic). *Journal of Insect Conservation* 25: 585–596. <https://doi.org/10.1007/s10841-021-00325-8>
- Kankare M, Stefanescu C, van Nouhuys S, Shaw MR (2005a) Host specialization by *Cotesia* wasps (Hymenoptera: Braconidae) parasitizing species-rich Melitaeini (Lepidoptera: Nymphalidae) communities in north-eastern Spain. *Biological Journal of the Linnean Society*, 86: 45–65. <https://doi.org/10.1111/j.1095-8312.2005.00523.x>
- Kankare M, Van Nouhuys S, Gaggiotti O, Hanski I (2005b) Metapopulation genetic structure of two coexisting parasitoids of the Glanville fritillary butterfly. *Oecologia* 143: 77–84. <https://doi.org/10.1007/s00442-004-1782-1>
- Kankare M, Van Nouhuys S, Hanski I (2005c) Genetic divergence among host-specific cryptic species in *Cotesia melitaearum* aggregate (Hymenoptera: Braconidae), parasitoids of checkerspot butterflies. *Annals of the Entomological Society of America* 98: 382–394. [https://doi.org/10.1603/0013-8746\(2005\)098\[0382:GDAHCS\]2.0.CO;2](https://doi.org/10.1603/0013-8746(2005)098[0382:GDAHCS]2.0.CO;2)
- Kester KM, Barbosa P (1991) Post-emergence learning in the insect parasitoid, *Cotesia congregata* (Say) (Hymenoptera: Braconidae). *Journal of Insect Behavior* 4: 727–742. <https://doi.org/10.1007/BF01052227>
- Klapwijk MK, Lewis OT (2014) Spatial ecology of host–parasitoid interactions: a threatened butterfly and its specialised parasitoid. *Journal of Insect Conservation* 18: 437–445. <https://doi.org/10.1007/s10841-014-9653-5>
- Konvička M, Hula V, Fric ZF (2003) Habitat of pre-hibernating larvae of the endangered butterfly *Euphydryas aurinia* (Lepidoptera: Nymphalidae): What can be learned from vegetation composition and architecture? *European Journal of Entomology* 100: 313–322. <https://doi.org/10.14411/eje.2003.050>
- Korb S, Bolshakov LV, Fric ZF, Bartoňová A (2016) Cluster biodiversity as a multidimensional structure evolution strategy: Checkerspot butterflies of the group *Euphydryas aurinia* (Rottemburg, 1775) (Lepidoptera: Nymphalidae). *Systematic Entomology* 41: 441–457. <https://doi.org/10.1111/syen.12167>
- Larsen N (1992) Higher order interactions in 23S rRNA. *Proceedings of the National Academy of Sciences of the United States of America* 89: 5044–5048. <https://doi.org/10.1073/pnas.89.11.5044>
- La Salle J, Gauld ID (1991) Parasitic Hymenoptera and the biodiversity crisis. *Redia* 74: 315–334.
- Lei G-C, Hanski I (1997) Metapopulation Structure of *Cotesia melitaearum*, a Specialist Parasitoid of the Butterfly *Melitaea cinxia*. *Oikos* 78: 91–100. <https://doi.org/10.2307/3545804>
- Lincoln DE, Newton TS, Ehrlich PR, Williams KS (1982) Coevolution of the checkerspot butterfly *Euphydryas chalcedona* and its larval food plant *Diplacus aurantiacus*: Larval response to protein and leaf resin. *Oecologia* 52: 216–223. <https://doi.org/10.1007/BF00363840>
- Meister H, Lindman L, Tammaru T (2015) Testing for local monophagy in the regionally oligophagous *Euphydryas aurinia* (Lepidoptera: Nymphalidae). *Journal of Insect Conservation* 19: 691–702. <https://doi.org/10.1007/s10841-015-9792-3>
- Munguira ML, Martín J, García-Barros E, Viejo JL (1997) Use of space and resources in a Mediterranean population of the butterfly *Euphydryas aurinia*. *Acta Oecologica* 18: 597–612. [https://doi.org/10.1016/S1146-609X\(97\)80044-6](https://doi.org/10.1016/S1146-609X(97)80044-6)

- Nair A, Fountain T, Ikonen S, Ojanen SP, van Nouhuys S (2016) Spatial and temporal genetic structure at the fourth trophic level in a fragmented landscape. *Proceedings of the Royal Society of London B* 283: e20160668. <https://doi.org/10.1098/rspb.2016.0668>
- Ojanen SP, Nieminen M, Meyke E, Pöyry J, Hanski I (2013) Long-term metapopulation study of the Glanville fritillary butterfly (*Melitaea cinxia*): survey methods, data management, and long-term population trends. *Ecology and Evolution* 3: 3713–3737. <https://doi.org/10.1002/ece3.733>
- Pakarinen SP (2011) Host-parasitoid relationship in different *Cotesia melitaeorum* and *Melitaea cinxia* populations around the Baltic Sea. Master's Thesis, Department of Biological and Environmental Sciences, University of Helsinki, 86 pp.
- Porter K (1979) A third generation of *Apanteles bignellii* Marsh. (Hym., Braconidae). *Entomologist's Monthly Magazine* 114: e214.
- Porter K (1981) The population dynamics of small colonies of the butterfly *Euphydryas aurinia*. – PHD thesis, Oxford University.
- Porter K (1983) Multivoltinism in *Apanteles bignellii* and the influence of weather on synchronisation with its host *Euphydryas aurinia*. *Entomologia Experimentalis et Applicata* 34: 155–162. <https://doi.org/10.1111/j.1570-7458.1983.tb03311.x>
- R Core Team (2018) R: A language and environment for statistical computing. R Foundation for Statistical Computing, Vienna. <https://www.R-project.org/>
- Rougerie R, Smith MA, Fernandez-Triana J, Lopez-Vaamonde C, Ratnasingham S, Hebert PDN (2011) Molecular analysis of parasitoid linkages (MAPL): gut contents of adult parasitoid wasps reveal larval host. *Molecular Ecology* 20: 179–186. <https://doi.org/10.1111/j.1365-294X.2010.04918.x>
- Shaw MR, Stefanescu C, Van Nouhuys S (2009) Parasitoids of European butterflies. In: Settele J, Shreeve TG, Konvicka M, van Dyck H (Eds) *Ecology of Butterflies in Europe*. Cambridge University Press, Cambridge, 130–156.
- Singer MC, Ehrlich PR (1979) Population dynamics of the checkerspot butterfly *Euphydryas editha*. *Fortschritte der Zoologie* 25: 53–60.
- Singer MC, Stefanescu C, Pen I (2002) When random sampling does not work: standard design falsely indicates maladaptive host preferences in a butterfly. *Ecology Letters* 5: 1–6. <https://doi.org/10.1046/j.1461-0248.2002.00282.x>
- Stamp NE (1981) Effect of group size on parasitism in a natural population of the Baltimore checkerspot *Euphydryas phaeton*. *Oecologia* 49: 201–206. <https://doi.org/10.1007/BF00349188>
- Stefanescu C, Planas J, Shaw MR (2009) The parasitoid complex attacking coexisting Spanish populations of *Euphydryas aurinia* and *Euphydryas desfontainii* (Lepidoptera: Nymphalidae, Melitaeini). *Journal of Natural History* 43: 553–568. <https://doi.org/10.1080/00222930802610444>
- Tájek P, Tenčík A, Konvicka M, John V (2023) Vegetation changes at oligotrophic grasslands managed for a declining butterfly. *Nature Conservation* 52: 23–46. <https://doi.org/10.3897/natureconservation.52.90452>
- Toro-Delgado E, Hernández-Roldán J, Dincă V, Vicente JC, Shaw MR, Quicke DL, Vodá R, Albrecht M, Fernández-Triana J, Vidiella B, Valverde S, Dapporto L, Hebert PDN, Talavera G, Vila R (2022) Butterfly–parasitoid–hostplant interactions in Western Palaearctic

- Hesperiidae: a DNA barcoding reference library. *Zoological Journal of the Linnean Society* 196: 757–774. <https://doi.org/10.1093/zoolinnean/zlac052>
- Yu DSK, van Achterberg C, Horstmann K (2012) *Taxapad*, Ichneumonoidea. Vancouver. <http://www.taxapad.com>
- Van Nouhuys S, Lei G (2004) Parasitoid-host metapopulation dynamics: the causes and consequences of phenological asynchrony. *Journal of Animal Ecology* 73: 526–535. <https://doi.org/10.1111/j.0021-8790.2004.00827.x>
- Van Swaay C, Cuttelod A, Collins S, Maes D, López Munguira M, Šašić M, Settele J, Verovnik R, Verstrael T, Warren M, Wiemers M, Wynhof I (2010) *European Red List of Butterflies*. Luxembourg: Publications Office of the European Union.
- Wahlberg N, Kullberg J, Hanski I (2001) Natural history of some Siberian Melitaeine butterfly species (Nymphalidae: Melitaeini) and their parasitoids. *Entomologica Fennica* 12: 72–77. <https://doi.org/10.33338/ef.84102>
- Warren MS (1994) The UK status and suspected metapopulation structure of a threatened European butterfly, the marsh fritillary *Eurodryas aurinia*. *Biological Conservation* 67: 239–249. [https://doi.org/10.1016/0006-3207\(94\)90615-7](https://doi.org/10.1016/0006-3207(94)90615-7)
- Wirta HK, Hebert PDN, Kaartinen R, Prosser SW, Várkonyi G, Roslin T (2014) Complementary molecular information changes our perception of food web structure. *Proceedings of the National Academy of Sciences* 111: 1885–1890. <https://doi.org/10.1073/pnas.1316990111>
- Zhu YL, Yang F, Yao ZW, Wu YK, Liu B, Yuan HB, Lu YH (2019) A molecular detection approach for a cotton aphid-parasitoid complex in northern China. *Scientific Reports* 9: e15836. <https://doi.org/10.1038/s41598-019-52266-7>
- Zimmermann K, Fric Z, Jiskra P, Kopeckova M, Vlasanek P, Zapletal M, Konvicka M (2011) Mark–recapture on large spatial scale reveals long distance dispersal in the Marsh Fritillary, *Euphydryas aurinia*. *Ecological Entomology* 36: 499–510. <https://doi.org/10.1111/j.1365-2311.2011.01293.x>

Supplementary material I

List of sampled colonies of *E. aurinia*

Authors: Václav John, Martin Konvička

Data type: xlsx

Explanation note: Spreadsheet with information on all 97 *E. aurinia* colonies monitored in western Czech Republic in 2001–2021, with caterpillar webs counts for individual years. The fourteen colonies sampled for hymenopteran parasitoids are indicated in red.

Copyright notice: This dataset is made available under the Open Database License (<http://opendatacommons.org/licenses/odbl/1.0/>). The Open Database License (ODbL) is a license agreement intended to allow users to freely share, modify, and use this Dataset while maintaining this same freedom for others, provided that the original source and author(s) are credited.

Link: <https://doi.org/10.3897/jhr.97.113231.suppl1>

Corrigendum: Ulmer JM, Janšta P, Azar D, Krogmann L (2023) At the dawn of megadiversity – Protoitidae, a new family of Chalcidoidea (Hymenoptera) from Lower Cretaceous Lebanese amber. Journal of Hymenoptera Research 96: 879–924. doi:10.3897/jhr.96.105494

Jonah M. Ulmer^{1,2}, Petr Janšta^{1,3}, Dany Azar^{4,5}, Lars Krogmann^{1,2}

1 Department of Entomology, State Museum of Natural History Stuttgart, Rosenstein 1, 70191 Stuttgart, Germany **2** Institute of Biology, Biological Systematics (190w), University of Hohenheim, Stuttgart, Germany **3** Department of Zoology, Faculty of Science, Charles University, Prague, Czech Republic **4** State Key Laboratory of Palaeobiology and Stratigraphy, Nanjing Institute of Geology and Palaeontology, Chinese Academy of Sciences, Nanjing, China **5** Lebanese University, Faculty of Sciences II, Department of Natural Sciences, Fanar, Matn, Lebanon

Corresponding author: Jonah M. Ulmer (jonah.ulmer@gmail.com)

Academic editor: Michael Ohl | Received 8 November 2023 | Accepted 10 November 2023 | Published 30 January 2024

<https://zoobank.org/B047674B-27DF-44A6-93E9-A8602565E211>

Citation: Ulmer JM, Janšta P, Azar D, Krogmann L (2024) Corrigendum: Ulmer JM, Janšta P, Azar D, Krogmann L (2023) At the dawn of megadiversity – Protoitidae, a new family of Chalcidoidea (Hymenoptera) from Lower Cretaceous Lebanese amber. Journal of Hymenoptera Research 96: 879–924. doi:10.3897/jhr.96.105494. Journal of Hymenoptera Research 97: 43–44. <https://doi.org/10.3897/jhr.97.115499>

The recently published description of the fossil Chalcidoidea family Protoitidae, alongside the genus *Protoita* (Ulmer et al. 2023), failed to declare a type species for the genus. Under ICZN articles 13.2 and 13.3, this renders both the names *Protoita* and Protoitidae as *nomina nuda*. Below we formally define and validate the family Protoitidae, and *Protoita*, the type genus, with the taxon *Protoita noyesi*, as the type species. Under ICZN Article 16.1, both of these new names take their authorship and date from the publication of this corrigendum, rather than from the original publication. A new supplementary table including the updated fossil taxonomy is also provided.

Systematic paleontology

Protoitidae Ulmer & Krogmann 2023, fam. nov.

Type genus. *Protoita* gen. nov. Ulmer & Krogmann 2023.

Diagnosis. See Ulmer et al. 2023 p. 889.

***Protoita* Ulmer & Krogmann 2023, gen. nov.**

Type species. *Protoita noyesi* Ulmer & Krogmann 2023.

Diagnosis. See Ulmer et al. 2023 p. 890.

References

Ulmer JM, Janšta P, Azar D, Krogmann L (2023) At the dawn of megadiversity – Protoitidae, a new family of Chalcidoidea (Hymenoptera) from Lower Cretaceous Lebanese amber. Journal of Hymenoptera Research 96: 879–924. <https://doi.org/10.3897/jhr.96.105494>

Supplementary material I

Updated checklist of fossil Chalcidoidea data

Authors: Jonah M. Ulmer

Data type: pdf

Explanation note: Updated listing of occurrence data for Chalcidoidea fossils used for making time series plot.

Copyright notice: This dataset is made available under the Open Database License (<http://opendatacommons.org/licenses/odbl/1.0/>). The Open Database License (ODbL) is a license agreement intended to allow users to freely share, modify, and use this Dataset while maintaining this same freedom for others, provided that the original source and author(s) are credited.

Link: <https://doi.org/10.3897/jhr.97.115499.suppl1>

A DNA-barcoding-based approach to quantitatively investigate larval food resources of cavity-nesting wasps from trap nests

Luisa Timm¹, Johanna Schaal², Manuela Sann²

1 Department of Entomology, State Museum of Natural History, Rosenstein 1, 70191 Stuttgart, Germany

2 Department of Chemical Ecology, Institute of Biology, University of Hohenheim, Garbenstr. 30, 70593 Stuttgart, Germany

Corresponding author: Manuela Sann (manuela.sann@uni-hohenheim.de)

Academic editor: Michael Ohl | Received 15 December 2023 | Accepted 24 January 2024 | Published 30 January 2024

<https://zoobank.org/47BA94FB-2105-4C68-9CD4-EC7359F81328>

Citation: Timm L, Schaal J, Sann M (2024) A DNA-barcoding-based approach to quantitatively investigate larval food resources of cavity-nesting wasps from trap nests. *Journal of Hymenoptera Research* 97: 45–56. <https://doi.org/10.3897/jhr.97.117410>

Abstract

Artificial nesting resources, also known as trap nests, have proven to be an ideal method for monitoring cavity-nesting bees and wasps, their collected food resources, and natural enemies. Nowadays, trap nests are frequently used to assess responses to environmental and biodiversity changes based on multi-trophic interaction networks. Here, we reconstructed quantitative trophic interaction networks of five apoid wasps (*Trypoxylon clavicerum*, *Passaloecus corniger*, *Passaloecus gracilis*, *Psenulus fuscipennis*, *Isodontia mexicana*) and two vespid wasp species (*Ancistrocerus nigricornis*, *Microdynerus parvulus*) using DNA barcoding. Sampling the nests during their construction period allowed us to give an accurate count and identification of the provided food items. We recovered highly resolved bi- and tripartite networks including wasp-beetle larva, wasp-cricket, natural enemy-wasp-moth larva, natural enemy-wasp-spider, and natural enemy-wasp-aphid associations. The latter include aphid species that are known as agricultural and forest pests. Although the quantitative sampling of nests entails increased time costs, it enables not only high-quality DNA barcoding but also to reconstruct quantitative interaction networks. Thus, our approach is a highly promising monitoring tool for gaining deeper knowledge on the ecology, habitat requirements and the impact of environmental and biodiversity change on cavity-nesting bees and wasps.

Keywords

Cavity-nesting, DNA barcoding, food resources, tripartite, wasps

Introduction

Bees and wasps play fundamental economic and ecological roles, e.g. as pollinators or to control other arthropod populations including agricultural pest species (Harris 1994; Ollerton et al. 2006; Klein et al. 2007; Fornoff et al. 2023). However, due to diverse anthropogenic factors, bees and wasps are in decline (Senapathi et al. 2015; Hallmann et al. 2017; Trapp et al. 2017; Goulson 2019; Powney et al. 2019; Dicks et al. 2021; Zattara and Aizen 2021). Studying bee or wasp species interactions by means of artificial nesting sites (hereafter referred to as trap nests) is a standardized approach (Staab et al. 2018) to identify and assess environmental drivers associated with population declines. This necessarily includes an in-depth view on trophic interactions, acting bottom-up or top-down on the respective populations, and should be more informative than analyzing co-occurring communities at sampling locations e.g., nesting sites only (Blanchet et al. 2020). Here, we investigate nests of cavity-nesting vespid and apoïd wasp species by quantifying their collected food resources as larval provisions, and their natural enemies within a subset of nest cells, to reconstruct highly resolved quantitative multi-trophic interaction networks. The morphological identification of food resources provided to the larvae can be challenging, as insect taxonomists are rare (Hochkirch et al. 2022) or food items can be morphologically unrecognizable, when only parts are left for determination (Fornoff et al. 2023). Thus, we applied DNA barcoding (Turčinavičienė et al. 2016) to overcome these difficulties. In addition, utilizing openable and resealable trap nests allows minimal invasive sampling, collecting fresh material for DNA barcoding and a direct ecological observation of cavity-nesting wasps.

Material and methods

Sample collection

Samples were taken from trap nests set at three different sites in the close surroundings of the University of Hohenheim, Germany from May to August 2022 and 2023 at a weekly base (Suppl. material 5 and Suppl. material 4: table S13). Trap nests are designed to be easily openable and consist of several MDF (medium density fiberboard) boards with ten milled furrows each, covered with a removable acrylic glass, enabling a minimal invasive investigation of a respective nest. Each furrow represents one nest consisting of several nest cells (Fig. 1B–D). Furrows have a diameter of 2.0–9.0 mm to address different sized wasps (Suppl. material 2: table S7). During nest construction and provisioning, a subset of the nest i.e., recently finished nest cells were randomly sampled. Particularly, the whole content of one or a maximum of two nest cells comprising the wasp larva as well as its food provision and potential natural enemies were sampled while leaving remaining nest cells intact. Larvae and food provision were transferred into 100% pure ethanol using sterile forceps and subsequently stored at -20 °C until further processing. Sampling nest cells during nest construction allowed the collection of full-sized and freshly col-

lected prey arthropods before being consumed by the larval wasp. Additionally, one reed stem, also part of the trap nests, was opened and sampled as described before. Please note, in rare cases sampling had to be done for fully constructed nests comprising significantly older larval stages and thus, contained only a few prey individuals or prey remains.

Sample preparation and DNA barcoding

From 19 wasp nests, we sampled a total of 20 nest cells comprising 20 wasp larvae, 361 prey individuals, and six natural enemies (individuals of the natural enemy *Pronotalia* sp. were not counted due to their high number). We separated prey morphotypes under a microscope and selected one specimen per morphotype for the subsequent DNA extraction. Thus, a total of 60 individuals comprising selected prey specimens and wasp larvae were processed for DNA barcoding. We stored the remaining morphotype individuals as voucher specimens.

Genomic DNA (gDNA) was extracted using the nexttec™ 1-Step Tissue & Cells Isolation Kit following the manufactures' protocol with an incubation at 56 °C for 30 min. DNA samples were stored at -20 °C until further processing.

Polymerase chain reactions (PCR) targeting the cytochrome C oxidase I (COI) gene fragment were conducted with the established standard primer pairs HCO2198/LCO1490 (Folmer et al. 1994) and LepF1/LepR1 (Hebert et al. 2003) (sequences in Suppl. material 1: table S1). PCR reactions were set up using the ROTI®Pol TagS Red-Mix in a total reaction volume of 25 µl with 4 or 2 µl template DNA for HCO/LCO and Lepf1/LepR1 reactions respectively (see Suppl. material 1: tables S2, S3). The PCR conditions with HCO/LCO were set as bottom-up reaction starting with 1 min at 94 °C, followed by 15 cycles of 1 min denaturation at 94 °C, 1 min annealing at 40 °C and 1 min elongation at 72 °C and 20 cycles with an annealing temperature of 45 °C and same elongation and denaturation temperatures and times subsequently. The final elongation was set for 5 min at 72 °C. LepF1/LepR1 conditions are included in the supplements (Suppl. material 1: table S5). PCR products were enzymatically purified using the Illustra Exoprostar 1-Step mix, following manufactures protocols and afterwards sequenced on a Sanger-sequencing platform at Microsynth Seqlab GmbH Göttingen, Germany.

Resulting raw DNA sequences were manually edited using Geneious Prime 2023.0.4 (<https://www.geneious.com>) and searched against the National Center for Biotechnology Information (NCBI) database using the Nucleotide collection (nt/nr) database of the Basic Local Alignment Search Tool BLAST with the following option: highly similar sequences (megablast) (Altschul et al. 1990; Camacho et al. 2009).

Data analysis

The visualization of interactions between the wasp species, their prey and their natural enemies was carried out using R version 4.3.1 (R Core Team 2023) with the R package “bipartite” (Dormann et al. 2008).



Figure 1. Nesting site and sample collection procedure: **A** example of a trap nest placed in the Botanical Garden of the University of Hohenheim, Stuttgart, Germany **B, C** nests of *Passaloecus gracilis* and *Isodontia mexicana*. One nest comprises several nest cells, which are separated by a given nesting material e.g. silky membran (**B**) or dry grass fragments (**C**) **E** morphotyped aphids **F** morphotyped spiders.

Results

We identified seven species of cavity-nesting wasps comprising one species of the apoïd family Crabronidae (*Trypoxylon clavicerum*), two species of Pemphredonidae (*Passaloecus corniger* and *Passaloecus gracilis*), one species of Psenidae (*Psenulus fuscipennis*), one species of Sphecidae (*Isodontia mexicana*) and, two species of vespïd wasps belonging to the

family Vespidae (*Ancistrocerus nigricornis* and *Microdynerus parvulus*) (Suppl. material 2: table S6). The latter two species provisioned their larvae with two different species of Lepidoptera (larvae) (Suppl. material 3: table S11) and one species of Coleoptera (larvae) (Suppl. material 3: table S12), respectively. The spider-hunting wasp *T. clavicercum* collected nine different species of Araneae across three different families. Six species of the family Linyphiidae, one species of Araneidae and two species of Tetragnathidae were identified (Suppl. material 3: table S8). The average number of collected prey individuals in *T. clavicercum* nests was 32.25 spiders per nest cell ($n = 4$, $SD = 15.52$). Please note, in case only prey remains were available counting nest content was not feasible. The herbivore-hunting wasps *Passaloecus* and *Psenulus* collected nine different species of Aphididae (Suppl. material 3: table S9). The cricket-hunting wasps *Isodontia mexicana* provided its larvae with two species of the genus *Meconema* (Tettigoniidae) (Suppl. material 3: table S10). Furthermore, four species of natural enemies were detected comprising one individual of the parasitoid wasp *Nematopodius* sp., two of the cuckoo-wasp *Trichbrysis cyanea* (*P. corniger* and *T. clavicercum*), more than 40 individuals of the chalcid wasp *Pronotalia* sp. (*A. nigricornis*) and two individuals of *Pseudomalus auratus* (*P. gracilis*).

Quantitative multi-trophic networks

The spider-hunting wasp *T. clavicercum* collected the most diverse set of different species as larval food resources (Fig. 2A). Here, each investigated nest cell included at least two but typically three different spider species with varying composition between the nests. Nest cells of the aphid-hunting wasp *P. gracilis* were provided with an average number of 30 aphids ($n = 3$, $SD = 1$) comprising only one species: *Aphis ruborum*.

The aphid-hunter *P. fuscipennis* collected five different species of Aphididae, and most of the nest cells contained only a single species (Fig. 2B). The vespid wasp *A. nigricornis* collected eleven Lepidoptera larvae in the investigated nest cell, comprising two different species: *Argyresthia pruniella* and *Hedya pruniana*. The cricket-hunter *I. mexicana* provided eight individuals of the genus *Meconema*, in one nest cell comprising seven of the species *Meconema meridionale* and one *Meconema thalassinum* (Fig. 2C).

Regarding *P. corniger*, nests were sampled several days after provisioning causing prey items to be partly consumed by the larva. Thus, counting collected aphids was not feasible. However, three different species of Aphididae were identified in the larval provisions (Fig. 2B). Furthermore, counting of prey individuals was not feasible for the vespid wasp *M. parvulus*. Here, we identified one larva of the weevil *Tychius picirostris* provided as a larval provision.

Discussion

Quantitative multi-trophic interaction networks provide valuable insights into the feeding ecology of diverse cavity-nesting Hymenoptera and enable conclusions to be drawn about their responses to environmental and biodiversity changes (Staab et

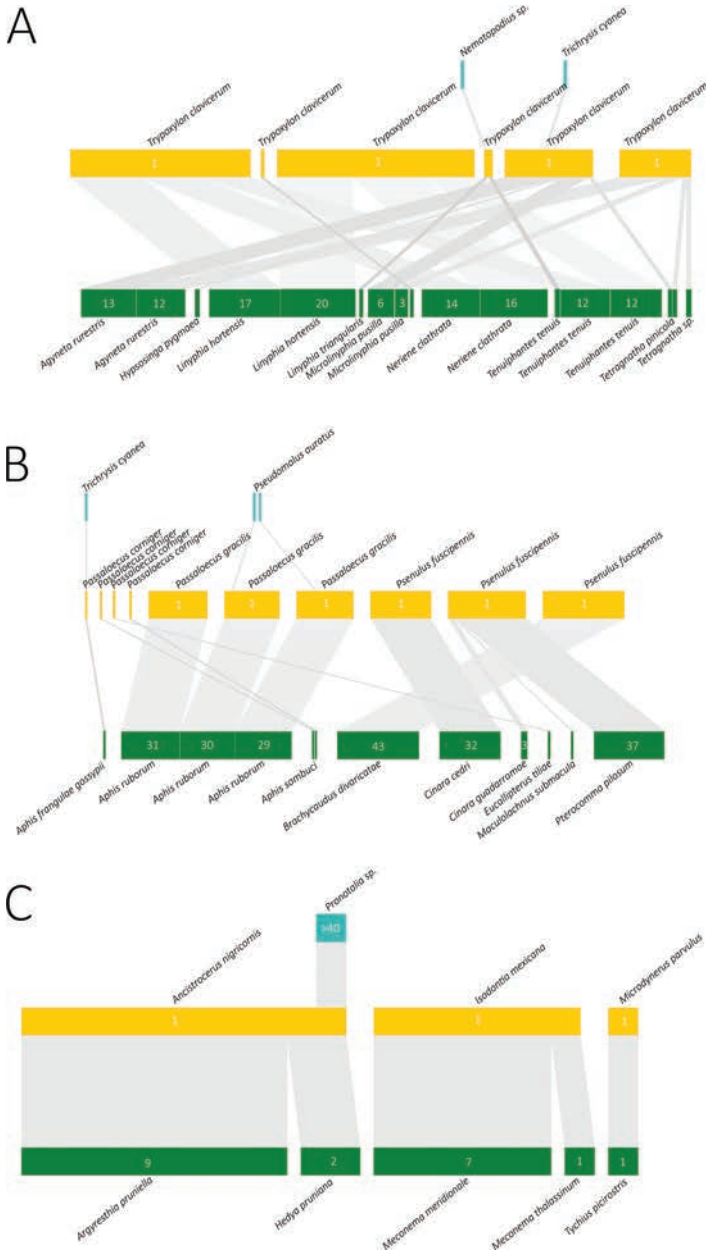


Figure 2. Tri-trophic interaction networks of the studied vespid and apoid wasp species comprising identified prey species and natural enemies. Interaction networks were conducted for the **A** spider-hunting apoid wasp *T. clavicernum* **B** aphid-hunting apoid wasp species *P. corniger*, *P. gracilis* and *P. fuscipennis* and **C** Lepidoptera-hunting vespid wasp *A. nigricornis*, cricket-hunting apoid wasps *I. mexicana* and weevil-hunting vespid wasp *M. parvulus*. Yellow boxes represent the nest cell and the respective wasp larva, blue boxes the natural enemies and green boxes the prey species and the number of prey individuals per species per nest cell. Boxes with no number represent one individual only. The natural enemy *Pronotalia* sp. was not counted due to a high and randomly distributed number of individuals in the nest cell (> 40). Connections of nests and prey species are marked with grey bars.

al. 2018; Fornoff et al. 2023). The here applied minimally-invasive approach allows us to gain comprehensive insides into the larval food provisions of apoid and vespid wasps and increases our knowledge about important feeding links. A major advantage and novelty of the method used here is the quantification of the prey specimens. Linking the quantity and identity of all interaction partners allows e.g., to study individual-based interactions, observe direct feeding links or, interpret the dependence of higher trophic levels on the levels below (Fornoff et al. 2023). Furthermore, this approach facilitates the extraction of high quality and quantity gDNA for subsequent DNA barcoding, given prey items are sampled directly after provisioning. Data analyses requiring higher-quality gDNA also become possible e.g., genetic gut content analyses of prey arthropods. The here presented approach requires a minimum of lab expertise and equipment and thus, might be also interesting for biologist with little or no molecular expertise. In our study, the procedure from sorting morphotypes of prey items to laboratory work to receiving the raw DNA sequence required 15 to 20 minutes hands-on time per sample. However, apart from sorting morphotypes several samples can be processed in the laboratory at the same time. Thus, a common sample size consisting of 96 samples can be prepared for sequencing within one day. Sequencing can be outsourced and requires around 24 hours depending on the sequencing company.

To the best of our knowledge, our approach further allowed the identification of so far unknown or unpublished feeding links: The spider-hunting apoid wasp *T. clavicerum* is known to provide its larvae with spiders of the families Araneidae, Linyphiidae, Tetragnathidae and Dictynidae (Fornoff et al. 2023). Here we expand the family-associated species list given by Fornoff et al. (2023) by five species namely *Hysosinga pygmaea*, *Linyphia hortensis*, *Microlinyphia pusilla*, *Neriena clathrata* and *Tenuiphantes tenuis*. Furthermore, we newly found *Brachycaudus divaricatae* and *Pterocomma pilosum* as host species for the aphid-hunting wasp *P. fuscipennis* as well as *Aphis frangulae gossypii* and *Eucallipterus tiliae* for *P. corniger*. The vespid wasp *A. nigricornis*, known to provide Lepidoptera larvae as larval provision was found to provide larvae of the cherry fruit moth *Argyresthia pruniella* (Argyresthiidae) and the plum tortrix *Hedya pruniana* (Tortricidae). Interestingly, several of the here identified prey species are known as agricultural pests e.g., *A. ruborum* (collected by *P. gracilis*), a potential pest of *Rubus* and *Fragaria* (Alford 2014; Riddick et al. 2019); *C. cedri* (collected by *P. fuscipennis*) a pest on *Cedrus* species (Ji et al. 2021); and *A. pruniella* and *H. pruniana* (collected by *A. nigricornis*), both mainly feeding on trees of the genus *Prunus* (Řezáč 1964). Especially, *A. pruniella* is known to cause high levels of damage to *Prunus* trees, in addition to acting as pest on other orchard crops (Řezáč 1964). Nest cells belonging to the apoid wasps *P. gracilis* and *P. fuscipennis* were mostly found to be filled exclusively with aphids belonging to one species, which probably reflects their agglomerations on the host plant. Given the potential pest risk of some of these aphids, a targeted installation of trap nests might be helpful to control their abundances.

In summary, the combination of standardized trap nest monitoring and DNA barcoding is a useful approach to comprehensively investigate the biology of cavity-nesting Hymenoptera and their interaction partners.

Author contributions

Luisa Timm: Conceptualization, Data curation, formal analysis, investigation, visualization, writing – original draft, Writing – review and editing. Johanna Schaal: Data curation, investigation. Manuela Sann: Conceptualization, Data curation, formal analysis, Funding acquisition, Project administration, Resources, Writing – review and editing.

Data availability statement

Data are deposited as supplementary files. All raw sequencing data are available for download from Mendeley repository: DOI: 10.17632/vjttmbkxpx.1.

Acknowledgements

The data acquisition was funded with the support of the Stiftung Naturschutzfonds Baden-Württemberg with earmarked funds of the Glücksspirale. We thank Prof. Dr. Lars Krogmann and Prof. Dr. Johannes Steidle for providing lab facilities and lab resources. We are grateful to Dr. Helmut Dalitz and Dr. Robert Gliniars as well as Katrin Besemer, Sabine Benz, Thomas Ruopp, Franz-Steffen Glatz, Abdullah Ahmed and Dirk Heinrichs for providing space and helping set up the trap nests in the Botanical Garden at the University of Hohenheim. For the construction of the trap nests, we thank the team of the carpentry and metal workshop of the University of Hohenheim. We thank Dr. Michael C. Orr for proofreading the manuscript.

References

- Altschul SF, Gish W, Miller W, Myers EW, Lipman DJ (1990) Basic local alignment search tool. *Journal of Molecular Biology* 215: 403–410. [https://doi.org/10.1016/S0022-2836\(05\)80360-2](https://doi.org/10.1016/S0022-2836(05)80360-2)
- Alford DV (2014) *Pests of fruit crops: a colour handbook*, 2nd ed. Plant protection handbook series. CRC Press-Taylor & Francis (Boca Raton, FL).
- Blanchet FG, Cazelles K, Gravel D (2020) Co-occurrence is not evidence of ecological interactions. *Ecology Letters* 23: 1050–1063. <https://doi.org/10.1111/ele.13525>
- Camacho C, Coulouris G, Avagyan V, Ma N, Papadopoulos J, Bealer K, Madden TL (2009) BLAST+: architecture and applications. *BMC Bioinformatics* 10: 1–9. <https://doi.org/10.1186/1471-2105-10-421>
- Dicks LV, Breeze TD, Ngo HT, Senapathi D, An J, Aizen MA, Basu P, Buchori D, Galetto L, Garibaldi LA, Gemmill-Herren B, Howlett BG, Imperatriz-Fonseca VL, Johnson SD, Kovács-Hostyánszki A, Kwon YJ, Lattorff HMG, Lungharwo T, Seymour CL, Vanbergen AJ, Potts SG (2021) A global-scale expert assessment of drivers and risks associated with

- pollinator decline. *Nature Ecology & Evolution* 5: 1453–1461. <https://doi.org/10.1038/s41559-021-01534-9>
- Dormann CF, Gruber B, Fründ J (2008) Introducing the bipartite package: analysing ecological networks. *RNews* 8: 8–11.
- Folmer O, Black M, Hoeh W, Lutz R, Vrijenhoek R (1994) DNA primers for amplification of mitochondrial cytochrome c oxidase subunit I from diverse metazoan invertebrates. *Molecular Marine Biology and Biotechnology* 3: 294–299.
- Fornoff F, Halla W, Geiger S, Klein A-M, Sann M (2023) DNA barcoding resolves quantitative multi-trophic interaction networks and reveals pest species in trap nests. *Insect Conservation and Diversity* 16(5): 725–731. <https://doi.org/10.1111/icad.12664>
- Goulson D (2019) The insect apocalypse, and why it matters. *Current Biology* 29: R967–R971. <https://doi.org/10.1016/j.cub.2019.06.069>
- Hallmann CA, Sorg M, Jongejans E, Siepel H, Hoffland N, Schwan H, Stenmans W, Müller A, Sumser H, Hürren T, Goulson D, de Kroon H (2017) More than 75 percent decline over 27 years in total flying insect biomass in protected areas. *PLOS ONE* 12: e0185809. <https://doi.org/10.1371/journal.pone.0185809>
- Harris AC (1994) *Ancistrocerus gazella* (hymenoptera: Vespoidea: Eumenidae): a potentially useful biological control agent for leafrollers *Planotortrix octo*, *P. excessana*, *Ctenopseustis obliquana*, *C. herana*, and *Epiphyas postvittana* (Lepidoptera: Tortricidae) in New Zealand. *New Zealand Journal of Crop and Horticultural Science* 22: 235–238. <https://doi.org/10.1080/01140671.1994.9513832>
- Hebert PDN, Cywinska A, Ball SL (2003) Biological identifications through DNA barcodes. *Proceeding of the Royal Society London Series* 270: 313–321. <https://doi.org/10.1098/rspb.2002.2218>
- Hochkirch A, Casino A, Penev L, Allen D, Tilley L, Georgiev T, Gospodinov K, Barov B (2022) European red list of insect taxonomists. Luxembourg: Publications Office of the European Union. <https://doi.org/10.2779/364246>
- Ji Y, Li G, Zhou C, Yin S (2021) Influence of temperature on the development and reproduction of *Cinara cedri* (Hemiptera: Aphidoidea: Lachninae). *Bulletin of Entomological Research* 111: 579–584. <https://doi.org/10.1017/S0007485321000419>
- Klein A-M, Vaissiere BE, Cane JH, Steffan-Dewenter I, Cunningham SA, Kremen C, Tscharntke T (2007) Importance of pollinators in changing landscapes for world crops. *Proceedings of the Royal Society B: Biological Sciences* 274: 303–313. <https://doi.org/10.1098/rspb.2006.3721>
- Ollerton J, Johnson SD, Hingston AB (2006) Geographical variation in diversity and specificity of pollination systems. In: Waser NM, Ollerton J (Eds) *Plant-Pollinator Interactions: from Specialization to Generalization*. University of Chicago Press (Chicago), 283–308.
- Powney GD, Carvell C, Edwards M, Morris RK, Roy HE, Woodcock BA, Isaac NJB (2019) Widespread losses of pollinating insects in Britain. *Nature Communications* 10: 1–6. <https://doi.org/10.1038/s41467-019-08974-9>
- R Core Team (2023) *R: A Language and Environment for Statistical Computing*. R Foundation for Statistical Computing, Vienna. <https://www.R-project.org/>
- Řezáč M (1964) Die Schädlichkeit und die Parasiten der auf den mitteleuropäischen Obstbaumarten lebenden *Argyresthia*-Arten und die Möglichkeit ihrer Bekämpfung. *Zoologické listy - Folia zoologica* 13: 57–72.

- Riddick EW, Miller GL, Owen CL, Bauchan GR, Schmidt JM, Garipey T, Brown, RL, Grodowitz MJ (2019) Discovery of *Aphis ruborum* (Hemiptera: Aphididae) and *Aphelinus varipes* (Hymenoptera: Aphelinidae) on Cultivated Strawberry in Mississippi, USA. *Journal of Insect Science* 19(3): 17. [1–6] <https://doi.org/10.1093/jisesa/iez045>
- Senapathi D, Carvalheiro LG, Biesmeijer JC, Dodson CA, Evans RL, McKerchar M, Morton RD, Moss ED, Roberts SPM, Kunin WE, Potts SG (2015) The impact of over 80 years of land cover changes on bee and wasp pollinator communities in England. *Proceedings of the Royal Society B: Biological Sciences* 282: 20150294. <https://doi.org/10.1098/rspb.2015.0294>
- Staab M, Pufal G, Tscharnkte T, Klein A-M (2018) Trap nests for bees and wasps to analyse trophic interactions in changing environments – a systematic overview and user guide. *Methods in Ecology and Evolution* 9: 2226–2239. <https://doi.org/10.1111/2041-210X.13070>
- Trapp J, McAfee A, Foster LJ (2017) Genomics, transcriptomics and proteomics: enabling insights into social evolution and disease challenges for managed and wild bees. *Molecular Ecology* 26: 718–739. <https://doi.org/10.1111/mec.13986>
- Turčinavičienė J, Radzevičiūtė R, Budrienė A, Budrys E (2016) Species identification and genetic differentiation of European cavity-nesting wasps (Hymenoptera: Vespidae, Pompilidae, Crabronidae) inferred from DNA barcoding data. *Mitochondrial DNA Part A* 27: 476–482. <https://doi.org/10.3109/19401736.2014.905827>
- Zattara EE, Aizen MA (2021) Worldwide occurrence records suggest a global decline in bee species richness. *One Earth* 4: 114–123. <https://doi.org/10.1016/j.oneear.2020.12.005>

Supplementary material I

PCR Conditions

Authors: Luisa Timm, Johanna Schaal, Manuela Sann

Data type: docx

Explanation note: **table S1.** Primer Sequences; **table S2.** total master-mix and volume for PCR reaction with HCO/LCO primers; **table S3.** total master-mix and volume for PCR reaction with LepF1/LepR1 primers; **table S4.** PCR conditions for HCO/LCO primers; **table S5.** PCR conditions for LepF1/LepR1 primers.

Copyright notice: This dataset is made available under the Open Database License (<http://opendatacommons.org/licenses/odbl/1.0/>). The Open Database License (ODbL) is a license agreement intended to allow users to freely share, modify, and use this Dataset while maintaining this same freedom for others, provided that the original source and author(s) are credited.

Link: <https://doi.org/10.3897/jhr.97.117410.suppl1>

Supplementary material 2

Barcode and nest information

Authors: Luisa Timm

Data type: xlsx

Explanation note: **table S6**. Barcode information. Results of BLAST search against the National Center for Biotechnology Information (NCBI) database using the Nucleotide collection (nt/nr) database of the Basic Local Alignment Search Tool BLAST with the following option: highly similar sequences (megablast) (Altschul et al. 1990; Camacho et al. 2009); **table S7**. Nest information.

Copyright notice: This dataset is made available under the Open Database License (<http://opendatacommons.org/licenses/odbl/1.0/>). The Open Database License (ODbL) is a license agreement intended to allow users to freely share, modify, and use this Dataset while maintaining this same freedom for others, provided that the original source and author(s) are credited.

Link: <https://doi.org/10.3897/jhr.97.117410.suppl2>

Supplementary material 3

Infos on arthropods

Authors: Luisa Timm

Data type: xlsx

Explanation note: **table S8**. Collected Araneae in nests of *Trypoxylon clavicerum*. Information based on "Spinnen Forum Wiki" > wiki.arages.de <; **table S9**. Collected Aphididae of *Passaloecus corniger*, *Passaloecus gracilis* and *Psenulus fuscipennis*. Information based on Dr. Willem N. Ellis "Leafminers and plant galls of Europe" > <https://bladmineerders.nl><, if not differently indicated; **table S10**. Collected Tettigonidae of *Isodontia mexicana*. Information based on J.Fischer et al. "Die Heuschrecken Deutschlands und Nordtirols, Bestimmen - Beobachten - Schützen"; **table S11**. Collected Lepidoptera of *Ancistrocerus nigricornis*. Information based on ><https://lepiforum.org><; **table S12**. Collected *Tychius picirostris* of *Microdynerus parvulus*. Information based on Karl Wilhelm Harde, Frantisek Severa und Edwin Möhn: "Der Kosmos Käferführer: Die mitteleuropäischen Käfer".

Copyright notice: This dataset is made available under the Open Database License (<http://opendatacommons.org/licenses/odbl/1.0/>). The Open Database License (ODbL) is a license agreement intended to allow users to freely share, modify, and use this Dataset while maintaining this same freedom for others, provided that the original source and author(s) are credited.

Link: <https://doi.org/10.3897/jhr.97.117410.suppl3>

Supplementary material 4

Information on sampling sites

Authors: Luisa Timm

Data type: xlsx

Explanation note: **table S13**. Information on sampling sites at the University of Hohenheim.

Copyright notice: This dataset is made available under the Open Database License (<http://opendatacommons.org/licenses/odbl/1.0/>). The Open Database License (ODbL) is a license agreement intended to allow users to freely share, modify, and use this Dataset while maintaining this same freedom for others, provided that the original source and author(s) are credited.

Link: <https://doi.org/10.3897/jhr.97.117410.suppl4>

Supplementary material 5

Trap nests locations

Authors: Luisa Timm, Manuela Sann

Data type: png

Explanation note: supplementary image.

Copyright notice: This dataset is made available under the Open Database License (<http://opendatacommons.org/licenses/odbl/1.0/>). The Open Database License (ODbL) is a license agreement intended to allow users to freely share, modify, and use this Dataset while maintaining this same freedom for others, provided that the original source and author(s) are credited.

Link: <https://doi.org/10.3897/jhr.97.117410.suppl5>



A newly recorded genus *Microdynerus* Thomson, 1874 and a review of its related genus *Leptochilus* de Saussure, 1853 (Hymenoptera, Vespidae, Eumeninae) from China

Yue Bai¹, Bin Chen¹, Ting-Jing Li¹

¹ Chongqing Key Laboratory of Vector Insects, Institute of Entomology and Molecular Biology, College of Life Science, Chongqing Normal University, Chongqing 401331, China

Corresponding author: Ting-Jing Li (ltjing1979@hotmail.com)

Academic editor: Michael Ohl | Received 3 September 2023 | Accepted 29 January 2024 | Published 9 February 2024

<https://zoobank.org/727CB19F-EC87-4F6F-AEA5-1B696C959040>

Citation: Bai Y, Chen B, Li T-J (2024) A newly recorded genus *Microdynerus* Thomson, 1874 and a review of its related genus *Leptochilus* de Saussure, 1853 (Hymenoptera, Vespidae, Eumeninae) from China. *Journal of Hymenoptera Research* 97: 57–83. <https://doi.org/10.3897/jhr.97.112108>

Abstract

In this paper, the genus *Microdynerus* Thomson 1874 is newly recorded from China with one species *Microdynerus* (*Pseudomicrodynerus*) *parvulus* (Herrich-Schäffer, 1838). Furthermore, a total of ten species of the genus *Leptochilus* de Saussure is recorded from China, including one new species, i.e., *Leptochilus* (*Lionotulus*) *angulus* **sp. nov.**, which is described and illustrated in detail. Of the remaining nine *Leptochilus* species three are recorded here for the first time from China, i.e., *L. (Lionotulus) argentifrons* (Kostylev, 1935), *L. (Lionotulus) callidus* (Kostylev, 1940), and *L. (Lionotulus) locuples* Giordani Soika, 1970, whereas the remaining six species, i.e., *L. (Lionotulus) chinensis* Gusenleitner, 2001, *L. (Lionotulus) gobicus* (Kostylev, 1940), *L. (Lionotulus) babyrganus* Kurzenko, 1977, *L. (Lionotulus) incertus* (Kostylev, 1940), *L. (Lionotulus) kozlovi* Kurzenko, 1977, and *L. (Neoleptochilus) tibetanus* Giordani Soika, 1966, have been documented from China before. All treated species are diagnosed and illustrated. Finally, a key to the Chinese species of the two related genera is provided.

Keywords

China, Eumeninae, Hymenoptera, *Leptochilus*, *Microdynerus*, new record, new species

Introduction

The genus *Microdynerus* Thomson, 1874 in the subfamily Eumeninae contains three subgenera with 53 valid species and six subspecies (Carpenter, unpublished). The non-entotypical subgenus *Microdynerus* (*Microdynerus*) is distributed mainly in the Palearctic Region with the exception of a few species occurring in Nearctic Region. The distribution of the other two subgenera *M.* (*Pseudomicrodynerus*) and *M.* (*Alastorynerus*), both of them currently comprising only four species each, is limited to Palearctic Region. Both were first described as genera by Blüthgen (1938) and then downgraded to the subgeneric level by Carpenter (1986) and Gusenleitner (1997) respectively. Species of the genus are usually small (4.5–7.5 mm) and show often a medially transverse raised bulge on the metanotum, which gives them a superficially similar appearance to the genus *Leptochilus* de Saussure 1853. In fact, some species of these two genera were confused before (Arens 2001). To date, there was no record of *Microdynerus* in China, whereas, the *Leptochilus* was known from China by six species. In our collections of Chinese eumenids, two specimens of the genus *Microdynerus* were initially misidentified and mixed with those of *Leptochilus*.

Leptochilus is a larger group distributed in most of global zoogeographic regions (except Australian Region), containing six subgenera with 198 species: *L.* (*Euleptochilus*) Blüthgen, *L.* (*Leptochilus*) de Saussure, *L.* (*Lionotulus*) Blüthgen, *L.* (*Neoleptochilus*) Blüthgen, *L.* (*Sarochilus*) Gusenleitner, and *L.* (*Zendalia*) Robertson. Among the known species, more than 130 species belonging to the first five subgenera above occur in the Palearctic Region (Fateryga 2018; Fateryga and Fateryga 2021). The distribution of the remaining subgenus *L.* (*Zendalia*) Robertson 1928, however, is restricted to the Nearctic and Neotropical regions. The taxonomic development of the genus *Leptochilus* was shaped by Blüthgen (1938–1967), Parker (1966), Giordani Soika (1938–1986), Gusenleitner (1966–2017), and others. Since the 1970s, a large number of species in this genus had been described by Gusenleitner (1973, 1976, 1977, 1979, 1995, 2001, 2002, 2006) and Giordani Soika (1970, 1976, 1979, 1986). In China, five species of the subgenus *L.* (*Lionotulus*) and one of the subgenus *L.* (*Neoleptochilus*) were sporadically recorded (Kostylev 1940; Giordani Soika 1966; Kurzenko 1977; Gusenleitner 2001).

In the present paper, the genus *Microdynerus* with the species *M.* (*Pseudomicrodynerus*) *parvulus* (Herrich-Schäffer, 1838) was newly recorded and illustrated in China. Furthermore, all known species of the genus *Leptochilus* in China are systematically revised and ten species belonging to the two subgenera *L.* (*Lionotulus*) and *L.* (*Neoleptochilus*) are recognized from Xinjiang, Xizang, Qinghai, Gansu, and Inner Mongolia of China. Based on the pertinent literature and available specimens, one of these species in *Leptochilus* are identified as new to science and three are new records. The new species is described and illustrated in detail, and nine other species of *Leptochilus* are provided with diagnosis and figures. A key to the Chinese species of the two genera *Microdynerus* and *Leptochilus* is given. Finally, a distribution map (Fig. 95) of all known species of these two genera *Leptochilus* and *Microdynerus* in China is provided.

Materials and methods

The specimens examined in our study are deposited in the Institute of Entomology and Molecular Biology, Chongqing Normal University, Chongqing, China (CNU), and Zoological Institute in St. Petersburg, Russia. Descriptions and measurements were made under a stereomicroscope (Olympus SZ61).

Once a male specimen was available, we softened the specimen and directly dissected the genitalia with a dissecting needle for comparison, and then stored it in anhydrous alcohol for subsequent review. Male genitalia were extracted from softened specimens and directly dissected with a dissecting needle for comparison, and then stored it in anhydrous alcohol for subsequent review.

All photos and measurements were taken with Keyence VHX-5000 digital microscope and Photoshop CS 6 was used to compile the photo plates. Body length was measured from the anterior margin of the head to the posterior margin of metasomal tergum 2. If the pinned specimens were not horizontally oriented, a segmented approach was adopted to measurement. For the density description of punctures, “sparsely” means that interspaces are larger than one puncture diameter, “moderately” means equal to the diameter, and “densely” means less than one diameter. The abbreviations used in the text are shown as follows: A (1, 2, ...) for antennal joints, T (1, 2, ...) for metasomal terga, S (1, 2, ...) for metasomal sterna.

Descriptions and keys are based on available specimens and the most pertinent literature, among which keys in Gusenleitner (1993) and Selis (2023) and descriptions in Giordani Soika (1966), Kurzenko (1977) and Gusenleitner (2021) have been applied mainly. The species discussed are alphabetically listed in the text. The used terminology principally follows Carpenter (1981 (1982)).

Results

Genus *Leptochilus* de Saussure, 1853

Leptochilus de Saussure, 1853: 233; Giordani Soika 1938: 2–14; 1941: 7–13; Parker 1966: 151–229; van der Vecht and Fischer 1972: 42–53.

Type species. *Pterochilus mauritanus* [!] [= *Pterochilus mauritanicus* Lepeletier, 1841], by subsequent designation of Ashmead 1902.

Diagnosis. Body length < 9.0 mm; without epicnemial carina; axillary fossa of scutellum oval, broader than long; metanotum with horizontal carina between dorsally and posterior surfaces; propodeum with submarginal carina projecting as rounded lobe above valvula and bilamellate; T1 depressed subapically, gradually widened with lateral sides divergent in dorsal view; T2 with flat or concave apical lamella.

Distribution. Worldwide except Australian region.

***Leptochilus (Lionotulus) angulus* Bai, Chen & Li, sp. nov.**

<https://zoobank.org/501C27FC-7DE5-4667-BA21-EF1A0A4EC4CC>

Figs 1–9

Material examined. *Holotype*, ♀, CHINA, Inner Mongolia, Urad Front Banner, Xin an Town, Shulin Village, 40.945°N, 108.633°E, 989 m, 3.VIII.2016, Zhenxia Ma (CNU); *paratypes*, 3♀♀, same data as holotype.

Diagnosis. This species resembles *L. (L.) callidus* (Kostylev, 1940) with similar clypeus punctures (Figs 2, 3, 19) and occipital carina (Figs 4, 24). It can be distinguished from the related species and other members of the genus by the following character combination: pronotal carina transparent and obvious (Fig. 5), propodeum with long and undeveloped carina between dorsal and posterior surfaces, posterior surface with oblique and long striae, propodeal carina as long as propodeal concavity (Fig. 7).

Description. Female. Body length 5.5–6.3 mm (Fig. 1), forewing length 5.4–6.2 mm; black, with the following parts light yellow: basal spot of clypeus (or not), an anterior interrupted band of pronotum dorsally, most of tegula except the median transparent part, apical margin of scutellum, small dorsal spots of mesopleuron (or not), apical margin of femora, tibiae (slightly dark at apical margin) and tarsi, apical bands of T1–T2 (T1 subterminal part ferruginous or not), apical small spots on both sides of S2, and apical spots of T3–T5 in the middle (or not).

Head. In front view, clypeus wider than long (1.4×), and apically with emargination wider than depth (2.2×–2.5×) (Figs 2, 3), clypeus laterally with dense short white setae; clypeus with small and dense punctures basally, and with bigger and coarser punctures on apical half; frons, vertex and gena with coarse and dense punctures; occipital carina forming obvious angle latero-ventrally (Fig. 4).

Mesosoma. Mesosoma with irregular coarse punctures, interspaces between punctures with minute punctures; mesoscutum on anterior half and mesopleuron ventrally with sparse punctures (Figs 1, 6); pronotal carina transparent and obvious (Fig. 5); metapleuron and lateral surfaces of propodeum with unbroken finely horizontal striae, and lateral surface of propodeum densely striate mixed with irregular punctures (Fig. 6); propodeum with long and undeveloped carina between dorsal and posterior surfaces (Fig. 7); posterior surface with oblique and long striae, propodeal carina present in lower part and half as long as propodeal concavity (Fig. 7).

Metasoma. Metasoma leathery, with smaller and sparser punctures than those on head and mesosoma (Figs 8, 9); punctures of T1 larger than the second metasomal segment, punctures of metasomal segments 2–3 larger than those on metasomal segments 4–6; in dorsal view, the first metasomal segment semi-circular (Fig. 1); the second one with wide apical lamellae and with a row of great punctures at base of lamellae, interspaces between punctures short carina-formed; S2 weak convex in lateral view (Fig. 8), with shallow and long longitudinal medial furrows at base (Fig. 9).

Male. Unknown.

Distribution. China (Inner Mongolia).

Etymology. The specific name *angulus* is derived from Latin word: *angulus*, referring to occipital carina forming obvious angle latero-ventrally.



Figures 1–9. *Leptochilus (Lionotulus) angulus* sp. nov., holotype (♀) **1** habitus in dorsal view **2, 3** head in frontal view **4** gena in lateral view **5** vertex and pronotum **6** mesosoma in lateral view **7** propodeum in posterior view **8, 9** metasoma in lateral view.

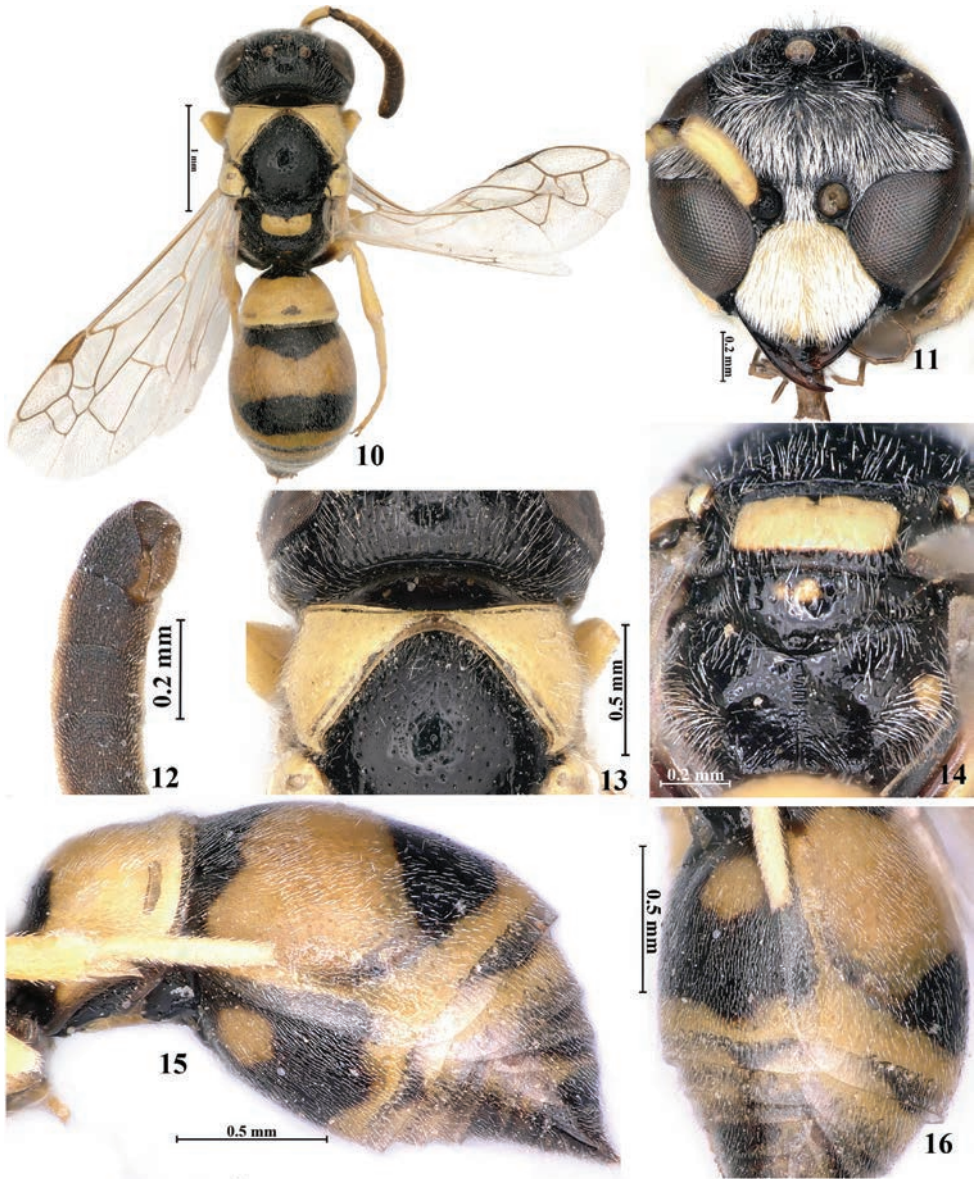
***Leptochilus (Lionotulus) argentifrons* (Kostylev, 1935)**

Figs 10–16

Microdynerus argentifrons Kostylev, 1934: 137; Kostylev 1940: 37; van der Vecht and Fischer 1972: 45.

Material examined. 1♂, CHINA, Xinjiang, Bayinguoleng Mongolian Autonomous Prefecture, Ruoqiang County, 14.V.2010, Zhaohui Luo (CNU).

Diagnosis. Female body length 5.0 mm; male body length 4.5 mm, forewing 4.3 mm (Fig. 10); body with small and sparse punctures, interspaces between punctures



Figures 10–16. *Leptochilus (Lionotulus) argentifrons* (Kostylev, 1935) ♂ **10** habitus in dorsal view **11** head in frontal view **12** part of antenna **13** vertex and pronotum **14** propodeum in posterior view **15, 16** metasoma in lateral view.

polished (Fig. 10); with obvious white setae; black, with the following parts yellow: clypeus, scape, flagellum except dorsally, pronotum, tegula, parategula, scutellum at posterior half, posterodorsal spot of mesopleuron, legs (except basal margins of femora), mostly on apical margin of T1, wide band in the part middle area of T2, lateral

spot of S2, apical bands of metasomal segments 2–5. In front view, frons with dense setae (Fig. 11); clypeus wider than long, apically with deep emargination in male, and emargination wider than depth (1.8×); A13 sharp at the apex (Fig. 12); ocelli large; occipital carina curved latero-ventrally. Pronotal carina obvious (Fig. 13); propodeum smooth (Fig. 14), with boundary between dorsal and posterior surfaces, but without carina; propodeal carina present in lower half, and less than 1/2 of propodeal concavity. Metasomal segments 2–4 with wide apical lamellae and the second metasomal segment with a row of great punctures at base, interspaces between punctures short carina-formed (Fig. 15); S2 weak convex in lateral view, with shallow and short longitudinal medial furrows at base (Fig. 16).

Distribution. China (new record: Xinjiang), Turkmenistan.

Leptochilus (Lionotulus) callidus (Kostylev, 1940)

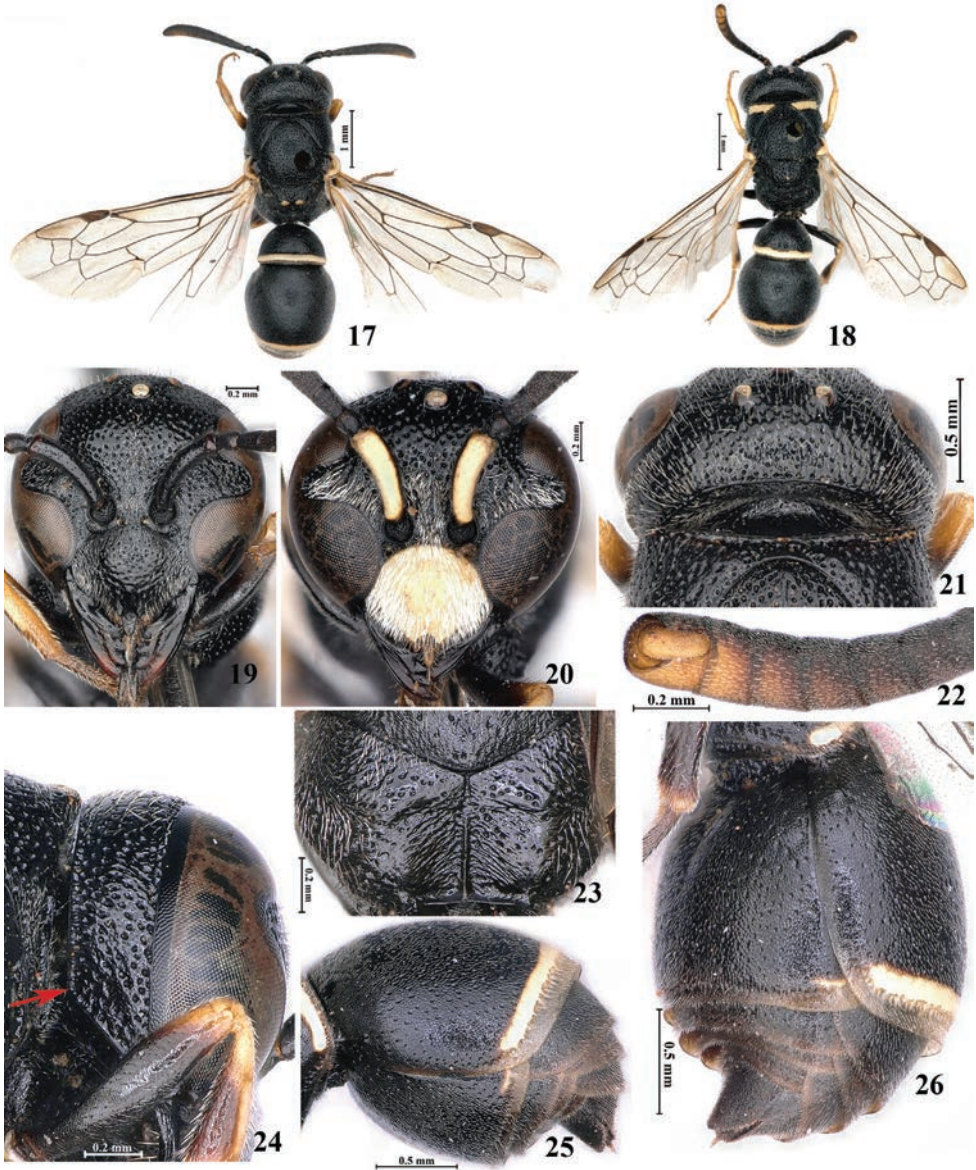
Figs 17–26

Odynerus callidus Kostylev, 1940: 33.

Leptochilus callidus: van der Vecht and Fischer 1972: 46.

Material examined. 1♀, 1♂, CHINA, Inner Mongolia, Ewenki Autonomous Banner, Yimin Town, Five Pastureland, 8.VIII.2006, Tingjing Li (CNU); 2♂♂, CHINA, Ningxia, Yinchuan City, Helan County, Jinshan Township, Lujiawazi, 38.694°N, 106.174°E, 1117 m, 21.VII.2020, Yujiang Yao, Rongyuan Zhang (CNU); 1♂, CHINA, Ningxia, Wuzhong City, Yanchi County, Huamachi Town, Yikeshu Village, 37.891°N, 107.434°E, 1312 m, 25.VII.2020, Qianchen Wang, Rongyuan Zhang (CNU).

Diagnosis. Female body length 6.1 mm, forewing 5.7 mm (Fig. 17); male body length 4.9–5.5 mm, forewing 4.4–5.0 mm (Fig. 18); black, with the following parts light yellow: clypeus of male, scape ventrally in male, an anterior interrupted band of pronotum dorsally in male, outer margin of tegula, two spots on posterior margin of scutellum in female, apical margin of femora, tibiae (slightly dark ventrally) and tarsi, apical bands of T1–T2, apical small spots of S2 laterally; A8–A12 ventrally deep yellow. In front view, clypeus wider than long (1.3× in female, 1.1× in male), and apically with shallow emargination wider than depth (2.9× in female, 2.7× in male) (Figs 19, 20); clypeus in female with sparse and coarse punctures, interspaces between punctures with transverse wrinkles on apical half (Fig. 19), clypeus in male with sparse and small punctures (Fig. 20); clypeus and frons at lower part in male with dense white setae (Fig. 20); A13 almost parallel on both sides at the apex (Fig. 22); frons, vertex and gena with coarse and irregular punctures; frons punctures in male larger than those in female; occipital carina forming obvious angle latero-ventrally (Fig. 24). Mesosoma with irregular and coarse punctures, interspaces between punctures with minute punctures; posterior margin of mesoscutum and mesopleuron dorsally with dense punctures, interspaces between punctures reticulate; pronotal carina non-transparent and obvious (Fig. 21); metapleuron dorsally with coarse horizontal striae, ventrally leathery and



Figures 17–26. *Leptochilus (Lionotulus) callidus* (Kostylev, 1940) ♀ **17, 19, 21, 23–26** ♂ **18, 20, 22**. **17, 18** habitus in dorsal view **19, 20** head in frontal view **21** vertex and pronotum **22** part of antenna **23** propodeum in posterior view **24** gena in lateral view **25, 26** metasoma in lateral view.

with irregular fine striae; propodeum dorsally with coarse and dense punctures; carina degenerate between dorsal and posterior surfaces (Fig. 23); posterior surface with long and oblique striae mixed with coarse punctures, propodeal carina present in lower part and about 2/3 of propodeal concavity (Fig. 23). Metasoma leathery, with small and

sparse punctures; the second metasomal segment with wide apical lamellae and there with a row of great punctures at base, interspaces between punctures short carina-formed (Fig. 25); S2 weak convex in lateral view (Fig. 25), with shallow longitudinal medial furrows at base, and half as long as S2 (Fig. 26).

Distribution. China (new record: Inner Mongolia, Ningxia), Central Asia from Lake Aral to Gobi Desert.

***Leptochilus (Lionotulus) chinensis* Gusenleitner, 2001**

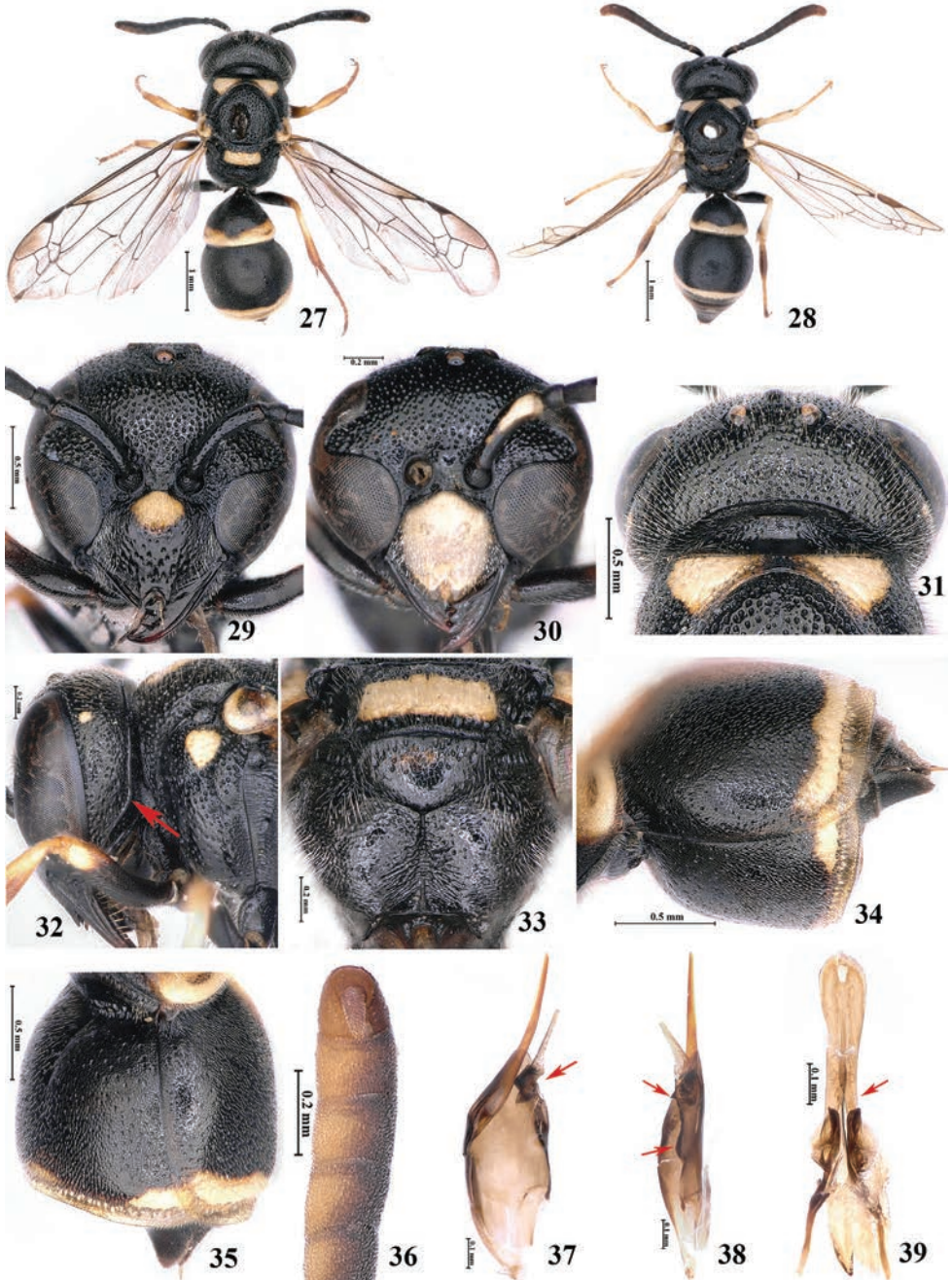
Figs 27–39

Leptochilus chinensis Gusenleitner, 2001: 239.

Material examined. 1♀, CHINA, Inner Mongolia, Hohhot, Horinger County, Suojiayao Village, 40.570°N, 111.966°E, 1230 m, 25.VII.2019, Xue Zhang (CNU); 2♂♂, CHINA, Inner Mongolia, Hohhot, Wuchuan County, Daqingshan Town, Sanchakou Village, 41.003°N, 111.533°E, 1661 m, 23.VII.2019, Pan Huang (CNU); 2♂♂, CHINA, Inner Mongolia, Hohhot, Wuchuan County, Daqingshan Town, Dongyaozi, 40.930°N, 111.393°E, 1503 m, 24.VII.2019, Xue Zhang (CNU); 1♂, CHINA, Inner Mongolia, Tongliao city, Daqinggou, 11.VIII.2006, Ming Luo (CNU).

Diagnosis. Female body length 5.5 mm (Fig. 27); male body length 4.5–4.8 mm, forewing 4.3–4.5 mm (Fig. 28); black, with the following parts yellow: clypeus basal marking in female, complete clypeus in male, scape ventrally in male, small spot of gena, two anterior marking of pronotum dorsally, spot of mesopleuron dorsally, tegula, posterior margin of scutellum, apical margin of femora, tibiae and tarsi, narrow apical bands of T1–T2 (broader of T1 laterally), broken apical bands of S2. In front view, clypeus wider than long (1.4× in female, 1.1× in male), and apically emargination wider than depth (2.3× in female, 1.8× in male) (Figs 29, 30); clypeus in female with sparse and coarse punctures on basal half, with dense and larger punctures on apical half (Fig. 29); clypeus in male with sparse and small punctures, with dense white setae (Fig. 30); frons, vertex and gena with coarse and dense punctures, occipital carina curved latero-ventrally (Fig. 32); A13 sharp at the apex (Fig. 36). Mesosoma with coarse and dense punctures; pronotal carina degenerate (Fig. 31); metapleuron and lateral surfaces of propodeum with unbroken finely horizontal striae; propodeum posterior surfaces with wide propodeal concavity, with long and oblique striae laterally, propodeal carina present in lower part, and short about 1/3 as long as the propodeal concavity (Fig. 33); hind tarsus in male swollen (Fig. 28). Metasoma leathery, with sparse and small punctures (Figs 27, 28); the second metasomal segment with wide apical lamellae and there with a row of great punctures at base, interspaces between punctures short carina-formed (Fig. 34); S2 strong convex in lateral view (Fig. 34), with deep longitudinal medial furrows at base (Fig. 35); volsella with lateral processes in the middle and basal parts (Figs 37, 38), penis valve slightly narrow in the middle part, with depression at the top (Fig. 39).

Distribution. China (Inner Mongolia, Shaanxi, Ningxia).



Figures 27–39. *Leptochilus (Lionotulus) chinensis* Gusenleitner, 2001 ♀ **27, 29, 31–35** ♂ **28, 30, 36–39**. **27, 28** habitus in dorsal view **29, 30** head in frontal view **31** vertex and pronotum **32** gena in lateral view **33** propodeum in posterior view **34, 35** metasoma in lateral view **36** part of antenna **37, 38** volsella **39** penis valve.

***Leptochilus (Lionotulus) gobicus* (Kostylev, 1940)**

Figs 40–45

Odynerus gobicus Kostylev, 1940: 36.*Leptochilus gobicus*; van der Vecht and Fischer 1972: 47.

Material examined. *Holotype*, ♂, Tzoto, Alachan, Gobi, 9.V.1908, P. Kozlov! (Zoological Institute in St. Petersburg); *paratype*, 1♀, same data as holotype.

Diagnosis. Female body length 5.5 mm (Fig. 40); black, with the following parts yellow: small spot of gena, A6–A13 of male, two anterior small spots of pronotum dorsally, outer margin of tegula, posterior margin scutellum in male, apical margin of femora, part of tibiae and tarsi (hind tarsus dorsally brown), narrow apical bands of T1–T2, apical spots of S2 laterally. Body with sparse white setae, and with minute and sparse punctures (Figs 40, 41); clypeus wider than long (1.3× in female, 1.1× in male), and apically emargination wider than depth (3.0× in female, 1.9× in male) (Figs 42, 43); clypeus in female with sparse and shallow punctures, base of emargination without punctures and smooth (Fig. 42); clypeus in male with dense setae (Fig. 43); frons, vertex and gena with coarse and sparse punctures. Punctures of mesosoma coarser and denser than those on head and metasoma; pronotal carina unobvious (Figs 40, 41); A13 sharp at the apex (Fig. 45); the first hind tarsus in male swollen (Fig. 44). Metasoma leathery, with sparse and small punctures; the second metasomal segment with wide apical lamellae and there with a row of great punctures at base, interspaces between punctures short carina-formed (Fig. 44); S2 weakly convex in lateral view (Fig. 44).

Distribution. China (Inner Mongolia).

***Leptochilus (Lionotulus) habyrganus* Kurzenko, 1977**

Figs 46–57

Leptochilus habyrganus Kurzenko, 1977: 550.

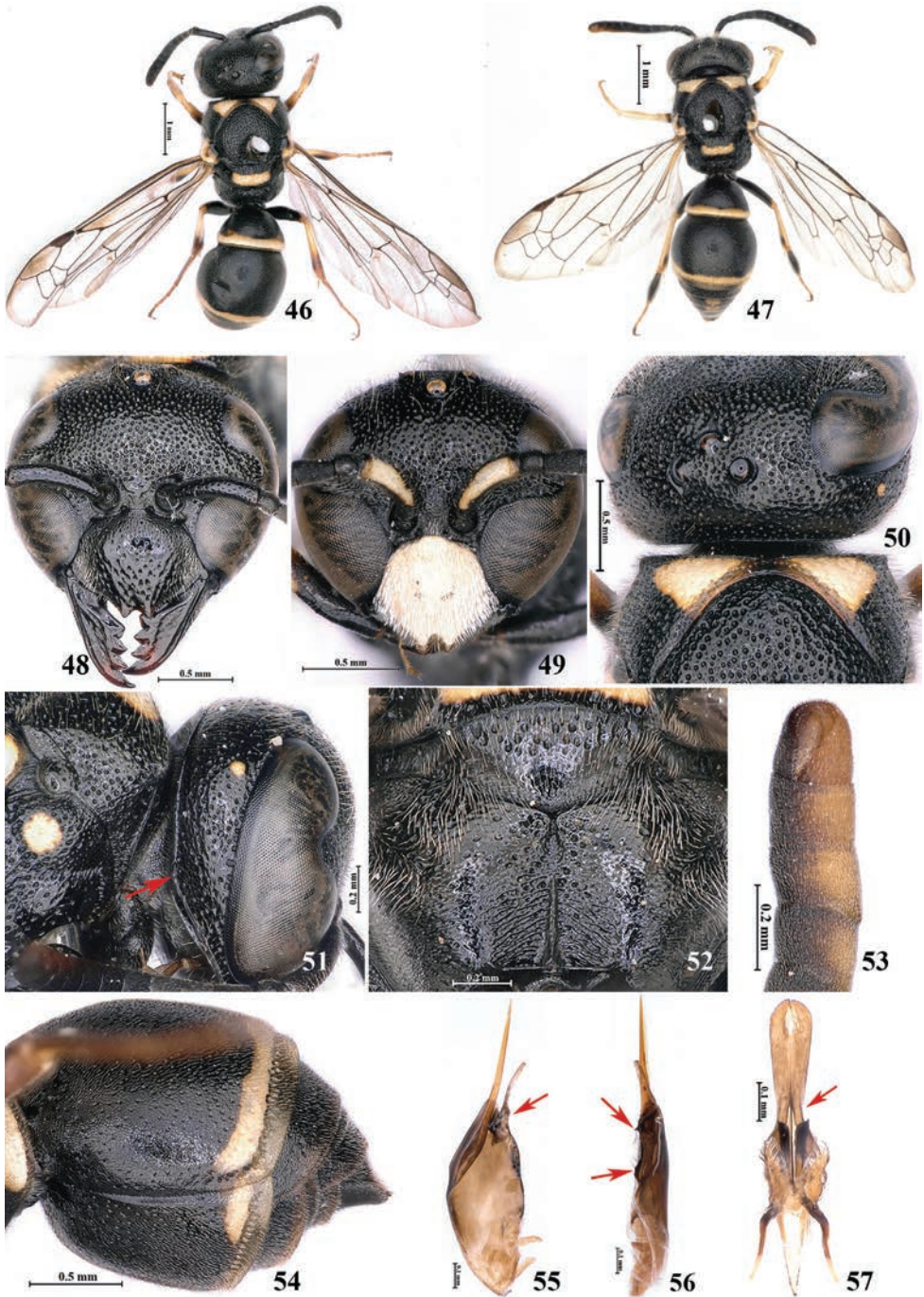
Material examined. 2♀♀, CHINA, Gansu Province, Weiwu City, Qilian Town, Qilian Township, 37.678°N, 102.422°E, 2354 m, 5.VII.2019, Xue Zhang (CNU); 1♀, 1♂, CHINA, Inner Mongolia, Hohhot, Wuchuan County, Daxiyaozi, 41.046°N, 111.483°E, 1732 m, 23.VII.2019, Xue Zhang (CNU); 1♀, 2♂♂, CHINA, Inner Mongolia, Baotou City, Guyang County, Near Dadeheng, 41.130°N, 110.321°E, 1570 m, 21.VII.2019, Rongyuan Zhang (CNU); 1♂, CHINA, Inner Mongolia, Hohhot, Wuchuan County, Daqingshan Town, Sanchakou Village, 41.003°N, 111.533°E, 1661 m, 23.VII.2019, Pan Huang (CNU); 1♂, CHINA, Inner Mongolia, Hohhot, Wuchuan County, Daqingshan Town, Dongyaozi, 40.930°N, 111.393°E, 1503 m, 24.VII.2019, Xue Zhang (CNU).



Figures 40–45. (taken by Alexander V. Fateryga). *Leptochilus (Lionotulus) gobicus* (Kostylev, 1940). holotype (♂) **41, 43–45** paratype (♀) **40, 42, 40, 41** habitus in dorsal view **42, 43** head in frontal view **44** habitus in lateral view **45** part of antenna.

Diagnosis. Female body length 5.4–6.3 mm, forewing 5.0–5.8 mm (Fig. 46); male body length 4.3–4.9 mm, forewing 4.0–4.6 mm (Fig. 47). This species resembles *L. (L.) chinensis* Gusenleitner, 2001 with similar coloration (Figs 27, 28, 46, 47), antenna (Figs 36, 53), occipital carina (Figs 32, 51), pronotal carina (Figs 31, 50), hind tarsi in male (Figs 28, 47) and S2 (Figs 34, 54). Male genitalia are different from *L. (L.) chinensis* Gusenleitner, 2001 (Figs 37–39, 55–57) by penis valve obvious narrow in the middle part, depression deeper than above at the top (Fig. 57). In addition, it can be distinguished from the related species and other members of the genus by the following character combination: in front view clypeus wider than long (1.1× in female, 1.2× in male), apically emargination wider than depth (2.6× in female, 1.8× in male) (Figs 48, 49), propodeum posterior surface with finely and oblique striae mixed with sparse punctures, propodeal concavity shallow, and propodeal carina present in lower part, and long about 2/3 as long as the propodeal concavity (Fig. 52).

Distribution. China (Inner Mongolia, Gansu, Qinghai).



Figures 46–57. *Leptochilus (Lionotulus) habyriganus* Kurzenko, 1977 ♀ **46, 48, 50–52, 54** ♂ **47, 49, 53, 55–57.** **46, 47** habitus in dorsal view **48, 49** head in frontal view **50** vertex and pronotum **51** gena in lateral view **52** propodeum in posterior view **53** antenna **54** metasoma in lateral view **55, 56** volsella **57** penis valve.

***Leptochilus (Lionotulus) incertus* (Kostylev, 1940)**

Figs 58–60

Odynerus incertus Kostylev, 1940: 33.*Leptochilus incertus*; van der Vecht and Fischer 1972: 47.

Material examined. *Holotype*, ♀, Bain-Houdouk, Nord Alachan, Mongolic, 20.V.1909, P. Kozlv! (Zoological Institute in St. Petersburg).

Diagnosis. Female body length 5.5 mm (Fig. 58); black, with the following parts light yellow: base half of clypeus, scape ventrally, pronotum dorsally in the front half, tegula, scutellum at posterior half, dorsal spot of mesopleuron, apical margins of femora, tibiae and tarsi, apical bands of both T1–T2 and S2 (band of T1 expand on both side and T2 with medial spots laterally). In front view, clypeus wider than long, and apically with shallow and wide emargination (Fig. 60); with large and dense punctures on apical half, with obvious white setae; frons with dense setae on lower half; frons, vertex and gena with small and sparse punctures. Punctures of mesosoma larger than those on head and metasoma (Fig. 59); pronotal carina obvious (Fig. 58). Metasoma leathery, with small and sparse punctures; the second metasomal segment with wide apical lamellae and there with a row of great punctures at base, interspaces between punctures short carina-formed (Fig. 59); S2 weakly convex in lateral view, with shallow longitudinal medial furrows at base (Fig. 59).

Male. Unknown.

Distribution. China (Inner Mongolia).

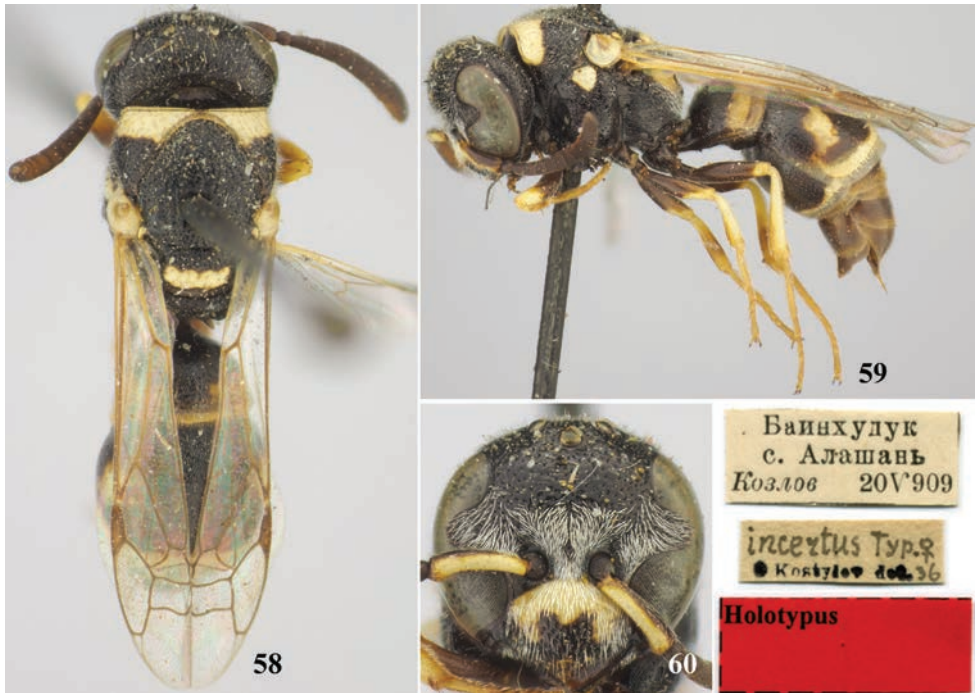
***Leptochilus (Lionotulus) kozlovi* Kurzenko, 1977**

Figs 61–71

Leptochilus kozlovi Kurzenko, 1977: 547.

Material examined. 2♀♀, 1♂♂, CHINA, Xinjiang, Ili Kazak Autonomous Prefecture, Huocheng County, Qingshuihe Town, Shuanggouyi village, 44.182°N, 80.685°E, 688 m, 26.VII.2019, Jie Chen (CNU); 1♂♂, CHINA, Xinjiang, Karamay, jinlong town, Near G217 and S201 of Ayikule Reservoir, 45.526°N, 84.916°E, 279 m, 23.VII.2019, Tingjing Li, Qian Han, Jie Chen (CNU).

Diagnosis. Female body length 4.3–5.2 mm, forewing 4.5–4.6 mm (Fig. 61); male body length 4.3–4.6 mm, forewing 4.1–4.3 mm (Fig. 62); black, with the following parts yellow: clypeus in male, scape ventrally in female, wholly scape in male, anterior half of pronotum, tegula, parategula, apical half of scutellum, apical margin of femora, tibiae (slightly dark apical margin) and most of tarsi, apical bands of both T1–T2 and S2 (broader of T1 laterally), apical margin of T3–T5 with short bands or spots (apical margin of T6 in male); A6–A13 ventrally deep yellow. Body with dense and coarse



Figures 58–60. (taken by Alexander V. Fateryga). *Leptochilus* (*Lionotulus*) *incertus* (Kostylev, 1940). holotype (♀) **58** habitus in dorsal view **59** habitus in lateral view **60** head in frontal view.

punctures, interspaces between punctures reticulate; clypeus wider than long (1.3× in female, 1.0× in male), apically with shallow emargination wider than depth (2.8× in female, 2.6× in male) (Figs 63, 64); clypeus in female with sparse and coarse punctures, base of emargination without punctures and smooth (Fig. 63); clypeus in male with sparse and small punctures, dense white setae (Fig. 64); frons on lower half in male with dense white setae; occipital carina slightly curved latero-ventrally (Fig. 66); A13 sharp at the apex (Fig. 71). Pronotal carina transparent and obvious (Fig. 65); metapleuron and lateral surfaces of propodeum with unbroken coarse horizontal striae mixed with coarse punctures (Fig. 67); propodeum with developed and long carina between dorsal and posterior surfaces (Fig. 68), posterior surface with coarse and oblique striae mixed with coarse punctures, propodeal carina weakly present in lower part and less than half of propodeal concavity. Punctures of metasomal segments 3–7 sparser than those on metasomal segments 1–2; the second metasomal segment with wide apical lamellae and with a row of great punctures at base, interspaces between punctures long carina-formed extending almost to the top (not reaching apical margin) (Fig. 69); S2 weakly convex in lateral view, with shallow and short longitudinal medial furrows at base (Fig. 70).

Distribution. China (Xinjiang).



Figures 61–71. *Leptochilus (Lionotulus) kozlovi* Kurzenko, 1977 ♀ **61, 63, 65–70** ♂ **62, 64, 71**. **61, 62** habitus in dorsal view **63, 64** head in frontal view **65** vertex and pronotum **66** gena in lateral view **67** mesosoma in lateral view **68** propodeum in posterior view **69, 70** metasoma in lateral view **71** part of antenna.

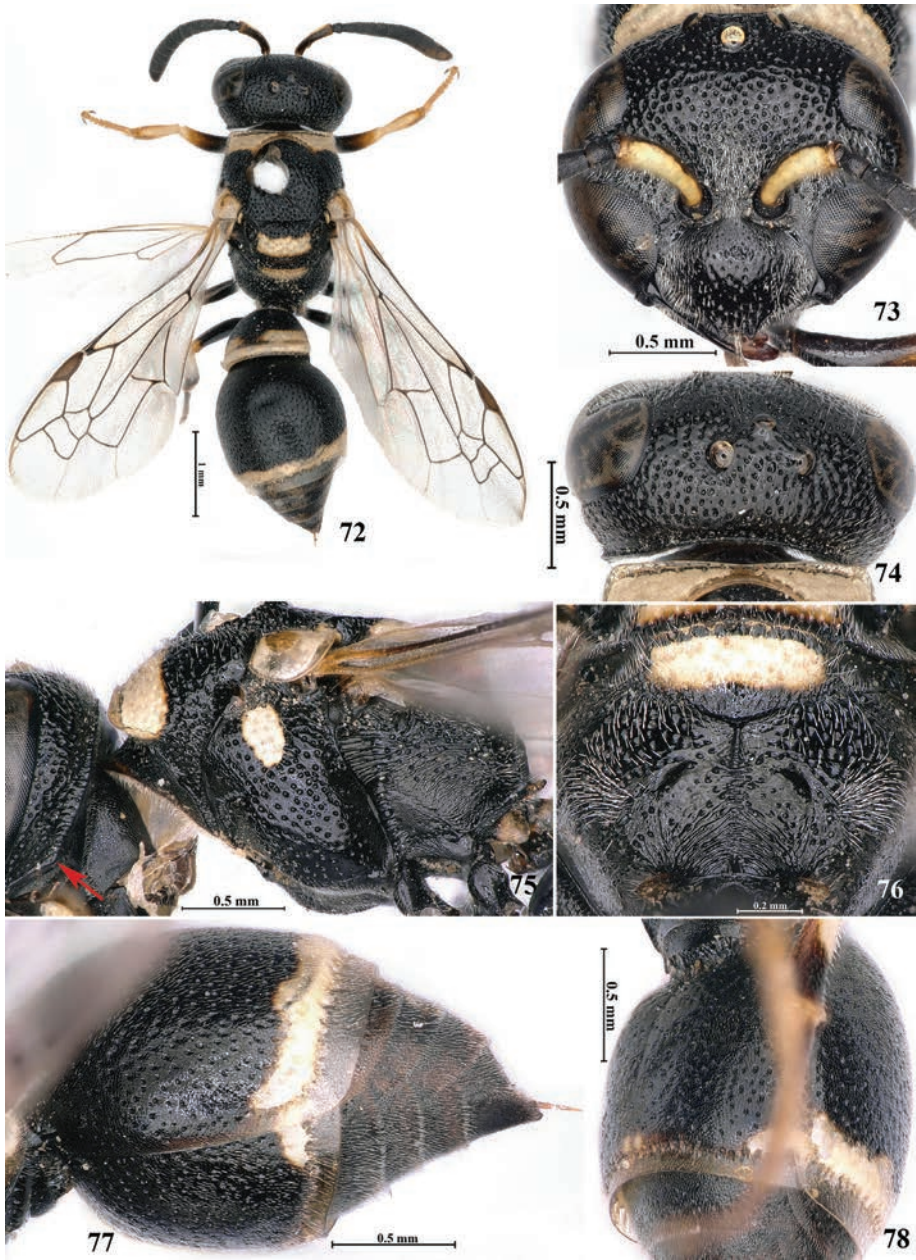
***Leptochilus (Lionotulus) locuples* Giordani Soika, 1970**

Figs 72–78

Leptochilus locuples Giordani Soika, 1970: 70; van der Vecht and Fischer 1972: 48.**Material examined.** 1 ♀, CHINA, Gansu Province, Zhangye City, Gaotai County, Heiquan Town, Yanzhibao Village, 39.607°N, 99.654°E, 1319 m, 1.VII.2019, Xue Zhang (CNU).**Diagnosis.** Female body length 5.5 mm, forewing 4.9 mm (Fig. 72); black, with the following parts whitish yellow: scape ventrally, pronotum dorsally at anterior half, tegula, parategula, scutellum at posterior half, posterior oblique plane of metanotum, dorsal spot of mesopleuron, apical margins of femora, tibiae and tarsi, apical bands of T1–T2 (band of T1 extended on lateral side) and apical small spots of S2 laterally. Body with dense and coarse punctures; in front view, clypeus wider than long (1.3×), and apically emargination wider than depth (2.9×) (Fig. 73); clypeus with large and dense punctures on apical half, with minute and dense punctures on basal half, outer margin with white setae; frons with dense setae at the lower half (Fig. 73); occipital carina developed and forming obvious angle latero-ventrally (Fig. 75). Pronotal carina developed and transparent (Fig. 74); metapleuron with horizontal striae dorsally and leathery ventrally (Fig. 75); propodeum with short and curved carina between dorsal and posterior surfaces, lateral surfaces with fine striae mixed with sparse punctures; without propodeal carina, and sparsely punctate on upper half, propodeal concavity only present in upper part, and obliterate and with oblique striae in lower half crossing posterior surface (Fig. 76). Metasoma leathery, with large and coarse punctures (Fig. 77); the second metasomal segment with wide apical lamellae and with a row of great punctures at base, interspaces between punctures short carina-formed (Fig. 77); S2 weakly convex in lateral view, with shallow longitudinal medial furrows at base, and slightly longer than half of S2 (Fig. 78).**Male.** Unknown.**Distribution.** China (new record: Gansu), Turkmenistan.***Leptochilus (Neoleptochilus) tibetanus* Giordani Soika, 1966**

Figs 79–85

Leptochilus tibetanus Giordani Soika, 1966: 99; van der Vecht and Fischer 1972: 53.**Material examined.** 7 ♀♀, CHINA, Xizang, Linzhi City, Milin County, Wolong Town, 4.VIII.2014, Tingjing Li (CNU); 1 ♀, CHINA, Xizang, Linzhi City, Bayi Town, Bujiu Township, Duodang Village, 5.VIII.2014, Tingjing Li (CNU).**Diagnosis.** Female body length 6.0–6.8 mm, forewing 5.5–6.0 mm (Fig. 79); male body length 4.5–5.5 mm; body with obvious white setae, and the setae on the head and mesosoma longer than those on the metasoma; black, with the following parts yellow: base band of clypeus in female, wholly clypeus in male, scape line in male ventrally; small spot of gena near eye, an anterior interrupted band of pronotum



Figures 72–78. *Leptochilus (Lionotulus) locuples* Giordani Soika, 1970 ♀ **72** habitus in dorsal view **73** head in frontal view **74** vertex and pronotum **75** gena and mesosoma in lateral view **76** propodeum in posterior view **77, 78** metasoma in lateral view.

dorsally, tegula, parategula, scutellum on posterior half, dorsal spots of mesopleuron, apical margin of femora, tibiae base and dorsally, tarsi, apical bands of T1–T5 (apical bands of T3–T5 incomplete), T2 laterally with circular and medial spots, apical



Figures 79–85. *Leptochilus (Neoleptochilus) tibetanus* Giordani Soika, 1966 ♀ **79** habitus in dorsal view **80** head in frontal view **81** vertex and pronotum **82** mesosoma in lateral view **83** gena in lateral view **84** propodeum in posterior view **85** metasoma in lateral view.

bands of S2–S5. Body with sparse white setae; in front view, clypeus in female slightly wider than long, and apically with semicircular emargination wider than depth (2×) (Fig. 80), emargination in male wider than in female; clypeus in female with small and sparse punctures, and interspaces between punctures with smaller punctures, with dense white setae laterally (Fig. 80), wholly with dense white setae in male; frons

and vertex with coarse and dense punctures, interspaces between punctures reticulate (Figs 80, 81); punctures on gena sparser and smaller than above, interspaces between punctures leathery, occipital carina curved latero-ventrally (Fig. 83); A13 sharp apically. Mesosoma with coarse punctures, interspaces between punctures finely punctate; punctures of pronotum and mesoscutum dense; other part of mesosoma with sparse punctures; pronotal carina narrow extremely (Fig. 81); metapleuron and lateral surfaces of propodeum with unbroken finely horizontal striae (Fig. 82); propodeum with long and dense setae, and without carina between dorsal and posterior surfaces (Fig. 84); propodeal concavity deep, propodeal carina present in lower part and less than half of propodeal concavity (Fig. 84). Metasoma with sparse and coarse punctures (Fig. 85); metasomal segments 1–3 punctures larger than those on metasomal segments 4–6; the second metasomal segment with apical lamellae and there with a row of great punctures at base, interspaces between punctures normal, not carina-formed (Fig. 85); S2 weak convex in lateral view, with shallow longitudinal medial furrows at base.

Distribution. China (Xizang).

Genus *Microdynerus* Thomson, 1874

Microdynerus Thomson, 1874: 58.

Type species. *Odynerus exilis* Herrich-Schäffer, 1839, by subsequent designation of Jones 1937.

Diagnosis. Female without cephalic foveae (Fig. 88); pronotum with anterior face usually densely punctate; mesosoma long, mesoscutum longer than wide; inner side of the trailing edge of tegula straight and not extended (except *Microdynerus robustus*); posterior face of propodeum without wide deep vertical cavity, with submarginal carina and vavula not projecting; T1 wider than long; T1–T2 with apical bands, T2 apically not carina-formed or without foveae, S2 without longitudinal furrow (Fig. 94).

Distribution. Palearctic and Nearctic Region.

Microdynerus (*Pseudomicrodynerus*) *parvulus* (Herrich-Schäffer, 1838)

Figs 86–94

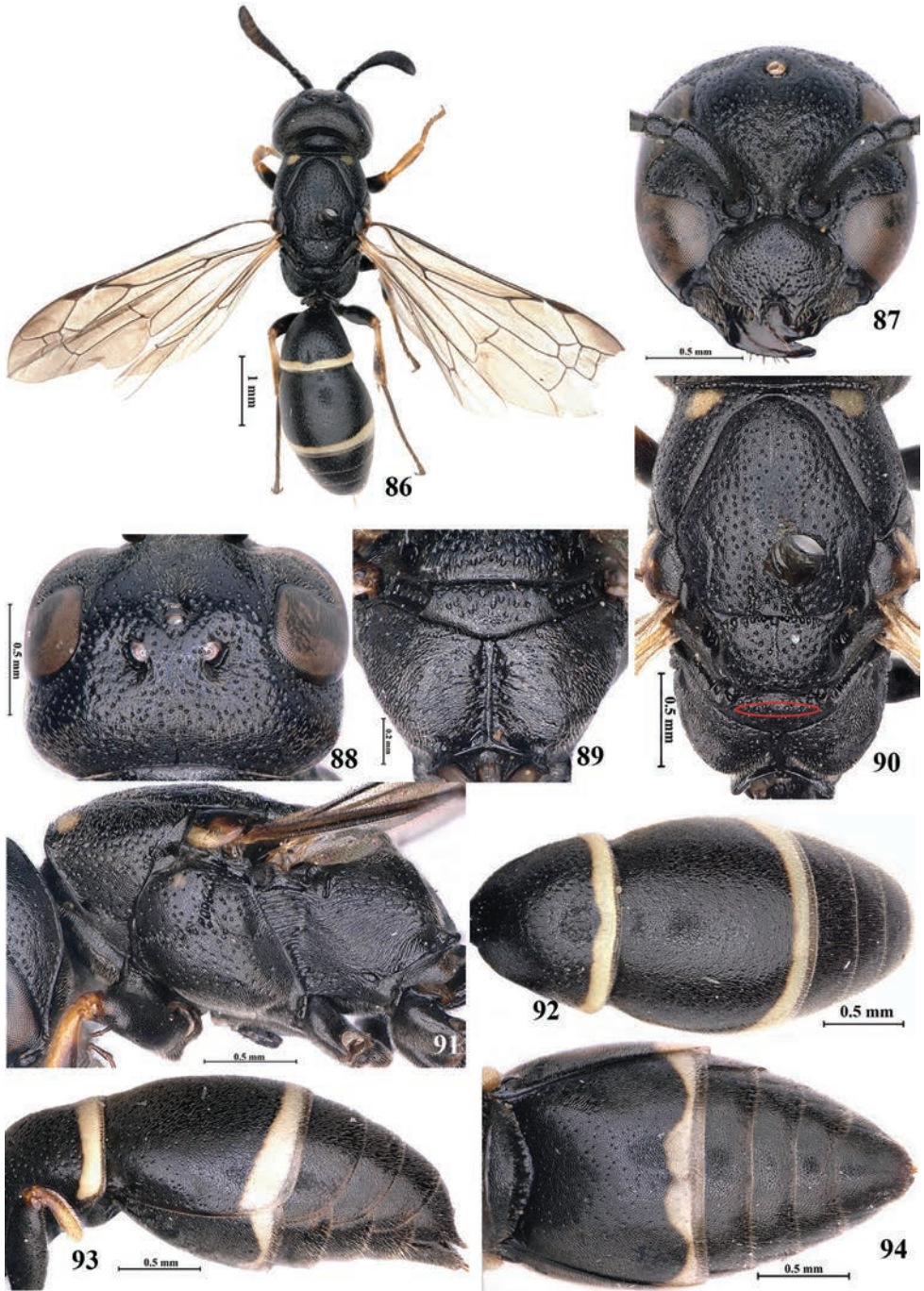
Odynerus parvulus Herrich-Schäffer, 1838: 19.

Odynerus helvetius de Saussure, 1855: pl. XIII fig. 6; 1856: 295; Berland 1928: 63, figs. 104–108.

Microdynerus bifidus Morawitz, 1885: 177; Kostylev 1929: 82.

Pseudomicrodynerus helvetius; Blüthgen, 1938 (1937): 276; 1938: 446; 1952: 353; 1961: 66, 93; van der Vecht and Fischer 1972: 37.

Microdynerus parvulus; Castro, 1997: 5; Gusenleitner 2008: 38.



Figures 86–94. *Microdynerus parvulus* (Herrich-Schäffer, 1838) ♀ **86** habitus in dorsal view **87** head in frontal view **88** vertex **89** propodeum in posterior view **90** mesosoma in dorsal view **91** mesosoma in lateral view **92** metasoma in dorsal view **93** metasoma in lateral view **94** metasoma in ventral view.

Material examined. 2♀♀, CHINA, Xinjiang, Changji Hui Autonomous Prefecture, Qinghe county, Qinghe town, Ale Township, Akelangke Village, 46.690°N, 90.369°E, 1256 m, 19.VII.2019, Qian Han (CNU).

Diagnosis. Body length 5.5–5.8 mm, forewing 5.4–5.5 mm (Fig. 86); interspaces between punctures leathery; black, with the following parts whitish yellow: whole clypeus in male, antenna ventrally in male, two anterior spots of pronotum dorsally (or not), outer margin of tegula, apical bands of both T1–T2 and S2, apical spot of S3 laterally (or not), part of tibiae; mandibular teeth ferruginous in male. Body with sparse and small punctures; in front view, head slightly subquadrate, two lateral margin almost parallel (Fig. 87), in dorsal view head thick, vertex prolonged (Fig. 88); mandible enlarged and angular, the outer edge curved (Fig. 87); clypeus punctate, interspaces between big punctures densely micropunctate, and sparser at apex, clypeus wider than long (1.3× in female), apically with deep U-styled emargination wider than depth (1.5× in female) (Fig. 87); interantennal carina at the same level as frons; in female A6–A12 thick and short, A13 in male wide and flat, backward reaching apical margin of A9; frons wide and swollen, with a medial longitudinal furrow from anterior-ocellus to base of interantennal carina; frons, vertex and gena with sparse and deep punctures, interspaces with extremely minute punctures (Fig. 88); occipital carina curved latero-ventrally (Fig. 91). Mesosoma with sparse and deep punctures, interspaces with extremely minute punctures (Fig. 90); sharp angle of pronotal carina at humeral angle, and pronotal carina posteriorly with a row of short longitudinal carinae; mesoscutum with two longitudinal furrows of punctures on posterior margin; anterior margin of scutellum with a row of dense punctures, and with a shallow longitudinal furrow in the middle; metanotum medially with transverse raised bulge (Fig. 90); propodeal furrow deep, propodeal carina in the furrow developed and complete (Fig. 89). Metasoma leathery, punctures smaller and shallower than those on head and mesosoma, punctures on T1 a little larger and deeper than the second metasomal segment, and those on metasomal segments 3–6 indistinct (Figs 7–9); in dorsal view, the first metasomal segment bell-shaped, the second one with narrow apical lamellae; S2 concave basally, and flat in lateral view (Fig. 94).

Distribution. China (new record: Xinjiang), England, France, Spain, Italy, Switzerland, Germany, Austria, Belarus, Ukraine, Russia.

Key to the Chinese species of the two genera *Leptochilus* de Saussure and *Microdynerus* Thomson

- 1 Mandible enlarged and angular in outer edge, head in frontal view subquadrate (Fig. 87); mesosoma prolonged, mesoscutum longer than wide (Fig. 90); propodeum with submarginal carina and vavula not projecting (Fig. 90) ***Microdynerus (Pseudomicrodynerus) parvulus (Herrich-Schäffer, 1838)***
- Mandible narrow and slightly curved in outer edge, head in frontal view rounded (Figs 2–3, 11, 19, 20); mesosoma shorter, mesoscutum about as long as wide; propodeum with submarginal carina and vavula projecting (Fig. 82) **2**

- 2 T1 long and bell-shaped (Fig. 79), longer than wide; the second metasomal segment with wide apical lamellae and with a row of great punctures at base, interspaces between punctures not carina-formed (Fig. 85).....
..... ***Leptochilus (Neoleptochilus) tibetanus* Giordani Soika, 1966**
- T1 short and semi-circular (Figs. 1, 10, 17, 18), wider than long; the second metasomal segment with wide and concave apical lamellae and with a row of great punctures at base of lamellae, interspaces between punctures carina-formed (Figs 8–9) **3**
- 3 The second metasomal segment with large and coarse punctures (Figs 69, 77)..... **4**
- The second metasomal segment with small and shallow punctures (Figs 8, 15, 25, 35, 54)..... **5**
- 4 Occipital carina developed and forming obvious angle latero-ventrally (Fig. 75); propodeum with short and curved carina between dorsal and posterior surfaces (Fig. 76); interspaces between apical punctures of the second metasomal segment with short carina-formed (Fig. 77).....
..... ***Leptochilus (Lionotulus) locuples* Giordani Soika, 1970**
- Occipital carina obviously curved latero-ventrally (Fig. 66); propodeum with developed carina between dorsal and posterior surfaces (Fig. 68); interspaces between apical punctures of the second metasomal segment with carina-formed extending almost to the top (Fig. 69).....
..... ***Leptochilus (Lionotulus) kozlovi* Kurzenko, 1977**
- 5 Ocelli large, almost as big as diameter of antennal socket (Fig. 11); body wholly finely and sparsely punctate, smooth, and with a large area of yellow markings (Fig. 10) ***Leptochilus (Lionotulus) argentifrons* (Kostylev, 1935)**
- Ocelli smaller than diameter of antennal socket (Figs 19, 20); body wholly coarsely punctate, leathery, and with a smaller area of yellow markings than the above **6**
- 6 Occipital carina obviously angle latero-ventrally (Figs 4, 24)..... **7**
- Occipital carina curved latero-ventrally (Figs 32, 51, 59) **8**
- 7 Pronotal carina transparent; propodeum with obvious carina between dorsal and posterior surfaces, propodeal carina half as long as propodeal concavity (Fig. 7)..... ***Leptochilus (Lionotulus) angulus* sp. nov.**
- Pronotal carina non-transparent; propodeum carina between dorsal and posterior surfaces longer than the above species, about 2/3 as long as the propodeal concavity (Fig. 23) ***Leptochilus (Lionotulus) callidus* (Kostylev, 1940)**
- 8 Clypeus apically with shallow and wide emargination; frons with dense setae on lower half (Fig. 60); male unknown
..... ***Leptochilus (Lionotulus) incertus* (Kostylev, 1940)**
- Apical emargination of clypeus deeper and narrower than the above; frons with sparse setae on lower half (Fig. 48); the first hind tarsus in male swollen (Figs 28, 44, 47) **9**

- 9 Female clypeus with minute and dense punctures basally, and with coarser and bigger punctures apically (Figs 29, 48); in lateral view, S2 of both sexes strongly convex basally (Figs 34, 54) **10**
- Female clypeus wholly with small and sparse punctures (Fig. 42); in lateral view, S2 of both sexes slightly convex basally (Fig. 44)
..... ***Leptochilus (Lionotulus) gobicus* (Kostylev, 1940)**
- 10 Propodeal concavity deep, propodeal carina less than half of propodeal concavity (Fig. 33); penis valve slightly narrow in the middle part, with depression at the top (Fig. 39)..... ***Leptochilus (Lionotulus) chinensis* Gusenleitner, 2001**
- Propodeal concavity shallow, propodeal carina more than half of propodeal concavity (Fig. 52); penis valve obvious narrow in the middle part, depression deeper than the above at the top (Fig. 57)
..... ***Leptochilus (Lionotulus) habyriganus* Kurzenko, 1977**



Figure 95. A distribution map of all known species of these two genera *Leptochilus* and *Microdynerus* in China.

Acknowledgements

We are very grateful to Dr. Alexander V. Fateryga (Branch of the Kovalevsky Institute of Biology of the Southern Seas of RAS, Feodosiya, Russia) for helping us to take photos of type specimens deposited in the Zoological Institute in St. Petersburg. We are also grateful to Prof. James M. Carpenter (American Museum of Natural History, New York, USA), Marco Selis (Viterbo, Italy) and another anonymous reviewer

for providing their important comments on this study. And we sincerely thank Dr. Zhaohui Luo (Xinjiang Institute of Ecology and Geography, Chinese Academy of Sciences, Urumqi, China) for providing us with the specimens deposited in the insect collections under her care. This study was funded by Science & Technology Fundamental Resources Investigation Program (Grant No. 2022FY202100) and the National Natural Science Foundation of China (Nos: 31772490, 31372247, 31000976).

References

- Arens W (2001) The female of *Leptochilus aegineticus* Gusenleitner, 1970, hitherto incorrectly known as *Microdynerus globosus* Gusenleitner, 1997 (Hymenoptera, Eumenidae). Linzer Biologische Beiträge 33(1): 257–261.
- Berland L (1928) Faune de France 19. Hymenopteres vespiformes. II. (Eumenidae, Vespidae, Masaridae, Bethyliidae, Dryinidae, Embolemidae). Faune France 19: [viii +] 208.
- Blüthgen P (1938) [1937] Systematisches Verzeichnis der Faltenwespen Mitteleuropas, Skandinaviens und Englands. Konowia, Vienna 16: 270–295.
- Blüthgen P (1938) Beiträge zur Kenntnis der paläarktischen Eumeniden (Hymenoptera, Vespidae). Deutsche Entomologische Zeitschrift 1938: 434–496. <https://doi.org/10.1002/mmnd.193819380208>
- Blüthgen P (1943) Taxonomische und biologische Notizen über paläarktische Faltenwespen (Hymenoptera, Vespidae). Stettiner Entomologische Zeitung 104: 149–158.
- Blüthgen P (1952) Eränzungen zur Faltenwespenfauna der Schweiz. Mitteilungen der Schweizerischen Entomologischen Gesellschaft 25: 349–353.
- Blüthgen P (1953) Portuguese and Spanish wasps (Hymenoptera, Vespoidea). Memórias e Estudos do Museu Zoológico da Universidade de Coimbra 218: 1–23.
- Blüthgen P (1955) New Diploptera from Israel and the Near East. I. Bulletin of the Research Council of Israel 5B: 24–31.
- Blüthgen P (1961) Die Faltenwespen Mitteleuropas (Hymenoptera, Diploptera). Abhandlungen der Deutschen Akademie der Wissenschaften zu Berlin. Klasse für Chemie, Geologie und Biologie (2): 1–252. <https://doi.org/10.1515/9783112537084>
- Blüthgen P (1967) Faltenwespen aus Bulgarien (Hymenoptera, Diploptera). Bulletin de l'Institut de Zoologie et Muséum 23: 229–234.
- Carpenter JM (1981) [1982] The phylogenetic relationships and natural classification of the Vespoidea (Hymenoptera). Systematic Entomology 7: 11–38. <https://doi.org/10.1111/j.1365-3113.1982.tb00124.x>
- Carpenter JM (1986) A synonymic generic checklist of the Eumeninae (Hymenoptera: Vespidae). Psyche (Cambridge) 93(1–2): 61–90. <https://doi.org/10.1155/1986/12489>
- Castro L (1997) Insecta: Hymenoptera. Fam. 3a: Vespidae: Eumeninae. Catalogus de la Entomofauna Aragonesa 16: 3–8.
- de Saussure H (1852–1853) Etudes sur la famille des Vespides. 1. Monographie des guepes solitaires ou de la tribu des Eumeniens, comprenant la classification et la description de toutes

- les especes connues jusqu'a ce jour, et servant de complement au manuel de Lepeletier de Saint-Fargeau. Masson & Cherbuliez, Paris & Geneva, [lii +] 286 pp.
- de Saussure H (1854–1856) Études sur la Famille des Vespides 3. Geneva & Paris, 352 pp.
- Fateryga AV (2018) First data on the bionomics of the solitary wasp *Leptochilus membranaceus* (Morawitz) (Hymenoptera, Vespidae: Eumeninae). Entomological Review 98(3): 283–289. <https://doi.org/10.1134/S0013873818030053>
- Fateryga AV, Fateryga VV (2021) A further study of the nesting biology of *Leptochilus* (*Neoleptochilus*) *regulus* (de Saussure, 1855) (Hymenoptera, Vespidae, Eumeninae). Journal of Hymenoptera Research 84: 75–86.
- Herrich-Schäffer GAW (1838) Fauna Insectorum Germaniae initia, oder, Deutschlands Insects 154: 19. [pl 19]
- Kostylev G (1929) Materialien zur Kenntnis der Vespidenfauna Armeniens. Rev. russe Entomol, Leningrad 23: 76–82.
- Kostylev G (1935) [1934] Neue und wenig bekannte mittelasiatische Wespidenarten (Hym.). In Russian with German descriptions. Archive of the Zoological Museum of Moscow State University 1: 117–146.
- Kostylev G (1940) Espèces nouvelles et peu connues de Vespides, d'Euménides et de Masarides paléarctiques (Hymenoptera). II. Bulletin de la Société des naturalistes de Moscou, Section biologique (N.S.) 49: 24–42.
- Kurzenko NV (1977) Eumenid wasps (Hymenoptera, Eumenidae) of the Mongolian People's Republic and adjacent regions of China and southern Siberia. Insects of Mongolia 5: 537–582.
- Giordani Soika A (1938) Diagnosi di nuovi Eumenini mediterranei. Bollettino della Societa Veneziana di Storia Naturale, Venice 2: 2–14.
- Giordani Soika A (1941) Diagnosi di nuovi *Leptochilus* dell'Africa minore (Hymenotera, Vespidae). Bollettino della Società Entomologica Italiana. Florence, Genoa 78: 7–13.
- Giordani Soika A (1953) Hyménoptères récoltés par une mission Suisse au Maroc (1947). Eumeninae. Bulletin de la Société des Sciences Naturelles du Maroc, Rabat 32: 235–267.
- Giordani Soika A (1966) Eumenidi raccolti dalla spedizione Schaefer nel Tibet meridionale e Sikkim. Bollettino del Museo Civico di Storia Naturale di Venezia 17: 97–112.
- Giordani Soika A (1970) Missione Giordani Soika in Iran 1965, III. Contributo Alla Conoscenza Degli Eumenidi Del Medio Oriente. Parte I- Sistematica. Bollettino del Museo Civico di Storia Naturale di Venezia 20/21: 27–183.
- Giordani Soika A (1979) Eumenidi raccolti nell'Arabia meridionale da K. Guichard. Bollettino del Museo Civico di Storia Naturale di Venezia 30: 271–285.
- Giordani Soika A (1986) Eumenidi Paleartici nuovi o poco noti. Bollettino del Museo Civico di Storia Naturale di Venezia 35: 91–162.
- Gusenleitner J (1970) Notes on some new Eumenidae from Israel (Hymenoptera, Vespoidea). Israel Journal of Entomology 5: 55–61.
- Gusenleitner J (1973) Bemerkenswertes Ober Faltenwespen 5. (Diploptera, Hymenoptera). Nachrichtenblatt der Bayerischen Entomologen 22(6): 118–120.
- Gusenleitner J (1976) Bemerkenswertes uber Faltenwespen 6. (Diploptera, Hymenoptera). Nachrichtenblatt der Bayerischen Entomologen 25(6): 112–119.

- Gusenleitner J (1977) Neue *Leptochilus*-Arten aus Anatolien und Nordafrika. Linzer Biologische Beiträge 9(1): 163–178.
- Gusenleitner J (1979) Die Arten der Untergattung *Neoleptochilus* Bluthgen, 1961 auf der Iberischen Halbinsel (Eumenidae, Hym.). Linzer Biologische Beiträge 11(1): 95–103.
- Gusenleitner J (1985) Neue *Leptochilus*-Arten aus dem Mittelmeergebiet und dem Iran (Hymenoptera, Eumenidae). Entomofauna 6: 81–101.
- Gusenleitner J (1993) Bestimmungstabellen mittel- und südeuropäischer Eumeniden (Vespoidea, Hymenoptera) Teil 1: Die Gattung *Leptochilus* Saussure 1852. Linzer Biologische Beiträge 25(2): 745–769.
- Gusenleitner J (1995) Bemerkungen über die gattung *Leptochilus* Saussure 1852 und Beschreibung neuer Arten dieser Gattung. (Hymenoptera, Vespoidea, Eumenidae). Linzer Biologische Beiträge 27(1): 169–181.
- Gusenleitner J (1997) Bestimmungstabellen mittel- und südeuropäischer Eumeniden (Vespoidea, Hymenoptera) Teil 7: Die Gattungen *Microdynerus* Thomson 174 und *Eumicrodynerus* Gusenleitner 1972. Linzer Biologische Beiträge 29(2): 779–797.
- Gusenleitner J (2001) A new *Leptochilus* species from China (Hymenoptera: Eumenidae). Linzer Biologische Beiträge 33(1): 239–241.
- Gusenleitner J (2002) New or notable Vespoidea from the Near East (Hymenoptera: Eumenidae, Masaridae). Linzer Biologische Beiträge 34(1): 335–343.
- Gusenleitner J (2006) Eumeninae collected in Pakistan. Linzer Biologische Beiträge 38(2): 1295–1305.
- Gusenleitner J (2008) Vespidae (Insecta: Hymenoptera). In: Schuster, R. (Hrsg.), Biosystematics and Ecology Series No. 24. Checklisten der Fauna Österreichs 3: 31–40.
- Gusenleitner J (2017) Über bemerkenswerte Faltenwespen aus der äthiopischen Region. Teil 11 (Hymenoptera, Vespidae: Eumeninae). Linzer Biologische Beiträge 49(2): 1147–1155.
- Morawitz F (1885) Eumenidarum species novae. Horae Societatis Entomologicae Rossicae. Rossicae 19: 135–181.
- Parker FD (1966) A revision of the North American species in the genus *Leptochilus* (Hymenoptera: Eumenidae). Miscellaneous publications of the Entomological Society of America 5: 153–229. <https://doi.org/10.4182/ASHC3002.5-4.153>
- Selis M (2023) Illustrated key to the genera and a checklist of Italian Vespidae (Hymenoptera). Fragmenta Entomologica 55(1): 63–88.
- Thomson CG (1874) *Vespa* Linn., Hymenoptera Scandinaviae 3: 1–94.
- van der Vecht J, Fischer FCJ (1972) Hymenopterorum Catalogus. Pars 8. Palaearctic Eumenidae. Hymenopterorum Catalogus 8: 1–199.

Erimerinae, a prior name to Microdontomerinae (Hymenoptera, Torymidae) with the description of a new genus and three new species from Iran

Hossein Lotfalizadeh¹, Zohreh Mirzaee^{2,3}, Gholamreza Tavakoli-Korghond⁴,
Petr Janšta^{5,6}, Jean-Yves Rasplus⁷

1 Insect Taxonomy Research Department, Iranian Research Institute of Plant Protection (IRIPP), AREEO, Tehran, Iran **2** Biology Department, Faculty of Sciences, Shiraz University, Shiraz, Iran **3** Senckenberg German Entomological Institute, Eberswalder Str. 90, 15374 Müncheberg, Germany **4** Department of Plant Protection, South-Khorasan, Agricultural and Natural Resources Research & Education Center, AREEO, Birjand, Iran **5** Department of Zoology, Faculty of Science, Charles University, Prague, Czech Republic **6** Department of Entomology, State Museum of Natural History Stuttgart, Stuttgart, Germany **7** CBGP, University of Montpellier, CIRAD, INRA, IRD, Montpellier SupAgro, Montpellier, France

Corresponding author: Hossein Lotfalizadeh (hlotfalizadeh@gmail.com)

Academic editor: Ankita Gupta | Received 1 November 2023 | Accepted 27 January 2024 | Published 21 February 2024

<https://zoobank.org/827B35CC-A116-4EBA-AB13-19C72EBC0D34>

Citation: Lotfalizadeh H, Mirzaee Z, Tavakoli-Korghond G, Janšta P, Rasplus J-Y (2024) Erimerinae, a prior name to Microdontomerinae (Hymenoptera, Torymidae) with the description of a new genus and three new species from Iran. Journal of Hymenoptera Research 97: 85–103. <https://doi.org/10.3897/jhr.97.115028>

Abstract

Erimerinae has been proposed as a subfamily group name prior to Microdontomerinae and the latter was considered as a junior synonym of Erimerinae. A new genus, *Perserimerus* Lotfalizadeh & Rasplus, **gen. nov.**, and three new species, *Perserimerus marginalis* Lotfalizadeh & Rasplus, **sp. nov.**, *Microdontomerus iriphagus* Lotfalizadeh & Janšta, **sp. nov.**, and *M. quadrimaculatus* Lotfalizadeh & Rasplus, **sp. nov.**, are described from Iran. Diagnostic characters of the new genus and newly described species are provided and compared with morphologically similar genera and species. *Microdontomerus iriphagus* and *M. quadrimaculatus* were reared from oothecae of *Iris oratoria* (Linnaeus, 1785) (Mantodea) and galls of *Stefaniola similata* Mamaev, 1972 (Diptera: Cecidomyiidae) on *Haloxylon ammodendron* C.A. Mey, respectively. A key to the known species of *Microdontomerus* of Iran is provided.

Keywords

Galls, *Haloxylon*, Mantid egg cases, Microdontomerinae, new genus, new species, parasitoid

Introduction

The family Torymidae consists of six subfamilies including Erimerinae (Crawford, 1914; Microdontomerinae sensu Janšta et al., 2018; for synonymy details see Results). Erimerinae have a broad range of hosts spanning primary parasitoids of various life stages of gall-maker insects (mostly Hymenoptera and Diptera), several Lepidoptera, Coleoptera, Apoidea, and also of Mantodea (Grissell 1995; Janšta et al. 2016, 2018). They are also known as hyperparasitoids of Lepidoptera and Coleoptera larvae (Janšta et al. 2016). One species, *Microdontomerus anthonomi* (Crawford), has been reported to have negative effect on biocontrol agent of *Bangasternus orientalis* (Capiomont) (Coleoptera: Curculionidae) and *Urophora affinis* Fraunfeld (Diptera: Tephritidae) introduced to the U.S. from Europe for biological control program against spotted knapweed (*Centaurea stoebe* L.) and diffuse knapweed (*C. diffusa* Lam.) (Turner et al. 1990).

The genus *Microdontomerus* Crawford, 1907 includes seven species in the Palaearctic region (Table 1). Only two species, *M. albipes* (Giraud, 1870) and *M. annulatus* (Spinola, 1808), have been reported from Iran so far (Lotfalizadeh and Gharali 2005; Fallahzadeh et al. 2009; Nazemi Rafie and Lotfalizadeh 2012). This genus appears more diverse in the Nearctic region where it includes 19 species (Grissell 2005; Janšta et al. 2016).

During our recent collections in different regions of Iran we have been discovered some taxa that do not correspond with the known genera and species of the subfamily Erimerinae. These include one new genus with remarkable morphological characters and two interesting *Microdontomerus* species reared from two different hosts. These three new taxa are described in the presented paper.

Materials and methods

Examined specimens were either reared from hosts (oothecae of Mantodea, galls of Cecidomyiidae, Diptera) or collected by Malaise trap from Sistan & Balauchestan, Isfahan, Khuzestan and South-Khorasan provinces during 2015–2019.

Table 1. Species of *Microdontomerus* known in the Palaearctic region (Picard 1930; Steffan 1967; Janšta et al. 2016; Doğanlar 2016; Noyes 2019).

Species	Hosts	References
<i>M. albipes</i> (Giraud, 1870)	Lepidoptera: Gelechiidae	Noyes (2019)
<i>M. altinekinesis</i> Doğanlar, 2016	Unknown	Doğanlar (2016)
<i>M. annulatus</i> (Spinola, 1808)	Diptera: Cecidomyiidae and Tephritidae; Hymenoptera: Cynipidae; Lepidoptera: Tortricidae	Noyes (2019)
<i>M. direklinensis</i> Doğanlar, 2016	Unknown	Doğanlar (2016)
<i>M. gurcukoyensis</i> Doğanlar, 2016	Unknown	Doğanlar (2016)
<i>M. iridis</i> (Picard, 1930)	Mantodea: Mantidae	Picard (1930), Janšta et al. (2016)
<i>M. ovivorus</i> (Steffan, 1967)	Coleoptera: Buprestidae	Steffan (1967)

Altogether, we examined 72 specimens (48 females and 24 males), all were card mounted. Identifications were realized using Grissell (2005), Doğanlar (2016) and Janšta et al. (2016). Harris (1979) was followed for the terminology of sculpture. Examination of the external morphology of dry-mounted specimens was done using a Leica M205C research stereomicroscope with a maximum magnification of 180×. External morphology was illustrated using a Keyence VHX-5000 digital microscope. Artifacts removal, background standardization and plate assembling were done in Photoshop CS4. Specimens examined during this study are deposited in the following collections:

- CBGP** Centre de Biologie pour la Gestion des Populations, Montferrier-sur-Lez, France.
HMIM Hayk Mirzayans Insect Museum, Iranian Research Institute of Plant Protection, Tehran, Iran.
SMNS State Museum of Natural History Stuttgart, Germany.

Morphological terminology follows Gibson et al. (1997) and Janšta et al. (2016). All measurements were made with special reference to the correct orientation following Janšta et al. (2016). Abbreviations of used morphological characters are:

anl₁–anl₃	anellus 1–3;
clv₁–clv₃	clavomere 1–3;
fu₁–fu₆	funicular 1–6;
Gt₁–Gt₆	gastral tergite 1–6;
LOL (lateral ocellar line)	minimum distance between the anterior and a posterior ocellus;
MPS	multiporous plate sensilla;
mv	marginal vein;
OI (ovipositor index)	ratio of ovipositor length to length of metatibia;
OOL (ocello-ocular line)	distance between the posterior ocellus and the eye;
pmv	postmarginal vein;
POL	distance between posterior ocelli;
st	stigma;
stv	stigmatal vein;
tsc	terminal spine.

Results

Nomenclatory remarks

The following described genus and all species belong to the subfamily Erimerinae (Hymenoptera: Torymidae). Erimerinae was described by Crawford (1914). Later, Grissell (1995) recognized the subfamily just as a clade in the tribe Microdontomerini. Subsequently, Janšta et al. (2018) reclassified Microdontomerini *sensu* Grissell (1995) as the

subfamily Microdontomerinae. However, as *Erimerus* is the type genus of the subfamily group name Erimerinae (Crawford, 1914) and Erimerinae has been proposed as a subfamily group name prior to Microdontomerinae, we treat Microdontomerinae as a junior synonym of Erimerinae.

Descriptions

Perserimerus Lotfalizadeh & Rasplus, gen. nov.

<https://zoobank.org/05F35775-6A17-4495-9273-BC832B8DD566>

Figs 1, 2

Type species. *Perserimerus marginalis* Lotfalizadeh & Rasplus, sp. nov., by present designation.

Etymology. The generic name is composed of the Latin prefix “*Pers*”, referring to the old name of Iran (Persia) and the genus “*Erimerus*”. Masculine gender.

Description. Body metallic green, laterally with cooery to dark blue-violet (Fig. 1A), dorsally with cooery reflection (Fig. 1B). Head and mesosoma finely reticulate, metasoma alutaceous. Head 1.36× as broad as high; 1.88× as broad as long. Occipital carina not developed. Anterior margin of clypeus nearly straight. Scrobes bare and finely sculptured relative to the rest of face. Toruli inserted above the ventral level of eye. OOL about 0.56× as long as LOL. POL about 3× as long as OOL. Antenna (Fig. 2A) with scape not reaching anterior ocellus; flagellum with three anelli and five funiculars, all funiculars transverse. Clava four segmented with fourth segment forming distinct terminal spine (Fig. 2A, C; tsc). Pronotum forming a collar. Mesonotum 1.27× as long as broad. Notauli complete. Propodeum with delicate reticulate sculpture, without median carina. Fore wing (Fig. 1A) bare in basal half with speculum reaching stigmal vein; marginal vein 1.8× as long as postmarginal vein and 4.5× as long as stigmal vein; marginal and postmarginal veins distinctly triangularly enlarged, marginal vein about 2.6× as long as its broadest part (Fig. 2B); stigmal vein very short and stigmal uncus nearly closes to postmarginal vein. Hind femur simple, without subapical tooth; hind tibia with one apical spur. Metasoma sessile, with short petiole; tip of hypopygium almost reaching two-thirds of metasoma (Fig. 1A); Gt_1 – Gt_6 not incised medially. Ovipositor 0.31× as long as gaster. OI 0.79.

In the key to genera of Toryminae by Grissell (1995), the new genus run to the Afrotropical and Australian genus *Echthrodape* Burks (couplet 30) by having marginal and postmarginal vein conspicuously thickened relative to submarginal vein (marginal and postmarginal veins distinctly triangularly enlarged, 2.25× and 2.6× as long as broad, respectively). However, *Perserimerus*, gen. nov., clearly differs from *Echthrodape* by the presence of three anelli, a well-developed terminal spine on clava, the absence of occipital carina, the marginal vein reaching margin of wing and malar space not longer than the breadth of oral fossa. Further, *Echthrodape* exhibits uniformly widened marginal and postmarginal veins (Grissell 1995; figs 374–375), while in *Perserimerus*, gen. nov., marginal and postmarginal veins are triangularly thickened (Fig. 2B).

Persemerus, gen. nov., is similar to *Erimerus* as for both genera the reduction of a few apical flagellar segments to anelli, clava with terminal spine and hind tibia with only one spur are characteristic. However, none of the *Erimerus* species has marginal and postmarginal vein widened throughout. Furthermore, *Erimerus* has body including metasoma densely reticulated and hence dull and not shiny.

Host association. Unknown.

***Persemerus marginalis* Lotfalizadeh & Rasplus, sp. nov.**

<https://zoobank.org/E3E12CA8-9EDB-4B2C-8185-5EFAFF267471>

Figs 1, 2

Material examined. Holotype: IRAN • ♀; Sistan & Bluchestan province, near to Hamun Lake, 30.iv.2015, sweeping net on *Tamarix*, E. Rakhshani leg. (deposited in HMIM).

Etymology. The species name refers to the unique shape of the marginal and post-marginal veins.

Description. Female (Fig. 1A): Body length including ovipositor 1.24 mm; length of ovipositor 0.18 mm.

Colour. Head, mesosoma, metasoma and all coxae metallic green, dorsally with coppery, laterally with coppery to dark blue violet reflection (Fig. 1A). Pedicel brown with metallic reflection. Scape, tegula, all femora distally, entire fore- and mesotibia, metatibia apically and distally, tarsi and wing venation pale yellow. Flagellum dark brown with apical part of clava bright brown to yellow, pro- and mesofemur and metatibia medially brown. Metafemur dark with metallic reflection. Fore wing hyaline, setae brown.

Head. Head 1.36× as broad as high; 1.88× as broad as long; 1.12× as broad as mesonotum at its widest part in dorsal view. Temple short, strongly converging, 0.23× as long as eye. Eyes separated by 1.06× their own height, eye 1.78× as high as long. Head with fine reticulate sculpture with thin, short, pale setae on face, vertex and temple; scrobes more finely reticulate, without setae. Clypeus with anterior margin nearly straight; ventral part of clypeus smooth. Malar space 0.41× as long as eye height. Occipital carina absent (Fig. 1B). POL 3× OOL, OOL 0.56× LOL.

Antenna (Fig. 2A). Scape 5.38× as long as broad, not reaching ventral margin of anterior ocellus; pedicel 1.25× as long as broad; toruli inserted slightly above ventral level of eye. Combined length of pedicel and flagellum shorter than breadth of head (0.78× as long as breadth of head). Flagellum with three ring-like anelli, distinctly wider than long; first anellus (an₁) smaller, other gradually larger toward third one; remaining flagellomeres distinctly transverse, with Fu₁ 1.66× as broad as long, as wide as pedicel; fu₂–fu₅ of about same dimensions, 2.00–2.33× as broad as long, bearing only one row of MPS; clava 2× longer than broad, with three clavomeres (clv₁–clv₃) and terminal spine; antennal formula 1,1,3,5,3 (Fig. 2A).

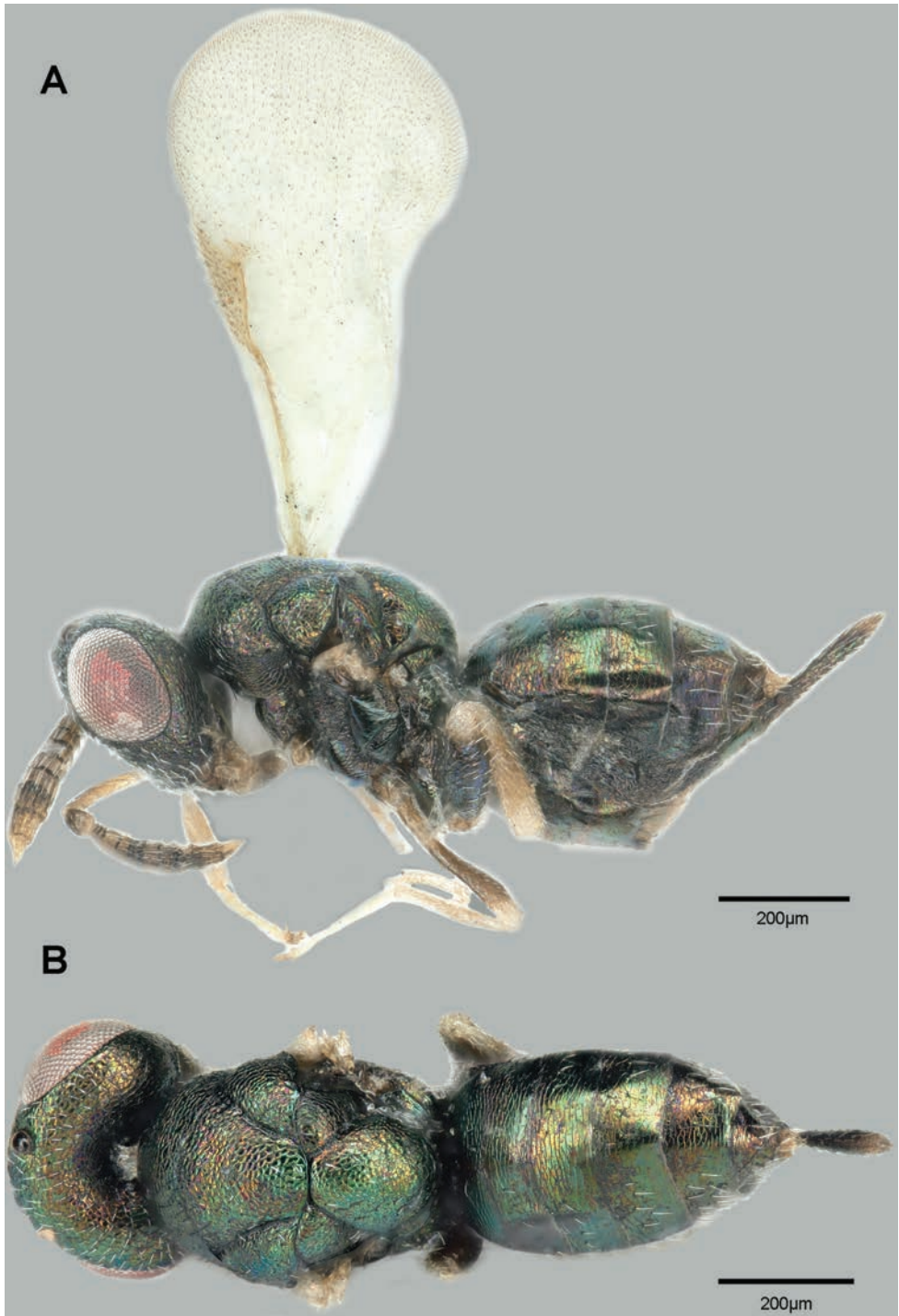


Figure 1. *Perseimerus marginalis*, female holotype **A** habitus, lateral view **B** habitus, dorsal view.

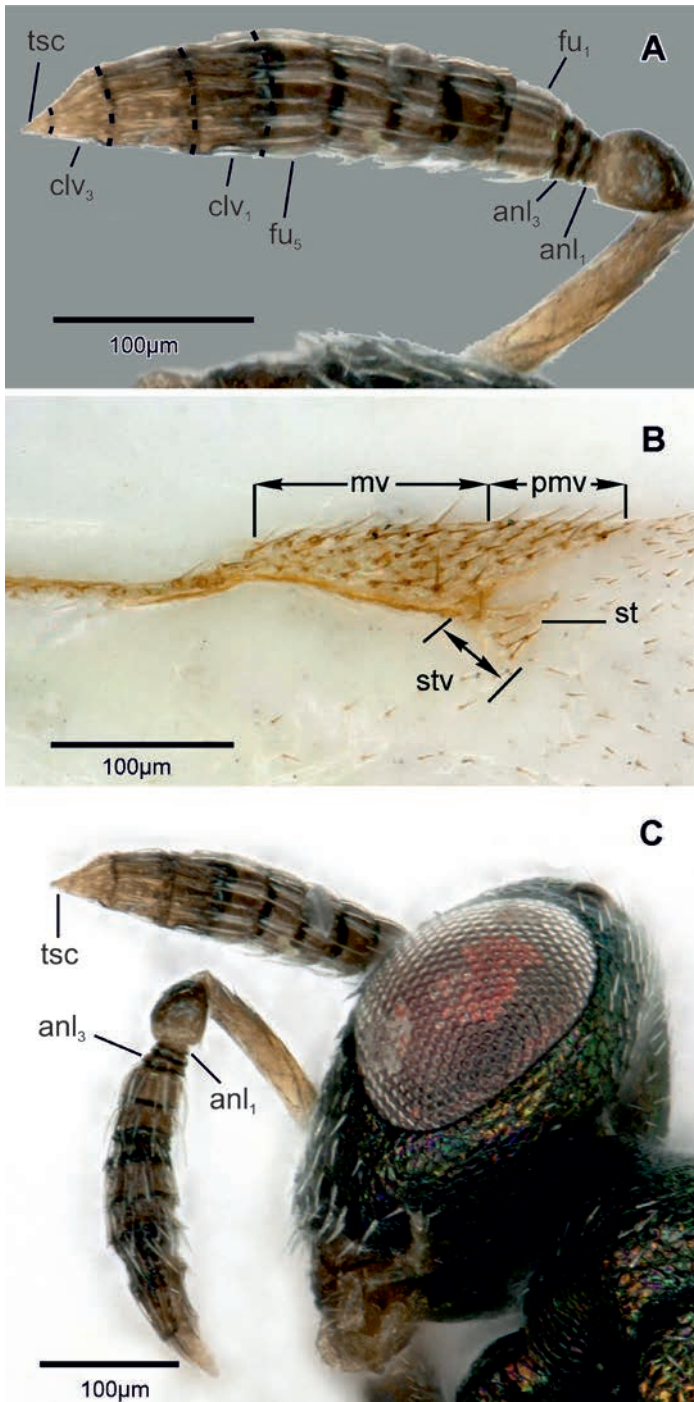


Figure 2. *Perseimeris marginalis*, female holotype **A** antenna, lateral view **B** fore wing, venation **C** head, lateral view (anl_{1,3} – anellus 1, 3; clv_{1,3} – clavomere 1, 3; fu_{1,5} – funicular 1, 5; mv – marginal vein; pmv – postmarginal vein; st – stigma; stv – stigmatal vein; tsc – terminal spine).

Mesosoma (Fig. 1A, B). Mesosoma 1.35× as long as broad. Pronotum 0.82× as broad as mesoscutum. Pronotum and mesoscutum entirely reticulate, and covered with thin, short, pale setae. Notauli complete, distinct and not obliterated by sculpture. Mesoscutellum 1.11× as long as broad, without frenal area, broadly abutting mesoscutum and separating axillae. Mesoscutellum and axilla more sparsely covered with setae. Hind leg with coxa 1.85× as long as broad, alutaceous, with sparse setae dorsally and ventrally; metafemur 3.8× as long as broad, simple, without subapical tooth; metatibia 4.25× as long as broad, with one apical spur. Fore wing 1.94× as long as wide, hyaline, with dense brown setae on distal half; speculum broad and reach below marginal vein; costal cell bare; marginal vein 1.8× as long as postmarginal vein and 4.5× as long as stigmal vein; marginal and postmarginal veins distinctly triangularly enlarged, 2.25× and 2.6× as long as broad, respectively; stigmal vein very short and stigma nearly closes to marginal and postmarginal veins (Fig. 2B).

Metasoma (Figs 1A, B) excluding ovipositor 1.14× as long as mesosoma. Petiole very short. Gaster with shallow alutaceous sculpture; Gt_1 – Gt_6 not incised medially; tip of hypopygium almost reaching two-third of gaster; ovipositor short, 0.31× as long as gaster. OI 0.79.

Male. Unknown.

Distribution. Palearctic: Iran.

Biological association. This species was swept on *Tamarix* and could be parasitoid of associates of this shrub, such as gall-makers or other phytophages.

***Microdontomerus iriphagus* Lotfalizadeh & Janšta, sp. nov.**

<https://zoobank.org/D5CE0234-A11D-47EE-AE9D-DB41A04A2F98>

Figs 3–5

Material examined. Holotype: IRAN • ♀; Isfahan province, Tiran-Daran Highway (32°42'36"N, 51°11'07"E), ex *Iris oratoria* oothecae, Z. Mirzaee (deposited in HMIM). **Paratypes:** IRAN • same as holotype (23♀♀, 1♂♂, HMIM; 1♀, 1♂, SMNS; 1♀, CBGP); Khuzestan province, Deh-dez (31°44'37"N, 50°11'52"E), ex *I. oratoria* oothecae (19♀♀, 5♂♂), Z. Mirzaee (HMIM).

Etymology. The species name refers to the mantid host.

Diagnosis. Head almost circular in frontal view, about 1.13× as broad as high (Fig. 4C); 2.14× as broad as long. Anterior margin of clypeus straight and recessed relative to oral margin. Scrobes bare and finely sculptured relative to the rest of face. Toruli inserted above ventral level of eye. OOL about 0.85× as long as LOL. POL about 2.82× as long as OOL (Fig. 5B). Antenna in female with scape not reaching anterior ocellus; flagellum with one anellus and seven funicular segments, all funicular segments transverse (Fig. 4A). Pronotum and mesoscutum reticulate, mesoscutellum coriaceous and less sculptured in contrast to aforementioned (Fig. 5B). Fore wing (Fig. 5C) with speculum reaching end of marginal vein; costal cell dorsally with 1–2 rows of setae along anterior margin, cubital cell without setae and basal cell at most with few setae

along anterior margin; basal and cubital line of setae complete; marginal vein less than $2\times$ as long as postmarginal vein and more than $2.5\times$ as long as stigmal vein. All tarsi slightly longer than tibiae, metafemur simple, without any tooth. Metasoma with hypopygium reaching near to end of gaster (Fig. 3A); Gt_1 incised medially, Gt_2 – Gt_3 distinctly emarginate medially, Gt_4 – Gt_5 slightly emarginated (Fig. 5D). Ovipositor about $0.65\times$ as long as body; OI 2.3.

Comments. *Microdontomerus iriphagus*, sp. nov., was reared from oothecae of *Iris oratoria* (Linnaeus, 1785) (Mantodea) in 2018–2019 and has already been reported as *Microdontomerus* sp. by Mirzaee et al. (2021). It is similar to *M. iridis*, but *M. iriphagus* possesses one anellus while *M. iridis* has two anelli Fig. 4A, B; also *M. iriphagus* differs from *M. iridis* in having brownish-yellow metasoma with a pair of oval pale-yellow spots on all tergites (Fig. 5D) (entirely metallic in *M. iridis*), yellowish legs (Fig. 3A) (at least metallic coxae in *M. iridis*), pale scape (Fig. 4A) (dark-brown in *M. iridis*). *Microdontomerus iriphagus* has also shorter ovipositor with OI about 2.3 (OI-2.5 to 2.9 in *M. iridis*) and OOL only about $0.85\times$ LOL (about the same in *M. iridis*).

Microdontomerus iriphagus, sp. nov., is similar to *M. gurcukoyensis* Doğanlar, 2016 in having yellowish antennae and legs but these species can be easily separated by the coloration of their metasoma (brownish and yellowish basally in *M. gurcukoyensis*); the scape yellowish and the metallic flagellomeres (yellowish in *M. gurcukoyensis*), with whitish-yellow fore coxa (concolorous with body in *M. gurcukoyensis*). The ovipositor of *M. iriphagus* is also slightly longer with an OI about 2.3, while *M. gurcukoyensis* has an OI=1.66 (Doğanlar 2016).

Description. Female (Fig. 3A): Body length excluding ovipositor 2.10 mm (including ovipositor 3.50 mm [3.2–4.4 mm]); length of ovipositor 1.40 mm.

Colour. Head, mesosoma, meso- and metacoxa metallic green (except distal part); metasoma brownish-yellow laterally, pale-yellow dorsally on all tergites, with pair of dark brown spots dorsolaterally on each tergite. Spots connecting medially on Gt_1 and G_{16-7} (Fig. 5D). Scape, tegula, legs (except most of meso- and metacoxa and metafemur) pale yellow. Tarsomeres brownish distally. Metafemur rightly brown yellow. Distal part of scape brown with slight metallic reflection, pedicel black with distinct metallic reflection, flagellum dark brown; ovipositor brownish yellow, ovipositor sheath dark brown. Fore wing hyaline, wing venation yellowish-brown, setae dark-brown.

Head. Head $1.13\times$ as broad as high (Fig. 4C); $2.14\times$ as broad as long in dorsal view and $1.83\times$ in lateral view (Fig. 5A); $1.10\times$ as broad as mesonotum at its widest part in dorsal view. Without occipital carina. Temple short, strongly converging, $0.3\times$ as long as eye. Eyes separated by $1.17\times$ their own height, eye $1.45\times$ as high as long. Head reticulate with thin, short, silvery setae on face; scrobes more finely reticulate, without setae. Torulus separated by $1\times$ their own diameter; clypeus with anterior margin nearly straight and recessed relative to corners of oral fossa; ventral part of clypeus finely reticulate. Malar space $0.5\times$ as long as eye height. POL $2.82\times$ OOL, OOL $0.85\times$ LOL (Fig. 5B).

Antenna (Fig. 4A). Scape $3.2\times$ as long as broad and pedicel about as long as broad, the former not reaching ventral margin of anterior ocellus; torulus inserted above ventral level of eye. Combined length of pedicel and flagellum as long as breadth of head.

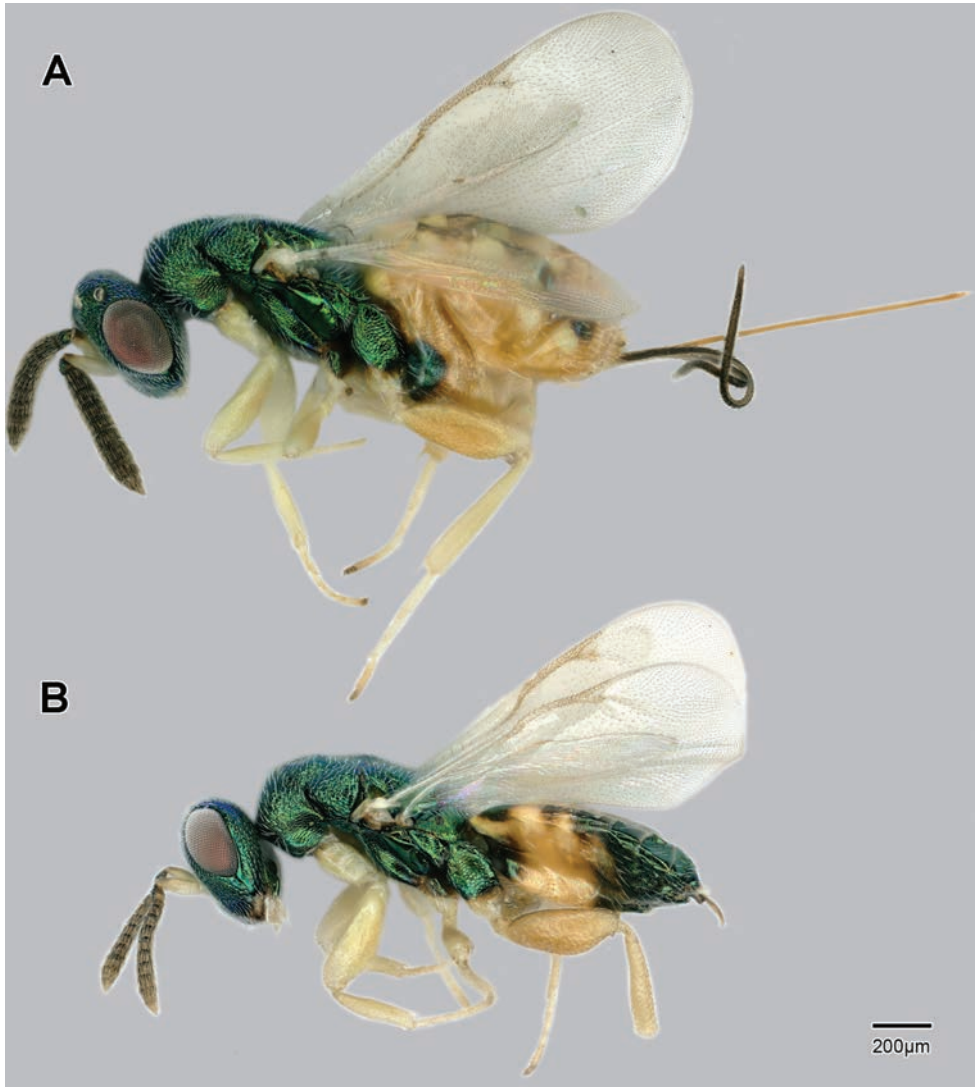


Figure 3. *Microdontomerus iriphagus* **A** female habitus, lateral view **B** male habitus, lateral view.

Flagellum with one anellus; all flagellomeres distinctly transverse, with fu_1 the smallest, $0.71\times$ as long as broad, $1.4\times$ as wide as pedicel, and bearing only few MPS; fu_2 – fu_6 of about same dimensions, $0.55\times$ as long as broad.

Mesosoma (Figs 5A, B) $1.31\times$ as long as broad. Pronotum $0.73\times$ as broad as mesoscutum. Pronotum and mesoscutum entirely and uniformly reticulate, and covered with thin, short, silvery setae (Fig. 5B). Mid lobe of mesoscutum posteriorly and entire mesoscutellum flattened dorsally. Notaulus distinctly impressed and obliterated by sculpture. Mesoscutellum $0.9\times$ as long as broad, broadly abutting mesoscutum and separating axillae. Frenal area not separated but relatively distinct with coriaceous

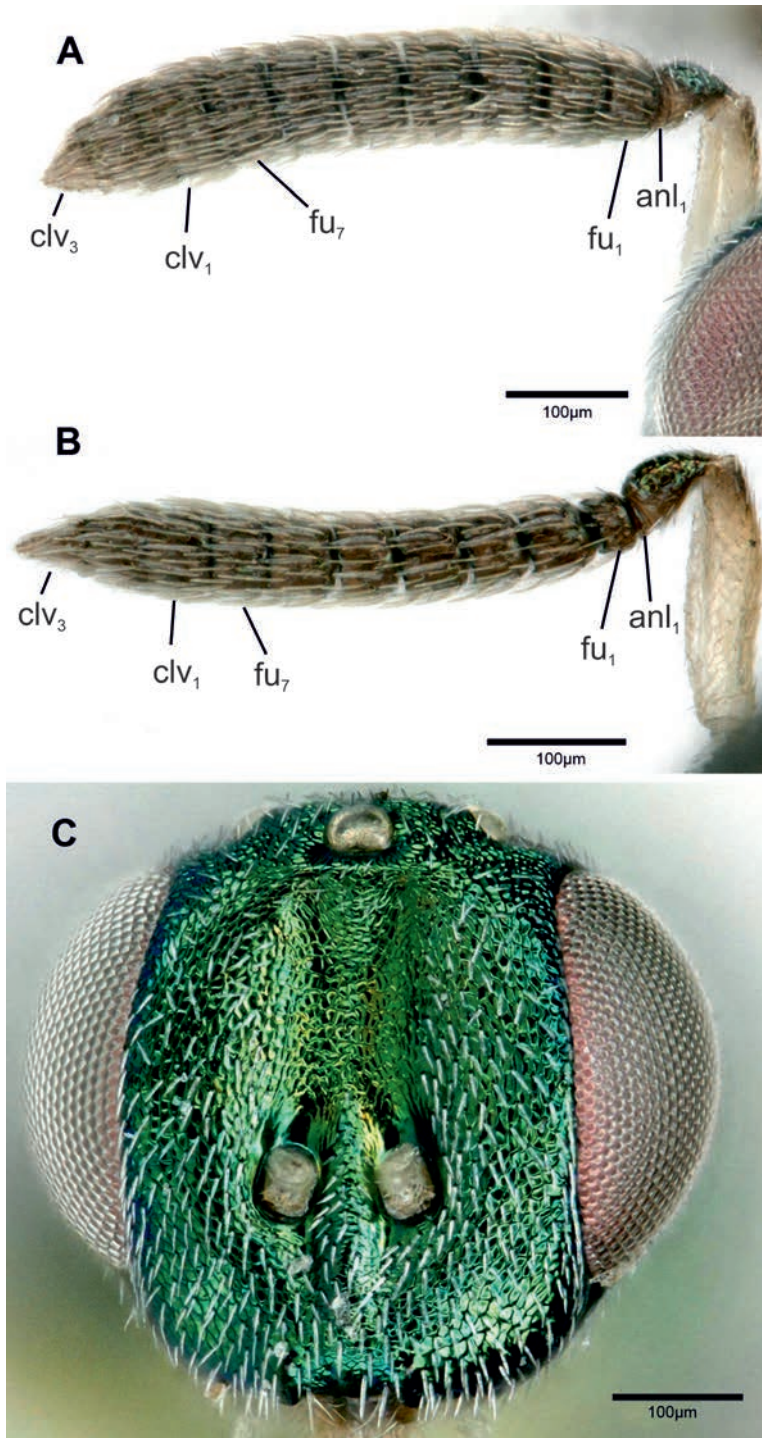


Figure 4. *Microdontomerus iriphagus* **A** female antenna, lateral view **B** male antenna, lateral view **C** male head, frontal view (anl_1 – anellus 1; $clv_{1,3}$ – clavomere 1, 3; $fu_{1,7}$ – funicular 1, 7).

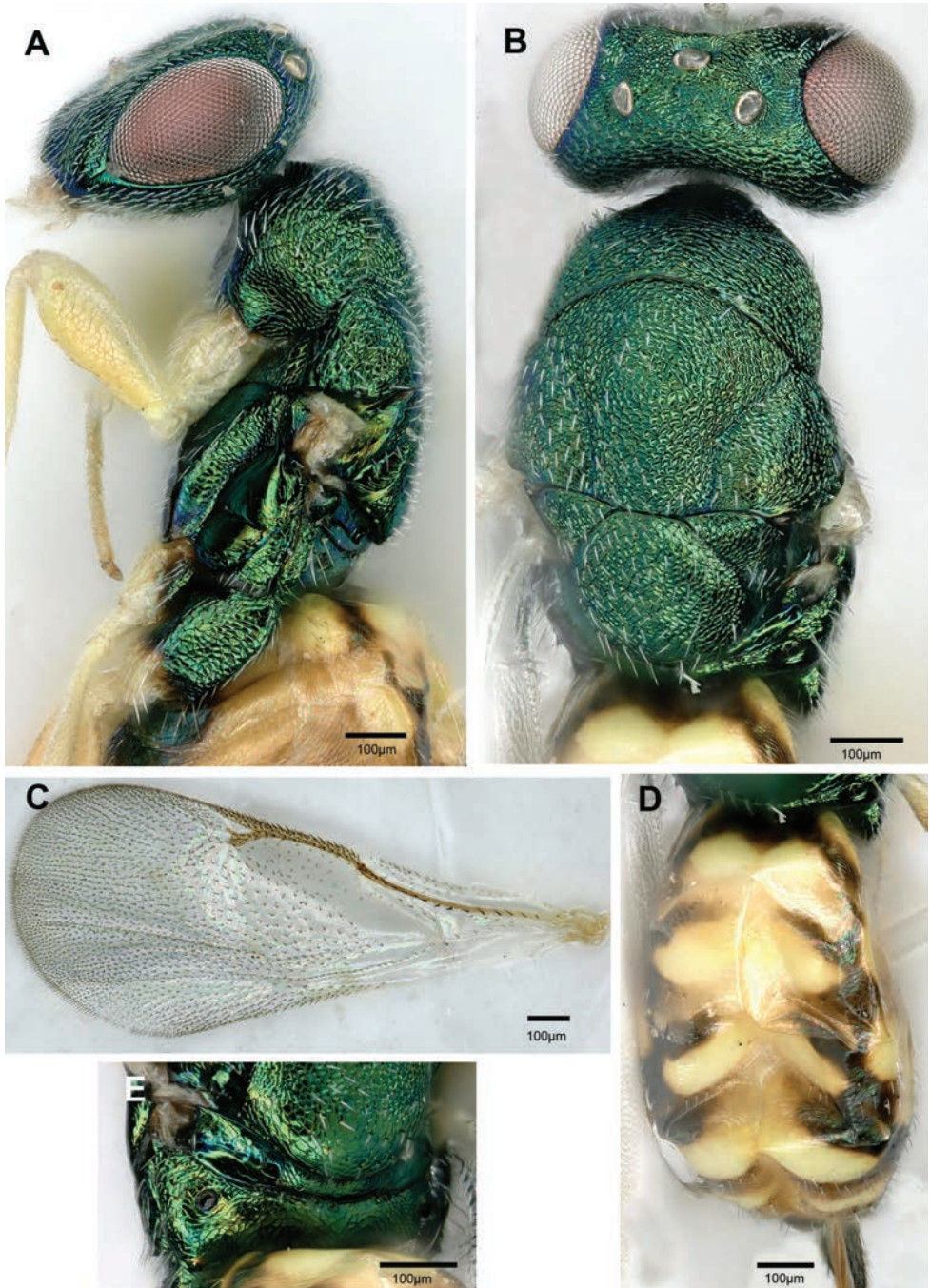


Figure 5. *Microdontomerus iriphagus*, female **A** mesosoma, lateral view **B** mesosoma, dorsal view **C** fore wing **D** metasoma, dorsal view **E** propodeum, dorsal view.

sculpture (Fig. 5E). Propodeum delicately reticulate, without median carina (Fig. 5E). Profemur 3.6× as long as broad. Metacoxa reticulate, covered by setae dorsally and ventrally, 2.3× as long as broad; metafemur 2.8× as long as broad, without any tooth; metatibia 4.68× as long as broad; metatarsus long, as long as metatibia (Fig. 3A). Fore wing 2.25× as long as wide, hyaline, with densely setose on disc; speculum reaching end of marginal vein; costal cell dorsally with 1–2 rows of short setae along anterior margin, and 3–4 rows at end of cell, basal and cubital cell bare; basal and cubital line of setae complete; marginal vein 1.93× as long as postmarginal vein and 2.7× as long as stigmal vein; venation pale brown (Fig. 5C).

Metasoma (Fig. 5D) 1.3× as long as mesosoma, with superficially alutaceous sculpture dorsally and laterally. Petiole very short. Gt_1 incised medially, Gt_2 – Gt_3 distinctly emarginate medially, Gt_4 – Gt_5 slightly emarginate medially. Tip of hypopygium almost reaching near to apex of gaster (Fig. 3A). OI 2.3.

Male (Fig. 3B). Length of body 1.68 mm (1.6–2.2 mm). Similar to females except following: metasoma concolor of mesosoma except brownish-yellow sub-basal band, laterally extending from Gt_1 to proximal part of Gt_3 . Funicular segments less transverse than in the female. Fu_2 – fu_7 about 0.60–0.71× as long as broad, with first flagellomere shortest; clava 1.86× as long as broad (Fig. 4B). Pro- and metafemur distinctly swollen, respectively 2.94 and 2.27× as long as broad, the latter distinctly serrate posteriorly.

Distribution. Palaearctic: Iran.

Biological association. This species represents an association with an uncommon host for Erimेरinae, the mantids ootheca of *Iris oratoria* (Linneaus, 1758) (Mantodea), as well as another species of the genus *Microdontomerus* in the Mediterranean basin, *Microdontomerus iridis* (Picard 1930) (Janšta et al. 2016).

***Microdontomerus quadrimaculatus* Lotfalizadeh & Rasplus, sp. nov.**

<https://zoobank.org/1560E7D1-6B8B-4A3B-BDC8-D6C23CB4F23D>

Figs 6–7

Material examined. Holotype: IRAN • ♀; South-Khorasan province, Khoosf (32°77'N, 58°85'E, 1300 m), 5.iv.2018, galls on *Haloxylon ammodendron*; Tavakkoli-Korghond, G. leg. (deposited in HMIM). **Paratypes:** IRAN • same as holotype, 1♀ (deposited in HMIM).

Etymology. A reference to the four pale-yellow oval spots on the gastral tergites that is characteristic of this species.

Diagnosis. Head about 1.18× as broad as high and 1.66–1.72× as broad as long. Anterior margin of clypeus straight and slightly protruded relative to corners of oral fossa. Scrobes bare and finely sculptured relative to the rest of face. Toruli inserted distinctly above ventral level of eye. POL about 3.05× as long as OOL and OOL about 0.72× as long as LOL. Antenna with scape not reaching anterior ocellus; flagellum

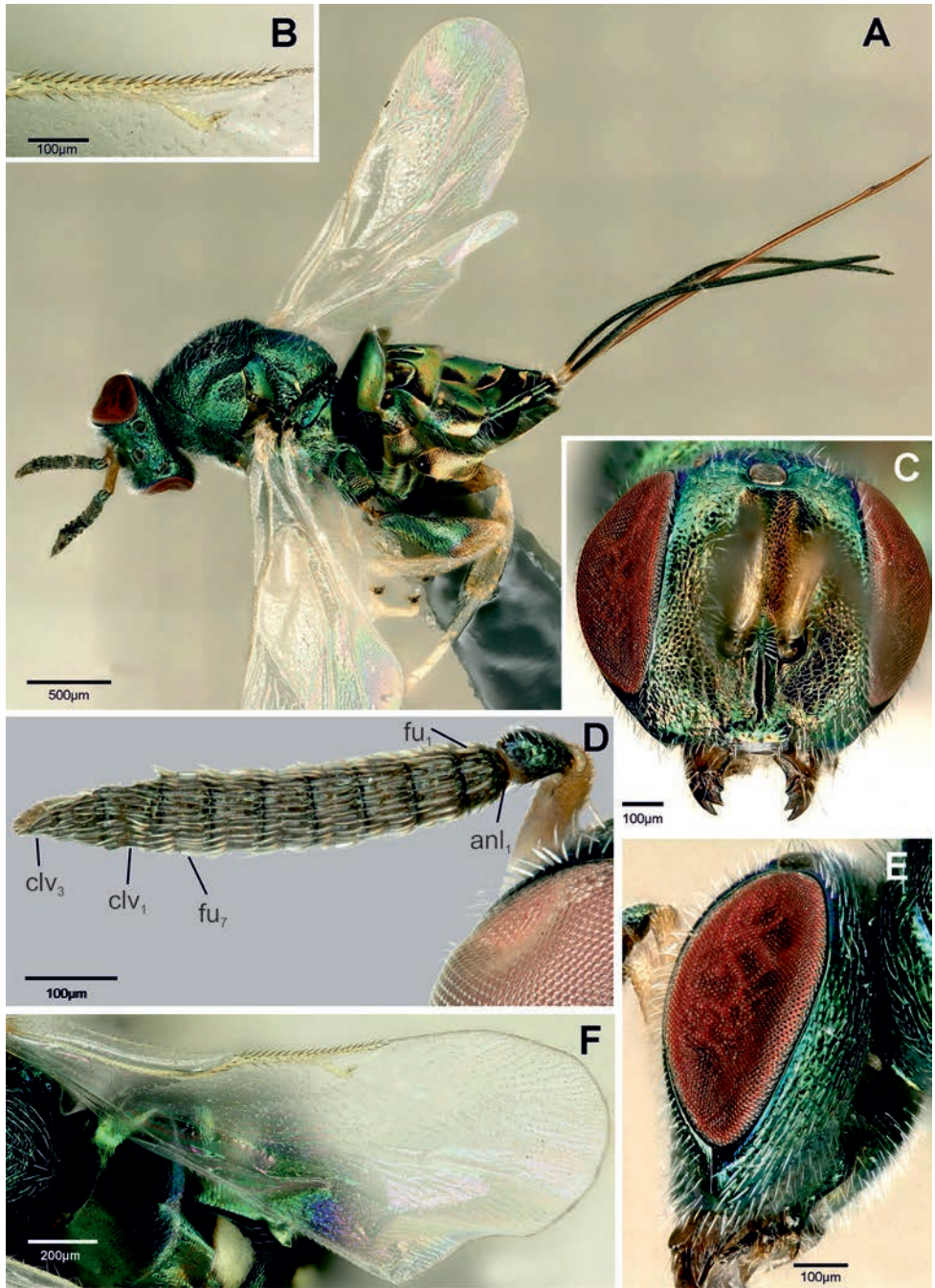


Figure 6. *Microdontomerus quadrimaculatus*, female **A** female habitus, lateral view **B** fore wing venation **C** head, frontal view **D** female antenna, lateral view **E** head, lateral view **F** fore wing (anl₁ – anellus 1; clv_{1,3} – clavomere 1, 3; fu_{1,7} – funicular 1, 7).

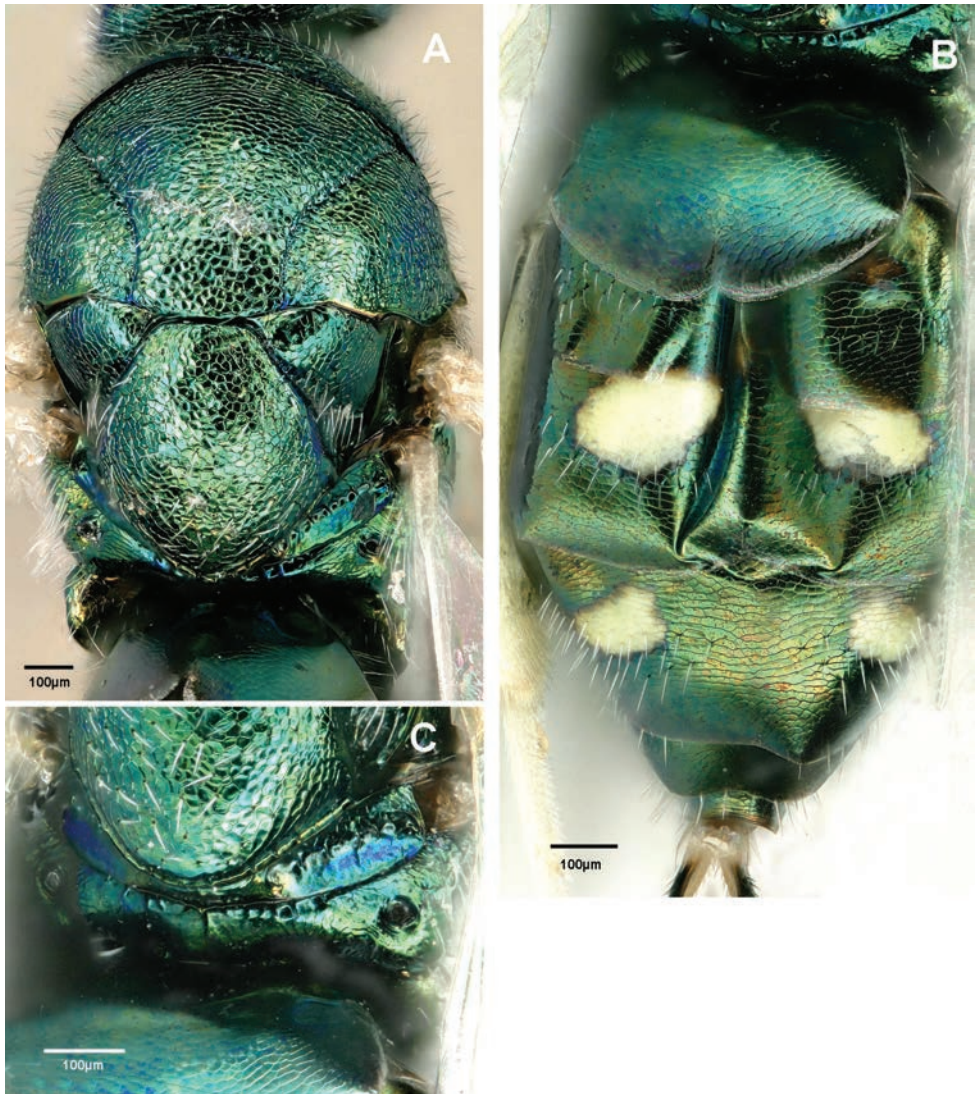


Figure 7. *Microdontomerus quadrimaculatus*, female **A** mesosoma, dorsal view **B** metasoma, dorsal view **C** propodeum, dorsal view.

with one anellus and seven funicular segments, all funicular segments transverse. Mesonotum entirely reticulate. Fore wing with speculum reaching end of marginal vein; costal cell dorsally with three rows of setae along anterior margin, cubital cell without setae and basal cell at most with few setae along anterior margin; basal and cubital line of setae complete; marginal vein $1.33\times$ as long as postmarginal vein and $2.66\times$ as long as stigmal vein. All tarsi slightly longer than tibiae, metafemur simple, without any tooth. Metasoma with hypopygium reaching almost end of gaster; Gt_1 incised medi-

ally, Gt_2 – Gt_3 distinctly emarginate medially, Gt_3 – Gt_4 with a pair of whitish spots, Gt_4 – Gt_5 slightly emarginate. Ovipositor $0.95\times$ as long as body; OI 3.75.

Description. Female (Fig. 6A): Body length including ovipositor 5.25 mm; length of ovipositor 2.5 mm.

Colour. Head, mesosoma, meso- and metacoxa and metasoma metallic blue-green with coppery reflection (Fig. 6A). Gt_3 – Gt_4 with a pair of pale-yellow oval spots. Pedicel concolorous with body with metallic green reflection, flagellum dark-brown with slight metallic reflection. Scape, tegula, all femur distally, metatibia and tarsi pale yellow. Pro- and metacoxa concolorous with body, mesocoxa brown. Fore wing hyaline, wing venation pale yellow, setae brown.

Head (Fig. 6C). Head $1.18\times$ as broad as high; $1.66\times$ as broad as long in dorsal view and $1.74\times$ in lateral view (Fig. 6E); $1.04\times$ as broad as mesonotum at its widest part in dorsal view. Head reticulate with thin, short, silvery setae on face, vertex and temple which are slightly longer than two meshes of the reticulation; scrobe more finely reticulate, without setae. Eyes separated by $0.82\times$ their own height, eye $1.88\times$ as high as long. Clypeus with anterior margin distinctly straight and slightly protruded relative to corners of oral fossa; ventral part of clypeus smooth (Fig. 6C). Malar space $0.29\times$ as long as eye height. Occipital carina absent. POL $3.05\times$ OOL, OOL $0.72\times$ LOL.

Antenna (Fig. 6D). Scape $5.33\times$ as long as broad, not reaching ventral margin of anterior ocellus; pedicel $1.16\times$ as long as broad; torulus inserted distinctly above ventral level of eye. Combined length of pedicel and flagellum $0.70\times$ as long as breadth of head. Flagellum with one ring-like anellus; remaining flagellomeres distinctly transverse, with fu_1 the smallest, $0.57\times$ as long as broad, wider than pedicel, and bearing only few MPS; fu_2 – fu_7 of about same dimensions, 0.58 – $0.65\times$ as long as broad.

Mesosoma (Fig. 7A). Mesosoma $1.3\times$ as long as broad. Pronotum $0.81\times$ as broad as mesoscutum. Pronotum and mesoscutum entirely reticulate, and covered with thin, short, silvery setae. Notaulus complete and distinctly impressed. Mesoscutellum as long as broad, without frenal area. Mesoscutellum and axilla more sparsely covered with setae. Propodeum mainly smooth, slightly reticulate laterally, with incomplete and barely visible median carina in basal part (Fig. 7C). Hind leg with coxa reticulated, covered by setae dorsally and ventrally, $1.8\times$ as long as broad; metafemur $3.20\times$ as long as broad, without any tooth; metatibia $4\times$ as long as broad; metatarsus long, $1.16\times$ as long as metatibia. Fore wing $2.4\times$ as long as wide, hyaline, densely setose on disc; speculum reaching end of marginal vein; costal cell dorsally with three rows of setae along anterior margin, basal and cubital cell bare; basal and cubital line of setae complete; marginal vein $1.33\times$ as long as postmarginal vein and $2.66\times$ as long as stigmal vein; venation pale yellow (Figs 6A, F).

Metasoma (Fig. 6B). Metasoma $1.23\times$ as long as mesosoma (but somewhat collapsed), with very shallow alutaceous sculpture. Petiole very short, strongly transverse. Gt_1 incised medially, Gt_2 – Gt_3 distinctly emarginate medially, Gt_4 – Gt_5 slightly emarginate medially. Tip of hypopygium almost reaching apex of gaster. OI 3.75.

Distribution. Palearctic: Iran.

Biological association. This species was reared from galls of *Stefaniola similata* Mamaev, 1972 (Diptera: Cecidomyiidae) on *Haloxylon ammodendron* C.A. Mey in the eastern Iran.

Key to the species of the genus *Microdontomerus* in Iran (females)

- 1 Metasoma brownish-yellow with a pair of pale-yellow oval spots on every tergite (Fig. 5D) *M. iriphagus* sp. nov.
- Metasoma concolorous with mesosoma and with distinct metallic reflection (Fig. 6A) **2**
- 2 Ovipositor sheaths short, as long as metasoma or slightly (about 1.3 times) longer than metasoma *M. albipes* (Giraud, 1870)
- Ovipositor sheaths long, as long as the combined length of meso- and metasoma (Fig. 6A) **3**
- 3 Gt₃₋₄ with a pair of whitish spots (Fig. 7B); marginal vein 1.33× and 2.66× as long as postmarginal and stigmal vein, respectively (Fig. 6B) *M. quadrimaculatus* sp. nov.
- All gastral tergites metallic green without contrasted spots; marginal vein about 2.14× and 4.0× as long as postmarginal and stigmal vein, respectively. *M. annulatus* (Spinola, 1808)

Discussion

Previously, the genus *Oopristus* Steffan, 1968 (Hymenoptera: Torymidae) was originally described from Iran (Steffan 1968; Lotfalizadeh and Gharali 2005). *Perseimerus* Lotfalizadeh & Rasplus, gen. nov., is the second genus found for the first time in Iran. Considering Iran's significant diversity of ecological and bioclimatic conditions, the presence of further undescribed taxa are awaiting discovery.

Among the described taxa, *M. quadrimaculatus*, sp. nov., was reared from galls of *Stefaniola similata* on saxaul shrubs, *Haloxylon ammodendron*. Saxaul shrubs are distributed in the Central and Eastern deserts and arid environments of Iran, where it is mostly used for wind control and sandy soil maintenance. The first attempt to study the pests and their associated parasitoids of saxauls was carried out by Lotfalizadeh et al. (2019). These shrubs are seriously endangered by a few pest insects including the mealybug *Anophococcus abaii* (Danzig, 1990) (Hemiptera: Eriococcidae) and *S. similata*. Our knowledge on the natural enemies of these pests is still limited. *Microdontomerus quadrimaculatus* may potentially play a role in a control of *S. similata*, as it was discovered for example for *Mesopolobus quadrimaculatus* Dzhankomen (Hymenoptera: Pteromalidae), a parasitoid of *Stefaniola* spp. on *Haloxylon* spp., in China (Li et al. 2018). However, further investigation of efficiency of *M. quadrimaculatus* as a natural enemy of *S. similata* is needed.

About 27 species of chalcidoid species worldwide have been reported from Mantodea ootheca (Janšta et al. 2016; Noyes 2019; Mirzaee et al. 2021). Most of these species belongs to the subfamily Podagrioninae (Torymidae), highly specialized mantids' parasitoids, where many species are still awaiting their description (Janšta, pers. observ.). However, association of *M. iriphagus* Lotfalizadeh & Janšta, sp. nov., as well as *M. iridis* (Janšta et al. 2016) (both Erimerinae) represent rather biological exceptions within their own clade, their morphology does not show any special adaptations to the hosts, and we do not expect that many species remain to be discovered.

Acknowledgements

We would like to thanks Dr. E. Rakhshani (University of Zabol, Iran) for sharing his collection with us and providing type specimen of *Peserimerus marginalis*. This work was supported by grants of the Ministry of Education, Youth and Sports of the Czech Republic no. SVV 266686/2024 and of the PRIMUS Research Programme (Charles University, no. PRIMUS/24/SCI/015) (both for PJ). Hossein Lotfalizadeh was supported by a grant from the Iranian Agricultural Research, Education and Extension Organisation (AREEO), project No 25554/200.

References

- Crawford JC (1914) Notes on the chalcidoid family Callimomidae. Proceedings of the Entomological Society of Washington 16: 122–126.
- Doğanlar M (2016) Species of *Microdontomerus* (Crawford, 1907) and *Eridontomerus* (Crawford, 1907) (Hymenoptera: Torymidae: Microdontomerini) from Turkey, with descriptions of new species. Entomofauna 37: 505–520.
- Fallahzadeh M, Narendran TC, Saghaei N (2009) Insecta, Hymenoptera, Chalcidoidea, Eurytomidae and Torymidae in Iran. Check List, Campinas 5(4): 830–839. <https://doi.org/10.15560/5.4.830>
- Gibson GAP, Huber JT, Woolley JB (1997) Annotated keys to the genera of Nearctic Chalcidoidea (Hymenoptera). National Research Council Research Press, Ottawa, 794 pp.
- Grissell E (1995) Toryminae (Hymenoptera: Chalcidoidea: Torymidae): a redefinition, generic classification, and annotated world catalog of species. Memoirs on Entomology, International 2: 1–470.
- Grissell E (2005) A review of North American species of *Microdontomerus* Crawford (Torymidae: Hymenoptera). Journal of Hymenoptera Research 14(1): 22–65.
- Harris RA (1979) A glossary of surface sculpturing. Occasional Papers in Entomology 28: 1–31.
- Janšta P, Delvare G, Krogmann L, Schütte K, Peters R (2016) Systematics, biology and distribution of *Microdontomerus iridis* (Picard, 1930) comb. n. (Hymenoptera, Torymidae, Toryminae, Microdontomerini), a parasitoid of Mantodea oothecae. Journal of Hymenoptera. Research 48: 1–18. <https://doi.org/10.3897/JHR.48.7470>

- Janšta P, Cruaud A, Delvare G, Genson G, Heraty J, Křížková B, Rasplus J-Y (2018) Torymidae (Hymenoptera, Chalcidoidea) revised: molecular phylogeny, circumscription and reclassification of the family with discussion of its biogeography and evolution of life-history traits. *Cladistics* 34: 627–651. <https://doi.org/10.1111/cla.12228>
- Li Q, Dzhankmen KA, Triapitsyn SV, Hu H (2018) Parasitoids reared from galls of *Stefaniola* sp. (Diptera, Cecidomyiidae) on *Haloxylon* spp. in China, with redescription of *Mesopolobus quadrimaculatus* Dzhankmen (Chalcidoidea, Pteromalidae). *Turkish Journal of Zoology* 42: 263–268. <https://doi.org/10.3906/zoo-1709-13>
- Lotfalizadeh H, Gharali B (2005) Introduction to the Torymidae fauna (Hymenoptera: Chalcidoidea) of Iran. *Zoology in the Middle East* 36: 67–72. <https://doi.org/10.1080/09397140.2005.10638129>
- Lotfalizadeh H, Tavakoli-Korghond G, Mokhtari A (2019) On the parasitoid complex (Hymenoptera: Chalcidoidea) of *Anophococcus abaii* (Hemiptera: Eriococcidae), with description of *Metaphycus anophococci* Lotfalizadeh, n. sp. *Annales de la Société entomologique de France* (N.S 55): 317–326. <https://doi.org/10.1080/00379271.2019.1621204>
- Mirzaee Z, Lotfalizadeh H, Sadeghi S (2021) Chalcidoid parasitoids (Hymenoptera: Torymidae and Eupelmidae) of mantids (Mantodea) oothecae in Iran. *Phytoparasitica* 50: 487–499. <https://doi.org/10.1007/s12600-021-00965-1>
- Nazemi Rafie J, Lotfalizadeh H (2012) Identification and diversity of torymid wasps (Hym.: Chalcidoidea, Torymidae) of Kurdistan Province. *Proceedings of 20th Iranian Plant Protection Congress*, 105–105.
- Noyes JS (2019) Universal Chalcidoidea Database. <http://www.nhm.ac.uk/research-curation/research/projects/chalcidoids/> [accessed on 7 Jul 2023]
- Picard F (1930) Sur deux Hyménoptères chalcidides nouveaux, parasites dans des oothèques de Mantides. *Bulletin de la Société Entomologique de France* 35: 87–90. <https://doi.org/10.3406/bsef.1930.28262>
- Steffan JR (1967) *Paraholaspis ovivora* n. sp. (Hym., Torymidae) parasites des oeufs de bu-preste *Steraspis speciosa* Klug. *Entomophaga* 12(2): 149–152. <https://doi.org/10.1007/BF02370611>
- Steffan JR (1968) Observations sur *Chalcedectus sinaiticus* (Ms.) et descriptions de *C. balachowskyi* sp. n. (Hym. Chalcedectidae) et d'*Oopristus safavii* gen. n., sp. n. (Hym. Torymidae), deux parasites d'importance économique en Iran. *Entomophaga* 13: 209–216. <https://doi.org/10.1007/BF02371816>
- Turner CE, Grissell EE, Cuda JP, Casanave K (1990) *Microdontomerus anthonomi* (Crawford) (Hymenoptera: Torymidae), an indigenous parasitoid of the introduced biological control insect *Bangasternus orientalis* (Capiomont) (Coleoptera: Curculionidae) and *Urophora affinis* Fraunfeld (Diptera: Tephritidae). *Pan-Pacific Entomologist* 66: 162–166.

Description and mitochondrial genome sequencing of a new species of inquiline gall wasp, *Synergus nanlingensis* (Hymenoptera, Cynipidae, Synergini), from China

Yu-Bo Duan^{1*}, Yan-Jie Wang^{1*}, Dao-Hong Zhu¹, Yang Zeng¹, Xiu-Dan Wang¹

¹ *Laboratory of Insect Behavior and Evolutionary Ecology, College of Life Science and Technology, Central South University of Forestry and Technology, Changsha, Hunan, China*

Corresponding authors: Yang Zeng (zengyangsile@163.com); Xiu-Dan Wang (t20192464@csuft.edu.cn)

Academic editor: Miles Zhang | Received 24 January 2024 | Accepted 26 February 2024 | Published 11 March 2024

<https://zoobank.org/DE0BABB9-F338-468A-8148-90BD1562E3A6>

Citation: Duan Y-B, Wang Y-J, Zhu D-H, Zeng Y, Wang X-D (2024) Description and mitochondrial genome sequencing of a new species of inquiline gall wasp, *Synergus nanlingensis* (Hymenoptera, Cynipidae, Synergini), from China. *Journal of Hymenoptera Research* 97: 105–126. <https://doi.org/10.3897/jhr.97.119433>

Abstract

A new species of inquiline gall wasp, *Synergus nanlingensis* Wang & Zeng, **sp. nov.**, which was reared from galls on *Castanopsis eyrei* Tutch (Fagaceae) collected in Guangdong Province, China, is described and illustrated herein along with its mitochondrial genome. The mitogenome of *S. nanlingensis* is 16,604 base pairs in length and comprises 37 genes, which is typical of mitogenomes. One large control region was detected in the *S. nanlingensis* mitogenome, which differed from that reported for other Cynipidae species. Similar to other Cynipidae species, *S. nanlingensis* has the same four common gene rearrangement events; however, it shows some differences, as follows: *trnS1* is downstream of *Cytb*; *trnS2* is upstream of *nad1*; and *trnC* is downstream of *rrnS*. Phylogenetic analysis using *COI*, *CytB*, and *28S-D2* sequences confirmed that *S. nanlingensis* is a distinct species belonging to the genus *Synergus* Hartig.

Keywords

Castanopsis, gall wasp, mitogenome, morphology, phylogenetic analysis

* These authors contributed equally.

Introduction

Cynipids or gall wasps (Hymenoptera: Cynipoidea, Cynipidae) are the second largest radiation of gall-inducing insects, with about 1400 described species (Ronquist et al. 2015; Lobato-Vila et al. 2022a). They are widely distributed worldwide, mainly throughout the Holarctic region (Nearctic and Palearctic), and most species are gall inducers on different host plants (Melika and Abrahamson 2002; Ronquist et al. 2015; Lobato-Vila et al. 2022b). Gall induction starts after the oviposition where this interaction between the female wasp and the plant tissue triggers gall formation, and larval activity (chewing, feeding) promotes gall growth and subsequent transformations of the gall structure (Csóka et al. 2005). This can affect the growth of the host plant, even causing host death (Duffet 1968). The gall protects the larvae from not only predatory insects, but also insecticides, posing difficulties for their chemical control (Moriya et al. 2003; Chiara et al. 2018). Some cynipoids can significantly impact the forestry industry. For example, *Dryocosmus kuriphilus* Yasumatsu is a worldwide invasive pest that causes serious damage to chestnut trees (Zhu et al. 2007; Yang et al. 2021), while damage by *Diplolepis abei* Pujade-Villar & Wang causes significant economic losses to the rose horticulture industry in Northwest China (Guo et al. 2013; Lobato-Vila et al. 2020).

By contrast, nearly 240 species of cynipids (Lobato-Vila et al. 2022b), termed inquilines, are unable to trigger gall growth; instead, they develop inside galls induced by other gall wasps, forming an advantageous relationship that benefits only the inquilines and that can even cause the death of the gall inducer (Duffet 1968; Péntzes et al. 2009; Bozsó et al. 2015). Inquilines are distributed into four tribes: Synergini *sensu stricto*, Ceroptresini, Diastrophini, and Rhoophilini (Ronquist et al. 2015; Lobato-Vila et al. 2022a). *Synergus* Hartig is the most speciose genus in Synergini, with about 130 species known worldwide (Schwéger et al. 2015; Pujade-Villar et al. 2017; Lobato-Vila et al. 2020). Most *Synergus* species are associated with galls induced by gall wasps of the tribe Cynipini on Fagaceae (principally *Quercus* spp.). In Europe, the 22 species of Fagaceae (Schwarz 1993; Tutin 1993; Tutin and Akeroyd 1993) are known to host at least 30 species of *Synergus* (Melika 2006; Péntzes et al. 2012). By comparison, there are 294 species of Fagaceae in seven genera in mainland China, including 163 endemic and at least three introduced (Huang et al. 1999). However, only 17 *Synergus* species are known from mainland China (Lobato-Vila et al. 2022a), thus, it is thought that the species diversity of *Synergus* in mainland China is likely to be higher than current estimates (Abe 2007; Liu et al. 2012).

The mitochondrial genome of most insects is a double-stranded circular structure DNA molecule comprising 13 protein-coding genes, 22 transfer RNAs (tRNAs), two ribosomal RNA (rRNA) genes, and a major noncoding sequence called ‘Control Region’ (CR) (Cameron 2014). Given the maternal mode of inheritance and conserved gene components, the insect mitochondrial genome is a molecular marker widely used in phylogenetic construction (Cameron 2014). However, gene rearrangements have been found frequently in Hymenoptera (Wei et al. 2014; Chen et al. 2018), not only for tRNA genes but also for protein-coding genes (PCGs) (Simon et al. 2006; Tang et

al. 2019). Gene rearrangements, including transpositions, inversions, and inverse transpositions in the mitogenome, are common in certain insect groups, can be an informative feature for phylogenetic reconstruction (Cameron 2014; Feng et al. 2020). For example, Tang et al. (2019) analyzed 83 full or partial mitochondrial genomes to resolve relationships among all major clades of Hymenoptera with high support, confirming the phylogenetic position of Cynipoidea in Proctotrupomorpha as previously hypothesized by Heraty et al. (2011). Despite these advances, complete or nearly complete mitogenome sequences remain scarce for Cynipidae, with just seven species documented, including only two from Synergini (Tang et al. 2019; Xue et al. 2020; Pang et al. 2022; Shu et al. 2022; Zhong and Zhu 2022; Mozhaitseva et al. 2023; Su et al. 2023).

In this study, we describe a new species of the genus *Synergus* from China. The completed mitogenome of this new species was sequenced and annotated, and mitogenome structure and gene rearrangements in this lineage were analyzed. Additionally, phylogenetic analyses were conducted using *COI*, *Cytb*, and *28S-D2* sequences to delineate the evolutionary relationships between this new species and existing species from the Palearctic region within *Synergus*.

Materials and methods

Specimen collection

A total of 142 galls were collected in September 2023, from branches of *Castanopsis eyrei* Tutch on the summit of Xiaohuang Mountain, Guangdong Province, China. The galls were kept in insect mesh bags with moistened cotton and placed in meshed rearing cages. These cages were placed in the laboratory environment under room temperature conditions. To maintain humidity, the cages were misted with water every 1.5 days, and the humidifying cotton was frequently replaced until the emergence of insects. Adult wasps were directly preserved in 100% ethanol within two days after emergence and frozen at -80°C for morphological and molecular studies.

Morphological observations

Specimens for conventional morphological examination were air-dried at room temperature and mounted to pinned triangular card paper. They were then photographed with a Leica M205C microscope system equipped with Leica DMC6200 digital camera (Leica Inc., Wetzlar, Germany) attached to a computer. The illustration was made using the Procreate application on an iPad Air 3, utilizing an Apple Pencil and based on a magnified photograph of the tarsal claw.

The terminology used to describe the morphology of specimens follows that used in other studies on gall wasps (Harris 1979; Ronquist and Nordlander 1989; Ronquist 1995; Melika 2006) as follows: abbreviations: F1–F13 = 1st and subsequent flagellomeres; post-ocellar distance (POL) = distance between the posterior ocelli; ocellar-ocular

distance (OOL) = distance from the outer margin of a posterior ocellus to the inner margin of the compound eye; lateral-frontal ocelli distance (LOL) = distance between the lateral and frontal ocellus. The width of the radial cell of the forewing was measured from the margin of the wing to the Rs vein.

Type specimens are housed in the Insect Collection of the Central South University of Forestry and Technology (CSUFT), Changsha city, Hunan province, China.

DNA extraction and sequencing

Before DNA extraction, specimens were washed in sterile water to avoid surface contamination. Total DNA was then extracted using SDS/proteinase K digestion and phenol-chloroform extraction. The extracted DNA pellets were air-dried, resuspended in 20 μ L sterile water, and stored at 4 °C for PCR and sequencing. Insect universal primers designed by Folmer et al. (1994), Simon et al. (1994), Schw eger et al. (2015), and Tavakoli et al. (2019) (Suppl. material 1) were used to amplify partial fragments of the mitochondrial *rrnL*, *COI*, *Cytb*, and *28s-D2* genes. The PCR products were purified and sequenced using the Sanger method by Wuhan Icongene Co, Ltd (Wuhan, China). GDcox1F, GDcox1R, GDrrnLF, GDrrnLR, and GDcytbR were designed to amplify the remaining genome by long PCR (Suppl. material 2). The reaction mixture comprised: 0.4 μ L APEX (AG, Dalian, China), 10 μ L buffer mixture, 0.4 μ L of each primer, and 0.5 μ L of DNA; water was added to each reaction to a final volume of 20 μ L. Amplification was conducted using a C1000 Touch Thermal Cycler (Bio-Rad, Hercules, CA, USA). The cycling conditions were as follows: 98 °C for 1 min, 34 cycles of 98 °C for 10 s, 55 °C for 30 s, and 68 °C for 10 min. Two amplification strategies were used to obtain the complete mitogenome sequence. First, PCR amplification was performed using four specific long PCR primer combinations: GDrrnLF/GDcox1F, GDrrnLR/GDcox1R, GDrrnLF/GDcox1R, and GDrrnLR/GDcox1F. However, only GDrrnLF/GDcox1F resulted in a desired outcome. A clear single band was obtained using the primer combination GDcytbR/GDcox1R. These PCR products were then purified and sequenced.

The primer walking method was used to determine the sequence for each long PCR product using an ABI 3730XL DNA sequencer (Applied Biosystems, Foster City, CA, USA) by Wuhan Icongene Co, Ltd. Long PCR fragments were sequenced directly with the PCR primers and internal primers (Suppl. material 3). Sequences were assembled using SeqMan Pro 7.1.0 (Burland, 2000), then checked and corrected manually. The same site with different nucleotides was used to check the original sequencing peak map or to resequence the products to determine the nucleotides of the site.

Genome annotation and analyses

The initial mitogenome annotations were conducted using MITOS on Galaxy (https://usegalaxy.org/root?tool_id=toolshed.g2.bx.psu.edu%2Frepos%2Fiuuc%2Fmitos%2Fmitos%2F2.1.3%20galaxy0). PCGs were identified by ORFFinder in NCBI (www.ncbi.nlm.nih.gov). rRNA genes were confirmed by sequence comparison with

published mitochondrial rRNA sequences from *Synergus* sp. (Tang et al. 2019), and *Dryocosmus liui* Pang, Su & Zhu (Hymenoptera: Cynipidae) (Su et al. 2023). Control regions (CRs) were confirmed by the boundaries of *trnS2* and *trnC*. Codon usage and relative synonymous codon usage (RSCU) of 13 PCGs in the specimens were calculated using PhyloSuite v1.2.2. The RSCU figure was drawn using the ggplot2 package (Hadley 2009); a plugin of Rscript 3.4.4 (Zhong and Zhu 2022). The nucleotide composition and AT/GC skew were calculated using PhyloSuite.

Analyses of phylogenetic relationship and pairwise genetic distance

To assess the taxonomic position of *Synergus nanlingensis* within the genus *Synergus*, we incorporated *S. nanlingensis* into the clade of *Synergus* species from the Palearctic region as recovered by Lobato-Vila et al. (2022a). This clade was strongly supported as monophyletic. New species specificity and whether the morphological similarities reflected the phylogenetic relationship based on molecular data were determined using the method of Lobato-Vila et al. (2021). Specifically, the *COI*, *Cytb*, and *28S-D2* sequences of 31 Palearctic *Synergus* species and two additional species of other cynipid genera were used as outgroups (Suppl. material 4). Sequences were aligned using MAFFT (Kato et al. 2002) and those from each gene (660 bp of *COI*, 450 bp of *Cytb*, and 574 bp of *28S-D2*) were concatenated in a single matrix (1684 bp) using PhyloSuite.

This concatenated matrix of molecular data sets was analyzed based on the model-based phylogenetic approaches Bayesian Inference (BI) and Maximum Likelihood (ML). To determine the best partitions and models, the data sets were also analyzed using ModelFinder (Kalyaanamoorthy et al. 2017). For BI analysis, four simultaneous Markov chains were run for 10 million generations, with tree sampling occurring every 1,000 generations, and a burn-in of 25% of the trees in MrBayes 3.2.7 (Huelsenbeck and Ronquist 2001). For ML analyses, a total of 10,000 bootstrap replicates were obtained with the auto model applied to all partitions in IQ-tree2.2.2.7 (Nguyen et al. 2015). The final tree was rooted using the outgroup.

Results

Morphology-based taxonomy

Synergus nanlingensis Wang & Zeng, 2023, sp. nov.

<https://zoobank.org/982D4466-0B8A-4F8B-BD6B-938871C8417B>

Figs 1, 2

Holotype. Female, CHINA, Guangdong Province, Shaoguan City, 24-09-2022, reared from galls collected in 1-9-2022, leg. Y. Zeng, L. Liu and Y. Duan. Paratypes: three females and 13 males, same as holotype, housed in CSUFT (the holotype and two male paratypes were dried and mounted, while the other paratypes were deposited in 99% ethanol in a freezer at -80°C).

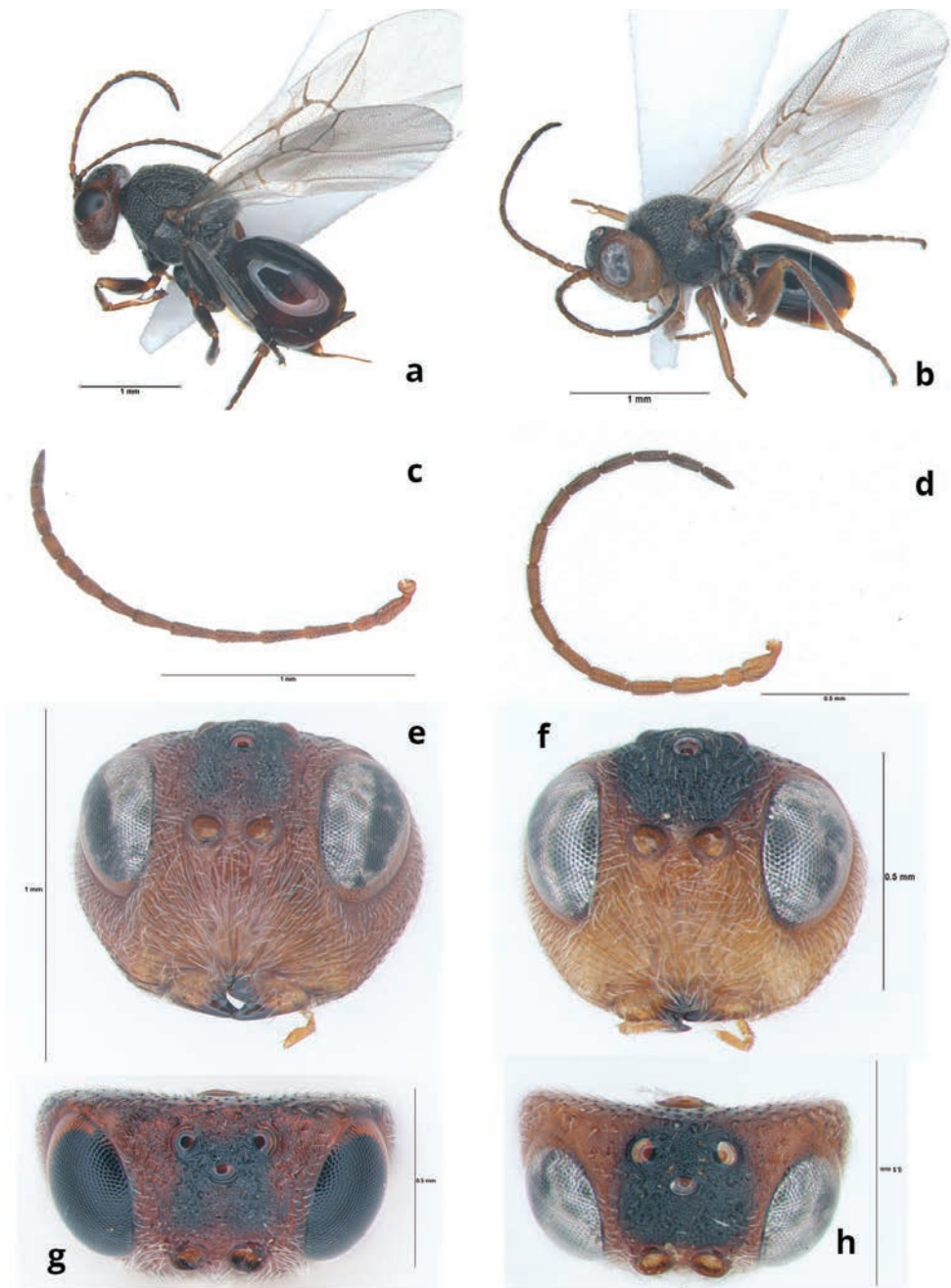


Figure 1. *Synergus nanlingensis* Wang & Zeng, 2023, sp. nov. **a** general habitus (♀) **b** general habitus (♂) **c** antenna (♀) **d** antenna (♂) **e** head in anterior view (♀) **f** head in anterior view (♂) **g** head in dorsal view (♀) **h** head in dorsal view (♂).

Diagnosis. *Synergus nanlingensis* Wang & Zeng, sp. nov., most closely resembles *Synergus hupingshanensis* (Liu, Yang & Zhu) is part of a group characterized by a completely opened radial cell, tarsal claws with a basal lobe and lateral pronotal carina present. However, it can be differentiated from *S. hupingshanensis* by the following morphological features: (1) The first flagellomere (F1) of *S. nanlingensis* is nearly equal in length to the second flagellomere (F2), whereas in *S. hupingshanensis*, F1 1.3× as long as F2; (2) the head of *S. nanlingensis* reddish brown with the frons and the center of the occiput being black, whereas head of *S. hupingshanensis* entirely orange without such black markings; and (3) scutellar foveae in *S. nanlingensis* are smooth and shiny at the bottom, whereas in *S. hupingshanensis* are roughly sculptured.

Description. Female; body length: 2.6–3.2 mm ($N = 10$).

Color (Figs 1a, 2c): head reddish brown, except frons, mandible teeth, and center of occiput black; antennae reddish brown. Mesosoma, legs, and metasoma black, with tarsus and distal part of body reddish brown. Wings hyaline with distinct brown veins.

Head (Figs 1e, g, 2a, c): transverse ellipse in front view (the widest of head near middle), 1.2× as wide as high, slightly broader than mesosoma in the anterior view, 1.2× wider than long as seen from above; frons slightly elevated from lateral view; lateral frontal carinae inconspicuous or absent, with rugose sculpture between the compound eye and frons; frons surface densely punctate with deep punctures and sparse setae (Fig. 1g). Eyes 1.6× as high as wide; height of eye 1.5× as high as length of malar space (Fig. 1e). Lower face densely setose, radiating from the clypeus toward basal margin of compound eye and antennal toruli. Gena broadened behind eyes, with punctures and white sparse setae. Middle of clypeus slightly impressed; anterior tentorial pit large and distinct; epistomal sulcus and clypeopleurostomal line indistinct; malar sulcus absent. Transfacial distance longer than the height of the compound eye; diameter of torulus shorter than the diameter of toruli and about half the distance between the inner margin of the eye and torulus (Fig. 1e). POL: OOL: LOL=2.2:1.8:1; LOL approximately as long as the diameter of the lateral ocellus. Ocelli ovate, all three similar in size (Fig. 1e). Occiput smooth; postgena with setae.

Antenna (Fig. 1c): 12 flagellomeres, pedicel 1.8× as long as broad, F1 longer than F2. F1–F12:14:13:13:13:11:10:9:8:8:7:7:10. Placoid sensillae distinct on F5–F12.

Mesosoma (Fig. 2d–f): 1.3× as long as high on the lateral view (Fig. 2d), with dense pubescence. Length of the middle part of pronotum is one-third that of the outer lateral margin; pronotum punctate, laterally areolate-rugulose, lateral carina distinct. Mesoscutum 1.4× as wide as long (measuring along the anterior edge of tegulae), surface areolate-rugose, center with a transverse rugae, covered with densely yellow setae. Notauli percurrent and distinct, somewhat convergent posteriorly; anterior parallel line, parapsidal line, and median mesoscutal line indistinct, barely traceable (Fig. 2e). Scutellar foveae elongate ovate, bottom smooth and shiny, deeply impressed, with short sparse white setae, separated by distinct central carina. Mesopleuron hairless, finely striated ventrally and carinate-rugose dorsally. Metapleural sulcus reaches posterior margin of mesopectus in the most upper 1/4 of its height (Fig. 2d). Propodeum smooth coriaceous, with short sparse white setae. Lateral propodeal carinae slightly impressed basally and slightly convergent distally (Fig. 2f).

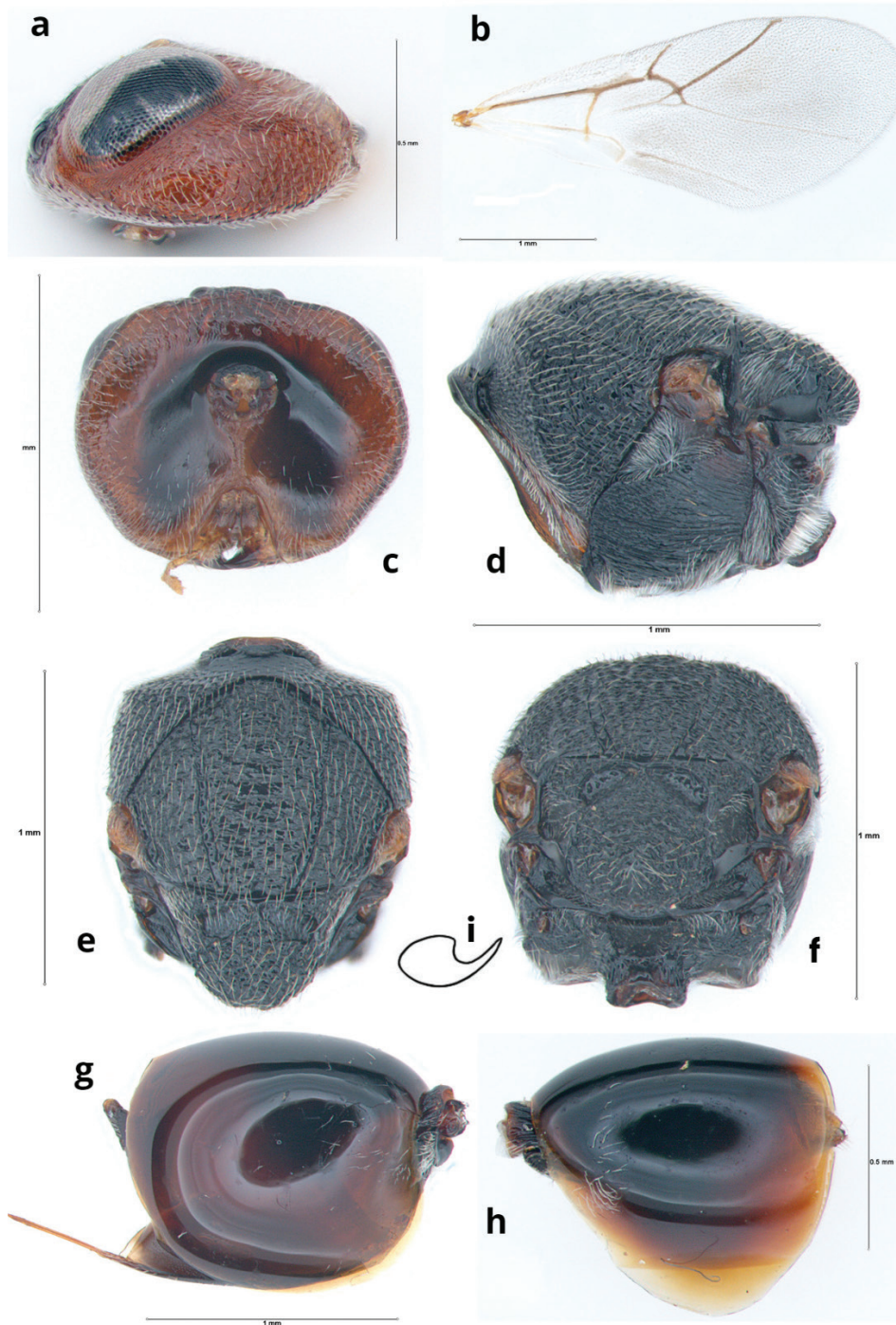


Figure 2. *Synergus nanlingensis* Wang & Zeng, 2023, sp. nov. **a** head in lateral view (♀) **b** fore wing (♀) **c** head in posterior view (♀) **d** mesosoma, lateral view (♀) **e** mesosoma, dorsal view (♀) **f** propodeum, dorsal view (♀) **g** metasoma, lateral view (♀) **h** metasoma, lateral view (♂) **i** tarsal claw.

Legs: Tarsal claws with a small basal lobe (Fig. 2i).

Forewing (Fig. 2b): hyaline and densely setose, approximately as long as body length. All veins well pigmented. Radial cell open, about 2.9× as long as broad; R1 does not reach wing margin; Rs curved toward to posterior distally.

Metasoma (Fig. 2g): slightly shorter than the head and mesosoma combined, and 1.2× as long as high; petiole sulcate; syntergite almost completely covering remaining tergites, surface smooth and mainly glabrous, with few white setae anterolaterally, and a postero-dorsal area without setae and micropunctures. Subsequent tergites and hypopygium micropunctate; prominent part of ventral spine of hypopygium small, with few lateral setae.

Male (Figs 1b, d, f, g, 2h): similar to the female, but body length 1.9–2.2 mm ($N = 6$); head, legs, and distal part of abdomen yellowish brown; frons, mandible teeth, mesosoma, basal part of abdomen, and hind coxa black.

Antenna: 13 flagellomeres, pedicel 1.4 times as long as broad. F1–F13: 16:13:14:14:14:13:13:12:11:10: 11. Metasoma elongated, shorter than the head and mesosoma combined.

Biology. Specimens of *S. nanlingensis* were collected from galls found on branches of *Castanopsis eyrei* on the summit of Xiaohuang Mountain 1,600 m above sea level. Galls are nearly spherical in shape, range in diameter from 15 to 35 mm, and are hard and strongly lignified (Fig. 3). Galls appear in July and inquilines emerged from late September to October. The gall inducer of the gall which yielded *S. nanlingensis* is unconfirmed.

Distribution. Shaoguan City, Guangdong Province, China.

Etymology. The specific epithet refers to the type locality.

Genome organization and base composition

The total length of the complete mitogenome of *S. nanlingensis* is 16,604 bp (GenBank accession OR978581). The mitochondrial genome contains the typical gene repertoire of 13 PCGs, two rRNA genes, and 22 tRNA genes (Fig. 4). There are eight overlapping regions, ranging in size from 1 to 7 bp. The mitogenome contains 20 intergenic spacers, with lengths ranging from 1 to 336 bp. The longest gene spacer is between *Cox2* and *trnD* (Table 1). The nucleotide content of the *S. nanlingensis* mitogenome is as follows: 44.2% A, 5.6% G, 42% T, and 8.2% C; the total A + T percentage is 86.2%, AT skew is 0.026 and GC skew is -0.191, which is consistent with that in other Hymenoptera (Wei et al. 2010; Chen et al. 2018).

Protein-coding genes and codon usage

The total length of the 13 PCGs of *S. nanlingensis* is 11,037 bp. Five PCGs (*nad1*, *nad2*, *nad4L*, *nad4*, and *nad5*) are encoded by the minority strand (N-strand), and the other eight genes are encoded by the majority strand (J-strand) (Table 1). The overall A + T content in PCGs is 84.7%, ranging from 77.4% (*cox1*) to 91.8% (*nad6*). The AT skew of the PCGs is -0.102, and the GC skew is 0.03. A very high A + T content (94.9%) is found at the third codon of PCGs.

Table 1. Annotation of the *Synergus nanlingensis* Wang & Zeng, 2023, sp. nov. mitochondrial genome.

Gene	Positions	Size	Strand	Nucleotides Intergenic	Anti or Start codon	Stop codon	A+T(%)
trnS2	1–68	68	–	-2	TGA		89.7
nad1	67–1005	939	–	73	ATT	TAG	85
trnL1	1079–1144	66	–	1	TAG		92.4
trnI	1146–1215	70	–	5	GAT		85.7
trnL2	1221–1291	71	–	-1	TAA		90.1
trnW	1291–1358	68	–	3	TCA		91.2
trnM	1362–1427	66	+	-5	CAT		89.4
trnQ	1423–1491	69	–	2	TTG		87
nad2	1494–2501	1008	–	24	ATT	TAA	91.7
trnY	2526–2592	67	–	4	GTA		86.6
trnV	2597–2664	68	+	12	TAC		94.1
cox1	2677–4212	1536	+	117	ATT	TAA	77.4
cox2	4330–5016	687	+	336	ATA	TAA	83.9
trnK	5353–5424	72	+	6	TTT		87.5
trnD	5431–5503	72	+	0	GTC		94.5
atp8	5504–5665	161	+	-6	ATT	TAA	87.7
atp6	5659–6333	675	+	1	ATG	TAA	83.7
cox3	6335–7122	788	+	3	ATG	TA	80.5
trnG	7126–7198	73	+	0	TCC		94.5
nad3	7199–7534	336	+	31	ATT	TAA	87.8
trnA	7566–7636	71	+	-3	TGC		87.3
trnR	7634–7703	70	+	0	TCG		88.6
trnN	7704–7771	68	+	1	GTT		83.8
trnF	7773–7836	64	+	-2	GAA		92.2
trnE	7835–7901	67	–	0	TTC		97
nad5	7902–9572	1671	–	0	ATT	TAA	87.4
trnH	9573–9646	74	–	7	GTG		89.2
nad4	9654–10967	1314	–	-7	ATG	TAA	85.5
nad4L	10961–11236	276	–	12	ATT	TAA	90.6
trnT	11249–11312	64	+	-1	TGT		92.2
trnP	11312–11378	67	–	81	TGG		88.1
nad6	11460–11969	510	+	3	ATT	TAA	91.8
cytb	11973–13109	1137	+	0	ATG	TAA	80.9
trnS1	13110–13171	62	+	76	TCT		87.1
rrnL	13248–14628	1381	–	0			88.8
rrnS	14629–15461	833	–	0			90.1
trnC	15462–15530	69	+	0	GCA		91.3
CR	15531–16604	1066					84.6

Notes: + indicates the gene is coded on majority strand while – indicates the gene is coded on minority strand.

In *S. nanlingensis*, eight genes (*cox1*, *nad1*, *nad2*, *nad3*, *nad4L*, *nad5*, *nad6*, *atp8*) are initiated with ATT, four genes (*atp6*, *nad4*, *cob*, and *cox3*) with ATG, and *Cox2* initiated with ATA. All PCGs use ATN as the starting codon, similar to that reported for other Hymenoptera (Tang et al. 2019). Most PCGs from *S. nanlingensis* terminate with stop codons TAA, whereas *Cox3* ends with TA and *nad1* with TAG.

The relative synonymous codon usage in all 13 PCGs is shown in Fig. 5. As reported for previously studied Cynipidae species, the most common amino acids are leucine (Leu2) and serine (Ser2). The least common codons are CUG-Leu1 and CUC-Leu1.

tRNA and rRNA

In total, 22 tRNA genes were identified in the mitogenome of *S. nanlingensis*, ranging in size from 62 bp to 74 bp and accounting for 1,507 bp in total concatenated length (Table 1). Of the tRNA genes, 12 are located on the H-strand whereas ten tRNA genes are located on the L-strand. Of these tRNA genes, 21 can be folded into a conventional cloverleaf secondary structure, whereas *trnS1* lack the dihydrouridine arm (D-arm). This feature has also been reported for *Andricus mairei* (Kieffer) (Zhong and Zhu 2022). The lack of the D-arm in *trnS1* is a common feature of most metazoans (Kahnt et al. 2015; Du et al. 2017). In the mitochondrial tRNA secondary structures of *S. nanlingensis*, seven mismatched base pairs were detected: five G-U pairs, one G-A pair, and one A-A pair. As reported for other Cynipoidea species (Mao et al. 2015; Tang et al. 2019; Xue et al. 2020; Su et al. 2023), *rrnL* and *rrnS* are next to each other and both are located in the L-strand in *S. nanlingensis*, with lengths of 1,381 bp and 833 bp, respectively.

Noncoding sequences (CR)

A large CR was detected in *S. nanlingensis* mitogenome, located between *trnC* and *trnS2*. The CR is 1073 bp in length and its AT content was 84.6%. It has three 166-bp non-tandem repeat units, one 36-bp A + T-rich region (AT% = 94.3%) and one 32-bp A + T-rich region (AT% = 90.6%) (Fig. 6).



Figure 5. Relative synonymous codon usage (RSCU) of *Synergus nanlingensis* Wang & Zeng, 2023, sp. nov. mitochndrial genome. Codon families are labeled on the x-axis. Values on the top of the bars indicate the percentage of each amino acid used for the construction of 13 protein-coding genes (PCGs).

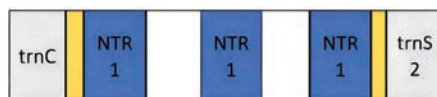


Figure 6. Structures of control regions in the mitogenome of *Synergus nanlingensis* Wang & Zeng, 2023, sp. nov. Abbreviation: NTR, nontandem repeat. Yellow shows A + T-rich regions.

Gene arrangements

Compared with the ancestral mitogenome arrangement, rearrangements of *S. nanlingensis* mitogenome involve tRNA genes, rRNA genes, and PCGs. Su et al. (2023) compared the reported mitochondrial gene rearrangements of gall wasps and found four rearrangement events: *trnE* and *trnF* had inverted and swapped positions; *rrnL* and *rrnS* moved into the *cob*–*nad1* junction; a novel tRNA gene cluster *trnL1*–*trnI*–*trnL2*–*trnW*–*trnM*–*trnQ* was formed between *nad1* and *nad2*; and *trnV* was inverted and moved to the *nad2*–*cox1* junction. These four rearrangements are also found in *S. nanlingensis*. However, unlike gall wasps with two CRs (Xue et al. 2020; Pang et al. 2022; Zhong and Zhu 2022; Su et al. 2023), mitochondrial genes of *S. nanlingensis* have the following differences: *trnS1* is downstream of *Cytb*; *trnS2* is upstream of *nad1*; and *trnC* is downstream of *rrnS* (Fig. 7).

DNA taxonomy and phylogenetic relationship

The genetic distance between *Synergus nanlingensis* and other *Synergus* species is long (Suppl. material 5). The topology of our phylogenetic tree mostly coincides with that recovered by Lobato-Vila et al. (2022a) (Fig. 8) and supports *S. nanlingensis* as a distinct species, clustering it with other Palearctic *Synergus*. Different analytical approaches (BI and ML) did not affect the topology but did affect the level of node support (Suppl. material 7). *Synergus nanlingensis* is recovered as a sister species of *Synergus itoensis* Abe, Ide & Wachi, although this relationship is not highly supported.

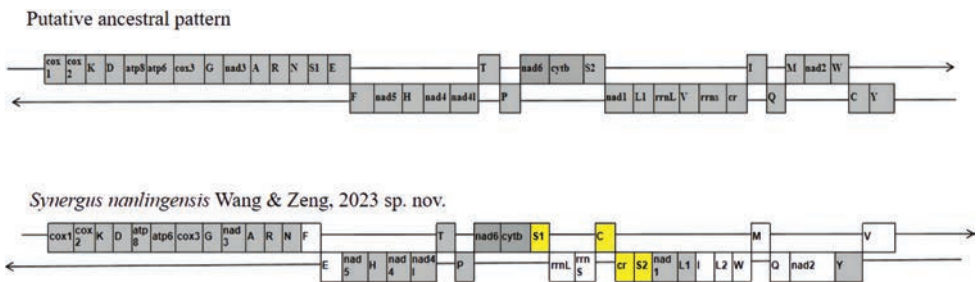


Figure 7. Mitochondrial genome organization and gene rearrangement in *Synergus nanlingensis* Wang & Zeng, 2023, sp. nov. compared with the ancestral type of the insect mitochondrial genome. All abbreviations are the same as in Table 1 in the main text. Arrow pointing to the right represents the J-strand and arrow pointing to the left represents the N-strand. Genes are drawn in their original order; intergenic distances are not included, and sizes of genes are not to scale. Yellow boxes indicate genes with different positions from two control regions reported in Cynipidae, and white boxes indicate genes that are different in terms of both position and strand associations from the putative ancestral pattern. Gray boxes show conserved gene blocks.

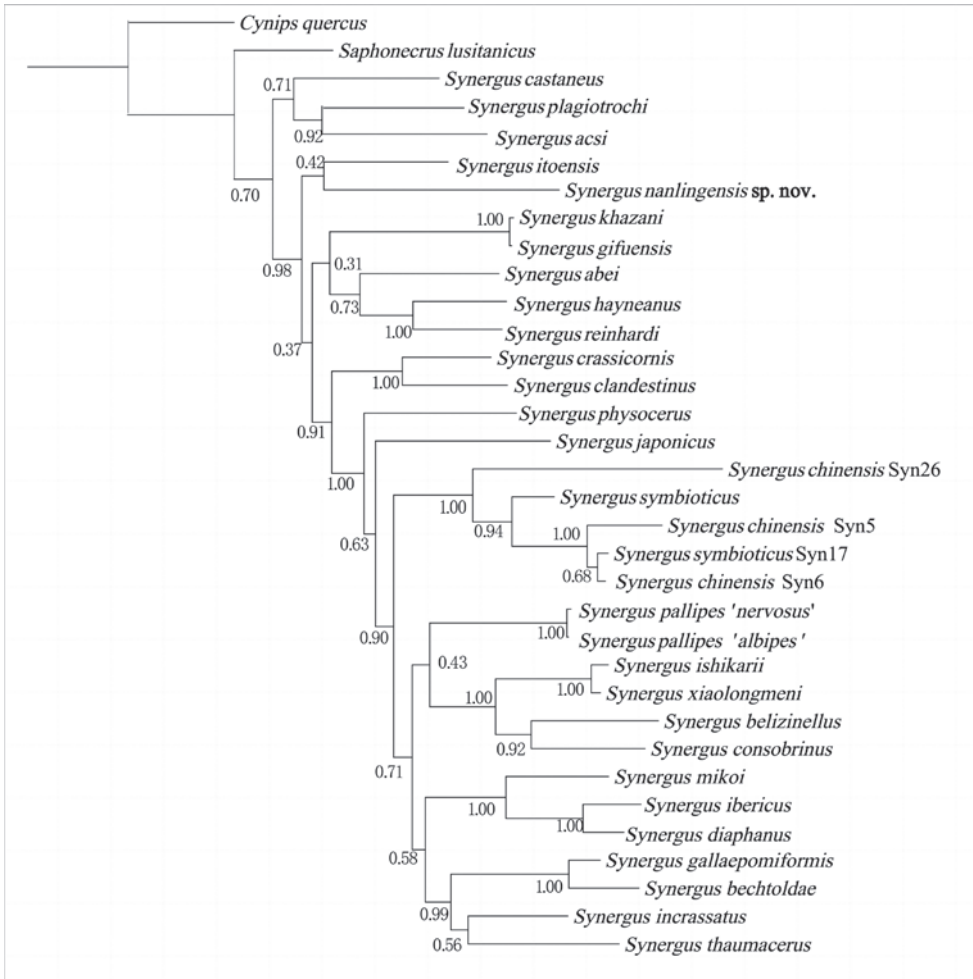


Figure 8. Bayesian analysis of the MAFFT alignment data set inferred from the *COI* + *Cytb* + *28S-D2* data sets. Posterior probabilities are shown at each node.

Discussion

The discovery of *Synergus nanlingensis*, a new species found in China, marks a significant contribution to the biodiversity of the family Cynipidae, especially among inquiline. Currently, little is known about the gall wasp species associated with *Castanopsis*, with only two *Synergus* species, *S. hupingshanensis* and *S. kawakamii* (Tang & Melika), reported so far (Schwéger et al. 2015; Lobato-vila et al. 2022a). Given the rich diversity of species and endemics within *Castanopsis* and Fagaceae in China (Xu et al. 2022), further research in this region is expected to uncover more new species associated with these hosts.

Phylogenetic tree analysis robustly confirms the status of *S. nanlingensis* as a member of the genus *Synergus*. Although an open radial cell in the forewing is not a typical characteristic of *Synergus*, the species was confirmed as a member based on the presence of the female antenna with 12 flagellomeres, the complete notaulus, and presence of an incomplete lateral frontal carina (Schweger et al. 2015); placing it within a group characterized by a fully open radial cell, basally lobed claws, and the presence of a lateral thoracic carina (Lobato-Vila et al. 2020). Interestingly, no Cynipini were reared from the same galls as *S. nanlingensis*, despite three years of collections made in different months. This phenomenon was also observed in the breeding records of *S. hupingshanensis*, where no expected gall-inducers were reared from two years of field collections (Liu et al. 2012). The reasons for the lack of expected gall inducers for these two species are still unknown and warrant further experimental investigation to determine whether or not they are inducers or inquilines as its currently known sister species *S. itoensis* is one of the few known rare cases of *Synergus* that have secondarily reverted back to gall induction (Abe and Wachi 2011). Gobbo et al. (2020) have compared the genome of *S. itoensis* with that of three other related *Synergus* inquilines, and found that there were distinct genetic differences between gall inducers and inquilines. Therefore, further study on the mitogenome or genome comparison between Chinese *Synergus* and known gall inducers and inquilines will provide molecular evidence for speculating whether they have gall inducing ability.

This study presents the first complete mitochondrial genome reported for a species of *Synergus*. In the mitochondrial genome of *S. nanlingensis*, general characteristics and typical rearrangement events of Cynipidae species were observed (Zhong and Zhu 2022; Su et al. 2023), but some differences were also noted. For instance, a long intergenic spacer of 366 bp between *Cox2* and *trnD* was observed in *S. nanlingensis*. Such long intergenic spacers have also been found in the mitochondrial genomes of other Hymenoptera insects, possibly as a result of gene rearrangement (Chen et al. 2018; Zhong and Zhu 2022). While TAA is commonly used as a stop codon in arthropod mitogenomic PCGs, variations such as TA, a single T, and more uniquely, TAG, have been observed (Yamauchi et al. 2002). In *S. nanlingensis*, *Cox3* ends with TA and *nad1* with TAG, aligning with stop codon usage in two previously known Synergini mitogenomes (Tang et al. 2019; Shu et al. 2022). Prior research identified two control regions (CR1 and CR2) in Cynipoidea, with CR2 being a partially inverted repeat of CR1 (Mao et al. 2015; Zhong and Zhu 2022; Su et al. 2023). This led to speculation that inverted, duplicated CRs might be characteristic of the Cynipoidea mitochondrial genome. However, only one control region was found in the *S. nanlingensis* mitogenome, consistent with the two known mitogenomes of Synergini. Remarkably, this study provides a complete sequencing of the control region, which were never described before. Whether these features and gene rearrangement serve as distinguishing characteristics within Synergini requires further data support.

Acknowledgements

This study is supported by the National Key Research and Development Program of China (2018YFE0127100). We thank International Science Editing (<http://www.internationalscienceediting.com>) for editing this manuscript. We sincerely thank Zongjun Liu, Yong Xie, Jia-dong Zhang, Zhi-ping Zhou and other staff of the Nanling National Nature Reserve for their selfless help in collecting specimens.

References

- Abe Y (2007) Parallelism in secondary loss of sex from a heterogonic life cycle on different host plants in the *Andricus mukaigawae* complex (Hymenoptera: Cynipidae), with taxonomic notes. *Journal of Natural History* 41(8): 473–480. <https://doi.org/10.1080/00222930701192122>
- Abe Y, Ide T, Wachi N (2011) Discovery of a new gall-inducing species in the inquiline tribe Synergini (Hymenoptera: Cynipidae): inconsistent implications from biology and morphology. *Annals of the Entomological Society of America* 104: 115–120. <https://doi.org/10.1603/AN10149>
- Bozsó M, Tang CT, Péntzes Z, Yang, MM, Bihari P, Pujade-Villar J, Schwéger S, Melika G (2015) A new genus of cynipid inquiline, *Lithosaphonecrus* Tang, Melika & Bozsó (Hymenoptera: Cynipidae: Synergini), with description of four new species from Taiwan and China. *Insect Systematics & Evolution* 46(1): 79–114. <https://doi.org/10.11646/zootaxa.5060.1.6>
- Burland TG (2000) DNASTAR's Lasergene sequence analysis software. *Methods in Molecular Biology* 132: 71–91. <https://doi.org/10.1385/1-59259-192-2:71>
- Cameron SL (2014) Insect mitochondrial genomics: Implications for evolution and phylogeny. *Annual Review of Entomology* 59: 95–117. <https://doi.org/10.1146/annurev-ento-011613-162007>
- Chen L, Chen PY, Xue PY, Hua HQ, Li YX, Zhang F, Wei SJ (2018) Extensive gene rearrangements in the mitochondrial genomes of two egg parasitoids, *Trichogramma japonicum* and *Trichogramma ostriniae* (Hymenoptera:Chalcidoidea:Trichogrammatidae). *Scientific Reports* 8(1): 7034. <https://doi.org/10.1038/s41598-018-25338-3>
- Chiara F, Ester F, Marianna P, Matteo AS, Alberto A (2018) Effectiveness of *Torymus sinensis*: a successful long-term control of the Asian chestnut gall wasp in Italy. *Journal of Pest Science* 92: 353–359. <https://doi.org/10.1007/s10340-018-0989-6>
- Csóka G, Stone GN, Melika G (2005) Biology, ecology and evolution of gall inducing Cynipidae. In: Raman A, Schaefer CW, Withers TM (Eds) *Biology, ecology and evolution of gall-inducing arthropods*. Science Publishers, Inc. Enfield, New Hampshire, 569–636.
- Duffet GH (1968) Some new interrelationships of Hymenoptera over-wintering within the galls of *Andricus kollari* (Hartig). *The Entomologist's Monthly Magazine* 105: 1259–1261.
- Du YM, Dai W, Dietrich CH (2017) Mitochondrial genomic variation and phylogenetic relationships of three groups in the genus *Scaphoideus* (Hemiptera: Cicadellidae: Deltocephalinae). *Scientific Reports* 7: 16908. <https://doi.org/10.1038/s41598-017-17145-z>

- Feng Z, Wu Y, Yang C, Gu X, Wilson JJ, Li H, Cai W, Yang H, Song F (2020) Evolution of tRNA gene rearrangement in the mitochondrial genome of ichneumonoid wasps (Hymenoptera, Ichneumonoidea). *International Journal of Biological Macromolecules* 164: 540–547. <https://doi.org/10.1016/j.ijbiomac.2020.07.149>
- Folmer O, Black M, Hoeh W, Lutz R, Vrijenhoek R (1994) DNA primers for amplification of mitochondrial cytochrome oxidase subunit I from diverse metazoan invertebrates. *Molecular Marine Biology and Biotechnology* 3(5): 294–299.
- Guo R, Wu BM, Zhang WL, Wang YQ, Wang YP (2013) First discovery of an invasive gall-former insect pest *Diplolepis rosae*, in China. *Chinese Journal of Applied Entomology* 50(2): 500–504. [in Chinese] <https://doi.org/10.7679/j.issn.2095-1353.2013.069>
- Gobbo E, Lartillot N, Hearn J, Stone GN, Abe Y, Wheat CW, Ide T, Ronquist F (2020) From inquilines to gall inducers: Genomic signature of a life-style transition in synergus gall wasps. *Genome Biology and Evolution* 12(11): 2060–2073. <https://doi.org/10.1093/gbe/evaa204>
- Hadley W (2009) ggplot2, elegant graphics for data analysis. Springer, New York, America. https://doi.org/10.1111/j.1467-985X.2010.00676_9.x
- Harris R (1979) A glossary of surface sculpturing. State of California, Department of Food and Agriculture. *Occasional Papers in Entomology* 28: 1–31.
- Heraty J, Ronquist F, Carpenter JM, Hawks D, Schulmeister S, Dowling AP, Murray D, Munro J, Wheeler WC, Schiff N, Sharkey M (2011) Evolution of the hymenopteran megara-diation. *Molecular Phylogenetics and Evolution* 60:73–88. <https://doi.org/10.1016/j.ympev.2011.04.003>
- Huang C, Chang Y, Hsu Y, Jen H (1999) Fagaceae. In: Chun WY, Huang CC (Eds) *Fl. Reipubl. Popularis Sin*, 332 pp.
- Huelsenbeck JP, Ronquist F (2001) MRBAYES: Bayesian inference of phylogenetic trees. *Bioinformatics* 17(8): 764–755. <https://doi.org/10.1093/bioinformatics/17.8.754>
- Kahnt B, Gerth M, Paxton RJ, Bleidorn C, Husemann M (2015) The complete mitochondrial genome of the endemic and highly specialized South African bee Species *Rediviva intermixta* (Hymenoptera: Melittidae), with a comparison with other bee mitogenomes. *Biological Journal of The Linnean Society* 116(4): 940–953. <https://doi.org/10.1111/BIJ.12627>
- Kalyaanamoorthy S, Minh BQ, Wong TKF, von Haeseler A, Jermini LS (2017) ModelFinder: fast model selection for accurate phylogenetic estimates. *Nature Methods* 14: 587–589. <https://doi.org/10.1038/nmeth.4285>
- Katoh K, Misawa K, Kuma K, Miyata T (2002) MAFFT: a novel method for rapid multiple sequence alignment based on fast Fourier transform. *Nucleic Acids Research* 30(14): 3059–3066. <https://doi.org/10.1093/nar/gkf436>
- Liu Z, Yang XH, Zhu DH, He YY (2012) A new species of *Saphonecrus* (Hymenoptera, Cynipoidea) associated with plant galls on *Castanopsis* (Fagaceae) in China. *Annals of the Entomological Society of America* 105(4): 555–561. <https://doi.org/10.1603/AN12021>
- Lobato-Vila I, Caicedo G, Rodríguez PA, Pujade-Villar J (2020) The inquiline oak gall wasp (Hymenoptera: Cynipidae) fauna from Colombia: new data and species. *The Canadian Entomologist* 152(2): 131–144. <https://doi.org/10.4039/tce.2019.77>
- Lobato-Vila I, Wang YP, Melika G, Guo R, Ju XX, Pujade-Villar J (2021) A review of the species in the genus *Synergus* Hartig (Hymenoptera: Cynipidae: Synergini) from mainland

- China, with an updated key to the Eastern Palaearctic and Oriental species. *Journal of Asia-Pacific Entomology* 24(1): 341–362. <https://doi.org/10.1016/j.aspen.2020.11.014>
- Lobato-Vila I, Bae J, Roca-Cusachs M, Kang M, Jung S, Melika G, Péntzes Z, Pujade-Villar J (2022a) Global phylogeny of the inquiline gall wasp tribe Synergini (Hymenoptera: Cynipoidea: Cynipidae): first insights and establishment of a new cynipid tribe. *Zoological Journal of the Linnean Society* 195(4): 1338–1354. <https://doi.org/10.1093/zoolinnean/zlab085>
- Lobato-Vila I, Sala-Nishikawa A, Melika G, Stone GN, Tang CT, Yang MM, Fang ZQ, Zhu Y, Wang YP, Jung S, Nicholls JA, Pujade-Villar J (2022b) A catalogue, revision, and regional perspective of Eastern Palaearctic and Oriental oak gall wasps and their inquilines (Hymenoptera: Cynipidae: Cynipini, Synergini, Ceroptresini). *Zootaxa* 5161: 1–71. <https://doi.org/10.11646/zootaxa.5161.1.1>
- Mao M, Gibson T, Dowton M (2015) Higher-level phylogeny of the Hymenoptera inferred from mitochondrial genomes. *Molecular Phylogenetics and Evolution* 84: 34–43. <https://doi.org/10.1016/j.ympev.2014.12.009>
- Melika G (2006) Gall wasps of Ukraine, Cynipidae. *Vestnik zoologii (Supplement)* 21(1): 300.
- Melika G, Abrahamson WG (2002) Review of the world genera of oak cynipid wasps (Hymenoptera: Cynipidae: Cynipini). In: Melika G, Thuróczy C (Eds) *Parasitic Wasps: Evolution, Systematics, Biodiversity and Biological Control*. Agroiinform, Budapest, 150–190.
- Moriya S, Shiga M, Adachi I (2003) Classical biological control of the chestnut gall wasp in Japan. In: Van Driesche RG (Eds) *Proceedings of the 1st international symposium on biological control of arthropods, Hawaii, 14–18 January 2002*. USDA Forest Service, Washington, DC, USA, 407–415.
- Mozhaitseva K, Tourrain Z, Branca A (2023) Population genomics of the mostly thelytokous *Diplolepis rosae* (Linnaeus, 1758) (Hymenoptera: Cynipidae) reveals population-specific selection for sex. *Genome Biology and Evolution* 15(10): evad185. <https://doi.org/10.1093/gbe/evad185>
- Nguyen LT, Schmidt HA, von Haeseler A, Minh BQ (2015) IQ-TREE: a fast and effective stochastic algorithm for estimating maximum-likelihood phylogenies. *Molecular Biology and Evolution* 32(1): 268–274. <https://doi.org/10.1093/molbev/msu300>
- Pang Y, Su CY, Zhu JQ, Yang XH, Zhong JL, Zhu DH, Liu ZW (2022) A new species of *Andricus* Hartig, 1840 (Hymenoptera, Cynipidae) from China, with references to DNA taxonomy and Wolbachia infection. *ZooKeys* 1134: 52–73. <https://doi.org/10.3897/zookeys.1134.89267>
- Péntzes Z, Tang P, Bihari P, Bozsó M, Schwéger S, Melika G (2012) Oak associated inquilines (Hymenoptera, Cynipidae, Synergini). *TISCIA Mono* 11: 1–76.
- Péntzes Z, Melika G, Bozsóki Z, Bihari P, Mikó I, Tavakoli M, Pujade-Villar J, Fehér B, Fülöp D, Szabó K, Bozsó M, Sipos B, Somogyi K, Stone GN (2009) Systematic re-appraisal of the gall-usurping wasp genus *Synophrus* Hartig, 1843 (Hymenoptera: Cynipidae: Synergini). *Systematic Entomology* 34(4): 688–711. <https://doi.org/10.1111/j.1365-3113.2009.00482.x>
- Pujade-Villar J, Wang YP, Chen T, Shen J, Ferrer-Suay M (2017) Description of a new *Synergus* species from China and comments on other inquiline species (Hymenoptera: Cynipidae: Synergini). *Zootaxa* 4341(1): 56–66. <https://doi.org/10.11646/zootaxa.4341.1.4>

- Ronquist F (1995) Phylogeny and early evolution of the Cynipoidea (Hymenoptera). *Systematic Entomology* 20: 309–335. <https://doi.org/10.1111/j.1365-3113.1995.tb00099.x>
- Ronquist F, Nieves-Aldrey JL, Buffington ML, Liu Z, Liljeblad J, Nylander JA (2015) Phylogeny, evolution and classification of gall wasps: the plot thickens. *PLOS ONE* 10(5): 1–40. <https://doi.org/10.1371/journal.pone.0123301>
- Ronquist F, Nordlander G (1989) Skeletal morphology of an archaic cynipoid, *Ibalia rufipes* (Hymenoptera: Ibalidae). *Entomologica Scandinavica* 19(4): 1–60. <https://doi.org/10.1002/arch.940100408>
- Schwarz O (1993) *Quercus* L. In: Tutin TG, Heywood VH, Burges NA, Valentine DH, Walters SM, Webb DA (Eds) *Flora Europaea*, Vol. 1: Lycopodiaceae to Platanaceae. Cambridge University Press, Cambridge, 72–76.
- Schwéger S, Melika G, Tang CT, Bihari P, Bozsó M, Stone GS, Nicholls JA, Péntzes Z (2015) New species of cynipid inquelines of the genus *Synergus* (Hymenoptera: Cynipidae: Synergini) from the Eastern Palaearctic. *Zootaxa* 3999(4): 451–497. <https://doi.org/10.11646/zootaxa.3999.4.1>
- Shu X, Li Z, Yuan R, Tang P, Chen X (2022) Share novel gene rearrangements in the mitochondrial genomes of cynipoid wasps (Hymenoptera: Cynipoidea). *Genes (Basel)* 13(5): 914. <https://doi.org/10.3390/genes13050914>
- Simon C, Frati F, Beckenbach A, Crespi B, Liu H, Flook P (1994) Evolution, weighting, and phylogenetic utility of mitochondrial gene sequences and a compilation of conserved polymerase chain reaction primers. *Annals of the Entomological Society of America* 87: 651–701. <https://doi.org/10.1093/aesa/87.6.651>
- Simon C, Buckley TR, Frati F, Stewart JB, Beckenbach AT (2006) Incorporating molecular evolution into phylogenetic analysis, and a new compilation of conserved polymerase chain reaction primers for animal mitochondrial DNA. *Annual Review of Ecology, Evolution, and Systematics* 37(1): 545–579. <https://doi.org/10.1146/annurev.ecolsys.37.091305.110018>
- Su CY, Zhu DH, Abe Y, Ide T, Liu ZW (2023) The complete mitochondrial genome and gene rearrangements in a gall wasp species, *Dryocosmus liui* (Hymenoptera: Cynipoidea: Cynipidae). *Peer J* 11: e15865. <https://doi.org/10.7717/peerj.15865>
- Tang P, Zhu JC, Zheng BY, Wei SJ, Michael S, Chen X.X, Alfried P (2019) Mitochondrial phylogenomics of the Hymenoptera. *Molecular Phylogenetics and Evolution* 131(1): 8–18. <https://doi.org/10.1016/j.ympev.2018.10.040>
- Tavakoli M, Khaghaninia S, Melika G, Stone GN, Hosseini-Chegeni (2019) Molecular identification of *Andricus* species (Hymenoptera: Cynipidae) inducing various oak galls in Central Zagros of Iran., *Mitochondrial DNA Part A* 30(5): 713–720. <https://doi.org/10.1080/124701394.2019.1622693>
- Tutin TG (1993) *Castanea* Miller. In: Tutin TG, Heywood VH, Burges NA, Valentine DH, Walters SM, Webb DA (Eds) *Flora Europaea*, vol. 1: Lycopodiaceae to Platanaceae. - Cambridge University Press, Cambridge, 72 pp.
- Tutin TG, Akeroyd JR (1993) *Fagus* L. In: Tutin TG, Heywood VH, Burges NA, Valentine DH, Walters SM, Webb DA (Eds) *Flora Europaea*, Vol. 1: Lycopodiaceae to Platanaceae. - Cambridge University Press, Cambridge, 72 pp.
- Wei SJ, Li Q, van Achterberg K, Chen XX (2014) Two mitochondrial genomes from the families Bethyridae and Mutillidae: Independent rearrangement of protein-coding genes and

- higher-level phylogeny of the Hymenoptera. *Molecular Phylogenetics and Evolution* 77: 1–10. <https://doi.org/10.1016/j.ympev.2014.03.023>
- Wei SJ, Shi M, Sharkey MJ, van Achterberg C, Chen XX (2010) Comparative mitogenomics of Braconidae (Insecta, Hymenoptera) and the phylogenetic utility of mitochondrial genomes with special reference to holometabolous insects. *BMC Genomics* 11: 371. <https://doi.org/10.1186/1471-2164-11-371>
- Xu W, Yang T, Li ZH, Zhou P (2022) Distribution pattern of plant community species diversity along altitudinal gradients in Nanling mountains, Guangdong. *Forestry and Environmental Science* 38(1): 9–17. [in Chinese]
- Xue S, Zhang Y, Gao S, Lu S, Wang J, Zhang K (2020) Mitochondrial genome of *Trichagalma acutissimae* (Hymenoptera: Cynipoidea: Cynipidae) and phylogenetic analysis. *Mitochondrial DNA B* 5(1): 1073–1074. <https://doi.org/10.1080/23802359.2020.1721366>
- Yamauchi MM, Miya MU, Nishida M (2002) Complete mitochondrial DNA sequence of the Japanese spiny lobster *Panulirus japonicus* (Crustacea, Decapoda). *Gene* 295(1): 89–96. [https://doi.org/10.1016/s0378-1119\(02\)00824-7](https://doi.org/10.1016/s0378-1119(02)00824-7)
- Yang XH, Li XM, Zhu DH, Zeng Y, Zhao LQ (2021) The diversity and dynamics of fungi in *Dryocosmus kuriphilus* community. *Insects* 12(5): 426. <https://doi.org/10.3390/insects12050426>
- Zhong JL, Zhu DH (2022) Detection of two different mitochondrial genomes in a gall wasps species, *Andricus mairei* (Hymenoptera: Cynipoidea: Cynipidae). *Journal of Asia-Pacific Entomology* 25(4): 101987. <https://doi.org/10.1016/j.aspen.2022.101987>
- Zhu DH, He YY, Fan YS, Ma MY, Peng DL (2007) Negative evidence of parthenogenesis induction by *Wolbachia* in a gallwasp species, *Dryocosmus kuriphilus*. *Entomologia Experimentalis et Applicata* 124(3): 279–284. <https://doi.org/10.1111/j.1570-7458.2007.00578.x>

Supplementary material I

List of universal insect mitochondrial short fragments of the *cox1*, *cob*, *rrnL* and *D2* genes primers used for long PCR primer developments

Authors: Yu-Bo Duan, Yan-Jie Wang, Dao-Hong Zhu, Yang Zeng, Xiu-Dan Wang

Data type: docx

Copyright notice: This dataset is made available under the Open Database License (<http://opendatacommons.org/licenses/odbl/1.0/>). The Open Database License (ODbL) is a license agreement intended to allow users to freely share, modify, and use this Dataset while maintaining this same freedom for others, provided that the original source and author(s) are credited.

Link: <https://doi.org/10.3897/jhr.97.119433.suppl1>

Supplementary material 2

List of PCR primers used in this study

Authors: Yu-Bo Duan, Yan-Jie Wang, Dao-Hong Zhu, Yang Zeng, Xiu-Dan Wang

Data type: docx

Copyright notice: This dataset is made available under the Open Database License (<http://opendatacommons.org/licenses/odbl/1.0/>). The Open Database License (ODbL) is a license agreement intended to allow users to freely share, modify, and use this Dataset while maintaining this same freedom for others, provided that the original source and author(s) are credited.

Link: <https://doi.org/10.3897/jhr.97.119433.suppl2>

Supplementary material 3

List of PCR primers and sequencing primers used in this study

Authors: Yu-Bo Duan, Yan-Jie Wang, Dao-Hong Zhu, Yang Zeng, Xiu-Dan Wang

Data type: docx

Copyright notice: This dataset is made available under the Open Database License (<http://opendatacommons.org/licenses/odbl/1.0/>). The Open Database License (ODbL) is a license agreement intended to allow users to freely share, modify, and use this Dataset while maintaining this same freedom for others, provided that the original source and author(s) are credited.

Link: <https://doi.org/10.3897/jhr.97.119433.suppl3>

Supplementary material 4

Summary of taxonomic groups used in Fig. 8

Authors: Yu-Bo Duan, Yan-Jie Wang, Dao-Hong Zhu, Yang Zeng, Xiu-Dan Wang

Data type: docx

Copyright notice: This dataset is made available under the Open Database License (<http://opendatacommons.org/licenses/odbl/1.0/>). The Open Database License (ODbL) is a license agreement intended to allow users to freely share, modify, and use this Dataset while maintaining this same freedom for others, provided that the original source and author(s) are credited.

Link: <https://doi.org/10.3897/jhr.97.119433.suppl4>

Supplementary material 5

Pair-wise COI sequence distances in *Synergus*

Authors: Yu-Bo Duan, Yan-Jie Wang, Dao-Hong Zhu, Yang Zeng, Xiu-Dan Wang

Data type: docx

Copyright notice: This dataset is made available under the Open Database License (<http://opendatacommons.org/licenses/odbl/1.0/>). The Open Database License (ODbL) is a license agreement intended to allow users to freely share, modify, and use this Dataset while maintaining this same freedom for others, provided that the original source and author(s) are credited.

Link: <https://doi.org/10.3897/jhr.97.119433.suppl5>

Supplementary material 6

Predicted folding pattern for tRNAs of *Synergus nanlingensis* mitochondrial genome

Authors: Yu-Bo Duan, Yan-Jie Wang, Dao-Hong Zhu, Yang Zeng, Xiu-Dan Wang

Data type: docx

Copyright notice: This dataset is made available under the Open Database License (<http://opendatacommons.org/licenses/odbl/1.0/>). The Open Database License (ODbL) is a license agreement intended to allow users to freely share, modify, and use this Dataset while maintaining this same freedom for others, provided that the original source and author(s) are credited.

Link: <https://doi.org/10.3897/jhr.97.119433.suppl6>

Supplementary material 7

Maximum Likelihood tree were inferred from the datasets *COI* + *Cytb* + *28S-D2* using IQ-tree

Authors: Yu-Bo Duan, Yan-Jie Wang, Dao-Hong Zhu, Yang Zeng, Xiu-Dan Wang

Data type: doc

Copyright notice: This dataset is made available under the Open Database License (<http://opendatacommons.org/licenses/odbl/1.0/>). The Open Database License (ODbL) is a license agreement intended to allow users to freely share, modify, and use this Dataset while maintaining this same freedom for others, provided that the original source and author(s) are credited.

Link: <https://doi.org/10.3897/jhr.97.119433.suppl7>

Annotated checklist of the megachilid bees of Corsica (Hymenoptera, Megachilidae)

Romain Le Divelec^{1,2}, Alexandre Cornuel-Willermoz³,
Matthieu Aubert², Adrien Perrard^{4,5}

1 Laboratory of Zoology, Research Institute for Biosciences, University of Mons, Place du parc 20, 7000, Mons, Belgium **2** Observatoire des Abeilles, 68 rue du Onze Novembre, 59148, Flines-lez-Raches, France **3** Office de l'Environnement de la Corse, Observatoire Conservatoire des Invertébrés de Corse, 14 avenue Jean Nicoli, 20250, Corte, France **4** Institut d'Ecologie et des Sciences de l'Environnement de Paris, UMR 7618 CNRS, Sorbonne Université, INRAE, IRD, UPEC, 4 Place Jussieu, 75005 Paris, France **5** Université Paris Cité, 45 Rue des Saints-Pères, 75006 Paris, France

Corresponding author: Romain Le Divelec (romainledivelec@hotmail.fr)

Academic editor: C. K. Starr | Received 23 October 2023 | Accepted 9 February 2024 | Published 25 March 2024

<https://zoobank.org/7EC88083-162B-450D-AB00-2DAF559F8D3E>

Citation: Le Divelec R, Cornuel-Willermoz A, Aubert M, Perrard A (2024) Annotated checklist of the megachilid bees of Corsica (Hymenoptera, Megachilidae). Journal of Hymenoptera Research 97: 127–189. <https://doi.org/10.3897/jhr.97.114614>

Abstract

Corsica stands as one of the largest Mediterranean Islands and has been the exploration ground for renowned entomologists like Charles Ferton. However, no synthesis on Corsican bees has been published so far. To fill this gap in knowledge, we propose an overview of the megachilid bee fauna of the island based on fieldwork, a thorough examination of material housed at the Muséum national d'Histoire naturelle (MNHN, Paris), data compilation from various collections and a comprehensive review of existing literature. We reviewed 5,886 specimens and we extracted 279 additional data from literature sources. These data confirm the presence in Corsica of 91 species of which two are endemic, including *Hoplitis corsaria* (Warncke, 1991) which is elevated to species rank stat. nov. One new synonymy is established: *Megachile lucidifrons* Ferton, **syn. nov.** of *Megachile albocristata* Smith, 1853. The presence in Corsica of 19 species is regarded as dubious or erroneous. Finally, the types of Megachilid bees housed at MNHN and described based on Corsican material are illustrated. Lectotypes are designated for *Megachile sicula* var. *corsica* Benoist, 1935, *Osmia corsica* Ferton, 1901, *Osmia erythrogastra* Ferton, 1905, *Osmia lanosa* Pérez, 1879, and *Osmia lineola* Pérez, 1895.

Keywords

Anthophila, Apoidea, mediterranean islands

Introduction

Bees (Apoidea, Anthophila) are essential pollinators, given their pivotal role in pollinating a wide variety of plants and their high level of specialization and dependence on specific flora for both larval and adult nutrition (Willmer 2011). This diverse group encompasses approximately 20,000 species globally, classified into seven families: Andrenidae, Apidae, Colletidae, Halictidae, Mellitidae, Megachilidae, and Stenotritidae. Notably, bee biodiversity hotspots are concentrated in regions with Mediterranean and xeric climates, including the Mediterranean basin (Orr et al. 2021). Despite their ecological significance, recent efforts in compiling checklists have highlighted a significant knowledge gap regarding bee diversity in Mediterranean islands (e.g. Varnava et al. 2019; Nobile et al. 2021). Particularly, the fauna of the Corsican Island remains largely unexplored.

Spanning 8,722 km², Corsica ranks as the fourth-largest Mediterranean island. Its topography is dominantly shaped by expansive mountain ranges covering much of the land, with the highest peak reaching 2,710 m. The prevailing climate is largely Mediterranean, characterized by hot and arid summers, erratic rainfall patterns, and the potential for intense rain events in autumn and spring. However, at higher elevations, the climate takes on an alpine character, marked by lower temperatures (DREAL 2017). The varied elevation gradients contribute to a diverse range of habitats, encompassing coastal dune grasslands, elevated pine and beech forests, and various maquis or shrub thickets. This mosaic of habitats, coupled with Corsica's prolonged isolation from the mainland, fosters a rich array of fauna and flora, including numerous endemic species (Sabiani 2004).

The main investigations into Corsican wild bees occurred mainly from the late XIXth century to the early XXth century. During this period, Charles Ferton (1856–1921), a military professional stationed at the Bastion of Bonifacio from 1895 until his passing in 1921, published a series of notes and descriptions introducing new species (Ferton 1923). Starting in 1895, C. Ferton devoted considerable time observing and collecting wasps and bees in the Bonifacio area, although he also collected in other parts of the island. His extensive collection, now housed at the Muséum national d'Histoire naturelle (MNHN) in Paris, represents the largest collection of Corsican material. Additionally, C. Ferton published approximately thirty studies and notes on the diversity and behaviour of bees and wasps. Following Ferton's era, few surveys were conducted in Corsica. The literature on Corsican Anthophila is therefore particularly scarce, difficult to access and disjointed, often dealing only with a few isolated taxa. Only a handful of works have undertaken a comprehensive review of certain genera (Rasmont and Adamski 1995: Bumblebees; Terzo et al. 2007: *Ceratina* Latreille, 1802; Liongo Li Enkulu 1988: *Megachile* Latreille, 1802).

In 2016, a research initiative led by C. Villemant, C. Fontaine, and A. Perrard (MNHN) aimed to investigate mimicry in Aculeata communities in Bonifacio. This project marked the beginning of the restoration and examination of Corsican material from Ferton's collection. From 2016 onwards, extensive and collaborative sampling efforts resulted in an additional substantial influx of new data for the island, prompting the need for an updated checklist of Corsican bees, given the absence of synthesis works. For our first contribution to a comprehensive review of Corsican bees, we focused on the Megachilidae. The compilation of 65 publications suggests the presence

of up to 90 taxa in Corsica. Many of these records, however, are questionable or outdated, relying on unclear nomenclature or species concepts. Recognizing the significant disparity between modern and historical taxonomies, a thorough revision of these records was imperative. Based on a bibliographic synthesis and an extensive review of collection material we propose an updated checklist of Corsican Megachilidae.

Material and methods

Study of the collections housed at MNHN

The historical data presented in this article predominantly stem from the examination of Charles Ferton's collection. This material was initially stored in numerous boxes organized by locality and date within a distinct section of the MNHN collection (Fig. 1). It underwent labelling, taxonomic identification to the lowest level (species or subspecies), and digitization of the label data. The Corsican segment of Ferton's collection encompasses over 14,000 Aculeate specimens, including 2,038 Megachilidae specimens, constituting approximately one-third of his entire Aculeate collection. The remaining two-thirds primarily originates from Algeria and Mainland France. Ferton's collection also includes five handwritten books containing field trip details and observations (Figs 2, 3). Only the book for the years 1911–1920 is missing. An important part of his collection is directly linked to these manuscripts. Ferton's practice of annotating page numbers on original locality labels facilitated the connection between detailed observations in the manuscripts and the corresponding specimens in his collection. The final two manuscripts primarily focused on Corsica have been particularly helpful for encoding the data associated to the specimens by offering insights into collecting methods and localities. In addition to Ferton's collection, 337 Megachilidae specimens from Corsica were identified in various parts of the MNHN collections, including those of R. Benoist (material collected between 1920 and 1940), E. G. Dehaut (material collected by G. Bénard between 1909 and 1910), and J. Sichel (material collected in the 1860s without specifying localities). Several other collections, including those of J. Barbier, L. de Berland, J. Casewitz-Weulersse, J. de Gaulle, J. Hamon, S. Kelnert-Pillault, A. L. M. Lepeletier de Saint-Fargeau, and H. Nouvel, also contain a limited number of specimens from Corsica.

Recent sampling

The study of historical collections was completed by recent samplings conducted within three different programs by (1) A standardized sampling initiative aimed at exploring bee and wasp communities was undertaken in 2017. Monthly sampling occurred from March to November 2017 in seven localities of Bonifacio explored by C. Ferton, using active netting and bi-weekly pan-trapping following the Westphal protocol (Westphal et al. 2008). The collected material was deposited at MNHN and the collections of the Observatoire Conservatoire des Invertébrés de Corse (OCIC),



Figures 1–3. Collection and catalogue of C. Ferton **1** example of box housing unidentified specimens collected and mounted by C. Ferton **2** manuscript of C. Ferton with morphological notes **3** manuscript detailing observations about the nesting of some Megachilid bees (in red, additional information added by C. Ferton subsequent to the initial black draft).

branch of the Office de l'Environnement de la Corse (OEC). (2) Between 2019 and 2021, bees were collected for two to four weeks per year across the island in the context of the expedition “La Planète Revisitée (Our Planet Revisited)–Corsica 2019–2022,” organized by MNHN. Collection methods included hand nets, pan traps, and Malaise traps. The collected specimens were distributed among one of the authors (RLD), MNHN, and OCIC. A barcoding program initiated during LPR expeditions resulted in the creation of dataset DS-MEGA1, available on BOLD (www.barcodinglife.org),

featuring 89 barcoded specimens representing 51 species. (3) Since 2019, OCIC has undertaken a territorial actions plan for pollinators, including the Corsican Honeybee (Cornuel-Willermoz and Andrei-Ruiz 2021). Over the past three years, this program conducted multiple surveys in 144 localities, encompassing 67 towns, primarily using active netting, supplemented by pan traps and malaise traps. The collected specimens were distributed among one of the authors (ACW), and OCIC.

Additional data gathering

Additional data was also obtained from various sources, including literature review, other collections, and an online forum. The review of the literature was based on 66 published works and provided 279 original data of Corsican Megachilidae, ranging from the short mention '*Corsica*' to the complete data. We also obtained data from J. Mann's collection in the Naturhistorisches Museum, Vienna, data from various museums and private collections thanks to A. Müller, E. Dufrêne, G. Le Goff and P. Vignac. Finally, we used the data from "Le Monde des Insectes" website (<https://insecte.org/>), restricting our research to records with pictures, to confirm the specimen identification.

Conventions of the checklist

We present the resulting data as an annotated checklist in which species are sorted by tribe and by genus. Under each species name are listed the literature records. These mentions include the original name used in the publication, the bibliographic reference, as well as the published localities. Additional comments are presented between square brackets. A question mark means that it was not possible to assign a record with confidence to a species. We used an asterisk (*) to highlight taxa for which Corsican data are reported for the first time in this study.

The original data we compiled for each species comprise the number of examined specimens (sorted by sex, 'NS' is indicated when sex is unknown), the collecting period and the list of municipalities. Detailed records were uploaded online in ten datasets on Cardobs (<https://cardobs.mnhn.fr/>) (IDs: 884FEA17-4810-3B88-E053-5014A8C0FB66, 87FCFAFA-BC57-0572-E053-5014A8C04A0C, 90768076-0CF5-15F2-E053-5014A8C08F4A, A766A82F-BE8D-556D-E053-2614A8C0C12D, BF62B36D-1D84-2F86-E053-3014A8C0EFF8, E4C9E0B0-B16B-04D9-E053-3014A8C043D8, EB611548-937C-63F5-E053-0514A8C02064, EB6380B5-805D-5935-E053-0514A8C08744, EFF30F3C-ACD5-6B6E-E053-0514A8C0121F, EFA34354-3736-7BE7-E053-0514A8C00AD2). They can be consulted and downloaded on the Openobs data portal (<https://openobs.mnhn.fr/>) and MNHN data portal (<https://science.mnhn.fr/>). Special attention is given to type material (last section) for which complete label data are cited. Different labels are separated by a double slash. Additional information on labels is given between square brackets. Sex of the types is provided before the label information.

The specimens examined in this study are summarized in Table 1. To assess the species richness of the island, we compared these data to the checklists of the three largest

Table 1. Numbers of examined specimens by species in decreasing order.

Tribe	Species	N	Tribe	Species	N
Megachilini	<i>Megachile argentata</i>	535	Osmiini	<i>Hoplitis praestans</i>	33
Osmiini	<i>Heriades crenulata</i>	512	Anthidiini	<i>Anthidium cingulatum</i>	29
Osmiini	<i>Osmia caeruleascens</i>	331	Megachilini	<i>Coelioxys inermis</i>	28
Osmiini	<i>Hoplitis corsaria</i>	265	Osmiini	<i>Hoplitis fasciculata</i>	24
Megachilini	<i>Megachile sicula</i>	257	Anthidiini	<i>Icteranthidium laterale</i>	23
Anthidiini	<i>Anthidiellum strigatum</i>	251	Anthidiini	<i>Anthidium florentinum</i>	21
Osmiini	<i>Heriades rubicola</i>	203	Osmiini	<i>Chelostoma rapunculi</i>	21
Osmiini	<i>Hoplitis anthocopoides</i>	186	Osmiini	<i>Osmia emarginata</i>	19
Osmiini	<i>Hoplitis bisulca</i>	167	Megachilini	<i>Megachile ericetorum</i>	18
Osmiini	<i>Osmia niveata</i>	167	Osmiini	<i>Osmia erythrogastra</i>	18
Osmiini	<i>Osmia rufobirta</i>	163	Anthidiini	<i>Pseudoanthidium melanurum</i>	16
Osmiini	<i>Hoplitis bihatata</i>	152	Megachilini	<i>Megachile rotundata</i>	14
Anthidiini	<i>Anthidium taeniatum</i>	142	Osmiini	<i>Hoplitis manicata</i>	14
Anthidiini	<i>Rhodanthidium septemdentatum</i>	117	Lithurgini	<i>Lithurgus chrysurus</i>	13
Osmiini	<i>Osmia ligurica</i>	116	Megachilini	<i>Coelioxys brevis</i>	13
Megachilini	<i>Megachile melanopyga</i>	112	Megachilini	<i>Megachile albocristata</i>	13
Osmiini	<i>Osmia bicornis bicornis</i>	107	Anthidiini	<i>Stelis nasuta</i>	12
Osmiini	<i>Osmia ferruginea</i>	100	Megachilini	<i>Coelioxys conoideus</i>	12
Megachilini	<i>Coelioxys afer</i>	98	Megachilini	<i>Coelioxys mandibularis</i>	12
Megachilini	<i>Megachile centuncularis</i>	89	Osmiini	<i>Osmia nasoproducta</i>	12
Osmiini	<i>Hoplitis adunca</i>	89	Osmiini	<i>Hoplitis tridentata</i>	11
Osmiini	<i>Osmia versicolor</i>	87	Anthidiini	<i>Anthidium oblongatum</i>	9
Osmiini	<i>Hoplitis cristatula</i>	82	Dioxyini	<i>Dioxyus cinctus</i>	9
Osmiini	<i>Osmia latreillei</i>	82	Megachilini	<i>Coelioxys acanthura</i>	8
Megachilini	<i>Megachile albisecta</i>	78	Anthidiini	<i>Stelis signata signata</i>	7
Osmiini	<i>Osmia submicans</i>	67	Megachilini	<i>Megachile deceptoria</i>	7
Osmiini	<i>Hoplitis aff. adunca</i>	61	Anthidiini	<i>Stelis murina</i>	6
Megachilini	<i>Megachile leachella</i>	59	Megachilini	<i>Coelioxys haemorrhoea</i>	6
Osmiini	<i>Hoplitis leucomelana</i>	58	Osmiini	<i>Chelostoma foveolatum</i>	6
Osmiini	<i>Chelostoma distinctum</i>	57	Osmiini	<i>Osmia cornuta cornuta</i>	6
Megachilini	<i>Megachile apicalis</i>	54	Anthidiini	<i>Stelis ornata ornata</i>	4
Osmiini	<i>Osmia signata signata</i>	54	Dioxyini	<i>Aglaopis tridentata</i>	4
Anthidiini	<i>Anthidium manicatum</i>	52	Anthidiini	<i>Stelis punctulatisima</i>	3
Osmiini	<i>Heriades truncorum</i>	50	Megachilini	<i>Megachile burdigalensis</i>	3
Osmiini	<i>Hoplitis perezii</i>	50	Megachilini	<i>Megachile versicolor</i>	3
Megachilini	<i>Megachile pusilla</i>	49	Anthidiini	<i>Stelis minuta</i>	2
Anthidiini	<i>Stelis breviscula</i>	47	Lithurgini	<i>Lithurgus cornutus</i>	2
Anthidiini	<i>Pseudoanthidium stigmaticorne</i>	43	Megachilini	<i>Coelioxys obtusus</i>	2
Osmiini	<i>Hoplitis acuticornis</i>	43	Osmiini	<i>Hoplitis ravouxi</i>	2
Osmiini	<i>Osmia aurulenta</i>	38	Osmiini	<i>Osmia melanogaster</i>	2
Osmiini	<i>Osmia scutellaris</i>	38	Anthidiini	<i>Icteranthidium grohmanni</i>	1
Osmiini	<i>Osmia tricornis</i>	37	Megachilini	<i>Coelioxys aurolimbatus</i>	1
Anthidiini	<i>Pseudoanthidium nanum</i>	36	Osmiini	<i>Osmia anceyi</i>	1
Megachilini	<i>Megachile lagopoda</i>	34	Osmiini	<i>Protosmia minutula</i>	1

mediterranean islands in Table 2: Sardinia, Sicily and Cyprus (Comba 2019; Varnava et al. 2020; Nobile et al. 2021; personal communication with Maurizio Cornalba). In order to estimate the completeness of our sampling effort of the Corsican Megachilid fauna, we used the Chao1 and abundance-based coverage estimators (ACE) (Chao 1984; Chao and Lee 1992; Colwell and Coddington 1994).

Table 2. Megachilidae diversity of the four largest Mediterranean islands.

Island	Corsica	Sardinia	Sicily	Cyprus
Size (km ²)	8722	24090	25711	9251
Genera	17	15	17	15
Species	91	91	129	91
Endemic/subendemic species	2(3*)	2(3*)	3	3
<i>Aglaopis</i>	1	1	0	0
<i>Anthidiellum</i>	1	1	1	2
<i>Anthidium</i>	5	3	8	5
<i>Chelostoma</i>	3	1	5	3
<i>Coelioxys</i>	10	8	14	12
<i>Dioxys</i>	1	2	3	2
<i>Eoanthidium</i>	0	0	0	1
<i>Heriades</i>	3	3	4	4
<i>Hoplitis</i>	15	15	19	9
<i>Icteranathidium</i>	2	0	2	2
<i>Lithurgus</i>	2	3	3	2
<i>Megachile</i>	15	18	20	17
<i>Osmia</i>	19	25	32	25
<i>Protosmia</i>	1	0	3	3
<i>Pseudoanthidium</i>	3	3	3	0
<i>Rhodanthidium</i>	2	2	3	1
<i>Stelis</i>	7	4	7	3
<i>Stenoheriades</i>	0	0	1	0
<i>Trachusa</i>	1	2	1	0

* including the undescribed *Hoplitis aff. adunca* mentioned in the present catalogue.

Results and discussion

Our synthesis is based on the examination of 5886 specimens (Table 1) and 279 data from the literature. It confirms the presence in Corsica of 91 species of Megachilidae, belonging to 17 different genera. Among them, twenty species and two genera are newly recorded in Corsica. Modern records are provided for 29 species which were only known from historical records. We could not get modern data for five species and further research is needed to clarify their presence in the island. Finally, the presence in Corsica of 19 species is regarded as dubious or erroneous.

It is noteworthy to highlight that *Megachile sculpturalis* Smith, 1853, an invasive Megachilid bee, has not been recorded in Corsica so far. This species arrived in France in 2008 (Vereecken and Barbier 2009) and is now widespread in a large part of Europe. It was recently found in Elba Island (Italy), only 50 km from Corsica (Ruzzier et al. 2020).

Based on our sample data, we found a Chao1 of 92.6 and an ACE of 92.955. Both estimators suggest that we detected most of the Megachilid species in the explored parts of the island. Additional efforts in the explored part may therefore result in few additional species for the checklist. However, the distribution of the data is uneven (Fig. 4) as Megachilidae data were available for only 131 of the 360 Corsican municipalities. Well-sampled sectors include Bonifacio, due to the Fertton data and the 2017 study, Vivario, and the coastline. These three areas concentrate a large proportion of the data. Under-sampled areas include the northwest (Cap Corse and Castagniccia region) and a

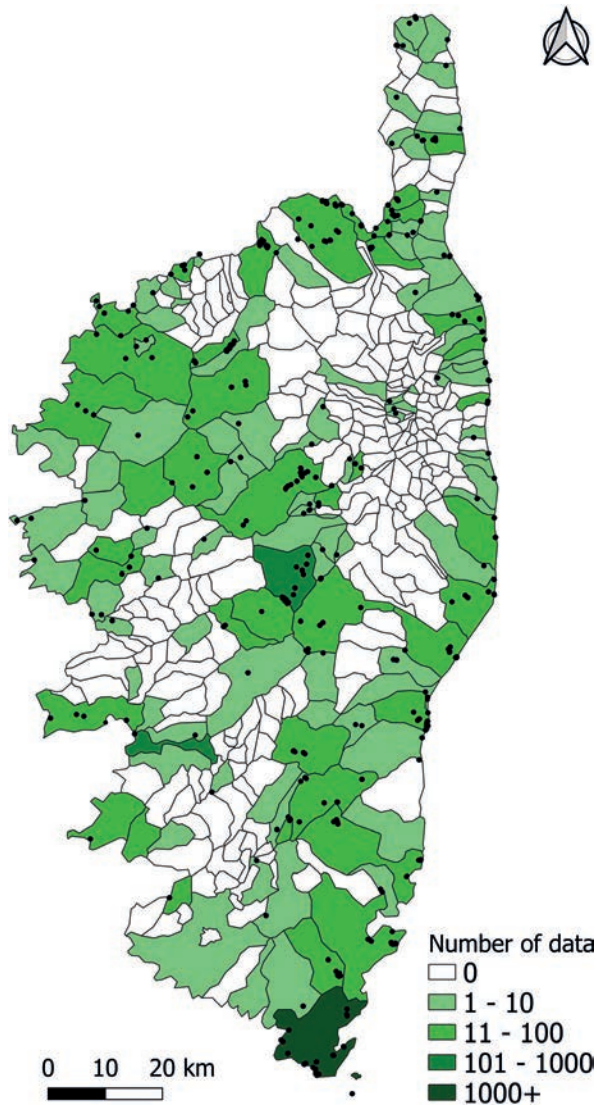


Figure 4. Distribution of the data in the different Corsican municipalities. Black dots are collecting stations with geographical coordinates. Municipalities for which we have imprecise collecting localities are highlighted in green (based on the quantity of data available).

large part of the southwest (Liamone and Taravo regions) probably due to the difficulty to access these rather remote regions. It is therefore possible that a few other species may be found in these areas. As such, the Territorial Actions Plan for wild pollinators defines these sectors as priority targets for more extensive inventories in the coming years.

In comparison to Megachilidae checklists from larger Mediterranean islands, Corsica exhibits notably high species richness (Table 2). Currently, only Sicily surpasses Corsica in Megachilidae diversity. This discrepancy can be attributed to the considerably larger size of Sicily and its proximity to the mainland, facilitating the establishment

of new species from the continent. Conversely, despite being almost 2.76 times larger than Corsica, Sardinia displays a similar species richness. Since Corsica and Sardinia are very close islands, it is not surprising to find a similar diversity. However, their fauna is not entirely overlapping, possibly due to their different geological histories and the different habitats found in the two islands. Notably, mountainous habitats such as alpine grasslands are present in Corsica but not in Sardinia. Additionally, most bees sampling effort in Sardinia seem to have been restricted to the north-western part of the island, with only a few sites which have been recently sampled in the rest of the island (Floris et al. 2000; Quaranta et al. 2004; Nobile et al. 2021). It is therefore likely that this similarity in diversity between Sardinia and Corsica roots from a lack of knowledge on the Megachilidae fauna of the larger island.

Below, we list the species present in Corsica, along with the dubious and erroneous records and the Corsican type material housed at MNHN. This checklist confirmed the expected high diversity of Megachilidae in Corsica and call for similar efforts to address the local diversity of the other bee families.

Checklist of the Corsican Megachilidae

Anthidiini Ashmead, 1899

***Anthidiellum* Cockerell, 1904**

1. *Anthidiellum strigatum strigatum* (Panzer, 1805)

Anthidium strigatum Panzer; Ferton (1901b: 92, 146): Bonifacio.

Anthidiellum strigatum (Panzer); Pagliano (1994: 392): Sotta.

Anthidiellum strigatum (Panzer); Kasperek (2022: 79): Corsica.

Material examined. 78♀, 165♂ & 8NS observed from April to October, between 1895 and 2021 in Albertacce, Aléria, Barbaggio, Asco, Bastelica, Bastia, Biguglia, Bonifacio, Calvi, Canale-di-Verde, Castellare-di-Casinca, Corbara, Corte, Coti-Chiavari, Evisa, Farinole, Figari, Furiani, Ghisonaccia, Ghisoni, Grosseto-Prugna, Lecci, Levie, Linguizzetta, Lucciana, Manso, Mausoléo, Ogliastro, Oletta, Olmi-Cappella, Palasca, Patrimonio, Penta-di-Casinca, Poggio-d'Oletta, Porto-Vecchio, Propriano, Quenza, Rospigliani, Saint-Florent, Santo-Pietro-di-Tenda, Sartène, Sorbollano, Tavera, Valle-di-Campoloro, Ventiseri, Vescovato, Vico, Vivario, Zicavo and Zonza.

***Anthidium* Fabricius, 1804**

2. *Anthidium cingulatum* Latreille, 1809

Anthidium cingulatum Latreille; Nadig and Nadig (1934: 27): Monte d'Oro.

Anthidium cingulatum Latreille; Warncke (1981: 335, Map 29): Corsica.

Anthidium cingulatum Latreille; Kasperek (2022: 93): Corsica.

Material examined. 13♀ & 16♂ observed from May to October between 1900 and 2022 in Balogna, Bocognano, Bonifacio, Corte, Ghisoni, La Porta, Lumio, Mausoléo, Nocario, Palasca, Quenza, Sisco, Talasani, Vivario and Zona.

3. *Anthidium florentinum* (Fabricius, 1775)*

Material examined. 15♀ & 6♂ observed from June to September between 2002 and 2022 in Ajaccio, Albertacce, Calacuccia, Castellare–di–Casinca, Lucciana, Propriano, Quenza, San-Giuliano, Talasani and Vico.

4. *Anthidium manicatum manicatum* (Linnaeus, 1758)

Anthidium manicatum Linnaeus; Ferton (1909a: 551–552): Bonifacio.

Anthidium manicatum (Linnaeus); Pagliano (1994: 396): Sotta.

Anthidium manicatum (Linnaeus); Kasperek (2022: 106): Corsica.

Anthidium manicatum (Linnaeus); Meunier et al. (2023): Corsica.

Material examined. 29♀ & 23♂ observed from May to October, between 1897 and 2021 in Aléria, Barbaggio, Bastelica, Bonifacio, Calacuccia, Casamaccioli, Castellare–di–Casinca, Corte, Ghisoni, Grosseto–Prugna, Lumio, Mausoléo, Meria, Palasca, Quenza, Santa–Maria–Poggio, Riventosa, Sisco, Tavera, Vivario and Zona.

5. *Anthidium oblongatum oblongatum* (Illiger, 1806)*

Material examined. 1♀ & 8♂ observed from June to July, between 2019 and 2021 in Bocognano, Casamaccioli, Quenza, Solaro and Zona.

6. *Anthidium taeniatum* Latreille, 1809*

Material examined. 45♀ & 97♂ observed from May to September, between 1895 and 2021 in Ajaccio, Bonifacio, Linguizzetta, Lucciana, Mausoléo, Patrimonio, Penta–di–Casinca, Prunelli–di–Fiumorbo, Sermano, Soveria, Talasani and Zona.

Icteranthidium Michener, 1948

7. *Icteranthidium grobmanni* (Spinola, 1838)

Icteranthidium grobmanni (Spinola); Pagliano (1994: 395): Col de Celaccia.

Icteranthidium grobmanni (Spinola); Kasperek (2022: 163): Corsica.

Material examined. 1♂ observed in September 2020 in Tavera.

8. *Icteranthidium laterale laterale* (Latreille, 1809)

Anthidium laterale Latreille; Stöckl (2000: 276): Corsica.

Icteranthidium laterale (Latreille); Kasperek (2022: 165): Corsica.

Material examined. 13♀ & 10♂ observed from July to September, between 1896 and 2022 in Balogna Bonifacio, Ghisoni, Rospigliani, Santo–Pietro–di–Venaco, Tavera, Vico and Vivario.

Pseudoanthidium Friese, 1898

9. *Pseudoanthidium melanurum* (Klug, 1832)

Pseudoanthidium melanurum (Klug); Kasperek (2022: 188): Corsica.

Material examined. 4♀ & 12♂ observed from May to June, between 2017 and 2020 in Borgo, Castellare–di–Casinca, Penta–di–Casinca and Venzolasca.

10. *Pseudoanthidium nanum* (Mocsáry, 1880)

? *Pseudoanthidium lituratum* (Panzer); Pagliano (1994: 398): Bastia.

Pseudoanthidium nanum (Mocsáry); Litman et al. (2021): Ajaccio, Bonifacio, Lecci, Sartène, Zicavo, Albertacce, Corte, Ghisoni, Lozzi, Palasca, Vivario.

Pseudoanthidium nanum (Mocsáry); Kasperek (2022: 191): Corsica.

Material examined. 21♀ & 15♂ observed from May to October, between 1901 and 2022 in Albertacce, Balogna, Bonifacio, Calacuccia, Corte, Coti–Chiavari, Ghisoni, Grosseto–Prugna, Mausoléo, Montegrosso, Palasca, Renno, Sartène, Ventiseri, Vivario and Zicavo.

Remark. *Pseudoanthidium nanum* has long been a challenging species complex before the revision of Litman et al. (2021). Two species of this complex occur in Corsica. It is therefore not possible to assign the record of Pagliano (1994) to one of these two species with confidence. Our data, partially published in Litman et al. (2021), confirmed the presence of this taxon in Corsica.

11. *Pseudoanthidium stigmaticorne* (Dours, 1873)

Anthidium lituratum Latr.; Pérez (1879: 213) [Misidentification]: Corsica.

Anthidium lituratum Latr.; Ferton (1901b: 88): Corsica.

Anthidium lituratum Latr. (= *peregrinum* Costa); Ferton (1909a: 552–553, 575, 578) [Misidentification]: Pianottoli–Caldarello.

Pseudoanthidium scapulare (Latreille); Scheuchl and Willner (2016: 791) [Misinterpretation of the record of Ferton (1909a)]: Corsica.

Pseudoanthidium stigmaticorne (Dours); Litman et al. (2021): Ajaccio, Bonifacio, Pianottoli–Caldarello, Propriano.

Pseudoanthidium stigmaticorne (Mocsáry); Kasperek (2022: 198): Corsica.

Material examined. 19♀ & 24♂ observed from May to September, between 1897 and 2019 in Ajaccio, Bonifacio, Pianottoli-Caldarello and Propriano.

Rhodanthidium Insensee, 1927

12. *Rhodanthidium septemdentatum* (Latreille, 1809)

Anthidium septemdentatum Latreille; Ferton (1909a: 551): Bonifacio.

Anthidium septemdentatum Latreille; Nadig and Nadig (1934: 26): Cap Corse.

Anthidium septemdentatum Latreille; Kusdas (1974: 160): Calvi.

Rhodanthidium septemdentatum (Latreille); Kasperek (2022: 223): Corsica.

Material examined. 51♀, 64♂ & 2NS observed from April to July, between 1895 and 2021 in Ajaccio, Bonifacio, Calacuccia, Castellare–di–Casinca, Chisa, Corte, Farinole, Galéria, Grosseto–Prugna, L'Île Rousse, Mausoléo, Palasca, Patrimonio, Pianottoli-Caldarello, Porri, Porto–Vecchio, Santa–Maria–Poggio, Riventosa, Santo–Pietro–di–Tenda, Sotta, Ventiseri, Venzolasca, and Zona.

13. *Rhodanthidium sticticum* (Fabricius, 1787)

Rhodanthidium sticticum (Fabricius); Kasperek and Lhomme (2019: 44): Porto–Vecchio.

Rhodanthidium sticticum (Fabricius); Kasperek (2022: 228): Corsica.

Remark. There is only one record from 1976 (Kasperek and Lhomme 2019). No modern record is known.

Stelis Panzer, 1806

14. *Stelis breviscula* Nylander, 1841*

Material examined. 19♀ & 28♂ observed from May to October, between 1895 and 2021 in Ajaccio, Asco, Bonifacio, Casaglione, Farinole, Figari, Galeria, Grosseto–Prugna, Ogliastro, Oletta, Olmi–Cappella, Palasca, Patrimonio, Porto–Vecchio, Propriano, Riventosa, Saint–Florent, Santo–Pietro–di–Tenda, Sisco, Sorbollano, Urtaca and Ventiseri.

15. *Stelis minuta* Lepeletier, 1825*

Material examined. 1 ♀ & 1 ♂ collected in 1909 in Ghisonaccia and Porto-Vecchio.

Remark. No modern record.

16. *Stelis murina* Pérez, 1884

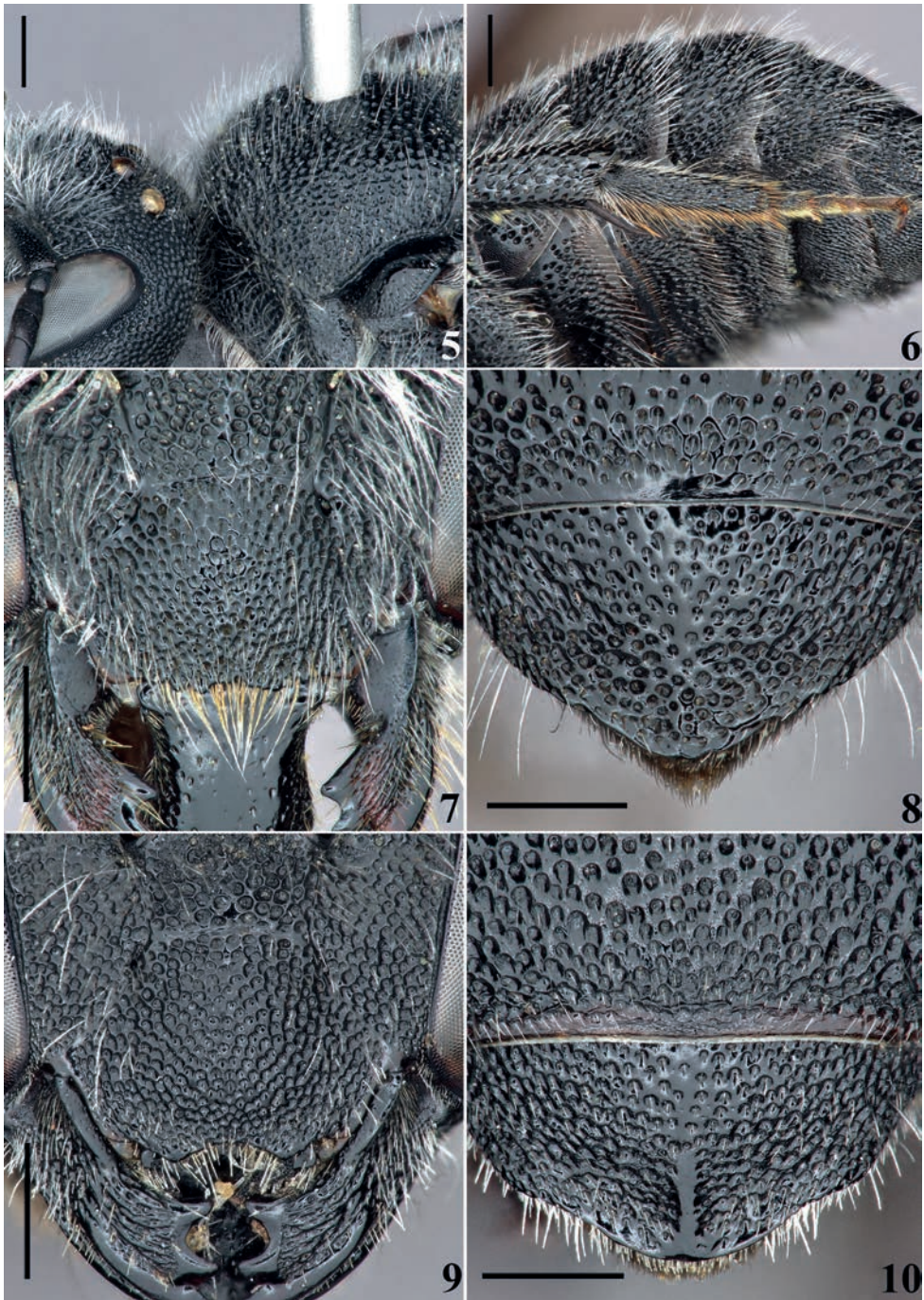
Figs 5–8

Stelis phaeoptera murina Pérez; Warncke (1992b: 356): Corsica.

Stelis phaeoptera (Kirby); Scheuchl and Willner (2016: 835): [quoting Warncke (1992b)].

Material examined. 2 ♀ & 4 ♂ observed from June to July, between 2019 and 2021 in Ghisoni, Mausoléo and Sisco.

Remark. Baker (1999) noted that the type material housed at MNHN does not include European specimens but only North African material in contradiction to the original description which also specifies material from France and Spain. The unpublished catalogue of Pérez mentions specimens from Bizerte (Tunisia) and La Chiffa (Algeria). Warncke (1992b) designated one of the females from Bizerte as lectotype. Blüthgen (1930) already noted that the original description of Pérez did not match well with a syntype he examined. As a matter of fact, the modern species concept of *S. murina* (Warncke 1992b; Baker 1999; Aguib et al. 2014; Kasperek 2015) does not match with its lectotype and paralectotypes (coll. Pérez, MNHN). The specimens from Corsica are similar to the types of *S. murina* (including lectotype). Both females and males of *S. murina* are hardly distinguishable from *S. phaeoptera* (Kirby, 1802). They can be distinguished from it by their entirely pure white pilosity (Figs 5, 6) [dirty white to brown in *S. phaeoptera*, notably darker on the vertex and mesoscutum], except on the inferior side of the tarsi where it is dark brown (Fig. 6) [yellow gold in *S. phaeoptera*, see fig. 7 in Aguib et al. 2014] and by their dark brown to black tibial spurs (Fig. 6) [ochreous in *S. phaeoptera*, see fig. 7 in Aguib et al. 2014]. Finally, the barcode generated for the Corsican *S. murina* matches that of Moroccan specimens and is highly divergent from the European sequences of *S. phaeoptera* available in BOLD (Le Divelec and Wood unpublished). A detailed review of this species group is required. Considering that *S. murina* sensu modern authors occurs in Crete (Le Divelec unpublished) and that it matches the original description of *S. murina cretica* Mavromoustakis, 1963, it should most probably be referred to as *S. cretica*. Unfortunately, the types of *S. murina cretica* could not be located in Mavromoustakis collection and are seemingly lost (Santerre pers. comm.). Non-type specimens from Crete identified by Mavromoustakis as *S. murina cretica* are preserved in his collection and are morphologically similar to *S. murina* sensu modern authors. The female of *S. cretica* can be easily distinguished from that of *S. murina* by the widely notched apical margin of the clypeus (Fig. 9) [with straight indentation in *S. murina* (Fig. 7)] and by the conspicu-



Figures 5–10. Comparative illustrations of *Stelis murina* Pérez and *Stelis cretica* Mavromoustakis (= *Stelis murina* sensu modern authors) **5–8** *Stelis murina* (from Corsica) **9, 10** *Stelis cretica* (from Crete) **5** pilosity of vertex and mesonotum **6** hind leg **7, 9** face **8, 10** tergum 6. Scale bars: 0.5 mm.

ous smooth medio-apical ridge on the last tergum (Fig. 10) [uniformly punctate in *S. murina* (Fig. 8)]. The male of *S. cretica* can be recognized by a notch bordered by a pair of teeth in the middle of the fourth sternum posterior margin (see fig. 4 in Aguib et al. 2014) [here with a conspicuous rake in *S. murina*, as in fig. 8 in Aguib et al. 2014].

BOLD process ID. LPRCW173-19 (BIN, BOLD:AEC2025).

17. *Stelis nasuta* (Latreille, 1809)

Material examined. 6♀ & 6♂ observed from May to June, between 1902 and 2020 in Asco, Bonifacio and Mausoléo.

Remark. The whitish light drawings of Corsican individuals are remarkably reduced if not absent.

18. *Stelis ornatula ornatula* (Klug, 1807)*

Material examined. 2♀ & 2♂ observed from June to July, between 1909 and 2020 in Palasca, Patrimonio, Sorbollano and Vico.

19. *Stelis punctulatissima punctulatissima* (Kirby, 1802)*

Material examined. 2♀ & 1♂ collected in June 2020 in Lucciana.

20. *Stelis signata signata* (Latreille 1809)*

Material examined. 3♀ & 4♂ observed from May to September, between 1974 and 2021 in Galeria, Ghisonaccia, Ghisoni, Manso, Oletta, Rospigliani and Ventiseri.

***Trachusa* Panzer, 1804**

21. *Trachusa byssina* (Panzer, 1798)

Trachusa byssina (Panzer); Kasperek (2022: 238): Corsica.

Remark. There is only one Corsican record (Kasperek 2022).

Dioxyini Cockerell, 1902

Aglaoapis* Cameron, 1901

21. *Aglaoapis tridentata* (Nylander, 1848)*

Material examined. 4♀ observed from June to September, between 2020 and 2021 in Ghisoni.

Remark. The morphology of the Corsican specimens is slightly different than that of the West palearctic specimens. The Corsican population might represent a distinct species. It was only observed in the Mountains where it seems to be very rare.

***Dioxys* Lepeletier & Serville, 1825**

22. *Dioxys cinctus* (Jurine, 1807)

Dioxys cincta Jurine; Friese (1895: 109): Corsica.

Dioxys cinctus (Jurine); Bogusch (2023, Fig. 8): Corsica.

Material examined. 4♀ & 5♂ observed from May to June, between 1902 and 2021 in Bonifacio, Ghisonaccia, Oletta, Porto–Vecchio and Ventiseri.

Lithurgini Newman, 1834

***Lithurgus* Berthold, 1827**

23. *Lithurgus chrysurus* Fonscolombe, 1834

Lithurge chrysurus Fonscolombe; Canovai et al. (2000: 78): Corsica.

Material examined. 9♀ & 4♂ observed from June to August, between 2003 and 2022 in Balogna, Canale–di–Verde, Coti–Chiavari, Mausoléo, Noceta, Rutali and Vico.

24. *Lithurgus cornutus fuscipennis* Lepeletier, 1841

Lithurgus cornutus (Fabricius); Dufrière et al. (2016: 18): Corsica.

Material examined. 2♀ observed from August to September, between 2020 and 2021 in Asco and Tavera.

Megachilini Latreille, 1802

***Coelioxys* Latreille, 1809**

25. *Coelioxys acanthura* (Illiger, 1806)

Coelioxys acanthura (Illiger); Ferton (1901b: 92): Bonifacio.

Coelioxys acanthura (Illiger); Warncke (1992a: 57): Corsica.

Coelioxys acanthura (Illiger); Pagliano (1994: 375): Algajola.

Material examined. 4♀ & 4♂ observed from June to August, between 1898 and 2021 in Bonifacio, Calvi, Coti–Chiavari, Palasca, Prunelli–di–Fiumorbo and Rutali.

26. *Coelioxys afer* Lepeletier, 1841

Coelioxys afer Lepeletier; Pagliano (1994: 375): Bastia.

Material examined. 53♀ & 45♂ observed from April to November, between 1895 and 2021 in Bonifacio, Evisa, Figari, Galeria, Grosseto–Prugna, Oletta, Palasca, Porto–Vecchio, Quenza, Saint–Florent, Santo–Pietro–di–Tenda, Sermano, Soveria, Talasani, Vero, Vescovato, Vivario, Zicavo and Zona.

27. *Coelioxys aurolimbatus aurolimbatus* Förster, 1853*

Material examined. 1♂ collected in July 2019 in Mausoléo.

Remark. This species is known from only one mountainous station.

28. *Coelioxys brevis* Eversmann, 1852

Coelioxys brevis Eversmann; Warncke (1992a: 53): Serra–di–Ferro, Linguizzetta.

Material examined. 8♀ & 5♂ observed from May to July, between 1972 and 2021 in Aléria, Ghisonaccia, Linguizzetta, Palasca, Solaro, Tallone and Ventiseri.

29. *Coelioxys conoideus* (Illiger, 1806)*

Material examined. 3♀ & 9♂ observed from July to September, between 1897 and 2019 in Cozzano, Mausoléo and Vivario.

Remark. This species has only been collected in mountains.

30. *Coelioxys echinatus* Förster, 1853

Coelioxys rufocaudatus Smith; Nadig and Nadig (1934: 62): Cap Corse.

Coelioxys echinata Förster; Warncke (1992a: 62): Corsica.

Remark. We could not confirm the occurrence of *C. echinatus* in Corsica. This species has been recorded twice in the past. It is unlikely to be confused with any other species, but we cannot exclude a confusion with *C. brevis*. We believe these records to be accurate for now.

31. *Coelioxys haemorrhhoa haemorrhhoa* Förster, 1853

Coelioxys haemorrhhoa Förster; Le Divelec and Dufrêne (2020: 6): Bonifacio.

Material examined. 3♀ & 3♂ observed from the end of May to September, between 1895 and 2017 in Bonifacio and Venzolasca.

32. *Coelioxys inermis* (Kirby, 1802)

Coelioxys acuminata Nylander; Ferton (1909a: 551): Bonifacio.

Coelioxys inermis (Kirby); Warncke (1992a: 65): Corsica.

Material examined. 10♀ & 18♂ observed from May to November, between 1896 and 2022 in Ajaccio, Asco, Balogna, Bonifacio, Corte, Evisa, Poggio-di-Venaco, Rospigliani, Vivario and Zonza.

33. *Coelioxys mandibularis* Nylander, 1848*

Material examined. 7♀ & 5♂ observed from May to October, between 2009 and 2021 in Bonifacio, Ghisonaccia, Levie, Mausoléo, Moncale, Olmi-Cappella, Palasca and Quenza.

34. *Coelioxys obtusus* Pérez, 1884*

Material examined. 1♀ & 1♂ observed in July 2019 in Palasca.

Megachile Latreille, 1802

35. *Megachile albisecta* (Klug, 1817)

Megachile sericans Fonscolombe; Ferton (1901b: 90–92, 145): Bonifacio.

Megachile albisecta Klug in Germar; Benoist (1940: 47): Corsica.

Creightonella albisecta (Klug); Liongo Li Enkulu (1988, Map 19): Corsica.

Creightonella albisecta (Klug); Pagliano (1994: 370): Sotta.

Material examined. 34♀ & 44♂ observed from June to September, between 1896 and 2022 in Balogna, Bonifacio, Coti-Chiavari, Ghisoni, Manso, Omessa, Palasca, Patrimonio, Piana, Propriano, Rospigliani, Rutali, Serra-di-Ferro and Vico.

36. *Megachile albocristata* Smith, 1853

Figs 39–42

Megachile (Chalicodoma) lucidifrons sp. nov.; Ferton (1905: 57–58): Bonifacio.

Megachile (Chalicodoma) lucidifrons Ferton; Ferton (1909b: 407): Bonifacio.

Chalicodoma albocristata Smith; Liongo Li Enkulu (1988, Map 20): Cap Corse.

Chalicodoma lucidifrons Ferton; Liongo Li Enkulu (1988, Map 44) [quoting Ferton (1905)].

Material examined. 9♀ & 4♂ observed from June to July, between 2019 and 2022 in Asco, Mausoléo, Santo-Pietro-di-Venaco, Sermano and Sisco.

Ecology. The ecology of *Megachile albocristata* is poorly known. The specimens were all observed in mountainous regions, specifically on sun-exposed rocky slopes covered with scrub vegetation (Fig. 11). These habitats featured prominent fractured rock formations and scree slopes where numerous individuals were observed in flight. During our investigations, we chanced upon a concealed nest beneath a boulder, situated within a cavity (Fig. 12). The layer (Fig. 13) covering the cells of the nest consist of a composite material comprising vegetable paste and ground gravels that the female takes great care to calibrate. The nesting behavior of *M. albocristata* appears to closely resemble that of *M. lefebvrei*, as detailed by Ferton (1909a: 544–547). It has been observed by Ferton on *Teucrium maritimum* (Lamiaceae). We observed this species visiting flowers of *Teucrium* in Mausoléo.

Remark. In Corsica, *M. albocristata* was previously known from only one uncertain historical record (Liongo Li Enkulu 1988). Our observations thus confirm the presence of this taxon in Corsica.

37. *Megachile apicalis* Spinola, 1808

Megachile apicalis Spinola; Ferton (1909a: 550): Bonifacio.

Megachile apicalis Spinola; Nadig and Nadig (1934: 26): Cap Corse.

Megachile apicalis Spinola; Liongo Li Enkulu (1988, Map 23): Corsica.

Material examined. 39♀ & 15♂ observed from from June to September, between 1895 and 2022 in Balogna, Bonifacio, Canale-di-Verde, Corte, Lucciana, Mausoléo, Oletta, Palasca, Patrimonio, Propriano, Rutali, Sartène and Vico.

48. *Megachile argentata schmiedeknechti* Costa, 1884

Figs 47–49

Megachile xanthopyga sp. nov.; Pérez (1895: 25).

Megachile xanthopyga Pérez; Ferton (1897: 48): Bonifacio.

Megachile xanthopyga Pérez; Ferton (1909a: 550): Bonifacio.

Megachile schmiedeknechti Costa; Nadig and Nadig (1934: 26): Cap Corse.

Megachile schmiedeknechti Costa; Benoist (1940: 65): Bonifacio, Vivario.

Megachile schmiedeknechti Costa; Rebmann (1968: 30): Corsica.

Megachile schmiedeknechti Costa; Kusdas (1974: 160): Calvi.

Megachile pilidens Alfken; Liongo Li Enkulu (1988, Map 54): Corsica.

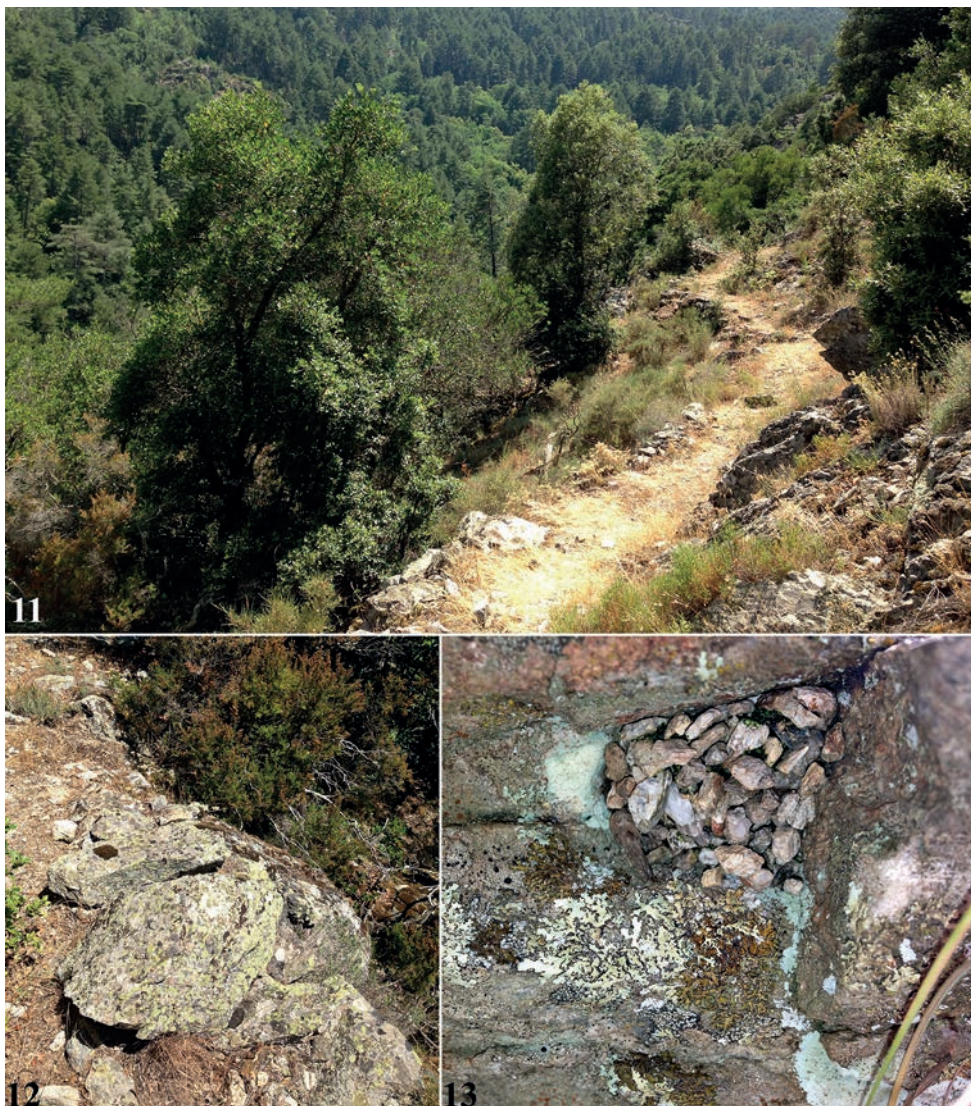
Megachile schmiedeknechti Costa; Liongo Li Enkulu (1988, Map 57): Corsica.

Megachile pilidens Alfken; Pagliano (1994: 373): Venzolasca.

Megachile schmiedeknechti Costa; Pagliano (1994: 374): Golfe de Liscia.

Megachile argentata schmiedeknechti Costa; Praz and Bénon (2023: 170): Corsica.

Material examined. 299♀, 234♂ & 2NS observed from April to October, between 1895 and 2022 in Ajaccio, Albertacce, Aléria, Asco, Balogna, Bastelica, Biguglia, Bonifacio,



Figures 11–13. Nesting site of *Megachile albocristata* **11** adret covered with sparse Oak wood (*Quercus ilex*) in the Tartagine valley (Mausoléo) **12** boulder sheltering a nest of *Megachile albocristata* **13** nest of *Megachile albocristata*.

Canale-di-Verde, Castellare-di-Casinca, Centuri, Conca, Coti-Chiavari, Evisa, Farinole, Figari, Ghisonaccia, Ghisoni, Grosseto-Prugna, La Porta, Lecci, Levie, Linguizzetta, Luciana, Mausoléo, Nocario, Noceta, Oletta, Palasca, Patrimonio, Penta-di-Casinca, Piana, Poggio-d'Oletta, Porto-Vecchio, Propriano, Quenza, Riventosa, Saint-Florent, Santo-Pietro-di-Tenda, Sartène, Sermano, Serra-di-Ferro, Sisco, Solaro, Sorbollano, Soveria, Talasani, Tavera, Ventiseri, Venzolasca, Vescovato, Vico, Vivario, Zicavo and Zona.

Remark. This taxon has been recently relegated to the status of a subspecies of *Megachile argentata* (Fabricius, 1793) (Praz and Bénon 2023). This subspecies occurs

in West Mediterranean islands such as Corsica, Sardinia, and Malta (Praz and Bénon 2023). Notably, both *M. a. argentata* (formerly identified as *M. pilidens*, now recognized as a synonym of *M. argentata*) and *M. a. schmiedeknechti* have been documented in Corsica (Liongo Li Enkulu 1988; Pagliano 1994). However, the distinction of these two taxa primarily relies on the colour of their pilosity which might pose challenge in discerning between old, discoloured specimens, particularly in males. Upon scrutinizing numerous specimens, we believe that the Corsican records of *M. pilidens* (= *M. a. argentata*) refer to *M. a. schmiedeknechti*.

38. *Megachile burdigalensis* Benoist, 1940*

Material examined. 1 ♀ & 2 ♂ observed from June to September, in 2020 in Bastelica, Oletta and Patrimonio.

39. *Megachile centuncularis centuncularis* (Linnaeus, 1758)

Megachile centuncularis Linnaeus; Ferton (1909a: 551): Bonifacio.

Megachile centuncularis (Linnaeus); Liongo Li Enkulu (1988, Map 27): Corsica.

Material examined. 58 ♀ & 31 ♂ observed from April to November, between 1895 and 2022 in Ajaccio, Balogna, Bonifacio, Corscia, Evisa, Ghisoni, Grosseto–Prugna, La Porta, Mausoléo, Oletta, Orto, Ota, Palasca, Porto–Vecchio, Riventosa, Rospigliani, San–Martino–di–Lota, Santo–Pietro–di–Venaco, Serra–di–Fiumorbo, Serra–di–Scopamène, Sisco, Sorbollano, Vivario and Zonza.

40. *Megachile deceptor*a Pérez, 1890

*Megachile deceptor*a Pérez; Liongo Li Enkulu (1988, Map 30): Cap Corse.

Material examined. 4 ♀ & 3 ♂ observed from May to July, between 2020 and 2021 in Ghisonaccia, Saint–Florent, Santo–Pietro–di–Tenda and Serra–di–Fiumorbo.

Remark. The species was only known from one historical data (Liongo li Enkulu 1988). Our observations thus confirm the presence of this taxon in Corsica.

41. *Megachile ericetorum* Lepeletier, 1841

Chalicodoma ericetorum (Lepeletier); Liongo Li Enkulu (1988, Map 32): Corsica.

Chalicodoma ericetorum melaleuca Zanden ssp. nov.; Zanden (1989: 72): Algajola.

Chalicodoma ericetorum (Lepeletier); Canovai et al. (2000: 78): Corsica.

Megachile ericetorum melaleuca Zanden; Le Goff (2004: 10): Vivario.

Material examined. 8 ♀ & 10 ♂ observed from May to September, between 1897 and 2021 in Ajaccio, Albertacce, Barrettali, Corte, Mausoléo, Riventosa, Sermano and Vivario.

Remark. The Corsican populations were assigned to the subspecies *M. ericetorum melaleuca* (Zanden, 1989) which is characterized by a pure white pilosity (dirty white to yellowish in the nominative subspecies). This subspecies has been synonymised with *M. ericetorum* by Praz and Dorchin (2018).

42. *Megachile lagopoda lagopoda* (Linnaeus, 1760)

Megachile lagopoda (Linnaeus); Liongo Li Enkulu (1988, Map 38): Corsica.

Megachile lagopoda (Linnaeus); Pagliano (1994: 372): Col de Celaccia.

Material examined. 13♀ & 21♂ observed from July to September, between 1896 and 2021 in Corscia, Ghisoni, Mausoléo, Piana, Quenza, Renno, Tavera, Vivario and Zicavo.

43. *Megachile leachella* Curtis, 1828

Figs 35–37

Megachile argentata var. *fossoria* Ferton, var. nov.; Ferton (1909a: 550): Bonifacio, Propriano.

Megachile dorsalis Pérez; Alfken (1923: 8): Corsica.

Megachile argentata Fabricius; Nadig and Nadig (1934: 26): Golfe de Sagone.

Megachile argentata var. *fossoria* Ferton; Benoist (1940: 66): Bonifacio, Vivario.

Megachile fossoria Ferton; Liongo Li Enkulu (1988, Map 35) [quoting Ferton (1909a)].

Megachile leachella Curtis; Liongo Li Enkulu (1988, Map 40): Corsica.

Megachile leachella Curtis; Pagliano (1994: 372): Bastia.

Megachile leachella Curtis; Meunier et al. (2023): Ajaccio.

Megachile leachella Curtis; Praz and Bénon (2023, supplementary material): Aléria, Borgo, Ghisonaccia.

Material examined. 30♀ & 29♂ observed from May to September, between 1897 and 2021 in Bonifacio, Calenzana, Cervione, Corbara, Farinole, Ghisonaccia, Grosseto–Prugna, Linguizzetta, Palasca, Penta–di–Casinca, Propriano, Santo–Pietro–di–Tenda, Solaro, Talasani, Tallone, Ventiseri, Vico and Zonza.

Remark. Schwarz and Gusenleitner (2011) delineated several forms of *M. leachella*. In the context of France, two distinct forms can be recognized: the variety *dorsalis* Pérez, 1880, prevalent in Southern France, and the variety *fossoria* Ferton, 1905, found in Corsica. Baker (in Liongo Li Enkulu 1988) proposed considering *M. fossoria* as a valid species. Nevertheless, the extensive variability exhibited by *M. leachella* across its entire distribution range complicates the clear demarcation of taxa. Praz and Bénon (2023) thus maintained the synonymy of this taxon with *M. leachella*.

44. *Megachile melanopyga melanopyga* Costa, 1863

Megachile melanopyga Costa; Benoist (1931, 63): Corsica.

Megachile melanopyga Costa; Liongo Li Enkulu (1988, Map 47): Corsica.

Megachile melanopyga Costa; Ebmer (1997: 52): Tavignano.

Material examined. 68♀ & 44♂ observed from April to November, between 1895 and 2022 in Ajaccio, Aléria, Balogna, Bastelica, Bocognano, Bonifacio, Calenzana, Castellare-di-Casinca, Coti-Chiavari, Croce, Ghisonaccia, Ghisoni, Grosseto-Prugna, Linguizzetta, Manso, Mausoléo, Moncale, Nocario, Oletta, Olmi-Cappella, Palasca, Patrimonio, Piana, Porto-Vecchio, Quenza, Santo-Pietro-di-Tenda, Sartène, Sorbollano, Sotta, Talasani, Tavera, Ventiseri, Vivario and Zona.

46. *Megachile pusilla* Pérez, 1884

Megachile pusilla Pérez; Ferton (1909a: 543): Bonifacio.

Megachile variscopa Pérez; Benoist (1940: 68): Corsica.

Megachile atratula Rebmann; Liongo Li Enkulu (1988, Map 24): Corsica.

Megachile albohirta (Brullé); Ornos et al. (2007: 121) [Misinterpretation]: Corsica.

Material examined. 29♀ & 20♂ observed from May to October, between 1895 and 2021 in Biguglia, Bonifacio, L'Île Rousse, Lucciana, Palasca, Poggio-d'Oletta, Propriano, Saint-Florent, Santo-Pietro-di-Tenda, Talasani and Ventiseri.

47. *Megachile rotundata* (Fabricius, 1793)

Megachile rotundata (Fabricius); Pagliano (1994: 374): Col de Celaccia.

Material examined. 6♀ & 8♂ observed from May to July, between 2002 and 2021 in Bonifacio, Coti-Chiavari, Grosseto-Prugna, Olmi-Cappella, Palasca and Ventiseri.

49. *Megachile sicula corsica* Benoist, 1935

Figs 43–45

Megachile sicula var. *perezi* Lichtenstein; Friese (1899: 39, 176): Corsica.

Megachile sicula Rossi; Ferton (1909a: 550): Bonifacio.

Megachile perezi Lichtenstein; Ferton (1909a: 550): Bonifacio.

Megachile perezi Lichtenstein; Friese (1911: 212): Corsica.

Megachile sicula f. *corsica* Benoist var. nov.; Benoist (1935: 103).

Chalicodoma sicula var. *corsica* Benoist; Benoist (1940: 45): Bonifacio.

Chalicodoma sicula Rossi; Kusdas (1974: 160): Calvi.

Chalicodoma corsica Benoist; Liongo Li Enkulu (1988, Map 29): Corsica.

Chalicodoma sicula Rossi; Liongo Li Enkulu (1988: 87, Map 62): Corsica.

Chalicodoma sicula perezi Lichtenstein; Liongo Li Enkulu (1988, Map 64): Corsica.

Chalicodoma sicula Rossi; Bürgis (1995: 27): Calvi.

Material examined. 187♀, 69♂ & 1NS observed from March to August, between 1855 and 2021 in Ajaccio, Albertacce, Aléria, Asco, Bonifacio, Corte, Evisa, Farinole, Galéria, Mausoléo, Porto-Vecchio, Saint-Florent, Santo-Pietro-di-Tenda, Serra-di-Ferro, Solaro, Sotta, Ventiseri, Vivario and Zona.

Remark. Following Tklačů's suggestions, Liongo Li Enkulu (1988) formally recognized the Corso-Sardinian variety as a distinct species. Subsequently, Rasmont et al. (1995) and Ornosu et al. (2007) adhered to this classification, designating *C. corsica* as a valid species. This taxonomic distinction lacks substantive morphological or molecular justifications, with only variations in the coloration of pilosity and integument being established (Benoist 1935, 1940). It is acknowledged that considerable variability exists in coloration and pilosity among several species within the *Chalicodoma* subgenus. In light of these considerations, we currently regard *C. corsica* as a subspecies of *M. sicula*. It is noteworthy that the CO1 sequence from a Corsican specimen stands isolated in comparison to the sequences available on BOLD for *M. sicula*, displaying a notable divergence from other clusters. A more comprehensive investigation is imperative to ascertain the precise taxonomic status of this Corsican taxon concerning other subspecies of *M. sicula*.

50. *Megachile versicolor* Smith, 1844

Megachile versicolor Smith; Liongo Li Enkulu (1988, Map 65): Corsica.

Megachile versicolor Smith; Pagliano (1994: 374): Bastia.

Material examined. 3♂ observed from May to June, between 2003 and 2017 in Oletta and Vivario.

Osmiini Newman, 1834

Chelostoma Latreille, 1809*

51. *Chelostoma distinctum* Stöckhert, 1929*

Material examined. 25♀ & 32♂ observed from March to June, between 1906 and 2021 in Ajaccio, Bastelicaccia, Cauro, Evisa, Ghisonaccia, Grosseto–Prugna, Lozzi, Murzo, Pianottoli–Caldarello, Poggio–di–Venaco, Santo–Pietro–di–Tenda, Sorbollano, Sermano, Sotta, Venzolasca, Zigliara and Zona.

Remark. The morphology of the Corsican specimens is slightly different than that of the other European specimens. The Corsican population might represent a distinct species.

52. *Chelostoma foveolatum* Schletterer, 1889*

Material examined. 6♀ observed in June 2003 in Grosseto–Prugna.

53. *Chelostoma rapunculi* Lepeletier, 1841*

Material examined. 9♀ & 12♂ observed from May to July, between 1897 and 2021 in Afa, Asco, Cateri, Corbara, Evisa, Grosseto–Prugna, Mausoléo, Olmi–Cappella, Quenza, Santa–Maria–Poggio, Sermano, Sorbollano, Vivario, Zigliara and Zona.

Heriades* Spinola, 1808*54. *Heriades crenulata* Nylander, 1856**

Heriades crenulata Nylander; Benoist (1931: 132): Corsica.

Eriades crenulatus Nylander; Kusdas (1974: 160): Calvi.

Heriades crenulata Nylander; Pagliano (1994: 379): Bastia.

Heriades crenulata Nylander; Marchal and Chardonnet (2001: 203): Serra-di-Fiumorbo.

Material examined. 247♀ & 265♂ observed from May to the beginning of November, between 1855 and 2021 in Ajaccio, Asco, Aullène, Bonifacio, Calenzana, Calvi, Cargèse, Corbara, Coti-Chiavari, Ersa, Farinole, Figari, Galéria, Ghisonaccia, Ghisoni, Grosseto-Prugna, Lecci, Linguizzetta, Mausoléo, Meria, Moncale, Oletta, Ota, Palasca, Patrimonio, Penta-di-Casinca, Piana, Poggio-di-Venaco, Poggio-d'Oletta, Porto-Vecchio, Propriano, Quenza, Saint-Florent, San-Martino-di-Lota, Santo-Pietro-di-Tenda, Serra-di-Ferro, Serra-di-Scopamène, Serriera, Sisco, Sorbollano, Sotta, Tavera, Ventiseri, Vivario and Zonza.

55. *Heriades rubicola* Pérez, 1890

Heriades rubicola Pérez; Benoist (1931: 132): Corsica.

Heriades rubicola Pérez; Pagliano (1994: 379): Venzolasca.

Material examined. 115♀ & 88♂ observed from May to October, between 1895 and 2021 in Aléria, Bonifacio, Calvi, Casaglione, Corbara, Ghisonaccia, Linguizzetta, Lumio, Moncale, Morosaglia, Ogliastro, Oletta, Palasca, Patrimonio, Penta-di-Casinca, Pietracorbara, Poggio-di-Venaco, Porto-Vecchio, Propriano, Saint-Florent, Santa-Maria-Poggio, Santo-Pietro-di-Tenda, Serra-di-Ferro, Talasani, Sisco, Venaco and Ventiseri.

56. *Heriades truncorum* (Linnaeus, 1758)

Heriades truncorum Linnaeus; Ferton (1901b: 93, 143): Propriano, Vivario.

Examined material. 30♀ & 20♂ observed from June to August, between 1896 and 2019 in Asco, Bonifacio, Evisa, Ghisoni, Mausoléo, Riventosa, Propriano, Serra-di-Ferro, Serra-di-Scopamène, Sorbollano, Vivario and Zicavo.

Hoplitis* Klug, 1807*57. *Hoplitis acuticornis* (Dufour & Perris, 1840)**

Osmia acuticornis Dufour & Perris; Benoist (1931: 41): Corsica.

Material examined. 31♀ & 12♂ observed from April to July, between 1895 and 2021 in Asco, Bonifacio, Borgo, Corte, Evisa, Mausoléo, Santo–Pietro–di–Venaco, Ventiseri, Vivario, Zicavo and Zona.

Remark. The morphology of the Corsican specimens is slightly different than that of the other European specimens. The Corsican population might represent a distinct species.

58. *Hoplitis aff. adunca* (Panzer, 1798)*

Material examined. 23♀ & 38♂ observed from May to June, between 1895 and 1907 in Bonifacio, Porto–Vecchio and Propriano.

Remark. This species will be described soon (Le Divelec in prep.). It seems to be restricted to Southern Corsica and Sardinia. No modern record is known for Corsica.

59. *Hoplitis adunca* (Panzer, 1798)

Osmia adunca Panzer; Radoszkowski (1887: 288): Corsica.

Osmia adunca Panzer; Benoist (1931: 36): Corsica.

Osmia morawitzi Pérez; Benoist (1931: 36) [Misidentification]: Corsica.

? *Osmia benoisti* Alfken; Warncke (1992: 115) [probably quoting Benoist (1931)]: Corsica.

Material examined. 44♀ & 45♂ observed from April to August, between 1895 and 2021 in Aléria, Bonifacio, Cervione, Corbara, Corte, Galeria, Ghisonaccia, Grosseto–Prugna, Lucciana, Oletta, Piana, Poggio–di–Venaco, Saint–Florent, Santo–Pietro–di–Tenda, Tallone, Ventiseri, Venzolasca, Vico, Vivario and Zona.

60. *Hoplitis anthocopoides* (Schenck, 1853)

Hoplitis anthocopoides Schenck; Scheuchl and Willner (2016: 435) [quoting Müller (2022a)].

Hoplitis anthocopoides Schenck; Müller (2022a): Corsica.

Material examined. 104 ♀ & 82♂ observed from May to August, between 1895 and 2021 in Ajaccio, Aléria, Aregno, Bonifacio, Borgo, Calvi, Casaglione, Centuri, Cervione, Corbara, Corscia, Corte, Ersa, Ghisonaccia, Grosseto–Prugna, L'Île Rousse, Lucciana, Lumio, Oletta, Palasca, Piana, Poggio–di–Venaco, Propriano, Santo–Pietro–di–Tenda, Serra–di–Ferro, Sotta, Ventiseri, Vico, Vivario and Zona.

61. *Hoplitis bihamata* (Costa, 1885)

Figs 51–53

Osmia corsica Ferton sp. nov.; Ferton (1901a: 61–63): Bonifacio, Monte Renoso.

Osmia corsica Ferton; Benoist (1931: 36): Corsica.

Osmia corsica Ferton; Nadig and Nadig (1934: 26): Monte d'Oro.

Osmia corsica Ferton; Stanek (1969: 28): Corsica.

Osmia marchali Pérez; Warncke (1992c: 109) [misidentification]: Col de Verde.

Material examined. 83♀ & 69♂ from April to September, between 1898 and 2021 in Asco, Barrettali, Bocognano, Bonifacio, Calvi, Casaglione, Corte, Evisa, Ghisoni, Mausoléo, Olcani, Patrimonio, Porto–Vecchio, Quenza, Santo–Pietro–di–Tenda, Serra–di–Scopamène, Sisco, Vivario and Zonza.

Remark. Corso-sardinian endemic.

62. *Hoplitis bisulca* (Gerstäcker, 1869)

Figs 59–61

Osmia lanosa Pérez; Ferton (1897: 42): Bonifacio.

Osmia lanosa Pérez; Ferton (1901b: 88–89): Bonifacio.

Osmia lanosa Pérez; Ferton (1905: 58–59): Bonifacio.

Osmia lanosa Pérez; Ferton (1909a: 538): Bonifacio.

Osmia bisulca Gerstäcker; Benoist (1931: 33): Corsica.

Material examined. 97♀ & 70♂ observed from May to August, between 1895 and 2021 in Bonifacio, Canale–di–Verde, Patrimonio and Zonza.

63. *Hoplitis corsaria* (Warncke, 1991), *stat. nov.*

Osmia crenulata Morawitz; Morawitz (1871: 208): Corsica.

Osmia crenulata Morawitz; Schmiedeknecht (1885–1886: 161): Corsica.

Osmia crenulata Morawitz; Ducke (1900: 171): Corsica.

Osmia crenulata Morawitz; Ferton (1901a: 63): Bonifacio.

Osmia crenulata Morawitz; Benoist (1931: 35): Corsica.

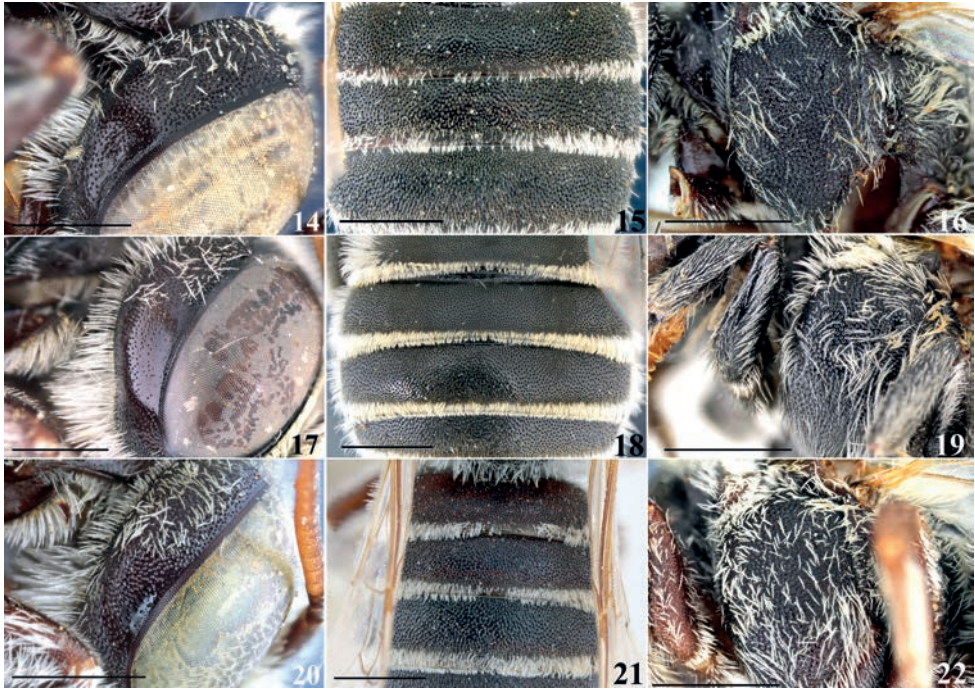
Osmia annulata corsaria Warncke *ssp. nov.*; Warncke (1991a: 734): Ajaccio.

Osmia annulata corsaria Warncke; Le Goff (2010: 7): Grosseto–Prugna.

Type material examined. *Holotype:* Corse 15-6-1981 [15.VI.1981] Ajaccio leg. Perraudin // Holotypus *Osmia annulata corsaria* War // Holotypus // ♂ // Coll. K. Warncke O. Ö. Landesmuseum Linz/Austria-egg.93. [Examined on pictures: <https://www.europeana.eu/fr>].

Material examined. 151♀ & 114♂ observed from May to July, between 1895 and 2021 in Ajaccio, Aléria, Aullène, Bonifacio, Canale–di–Verde, Coggia, Corbara, Ghisonaccia, Grosseto–Prugna, Lumio, Oletta, Palasca, Porto–Vecchio, Propriano, Sartène, Serra–di–Ferro, Sollacaro, Ventiseri, Venzolasca, Vico, Vivario and Zonza.

Remark. Old European records of *Osmia crenulata* (Morawitz, 1871) refer to *H. annulata* (Latreille, 1811) and not specifically to the East Mediterranean *H. annulata crenulata*. Corsican records only refer to *H. annulata corsaria*. *Hoplitis annulata* is a species complex. The morphology of the Corsican endemic *H. a. corsaria*, especially that of the



Figures 14–22. Comparative illustrations of *H. corsaria* (Warncke) and *H. annulata* (Latreille) **14–16** *H. annulata annulata* (Latreille) (from Spain) **17–19** *H. corsaria* (Warncke) (from Corsica) **20–22** *H. annulata crenulata* (Morawitz) (from Greece) **14, 17, 20** gena of male **15, 18, 21** gaster of female (**15** terga 2–4 **18** terga 1–4 **21** terga 1–3) **16, 19, 22** mesepisternum. Scale bars: 1 mm.

male, is remarkably distinct from that of the two other subspecies (Table 3). Plus, the CO1 sequences of the Corsican specimens are significantly diverging (around 3.7%) from the Iberian sequences of *H. annulata* published on BOLD. For these reasons, we consider *H. corsaria* to be a distinct species. The nominative subspecies and *H. a. crenulata* might also represent distinct species as they are morphologically different and have distinct nesting behaviour (Le Goff, 2010). However, the morphological differences are tenuous and without the examination of an extensive material or molecular evidence we cannot exclude intraspecific variability. *Hoplitis corsaria* is only known from Corsica to date.

BOLD process ID. LPRCW186-19, LPRCW187-19, LPRCI1815-21, LPRCI1824-21, LPRCI1968-21 (BIN, BOLD:AEC2169).

64. *Hoplitis cristatula* (van der Zanden, 1990)

Osmia cristata Fonscolombe; Fertton (1897: 42): Bonifacio.

Osmia cristata Fonscolombe; Fertton (1901b: 88): Bonifacio.

Osmia cristata Fonscolombe; Fertton (1909a: 538): Bonifacio.

Osmia cristata Fonscolombe; Benoist (1931: 34): Corsica.

Material examined. 48♀ & 34♂ observed from May to July, between 1895 and 2021 in Ajaccio, Aléria, Bonifacio, Calenzana, Casamaccioli, Coggia, Farinole, Grosseto–Prugna, L'Île Rousse, Ogliastro, Oletta, Santa–Maria–Poggio, Santo–Pietro–di–Tenda, Serra–di–Ferro, Vivario and Zona.

Table 3. Main morphological differences between *H. corsaria* and *H. annulata*.

Features	<i>H. corsaria</i>	<i>H. a. annulata</i>	<i>H. a. crenulata</i>
Gena punctuation	♀: Gena with shallow punctuation, more sparsely spaced by uneven interspaces that can reach the diameter of one puncture. ♂: Gena with remarkably minute and sparse punctuation, its lower half with large and almost impunctate area near outer orbit (Fig. 17).	♀: Gena with coarse and dense subcontiguous punctuation, with narrow linear interspaces. ♂: Gena with coarse subcontiguous punctuation, its lower half uniformly punctate, at most with a small impunctate area (Fig. 14).	♀: Gena with coarse and dense subcontiguous punctuation, with narrow linear interspaces. ♂: Gena with coarse subcontiguous punctuation, its lower half densely punctate, at most with a small impunctate area (Fig. 20).
Vertex length	Around two times the diameter of posterior ocellus	Around two times the diameter of posterior ocellus	More than two times the diameter of posterior ocellus
Mesepisternum punctuation	Punctuation sparse, punctures separated by conspicuous flat interspaces (dense around scrobal area) (Fig. 19).	Punctuation subcontiguous, mostly with linear to carina-shaped interspaces (Fig. 16).	Punctuation subcontiguous, mostly with carina-shaped interspaces (Fig. 22).
Metasoma	Punctuation of terga 2–4 fine and remarkably sparse (most interspaces > 1–2 puncture diameters) with conspicuous micropunctuation in-between, tegument smooth and shiny (Fig. 18).	Punctuation of terga 2–4 denser (interspace ≤ 1 puncture diameter) and somewhat coarser so the segment appears matte, micropunctuation hardly distinct, tegument of terga smooth, at most slightly shagreened basally (Fig. 15).	Punctuation of terga 2–4 denser (interspace ≤ 1 puncture diameter) and coarser so the segment appears matte, micropunctuation hardly distinct, tegument of terga shagreened, at least basally (Fig. 21).

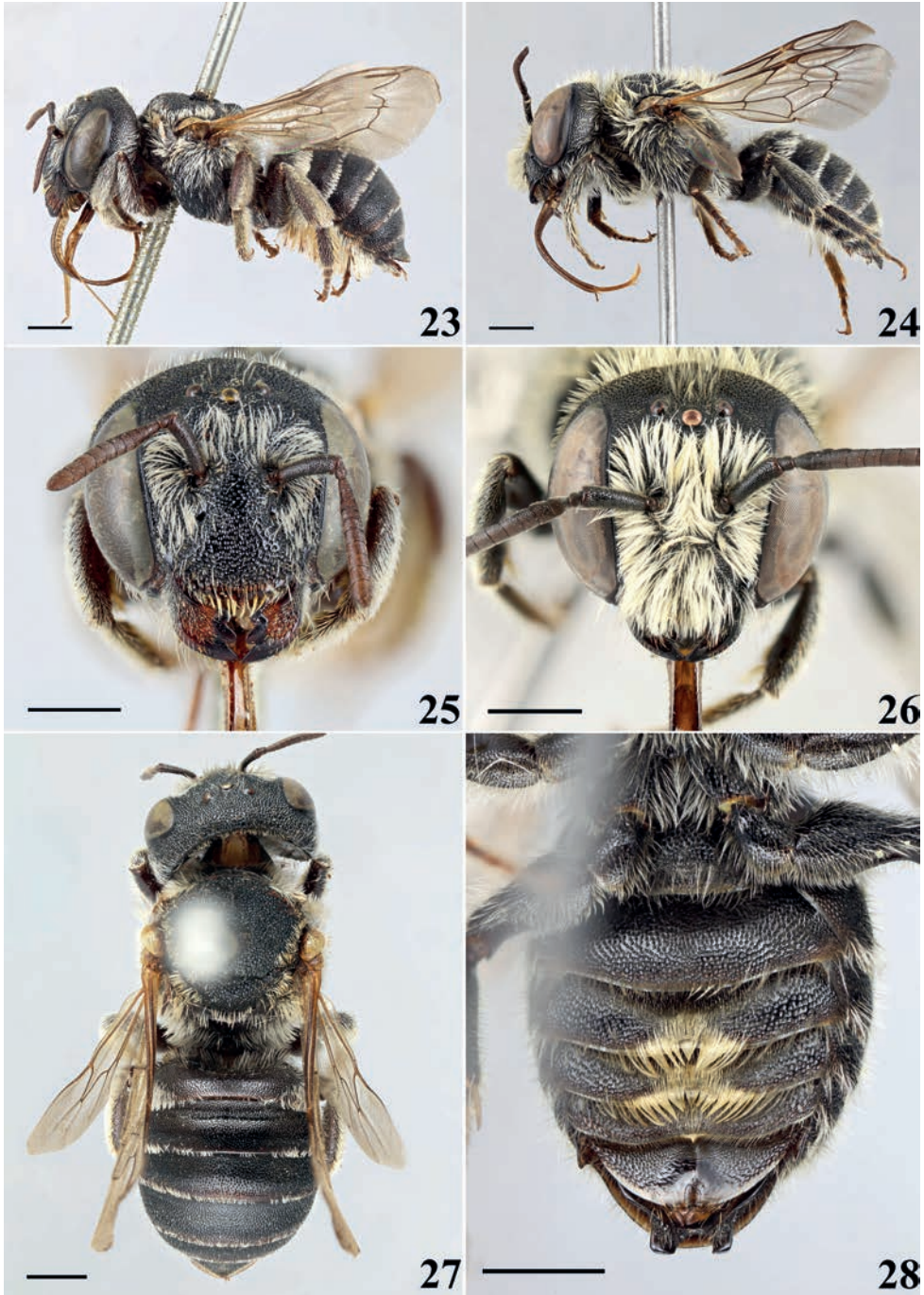
65. *Hoplitis fasciculata* (Alfken, 1934)

Figs 23–28

Hoplitis fasciculata (Alfken); Müller (2022a): Corsica.

Material examined. 13♀ & 11♂ observed from June to July, between 1899 and 2021 in Bonifacio, Propriano, Prunelli–di–Fiumorbo and Rutali.

Remark. The generic Corsican record of *H. fasciculata* mentioned on the website of Müller (2022a) comes from our records that are here published for the first time. Corsica represents the western limit of the distribution of this species. The female is easily distinguishable from other *Anthocopa* Lepeletier & Serville, 1825 by the white scopa (Fig. 23), the crenulate clypeus free margin (saw-edged) (Fig. 25) and the rugose areolate sculpture of the scutum (Fig. 27). The male can be recognized by the conspicuously bilobed tergum 7 (Fig. 28), the bidentate mandibule (Fig. 26). Its last sternum has a rounded apical margin and is apically depressed with a smooth and shiny area at the end of which is a small tubercle bearing a tuft of backwardly directed setae (Fig. 28).



Figures 23–28. *Hoplitis fasciculata* (Alfken) **23, 25, 27** female **24, 26, 28** male **23, 24** habitus in lateral view **25, 26** head in front view **27** habitus in dorsal view **28** gaster in ventral view. Scale bars: 1 mm

66. *Hoplitis leucomelana* (Kirby, 1802)

Osmia leucomelana Kirby; Warncke (1991b: 716): Ajaccio.

Hoplitis leucomelana (Kirby); Pagliano (1994: 383): Col de Celaccia.

Hoplitis leucomelana Kirby; Le Goff (2004: 11): Vivario.

Material examined. 33♀ & 25♂ observed from June to September, between 1896 and 2020 in Albertacce, Aullène, Biguglia, Bonifacio, Calacuccia, Casamaccioli, Coti–Chiavari, Evisa, Grosseto–Prugna, Oletta, Patrimonio, Piana, Sermano, Serra–di–Ferro, Serra–di–Fiumorbo, Sisco, Sorbollano, Tavera, Venaco, Vico, Vivario, Zigliara and Zonza.

67. *Hoplitis manicata* (Morice, 1901)

Hoplitis manicata Morice; Le Goff (2004: 19): Vivario (2B).

Material examined. 9♀ & 5♂ observed in June 2002 and 2003 in Vivario.

Remark. In Corsica, this species is only known from one station in the mountains of Vivario (Le Goff 2004). Corsica represents the western limit of the distribution of this species.

68. *Hoplitis perezii* (Ferton, 1895)

Osmia perezii Ferton; Ferton (1897: 42–43): Bonifacio.

Osmia perezii Ferton; Ferton (1901b: 89–90): Bonifacio.

Osmia perezii Ferton; Ferton (1909a: 538): Bonifacio.

Osmia perezii Ferton; Benoist (1931: 35): Corsica.

Anthocopa perezii (Ferton); Tkalcù (1969: 330): Bonifacio.

Material examined. 31♀ & 19♂ observed from May to July, between 1895 and 2021 in Bonifacio, Casamaccioli, Corte, Grosseto–Prugna and Sermano.

69. *Hoplitis praestans* (Morawitz, 1893)

Figs 63–66

Osmia praestans Morawitz; Dücke (1900: 110): Corsica.

Osmia lineola Pérez; Ferton (1901a: 63): Corsica.

Osmia praestans Morawitz; Friese (1911: 80): Corsica.

Osmia praestans Morawitz; Benoist (1931: 42): Corsica.

Osmia praestans Morawitz; Kusdas (1974: 160): Calvi.

Osmia praestans Morawitz; Warncke (1991b: 734): Calvi.

Material examined. 13♀ & 20♂ observed from May to July, between 1855 and 2021 in Bonifacio, Calvi, Ghisonaccia, Ghisoni, Linguizzetta, Mausoléo, Pianottoli-Caldarello, Ventiseri, Vivario and Zonza.

70. *Hoplitis ravouxi* (Pérez, 1902)

Hoplitis ravouxi (Pérez); Müller (2022a): Corsica.

Hoplitis loti Morawitz; Le Goff (2004: 11) [Misidentification]: Vivario.

Material examined. 1♀ observed in June 2003 in Vivario & 1♂ in May 2011 in Balogna.

71. *Hoplitis tridentata* (Dufour & Perris, 1840)

Osmia mocsaryi Friese; Ducke (1900: 154) [Misinterpretation]: Corsica.

Osmia mocsaryi Friese; Friese (1911: 92) [quoting Ducke (1900)]: Corsica.

Osmia mocsaryi Friese; Benoist (1931: 38) [quoting Ducke (1900)]: Corsica.

Material examined. 5♀ & 6♂ observed from May to June, between 1897 and 2021 in Borgo, Lucciana, Oletta, Sermano, Vescovato and Vivario.

Remark. This species has been recorded from Corsica under the name of *O. mocsaryi*, a species with which *H. tridentata* was regularly confused in the past (see below).

***Osmia* Panzer, 1806**

72. *Osmia anceyi* Pérez, 1879

Osmia anceyi Pérez; Müller (2018: 312): Verghia.

Material examined. 1♀ collected in June 2001 in Coti-Chiavari.

73. *Osmia aurulenta* (Panzer, 1799)

Osmia aurulenta (Panzer); Müller (2022a): Corsica.

Material examined. 33♀ & 5♂ observed from April to July, between 1897 and 2021 in Barbaggio, Bocognano, Ghisoni, Grosseto–Prugna, Lozzi, Lucciana, Palasca, Riventosa, Sartène, Sermano, Vico and Vivario.

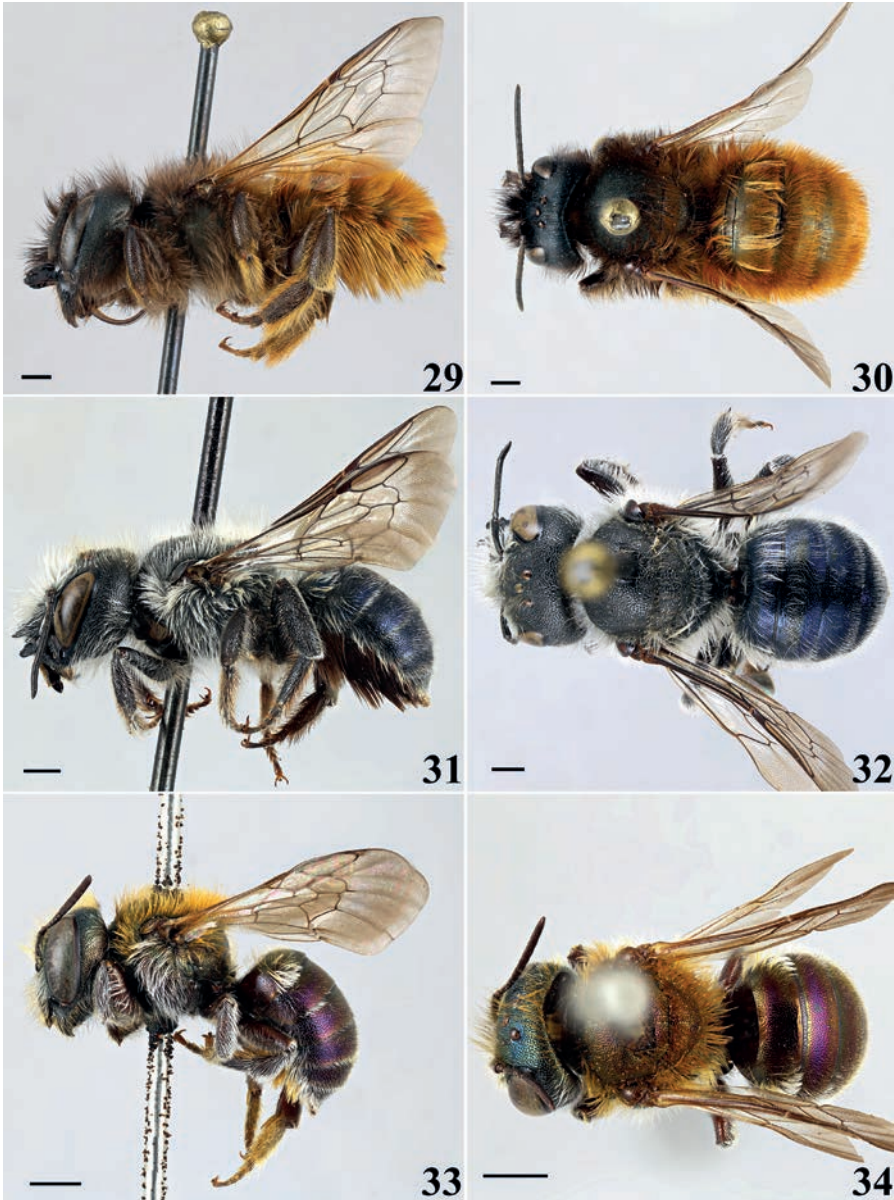
74. *Osmia bicornis bicornis* (Linnaeus, 1758)

Figs 29, 30

Osmia bicornis Latr.; Fertton (1911: 368): Bonifacio.

Osmia rufa rufa (Linnaeus); Peters (1977: 291): Ajaccio, Bastia, Calvi, Corte, Nonza, Monte d'Oro, Porto-Vecchio, Saint-Florent, Santo-Pietro-di-Venaco, Sari-Solenzara, Vivario.

Osmia bicornis globosa (Scopoli); Ungricht et al. (2008: 177): Corsica.



Figures 29–34. Remarkable variety of Corsican *Osmia* **29, 30** *Osmia bicornis bicornis* (Linnaeus) **31, 32** *Osmia latreillei iberoafricana* Peters **33, 34** *Osmia versicolor corrusca* Erichson **29, 31, 32** lateral view **30, 32, 34** dorsal view. Scale bars: 1 mm.

Material examined. 60♀ & 47♂ observed from March to June, between 1897 and 2021 in Bocognano, Bonifacio, Calacuccia, Casaglione, Corte, Ghisonaccia, Riventosa, Porto–Vecchio, Quenza, Serra–di–Ferro, Serra–di–Scopamène, Sollacaro, Sotta, Ventiseri, Vico, Vivario and Zona.

75. *Osmia caerulescens caerulescens* Linnaeus, 1758

Osmia aenea (Linnaeus); Ferton (1897: 40): Bonifacio.

Osmia cyanea (Fabricius); Ferton (1905: 93): Bonifacio.

Osmia aenea (Linnaeus); Ferton (1911: 368): Bonifacio.

Material examined. 222♀ & 109♂ observed from March to September, between 1855 and 2021 in Ajaccio, Albitreccia, Aléria, Asco, Aullène, Balogna, Biguglia, Bocognano, Bonifacio, Calenzana, Casaglione, Casamaccioli, Casanova, Centuri, Coggia, Corbara, Coti–Chiavari, Cozzano, Evisa, Farinole, Furiani, Galéria, Ghisonaccia, Ghisoni, Grosseto–Prugna, Linguizzetta, Lozzi, Lucciana, Mausoléo, Oletta, Olmi–Cappella, Palasca, Palneca, Patrimonio, Penta–di–Casinca, Pianottoli–Caldarello, Poggio–di–Venaco, Porto–Vecchio, Propriano, Prunelli–di–Fiumorbo, Quenza, Riventosa, Rogliano, Rutali, Saint–Florent, Santa–Maria–Poggio, Santo–Pietro–di–Tenda, Serra–di–Ferro, Serra–di–Fiumorbo, Sisco, Sorbollano, Sorbo–Ocagnano, Sotta, Tala-sani, Ventiseri, Vescovato, Vico, Vivario, Zicavo and Zona.

76. *Osmia cornuta cornuta* (Latreille, 1805)

Osmia cornuta (Latreille); Peters (1977: 337): Corsica.

Material examined. 3♀ & 3♂ observed from March to June, between 1976 and 2021 in Borgo, Grosseto–Prugna, Riventosa and Sotta.

77. *Osmia emarginata emarginata* Lepeletier, 1841

Osmia emarginata Lepeletier; Ferton (1901b: 85, 89): Evisa, Vivario.

Osmia emarginata emarginata Lepeletier; Tkalcù (1971: 224): Monte d’Oro, Vivario.

Osmia emarginata emarginata Lepeletier; Peters (1977: 310): Quenza, Rutali, Vivario.

Material examined. 12♀ & 7♂ observed from May to July, between 1897 and 2021 in Corte, Evisa, Lozzi, Serra–di–Ferro, Vivario, Zicavo and Zona.

78. *Osmia erythrogastra* Ferton, 1905

Figs 55–57

Osmia erythrogastra Ferton sp. nov.; Ferton (1905: 57): Bonifacio.

Osmia erythrogastra Ferton; Ferton (1909b: 407): Bonifacio.

Osmia erythrogastra Ferton; Benoist (1931: 33): Bonifacio.

Osmia erythrogastra Ferton; Müller (2020: 230): Bastia.

Material examined. 10♀ & 8♂ observed from May to August, between 1904 and 1964 in Bastia and Bonifacio.

Remark. No modern records.

79. *Osmia ferruginea* Latreille, 1811

Osmia igneopurpurea Costa; Ferton (1897: 39): Bonifacio.

Osmia ferruginea Lep.; Ferton (1899: 72): Bonifacio.

Osmia ferruginea Latreille; Ducke (1900: 212): Corsica.

Osmia ferruginea Lep.; Ferton (1901a: 65): Corsica.

Osmia ferruginea Lep.; Ferton (1901b: 143): Bonifacio.

Osmia ferruginea Lep.; Ferton (1905: 89–93): Bonifacio.

Osmia ferruginea Lep.; Ferton (1909a: 575, 577): Bonifacio.

Osmia ferruginea var. *igneopurpurea* Costa; Benoist (1931: 32): Corsica.

Osmia ferruginea igneopurpurea Costa stat. nov.; Warncke (1992d: 109): Corsica.

Material examined. 65♀ & 35♂ observed from March to June, between 1855 and 2020 in Barbaggio and Bonifacio.

Remark. The subspecies *igneopurpurea* Costa, 1882, has been documented in Corsica, Sardinia, Sicily, and Malta (Warncke 1992d). This subspecies is characterized by a dark scopa and dark hairs on the hind tibia. However, Corsican specimens exhibit significant variability, ranging from typical characteristics of the nominative subspecies to those of the subspecies *igneopurpurea*. The presence of numerous intermediate specimens further complicates the differentiation between subspecies. Given this variability, we suggest considering both dark and light hairy Corsican specimens of *O. ferruginea* as part of a single taxon. The subspecies *igneopurpurea* may just be a synonym of *Osmia ferruginea*.

80. *Osmia latreillei* (Spinola, 1806)

Figs 31, 32

Osmia latreillei (Spinola); Ducke (1900: 236): Corsica.

Osmia latreillei Lep.; Ferton (1905: 59, 93): Bonifacio.

Osmia latreillei (Spinola); Benoist (1931: 30): Corsica.

Osmia latreillei iberofrancana Peters; Tkalcù (1975b: 184): Corsica.

Osmia latreillei latreillei (Spinola); Ungricht et al. (2008: 153): Corsica.

Material examined. 35♀ & 47♂ observed from March to June, between 1895 and 2021 in Ajaccio, Bonifacio, Corte, Ghisonaccia and Riventosa.

Remark. Tkalcù (1975b) assigned the Corso-Sardinian populations to the subspecies *iberofrancana*. However, the situation remains unclear as he noted that these

populations exhibit intermediate characteristics, with some specimens closely resembling the nominate subspecies found in mainland France and Italy. Müller (2022a) argues that a subspecies rank is unjustified and proposes its synonymy with *O. latreillei*.

81. *Osmia ligurica* Morawitz, 1868

Osmia ligurica Morawitz; Kusdas (1974: 160): Calvi.

Material examined. 76♀ & 40♂ observed from May to August, between 1895 and 2021 in Albertacce, Aléria, Asco, Barbaggio, Bonifacio, Calacuccia, Castellare-di-Mercurio, Corte, Ghisonaccia, Grosseto-Prugna, Lumio, Mausoléo, Moncale, Oletta, Palasca, Patrimonio, Pianottoli-Caldarello, Porto-Vecchio, Propriano, Santo-Pietro-di-Tenda, Sermano, Serra-di-Ferro, Sisco, Sotta, Venaco, Ventiseri, Vivario and Zonza.

82. *Osmia melanogaster melanogaster* Spinola, 1808

Osmia notata (Fabricius); Benoist (1931: 28) [Misinterpretation, see Tkalcu 1975a]: Corsica.

Material examined. 2♂ collected in Ajaccio during the XIXth century (J. Pérez coll.).

Remark. No modern records.

83. *Osmia nasoproducta* Ferton, 1909

Figs 68–70

Osmia nasoproducta Ferton sp. nov.; (Ferton 1909b: 406–407): Bonifacio.

Material examined. 8♀ & 4♂ observed from March to June, between 1902 and 2017 in Bonifacio.

Remark. It is a rare and poorly known species. Its male was recently described (Le Goff 2016). The original description (Ferton 1909b) represented the only Corsican record until now.

84. *Osmia niveata* (Fabricius, 1804)

Osmia fulviventris var. *albiscopa* Alfken; Benoist (1931: 29): Corsica.

Osmia fulviventris Panzer; Kusdas (1974: 160): Calvi.

Osmia fulviventris niveata (Fabricius); Tkalcu (1975a: 307): Bastia, Porto-Vecchio, Ville-di-Pietrabugno.

Material examined. 114♀ & 53♂ observed from March to July, between 1896 and 2021 in Altagène, Bonifacio, Calenzana, Calvi, Centuri, Coggia, Corbara, Ersu, Grosseto-Prugna, Lozzi, Manso, Mausoléo, Olcani, Oletta, Osani, Palasca, Patrimonio,

Pianottoli-Caldarello, Poggio-di-Venaco, Porto-Vecchio, Prunelli-di-Fiumorbo, Quenza, Riventosa, Santo-Pietro-di-Tenda, Serra-di-Ferro, Sorbo-Ocagnano, Sotta, Venzolasca, Vivario and Zonza.

Remark. Corsican females, characterized by a pure white scopa, were previously considered a distinct subspecies named *O. niveata albiscopa*. However, the males are not distinguishable, and the barcode of Corsican specimens cannot be distinguished from other European counterparts. This suggests that the light hairy insular population is conspecific with mainland populations.

85. *Osmia rufohirta* Latreille, 1811

Osmia rufohirta Latreille; Ferton (1897: 37–39): Bonifacio.

Osmia rufohirta Latreille; Ferton (1899: 70–72): Bonifacio.

Osmia fossoria Pérez; Ducke (1900: 127) [Misinterpretation]: Corsica.

Osmia rufohirta Latreille; Ferton (1901b: 89, 145): Bonifacio.

Osmia rufohirta Latreille; Ferton (1905: 62, 83–95): Bonifacio.

Osmia rufohirta Latreille; Ferton (1909a: 579–580): Bonifacio.

Osmia rufohirta Latreille; Ferton (1911: 381–382): Bonifacio.

Osmia rufohirta Latreille; Benoist (1931: 40): Corsica.

Material examined. 101♀ & 62♂ observed from March to the beginning of July, between 1893 and 2021 in Bonifacio, Corte, Farinole, Patrimonio, Sermano and Vivario.

86. *Osmia scutellaris* Morawitz, 1868

Osmia scutellaris Morawitz; Le Goff (2004: 11): Vivario.

Osmia scutellaris Morawitz; Müller (2018: 320): Zonza.

Material examined. 19♀ & 19♂ observed from May to the beginning of July, between 1973 and 2021 in Bonifacio, Calacuccia, Casaglione, Grosseto-Prugna, Oletta, Palasca, Riventosa, Porto-Vecchio, Quenza, Santo-Pietro-di-Tenda, Sermano, Sotta, Vivario and Zonza.

87. *Osmia signata signata* Erichson, 1835

Osmia vidua Gerstäcker; Ferton (1897: 40–42): Bonifacio.

Osmia vidua Gerstäcker; Ferton (1901a: 64): Bonifacio.

Osmia vidua Gerstäcker; Benoist (1931: 27): Corsica.

Material examined. 34♀ & 20♂ observed from May to August, between 1895 and 2021 in Ajaccio, Bonifacio, Calenzana, Calvi, Coti-Chiavari, Grosseto-Prugna, Mausoléo, Olcani, Patrimonio, Porto-Vecchio, Propriano, Prunelli-di-Fiumorbo, Sartène, Serra-di-Ferro, Sollacaro and Sotta.

88. *Osmia submicans submicans* Morawitz, 1870

Osmia submicans submicans Morawitz; Tkalcù (1977: 94): Bonifacio.

Osmia submicans Morawitz; Zanden (1991: 65): Ajaccio, Saint–Florent.

Material examined. 51♀ & 16♂ observed from March to July, between 1898 and 2021 in Bonifacio, Galéria, Ghisonaccia, Ghisoni, Mausoléo, Muracciole, Oletta, Olmi–Cappella, Palasca, Riventosa, Porto–Vecchio, Sotta, Ventiseri, Vivario and Zonza.

89. *Osmia tricornis* Latreille, 1811

Osmia tricornis Latreille; Ferton (1901b: 97): Bonifacio.

Osmia tricornis Latreille; Ferton (1911: 368): Bonifacio.

Osmia tricornis Latreille; Benoist (1931: 23): Corsica.

Osmia tricornis Latreille; Kusdas (1974: 160): Calvi.

Osmia tricornis Latreille; Peters (1977: 337): Corsica.

Material examined. 12♀ & 25♂ observed from March to April, between 1896 and 2021 in Bonifacio, Calenzana, Corte and Santo–Pietro–di–Tenda.

90. *Osmia versicolor corrusca* Erichson, 1835

Figs 33, 34

Osmia versicolor Latreille; Ferton (1905: 85): Bonifacio.

Osmia versicolor Latreille; Kusdas (1974: 160): Calvi.

Osmia versicolor corrusca Erichson stat.nov.; Zanden (1984: 183): Bonifacio.

Material examined. 72♀ & 15♂ observed from February to the beginning of July, between 1895 and 2020 in Barbaggio, Bonifacio, Ghisonaccia and Patrimonio.

Remark. *Osmia v. corrusca* is allegedly restricted to Corsica, the Balearic Islands, the Iberian Peninsula and to North Africa (Warncke 1992d).

Protosmia Ducke, 1900*

91. *Protosmia minutula* (Pérez, 1896)*

Material examined. 1♂ observed in July 2019 in Mausoléo.

Dubious records

The Corsican records of *Megachile marginata* Smith, 1853 (as *Megachile picicornis* Morawitz), *M. pyrenaica* Pérez, 1890), *M. pyrenaica* Lepeletier, 1841 published by Liongo Li Enkulu (1988) could not be confirmed and are likely to be mistakes. The Corsican

record of *H. claviventris* (Thomson, 1872) published by Warncke (1988) most probably refers to *H. leucomelana*, a very common species in Corsica which is morphologically very similar. Finally, the presence of *O. notata* in Corsica is documented by Nadig and Nadig (1934) and Warncke (1988) who probably quoted the previous authors. These records most probably refer to the closely related *O. signata*, a common species in Corsica.

Erroneous records

Hoplitis benoisti (Alfken, 1935)

Osmia morawitzi Pérez; Benoist (1931: 36): Corsica.

Osmia benoisti Alfken; Warncke (1992: 115): Corsica.

Remark. The specimens reported by Benoist (1931) are preserved in his collection and belong to *H. adunca*. The Corsican record of Warncke (1992) is either a quotation of Benoist (1931) or refer to the new species, *H. aff. adunca*.

Hoplitis loti (Morawitz, 1867)

Osmia loti Morawitz; Ferton (1901a: 64): Bonifacio.

Hoplitis loti Morawitz; Le Goff (2004: 11) [= *H. ravouxi* (Pérez), Le Goff pers. comm.].

Remark. No such specimen has been located in Ferton's collection. It is a mountainous species, unlikely to occur in Bonifacio.

Hoplitis marchali (Pérez, 1902)

Osmia marchali Pérez; Warncke (1992c: 109): Col de Verde.

Remark. The specimen reported by Warncke (1992c) is preserved in his collection and belong to *H. bihamata*. *Hoplitis marchali* is present in the south of the Iberian Peninsula, North Africa, and Sicily (Warncke 1992c; Baldock et al. 2018).

Hoplitis mocsaryi (Friese, 1895)

Osmia mocsaryi Friese; Duce (1900: 154): Corsica.

Remark. Despite significant samplings in Corsica, no specimen of *H. mocsaryi* were observed. The specimen(s) originally recorded from Corsica could not be located. The original record of Duce (1900) was quoted by many authors (e.g. Friese 1911; Benoist 1931; Moczar 1958; Pagliano 1994; Rasmont et al. 1995, 2017; Ornos et al. 2007; Scheuchl and Willner 2016). However, Friese, Duce and Benoist misinterpreted the identity of the female of *H. mocsaryi* which they confused with *H. tridentata*. The

female of *H. mocsaryi* was actually described for the first time by Noskiewicz (1934). According to Noskiewicz (1934), Ducke also misidentified many males. Therefore, it seems more likely that *H. mocsaryi* was confused with *H. tridentata*.

***Megachile albohirta* (Brullé, 1839)**

Megachile albohirta (Brullé); Ornos et al. (2007: 121) [Misinterpretation]: Corsica.

Remark. The Corsican record of *Megachile albohirta* in Ornos et al. (2007) is a mistake that probably comes from a misinterpretation of the Corsican record of *M. variscopa* Pérez, 1895 by Benoist (1940). Following Tkalců (1993), Ornos et al. (2007) considered *M. variscopa* as a junior synonym of *M. albohirta*. However, they are two distinct species (Gonzalez et al. 2010; Praz 2017). *Megachile albohirta* is restricted to North Africa and Canary Islands (Brullé 1839; Nadig and Nadig 1933; Tkalců 1993) while *M. pusilla* (senior synonym of *M. variscopa*, see Praz and Bénon 2023) occurs in Western Europe (Soltani et al. 2017).

***Megachile lefebvrei* Lepeletier, 1841**

Megachile lefebvrei Lepeletier; Ferton (1920: 336): Bonifacio.

Chalicodoma lefebvrei lefebvrei Lepeletier; Tkalců (1975b: 187): Corsica.

Remark. No Corsican specimen was collected or examined during this study. *M. lefebvrei*, was vaguely reported from Corsica by Tkalců (1975b) who cites the dark form *M. lefebvrei lefebvrei*. Since no material was presented by the author, this could either be an error in the text or based on the paper of Ferton (1920). Ferton (1920) mentions an observation of *M. lefebvrei* in Bonifacio on July 31, 1915. However, only one Hymenoptera collected in 1915 is in his collection, suggesting that Ferton likely ceased his regular field trips in Corsica from 1915 onwards. Additionally, the date of observation seems unlikely. Upon comparing Ferton (1920) with the corresponding specimens in his collection, it becomes evident that he frequently switched the years 1915 and 1914. This discrepancy is not surprising, considering Ferton's passing during the preparation of the publication, leading to an incomplete revision of the draft. Finally, the entire publication focuses on Ferton's collecting activities in Algeria and occasionally in Provence. It appears more plausible to us that the specimen was observed in Nemours, where Ferton was definitely present in July 1914 and where the nominative form of *M. lefebvrei* is known to occur. In his box from the year 1914, a female of *M. lefebvrei* from Nemours is present with a label referring to his lost manuscript, where he had evidently recorded the observations reported in his publication.

***Megachile sicula sicula* (Rossi, 1792) and *Megachile s. perezi* Lichtenstein, 1880**

Megachile sicula var. *perezi* Lichtenstein; Friese (1899: 39, 176): Corsica.

Megachile sicula Rossi; Ferton (1909a: 550): Bonifacio.

Megachile perezii Lichtenstein; Ferton (1909a: 550): Bonifacio.

Megachile perezii Lichtenstein; Friese (1911: 212): Corsica.

Chalicodoma sicula Rossi; Liongo Li Enkulu (1988, p.87, Map 62): Corsica.

Chalicodoma sicula perezii Lichtenstein; Liongo Li Enkulu (1988, Map 64): Corsica.

Remark. Both *M. sicula* and *M. perezii* are mentioned in Corsica by Ferton and Friese. The record of *M. perezii* is a mistake as no specimen of *M. s. perezii* has been found in Ferton's collection. Liongo Li Enkulu (1988) also notes Corsican records for *C. corsica*, along with instances of *C. sicula sicula* (Rossi, 1792) and *C. s. perezii* (Lichtenstein, 1880). These two taxa are very close to *C. s. corsica* and are prone to confusion, particularly among males with highly variable pilosity. We believe that all these records exclusively pertain to *C. s. corsica*, which is the sole taxon we have observed on the island.

***Osmia caerulescens cyanea* (Fabricius, 1793)**

Osmia cyanea (Fabricius); Ferton (1905: 93): Bonifacio.

Remark. Ferton labelled his specimens of *O. caerulescens* with the name *cyanea*. The mention of *Osmia caerulescens cyanea* (Fabricius, 1793) is erroneous. This subspecies is strictly North African (Tkalců 1970).

***Osmia cyanoxantha* Pérez, 1879**

Osmia cyanoxantha Pérez; Benoist (1931: 31): Corsica.

Remark. No specimen of *O. cyanoxantha* has been located in MNHN collections. We believe that the record of Benoist resulted from a misidentification.

***Osmia koblii* Ducke, 1899**

Osmia koblii Ducke; Ferton (1905: 59) [Misinterpretation, see Peters (1977)]: Bonifacio.

Remark. No such specimen is in Ferton's collection. The Corsican record has moreover been invalidated by Peters (1977) who consider this species to be restricted to southern Italy and Sicily. It also occurs in Malta according to Müller (2022a).

***Osmia lhotelleriei* Pérez, 1887**

Osmia fossoria Pérez; Ducke (1900: 127) [Misinterpretation]: Corsica.

Remark. *Osmia fossoria* Pérez, junior synonym of *O. lhotelleriei*, is restricted to North Africa and Levant (Müller 2022). The record of Ducke (1900) refers to *O. rufohirta*.

Types of Megachilid bees described from Corsica and housed at MNHN

Megachile argentata var. *fossoria* Ferton, 1909

Figs 35–38

Megachile argentata var. *fossoria* Ferton, 1909a: p.550. Corsica: Bonifacio, Propriano (Lectotype designated by Schwarz and Gusenleitner (2011), MNHN).

Type material examined. Lectotype: ♀, MNHN Paris EY0000001710 // Terrain sable Propriano 20/6 99 [20.VI.1899] // Museum Paris Coll. Ferton // Lectotypus *Megachile argentata fossoria* Ferton M. Schwarz des. 2009 // = *Megachile leachella fossoria* Ferton, 1909 Le Divelec det. 2020; **Paralectotypes:** ♀, MNHN Paris EY0000001711 // Bonifacio 4/6 99 [04.VI.1899] dans nid page 286 *Megachile* // Museum Paris Coll. Ferton // Paralectotypus *Megachile argentata fossoria* Ferton M. Schwarz des. 2009 // = *Megachile leachella fossoria* Ferton, 1909 Le Divelec det. 2020; ♀, MNHN Paris EY0000001712 // Bonifacio 18/7 97 [18.VII.1897] dans nid trou sable feuilles collées-miel liquide œuf baignant page 190 *argentata* // Museum Paris Coll. Ferton // Paralectotypus *Megachile argentata fossoria* Ferton M. Schwarz des. 2009 // = *Megachile leachella fossoria* Ferton, 1909 Le Divelec det. 2020.

Current status. *Megachile* (*Eutricharaea*) *leachella* Curtis, 1828.

Megachile lucidifrons Ferton, 1905

Megachile (*Chalicodoma*) *lucidifrons* Ferton, 1905: p.57, ♀. Corsica: Bonifacio (Type lost).

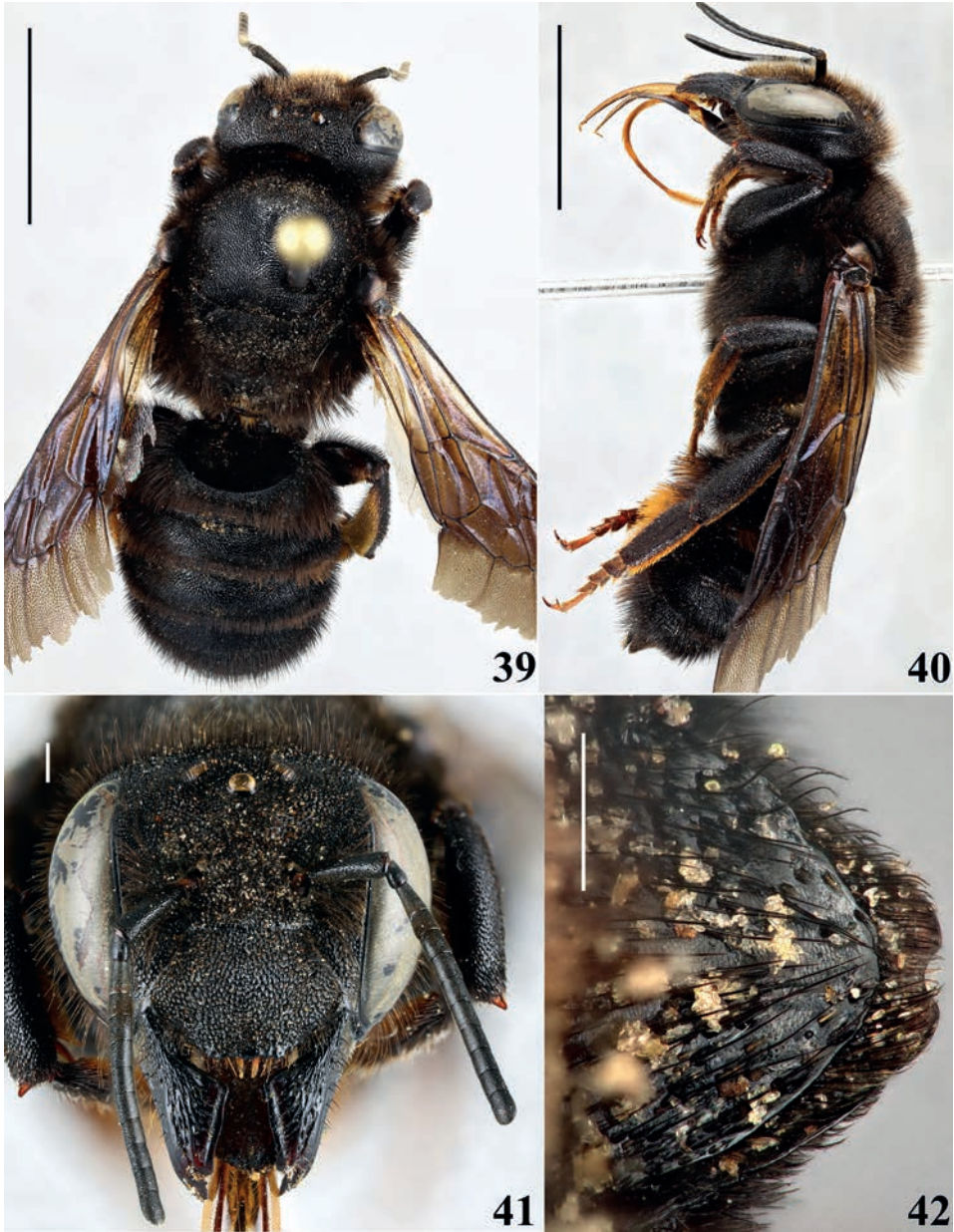
Remark. *Megachile lucidifrons* has been consistently listed in the works on French *Megachile* (Benoist 1935, 1940; Liongo Li Enkulu 1988; Rasmont et al. 1995) despite its uncertain identity (Ghisbain et al. 2023). It was described based on a single worn female from Bonifacio and belongs to the *lefebvrei* species-group (Benoist 1935). The holotype was last examined by Benoist (1940) but despite exhaustive research in MNHN collections and consultation of the loan logs, its whereabouts remain unknown. In a correspondence with B. Tkalcù, who sought to borrow the holotype, J. Kelner-Pillault (former curator of the Hymenoptera collections) mentioned her inability to locate it. The type is also not present in B. Tkalcù's collection (M. Schwarz, pers. comm.) and can be considered lost. A series of entirely black individuals of *Megachile* belonging to the *lefebvrei* species-group and matching the descriptions of Ferton (1905) and Benoist (1935) were collected in Corsica (Figs 39–42). No morphological differences were observed between these specimens and *M. albocristata*. Aside from the darker pilosity, the sculpture of the tegument, sterna, and genitalia is similar. The colour of the pilosity is highly variable in this subgenus



Figures 35–38. Lectotype of *Megachile argentata* var. *fossoria* Ferton **35** dorsal view **36** lateral view **37** head in front view **38** labels. Scale bars: 1 mm.

and cannot be relied upon for species differentiation. Consequently, we propose considering *M. lucidifrons* as a new junior synonym for *M. albocristata*.

Current status. – *Megachile* (*Chalicodoma*) *albocristata* Smith, 1853.

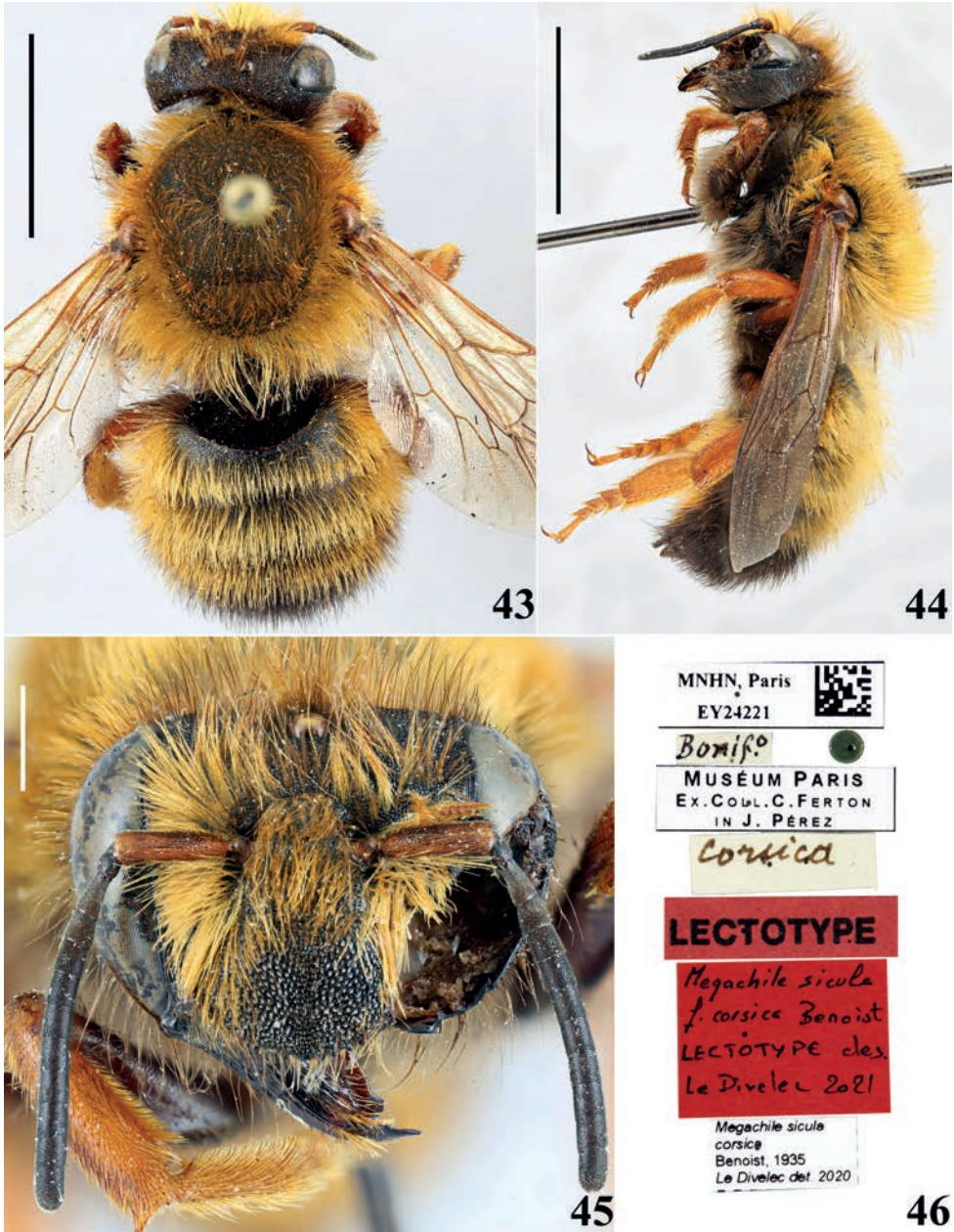


Figures 39–42. *Megachile alboicristata* Smith (Corsica, Mausoléo) **39** dorsal view **40** lateral view **41** head in front view **42** sternum 6. Black Scale bars: 5 mm. White Scale bars: 0.5 mm.

***Megachile sicula* var. *corsica* Benoist, 1935**

Figs 43–46

Megachile sicula f. *corsica* Benoist, 1935: p.103. Locality not indicated (Lectotype here designated, MNHN).



Figures 43–46. Lectotype of *Megachile sicula* var. *corsica* Benoist **43** dorsal view **44** lateral view **45** head in front view **46** labels. Black Scale bars: 5 mm. White Scale bars: 1 mm.

Type material examined. *Lectotype:* ♀, MNHN, Paris EY24221 // Bonif.^o [Bonifacio, Pérez's handwriting] // Muséum Paris Ex. Coll. C. Ferton in J. Pérez // *corsica* [Benoist's handwriting] // Lectotype // *Megachile sicula* f. *corsica* Benoist Lectotype des. Le Divelec 2021 // = *Megachile sicula corsica* Benoist, 1935 Le Divelec det. 2020; *Paralectotype:*

♂, MNHN, Paris EY24164 // Bonif^o [Bonifacio, Pérez's handwriting] // Ex. Coll. J. Pérez MNHN // Paralectotype // *Megachile sicula* f. *corsica* Benoist Paralectotype des. Le Divelec 2021 // = *Megachile sicula corsica* Benoist, 1935 Le Divelec det. 2020.

Remark. Benoist (1935) did not specify a locality in the original description but the taxon's name suggests it originates from Corsica. Benoist (1940) clarified the distribution of this taxon, indicating it is found in Bonifacio. Within Benoist's reference collection, there is a female and a male from Bonifacio, both labelled as "*corsica*" by Benoist himself. These specimens were acquired by Benoist from Pérez's collection, who, in turn, received them from C. Ferton. Other *M. sicula corsica* specimens in Benoist's collection originate from Ajaccio or Vivario. Notably, three specimens of Benoist's collection, borrowed by B. Tkalcú in 1965, have not been returned according to the loans log. However, they could not be located in Tkalcú's collection (M. Schwarz pers. comm.). Consequently, we designate the female from Bonifacio, labelled by Benoist, as the lectotype. Despite partial damage to the left eye, left mandible, and left leg from pests, the female is in overall good condition and perfectly matches the original description. The associated male from Bonifacio is chosen as paralectotype.

Current status. *Megachile (Chalicodoma) sicula corsica* Benoist, 1935.

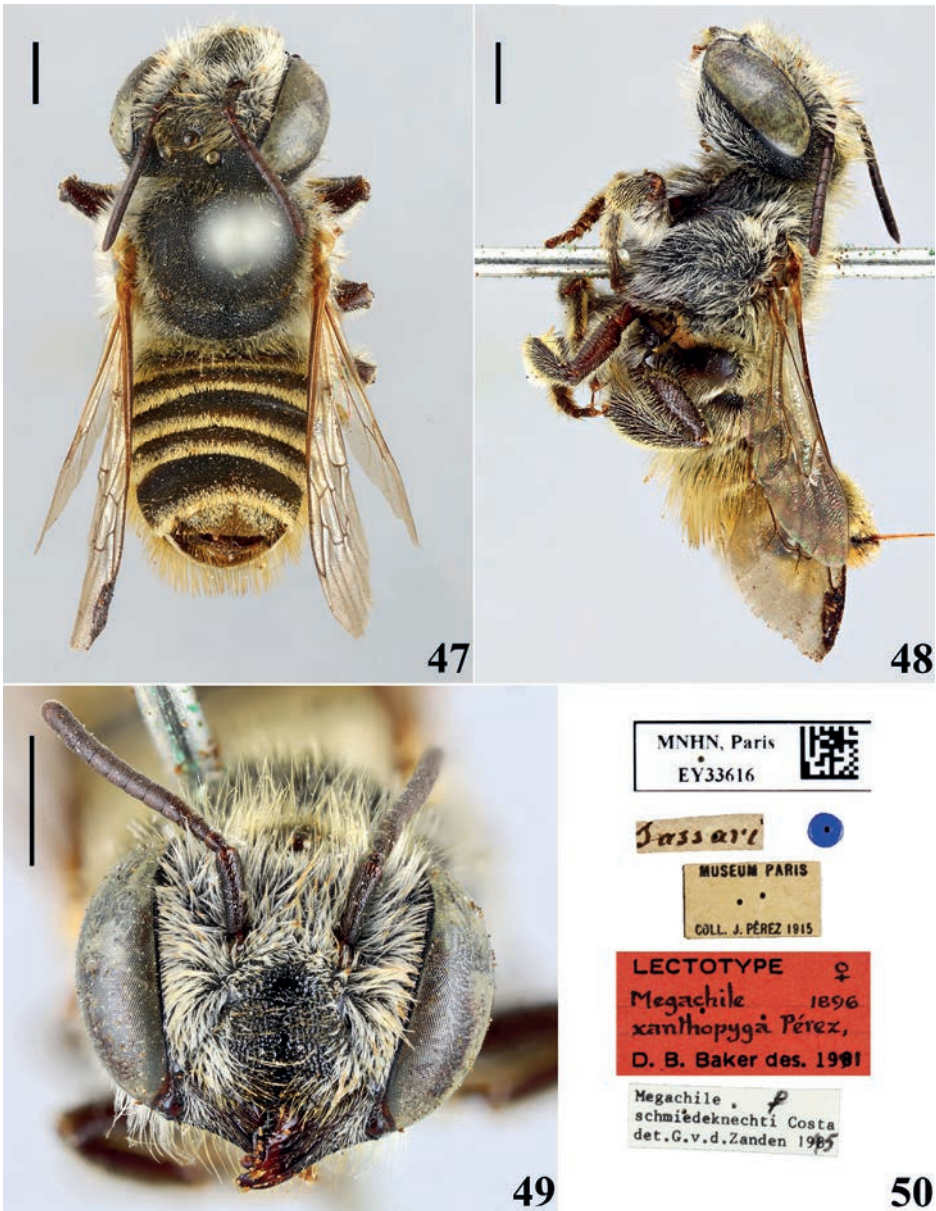
Megachile xanthopyga Pérez, 1895

Figs 47–50

Megachile xanthopyga Pérez, 1895: p.25, ♀♂. Locality not indicated (Lectotype designated by Praz and Bénon (2023), MNHN).

Type material examined. Lectotype: ♀, MNHN, Paris EY33616 // Sassari [Pérez's handwriting] // dark blue circle [May] // Museum Paris Coll. J. Pérez 1915 // Lectotype ♀ *Megachile xanthopyga* Pérez, 1896 D. B. Baker des. 1991 // *Megachile schmiedeknechti* Costa det. G. v. d. Zanden 1995; **Paralectotypes:** ♀, MNHN, Paris EY33617 // Sassari [Pérez's handwriting] // Museum Paris Coll. J. Pérez 1915 // Paralectotype ♀ *Megachile xanthopyga* Pér., 1896 D. B. Baker des. 1991 // *Megachile schmiedeknechti* Costa det. G. v. d. Zanden 1995; ♀, MNHN, Paris EY33618 // Sassari [Pérez's handwriting] // Museum Paris Coll. J. Pérez 1915 // Paralectotype ♀ *Megachile xanthopyga* Pér., 1896 D. B. Baker des. 1991 // *Megachile schmiedeknechti* Costa det. G. v. d. Zanden 1995; ♀, MNHN, Paris EY23891 // Bonifacio 15/8 [15.VIII., Ferton's label partly cut out] // Museum Paris Coll. J. Pérez 1915 // Paralectotype // *Megachile xanthopyga* J.P. Paralectotype des. Le Divelec 2021 // *Megachile schmiedeknechti* Costa det. G. v. d. Zanden 1995; ♀, MNHN, Paris EY23892 // Bonifacio 10/8 [10.VIII., Ferton's label partly cut out] // Museum Paris Coll. J. Pérez 1915 // Paralectotype // *Megachile xanthopyga* J.P. Paralectotype des. Le Divelec 2021 // *Megachile schmiedeknechti* Costa det. G. v. d. Zanden 1995; ♂, MNHN, Paris EY23894 // Bonifacio 30/7 [30.VII., Ferton's label partly cut out] // Museum Paris Coll. J. Pérez 1915 // Paralectotype // *Megachile xanthopyga* J.P. Le Divelec des. 2021.

Remark. No locality is specified in the original description. Pérez, in his original manuscript under *M. xanthopyga* (catalogue number 1732), mentions "Bonifacio, Sas-



Figures 47–50. Lectotype of *Megachile xanthopyga* Pérez **47** dorsal view **48** lateral view **49** head in front view **50** labels. Scale bars: 1 mm.

sari, ♀ mai-août, ♂ mai-juillet” (<https://science.mnhn.fr/catalogue/ey-bib-perez1/>). Praz and Bénon (2023) accepted and designated the Sardinian lectotype, along with two paralectotypes of *M. xanthopyga* labelled by D. Baker in 1991. Additionally, we have labelled as paralectotypes the three other specimens present under the *xanthopyga* head label in Pérez’s collection.

Current status. *Megachile (Eutricharaea) argentata schmiedeknechti* Costa, 1884.

***Osmia corsica* Ferton, 1901**

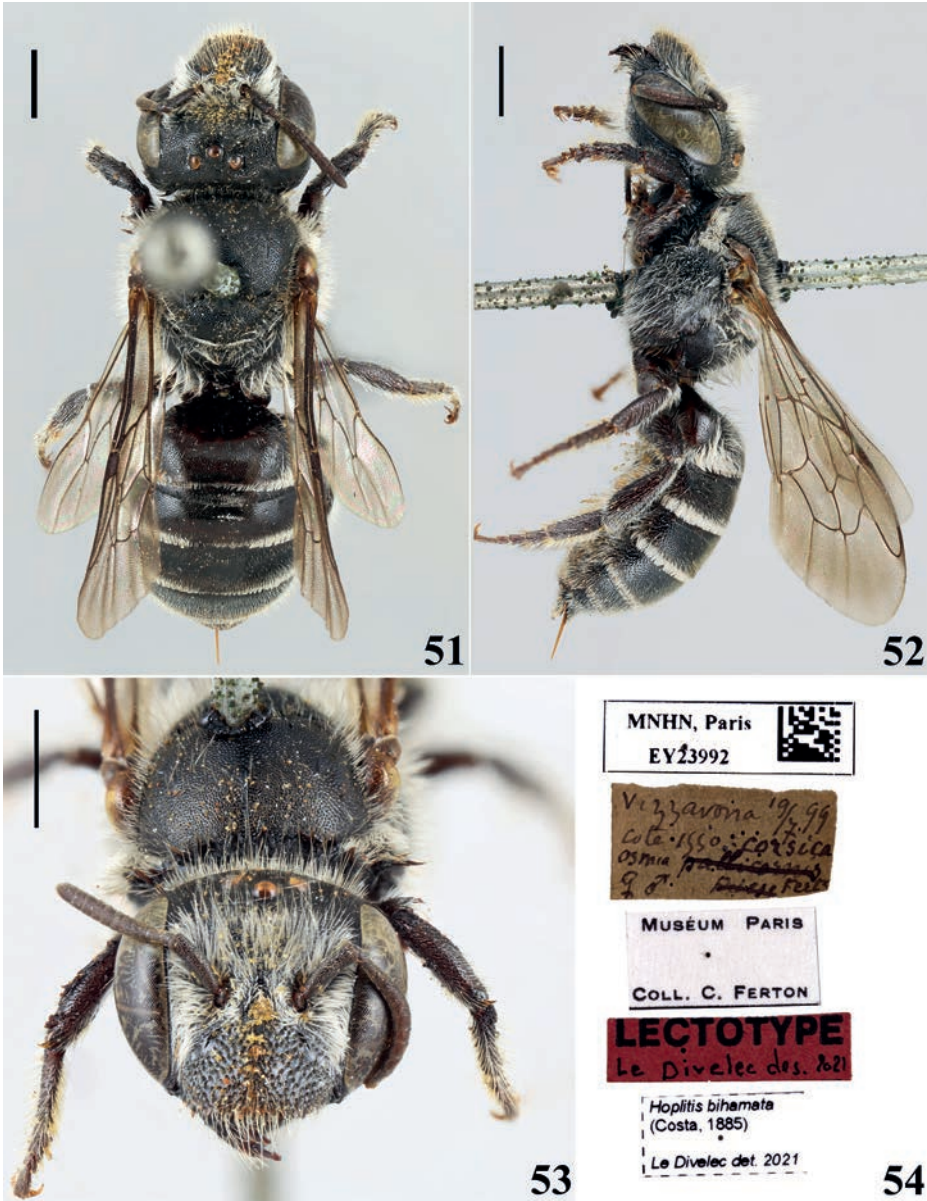
Figs 51–54

Osmia corsica Ferton, 1901: p.61, ♀♂. Corsica: Bonifacio, Monte Renoso (Lectotype here designated, MNHN).

Type material examined. Lectotype: ♀, MNHN, Paris EY23992 // Vizzavona 19/7 99 [19.VII.1899] cote 1550 [altitude] *Osmia corsica* Fert ♀♂ [the mention “*pallicornis* Friese” crossed out] // Muséum Paris Coll. C. Ferton // Lectotype Le Divelec des. 2021 // *Hoplitis bihamata* (Costa, 1885) Le Divelec det. 2021; **Paralectotypes:** ♀, MNHN, Paris EY23964 // Bonifacio 24/6 1900 [24.VI.1900] *corsica* Ferton ♀ // Muséum Paris Coll. C. Ferton // Paralectotype vdZ-1987 // Paralectotype valide Le Divelec 2021 // *Hoplitis bihamata* (Costa det. G. v. d. Zanden 1987 // *Hoplitis bihamata* (Costa, 1885) Le Divelec det. 2021; ♀, MNHN, Paris EY23968 // *Osmia corsica* Ferton ♀ Trinité (Bonifacio) 24/6 1900 [24.VI.1900] // Muséum Paris Coll. J. Vachal 1911 // Ex. Coll. C. Ferton // Paralectotype vdZ-1986 // Paralectotype valide Le Divelec 2021 // *Hoplitis bihamata* (Costa det. G. v. d. Zanden 1986 // *Hoplitis bihamata* (Costa, 1885) Le Divelec det. 2021; ♂, MNHN, Paris EY23972 // Vizzavona 19/7 1899 [19.VII.1899] cote 1550 [altitude] *Osmia corsica* ♂ // Muséum Paris Coll. C. Ferton // Paralectotype // *Osmia corsica* Ferton Paralectotype des. Le Divelec 2021 // *Hoplitis bihamata* (Costa, 1885) Le Divelec det. 2021; ♂, MNHN, Paris EY23982 // Bonifacio (Trinité) 17/6 00 [17.VI.1900] ♂ *corsica* [the mention “*pallicornis*” crossed out] // Muséum Paris Coll. C. Ferton // Paralectotype // *Osmia corsica* Fert. Paralectotype des. Le Divelec 2021 // *Hoplitis bihamata* (Costa, 1885) Le Divelec det. 2021; ♀, MNHN, Paris EY23994 // Fermant nid 19/7 99 [19.VII.1899] Vizzavona 1550 [altitude] *Osmia corsica* Fert. [the mention “*pallicornis* Friese” crossed out, four legs glued on the label] // Muséum Paris Coll. C. Ferton // Paralectotype // *Osmia corsica* Ferton Paralectotype des. Le Divelec 2021 // *Hoplitis bihamata* (Costa, 1885) Le Divelec det. 2021; ♀, MNHN, Paris EY23999 // Muséum Paris Bonifacio (Trinité) 17-6-1900 [17.VI.1900] Coll. C. Ferton // Paralectotype // *Osmia corsica* Ferton Paralectotype des. Le Divelec 2021 // *Hoplitis bihamata* (Costa, 1885) Le Divelec det. 2021; ♀, MNHN, Paris EY24001 // Muséum Paris Bonifacio (Trinité) 17-6-1900 [17.VI.1900] Coll. C. Ferton // Paralectotype // *Osmia corsica* Ferton Paralectotype des. Le Divelec 2021 // *Hoplitis bihamata* (Costa, 1885) Le Divelec det. 2021; ♀, MNHN, Paris EY24002 // Muséum Paris Bonifacio (Trinité) 17-6-1900 [17.VI.1900] Coll. C. Ferton // Paralectotype // *Osmia corsica* Ferton Paralectotype des. Le Divelec 2021 // *Hoplitis bihamata* (Costa, 1885) Le Divelec det. 2021.

Remark. An unpublished lectotype and some paralectotypes were labelled by G. v. d. Zanden in the eighties. He randomly selected specimens of *H. bihamata* in Ferton’s collection. Therefore, his lectotype is not part of the type series and cannot be accepted. We have designated one female in good condition as lectotype and selected 8 specimens collected by C. Ferton in the granitic part of Bonifacio (e.g. La Trinité) and in the Monte Renoso as paralectotypes, in accordance with the original description information.

Current status. *Hoplitis* (*Hoplitis*) *bihamata* (Costa, 1885).



Figures 51–54. Lectotype of *Osmia corsica* Ferton **51** dorsal view **52** lateral view **53** head in front view **54** labels. Scale bars: 1 mm.

***Osmia erythrogastra* Ferton, 1905**

Figs 55–58

Osmia erythrogastra Ferton, 1905: p.57, ♀♂. Corsica: Bonifacio, Santa-Manza (Lectotype here designated, MNHN).



Figures 55–58. Lectotype of *Osmia erythrogastra* Ferton **55** dorsal view **56** lateral view **57** head in front view **58** labels. Scale bars: 1 mm.

Type material examined. Lectotype: ♂, Museum Paris EY0000002285 // Bonifacio 26/6 04 [26.VI.1904] *erythrogastra* Ferton ♂ // Museum Paris Corse Bonifacio C. Ferton 1902 // Lectotype Le Divelec des. // *Os. Erythrogastra* Ferton, 1905 Lectotype des. Le Divelec 2021 // *Osmia erythrogastra* Ferton, 1905 Le Divelec det. 2021;

Paralectotypes: ♀, Museum Paris EY0000002284 // Bonifacio 26/6 04 [26.VI.1904] *erythrogastra* Ferton ♀ // Museum Paris Corse Bonifacio C. Ferton 1902 // *Anthocopa erythrogastra* (Ferton) ♀ det. G. v. d. Zanden 1987 // Paralectotype // *Os. Erythrogastra* Ferton, 1905 Paralectotype des. Le Divelec 2021 // *Osmia erythrogastra* Ferton, 1905 Le Divelec det. 2021; ♂, MNHN, Paris EY23930 // Bonifacio 26/6 04 [26.VI.1904] // Museum Paris Corse Bonifacio C. Ferton 1902 // Paralectotype // *Os. Erythrogastra* Ferton, 1905 Paralectotype des. Le Divelec 2021 // *Osmia erythrogastra* Ferton, 1905 Le Divelec det. 2021.

Remark. Ferton described this species based on four females and six males collected in the granitic area of Santa Manza on the June 26, 1904. Only two males and one female of this type series have been located. We designate as lectotype one male in good condition and bearing an original label.

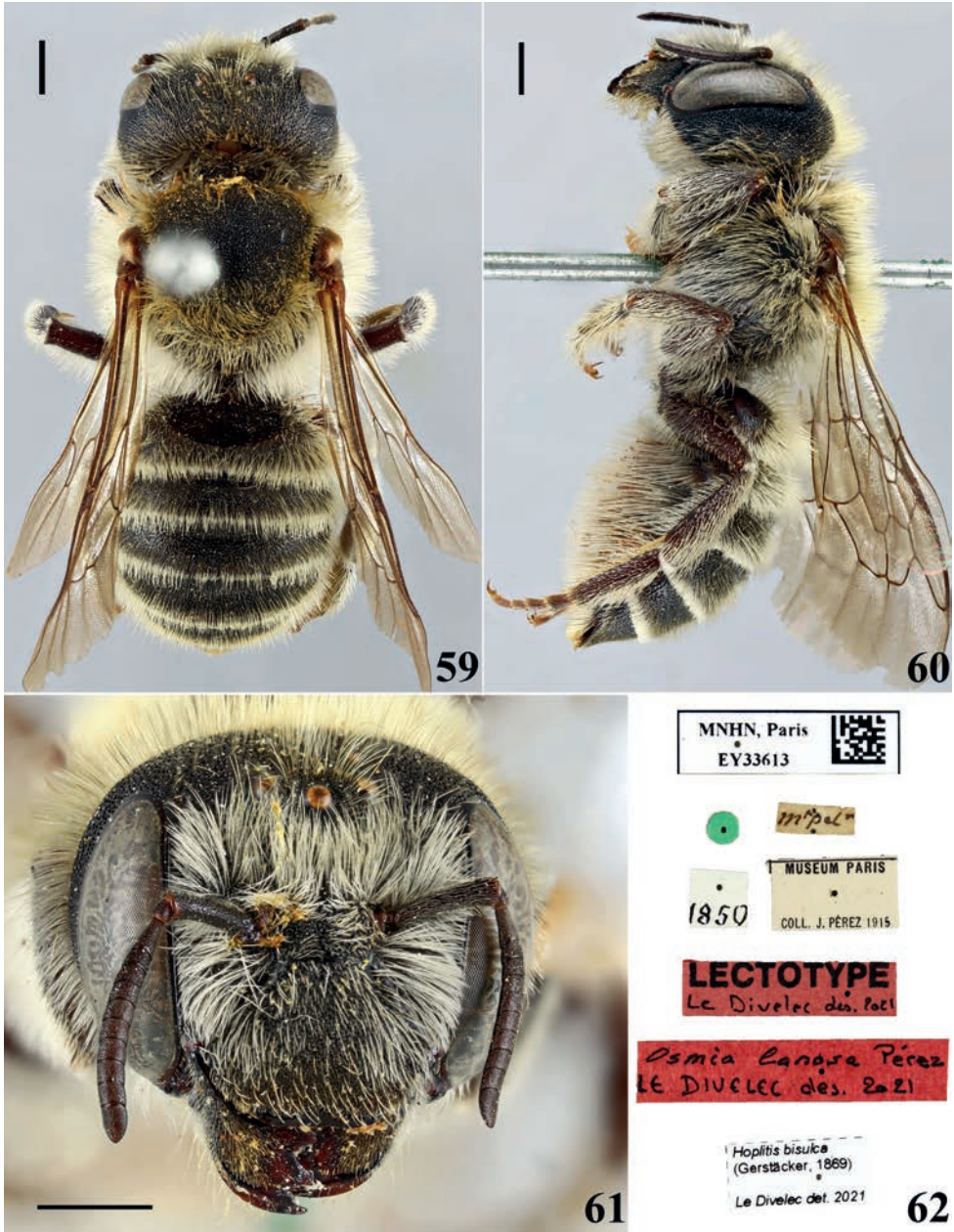
Current status. *Osmia* (*Erythrosmia*) *erythrogastra* Ferton, 1905.

Osmia lanosa Pérez, 1879

Figs 59–62

Osmia lanosa Pérez, 1879: p.194, ♀. Algeria and Southern France (Lectotype here designated, MNHN).

Type material examined. Lectotype: ♀, MNHN, Paris EY33613 // M'pel' [Montpellier] // green disc [June] // 1850 [Pérez's catalogue number] // Museum Paris Coll. J. Pérez 1915 // Lectotype Le Divelec des. 2021 // *Osmia lanosa* Pérez Le Divelec des. 2021 // *Hoplitis bisulca* (Gerstäcker, 1869) Le Divelec det. 2021; **Paralectotypes:** ♀, MNHN, Paris EY24179 // Bonifacio [cut out Ferton's label] // green disc [June] // 1850 [Pérez's catalogue number] // Museum Paris Coll. J. Pérez 1915 // Paralectotype // *Osmia lanosa* Pérez Paralectotype des. Le Divelec des. 2021 // *Hoplitis bisulca* (Gerstäcker, 1869) Le Divelec det. 2021; ♀, MNHN, Paris EY24180 // Bonifacio [cut out Ferton's label] // green disc [June] // 1850 [Pérez's catalogue number] // Museum Paris Coll. J. Pérez 1915 // Paralectotype // *Osmia lanosa* Pérez Paralectotype des. Le Divelec des. 2021 // *Hoplitis bisulca* (Gerstäcker, 1869) Le Divelec det. 2021; ♀, MNHN, Paris EY33605 // Alg. [Algeria] // 1850 [Pérez's catalogue number] // Museum Paris Coll. J. Pérez 1915 // Paralectotype // *Osmia lanosa* Pérez Paralectotype des. Le Divelec des. 2021; ♀, MNHN, Paris EY33606 // Marsr^{lc} [Marseille] // 1850 [Pérez's catalogue number] // Museum Paris Coll. J. Pérez 1915 // Paralectotype // *Osmia lanosa* Pérez Paralectotype des. Le Divelec des. 2021 // *Hoplitis bisulca* (Gerstäcker, 1869) Le Divelec det. 2021; ♀, MNHN, Paris EY33607 // Marsr^{lc} [Marseille] // 1850 [Pérez's catalogue number] // Museum Paris Coll. J. Pérez 1915 // Paralectotype // *Osmia lanosa* Pérez Paralectotype des. Le Divelec des. 2021 // *Hoplitis bisulca* (Gerstäcker, 1869) Le Divelec det. 2021; ♀, MNHN, Paris EY33608 // Marsr^{lc} [Marseille] // 1850 [Pérez's catalogue number] // Museum Paris Coll. J. Pérez 1915 // Paralectotype // *Osmia lanosa* Pérez Paralectotype des. Le Divelec des. 2021 // *Hoplitis bisulca* (Gerstäcker, 1869) Le Divelec det. 2021; ♀, MNHN, Paris EY33609 // Marsr^{lc} [Marseille] // green disc [June] // 1850 [Pérez's catalogue number] // Museum Paris Coll. J. Pérez 1915 //



Figures 59–62. Lectotype of *Osmia lanosa* Pérez **59** dorsal view **60** lateral view **61** head in front view **62** labels. Scale bars: 1 mm.

Paralectotype // *Osmia lanosa* Pérez Paralectotype des. Le Divelec des. 2021 // *Hoplitis bisulca* (Gerstäcker, 1869) Le Divelec det. 2021; ♀, MNHN, Paris EY33610 // Marsr^{le} [Marseille] // 1850 [Pérez's catalogue number] // Museum Paris Coll. J. Pérez 1915 //

Paralectotype // *Osmia lanosa* Pérez Paralectotype des. Le Divelec des. 2021 // *Hoplitis bisulca* (Gerstäcker, 1869) Le Divelec det. 2021; ♀, MNHN, Paris EY33611 // Marsr^{le} [Marseille] // 1850 [Pérez's catalogue number] // Museum Paris Coll. J. Pérez 1915 // Paralectotype // *Osmia lanosa* Pérez Paralectotype des. Le Divelec des. 2021 // *Hoplitis bisulca* (Gerstäcker, 1869) Le Divelec det. 2021; ♀, MNHN, Paris EY33612 // Marsr.^{le} [Marseille] // green disc [June] // 1850 [Pérez's catalogue number] // Museum Paris Coll. J. Pérez 1915 // Paralectotype // *Osmia lanosa* Pérez Paralectotype des. Le Divelec des. 2021 // *Hoplitis bisulca* (Gerstäcker, 1869) Le Divelec det. 2021.

Remark. More information about the type localities can be found in Pérez's manuscript catalogue (<https://science.mnhn.fr/catalogue/ey-bib-perez1/>): "Connue dans le midi oriental de la France et en Barbarie, en Corse, en Espagne. Montpellier. Marseille. Bonifacio. Barcelone. Vole en juin". In accordance with this information, we have selected the lectotype and 11 paralectotypes among the specimens under the *lanosa* head label in Pérez's collection. The female lectotype here designated is in good condition and matches with the current species concept of *H. bisulca*.

Current status. *Hoplitis (Anthocopa) bisulca* (Gerstäcker, 1869).

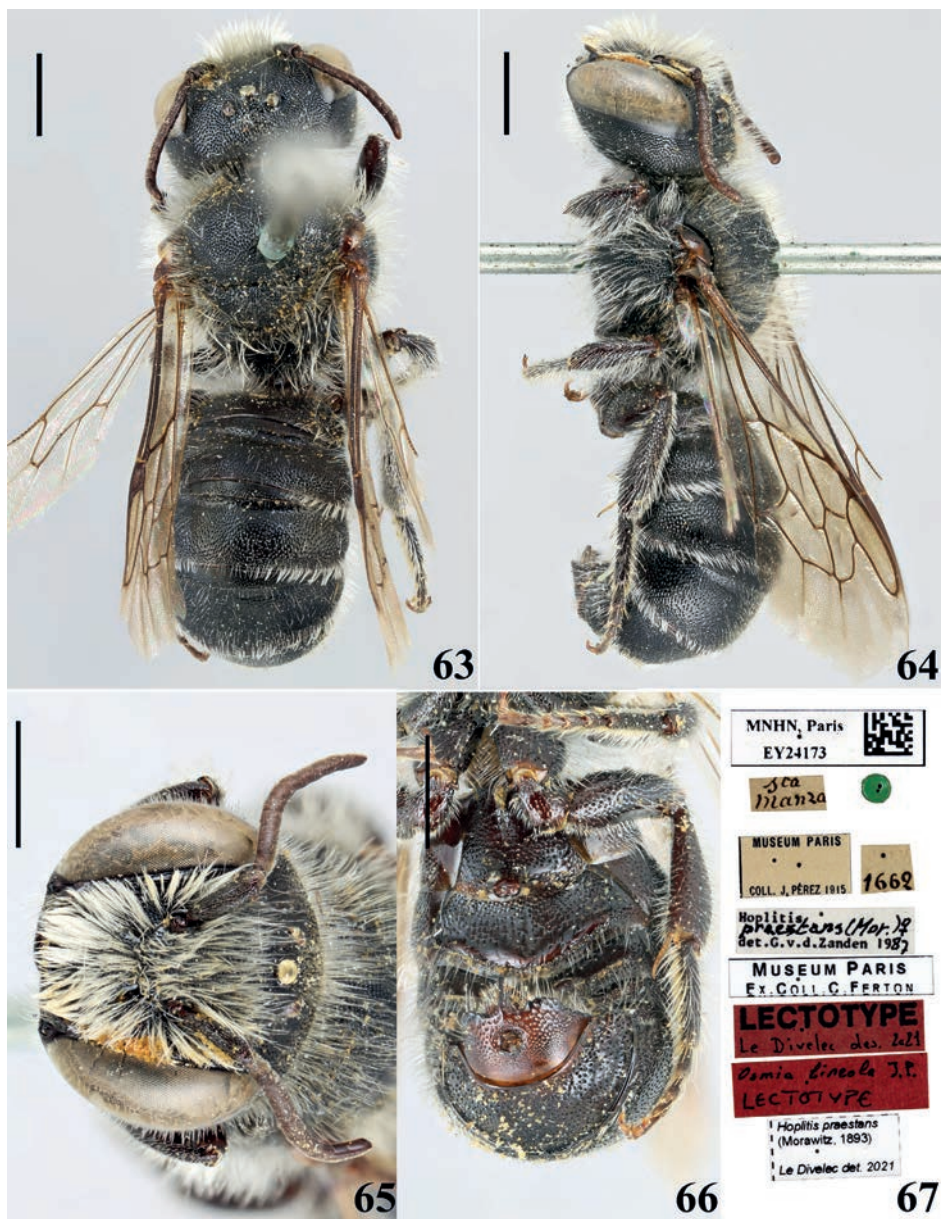
Osmia lineola Pérez, 1895

Figs 63–67

Osmia lineola Pérez, 1895: p.16, ♀♂. Locality not indicated (Lectotype here designated, MNHN).

Type material examined. Lectotype: ♂, MNHN, Paris EY24173 // S^{ta}Manza [Bonifacio, Santa-Manza] // green disc [June] // 1662 [Pérez's catalogue number] // Museum Paris Coll. J. Pérez 1915 // Museum Paris Ex. Coll. C. Ferton // Lectotype Le Divelec des. 2021 // *Osmia lineola* J.P. Lectotype // *Hoplitis praestans* (Mor.) ♀ det. G. v. d. Zanden 1987 // *Hoplitis praestans* (Morawitz, 1893) Le Divelec det. 2021; **Paralectotypes:** ♀, MNHN, Paris EY24172 // Bonif.^o [Bonifacio] // green disc [June] // 1662 [Pérez's catalogue number] // Museum Paris Coll. J. Pérez 1915 // Museum Paris Ex. Coll. C. Ferton // Paralectotype // *Osmia lineola* J.P. Paralectotype des. Le Divelec 2021 // *Hoplitis praestans* Mor. ♀ det. G. v. d. Zanden 1986 // *Hoplitis praestans* (Morawitz, 1893) Le Divelec det. 2021; ♂, MNHN, Paris EY33604 // Marsr^{le} [Marseille] // 439 // 1662 [Pérez's catalogue number] // Museum Paris Coll. J. Pérez 1915 // Paralectotype // *Osmia lineola* J.P. Paralectotype des. Le Divelec 2021 // *Hoplitis praestans* Mor. ♂ det. G. v. d. Zanden 1986 // *Hoplitis praestans* (Morawitz, 1893) Le Divelec det. 2021; ♀, MNHN, Paris EY33614 // Tibériade // *modesta* Ab. Tib. N°467 // 1662 [Pérez's catalogue number] // Museum Paris Coll. J. Pérez 1915 // Paralectotype // *Osmia lineola* J.P. Paralectotype des. Le Divelec 2021 // *Hoplitis praestans* (Mor.) ♀ det. G. v. d. Zanden 1986 // *Hoplitis praestans* (Morawitz, 1893) Le Divelec det. 2021.

Remark. Additional details regarding the type localities can be accessed in Pérez's manuscript catalogue (<https://science.mnhn.fr/catalogue/ey-bib-perez1/>): "♀ Tibériade (Abeille de Perrin). ♀ Bonifacio, Juin (Ferton), butinant sur le *Centaurea suaveolens*



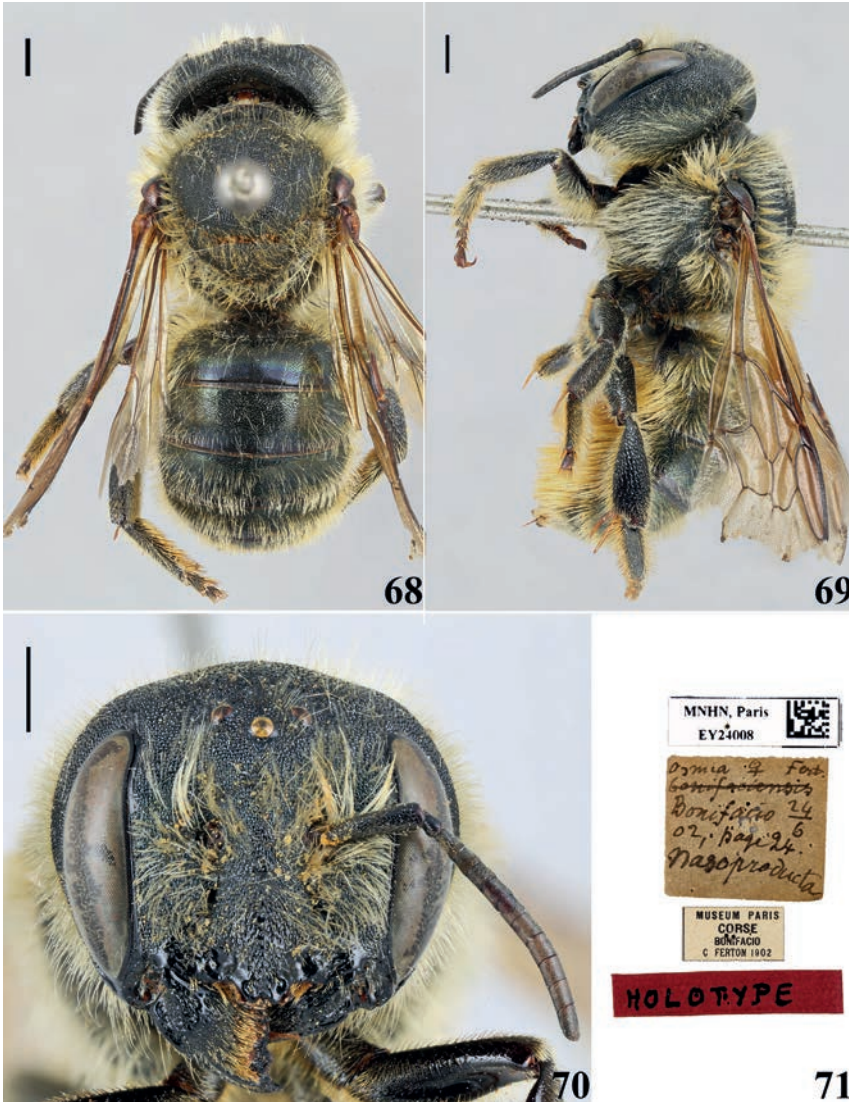
Figures 63–67. Lectotype of *Osmia lineola* Pérez **63** dorsal view **64** lateral view **65** head in front view **66** gaster in ventral view **67** labels. Scale bars: 1 mm.

(Ferton). ♂ Marseille et Corse (Santa–Manza)”. Within Pérez’s collection, only four specimens are located under the “*lineola*” head label, with two originating from Corsica (Ferton leg.). These specimens align with both the manuscript information and the original description. The male from Corsica in the best condition is designated as the lectotype, while the three remaining individuals are labelled as paralectotypes.

Current status. *Hoplitis (Alcidamea) praestans* (Morawitz, 1893).

***Osmia nasoproducta* Ferton, 1909**

Figs 68–71

Osmia nasoproducta Ferton, 1909b: p.406, ♀. Corsica: Bonifacio (Holotype, MNHN).**Type material examined. Holotype:** ♀, MNHN, Paris EY24008 // *Osmia* ♀ Fert. [the mention “*bonifaciensis*” crossed out] Bonifacio 24/06 02 [24.VI.1902], page 24 *nasoproducta* // Museum Paris Corse Bonifacio C. Ferton 1902 // Holotype.**Current status.** *Osmia* (*Helicosmia*) *nasoproducta* (Ferton, 1909).

Figures 68–71. Lectotype of *Osmia nasoproducta* Ferton **68** dorsal view **69** lateral view **70** head in front view **71** labels. Scale bars: 1 mm.

Acknowledgements

We are grateful to Andreas Müller, Gérard Le Goff, Eric Dufrière and Paul Vignac for sharing their data with us. Many thanks to Erwin Scheuchl and Maurizio Cornalba for our helpful exchanges. Thanks to Martin Schwarz for his help with the material preserved in Linz collections and to Rémi Santerre for his help with Mavromoustakis collection. We are grateful to Christophe Praz for improving this manuscript. Quentin Rome (PatriNat) kindly supported us with the uploading of our data on the INPN data portal. Special thanks to Claire Villemant, Agnèle Touret-Alby, Laurent Albenga, and Antoine Mantilleri for access to MNHN collections and to the photography setup of the department of terrestrial Arthropod's collections management (MNHN, Paris). Collecting specimens carried out in 2016–2017 was part of a program funded by the Labex BCDiv of MNHN, with the help of OCIC, OEC and the Conservatoire du Littoral de Corse du Sud. Thanks to Claire Villemant, Colin Fontaine, Marianne Elias, Benjamin Yguel, Marie-Cécile Ruiz and Viviane Sorba for joining or helping with the collecting in the campaigns of 2016 and 2017. The “Our Planet Revisited–Corsica 2019–2022” expedition was organized by MNHN (Paris) and funded by the Office Français de la Biodiversité (OFB) and the Collectivité de Corse (CdC). Many thanks to Julien Touroult, François Dusoulier and Jean Ichter for organizing these wonderful expeditions. Thanks to Claire Villemant, Bernardo F. Santos and Quentin Rome for collecting Megachilid bees during these expeditions. The present catalogue was realized within the “Inventaire national du patrimoine naturel (inpn.mnhn.fr)” project with funding from PatriNat (OFB, CNRS, MNHN).

References

- Aguib S, Louadi K, Schwarz M (2010) Le genre *Stelis* PANZER 1806 (Hymenoptera, Apoidea, Megachilidae) de l'Algérien avec une espèce nouvelle pour la faune de ce pays. *Entomofauna* 35(26): 553–572.
- Alfken JD (1923) Zur Kenntnis einiger Arten der *Megachile argentata*-Gruppe. *Acta Musaei Dzieduszciani* 9: 4–8.
- Baker DB (1999) On new stelidine bees from S. W. Asia and N. W. Africa, with a list of the Old-World taxa assigned to the genus *Stelis* Panzer, 1806 (Hymenoptera, Apoidea, Megachilidae). *Deutsche Entomologische Zeitschrift* 46(2): 231–242. <https://doi.org/10.1002/mmnd.4800460209>
- Baldock D, Wood TJ, Cross I, Smit J (2018) The bees of Portugal (Hymenoptera: Apoidea: Anthophila). *Entomofauna Supplement* 22: 1–164.
- Benoist R (1929) Les *Heriades* de la faune française (Hym. Apidae). *Annales de la Société Entomologique de France* 98: 131–141. <https://doi.org/10.1080/21686351.1929.12280329>
- Benoist R (1931) Les Osmies de la faune française (Hymenopt. Apidae). *Annales de la Société Entomologique de France* 100: 23–60. <https://doi.org/10.1080/21686351.1931.12280120>
- Benoist R (1935) Remarques sur quelques espèces du genre *Megachile* [Hymen. Apidae]. *Annales de la Société Entomologique de France* 104: 98–108.

- Benoist R (1940) Remarques sur quelques espèces de Mégachiles principalement de la faune française. *Annales de la Société Entomologique de France* 109: 41–88. <https://doi.org/10.1080/21686351.1940.12279433>
- Blüthgen P (1930) *Stelis phaeoptera* K. subsp. nov. *franconica* (Hym. Apidae). *Archiv für Insektenkunde des Oberrheingebietes u. der Angrenzenden Länder* 2: 277–278.
- Bogusch P (2023) European cuckoo bees of the tribe Dioxyini (Hymenoptera, Megachilidae): distribution, annotated checklist and identification key. *Journal of Hymenoptera Research* 96: 599–628. <https://doi.org/10.3897/jhr.96.104957>
- Brullé GA (1839) Insectes. In: Barker-Webb P, Berthelot S (Eds) *Histoire Naturelle des Îles Canaries* (Tome deux). Béthune, Paris, 54–95.
- Bürgis H (1995) *Leucopsis gigas* (Chalcidoidea: Leucopsidae) als Parasit der Mörtelbiene *Megachile sicula* (Apoidea: Megachilidae). *bembiX* 5: 27–32.
- Canovai R, Giannotti P, Giannetti S, Loni A, Raspi A, Santini L, Dellacasa M, Generani M, Pagliano G, Strumia F, Scaramozzino PL, Zuffi M, Baldaccini NE, Puglisi L, Battesti MJ, Brocard E (2000) Biodiversità: Compilazione delle specie dell'Entomofauna e dei piccoli vertebrati della Corsica e della Toscana Marittima. *Progretto interreg II. Toscana-Corsica, 1997–1999. L'attività scientifica delle Università di Pisa e Corte*: 75–86.
- Chao A (1984) Nonparametric estimation of the number of classes in a population. *Scandinavian Journal of statistics* 11(4): 265–270.
- Chao A, Lee SM (1992) Estimating the number of classes via sample coverage. *Journal of the American statistical Association* 87(417): 210–217. <https://doi.org/10.1080/01621459.1992.10475194>
- Colwell RK, Coddington JA (1994) Estimating terrestrial biodiversity through extrapolation. *Philosophical Transactions: Biological Sciences* 345: 101–118. <https://doi.org/10.1098/rstb.1994.0091>
- Comba M (2019) Hymenoptera: Apoidea: Antophila of Italy. Biogeographic Checklist of Italian Wild Bees with Notes on Taxonomy, Biology, and Distribution. <https://digilander.libero.it/mario.comba> [accessed on 12.10.2022]
- Cornuel-Willermoz A, Andrei-Ruiz MC (2021) Plan Territorial d'Actions en faveur des pollinisateurs sauvages et de l'abeille mellifère –Corse : 2021–2030. Office de l'Environnement de la Corse, Corte, 43 pp.
- Ducke A (1900) Die Bienengattung *Osmia* Panz. als Ergänzung zu Schmiedeknecht's "Apidae europaeae" Vol. II in ihren palaeartischen Arten monographisch bearbeitet. *Bericht des Naturwissenschaftlich-Medizinischen Vereins in Innsbruck* 25: 1–323.
- Dorchin A, Praz CJ (2018) Taxonomic revision of the Western Palearctic bees of the subgenus *Pseudomegachile* (Hymenoptera, Apiformes, Megachilidae, *Megachile*). *Zootaxa* 4524(3): 251–207. <https://doi.org/10.11646/zootaxa.4524.3.1>
- DREAL (2017) Le Profil Environnemental de la Corse, édition 2016. DREAL Corse, Corte, 236 pp.
- Dufrène E, Genoud D, Bourlet P (2016) Sur la distribution en France de *Lithurgus cornutus* Fabricius 1827 (Hymenoptera – Megachilidae -Lithurgini): Apport de données récentes. *OSMIA* 6: 16–21. <https://doi.org/10.47446/OSMIA6.5>
- Ebmer AW (1997) Hymenopterologische Notizen aus Österreich – 7 (Insecta: Hymenoptera: Apoidea). *Linzer Biologische Beiträge* 29: 45–62.

- Ferton C (1897) Nouvelles observations sur l'instinct des hyménoptères gastrilégides de France et de Corsica. Actes de la Société Linnéenne de Bordeaux 52: 37–50.
- Ferton C (1899) Sur les mœurs du *Chrysis dichroa* Dahlbom [Hymén.]. Bulletin de la Société Entomologique de France 1899: 70–73. <https://doi.org/10.3406/bsef.1899.22301>
- Ferton C (1901a) Description de l'*Osmia corsica*, n. sp. et observations sur la faune Corsica (Hymén.). Bulletin de la Société Entomologique de France 1901: 61–66. <https://doi.org/10.3406/bsef.1901.22776>
- Ferton C (1901b) Notes détachées sur l'instinct des Hyménoptères mellifères et ravisseurs avec la description de quelques espèces. Annales de la Société entomologique de France 70: 83–148.
- Ferton C (1905) Notes détachées sur l'instinct des hyménoptères mellifères et ravisseurs (3^e série) avec la description de quelques espèces. Annales de la Société Entomologique de France 74: 56–104. [pl. 3–4.]
- Ferton C (1909a) Notes détachées sur l'instinct des hyménoptères mellifères et ravisseurs (4^e série) avec la description de quelques espèces. Annales de la Société Entomologique de France 77: 535–586.
- Ferton C (1909b) Notes détachées sur l'instinct des hyménoptères mellifères et ravisseurs (5^e série) avec la description d'une espèce nouvelle. Annales de la Société Entomologique de France 78: 401–422.
- Ferton C (1911) Notes détachées sur l'instinct des hyménoptères mellifères et ravisseurs (7^e série) avec la description de quatre espèces nouvelles. Annales de la Société Entomologique de France 80: 351–412.
- Ferton C (1920) Notes détachées sur l'instinct des hyménoptères mellifères et ravisseurs (9^e série) avec la description de deux espèces nouvelles. Annales de la Société Entomologique de France 89: 329–375.
- Ferton C (1923) La vie des Abeilles et des Guêpes. Chiron, Paris, 376 pp.
- Floris I, Satta A, Lentini A (2000) Monitoring of insect pollinators in two different agricultural landscapes (Sardinia, Italy). Insect Social Life 3: 115–118.
- Friese H (1895) Die Bienen Europa's (Apidae europaeae) Theil I. Schmarotzerbienen. Friedländer und Sohn, Berlin, 218 pp.
- Friese H (1899) Die Bienen Europa's (Apidae europaeae) nach ihren Gattungen, Arten und Varietäten auf vergleichend morphologisch-biologischer Grundlage. Theil V: Solitäre Apiden: Genus *Lithurgus*, Genus *Megachile* (*Chalicodoma*). C. Lampe, Innsbruck und Imst, 228 pp.
- Friese H (1911) Apidae I. Megachilinae. Das Tierreich 28: 1–440.
- Ghisbain G, Rosa P, Bogusch P, Flaminio S, Le Divelec R, Dorchin A, Kasperek M, Kuhlmann M, Litman J, Mignot M, Müller A, Praz C, Radchenko VG, Rasmont P, Risch S, Roberts SPM, Smit J, Wood TJ, Michez D, reverté S (2023) The new annotated checklist of the wild bees of Europe (Hymenoptera: Anthophila). Zootaxa 5327(1): 001–147. <https://doi.org/10.11646/zootaxa.5327.1.1>
- Gonzalez VH, Engel MS, Hinojosa-Díaz IA (2010) A new species of *Megachile* from Pakistan, with taxonomic notes on the subgenus *Eutricharaea* (Hymenoptera: Megachilidae). Journal of the Kansas Entomological Society 83: 58–67. <https://doi.org/10.2317/JKES0905.16.1>
- Kasperek M (2015) The cuckoo bees of the genus *Stelis* Panzer, 1906 in Europe, North Africa and in the Middle East. A review and identification guide. Entomofauna Supplement 18: 1–144.

- Kasperek M (2022) The Resin and Wool Carder Bees (Anthidiini) of Europe. Chimaira, Frankfurt am Main, 290 pp.
- Kasperek M, Lhomme P (2019) Revision of the taxonomic status of *Rhodanthidium stictitum ordonezi* (Dusmet, 1915) an anthidiine bee endemic to Morocco (Apoidea: Anthidiini). Turkish Journal of Zoology 43: 43–51. <https://doi.org/10.3906/zoo-1809-22>
- Kusdas K (1974) Beitrag zur Kenntnis der Insektenfauna von Korsika. Zeitschrift der Arbeitsgemeinschaft Österreichischer Entomologen 24: 153–166.
- Le Divelec R, Dufrière E (2020) Sur l'identité du mâle de *Coelioxys coturnix* PÉREZ 1884 (Hymenoptera – Megachilidae). OSMIA 8: 5–10. <https://doi.org/10.47446/OSMIA8.1>
- Le Goff G (2004) *Hoplitis (Hoplitis) manicata* Morice, espèce nouvelle pour la faune des France et la peu commune *Megachile (Pseudomegachile) ericetorum melaleuca* Van der Zanden en Corse (Apoidea; Megachilidae; Megachilinae; Osmiini; Megachilini). L'Entomologiste 60: 9–12.
- Le Goff G (2010) Note sur la nidification dans le sol de quatre *Hoplitis* Klug du sous-genre *Annosmia* Warncke (Apoidea, Megachilidae, Osmiini). OSMIA 4: 5–10. <https://doi.org/10.47446/OSMIA4.2>
- Le Goff G (2016) Description du mâle d'*Osmia (Helicosmia) nasoproducta* Ferton 1909 (Apoidea – Megachilidae – Osmiini). OSMIA 6: 4–5. <https://doi.org/10.47446/OSMIA6.1>
- Liongo li Enkulu M (1988) Les Mégachiles (Hymenoptera, Apoidea) d'Europe et d'Afrique. Une étude écologique et agronomique. PhD thesis. Faculté Universitaire des Sciences Agronomiques, Gembloux, 247 pp.
- Litman JR, Fateryga AV, Griswold TL, Aubert M, Proshchalykin MY, Le Divelec R, Burrows S, Praz CJ (2021) Paraphyly and low levels of genetic divergence in morphologically distinct taxa: revision of the *Pseudoanthidium scapulare* complex of carder bees (Apoidea: Megachilidae: Anthidiini). Zoological Journal of the Linnean Society 195: 1287–1337. <https://doi.org/10.1093/zoolinlean/zlab062>
- Marchal P, Chardonnet G (2001) Sortie entomologique en Corse en mai 1998, liste des insectes récoltés, 2e note. Bulletin Mensuel de la Société Linnéenne de Lyon 70(10): 201–204. <https://doi.org/10.3406/linly.2001.11403>
- Meunier JY, Geslin B, Issertes M, Mahé G, Vyghen F, Labrique H, Dutour Y, Poncet V, Migliore J, Neve G (2023) Apoidea of the collections of Lyon, Aix-en-Provence, Marseille and Toulon Museums of Natural History (France). Biodiversity Data Journal 11: e99650. <https://doi.org/10.3897/BDJ.11.e99650>
- Morawitz F (1871) Neue suedeuropaeische Bienen. Horae Societatis Entomologicae Rossicae 8: 201–231.
- Müller A (2018) Palaearctic *Osmia* bees of the subgenus *Hoplosmia* (Megachilidae, Osmiini): biology, taxonomy and key to species. Zootaxa 4415(2): 297–329. <https://doi.org/10.11646/zootaxa.4415.2.4>
- Müller A (2020) Palaearctic *Osmia* bees of the subgenera *Hemiosmia*, *Tergosmia* and *Erythrosmia* (Megachilidae, Osmiini): biology, taxonomy and key to species. Zootaxa 4778(2): 201–236. <https://doi.org/10.11646/zootaxa.4778.2.1>
- Müller A (2022a) Palaearctic Osmiine Bees. <http://blogs.ethz.ch/osmiini> [accessed on 09.09.2022]

- Müller A (2022b) Palaearctic *Osmia* bees of the subgenera *Allosmia* and *Neosmia* (Megachilidae, Osmiini): biology, taxonomy and key to species. *Zootaxa* 5188(3): 201–232. <https://doi.org/10.11646/zootaxa.5188.3.1>
- Nadig A, Nadig A (1933) Beitrag zur Kenntnis der Hymenopterenfauna von Marokko und Westalgerien – Erster Teil: Apidae, Sphegidae, Vespidae. *Jahresbericht der Naturforschenden Gesellschaft Graubündens* 71: 37–107.
- Nadig A, Nadig A (1934) Beitrag zur Kenntnis der Orthopteren- und Hymenopterenfauna von Sardinien und Korsika. *Jahresbericht der Naturforschenden Gesellschaft Graubündens* 72: 3–40.
- Nobile V, Catania R, Niolu P, Pusceddu M, Satta A, Floris I, Flaminio S, Bella S, Quaranta M (2021) Twenty New Records of Bees (Hymenoptera, Apoidea) for Sardinia (Italy). *Insects* 12(7). <https://doi.org/10.3390/insects12070627>
- Ornosa C, Ortiz-Sánchez FJ, Torres F (2007) Catalogo de los Megachilidae del Mediterraneo occidental (Hymenoptera, Apoidea). II. Lithugini y Megachilini. *Graellsia* 63: 111–134. <https://doi.org/10.3989/graellsia.2007.v63.i1.85>
- Orr MC, Hughes AC, Chesters D, Pickering J, Zhu C-D, Ascher JS (2021) Global Patterns and Drivers of Bee Distribution. *Current Biology* 31: 451–458. <https://doi.org/10.1016/j.cub.2020.10.053>
- Pagliano G (1994) Catalogo degli Imenotteri italiani. IV. Apoidea: Colletidae, Andrenidae, Megachilidae, Anthophoridae, Apidae). *Memorie della Società Entomologica Italiana* 72: 331–467.
- Peters DS (1977) Systematik und Zoogeographie der west-paläarktischen Arten von *Osmia* Panzer, 1806 s.str., *Monosmia* Tkalců, 1974 und *Orientosmia* n. subgen. (Insecta: Hymenoptera: Megachilidae). *Senckenbergiana Biologica* 58: 287–346.
- Pérez J (1879) Contribution à la faune des apiaires de France. *Actes de la Société Linnéenne de Bordeaux* 33: 119–229.
- Pérez J (1895) Espèces Nouvelles de Mellifères de Barbarie. (Diagnoses préliminaires). Gounouilhou, Bordeaux, 64 pp.
- Praz CJ (2017) Subgeneric classification and biology of the leafcutter and dauber bees (genus *Megachile* Latreille) of the western Palearctic (Hymenoptera, Apoidea, Megachilidae). *Journal of Hymenoptera Research* 55: 1–54. <https://doi.org/10.3897/jhr.55.11255>
- Praz CJ, Bénon D (2023) Revision of the *leachella* group of *Megachile* subgenus *Eutricharaea* in the Western Palearctic (Hymenoptera, Apoidea, Megachilidae): A renewed plea for DNA barcoding type material. *Journal of Hymenoptera Research* 95: 143–198. <https://doi.org/10.3897/jhr.95.96796>
- Přidal A (2004) Checklist of the bees in the Czech Republic and Slovakia with comments on their distribution and taxonomy (Insecta: Hymenoptera: Apoidea). *Acta Universitatis Agriculturae et Silviculturae Mendelianae Brunensis* 52(1): 29–66. <https://doi.org/10.11118/actaun200452010029>
- Quaranta M, Ambroselli S, Barro P, Bella S, Carini A, Celli G, Cogoi P, Comba L, Comoli R, Felicioli A, Floris I, Intoppa F, Longo S, Maini S, Manino A, Mazzeo G, Medrzycki P, Nardi E, Niccolini L, Palmieri N, Patetta A, Piatti C, Piazza MG, Pinzauti M, Porporato M, Porrini C, Ricciardelli D'Albore G, Romagnoli F, Ruiui L, Satta A, Zandigiacomo P (2004) Wild bees in agroecosystems and semi-natural landscapes. 1997–2000 collection period in Italy. *Bulletin of Insectology* 57(1): 11–61.

- Radoszkowski O (1887) Sur quelques *Osmia* russes. Horae Societatis Entomologicae Rossicae 21: 275–293.
- Rasmont P, Ebmer P, Banaszak J, Zanden G (1995) Hymenoptera Apoidea Gallica. Liste taxonomique des abeilles de France, de Belgique, de Suisse et du Grand-Duché de Luxembourg. Bulletin de la Société Entomologique de France 100: 1–98.
- Rasmont P, Adamski A (1995) Les bourdons de la Corse (Hymenoptera, Apoidea, Bombinae). Notes Fauniques de Gembloux 31: 3–87. <https://doi.org/10.1080/21686351.1995.12277716>
- Rasmont P, Genoud D, Gadoum S, Aubert M, Dufrêne E, Le Goff G, Mahé G, Michez D, Pauly A (2017) Hymenoptera Apoidea Gallica: liste des abeilles sauvages de Belgique, France, Luxembourg et Suisse. http://www.atlashymenoptera.net/biblio/01500/414_Rasmont_et_al_2017_Hymenoptera_Apoidea_Gallica_2017_02_16.pdf [accessed on 27.06.2023]
- Rebmann O (1968) 3. Beitrag zur Kenntnis der Gattung *Megachile* Latr. (Hym. Apidae): Subgenus *Eutricharaea* und seine bisher bekanntgewordenen Arten. Deutsche Entomologische Zeitschrift 15: 21–48. <https://doi.org/10.1002/mmnd.19680150105>
- Ruzzier E, Menchetti M, Bortolotti L, Selis M, Monterastelli E, Forbicioni L (2020) Updated distribution of the invasive *Megachile sculpturalis* (Hymenoptera: Megachilidae) in Italy and its first record on a Mediterranean island. Biodiversity Data Journal 8: e57783. <https://doi.org/10.3897/BDJ.8.e57783>
- Sabiani T (2004) Encyclopaedia Corsicae (Vol. 1): Géologie – La mer – la terre. Edition Dumane, Corse, 812 pp.
- Scheuchl E, Willner W (2016) Taschenlexikon der Wildbienen Mitteleuropas. Quelle and Meyer, Wiebelsheim, 917 pp.
- Schmiedeknecht O (1885–1886) Genus *Osmia* Panz. Apidae Europaeae (Die Bienen Europa's) per Genera, Species et Varietates. Vol. 2. Friedländer, Berlin, 205 pp.
- Schwarz M, Gusenleitner F (2011) Beitrag zur Kenntnis der Gattung *Megachile* (Hymenoptera, Apoidea, Megachilinae). Entomofauna 32(15): 249–260.
- Soltani GG, Bénon D, Alvarez N, Praz CJ (2017) When different contact zones tell different stories: putative ring species in the *Megachile concinna* species complex (Hymenoptera: Megachilidae). Biological Journal of the Linnean Society 121: 815–822. <https://doi.org/10.1093/biolinnean/blx023>
- Stanek E (1969) Neue oder wenig bekannte *Osmia*-Arten aus dem Mittelmeergebiet (Hymenoptera, Apoidea, Megachilidae). Nachrichten des Naturwissenschaftlichen Museums der Stadt Aschaffenburg 78: 1–40. [pl. 1.]
- Stöckl P (2000) Synopsis der Megachilinae Nord- und Südtirols (Österreich, Italien) (Hymenoptera: Apidae). Berichte des Naturwissenschaftlich-medizinischen Vereins in Innsbruck 87: 273–306.
- Terzo M, Iserbyt S, Rasmont P (2007) Révision des Xylocopinae (Hymenoptera : Apidae) de France et de Belgique. Annales de la Société Entomologique de France 43: 445–491. <https://doi.org/10.1080/00379271.2007.10697537>
- Tkalců B (1969) Beiträge zur Kenntnis der Fauna Afghanistans. (Sammelergebnisse von O. Jakeš 1963–64, D. Povolný 1965, D. Povolný and Fr. Tenora 1966, J. Šimek, 1965–66, D. Povolný, J. Gaisler, Z. Šebek and Fr. Tenora 1967). Osmiini, Megachilidae, Apoidea, Hym. Casopis Moravského Musea Acta Musei Moraviae 54: 327–346.

- Tkalců B (1970) Typenrevision der von J.C. Fabricius beschriebenen paläarktischen Arten der Tribus Osmiini (Hymenoptera, Apoidea, Megachilidae). *Annotationes Zoologicae et Botanicae* 62: 1–15.
- Tkalců B (1971) Zur Identität zweier *Osmia*-Arten (Hymenoptera, Apoidea, Megachilidae). *Acta Entomologica Bohemoslovaca* 68: 222–230.
- Tkalců B (1975a) Revision der Europäischen *Osmia* (*Chalcosmia*)-Arten der *fulviventris*-Gruppe (Hymenoptera, Apoidea, Megachilidae). *Věstník Československé Společnosti Zoologické* 39: 297–317.
- Tkalců B (1975b) Sammelergebnisse der von RNDr. A. Hoffer geleiteten Algerien-Expeditionen in den Jahren 1971 und 1972 (Hymenoptera: Apoidea) 1. Teil: Megachilidae. *Zbornik Slovenského Národného Múzea* 21: 165–190.
- Tkalců B (1977) Taxonomische Notizen zu einigen paläarktischen Osmiini-Arten (Hymenoptera, Apoidea). *Acta Musei Moraviae* 62: 87–98.
- Tkalců B (1993) Neue Taxa der Bienen von den Kanarischen Inseln. Mit Bemerkungen zu einigen bereits bekannten Arten (Insecta, Hymenoptera, Apoidea). *Veröffentlichungen des Übersee-Museum Bremen* 12: 791–858.
- Ungricht S, Müller A, Dorn S (2008) A taxonomic catalogue of the Palaearctic bees of the tribe Osmiini (Hymenoptera: Apoidea: Megachilidae). *Zootaxa* 1865: 1–253. <https://doi.org/10.11646/zootaxa.1865.1.1>
- Varnava AI, Roberts SP, Michez D, Ascher JS, Petanidou T, Dimitriou S, Devalez J, Pittara M, Stavriniades MC (2020) The wild bees (Hymenoptera, Apoidea) of the island of Cyprus. *ZooKeys* 924: 1–114. <https://doi.org/10.3897/zookeys.924.38328>
- Vereecken NJ, Barbier E (2009) Premières données sur la présence de l'abeille asiatique *Megachile* (*Callomegachile*) *sculpturalis* Smith (Hymenoptera, Megachilidae) en Europe. *OSMIA* 3: 4–6. <https://doi.org/10.47446/OSMIA3.3>
- Warncke K (1981) Die Bienen des Kagenfurter Beckens. *Carinthia II* 171(91): 275–348.
- Warncke K (1988) Isolierte Bienenvorkommen auf dem Olymp in Griechenland (Hymenoptera, Apidae). *Linzer Biologische Beiträge* 20: 83–117.
- Warncke K (1991a) Die Bienengattung *Osmia* Panzer, 1806, ihre Systematik in der Westpaläarktis und ihre Verbreitung in der Türkei. 9. Die Untergattung *Annosmia* subg. n. *Linzer Biologische Beiträge* 23: 307–336.
- Warncke K (1991b) Die Bienengattung *Osmia* Panzer, 1806, ihre Systematik in der Westpaläarktis und ihre Verbreitung in der Türkei. 10. Die Untergattung *Alcidamea* Cress. *Linzer Biologische Beiträge* 23: 701–751.
- Warncke K (1992a) Die westpaläarktischen Arten der Bienengattung *Coelioxys* Lep. (Hymenoptera, Apoidea). *Bericht der Naturforschenden Gesellschaft Augsburg* 53: 31–77.
- Warncke K (1992b) Die westpaläarktischen Arten der Bienengattung *Stelis* Panzer, 1806 (Hymenoptera, Apidae, Megachilinae). *Entomofauna* 13(22): 341–376.
- Warncke K (1992c) Die westmediterranen Arten der Bienen *Osmia* subg. *Hoplitis* Klug, 1807. *Linzer Biologische Beiträge* 24: 103–121.
- Warncke K (1992d) Die Bienengattung *Osmia* Panzer, 1806 ihre Systematik in der Westpaläarktis und ihre Verbreitung in der Türkei. 11. Die Untergattung *Pyrosmia* Tkalců, 1975. *Linzer Biologische Beiträge* 24: 893–921.

- Willmer P (2011) *Pollination and Floral Ecology*. Princeton University Press, Princeton and Oxford, 778 pp. <https://doi.org/10.23943/princeton/9780691128610.001.0001>
- Zanden G (1984) Neue paläarktische Taxa der Familie Megachilidae (Hymenoptera, Apoidea, Megachilidae). *Reichenbachia* 22: 175–191.
- Zanden G (1989) Neue oder wenig bekannte Arten und Unterarten der palaearktischen Megachiliden (Insecta, Hymenoptera, Apoidea: Megachilidae). *Entomologische Abhandlungen Staatliches Museum für Tierkunde Dresden* 53: 71–86.
- Zanden G (1991) Systematik und Verbreitung der paläarktischen Arten der Untergattung *Caerulosmia* van der Zanden, 1989 (Hymenoptera, Apoidea, Megachilidae). *Linzer Biologische Beiträge* 23: 37–78.

A new species of *Uscanoidea* Girault (Hymenoptera, Trichogrammatidae), an egg parasitoid of *Monalonia dissimulatum* Distant (Hemiptera, Miridae)

Jean Gamboa^{1,2}, Lucía Pérez-Benavides^{1,2}, Esaú Ospina-Peñuela¹,
Francisco Serna², Gennaro Viggiani³

1 Laboratorio de Entomología Universidad de la Amazonia LEUA, Facultad de Ingeniería, Universidad de la Amazonia, sede Centro, Carrera 11, 5-69, Florencia, Caquetá, Colombia **2** Museo Entomológico UNAB, Facultad de Ciencias Agrarias, Universidad Nacional de Colombia, sede Bogotá, Carrera 30, 45-03, Bogotá D.C., Colombia **3** Laboratorio di Lotta biologica, Dipartimento di Agraria, Università degli Studi di Napoli “Federico II”, Via Università, 133, Portici, Napoli, Italia

Corresponding author: Jean Gamboa (j.gamboa@udla.edu.co)

Academic editor: Petr Janšta | Received 10 August 2023 | Accepted 15 January 2024 | Published 26 March 2024

<https://zoobank.org/49CE6CC2-4B5F-464A-8A8A-65CAA2A91605>

Citation: Gamboa J, Pérez-Benavides L, Ospina-Peñuela E, Serna F, Viggiani G (2024) A new species of *Uscanoidea* Girault (Hymenoptera, Trichogrammatidae), an egg parasitoid of *Monalonia dissimulatum* Distant (Hemiptera, Miridae). Journal of Hymenoptera Research 97: 191–206. <https://doi.org/10.3897/jhr.97.111008>

Abstract

A new species of *Uscanoidea* Girault (Hymenoptera: Trichogrammatidae), *Uscanoidea ricoi* Viggiani, Gamboa & Pérez-Benavides, **sp. nov.**, is described and illustrated. The species is a solitary egg parasitoid of *Monalonia dissimulatum* Distant (Hemiptera: Miridae), the main insect pest on cocoa crops. An identification key for the described *Uscanoidea* species of the world is provided. The new species has a high potential for the biological control of the true bug *M. dissimulatum* in cocoa plantations in the Neotropical region.

Keywords

Antennal club, biological control, cocoa, fore wing, genitalia

Introduction

During a research project in cocoa (*Theobroma cacao* L.-Malvaceae) agroforestry systems in Colombia, several specimens of a Trichogrammatidae (Hymenoptera: Chalcidoidea) emerged from eggs of *Monalonion dissimulatum* Distant (Hemiptera: Miridae) from cocoa pods. The parasitoid was identified as a member of the subfamily Oligositinae, tribe Chaetostrichini, which, according to Owen et al. (2007) comprises several genera, including *Adryas* Pinto & Owen, *Bloodiella* Nowicki, *Brachista* Walker, *Burksiella* De Santis, *Chaetostricha* Walker, *Kyuwia* Pinto & George, *Lathromeroidea* Girault, *Pseuduscana* Pinto, *Uscana* Girault, *Uscanoidea* Girault, *Zaga* Girault, and *Zagella* Girault. Morphological comparison among these genera indicated the inclusion of the parasitoid in *Uscanoidea*. At present, *Uscanoidea* includes 12 rather different species whose members are distributed in the Oriental, Nearctic, and Neotropical regions (Pinto 2006; Noyes 2022). From comparison of the collected specimens with described species in *Uscanoidea* it emerged that the egg parasitoid of *M. dissimulatum* represents a new species.

In the Neotropical region, *M. dissimulatum* is the phytophagous bug that causes the highest incidence of fruit damage in cocoa plantations (Lavabre 1977; Vélez 1997; Schuh 2002–2013). Nymphs and adults of *M. dissimulatum* are sucking bugs, producing punctures on cocoa pods (fruits) and feeding on the cells of the epicarp. When one to seven week old fruits 10 to 12 cm long are attacked, they turn black, harden, and die. Further, when maturing fruits are attacked, they produce small stunted seeds (almonds) (de Abreu 1977).

In South America, different cocoa agroecosystem productions are found, and most are considered agroforestry systems (Johns 1999; Sambuichi 2006; Suárez et al. 2018). In those plantations, which have a greater plant diversity and are managed under traditional technologies, most farmers do not control *M. dissimulatum* populations. However, the few that do employ synthetic insecticides. Considering this context, it is necessary to develop new pest management practices for phytophagous insects based on recognizing and using the natural diversity of beneficial insects associated with cocoa plantations, such as predators and parasitoids.

The aim of this paper is to describe a new species of *Uscanoidea*, which has potential value for *M. dissimulatum* pest control.

Methods

In the departments of Caquetá and Huila in Colombia, 251 cocoa plantations ranging from 1–32 hectares in size were sampled. In each plantation, a manual four-hour sampling was used to search for *Monalonion dissimulatum* eggs inside cocoa pods. Eggs of *M. dissimulatum* are typically inserted into cocoa pods, and localized by detecting the two lengthend aeropiles extending out from the anterior pole of the egg.

Cocoa pods containing *M. dissimulatum* eggs were collected in 23 localities, 12 in the municipalities of El Doncello, El Paujil, San Vicente del Caguán and Belén

de los Andaquíes in the Department of Caquetá, and 11 in the municipalities of Agrado, Colombia, Neiva, Timaná, Rivera, and Paicol in the Department of Huila. The cocoa pods were transported in plastic bags placed inside a styrofoam box to the Laboratory of Entomology of the University of the Amazonia (LEUA) in the city of Florencia, Caquetá.

Mature *Monalonia* eggs, typically yellowish-white in color, were extracted manually under Olympus SZ61 stereomicroscope, using a blade, forceps, a pin, and a fine-tipped paintbrush. The eggs were placed into 15 × 15 × 8 cm plastic boxes with a top opening on the lid and sealed with muslin for aeration, simulating brood chambers. After emergence, any adult parasitoids were preserved in ethanol 96% before point mounting. Additionally, some specimens were slide mounted following the protocol proposed by Woolley and Dal Molin (2017), with the following modifications: 1) wings were removed and deposited directly in clove oil; 2) the parasitoid bodies were rinsed in 10% KOH for 15 to 45 minutes depending on the degree of sclerotization in a water bath; 3) each specimen was immersed in 10% glacial acetic acid for about 3 minutes, and then into distilled water, sequentially into 35%, 50%, 75%, and 96% ethanol, and then clove oil diluted with 96% ethanol in 1:1 and 3:1 ratios for at least 15 min each; 4) each specimen was then transferred to clove oil for at least 30 min before slide mounting; 5) on the slides, each appendage and head were separated from the body, covered with a thin layer of Canada balsam, and finally covered with a coverslip; 6) lastly, the slide-mounted specimens were placed into a lab oven at 50 °C for 4 to 5 days. Dry specimens were studied under an Olympus SZ61 stereomicroscope at 90× magnification, and slide-mounted specimens were examined with an Olympus CX21 optical microscope at 400× magnification. Photographs were taken with a LEICA M205A stereomicroscope with a built-in camera and a HITACHI TM4000Plus II Environmental Scanning Electron microscope. A distribution map of the species of *Uscanoidea* was plotted with the software QGIS version 3.26.2.

The curatorship of all specimens was carried out following the protocols established in the LEUA: 1) specimens sizing less than 15 mm are point mounted; 2) specimens sizing less than 3 mm are slide-mounted within the mounting medium (Hoyer, entellan, canadian balsam) according to the specialist of the insect group; 3) labels on both point- and slide-mounted contain the basic information regarding locality, geographic coordinates, altitude, date, and collector. A second label contains scientific information of the host (scientific and family names), and collecting method.

Genus *Uscanoidea* was identified using the keys in Doutt and Viggiani (1968) and Pinto (2006). Terminology follows Doutt and Viggiani (1968), and Pinto (2006). The abbreviations used in the description are: c1: first club segment, c2: second club segment, c3: third club segment, c4: fourth club segment, c5: fifth club segment, md: metanotum disc, pd: propodeum disc, and eh: exit hole. The specimens described were deposited in the entomological collection LEUA in Florencia, Caquetá, Colombia, and in the entomological collection of the Università degli Studi di Napoli “Federico II,” Dipartimento di Agraria, Portici, Italy, (MUSA).

Results

Sixty eight individuals of *Uscanoidea ricoi*, sp. nov. were reared from the same (68) number of eggs of *Monalonion*, of which six were slide-mounted and the remainder point-mounted.

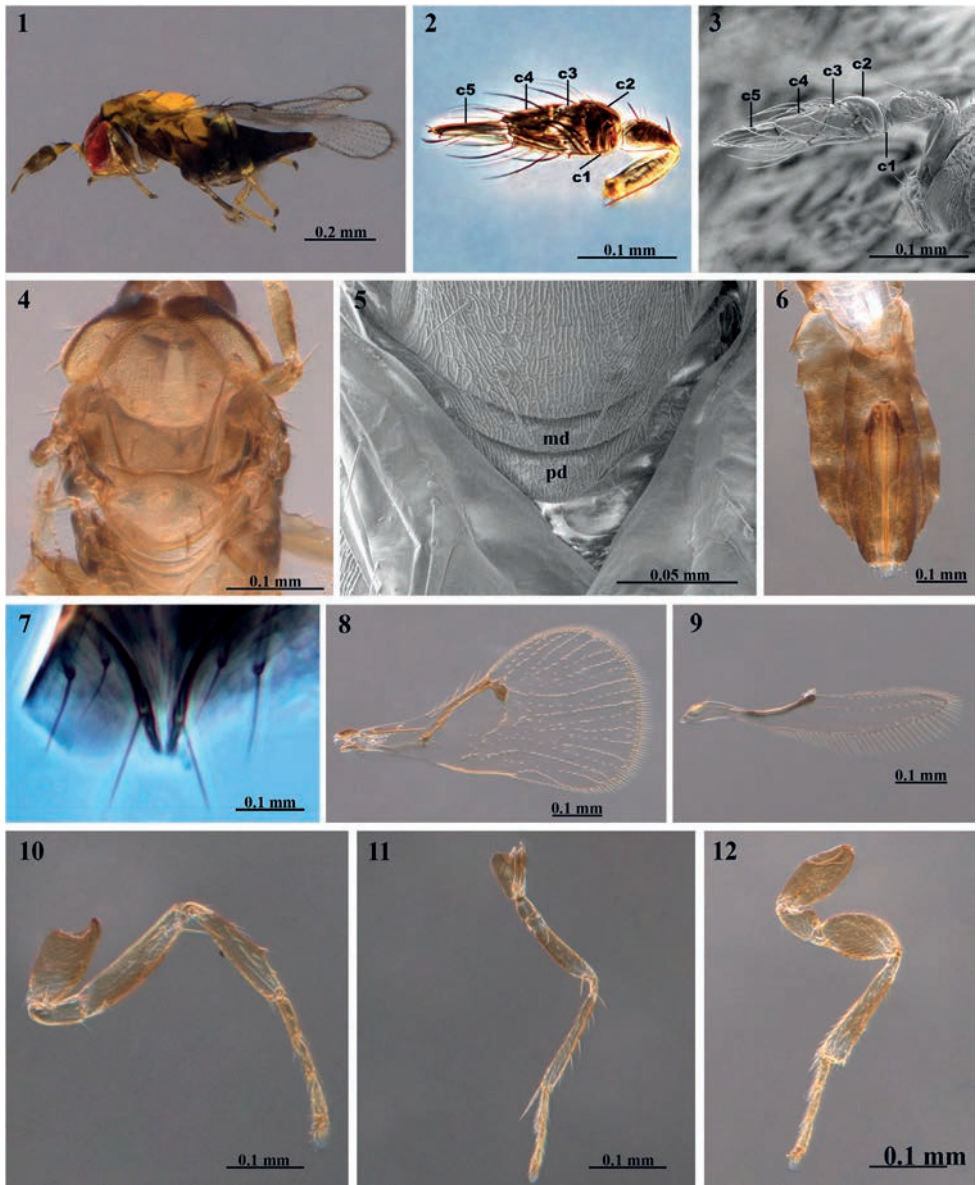
Taxonomy

Uscanoidea ricoi Viggiani, Gamboa & Pérez-Benavides, sp. nov.

<https://zoobank.org/ED75F2BA-35D7-4FC2-9902-4B5749FD861F>

Figs 1–30

Description. Female (Figs 1–12). **Colour:** Eyes red, vertex and face mostly yellow, occipital area black. Antenna dark brown, with scape, ventral aspect of the pedicel, and apical club segment lighter. Mesosoma. Pronotum black and yellow, mid lobe of mesoscutum, axillae, scutellum, metanotum and propodeum yellow. Pleural and ventral areas of mesosoma black or dark brown. Fore wing hyaline with dark brown venation. Legs mostly brown or dark brown, but with lighter parts on femur, tibia and tarsus. Metasoma (gaster) black. **Body length:** 0.7 mm. **Head.** As wide as mesosoma; mandible tridentate, maxillary palpus 1-segmented. Antenna (Fig. 2) with scape 4× as long as wide; pedicel slightly longer than half length of scape; 2 anelli; club conical, 3.5–4× as long as wide, asymmetrical 5-segmented; C1 (Fig. 2, c1) very short, somewhat longer than second anellus, ring-like and closely appressed to base of C2, without setae but with one lateral basiconic peg sensillum; C2 (Fig. 2, c2) asymmetrical, dorsal length 4× as long as ventral length, slightly wider than C3, with long setae (Fig. 3), distal margin with basiconic peg sensilla and one placoid sensillum; C3 asymmetrical, 0.8× as long as C2 and with setae and sensilla as for C2, but with a slightly curved placoid sensillum; C4 1.8× as long as C3 and with one distal basiconic peg sensillum; C5 tapered, narrow, 4–5× as long as wide, with 2 or 3 placoid sensilla, one prominent and as long as C5; terminal basiconic peg sensillum, and a short terminal seta. **Mesosoma.** 0.8× as long as metasoma; pronotum very short, with a few setae; mid lobe of mesoscutum subtrapezoidal (Fig. 4), 1.7× as long as scutellum, with faint reticulate sculpture and two pairs of rather short setae; scutellum with setae and sculpture as for mid lobe of mesoscutum; metanotum (Fig. 5, md) with disc slightly shorter (0.7×) than that of propodeum (Fig. 5, pd). Mesophragma apically concave. **Wings.** Fore wing (Fig. 8) 1.6× as long as wide; venation 0.58 wing length; Subcostal vein 1.3× marginal vein length, premarginal vein 0.6× Marginal vein length, Stigmal vein shorter than premarginal vein, with a short neck; costal cell 1.5× Marginal vein length and with a group of 6–8 setae, distally near the premarginal vein; 1 seta on the Subcostal vein, 2 setae on the premarginal vein and 3 main setae on the Marginal vein; disc with 17–20 regular and distinct rows of setae; radial sector 1 curved from stigma toward the wing base and with 7 or 8 setae; fringe with longest setae half the length of stigmal vein. Hind wing (Fig. 9) with 3 rows of setae on the disc. **Legs.** Fore leg: trochanter almost parallel-sided; femur narrow, 4–6× as long as wide with a rather long seta on the distal ventral; tibia front margin



Figures 1–12. *Uscanoidea ricoi* sp. nov., female **1** habitus, lateral view **2** antenna **3** setae on antenna **4** mesoscutum **5** metanotum and propodeum **6** metasoma **7** hypopygium **8** fore wing **9** hind wing **10** fore leg **11** mid leg **12** hind leg; c1 – first club segment, c2 – second club segment, md – metanotum disc; pd – propodeum disc.

with 3 spines, the middle one prominent (Fig. 10). Mid leg: fragile; tibia with a row of rather long setae on the external margin, somewhat shorter than the corresponding basitarsomere, one long seta on the distal ventral end, spur as long as basitarsomere (Fig. 11). Hind leg: robust; trochanter having a dorsal globular prominence; femur 2× as long as wide; tibia robust with spur as long as half basitarsus; tarsomeres

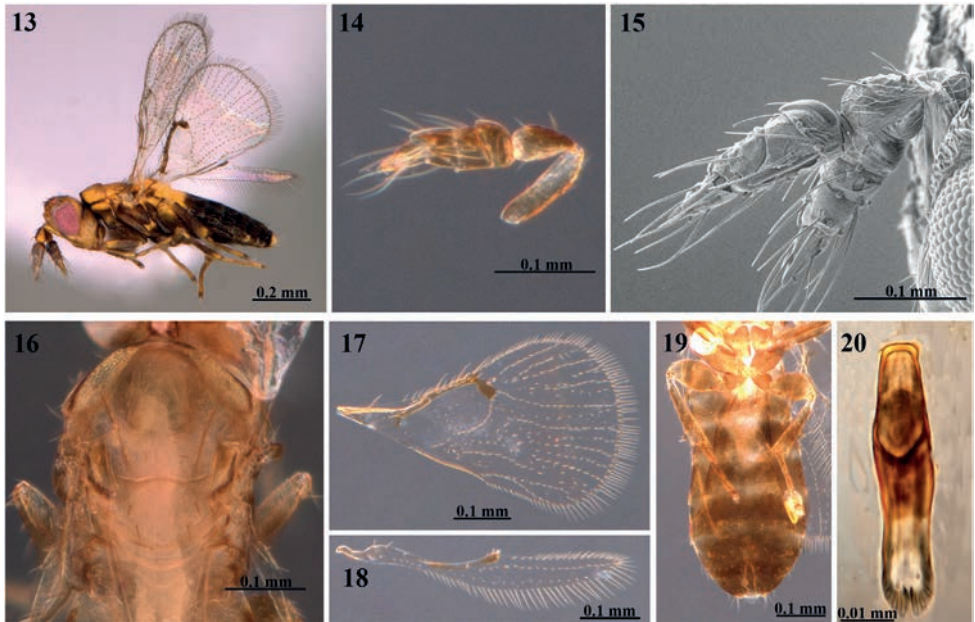
subequal (Fig. 12). **Metasoma.** Subconical (Fig. 6), ovipositor internally inserted at level of terga III-IV, not extruded; ovipositor length/hind tibia length ratio 1.76; hypopygium (Fig. 7) reaching the basal half of ovipositor, with two median converging ridges and two long, subapical setae.

Male (Fig. 13). Body coloration as the female. Antenna (Fig. 14) slightly shorter (3.0×) and with fewer asymmetrical segments than in female, C5 shorter, 2.5× as long as wide and with several long setae (Fig. 15), as on the preceding segments. Mesoscutum as female (Fig. 16). Fore wing fringe (Fig. 17) as long as stigmal vein length. Hind wing as the female (Fig. 18). Metasoma 1.3× as long as wide, with posterior apex less pointed than in female (Fig. 19). Genitalia (Fig. 20) simple, tubiform, slightly wider in the middle, basal 2/3rd brown, 4.4× as long as wide, length 0.125 mm, basal anterodorsal aperture 2× as long as wide; without ventral setae, parameres, volsellae, and aedeagal apodemes. Metatibia length/genitalia length ratio 1.7.

Etymology. The specific epithet is named in honor of Leonidas Rico Martínez, President (Rector) of Universidad de la Amazonia (Florencia, Caquetá, Colombia), (from 2011 to 2016). He supported the foundation of the LEUA, with the aim of investigating the diversity of insects present in the Colombian's Amazon.

Examined material. Holotype. COLOMBIA • ♀; Caquetá, El Doncello, Vda. Los Laureles, Fca. Los Matapollos; 01°41'53"N, 75°17'48"W; 620 m alt.; 30 Jul. 2022; E. Ospina and L. Pérez leg.; emerged from an egg of *Monalonion dissimulatum* collected in cacao pod; LEUA-51438. Holotype is deposited in Laboratory of Entomology of the University of the Amazonia (LEUA), Florencia, Caquetá, Colombia (LEUA), section Central Taxonomic Collection (CTC).

Paratypes. COLOMBIA • ♂ (**Allotype**); same data of holotype; LEUA-51442; deposited in LEUA • 2 ♀♀; same data of holotype; LEUA-51439/51440; LEUA • 5 ♀♀ and 4 ♂♂; Caquetá, El Doncello, Vda. La Ceiba, Fca. Bethel; 01°43'48"N, 75°16'55"W; 511 m alt.; 05 Jul. 2022; L. Pérez and E. Ospina leg.; emerged from egg of *Monalonion dissimulatum* collected in cacao pod; LEUA-51441; deposited in MUSA • 1 ♀; Caquetá, Belén de los Andaquíes, Vda. Agua Dulce, Fca. El Morichal; 01°20'34"N, 75°49'10"W; 328 m alt.; 13 Oct. 2021; L. Pérez and E. Ospina leg.; LEUA-51413; LEUA • 1 ♀; Caquetá, El Doncello, Vda. El Recreo, Fca. La Siberia; 01°42'53"N, 75°17'22"W; 452 m alt.; 06 Sep. 2022; Y. Rodríguez leg.; LEUA-51420; LEUA • 1 ♀ and 1 ♂; same collection data as for preceding; 18 Jul. 2021; L. Pérez and E. Ospina leg.; LEUA-51421/51422; LEUA • 1 ♂; Caquetá, El Doncello, Vda. La Ceiba, Fca. Bethel; 01°43'48"N, 75°16'55"W; 511 m alt.; 10 Ago. 2022; E. Ospina and L. Pérez leg.; LEUA-51408; LEUA • 5 ♀♀ and 3 ♂♂; same collection data as for preceding; 19 Jul. 2021; L. Pérez and E. Ospina leg.; LEUA-51959/51960/51961/51962/51963/51964/51965/51966; LEUA • 1 ♂; Caquetá, El Doncello, Vda. Los Laureles, Fca. Los Matapollos; 01°41'53"N, 75°17'48"W; 620 m alt.; 19 Jul. 2021; E. Ospina leg.; LEUA-51424; LEUA • 2 ♀♀ and 3 ♂♂; same collection data as for preceding; 06 Sep. 2022; L. Pérez leg.; LEUA-51426/51427/51428/51429/51430; LEUA • 1 ♂; Caquetá, El Doncello, Vda. Serranía, Fca. La Playa; 01°41'52"N, 75°18'05"W; 621 m alt.; 18 Jul 2021; L. Pérez and E. Ospina leg.; LEUA-51437; LEUA • 1 ♀ and 2 ♂♂; Caquetá, El Paujil, Vda. La Providencia, Fca. El Coralito; 01°32'23"N, 75°29'12"W; 320 m alt.; 20 Ago.



Figures 13–20. *Uscanoidea ricoi* sp. nov., male **13** habitus, lateral view **14** antenna **15** setae on antenna **16** mesoscutum **17** fore wing **18** hind wing **19** metasoma **20** genitalia.

2021; L. Pérez and E. Ospina leg.; LEUA/51969/51970/51971; LEUA • 1 ♀ and 1 ♂; Caquetá, El Paujil, Vda. La Rivera, Fca. La Fortuna; 01°36'50"N, 75°19'47"W; 663 m alt.; 18 Ago. 2021; L. Pérez and E. Ospina leg.; LEUA-51433/51434; LEUA • 1 ♀; Caquetá, San Vicente del Caguán, Vda. Alto Pocetas, Fca. La Chinita; 02°16'21"N, 74°40'40"W; 375 m alt.; 10 Sep. 2021; E. Ospina and L. Pérez leg.; LEUA-51976; LEUA • 2 ♀; Caquetá, San Vicente del Caguán, Vda. Buenos Aires, Fca. La Jardinera; 02°17'05"N, 74°40'46"W; 605 m alt.; 26 Sep. 2021; E. Ospina and L. Pérez leg.; LEUA-51406/51407; LEUA • 1 ♀; Caquetá, San Vicente del Caguán, Vda. La Reforma No. 2, Fca. La Victoria; 02°16'50"N, 74°41'44"W; 422 m alt.; 09 Oct. 2021; L. Pérez and E. Ospina leg.; LEUA-51423; LEUA • 2 ♀♀; Caquetá, San Vicente del Caguán, Vda. Sotará, Fca. Villanueva; 02°01'29"N, 74°51'42"W; 293 m alt.; 11 Sep. 2021; L. Pérez and E. Ospina leg.; LEUA-51412/51977; LEUA • 1 ♀; same collection data as for preceding, Fca. Parcela 4; 02°01'44"N, 74°50'55"W; 302 m alt.; 04 Oct. 2021; L. Pérez and E. Ospina leg.; LEUA-51435; LEUA • 2 ♀♀ and 2 ♂♂; Huila, Agrado, Vda. La Galda, Fca. El Trapiche; 02°14'52"N, 75°46'19"W; 827 m alt.; 23 Feb. 2022; E. Ospina and L. Pérez leg.; LEUA-51414/51415/51416/51417; LEUA • 2 ♀♀; same collection data as for preceding, Fca. Santana; 02°15'02"N, 75°46'23"W; 829 m alt.; 23 Feb. 2022; E. Ospina and L. Pérez leg.; E. Ospina and L. Pérez leg.; LEUA-51980/51981; LEUA • 1 ♀; Huila, Colombia, Vda. Horizonte Bajo, Fca. La Fortuna; 03°25'54"N, 74°46'05"W; 793 m alt.; 25 Ago. 2021; E. Ospina and L. Pérez leg.; LEUA-51410; LEUA • 4 ♀♀; Huila, Colombia, Vda. Ariari, Fca. La Esperanza; 03°25'58"N, 74°46'16"W; 782 m alt.; 25 Ago. 2021; E. Ospina and L. Pérez leg.; LEUA-51972/51973/51974/51975; LEUA

• 1 ♀ and 1 ♂; Huila; Neiva; Vda. Floragaita; Fca. El Tesoro; 02°52'45"N, 75°08'21"W; 928 m alt.; 26 Oct. 2021; E. Ospina and L. Pérez leg.; LEUA-51978/51979; LEUA • 1 ♂; Huila, Paicol, Vda. El Alto, Fca. Alemania; 02°27'12"N, 75°46'44"W; 916 m alt.; 15 May. 2022; E. Ospina and L. Pérez leg.; LEUA-51436; LEUA • 1 ♀; Huila, Timaná, Vda. Cascajal, Fca. Las Palmeras; 01°55'17"N, 75°56'59"W; 1250 m alt.; 28 May. 2022; L. Pérez and E. Ospina leg.; LEUA-51982; LEUA • 1 ♀ and 1 ♂; Huila, Rivera, Vda. El Guadual, Fca. La Primavera; 02°47'09"N, 75°14'03"W; 793 m alt.; 31 Jul. 2021; L. Pérez and E. Ospina leg.; LEUA-51431/51432; LEUA • 2 ♀♀ and 1 ♂; Huila, Rivera, Vda. Mesitas, Fca. La Balsa; 02°44'47"N, 75°14'57"W; 894 m alt.; 29 Jul. 2021; E. Ospina and L. Pérez leg.; LEUA-51409/51418; LEUA • 1 ♂; same collection data as for preceding; Fca. Caracolí; 02°44'49"N, 75°14'57"W; 869 m alt.; 28 Jul. 2021; E. Ospina and L. Pérez leg.; LEUA-51425; LEUA • 1 ♀ and 1 ♂; Huila; Rivera; Vda. El Viso; Fca. La Labranza; 02°45'22"N, 75°15'22"W; 760 m alt.; 28 Jul. 2021; E. Ospina and L. Pérez leg.; LEUA-51967/51968; LEUA. All additional material emerged from eggs of *Monalonia dissimulatum* collected in cocoa pod.

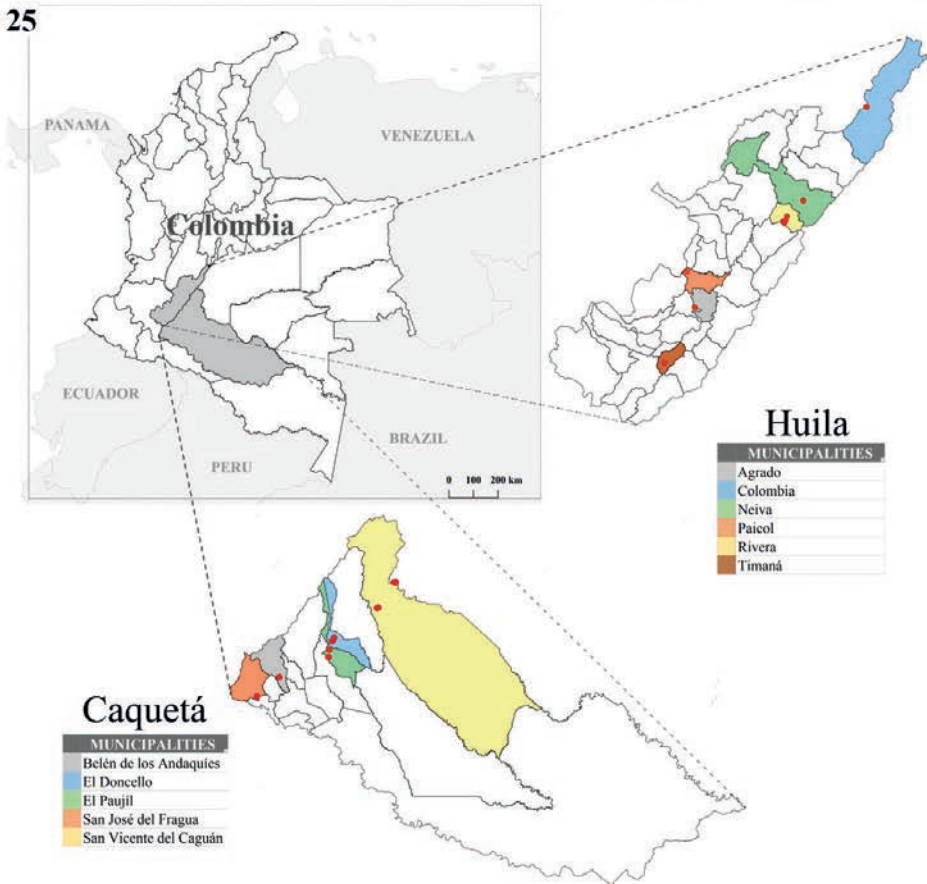
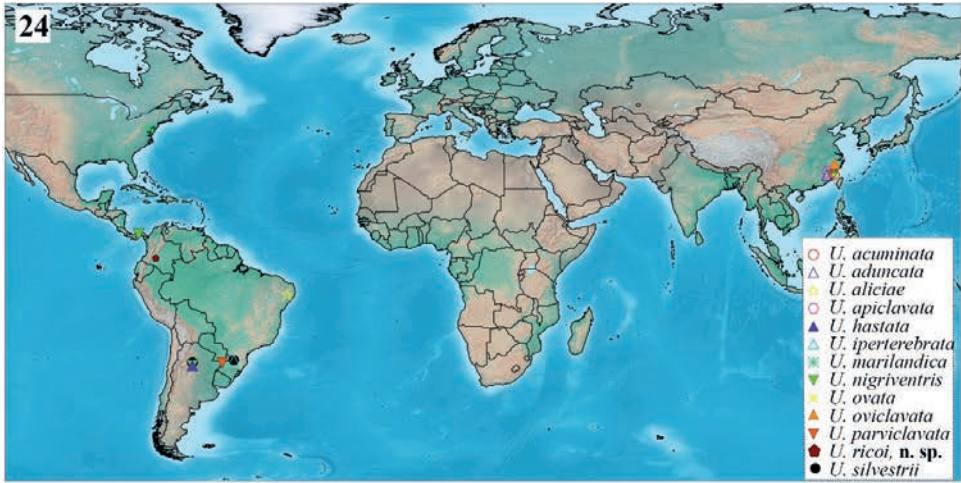
Biology. *Uscanoidea ricoi*, sp. nov., is a solitary parasitoid of eggs of *Monalonia dissimulatum* (Hemiptera: Miridae: Bryocorinae: Monaloniini) (Figs 21–23). Adult emergencies have been recorded in February, May, July, August, September and October. The parasitoid is multivoltine, like its host.

Distribution. Twelve species of *Uscanoidea* have been recorded worldwide: Argentina (4), Bermuda (1), Brazil (3), China (5), Jamaica (1), Panama (1), and United States of America (1) (De Santis 1979, 1989; Noyes 2022) (Fig. 24). *Uscanoidea ricoi*, sp. nov., is recorded from 23 localities in Colombia (Caquetá and Huila departments) (Fig. 25). Those localities are between 293 and 1,250 meters of altitude.

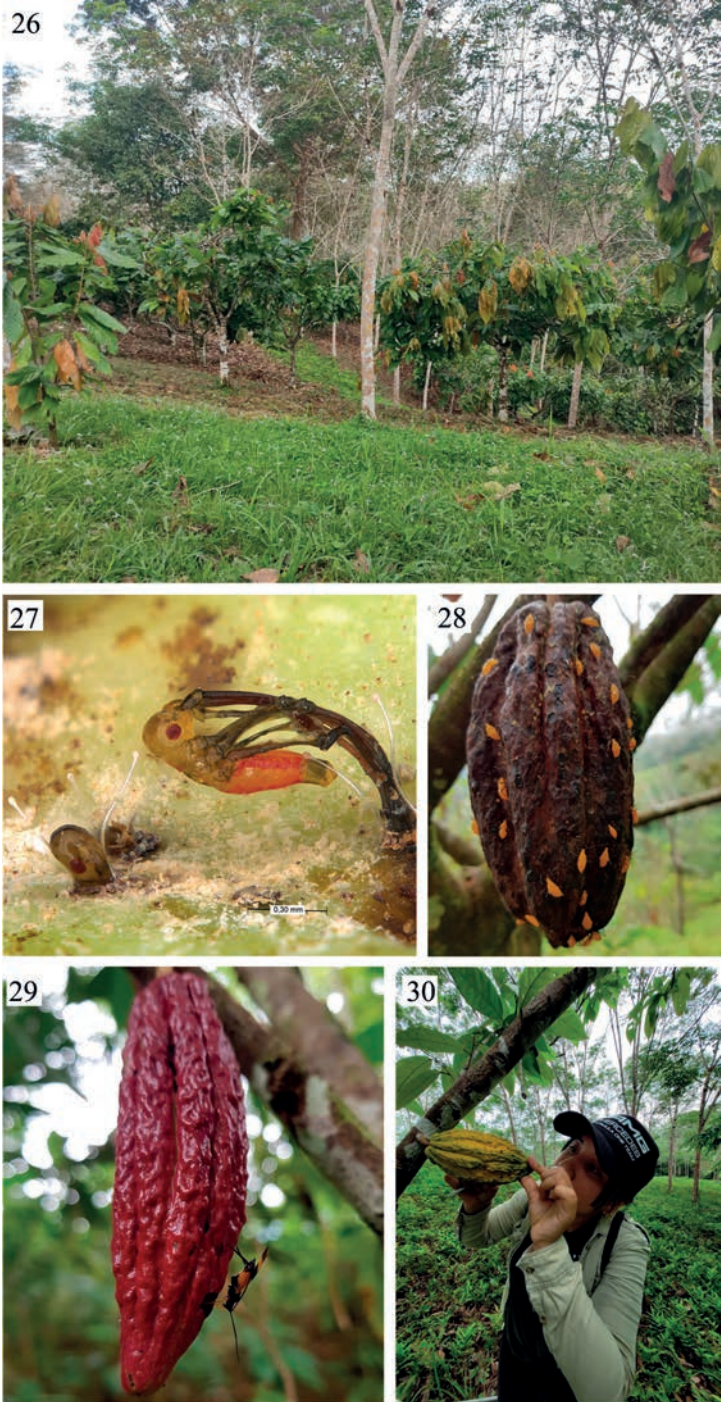
Habitat. Specimens of *Uscanoidea ricoi*, sp. nov., were collected in cocoa plantations intermixed within assortments of abundant vegetation (Fig. 26). In the region,



Figures 21–23. *Uscanoidea ricoi* sp. nov. emerging from *Monalonia dissimulatum* eggs **21** egg of *Monalonia dissimulatum* **22** egg of *Monalonia dissimulatum* with the emerging parasitoid *Uscanoidea ricoi* sp. nov. **23** egg of *M. dissimulatum* with exit hole of *U. ricoi* sp. nov.; eh – exit hole.



Figures 24, 25. Geographical distribution of *Uscanoidea* 24 all described *Uscanoidea* species 25 detail distribution of *Uscanoidea ricoi* sp. nov., in Colombia.



Figures 26–30. Habitat and host of *Uscanoidea ricoi* sp. nov. **26** cocoa plantations in agroforestry system **27** eggs at the moment of emergence of the nymphs of *Monalonia dissimulatum* **28** nymphs of *M. dissimulatum* host feeding on cocoa pod **29** adult of *M. dissimulatum* feeding on cocoa pod **30** collection of cocoa pods with *M. dissimulatum* eggs parasitized.

at least four types of traditional agroforestry systems for cocoa are recognized (1- complex diversified multistrata, 2- low diversity with regular trees, 3- low diversity with clustered trees, and 4- high density of Musaceae), depending on the diversity of the associated trees (Suárez et al. 2018). In the traditional cocoa agroforestry arrangements in Caquetá and Huila departments, plant species such as *Albizia guachapele* (Kunth) Dugand (Fabaceae), *Cariniana pyriformis* Miers (Lecythidaceae), *Cedrela odorata* L. (Meliaceae), *Citrus* spp. (Rutaceae), *Coffea arabica* L. (Rubiaceae), *Cordia alliodora* (Ruiz & Pav.) Oken (Cordiaceae), *Erythrina poeppigiana* (Walp.) O.F. Cook (Fabaceae), *Eugenia stipitata* McVaugh (Myrtaceae), *Hevea brasiliensis* (Willd. ex A. Juss.) Müll. Arg. (Euphorbiaceae), *Inga* spp. (Fabaceae), *Leucaena leucocephala* (Lam.) de Wit (Fabaceae), and *Theobroma grandiflorum* (Willd. ex Spreng.) K. Schum. (Malvaceae) are the most common trees and shrubs. Also, the diversity of associated herbs is high in the cacao plantations and *Musa* spp. (Musaceae) are commonly found there.

Most cocoa agroecosystems border on the introduced grasses *Brachiaria decumbens* Stapf (Poaceae) and *B. humidicola* (Rendle) Scheweick or border other agroecosystems such as *Saccharum officinarum* L. (Poaceae), *H. brasiliensis*, *C. arabica*, *Erythroxylum coca* Lam. (Erythroxylaceae) and *Musa paradisiaca* L. (Musaceae) or border stubble, secondary forests and primary forests. Extensive livestock production systems predominate in the region and there are high rates of deforestation.

Discussion

The genus *Uscanoidea* was described by Girault (1911) as follows: “A genus allied with and resembling *Uscana* Girault and *Uscanella* Girault but differing from the former in having a pointed conic-ovate abdomen which is longer than the thorax, in bearing a shorter somewhat swollen and compact 2-jointed antennal club and in lacking a ring-joint in the antennae; from the latter genus it is practically similar in the form of the antennae, but differs in the absence of the ring-joint, in the short marginal cilia of the fore wing, the more distinct and denser discal ciliation, the shorter marginal and stigmal veins and the longer, more pointed abdomen”. Douth and Viggiani (1968) revised the type material of both mentioned genera and made corrections to the original description. The distinction of *Uscanoidea* from *Uscana* was based mostly on the club number segments (3 in *Uscanoidea* and 4 in *Uscana*) and the length of the ovipositor (long in *Uscanoidea* and short in *Uscana*). After the type species *U. nigriventris* Girault, 2 new species from China were included in *Uscanoidea* (Lin 1994). The author defines both genera as having a 4-segmented club, but *Uscana* with “forewing moderately rounded, marginal vein slender and straight; 4 segments of club distinctly separated” and *Uscanoidea* with “forewing greatly broad and nearly truncate apically, marginal vein not very slender, usually with cluster of setae, club segmentation irregular and oblique, segmented differently in different view”. Pinto (2006) extends the limits of the genus including species with “male and female antennal club 5-segmented” and “propodeal disc and metanotum usually subequal in length”. The same author synonymizes the genus *Gnorimogramma* De Santis (1972) under *Uscanoidea*. The diagnosis of the latter genus by Pinto (2006)

includes in *Uscanoidea* only species having antenna with 2 anelli and 5 asymmetrical club segments; most of the other characteristics appear mostly of specific and not generic value. Consequently, at present, the genus *Uscanoidea sensu* Pinto remains a complex of heterogeneous species without a common identity. Particularly marked are the variations of the antennal shape shown in the known species included in the genus, which need further studies to confirm the present assessment of *Uscanoidea*. It is a matter of fact that the morphological differences between *Uscanoidea* and *Uscana* still remain uncertain. However, biologically the two genera are different, the known hosts of *Uscanoidea* are Hemiptera and of *Uscana* are Coleoptera (Bruchidae) (Fursov 1995).

Unfortunately, the type and syntype material of *U. nigriventris* are in very poor condition (Doutt and Viggiani 1968; Pinto 2006) and for other species, few specimens are available for advanced morphological and molecular studies. Of the 12 species at present included in *Uscanoidea*, 3 species, *U. aduncata* (Lin 1994), *U. aliciae* (De Santis 1972), *U. oviclavata* (Lin 1994) show funicular segments; the others 9 have no funicle. Among the latter, the type of the genus, *A. nigriventris* (Girault 1911), *U. hastata* (De Santis 1997), *U. ovata* Lin (1994) and *U. parviclavata* (De Santis 1997) have a short and long club. The new species *U. ricoi* is included in the group of *Uscanoidea* with a conic-ovate club, namely *U. acuminata* (Lin, 1994), *U. apiclavata* Lin (1994), *U. iperterebrata* Viggiani (1992), *U. marilandica* (Girault 1918) and *U. silvestrii* Viggiani (1992). Among the latter species, *U. ricoi* appears most allied to *U. apiclavata*, but is distinguishable for having female antennal scape longer (4× in *U. ricoi*; 3× in *U. apiclavata*), club C5 longer (4–5× in *U. ricoi*, 3× in *U. apiclavata*), and male with C5 shorter than in female (subequal in *U. apiclavata*); genitalia shorter (4.1× as long as wide in *U. ricoi*, 5.5× in *U. apiclavata*), slightly enlarged in the middle and not parallel sided; without ventral setae.

For the majority of the *Uscanoidea* species, biological data are lacking. However, what is known is that *U. aliciae* was reared from eggs of *Mahanarva (Ipiranga) rubicunda* (= *Mahanarva rubicunda indentata*) (Walker) (Hemiptera: Cercopidae) (De Santis 1972), both *U. parviclavata* and *U. silvestrii* were reared from eggs of *Campylenchia hastata* (Fabricius) (Hemiptera: Membracidae), and *U. silvestrii* was reared from eggs of an unidentified membracid (De Santis 1997). Lastly, Pinto (2006) included leafhoppers (Cicadellidae, Hemiptera) as hosts of *Uscanoidea*.

Key to identification for the known species of *Uscanoidea* of the world

- | | | |
|------|---|----------------------|
| 1 | Antenna with funicle and club..... | 2 |
| – | Antenna without funicle..... | 4 |
| 2(1) | Club elongate, 4.0× as long as wide; genitalia tubular, 4.0× as long as wide, with distal half very narrow..... | <i>U. aliciae</i> |
| – | Club ovate, less than 2.0× as long as wide..... | 3 |
| 3(2) | Genitalia with basal half ovate, with ventral medial keel and chelate structures..... | <i>U. aduncatum</i> |
| – | Genitalia tubular with a large anterodorsal aperture and with two ventral setae..... | <i>U. oviclavata</i> |

4(1)	Ovipositor longer than metasoma.....	5
–	Ovipositor not longer than metasoma.....	6
5(4)	Ovipositor base at level of mesocoxae.....	<i>U. silvestrii</i>
–	Ovipositor base at level of tegula.....	<i>U. iperterebrata</i>
6(4)	Fore wing fringe with longest setae as long as discal setae.....	7
–	Fore wing fringe with longest setae longer than discal setae.....	8
7(6)	Club 2.3× as long as wide; fore wing length/width ratio 5.0×	<i>U. hastata</i>
–	Club 1.7× as long as wide; fore wing length/width ratio 4.5×	<i>U. parviclavata</i>
8(6)	Fore wing infumate from base to level of stigma vein level	<i>U. ovata</i>
–	Fore wing hyaline.....	9
9(8)	Club at least 3.0× as long as wide.....	10
–	Club at most 2.0× as long as wide.....	<i>U. nigriventris</i>
10(9)	Female club with maximum length of C5 2.0× width.....	<i>U. acuminata</i>
–	Female club C5 at least 3.0× as long as wide	11
11(10)	Fore wing length/width ratio greater than 1.6.....	<i>U. marilandica</i>
–	Fore wing length/width ratio at most 1.6.....	12
12(11)	Female club segment C5 as long as in the male; genitalia tubular, parallel sided, 3.0× as long as wide, with two ventral setae	<i>U. apiclavata</i>
–	Female club segment C5 longer than in the male; genitalia tubular but not parallel sided, 4.4× as long as wide, without ventral setae.....	<i>U. ricoi</i>

Comments

The high anthropogenic pressure on natural ecosystems leads to cocoa agroforestry systems becoming the vegetation coverage that provides suitable habitats and food for different groups of insects. In a sampling carried out at the Matapollos farm located in El Doncello, Caquetá, 40 cocoa pods with *Monalonion dissimulatum* eggs were collected. From each pod, between 15 to 25 *M. dissimulatum* eggs were obtained, for a total of 719 eggs. The percentage of parasitoidism of *U. ricoi*, sp. nov., in *M. dissimulatum* eggs reached 87,9%. Therefore, it seems that cocoa in agroforestry system plantations ensures natural biological control of this phytophagous insect.

The parasitoid wasp *U. ricoi*, sp. nov., shows high potential as a biological agent against *M. dissimulatum* in cocoa plantations (Figs 27–29) since individuals have been found in different localities, agroforestry associations, and elevations, besides having a high percentage of the host eggs killed. In the future, new searches for *U. ricoi*, sp. nov., should be carried out in other localities in the Neotropical region (Fig. 30). Furthermore, studies of the biology and ecology of the parasitoid should be performed as a baseline for designing biological control management practices of the phytophagous insect pest *M. dissimulatum* in cocoa plantations.

This work corresponds to the first record, arguably the second record, of the plant bug parasitoid of *M. dissimulatum*. Moncayo (1957) recorded *Prophanurus* (= *Telenomus*) *bodkini* (Hymenoptera: Scelionidae) as an egg parasitoid of *M. dissimulatum*.

Prophanurus (= *Telenomus*) *bodkini* is incorrect as a taxonomic identity. Even so, during all these years in Colombia this incorrect information continues to be cited. We did an exhaustive search around the information included in Vélez (1997), to be able to make this statement. We even visited the entomological collection where Dr. Vélez worked and there is no evidence of this.

In Latin America, other *Monalonia* species harm crops of economic importance. Among others, *M. velezangeli* is a polyphagous pest insect in plantations of *Coffea arabica* L. (Rubiaceae), *Eucalyptus grandis* W. Hill (Myrtaceae), *Mangifera indica* L. (Anacardiaceae), *Persea americana* Mill. (Lauraceae), *Psidium guajaba* L. (Myrtaceae), and *Rubus glaucus* Benth. (Rosaceae) (Torres et al. 2012; Ocampo et al. 2018). Exhaustive searches for *Uscanoidea* parasitoids for different *Monalonia* species should be conducted.

Acknowledgments

We thank the Ministry of Science, Technology and Innovation (Ministerio de Ciencia, Tecnología e Innovación) – MINCIENCIAS and the General Royalty System (Sistema General de Regalías) – SGR for funding the Research Project “STUDY OF THE DIVERSITY, POPULATION DYNAMIC AND BIOTIC POTENTIAL OF PREDATORS AND PARASITOIDS THAT CONTROL TRUE BUGS OF THE GENUS *Monalonia* IN COCOA PLANTATIONS OF THE STATES OF HUILA AND CAQUETÁ FLORENCIA (ESTUDIO DE LA DIVERSIDAD, DINÁMICA POBLACIONAL Y POTENCIAL BIÓTICO DE DEPREDADORES Y PARASITOIDES CONTROLADORES DE CHINCHES VERDADERAS DEL GÉNERO *Monalonia* EN PLANTACIONES DE CACAO DE LOS DEPARTAMENTOS DE HUILA Y CAQUETÁ FLORENCIA)” [code BPIN 2020000100513], approved by Agreement Number 100 of November 24, 2020, from which this study has derived. To María Bermúdez, Yulieth Rodríguez, Loreisy Andrade, Eidy Martínez, and Sebastián Valencia for their support in sampling and laboratory activities. To Yennifer Carreño and Éric Córdoba for their support in taking photographs and preparing the figures for publication. To Lizeht Gamboa for the administrative support during the execution of the Research Project. To the Supervision Support Group of the Research Project, including Juan Suárez, Karen Obregón, Paulo Murcia, Olga González, and Diego Vega.

References

- de Abreu JM (1977) Mirídeos neotropicals associados ao cacaueiro. In: Lavabre EM (Ed.) Les mirídes du cacaoyer. Institut Français du Café et du Cacao, 85–106.
- De Santis L (1972) Nuevo género y nueva especie de Trichogrammatidae del Brasil (Hymenoptera Chalcidoidea). Archivos da Universidade Federal Rural do Rio de Janeiro 2: 37–39.
- De Santis L (1979) Catálogo de los Himenópteros Calcidoideos de América al sur de los Estados Unidos. Comisión de Investigaciones Científicas de la Provincia de Buenos Aires: 1–488.

- De Santis L (1989) Catalogue of the Chalcidoidea (Hymenoptera) of America South of the United States, second supplement. *Acta Entomológica Chilena* 15: 9–90.
- De Santis L (1997) Afelínidos y tricogramátidos de la colección del Dr. Alejandro A. Oglobin (Insecta, Hymenoptera) II. Segunda Comunicación. Sesión Ordinaria del Academia Nacional de Agronomía y Veterinaria 51: 7–17.
- Doutt R, Viggiani G (1968) The classification of the Trichogrammatidae (Hymenoptera: Chalcidoidea). *Proceedings of the California Academy of Sciences*, 4th series: 477–586.
- Fursov V (1995) A world review of *Uscana* species (Hymenoptera, Trichogrammatidae), potential biological control agents of bruchid beetles (Coleoptera, Bruchidae). *Le Colloques de l'INRA* 73: 15–17.
- Girault AA (1911) Synonymic and descriptive notes on the Hymenoptera Chalcidoidea with descriptions of several new genera and species. *Archiv fuer Naturgeschichte Berlin* 772(Bd. 1, Suppl. H. 2): 119–140.
- Girault AA (1918) North American Hymenoptera Trichogrammatidae. Privately printed Sydney, Australia: 1–11.
- Johns ND (1999) Conservation in Brazil's chocolate forest: The unlikely persistence of the traditional cocoa agroecosystem. *Environmental Management* 23: 31–47. <https://doi.org/10.1007/s002679900166>
- Lavabre EM (1977) Systematique des Miridae du cacaoyer. In: Lavabre EM (Ed.) *Les mirides du cacaoyer*. Institut Français du Café et du Cacao: 47–70.
- Lin N (1994) Systematic Studies of Chinese Trichogrammatidae (Hymenoptera: Chalcidoidea). Biological Control Research Institute, Fujian Agricultural University, 1–362.
- Moncayo ER (1957) Plagas del cacao en Antioquia y Santander. Tesis. Universidad Nacional de Colombia (Medellín).
- Noyes JS (2022) Universal Chalcidoidea Database. <https://ucd.chalcid.org/#/> [15 Jan 2023]
- Ocampo V, Durán J, Albornoz M, Forero D (2018) New plant associations for *Monalonion velezangeli* (Hemiptera: Miridae) in green urban areas of Bogotá (Colombia). *Acta Biológica Colombiana* 23: 205–208. <https://doi.org/10.15446/abc.v23n2.69374>
- Owen AK, George J, Pinto JD, Heraty JM (2007) A molecular phylogeny of the Trichogrammatidae (Hymenoptera: Chalcidoidea), with an evaluation of the utility of their male genitalia for higher level classification. *Systematic Entomology* 32: 227–251. <https://doi.org/10.1111/j.1365-3113.2006.00361.x>
- Pinto JD (2006) A review of the new world genera of Trichogrammatidae (Hymenoptera). *Journal of Hymenoptera Research* 15: 38–163.
- Sambuichi RHR (2006) Estrutura e dinâmica do componente arbóreo em área de cabruca na região cacaueira do sul da Bahia, Brasil. *Acta Botanica Brasilica* 20: 943–954. <https://doi.org/10.1590/S0102-33062006000400018>
- Schuh RT (2002–2013) On-Line Systematic Catalog of Plant Bugs (Insecta: Heteroptera: Miridae). <http://research.amnh.org/pbi/catalog/> [10 Jan 2023]
- Suárez JC, Ngo MA, Melgarejo, LM, Di Rienzo JA, Casanoves F (2018) First typology of cacao (*Theobroma cacao* L.) systems in Colombian Amazonia, based on tree species richness, canopy structure and light availability. *PLOS ONE* 13: e0191003. <https://doi.org/10.1371/journal.pone.0191003>

- Torres LF, Correa GA, Cartagena JR, Monsalve DA, Londoño ME (2012) Relationship of *Monalonion velezangeli* Carvalho & Costa (Hemiptera: Miridae) with the phenology of avocado (*Persea americana* Mill., cv. Hass). *Revista Facultad Nacional de Agronomía Medellín* 65: 6659–6665.
- Vélez R (1997) Plagas agrícolas de impacto económico en Colombia. Universidad de Antioquia (Medellín): 1–482.
- Viggiani G (1992) New species of Trichogrammatidae (Hymenoptera: Chalcidoidea) from South America. *Redia* 75: 253–265.
- Woolley JB, Dal Molin A (2017) Taxonomic revision of the *flavopalliata* species group of *Signiphora* (Hymenoptera: Signiphoridae). *Zootaxa* 4315: 1–150. <https://doi.org/10.11646/zootaxa.4315.1.1>

Redescription of *Apanteles mimoristae* (Hymenoptera, Braconidae), a parasitoid of the native pyralid cactus moth *Melitara* cf. *nephelepasa* in central Mexico

Renato Villegas-Luján¹, Robert Plowes², Lawrence E. Gilbert²,
Julio Cesar Rodríguez¹, Ricardo Canales-del-Castillo³, Gabriel Gallegos-Morales¹,
Martha P. España-Luna⁴, José Fernández-Triana⁵, Sergio R. Sanchez-Peña¹

1 Universidad Autónoma Agraria Antonio Narro, Saltillo, Coahuila, Mexico **2** University of Texas at Austin, Austin, Texas, USA **3** Universidad Autónoma de Nuevo León, San Nicolás de los Garza, Nuevo Leon, Mexico **4** Universidad Autónoma de Zacatecas, Zacatecas, Mexico **5** Canadian National Collection of Insects, Ottawa, Ontario, Canada

Corresponding author: Sergio R. Sanchez-Peña (sanchezcheco@gmail.com)

Academic editor: J. M. Jasso-Martínez | Received 18 December 2023 | Accepted 1 March 2024 | Published 26 March 2024

<https://zoobank.org/1B729C13-0B3A-4414-AFB0-BCB1A6130342>

Citation: Villegas-Luján R, Plowes R, Gilbert LE, Rodríguez JC, Canales-del-Castillo R, Gallegos-Morales G, España-Luna MP, Fernández-Triana J, Sanchez-Peña SR (2024) Redescription of *Apanteles mimoristae* (Hymenoptera, Braconidae), a parasitoid of the native pyralid cactus moth *Melitara* cf. *nephelepasa* in central Mexico. Journal of Hymenoptera Research 97: 207–228. <https://doi.org/10.3897/jhr.97.117514>

Abstract

Novel trophic associations have sometimes resulted in fortuitous and significant biological control. After the invasion of North America by the South American cactus moth, *Cactoblastis cactorum* (Berg) (Pyralidae: Phycitinae), it is pertinent to characterize the assemblage of local natural enemies that could utilize this moth in new host-parasitoid associations. Herein we report on *Apanteles mimoristae* Muesebeck (Braconidae: Microgastrinae), a North American gregarious endoparasitoid wasp attacking the caterpillar of the phycitine cactus moth *Melitara* cf. *nephelepasa* (Dyar) (Pyralidae: Phycitinae, also known as zebra worm), also native to North America; both collected in *Opuntia ficus-indica* (L.) Mill. (Cactaceae) cultivated fields at rural areas of Mexico City. We provide an updated morphological account for *A. mimoristae* visualized with light microscopy and scanning electron microscope (SEM); a fragment of its cytochrome oxidase subunit I (COI) gene sequence data is reported for the first time. Additionally, we analyze its taxonomical position relative to other *Apanteles* species from the Americas including those attacking cactus-feeding moths. Our analyses place *A. mimoristae* (from Mexico) in a clade with *A. esthercentenoae* Fernández-Triana (from Costa Rica), a parasitoid of both *Cromarcha stroudagnesia* Solis (Pyralidae) and *Palpita venatalis* (Schaus) (Crambidae) (non cactus-feeding), and in a sister clade to *A. opuntiarum* Martínez &

Berta (from Argentina) and *A. alexanderi* Brèthes (from Argentina and Uruguay), parasitoids of the cactus-feeding phycitines *Cactoblastis* and *Tucumania* respectively. Finally, we provide an updated key for the identification of *Apanteles* species recorded parasitizing cactus moth caterpillars in the American continent.

Keywords

Agriculture, biological control, ecosystem, invasive insect, North America, *Opuntia*, South America

Introduction

Novel trophic associations can result after dispersal and expansion of the geographical distribution of organisms. Some novel associations (e.g., infection, parasitism, parasitoidism, predation) sometimes bring about significant levels of mortality of phytophagous insects (Torres-Acosta et al. 1916; Felipe-Victoriano et al. 1917; Durocher-Granger et al. 2021) resulting (in the case of pests) in fortuitous or “new association” biological control (Sterling 1978; Hokkanen and Pimentel 1989). The South American cactus moth *Cactoblastis cactorum* (Berg) (Pyralidae: Phycitinae) is one of the most important herbivores of *Opuntia* Miller and related genera (prickly pears, Cactaceae) (Morrison et al. 2021). It poses a serious threat to *Opuntia* cacti in North America, both in their native natural communities and in commercial plantations (Starmer et al. 1988; Hight and Carpenter 2009). *Opuntia* (called nopal in Mexico) is widely consumed by the Mexican people since prehispanic times. The areas involved are of a continental scale and this implies that intensive measures like chemical control and physical destruction of *C. cactorum* are not feasible, making biological control by permanently established natural enemies (classical biological control) the most viable option (Habeck and Bennet 1990; Viguera and Portillo 2001).

North American *Opuntia* species are attacked by caterpillars of native cactus moths in the Pyralidae. Among these, the genus *Melitara* Walker is widespread in the deserts of northern Mexico and the southern and western United States; these insects usually bore into pads, are solitary and occasionally cause economic damage or plant dieback (Mann 1969; personal observations).

The study of local natural enemies is a key aspect in biocontrol of native and exotic insects (Morales-Galvez et al. 2022). Several species of Microgastrinae (Braconidae) are among the potential natural enemies considered for biological control of *C. cactorum*. Some species of *Apanteles* Foerster have been reported as parasitoids of pyralid cactus feeding moths, such as *Cactoblastis* Ragonot in South America, and the closely related genus *Melitara* in North America as well as *Loxomorpha* Amsel (= *Mimorista*) in the related family Crambidae (Muesebeck 1921). This family and the Pyralidae form the superfamily Pyraloidea. About half of described species of *Apanteles* are gregarious endoparasitoids of the host larval stage (Fernández-Triana et al. 2014; Varone et al. 2015; Figueroa et al. 2021). *Apanteles alexanderi* Brèthes,

A. mimoristae Muesebeck, *A. opuntiarum* Martínez & Bertha, and *Iconella etiellae* Viereck (a genus closely related to *Apanteles*) are among native Microgastrinae species parasitizing pyralid *Opuntia*-feeding moths in the American continent (Muesebeck 1921; Martínez et al. 2012; Fernández-Triana et al. 2013). Of those, only *A. opuntiarum* from Argentina has been studied as biological control agent of *C. cactorum* (Martínez et al. 2012). The most frequent reported hosts of another related wasp, *Apanteles megathymi* Riley, are butterfly larvae in the HesperIIDae (giant skippers like *Megathymus* spp.), but it has also been reported attacking the cactus zebra worm, *Melitara nephelapasa* (Dyar) and *Laniifera cyclades* (Druce) (Crambidae) in *Opuntia* spp (Mann 1969).

Apanteles mimoristae was described in the early 1900s based on four females and one male (Muesebeck 1921). However, the taxon is not well defined taxonomically: the original description is very short and incomplete, and it lacks illustrations and molecular information. Another important aspect in the Microgastrinae, as in other parasitoid wasp families, is the existence of cryptic species (Whitfield 1997; Hoy et al. 2000) making accurate species identification difficult even for specialists.

Indigenous parasitoids and other natural enemies may associate to invasive species (cactus moth in this context) to create new trophic relationships, exemplifying the so-called “new association biological control” (Hokkanen and Pimentel 1989). It is possible that indigenous *Apanteles* species parasitizing *Melitara*, like *A. mimoristae*, might exploit the invasive moth *C. cactorum* as a host. Our objective is to clarify and refine the description of *A. mimoristae* to better characterize the species and support its identification. DNA barcode sequences complemented by morphological comparison were used to investigate species boundaries. A key is provided to highlight the differences between *Apanteles* species reported to attack phycitine cactus moths in the American continent. The information presented here will serve as a foundation for investigations on the possible interactions of *A. mimoristae* in the zones invaded by *C. cactorum* in North America as an element in a biological control approach.

Materials and methods

Rearing material. Seventy caterpillars (larval stage) of zebra worm, *Melitara* cf. *nephelapasa* ranging from half-grown to fully grown were collected from prickly pear pads (*Opuntia ficus-indica* L. var. Milpa Alta) at commercial plots in Mexico City, central Mexico (19.191444, -99.003810) (Fig. 1) in the summer and fall of 2019 and 2020. These caterpillars were transported to the laboratory of the Universidad Autónoma Agraria Antonio Narro, and were placed individually in plastic containers, on a layer of moist filter paper at room temperature ($25^{\circ}\pm 2^{\circ}\text{C}$), 100% RH, and 12:12 h L:D, and fed daily fresh fragments of *O. ficus-indica* pads until they reached the adult stage or parasitoid emergence.

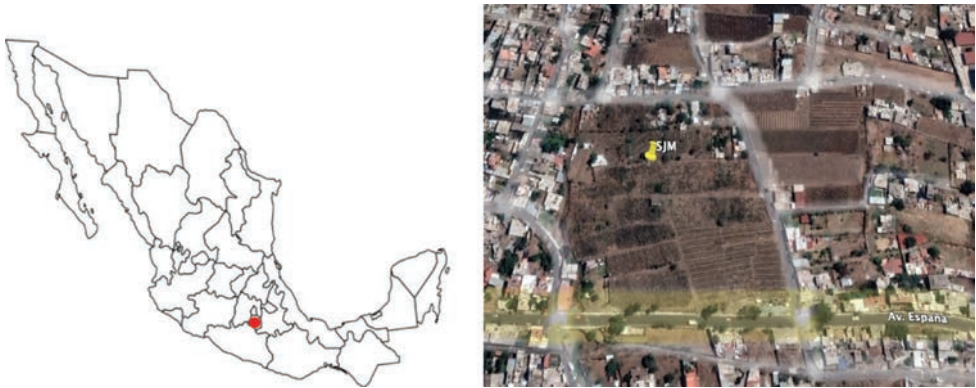


Figure 1. Collection site of *Apanteles mimoristae* from *Melitara cf. nephelapa* in cultivated fields of *Opuntia ficus-indica* (Cactaceae) in San Jerónimo Miactalán (SJM), in the municipality of Milpa Alta, Mexico City, MX (left). The cactus fields are partially surrounded by houses and other agricultural areas (right).

Morphological analysis

Parasitoid wasp. After emergence, adult wasps were preserved in 70% ethanol (for mounting and photographing) and 96% ethanol (for DNA analysis). Morphological terms and diagnostic structures followed Wharton (1997) and Wharton et al. (1997). Features were compared with the original description of *A. mimoristae* (Muesebeck 1921), and also Martínez et al. (2012) and Fernández-Triana et al. (2013, 2014).

Due to costs and travel limitations, it was not possible for the first author to examine the holotype of *A. mimoristae*. The Mexican material listed was examined by author JFT and compared to paratypes of *A. mimoristae* in the Canadian National Collection of Insects (CNC). They were also compared to the brief but valid description of the species by Muesebeck (1921). The geographical distribution of *Apanteles* species was obtained from Fernández-Triana et al. (2020). Morphological analysis and imaging used a microscope eye-piece Dino-Lite AM7025x camera (Dino-Lite, Los Angeles, USA) adapted on an Olympus SZ51stereoscope plus an Olympus 110 AL2X-2WD38 magnifying lens (Olympus, Fukuoka, Japan). Images were also obtained with a Hitachi TM-3000 scanning electron microscope (SEM) (Hitachi High-Tech Corp., Fukuoka, Japan). For measurements, the DinoXcope software version 2.3 (Dino-Lite) was used. Images were edited on ImageJ (National Institutes of Health, USA). All measurements are expressed in mm. Morphological terms and their abbreviations used are: SV = surface of the vertex, T1 = mediotergite 1, and T2 = mediotergite 2. Abbreviations of depositories are:

- UNAM** Colección Nacional de Insectos, Instituto de Biología, UNAM, Ciudad de México, México
- CNC** Canadian National Collection of Insects, Arachnids and Nematodes, Ottawa, Canada
- NMNH** National Museum of Natural History, Washington D.C., United States
- UT** University of Texas at Austin, United States

Melitara cf. *nephelepasa* caterpillars were identified following the description and geographical range reported in Mann (1969), collected in the host plant *O. ficus-indica*.

DNA extraction and PCR

Extraction, PCR conditions, and sequencing for the cytochrome oxidase subunit 1 (COI) were performed following Lopez-Monzon et al. (2019). Barcode sequences were obtained both at Brackenridge Field Laboratory, University of Texas (UT) at Austin, US (5 specimens) and at Facultad de Agronomía, Universidad Autónoma de Zacatecas (UAZ) at Zacatecas, MX (1 specimen).

Phylogenetic analysis

There were no known *A. mimoristae* sequences available before this work. A fragment of 628 base pairs (bp) of the cytochrome oxidase subunit I (COI) gene was obtained from all specimens at UT. The raw sequences were edited in Codon Code ver. 5.0.1 (Codon Code Corporation, Dedham, MA, US). The obtained sequences were aligned using ClustalW within the Molecular Evolutionary Genetics Analysis (MEGA) Version X software (Kumar et al. 2018), alongside a total of 152 sequences from *Apanteles* (Smith et al. 2008), supplemented with sequences from other *Apanteles* and related genera and species in the Braconidae retrieved through the Basic Local Alignment Search Tool (BLAST). Utilizing various exploratory phylogenetic trees derived from the Neighbor-Joining (NJ) and Maximum Likelihood (ML) algorithms, the alignment was refined to a subset of 33 sequences to ascertain the taxonomic and phylogenetic placement of *A. mimoristae* (Table 1). The phylogenetic relationship for the *Apanteles* species attacking cactus-feeding moths was then constructed by Maximum Likelihood (ML) algorithm using MEGA version X (Kumar et al. 2018) and parameter as GTR+I+G (General Time Reversible with invariant sites and a gamma distribution) an evolutionary model with 1,000 replicates. Model selection was performed using statistical and evolutionary analysis of multiple sequence alignments TOPALi v2 (Milne et al. 2009). In MrBayes ver.3.2.5 5 (Ronquist et al. 2012) we set partitions, first, second and third positions of COI, and models as selected by Partition Finder v1.1.1 (Lanfear et al. 2012) under the Bayesian information criterion (BIC) and the “all” search algorithm. For the first partition and second position the best model was GTR+I+G, and for the third partition the best model was HKY+I+G (Hasegawa-Kishino-Yano with invariant sites and a gamma distribution). We conducted the Bayesian phylogenetic analysis with nucmodel = 4by4, nruns = 2, nchains = 4, and sampled freq = 1000 (Sanchez-Peña et al. 2017), for one billion generations. We assessed convergence and stationarity in the Bayesian analysis using the “sump” command to examine log marginal likelihood plots, average standard deviation of split frequencies among runs, and the potential scale reduction factor for all parameters. Nodes that had posterior probabilities greater than 0.95, were considered well supported.

Table 1. Dataset of selected COI sequences of 33 species of Microgastrinae (*Apanteles* Förster, *Dolichogenidea* Viereck, *Glyptapanteles* Ashmead, *Iconella* Mason, and *Parapanteles* Ashmead) and their GenBank accession numbers utilized in the phylogenetic analysis. DNA voucher numbers [DHJPAR = Daniel H. Janzen and Winnie Hallwachs database at University of Pennsylvania; CNIN = Colección Nacional de Insectos, Universidad Nacional Autónoma de México (UNAM); USNM, National Museum of Natural History] * = *Apanteles* species parasitizing cactus moths in the Phycitinae on the American continent. A recent revision of the genus *Parapanteles* (Parks et al. 2020) indicated that it is not monophyletic, with species interspersed among *Apanteles* and closely related genera of Braconidae.

Microgastrinae species with COI sequence	Collection and voucher code	GenBank Accession number
<i>Apanteles</i> sp. Rodriguez48	DHJPAR0002317	KF462163
<i>Apanteles</i> sp. Rodriguez48	DHJPAR0047068	KF462208
<i>Apanteles</i> sp. Rodriguez106	DHJPAR0049396	KF462061
<i>Apanteles</i> sp. Rodriguez12	DHJPAR0047067	KF462166
<i>Apanteles</i> sp. Rodriguez169	DHJPAR0041984	JQ575692
<i>Apanteles</i> sp. Rodriguez69(3)	DHJPAR0039707	HQ926377
<i>Apanteles</i> sp. Rodriguez47	DHJPAR0002260	MT469770
<i>Apanteles</i> sp. Rodriguez47	DHJPAR0045169	KF462233
<i>Apanteles</i> sp. Rodriguez107	DHJPAR0034228	JQ853633
<i>Apanteles</i> sp. Rodriguez32	DHJPAR0048151	KF462206
<i>Apanteles</i> sp. Rodriguez158	DHJPAR0049161	KF461918
<i>Apanteles</i> sp. Rodriguez168	DHJPAR0045255	KF462252
<i>Apanteles</i> sp. Rodriguez68(2)	DHJPAR0004091	EU397563
<i>Apanteles</i> sp. Rodriguez33	DHJPAR0048132	KF462068
<i>Apanteles</i> sp. Rodriguez67	DHJPAR0049140	KF462152
* <i>Apanteles alexanderi</i>	CNIN1122	JX566790
* <i>Apanteles opuntiarum</i>	CNIN1113	JX566778
<i>Apanteles</i> sp. Rodriguez105 (<i>A. esthercentenoae</i>)	DHJPAR0005185	EU396687
* <i>Apanteles</i> Milpa Alta DF (<i>A. mimoristae</i>)		OQ676887
<i>Parapanteles</i> sp. Whitfield133	DHJPAR0020673	JQ850314
<i>Parapanteles</i> sp. Whitfield44	DHJPAR0030780	JQ854565
<i>Parapanteles</i> sp. Whitfield45(2)	DHJPAR0020128	EU397378
<i>Apanteles</i> sp. Rodriguez110	DHJPAR0005168	EU396741
<i>Parapanteles</i> sp. Whitfield102	DHJPAR0041787	MN645414
<i>Parapanteles</i> sp. Whitfield303	DHJPAR0012759	EU396804
<i>Parapanteles</i> sp. Whitfield302	DHJPAR0012793	EU396799
<i>Parapanteles</i> sp. Whitfield70	DHJPAR0020653	JQ853731
<i>Apanteles</i> sp. Rodriguez167	DHJPAR0045315	KF462011
<i>Apanteles</i> sp. Rodriguez169	DHJPAR0041984	JQ575692
<i>Iconella</i> sp. Whitfield05	DHJPAR0045362	KC685306
<i>Dolichogenidea</i> sp. Whitfield11	USNM00496786	JQ852381
<i>Glyptapanteles</i> sp. Whitfield175	DHJPAR0040014	JQ574612

Results

Material examined

Mexico, 15♀, 15♂ of *A. mimoristae*; Mexico City, Milpa Alta, San Jerónimo Mia-catlán; 19.191444, -99.003810, 2384 masl; 21.xi.2020; Renato Villegas leg.; zebra worm, *Melitara* cf. *nephelepasa* in commercial plots of *Opuntia ficus-indica* (Cactaceae) (prickly pear or nopal); GenBank: OQ676887.1 and OQ561741.1.

Redescription

Apanteles mimoristae Muesebeck, 1921

Note. Measurements from reared specimens in this work.

Female. Body length of $\bar{x}=2.94$ (2.805–3.097) (Figs 2–4).

Head. Transverse; antennae shorter than body, $\bar{x}=2.45$ (2.282–2.605), face smooth and eyes moderately setose in frontal view (Fig. 3A). SV finely wrinkled around the ocelli, but smooth and opaque between the ocelli (Figs 3B, 3C). Ocular–ocellar line/posterior ocellus diameter: 2.13–2.32. Intercellular distance/posterior ocellar diameter: 2.15–2.33. Antennal flagellomere 2 length/width: 2.06–2.46. Antennal flagellomere 14 length/width: 1.06–1.40. Length of antennal flagellomere 2/length of antennal flagellomere 14: 2.08–2.18.

Mesosoma. Dull black. Mesoscutum: indistinctly/irregularly punctate, profusely setose and markedly rugose, the roughness does not cover its surface in dorsal view (Fig. 3D). Scutellum: flat, dull, smooth, and setose. Pits in the scutoscutellar sulcus: 10. Mesopleura: anterior half punctate and pilose; posterior half smooth and polished. Propodeum: with rugae; with a well-defined broad median areola, inside of areola with marked wrinkles, and a transversal carina which does not reach the spiracle (Fig. 3D, E).



Figure 2. *Apanteles mimoristae* Muesebeck (Braconidae: Microgastrinae) female. Habitus.

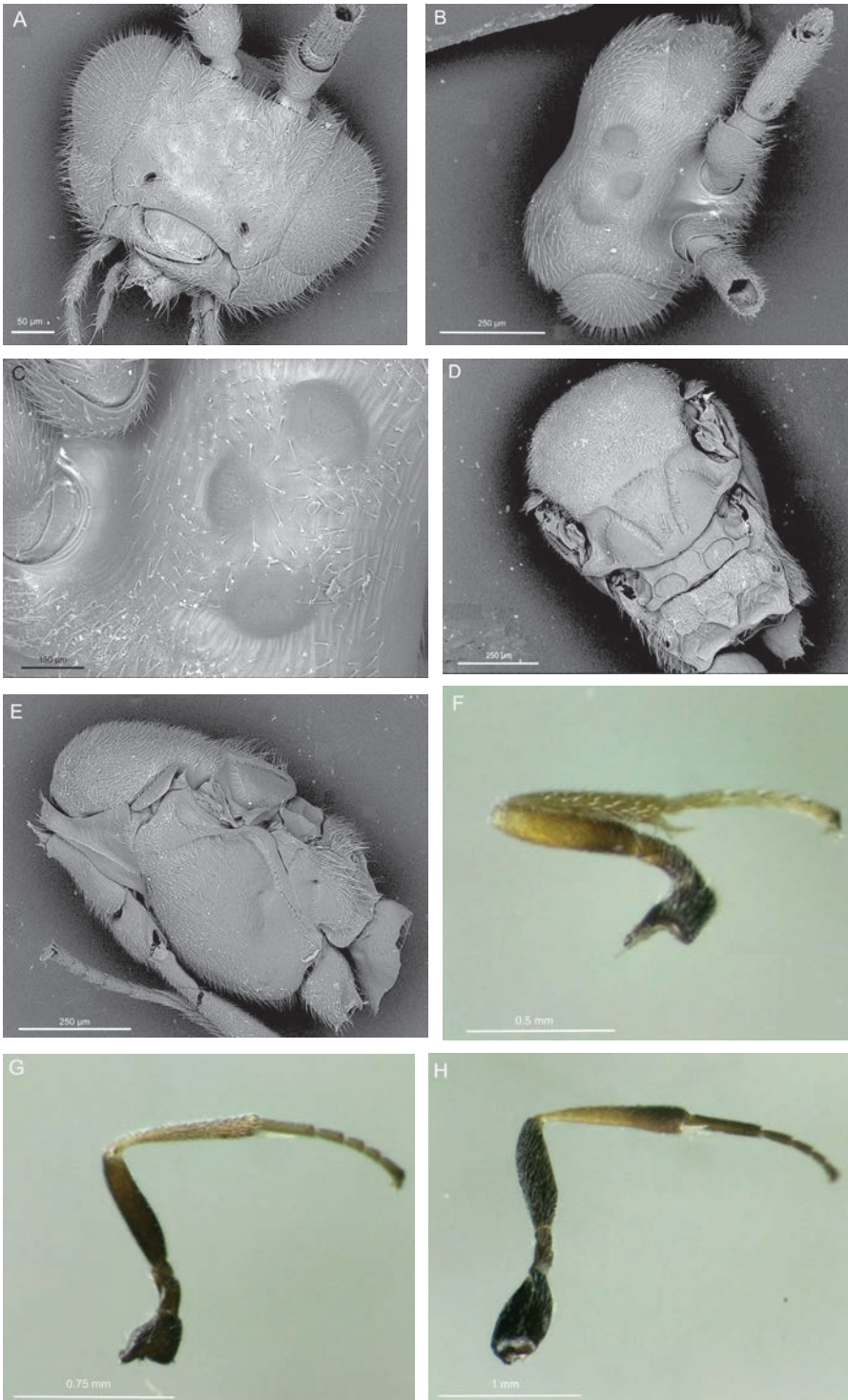


Figure 3. *Apanteles mimoristae* Muesebeck **A–C** head **A** frontal view **B** dorsal view **C** ocelli **D, E** mesosoma **D** dorsal view **E** lateral view **F–H** legs **F** anterior **G** medium **H** posterior.

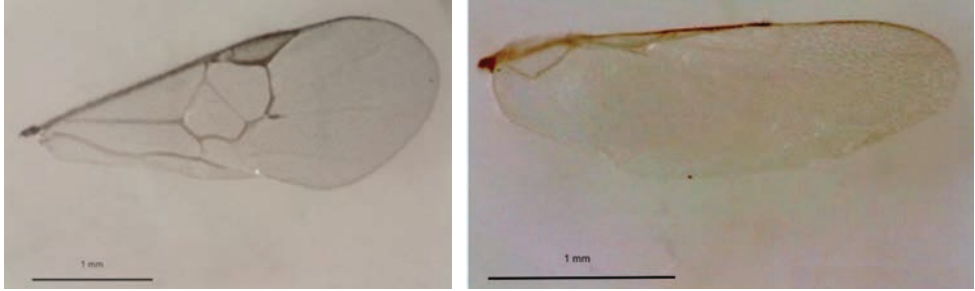


Figure 4. *Apanteles mimoristae* Muesebeck, female wings: forewing (left) and hindwing (right)

Legs: all coxae blackish; profemur: with less of the basal half dark brown and the rest dark yellow or light brown; mesofemur: more than half blackish and the rest dark brown; metafemur: entirely black; protibia: evenly light yellowish; mesotibia: basally yellowish and mostly light brown towards the apex; metatibia: color pattern varies from dark brown fading to light yellow from the base to the apex (Fig. 3E, H). Metatibia inner spur length slightly longer than half of metatarsus (Fig. 3H). Metafemur length/width: 2.92–3.16. Metatibia inner spur length/metatarsus length: 0.48–0.50. Wings: hyaline; translucent pterostigma with dark brown margins; veins transparent to dark brown (Fig. 4). Fore wing length: 3.61–3.65 mm. Fore wing veins length: r/2RS: 1.56–1.62, 2RS: 1.11–1.19, 2M/(RS+M)b: 0.78–0.85. Pterostigma length/width: 3.19–3.66. Anterior half of humeral complex whitish yellow, posterior half is light to dark brown; tegula pale to dark.

Metasoma. T1: elongated from above, wider at the base than at the apex, with marked wrinkles across all surface, mainly in the median area; barely setose, with two depressions on the posterior margin, more or less of the same size (Fig. 5A). T1 length/width at posterior margin: 2.42–2.50. T2: wider than long, smooth, without rugosities, with little setae in dorsal view and two groups of setae in lateral view (Fig. 5B, C). Width at posterior margin/length: 2.90–3.05. Ovipositor: mean length of sheaths = 0.895 mm (0.863–0.935); black, slightly wider at the base than at the apex, almost as long as the abdomen, smooth, opaque, moderately setose, and covering all the ovipositor (Fig. 5D). Ovipositor sheaths length/metatibial length: 0.833–1.02. Pleats in the hypopygium: at least 4.

Male. Very similar to female (Fig. 6), excepting smaller body size, \bar{x} = 2.696 (2.599–2.785); antennae longer than body, 3.008 (2.752–3.187).

Distribution. Mexico (Mexico City), United States (Texas and Florida).

Biology. Gregarious larva-prepupa koinobiont endoparasitoid.

Hosts. *Melitara* cf. *nephelepasa* (Pyralidae) feeding on *Opuntia ficus-indica* (Cactaceae); *Melitara junctolineella* Hulst (Pyralidae); *Loxomorpha flavidissimalis* (Grote) (Crambidae).

A list of selected morphological differences between *A. mimoristae* and four other *Apanteles* species parasitic on Pyralidae: Phycitine stem- and cladode borer larvae are summarized in Table 2. The dichotomous key provided below includes selected *Apanteles* species parasitizing phycitine cactus moths in North and South America.

Table 2. List of morphological features with measurements (mm) and rates in female specimens of known *Apanteles* species parasitizing pyraloid moths that mostly feed on cacti (*Opuntia*) in the Americas. NR = Not Reported.

Features / <i>Apanteles</i> species	<i>A. minoristae</i> Muesebeck (Muesebeck 1921, and this work)	<i>A. esthercentenoae</i> Fernández-Triana (Fernández-Triana et al. 2014) (not from <i>Opuntia</i> caterpillars)	<i>A. opuntiarum</i> Martínez & Berta (Martínez et al. 2012)	<i>A. alexanderi</i> Brèthes (Martínez et al. 2012)	<i>A. megathymyi</i> Riley (Fernández-Triana et al. 2014)
Body length	2.80–3.09	3.50–3.80	2.40–3.70	2.90–3.70	3.50–3.60
Ocular-ocellar line/ posterior ocellar diameter	2.13–2.32	2.00–2.20	NR	NR	1.40–1.60
Interocellar distance/posterior ocellar diameter	2.15–2.33	1.40–1.60	NR	NR	1.70–1.90
Antennal flagellomere 2 length/ width	2.06–2.46	2.60–2.80	NR	NR	2.60–2.80
Antennal flagellomere 14 length/ width	1.06–1.40	1.40–1.60	NR	NR	2.00–2.20
Length of antennal flagellomere 2/14	2.08–2.18	2.00–2.20	NR	NR	1.70–1.90
Metafemur length/width	2.92–3.16	3.00–3.10	NR	NR	3.20–3.30
Metatibia inner spur length / metabasis tarsus length	0.48–0.5	0.40–0.50	-0.40	0.40–0.50	0.40–0.50
Fore wing length	3.61–3.65	3.90–4.00	2.30–3.70	2.90–3.80	3.70–3.80
Length of fore wing veins:	1.56–1.62	2.00–2.30 or more	1.70–1.80	1.30–1.40	1.00 or less
r/2RS	1.11–1.19	1.70–1.80	NR	NR	1.40–1.60
2RS/2M	0.78–0.85	0.50–0.60	NR	NR	0.70–0.80
2M/(RS+M) b					
Pterostigma length/width	3.19–3.66	3.10–3.50	2.50	2.50–2.60	2.60–3.00
Pits in scutrocellular sulcus	10	11 or 12	9 or 10	9 or 10	7 or 8
T1 length/width at posterior margin	2.42–2.50	1.10–1.30	1.00	1.00	2.3–2.8
T2 width at posterior margin/ length	2.90–3.05/ 4.00 or more	3.60–3.90	3.20	3.10–3.20	2.80–3.10
Ovipositor sheaths length/ metatibial length	0.83–1.02	1.20–1.30	NR	1.40–1.50	1.40–1.50
Pleats in the hypopygium	4 or more	4 or more	NR	NR	4 or more

Key to *Apanteles* species parasitoids of Pyralidae: Phycitine stem- and cladode (*Opuntia*) borer larvae in the Western hemisphere

(After Muesebeck 1921; Martínez et al. 2012; Fernández-Triana et al. 2014, and this work).

- 1 Ovipositor sheaths shorter than metasoma..... **2**
 – Ovipositor sheaths as long as metasoma..... **4**
 2 Body length more than 3.50 mm; T1 sculptured, centrally with excavated area and transverse striation inside and/or a polished knob centrally on posterior margin of mediotergite. From North America, reported mainly parasitizing caterpillars of large-sized desert Hesperidae (giant skippers) in *Yucca* plants; also from Crambidae and Pyralidae infesting Cactaceae ***A. megathymi* Riley**
 – Body length 2.9–3.0 mm; T1 smooth or with partial faint punctae or small rugae. Parasitoids of stem-boring Pyraloids including *Opuntia*-feeding caterpillars (Pyralidae: Phycitinae) **3**
 3 T1 elongated, with two similar-sized depressions on the posterior margin, one at each corner (Fig. 5A, B); posterior half with a longitudinal fovea medially; sculpturing on T1 variable, smooth or closely and finely ruguloso-punctate or with faint wrinkles across the surface, mainly in the median area; T1 barely setose; T2 with short setae in dorsal view (Fig. 5B) and two groups of setae in lateral view (Fig. 5C). North American parasitoid of *Opuntia*-feeding caterpillars: *Loxomorpha* (Crambidae) and *Melitara* spp. (Pyralidae: Phycitinae) ***A. mimoristae* Muesebeck**
 – T1 approximately square, or only slightly longer than wide, with two apicolateral transverse depressions (fig. 13, Martínez et al. 2012, pp. 441); T1 punctate and occasionally rugulose medially. From temperate South America, parasitoid of *Opuntia*-feeding caterpillars (*Cactoblastis cactorum*, Pyralidae: Phycitinae) ***A. opuntiarum* Martínez & Berta**
 4 Body length more than 3.60 mm, T1 mostly sculptured, excavated area centrally with transverse striation inside and/or a polished knob centrally on posterior margin of mediotergite; T2 with some sculpture, mostly near posterior margin (fig. 150G, Fernández-Triana et al. 2014, pp. 482). From tropical forests in Central America; parasitoid of stem-boring Crambidae and Pyralidae (not in *Opuntia*) ***A. esthercentenoae* Fernández-Triana**
 – Body length less than 3.00 mm, T1 anteriorly smooth and rugose to rugulose (figs 6, 7, Martínez et al. 2012, pp. 438), T2 with faint but distinguishable rugosities (figs 6, 7, Martínez et al. 2012, pp. 438). From semiarid temperate South America; parasitoid of *Opuntia*-feeding caterpillars (*Tucumania* sp.; Pyralidae: Phycitinae) ***A. alexanderi* Brèthes**

Phylogenetic analysis

Five barcode sequences (COI) were obtained at UT; these were all were identical and differed by only one base pair from the single sequence obtained at UAZ (0.16%); such

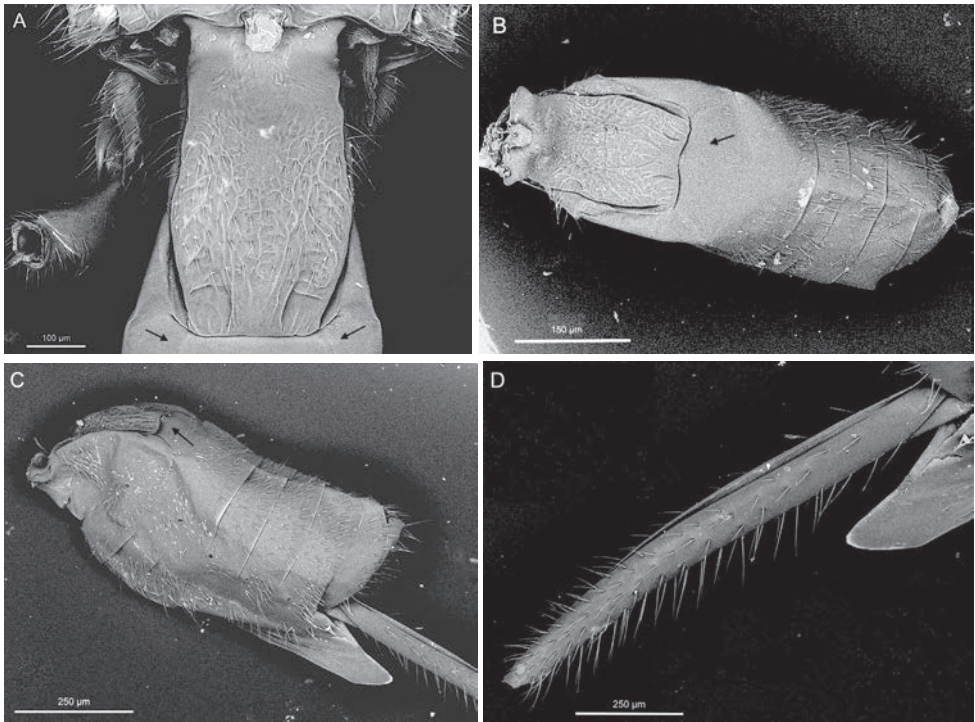


Figure 5. *Apanteles mimoristae* Muesebeck, female **A** T1, dorsal view, rough surface and posterior margin with two lateral depressions **B** metasoma dorsal view **C** metasoma lateral view, lateral setae on second and third tergite **D** ovipositor sheaths. Arrows in **A–C** indicate smooth surface of T2.

a low percentage of divergence should be considered intraspecific polymorphism. The Genbank accession numbers are OQ676887 (UT) and OQ561741 (UAZ). These are the first COI gene sequences reported for *A. mimoristae*.

BLAST searches of the UT sequence indicated highest similarity to *A. esthercentenoae* Fernández-Triana (2014) (Genbank sequences EU396681 and EU396684) (both as *Apanteles* sp. Rodríguez 105) with 92.33 and 92.32% identity respectively and 99% cover.

Phylogenetic trees were constructed using Bayesian and maximum likelihood analyses (Figs 7, 8 respectively) of previously published *Apanteles* sequences and sequences of *A. mimoristae* obtained in this work. In both trees, *A. mimoristae* and *A. esthercentenoae* (a parasitoid of the non cactus-feeding moths *Palpita venatalis* (Schaus) (Crambidae) and *Cromarcha stroudagnesia* Solis (Pyrilidae) in Costa Rica) belong in a sister group to *A. alexanderi* and *A. opuntiarum*, parasitoids of cactus-feeding phycitine Pyralidae in temperate South America. These relationships are expected considering the geographical distribution of these species pairs (North-Central America and South America respectively).

Field observations

In a collection, wasp larvae had already emerged from a dead zebra worm, preparing to pupate in the worm's gallery in a split-opened *O. ficus-indica* pad. The transparent



Figure 6. *Apanteles mimoristae* Muesebeck, male. Habitus.

cuticle of these wasp larvae reveals their striking blue or turquoise hemolymph indicating they were feeding on the hemolymph of the caterpillar host, which has the same characteristic color (Fig. 9).

Cocoons

In a field collection, a cluster of parasitic wasp cocoons was already formed and attached to the cuticle of the dead *M. cf. nephelypasa* caterpillar, inside a cactus pad; this cocoon mass was collected and incubated in the laboratory until adult emergence (Fig. 10). Cocoons were white/beige, elongated-oval, made of silk fibers, smooth. An irregular mass of cocoons was tightly packed (Fig. 10) and the cocoons were separated from each other. Some cocoons were adhered to the caterpillar cuticle, while other cocoons were inside the worm's gallery in a split-opened *O. ficus-indica* pad.

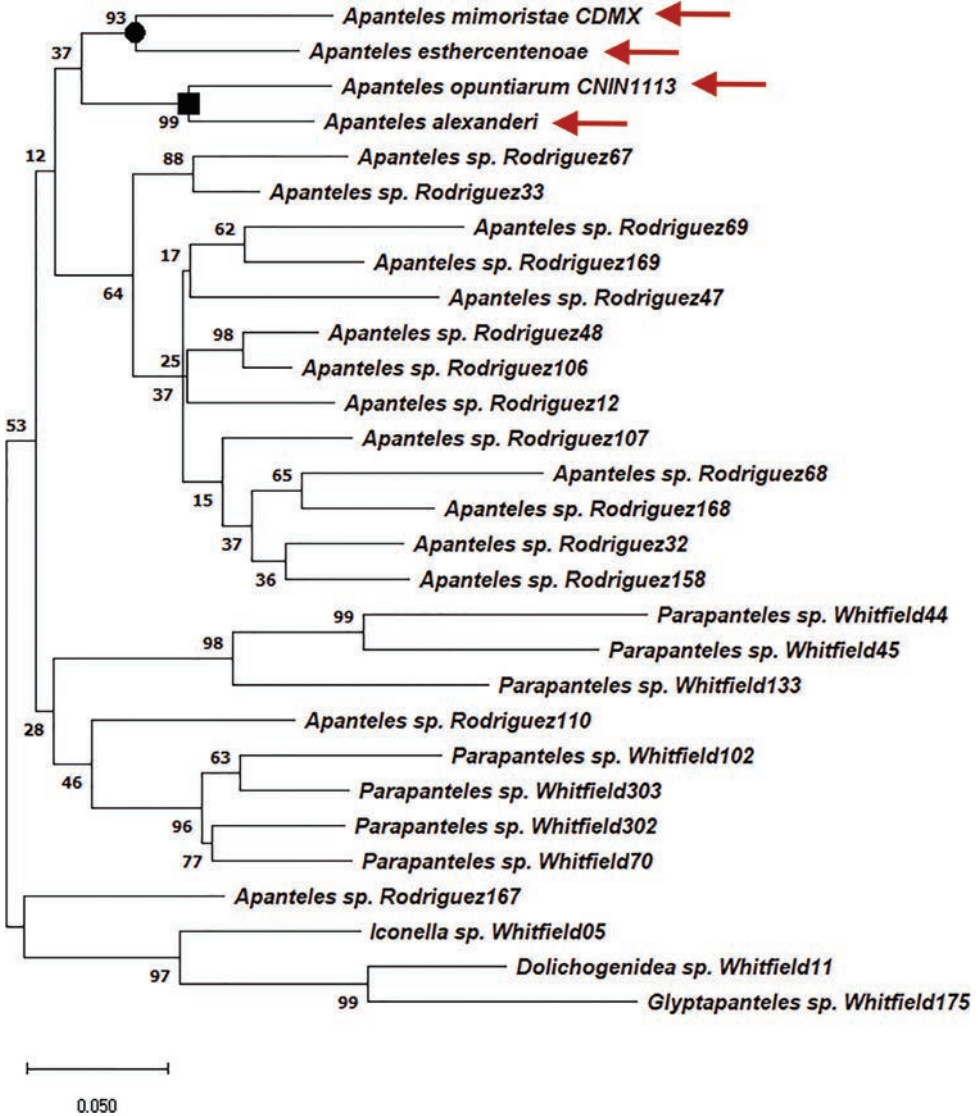


Figure 7. Bayesian tree for *Apanteles mimoristae* and related species. Arrows indicate *Apanteles mimoristae*, *A. esthercentenoae*, *A. alexanderi* and *A. opuntiarum*.

Discussion

Morphological analysis and diagnosis

Apanteles mimoristae can be distinguished from other *Apanteles* species, such as *A. alexanderi* and *A. opuntiarum*, which also attack phycitine moths feeding on *Opuntia*. They can be separated by the faint, but distinguishable rugosity on the second metasomal tergite (present in *A. alexanderi*, absent in *A. mimoristae* and *A. opuntiarum*), and the length of the ovipositor sheaths in relation to the metasoma (shorter in

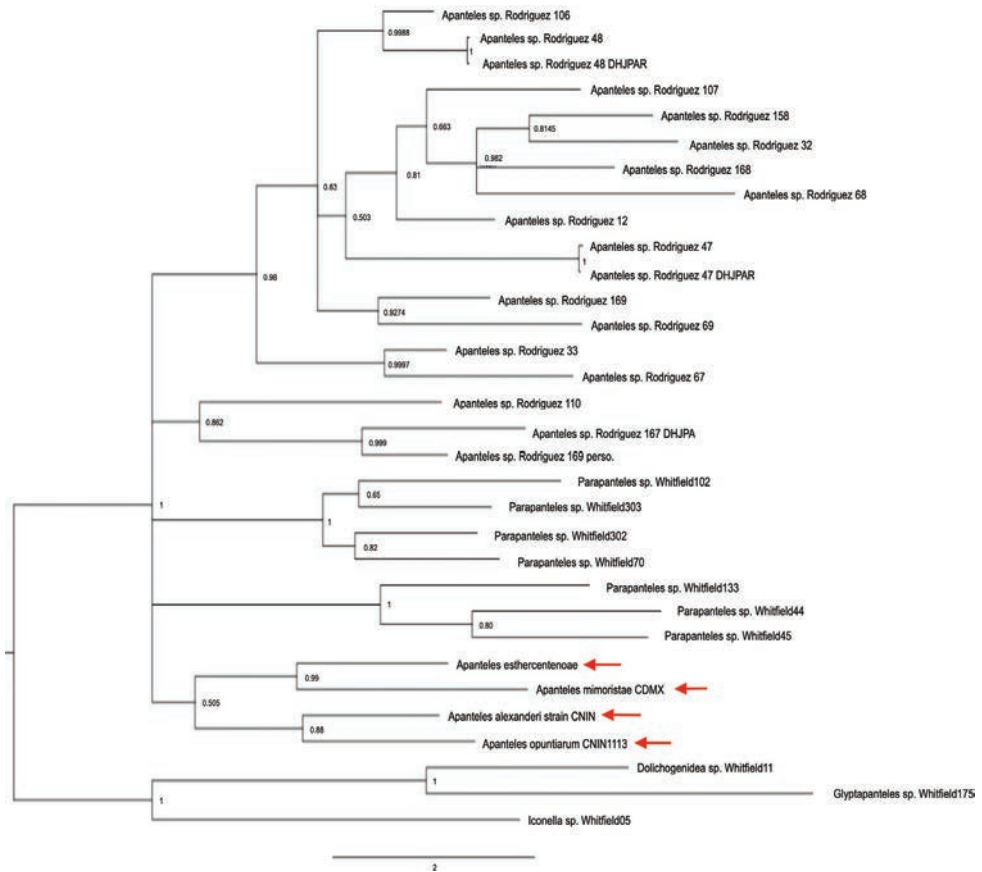


Figure 8. Maximum likelihood (1000 reps) tree for *Apanteles mimoristae* and related species. Arrows indicate *Apanteles mimoristae*, *A. esthercentenoae*, *A. alexanderi* and *A. opuntiarum*.



Figure 9. Turquoise-colored larvae of *Apanteles mimoristae* Muesebeck (Braconidae: Microgastrinae) next to a dead caterpillar of *Melitara cf. nephelepasa* (Pyrallidae) (zebra worm), inside an opened *Opuntia ficus-indica* (Cactaceae) pad. The blue-turquoise color of the wasp larvae indicates feeding on caterpillar hemolymph, which has a similar color. The arrow indicates the caterpillar's characteristic whitish stripes.



Figure 10. Adults of *Apanteles mimoristae* Muesebeck recently emerged from the irregular mass of cocoons (center). Both sexes emerged from a single caterpillar of the zebra worm, *Melitara* cf. *nephelepasa* (Pyralidae) feeding on *Opuntia ficus-indica* (Cactaceae) commercial plots from Milpa Alta, Mexico City, MX. The mass of cocoons in the center of the Petri dish shows compact, oval cocoons made up of tightly arranged silk threads.

A. opuntiarum and *A. alexanderi*, and longer in *A. mimoristae*). Also, their geographic distribution is distinctly different: *A. mimoristae* has been reported from Mexico and the United States, *A. alexanderi* from Argentina and Uruguay, and *A. opuntiarum* from Argentina (Fernández-Triana et al. 2020). Regarding related species like *A. esthercentenoae* (Costa Rica) and *A. megathymi* (Mexico and the United States), the following features present in *A. mimoristae* are diagnostic: the vertex is finely wrinkled around the ocelli but smooth between them; segment T1 has prominent and irregular roughness, and the posterior margin has two depressions of similar size, one at each corner; the second and third tergites are smooth and shiny (See key for additional features).

Molecular and phylogenetic analysis

Percent identity is a quantitative measure of the similarity between two sequences. Closely related species are expected to have a higher percentage of identity for a given sequence than distantly related species. The BLAST analysis indicated that the UT COI sequence has the highest similarity to *A. esthercentenoae* (Fernández-Triana 2014) (Genbank sequences EU396681 and EU396684) with 7.67% and 7.66% difference respectively and 99% cover. The identity percentages are quite low to be considered the same species. A threshold of around 2–3% difference is commonly considered to discriminate hymenopteran species using barcode sequences ((Martinez et al. 2012; Fernández-Triana et al. 2014; Sanchez-Peña et al. 2017). The difference in sequence identity between *A. mimoristae* and the Argentinian species *A. alexanderi* and *A. opuntiarum* is more than 12%. The interspecific variation between Argentinian species is 6.8–8.1%, whereas variation among these two species and species of the similar *A. leucostigmus* complex is 9.6–12.6% (Martinez et al. 2012).

The estimated number of undescribed *Apanteles* species parasitizing Pyraloids (Pyralidae and Crambidae) in the New World is exceedingly high (Fernández-Triana et al. 2014). There are very few DNA sequences available for *Apanteles* species currently described that attack cactus moths; thus, we consider that the sampling of *Apanteles* species related to *A. mimoristae* is very incomplete; as a result, the molecular analysis presented here is eminently alpha-taxonomical, while only preliminarily phylogenetic (Fernández-Triana et al. 2014).

Both phylogenetic trees (Figs 9, 10) show that *A. mimoristae* and *A. esthercentenoae* form a clade which is the sister group of the clade containing *A. alexanderi* and *A. opuntiarum*. This could be expected from geographical separation: the first two species live north of South America (Costa Rica, United States and Mexico), while the last two species are sympatric in temperate South America (Martínez et al. 2012; Fernández-Triana et al. 2014). The genera *Dolichogenidea*, *Glyptapanteles* and *Iconella* were placed in branches separated from *Apanteles* spp. including *Apanteles mimoristae* and related species.

Geographical distribution

The species *A. mimoristae* is clearly allopatric regarding *A. alexanderi* and *A. opuntiarum*: *A. mimoristae* inhabits warm North American deserts, while *A. alexanderi* and *A. opuntiarum* are found in similar areas of temperate South America. The type specimens of *A. mimoristae* were collected at Uvalde, Texas, US (Muesebeck 1921), where the dominant vegetation is microphyllous scrub, with cactus, oaks (*Quercus* L., Fagaceae), and mesquite (*Prosopis* L., Fabaceae). It has also been reported from Florida (Fernández-Triana et al. 2020). Here, *A. mimoristae* is confirmed in detail for the first time in central Mexico (Milpa Alta), specifically from commercial *Opuntia* farms. Original vegetation there is or was a semiarid grassy steppe and open forest of pine and oak trees. This finding expands the known distribution of the species, mak-

ing it the southernmost record to date. Regarding *A. esthercentenoae*, it has been found in Costa Rica (Área de Conservación Guanacaste, ACG) from natural vegetation in tropical seasonal dry forest. *Apanteles megathymi* has been reported from Mexico and the United States (several states) where the main vegetation is thorn scrub and cactus (Muesebeck 1921; Mann 1969; and Fernández-Triana et al. 2014).

Notes on *Melitara* spp., *A. mimoristae* and related species, and biological control of invasive cactus moth

Apanteles mimoristae is a gregarious endoparasitoid of caterpillars. The herbivore host reported here is *Melitara* cf. *nephelepasa*. It should be mentioned that the taxonomy of this *Melitara* species and related North American phycitines from *Opuntia* remained unsettled until recently. One recent online review (Simonsen and Brown 2015) synonymized *M. nephelepasa* (in part) with *Melitara subumbrella* (Dyar) and declared this and *M. junctolineella* “most similar species”. However, a substantial part of the literature traditionally refers to the central Mexico zebra worm populations as *M. nephelepasa* (Mann 1968; Arnaud 1978; Badii and Flores 2001) although the correct identity of these populations is probably not *M. nephelepasa* but perhaps *M. subumbrella* or *M. junctolineella* (Simonsen and Brown 2008; Moth Photographers Group 2023).

Muesebeck (1921) did not report whether the *A. mimoristae* specimens were solitary or gregarious. They emerged from a very similar or identical zebra worm species, *M. junctolineella* and from the *Opuntia* webworm *Loxomorpha flavidissimalis* (Grote) (Crambidae). The genus *Loxomorpha* was formerly known as *Mimorista*, hence the etymology of this wasp species, *A. mimoristae*. As for the parasitoids *A. alexanderi* and *A. opuntiarum*, each has a strong preference for the phycitines *Tucumania* and *Cactoblastis* respectively, in arid temperate South America (Martinez et al. 2012). *Apanteles esthercentenoae* has been reared from *Palpita venatalis* (Crambidae) and *Cromarcha stroudagnesia* (Pyrilidae), a stem borer. *Apanteles megathymi* mainly parasitizes borer larvae of some of the largest-sized known Hesperiiidae, the “giant skippers”: *Agathymus stephensi* (Skinner) and species of *Megathymus* like *M. coloradensis* (Fernández-Triana et al. 2014); it has also been reported from *M. nephelepasa* at San Luis Potosí state, central Mexico (Mann 1969). These five *Apanteles* species form a biologically heterogeneous assemblage of species with dissimilar environments and hosts. This suggests that many undescribed species might belong in this assemblage, and that our taxonomical sampling remains quite incomplete.

Regarding biological control of the invasive *C. cactorum*, it should be considered that *A. mimoristae* is very similar to *A. opuntiarum*, whose release in North America is being explored. Therefore, accurate identification of these wasps is essential. Future work should consider experiments exposing *C. cactorum* caterpillars to *A. mimoristae*, to determine their suitability as hosts of these wasps. The role of this and other possible new associations in biological control of *C. cactorum*, in areas where protection of susceptible species of Cactaceae is a concern should be investigated.

Author contribution statement

RVL: Conceptualization; Data curation; Formal analysis; Investigation; Methodology; Project administration; Resources; Software; Validation; Visualization; Writing – original draft. RP: Conceptualization; Funding acquisition; Investigation; Methodology; Project administration; Resources; Software; Visualization; LEG: Conceptualization; Data curation; Formal analysis; Investigation; Methodology; Project administration; Resources; Supervision; Validation; Writing – review and editing. JCR: Investigation; Methodology; Resources; Validation. GGM: Investigation; Methodology; Resources. RCC: Data curation; Investigation; Methodology; Resources; Validation. MPEL: Methodology; Resources. JFT: Investigation; Resources; Validation. SRSP: Conceptualization; Formal analysis; Funding acquisition; Investigation; Methodology; Project administration; Resources; Validation; Visualization; Writing – original draft; Writing – review & editing.

Acknowledgements

RVL and JCR are grateful to CONAHCYT for graduate scholarships. The Dirección de Investigación, Universidad Autónoma Agraria Antonio Narro (UAAAN) partially supported this research. UAAAN provided general logistic support. The support of Paloma Perry and CONTEX Award 2019-49, “Developing Biocontrol Strategies to Combat an Invasive Cactus-feeding Moth” (CONAHCYT-UT) is gratefully acknowledged.

References

- Arnaud Jr PH (1978) A host-parasite catalog of North American Tachinidae (Diptera). United States Department of Agriculture. Miscellaneous Publication 1319: 1–860.
- Badii MH, Flores AE (2001) Prickly pear cacti pests and their control in Mexico. *The Florida Entomologist* 84(4): 503–505. <https://doi.org/10.2307/3496379>
- Durocher-Granger L, Mfunne T, Musesha M, Lowry A, Reynolds K, Buddie A, Cafà G, Oford L, Chipabika G, Dicke M, Kenis M (2021) Factors influencing the occurrence of fall armyworm parasitoids in Zambia. *Journal of Pest Science* 94: 1133–1146. <https://doi.org/10.007/s10340-020-01320-9>
- Felipe-Victoriano M, Talamas EJ, Sanchez-Peña SR (2019) Scelionidae (Hymenoptera) parasitizing eggs of *Bagrada hilaris* (Hemiptera, Pentatomidae) in Mexico. *Journal of Hymenoptera Research* 73: 143–152. <https://doi.org/10.3897/jhr.73.36654>
- Fernández-Triana JL, Cardinal S, Whitfield JB, Hallwachs W, Smith MA, Janzen DH (2013) A review of the New World species of the parasitoid wasp *Iconella* (Hymenoptera, Braconidae, Microgastrinae). *ZooKeys* 321: 65–87. <https://doi.org/10.3897/zookeys.321.5160>
- Fernández-Triana JL, Whitfield JB, Rodríguez JJ, Smith MA, Janzen DH, Hallwachs WD, Hajibabaei M, Burns JM, Solis MA, Brown J, Cardinal S, Goulet H, Hebert PDN (2014)

- Review of *Apanteles* sensu stricto (Hymenoptera, Braconidae, Microgastrinae) from Area de Conservación Guanacaste, northwestern Costa Rica, with keys to all described species from Mesoamerica. *ZooKeys* 383: 1–565. <https://doi.org/10.3897/zookeys.383.6418>
- Fernández-Triana J, Shaw MR, Boudreault C, Beaudin M, Broad GR (2020) Annotated and illustrated world checklist of Microgastrinae parasitoid wasps (Hymenoptera, Braconidae). *ZooKeys* 920: 1–1089. <https://doi.org/10.3897/zookeys.920.39128>
- Figuerola JI, Correa-Méndez A, Osorio-Osorio R, Hernández-Hernández LU, De La Cruz-Lázaro E, Márquez-Quiroz C (2021) Field parasitism of the neotropical cornstalk borer, *Diatraea lineolata* (Walker), by *Apanteles diatraeae* Muesebeck. *Southwestern Entomologist* 46(1): 69–74. <https://doi.org/10.3958/0.59.046.0106>
- Habeck DH, Bennett FD (1990) *Cactoblastis cactorum* Berg (Lepidoptera: Pyralidae) a Phycitine new to Florida. Florida Department of Agriculture and Consumer Services, Division of Plant Industry (Gainesville, FL). Entomology Circular 333.
- Hight SD, Carpenter JE (2009) Flight phenology of male *Cactoblastis cactorum* (Lepidoptera: Pyralidae) at different latitudes in the southeastern United States. *The Florida Entomologist* 92(2): 208–216. <https://doi.org/10.1653/0.24.092.0203>
- Hokkanen HM, Pimentel D (1989) New associations in biological control: Theory and practice. *Canadian Entomologist* 121(10): 829–840. <https://doi.org/10.4039/Ent121829-10>
- Hoy MA, Jeyaprakash A, Morakote R, Lo PK, Nguyen R (2000) Genomic analyses of two populations of *Ageniaspis citricola* (Hymenoptera: Encyrtidae) suggest that a cryptic species may exist. *Biological Control* 17(1): 1–10. <https://doi.org/10.1006/bcon.1999.0775>
- Kumar S, Stecher G, Li M, Knyaz C, Tamura K (2018) MEGA X: Molecular evolutionary genetics analysis across computing platforms. *Molecular Biology and Evolution* 35(6): 1547–1549. <https://doi.org/10.1093/molbev/msy096>
- Lanfear R, Calcott B, Ho SY, Guindon S (2012) PartitionFinder: Combined selection of partitioning schemes and substitution models for phylogenetic analyses. *Molecular Biology and Evolution* 29(6): 1695–1701. <https://doi.org/10.1093/molbev/mss020>
- López-Monzón FJ, Plowes R, Sanchez-Peña SR (2019) First record of *Aphidius transcaspicus* Telenga (*Aphidius colemani* species group) in Mexico. *Southwestern Entomologist* 44(3): 795–798. <https://doi.org/10.3958/059.044.0327>
- Mann J (1969) Cactus feeding insects and mites. *Bulletin - United States National Museum* 256: 1–158. <https://doi.org/10.5479/si.03629236.256.1>
- Martínez JJ, Berta C, Varone L, Logarzo G, Zamudio P, Zaldívar-Riverón A, Aguilar-Velasco RG (2012) DNA barcoding and morphological identification of Argentine species of *Apanteles* (Hymenoptera: Braconidae), parasitoids of cactus-feeding moths (Lepidoptera: Pyralidae: Phycitinae), with description of a new species. *Invertebrate Systematics* 26(6): 435–444. <https://doi.org/10.1071/IS12060>
- Milne I, Lindner D, Bayer M, Husmeier D, McGuire G, Marshall DF, Wright F (2009) TOPALi v2: A rich graphical interface for evolutionary analyses of multiple alignments on HPC clusters and multi-core desktops. *Bioinformatics* 25(1): 126–127. <https://doi.org/10.1093/bioinformatics/btn575>
- Morales-Gálvez M, Villegas-Luján R, Plowes R, Gilbert L, Matson T, Gallegos-Morales G, Sanchez-Peña SR (2022) Natural egg parasitism by Scelionidae on a Phyci-

- tine cactus moth in Mexico. *The Florida Entomologist* 105(2): 174–177. <https://doi.org/10.1653/024.105.0212>
- Morrison CR, Plowes RM, Jones NT, Gilbert LE (2021) Host quality does not matter to native or invasive cactus moth larvae: Grave implications for North American prickly pears. *Ecological Entomology* 46(2): 319–333. <https://doi.org/10.1111/een.12964>
- Moth Photographers Group (2019) *Melitara subumbrella*. <https://mothphotographersgroup.msstate.edu/species.php?hodges=5973> [accessed 15 January 2024]
- Muesebeck CFW (1921) A revision of the North American species of ichneumon-flies belonging to the genus *Apanteles*. *Proceedings of the United States National Museum* 61(2436): 1–76. <https://doi.org/10.5479/si.00963801.2349.483>
- Parks K, Janzen DH, Hallwachs W, Fernández-Triana J, Dyer LA, Rodriguez JJ, Arias-Penna DC, Whitfield JB (2020) A five-gene molecular phylogeny reveals *Parapanteles* Ashmead (Hymenoptera: Braconidae) to be polyphyletic as currently composed. *Molecular Phylogenetics and Evolution* 150: 106859. <https://doi.org/10.1016/j.ympev.2020.106859>
- Ronquist FM, Teslenko M, van der Mark P, Ayres DL, Darling A, Höhna S, Larget B, Liu L, Suchard MA, Huelsenbeck JP (2012) MrBayes 3.2: Efficient Bayesian phylogenetic inference and model choice across a large model space. *Systematic Biology* 61(3): 539–542. <https://doi.org/10.1093/sysbio/sys029>
- Sanchez-Peña SR, Chacón-Cardosa MC, Canales-del-Castillo R, Ward L, Resendez-Pérez D (2017) A new species of *Trachymyrmex* (Hymenoptera, Formicidae) fungus-growing ant from the Sierra Madre Oriental of northeastern Mexico. *ZooKeys* (706): 73–94. <https://doi.org/10.3897/zookeys.706.12539>
- Simonsen TJ, Brown RL (2015) Cactus moths and their relatives (Pyralidae: Phycitinae). Mississippi Entomological Museum, Mississippi State University. <https://mississippientomologicalmuseum.org.msstate.edu/Researchtaxapages/CactusMoths/Introduction.html> [Accessed 15 January 2024]
- Starmer WT, Aberdeen V, Lachance MA (1988) The yeast community associated with decaying *Opuntia stricta* (Haworth) in Florida with regard to the moth, *Cactoblastis cactorum* (Berg). *Florida Scientist* 51: 7–11. <http://www.jstor.org/stable/24319982>
- Sterling WL (1978) Fortuitous biological suppression of the boll weevil by the red imported fire ant. *Environmental Entomology* 7(4): 564–568. <https://doi.org/10.1093/ee/7.4.564>
- Torres-Acosta RI, Humber RA, Sánchez-Peña SR (2016) *Zoophthora radicans* (Entomophthorales), a fungal pathogen of *Bagrada hilaris* and *Bactericera cockerelli* (Hemiptera: Pentatomidae and Triozidae): prevalence, pathogenicity, and interplay of environmental influence, morphology, and sequence data on fungal identification. *Journal of Invertebrate Pathology* (139): 82–91. <https://doi.org/10.1016/j.jip.2016.07.017>
- Townes H, Townes M (1960) Ichneumon-flies of America north of Mexico: 2. Subfamilies Ephialtinae, Xoridinae, and Acaenitinae. *Bulletin - United States National Museum* 216(2): 1–676. <https://doi.org/10.5479/si.03629236.216.1-2>
- Varone L, Logarzo GA, Martínez JJ, Navarro F, Carpenter JE, Hight SD (2015) Field host range of *Apanteles opuntiarum* (Hymenoptera: Braconidae) in Argentina, a potential bio-control agent of *Cactoblastis cactorum* (Lepidoptera: Pyralidae) in North America. *The Florida Entomologist* 98: 803–806. <https://doi.org/10.1653/024.098.0265>

- Vigueras AL, Portillo L (2001) Uses of *Opuntia* species and the potential impact of *Cactoblastis cactorum* (Lepidoptera: Pyralidae) in Mexico. *The Florida Entomologist* 84: 493–498. <https://doi.org/10.2307/3496377>
- Wharton RA, Marsh PM, Sharkey MJ (1997) Manual para los géneros de la familia Braconidae (Hymenoptera) del Nuevo Mundo. The International Society of Hymenopterists, Washington/DC, 447 pp.
- Whitfield JB (1997) Subfamily Microgastrinae. In: Wharton RA, Marsh PM, Sharkey MJ (Eds) *Manual of the New World genera of the family Braconidae (Hymenoptera)*. International Society of Hymenopterists, Kansas, 333–364.
- Yu DS, van Achterberg C, Horstmann K (2016) *World Ichneumonoidea. Taxonomy, biology, morphology and distribution (Braconidae)*. Taxapad: scientific names for information management. Ottawa, Ontario, Canada. <http://www.taxapad.Com>

First discovery of *Plutarchia* (Hymenoptera, Eurytomidae) in Palearctic region, with description of a new species from South Korea

Duk-Young Park¹, Seunghwan Lee^{1,2}

1 *Insect Biosystematics Laboratory, Department of Agricultural Biotechnology, Seoul National University, Seoul, 08826, Republic of Korea* **2** *Research Institute of Agricultural and Life Sciences, Seoul National University, Seoul, 08826, Republic of Korea*

Corresponding author: Seunghwan Lee (seung@snu.ac.kr)

Academic editor: Petr Janšta | Received 14 November 2023 | Accepted 5 March 2024 | Published 26 March 2024

<https://zoobank.org/22D7AF5B-7B43-4136-A6CF-1EE84016E25C>

Citation: Park D-Y, Lee S (2024) First discovery of *Plutarchia* (Hymenoptera, Eurytomidae) in Palearctic region, with description of a new species from South Korea. *Journal of Hymenoptera Research* 97: 229–239. <https://doi.org/10.3897/jhr.97.115524>

Abstract

The genus *Plutarchia* is discovered in the Palearctic region for the first time. In this study, we report a newly described and newly recorded species from South Korea: *P. fuscipennata* **sp. nov.**, and *P. malabarica* Narendran & Padmasenan, 1990, respectively. The host association of *Plutarchia malabarica* reared from leaf-miner flies (Diptera: Agromyzidae) attacking the seeds of *Pueraria lobata* (Willd.) Ohwi (Fabaceae) has been unknown until now. A key to the South Korean species and descriptions of the new species are also provided.

Keywords

Agromyzidae, East Asia, Fabaceae, new species, parasitoid

Introduction

The genus *Plutarchia* is a relatively small group within the family Eurytomidae and comprises 13 known species (Noyes 2019). Girault (1925) described this genus based on *P. bicarinativentris* from Australia. Subsequent species were recorded in the Palaeotropical region, with one in the Afrotropical region and the others in the Oriental region. However, this is not known in the Palearctic region.

This genus concept has undergone several morphological revisions, with new species added by Subba Rao (1974), Bouček (1988), Narendran (1994), and Lotfalizadeh et al. (2007). According to Lotfalizadeh et al. (2007), it has been placed within the genus *Philolema* clade based on morphological characters. However, owing to their unique characteristics, such as the projection of the mesopleuron, a procoxa with a large depression, and the fusion of 1st and 2nd gastral tergites with large basal pits, they have maintained an independent generic name.

The host of *Plutarchia* is not well known, but Bouček (1988) suggested that this genus is a parasitoid of dipterous puparia, particularly Agromyzidae. He pointed out that *P. indefensa* (Walker) was reared from *Melanagromyza* sp. (Diptera: Agromyzidae) in India, *P. bicarinativentris* was found in the pods of *Glycine clandestina* (Fabaceae) in Australia, and undescribed species were reared from *Ophiomyia phaseoli* (Diptera: Agromyzidae) in Papua New Guinea.

In this study, we report the genus *Plutarchia* in the Palearctic region for the first time by the new species and new record from South Korea.

Materials and methods

Adult specimens of *Plutarchia fuscipennata*, sp. nov., were collected using sweeping nets, and *P. malabarica* were reared from the puparia of Agromyzidae in the pods of *Pueraria lobata* (Willd.) Ohwi (Fabaceae). Most of the specimens were deposited at the Laboratory of Insect Biosystematics, Seoul National University, and one specimen of each species was deposited at the National Institute of Biological Resources. The abbreviations for the depositories of the specimens used in this study are as follows:

NIBR National Institution of Biological Resources;
SNU Laboratory of Insect Biosystematics, Seoul National University;
ZSIC Zoological Survey of India, Calcutta, India.

Specimens were examined with an Olympus SZ61 stereomicroscope and photographed with a DMC 5400 digital camera attached to a Leica Z16 APO motorized microscope. Serial images were combined using Zerene Stacker and digitally retouched using Adobe Photoshop CS6. Most morphological terms follow Lotfalizadeh et al. (2007) and Delvare et al. (2019).

Morphological abbreviations used in this paper as follows: **F1–FX**, funiculars 1–X; **MPS**, multiporous plate sensilla(e); **POL**, the distance between posterior ocelli; **LOL**, distance between anterior and posterior ocellus; **OOL**, minimal distance between posterior ocellus and inner orbit; **OD**, maximum diameter of posterior ocellus; **cc**, costal cell; **mv**, marginal vein; **pmv**, postmarginal vein; **stv**, stigmal vein; **GT1–GTX**, gastral tergites 1 to X.

Taxonomy

***Plutarchia* Girault, 1925**

Plutarchia Girault, 1925: 3. Type species: *Plutarchia bicarinativentris* Girault, 1925.

Key to South Korean species of *Plutarchia* Girault

- 1 Female **2**
- Male **3**
- 2 Head (Fig. 1D) with OOL more than 1.5× OD. Antenna with F2–5 slightly longer than wide and F6 almost square (Fig. 1B). Propodeum (Fig. 1E) areolate-rugose to reticulate medially with shallow medial depression. Fore wing (Fig. 1G) dark infusate basal half; vein dark brown..... ***P. fuscipennata* sp. nov.**
- Head (Fig. 3D) with OOL less than 1.5× OD. Antenna with F2–F5 distinctly longer than wide and F6 slightly longer than wide. Propodeum (Fig. 3G) areolate without medial depression. Fore wing (Fig. 3H) hyaline; vein pale brown ***P. malabarica* Narendran & Padmasenan**
- 3 Head (Fig. 2C) with POL less than 3.5× as long as OD. Antenna (Fig. 2B) stout having funicle with short petiole; clava at most 3.0× as long as wide. Propodeum (Fig. 2D) simply carinate to areolate-rugose with interspace somewhat reticulate. Petiole (Fig. 2D) almost smooth with inconspicuous sculpture; 3.2–3.4× as long as wide. Fore wing dark infusate basal half; vein dark brown ***P. fuscipennata* sp. nov.**
- Head (Fig. 4C) with POL more than 3.5× as long as OD. Antenna (Fig. 4B) slender having funicle with distinctly long petiole; clava at least 4.0× as long as wide. Propodeum (Fig. 4D) mixed with areolate-rugose and carinate-punctate. Petiole (Fig. 4D) reticulate-imbricate; 3.09–3.11× as long as wide. Fore wing hyaline; vein pale brown ***P. malabarica* Narendran & Padmasenan**

***Plutarchia fuscipennata* sp. nov.**

<https://zoobank.org/7F772ABA-90DA-44EB-AAB7-ED2C4E323832>

Figs 1A–H, 2A–D

Etymology. The species is named after the Latin *fusci* (dark) and *pennata* (wing), from the basally infusate wing of the new species.

Type material. *Holotype* SOUTH KOREA: ♀, San 1-6, Sujeom-dong, Gumi-si, Gyeongsangbuk-do, 36°07'40.6"N, 128°18'05.1"E, 23.vi.2015, Duk-Young Park (deposited in SNU). *Paratypes* SOUTH KOREA: 2♂, Irwolsan-gil, Galsan-ri, Jaesan-myeon, Bonghwa-gun, Gyeongsangbuk-do, 36°49'21.7"N, 129°05'05.3"E, 14.vii.2015, Duk-Young Park (each 1♂ in SNU and NIBR).

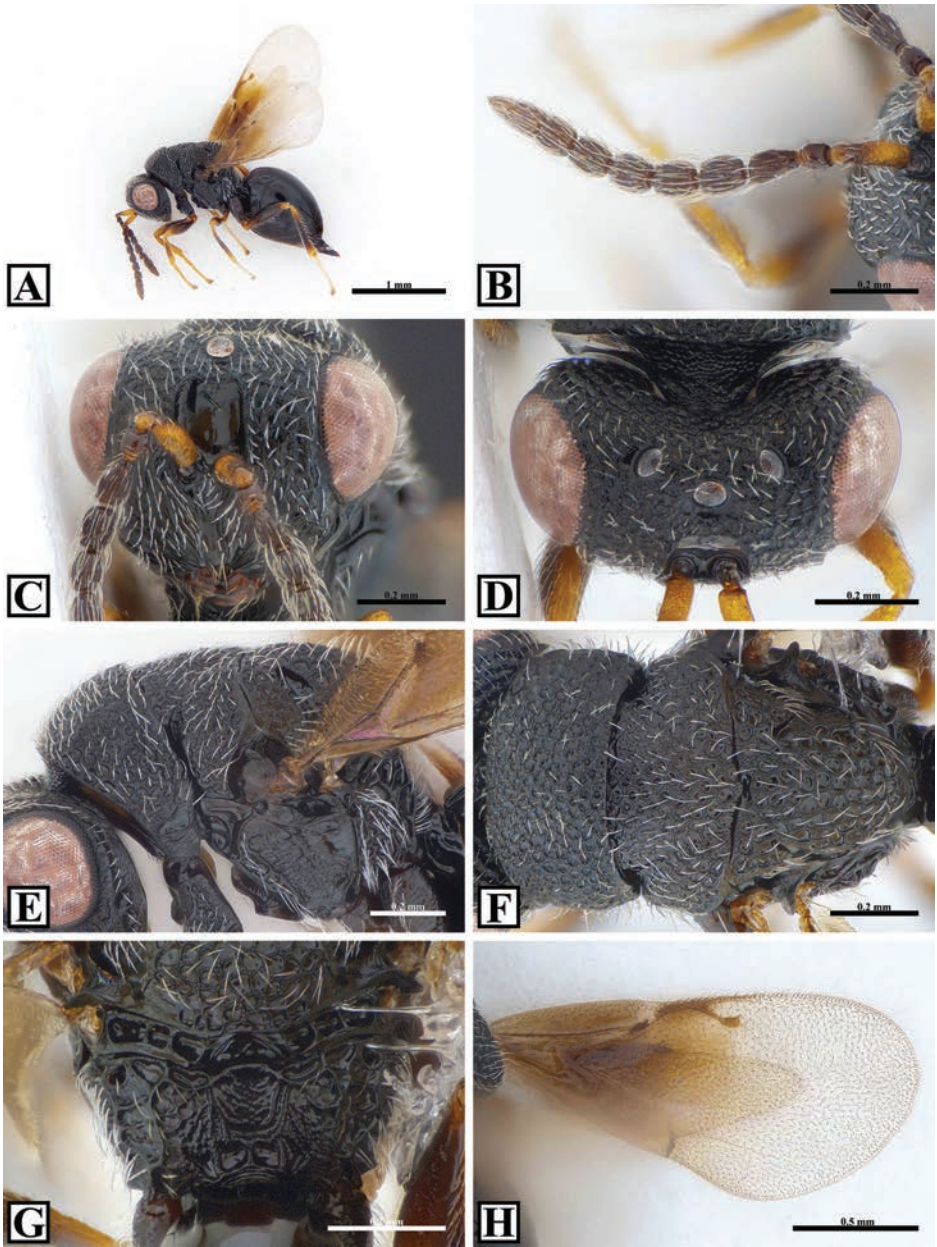


Figure 1. *Plutarchia fuscipennata*, holotype female **A** habitus, lateral view **B** antenna, dorsal view **C** head, frontal view **D** head, dorsal view **E** mesosoma, lateral view **F** mesosoma, dorsal view **G** propodeum, dorsal view **H** forewing.

Diagnosis. *Plutarchia fuscipennata* is easily distinguished from others by dark infuscate anterior half of the fore wing.

Description. Holotype female (habitus: Fig. 1A). Body length 2.49 mm, including ovipositor sheath. Body black except as follows: radicle and scape brownish-yellow with

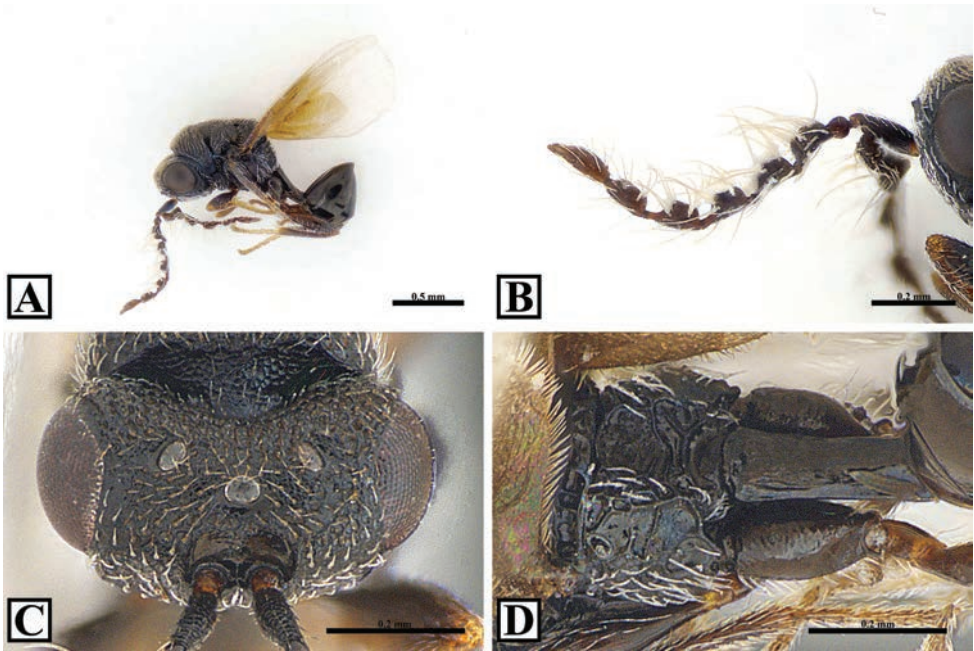


Figure 2. *Plutarchia fuscipennata*, paratype male **A** habitus, lateral view **B** antenna, lateral view **C** head, dorsal view **D** propodeum and petiole, dorsal view.

dark spot on dorsoapical region, funicle and clava dark brown except tip of clava slightly brightened; trochanter, basal and apical region of femora and tibiae, protarsus brownish-yellow, meso- and metatarsus whitish-yellow; fore wing with dark infuscate on basal half; vein and setae dark brown; ovipositor sheath dark with extreme apex reddish-brown.

Head (Fig. 1C–D) $1.3\times$ as wide as high in frontal view, $1.7\times$ as wide as long in dorsal view. Vertex areolate-reticulate to occiput regularly areolate; frons similar with vertex in sculpture, but lower face carinate gathered to lower margin; with lanceolate white setae. OOL: POL: LOL: OD = 1.6: 3.1: 1.4: 1.0. Preorbital carina weakly presented. Scrobal depression smooth with distinct carina laterally; scrobe not reaching to anterior ocellus. Malar space $0.47\times$ as long as height of eye; malar sulcus deep and oviform connected with malar depression. Gena with two deep puncture groove lines, lower punctures larger than the ones above; lateral outline of gena almost straight in frontal view; genal carina present.

Antenna (Fig. 1B) with scape minutely swollen anteromedially; $3.4\times$ as long as wide. Pedicel square. Anellus thin and smoothly connected with pedicel. Flagellum with six funiculars; F1 $1.7\times$ as long as wide; F2–F5 slightly longer than wide and F6 square; each funicular with single row of MPS; all setae subdecumbent. Clava with two visible clavomeres; $1.8\times$ as long as wide.

Mesosoma (Fig. 1E–G) $1.6\times$ as long as wide and $1.4\times$ as long as high; pronotum $2.2\times$ and mesoscutum $2.0\times$ as wide as long respectively; mesoscutellum $1.3\times$ as long as wide. Dorsal surface of mesosoma punctate with interspace reticulate, except medial region of pronotum with smaller punctures and mesoscutellum with larger

punctures. Notauli shallow. Anterior half of axilla fused with mesoscutellum, but distinguished by deep axillar groove posteriorly. Prepectus smooth with deep groove transversely. Tegula shallowly imbricate except smooth medially. Epicnemium well developed and double-hump shaped; adscrobal region areolate with interspace fine reticulate; femoral depression and mesepimeron variously carinate-areolate, but medial region of mesepimeron smooth. Metepimeron areolate with bearing long and lanceolate setae. Propodeum in approximately 95° angle to the plane of mesoscutellum; with median depression forming a single large square delimited by double carina, and two smaller squares attached at the bottom; fine reticulate submedially to areolate-rugose laterally. **Legs.** Procoxa with distinct S-shaped carina on anterior surface; with sparsely foveate-reticulate anteriorly to reticulate posteriorly. Mesocoxa somewhat smooth. Metacoxa shallowly imbricate; comparatively narrow and long, 2.1× as long as width; with two rows of setae. **Fore wing** (Fig. 1H). 2.33× as long as wide; cc: mv: pmv: stv = 3.1: 1.4: 1.2: 1.0; with basal half dark infuscate and vein dark brown; with dense dark setation on membrane.

Metasoma. Petiole wider than long in dorsal view. Gaster slightly longer than head+mesosoma; 1.6× as long as high. GT4 the longest; with inconspicuous sculpture on ventral half area. Syntergum slightly upturned.

Male (habitus Fig. 2A). Body length 1.39–1.43 mm. Morphologically similar to female except as following. Antenna (Fig. 2B) with scape dark to pedicel and flagellum dark brown; five funiculars and two clavomeres; funicle with short petiole; clava at most 3.0× as long as wide. Head (Fig. 2C) 1.68–1.70× as wide as long in dorsal view; OOL: POL: LOL: OD = 1.5–1.6: 3.2–3.4: 1.4–1.5: 1.0. Propodeum (Fig. 2D) simply carinate to areolate-rugose with interspace somewhat reticulate. Petiole (Fig. 2D) almost smooth with inconspicuous sculpture; 3.2–3.4× as long as wide.

Distribution. South Korea.

Biology. Unknown.

Remarks. Only one female and two males were collected using sweeping nets. The biology of this species has not been confirmed, but it would be similar to that of other species associated with Agromyzidae that attack Fabaceae.

Plutarchia malabarica Narendran & Padmasenan, 1990

Figs 3A–H, 4A–H

Plutarchia malabarica Narendran & Padmasenan, 1990: 115. Holotype ♀. Type locality: India (Kerala). Type depository: ZSIC, examined.

Material examined. SOUTH KOREA: 1♀1♂, Bunori Fortification, Hwado-myeon, Ganghwa-gun, Incheon, 37°35'28.1"N, 126°27'43.3"E, 20.ii.2021, Duk-Young Park, emerged from pupae of Agromyzidae sp. at 01.vi.2022 (1♀ in SNU and 1♂ in NIBR); 1♂, Ganghwa Island, San 185-3, Sagi-ri, Hwado-myeon, Ganghwa-gun, Incheon, 37°35'28.1"N, 126°27'43.3"E, 15.iii.2018, Jongwoo Kim (in SNU); 1♂, Dok moun-

tain fortress, Jigot-dong, Osan-si, Gyeonggi-do, 37°11'10.0"N, 127°01'17.9"E, 13.ix.2021, Duk-Young Park, emerged at 24.iv.2022 (in SNU).

Redescription. Female (habitus: Fig. 3A). Body length 2.08 mm, including ovipositor sheath. Body black except as follows: tip of scape, anterior half of pedicel, anellus and anterior half of clava dark brown; protibia, trochanters and trochantellus brownish-yellow; basal and apical tip of meso- and metatibia, and protarsus brown; meso- and metatarsus whitish-yellow; fore wing hyaline with vein pale brown; ovipositor sheath dark with apex yellowish-brown.

Head (Fig. 3C, D) 1.3× as wide as high in frontal view, 1.6× as wide as long in dorsal view. Vertex to occiput regularly areolate; frons areolate to lower face carinate gathered to lower margin; with linear to oblong white setae. OOL: POL: LOL: OD = 1.3: 3.4: 1.6: 1.0. Preorbital carina inconspicuous. Scrobal depression smooth with inconspicuous carina laterally; scrobe not reaching to anterior ocellus. Malar space 0.44× as long as height of eye in lateral view; malar sulcus indistinct; malar depression absent. Gena with two deep and narrow puncture groove lines; lateral outline of gena distinctly convex in frontal view; genal carina present.

Antenna (Fig. 3B). Scape minutely swollen anteromedially; 3.3× as long as wide. Pedicel 1.4× as long as wide. Anellus transverse. Six funiculars, but F6 almost combined with clava; F1 1.6× as long as wide; F2–F5 distinctly but F6 slightly longer than wide; each funicular with single row of MPS; all setae subdecumbent. Clava with two vague clavomeres; twice as long as wide.

Mesosoma (Fig. 3E–G) 1.5× as long as wide and 1.2× as long as high; pronotum, and mesoscutum 2.8× and 2.0× as wide as long respectively; mesoscutellum 1.4× as long as wide. Dorsal surface of mesosoma densely punctate except mesoscutellum with slightly larger punctures than mesoscutum. Notauli distinct and narrow. Anterior half of axilla fused with mesoscutellum, but distinguished by shallow and broad axillar groove posteriorly. Prepectus smooth with deep groove on ventral submarginal area. Tegula smooth medially to imbricate posteriorly. Epicnemium developed and one-hump shaped; adscrobal region areolate with interspace shallowly rough; femoral depression variously carinate-areolate and mesepimeron substrigulate. Metepimeron areolate-rugose with bearing long and linear erect white setae. Propodeum approximately 90° angle to the plane of mesoscutellum; with broad median area delimited by carina; callus areolate anteriorly to reticulate-rugose posteriorly. **Legs.** Procoxa with ambiguous S-shaped carina on anterior surface; with surface imbricate. Mesocoxa shallowly imbricate. Metacoxa imbricate; comparatively broad, 1.6× as long as width; with three rows of setae. **Fore wing** (Fig. 3H). 2.15× as long as wide; cc: mv: pmv: stv = 5.3: 1.3: 1.4: 1.0; with entirely hyaline and vein pale brown; with sparse dark setation on membrane.

Metasoma. Petiole wider than long in dorsal view. Gaster 1.5× as long as height; 1.1× as long as head+mesosoma. GT4 with entirely reticulate-imbricate except anterodorsally one-fourth area smooth. Syntergum not upturned.

Male (habitus Fig. 4A). Body length 1.57–1.76 mm. Morphologically similar to female except as following: antenna (Fig. 4B) with five funiculars and two clavomeres; funicle with distinctly long petiole; clava at least 4.0× as long as wide.

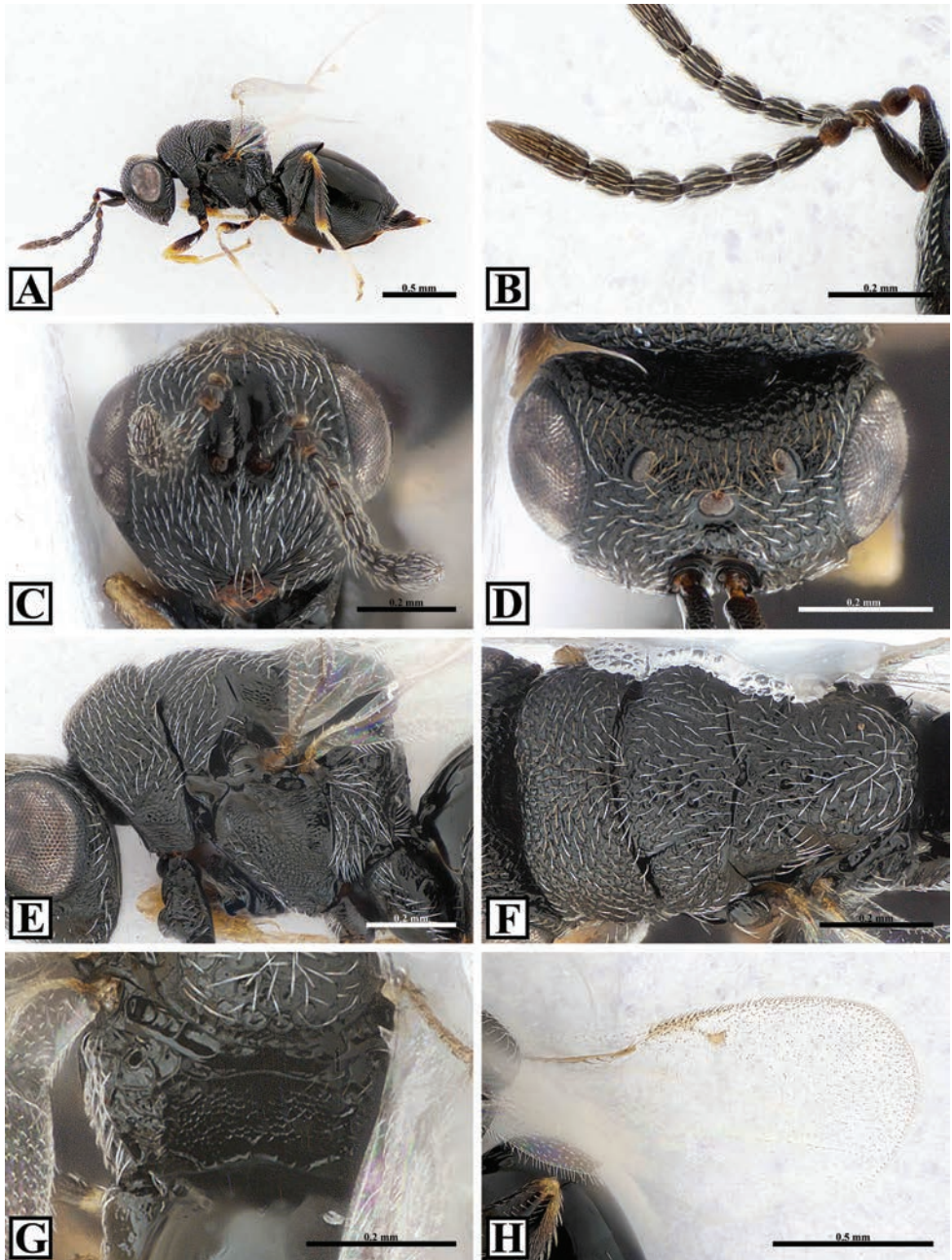


Figure 3. *Plutarchia malabarica*, female **A** habitus, lateral view **B** antenna, lateral view **C** head, frontal view **D** head, dorsal view **E** mesosoma, lateral view **F** mesosoma, dorsal view **G** propodeum, dorsal view **H** wing.

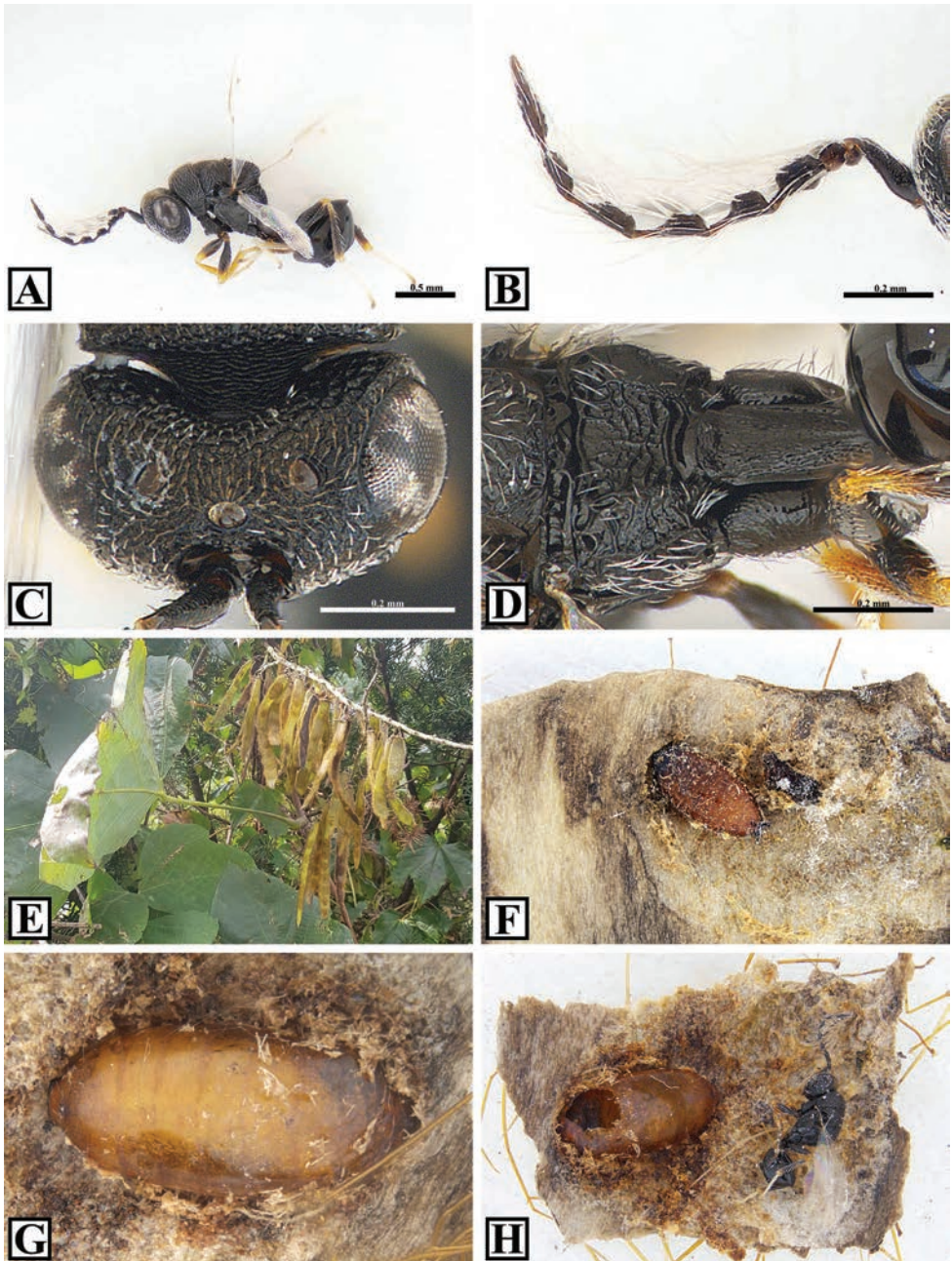


Figure 4. A–D *Plutarchia malabarica*, male **A** habitus, lateral view **B** antenna, lateral view **C** head, dorsal view **D** propodeum and petiole, dorsal view **E** leaves and pods of *Pueraria lobata* **F** pupa of Agromyzidae in pod of *Pu. lobata* **G** larva of *P. malabarica* in pupa of Agromyzidae **H** male habitus emerged from pupa of Agromyzidae.

Head (Fig. 4C) 1.77–1.80× as wide as length in dorsal view; OOL: POL: LOL: OD = 1.2–1.3: 3.7–3.8: 1.5–1.7: 1.0. Propodeum (Fig. 4D) mixed with areolate-rugose and carinate-punctate. Petiole (Fig. 4D) reticulate-imbricate; 3.09–3.11× as long as wide.

Variation. The length of the redescribed specimen (2.08 mm) in this study is slightly longer than that of the types (1.39–1.93 mm). Additionally, the POL/OOL ratio (2.62) is shorter compared to that of the holotype (3.22).

Distribution. South Korea (new record), India (Kerala).

Biology. We observed this species emerging from the cocoons of an unknown leaf-miner species (Diptera: Agromyzidae), which attacked the seeds of *Pueraria lobata* (Fabaceae). Seeds were collected during winter and subsequently stored under laboratory conditions. Owing to the controlled environment, adults of *P. malabarica* emerged earlier than expected from the pupae of Agromyzidae. However, their emergence is associated with oviposition by Agromyzidae on the seeds of *Pu. lobata*, which occurred from September to October, when *Pu. lobata* seed ripening process. The host record for *P. malabarica* is the first discovery of a host association for this species.

Discussion

Up to recently, *Plutarchia* was known to be distributed throughout the tropical (Oriental: Cambodia, India, Sri Lanka, Southern China; Australasian: Northern Australia; Afrotropical: Nigeria) to subtropical (Oriental: Nepal) zones of the Old World. Although this genus is mainly distributed in the Oriental region, its type species, *P. bicarinativentris*, was first discovered in Australia by Girault (1925). Another species, *P. giraulti*, was further identified in the Afrotropical region by Subba Rao (1974). However, the recent discovery of *P. fuscipennata* sp. nov., and *P. malabarica* in South Korea suggests that this genus may occupy a broader range across the Old World, including the temperate zone of the Palearctic region.

The biology of most *Plutarchia* species remains unknown; however, information exists for a few species. For example, *P. bicarinativentris* was reared from the pods of *Glycine clandestina* J. C. Wendl. (Fabaceae) in Australia (Bouček 1988) and is associated with *Ophiomyia* sp. (Agromyzidae) on *Tephrosia purpurea* (L.) Pers. (Fabaceae) in Cambodia (Lotfalizadeh et al. 2007). Additionally, *P. indefensa* was associated with *Melanagromyza* sp. (Agromyzidae), and *P. giraulti* was reared from an unidentified dipterous pupa on *Vigna unguiculata* (L.) Walp. (Fabaceae) (Subba Rao 1974). In this study, *P. malabarica* was reared from the pupae of Agromyzidae that attacked the seeds of *Pueraria lobata* (Fabaceae). Given the circumstances, *Plutarchia* may be a main parasitoid of Agromyzidae species associated with Fabaceae, as proposed by Bouček (1988).

Acknowledgements

We are grateful to reviewer, Dr. Hossein Lotfalizadeh, and subject editor, Dr. Petr Janšta, who helped improve the quality of this paper. This work was supported by a grant from the National Institute of Biological Resources (NIBR), funded by the Ministry of Environment (MOE) of the Republic of Korea (NIBR202203201 and NIBR202231206), by the Basic Science Research Program through the National Research Foundation of Korea (NRF), funded by the Ministry of Education (NRF2020R111A2069484), and by the Institute for Peace and Unification Studies (IPUS) at Seoul National University under the project of “Laying the Groundwork for Unification”.

References

- Bouček Z (1988) Australasian Chalcidoidea (Hymenoptera). A biosystematic revision of genera of fourteen families, with a reclassification of species. CAB International, Wallingford, Oxon, U.K., Cambrian News Ltd; Aberystwyth, Wales, 832 pp.
- Delvare G, Escola AR, Stojanova AM, Benoit L, Lecomte J, Askew RR (2019) Exploring insect biodiversity: the parasitic Hymenoptera, chiefly Chalcidoidea, associated with seeds of asphodels (Xanthorrhoeaceae), with the description of nine new species belonging to Eurytomidae and Torymidae. *Zootaxa* 4597(1): 1–90. <https://doi.org/10.11646/zootaxa.4597.1.1>
- Girault AA (1925) Indications (in new insects) of ruling power and law in nature: 3 pp private publication, Brisbane.
- Lotfalizadeh H, Delvare G, Rasplus J-Y (2007) Phylogenetic analysis of Eurytominae (Chalcidoidea: Eurytomidae) based on morphological characters. *Zoological Journal of the Linnean Society* 151: 441–510. <https://doi.org/10.1111/j.1096-3642.2007.00308.x>
- Narendran TC (1994) Torymidae and Eurytomidae of Indian subcontinent (Hymenoptera: Chalcidoidea). Zoological Monograph, Department of Zoology, University of Calicut, Kerala, India, 500 pp.
- Narendran TC, Padmasenan R (1990) A study on the Indian species of *Plutarchia* Girault (Hymenoptera: Eurytomidae). *Journal of the Bombay Natural History Society* 87: 114–122.
- Noyes JS (2019) Universal Chalcidoidea Database. World Wide Web electronic publication. <http://www.nhm.ac.uk/chalcidoids>
- Subba Rao BR (1974) Redescriptions of *Plutarchia* Girault and *Axanthosoma* Girault with the description of a new species *Plutarchia* from Nigeria (Eurytomidae: Hymenoptera). *Journal of Entomology (B)* 42(2): 199–206. <https://doi.org/10.1111/j.1365-3113.1974.tb00075.x>

A new species of the presocial potter wasp genus *Calligaster* de Saussure, 1852 (Hymenoptera, Vespidae, Eumeninae) from Vietnam

Cuong Quang Nguyen^{1,2}, Hoa Thi Dang^{1,2}, Lien Thi Phuong Nguyen^{1,2}

1 Institute of Ecology and Biological Resources, Vietnam Academy of Science and Technology, 18 Hoang Quoc Viet Road, Nghia Do, Cau Giay, Hanoi, Vietnam **2** Graduate University of Science and Technology, Vietnam Academy of Science and Technology, 18 Hoang Quoc Viet Road, Nghia Do, Cau Giay, Hanoi, Vietnam

Corresponding author: Lien Thi Phuong Nguyen (phuonglientit@gmail.com)

Academic editor: Michael Ohl | Received 23 January 2024 | Accepted 5 March 2024 | Published 28 March 2024

<https://zoobank.org/AF0919BC-B9E1-4713-8656-2B657BCBE17D>

Citation: Nguyen CQ, Dang HT, Nguyen LTP (2024) A new species of the presocial potter wasp genus *Calligaster* de Saussure, 1852 (Hymenoptera, Vespidae, Eumeninae) from Vietnam. Journal of Hymenoptera Research 97: 241–254. <https://doi.org/10.3897/jhr.97.119354>

Abstract

Taxonomic notes are presented on the genus *Calligaster* de Saussure (Vespidae: Eumeninae) from Vietnam. A new species, *Calligaster inflata* **sp. nov.** is described and figured together with its nest. The male genitalia are redescribed for *C. himalayensis*. A key is provided to all known species of the group in the Oriental Region.

Keywords

Calligaster, Eumeninae, key, new species, Oriental, Vietnam

Introduction

Potter wasps in the genus *Calligaster* have been considered to be one of several subsocial or presocial lineages as species fully progressive provision their brood (Cowan 1991). Their nests are made of many small pieces of leaves, as in the genus *Zethus* Fabricius, and they nest together with sisters (Nugroho et al. 2016). *Calligaster* is a small genus, with only six species distributed in the Oriental Region. Two of these species, *C. cyanoptera* de Saussure, 1855 and *C. viridipennis* Giordani Soika, 1960, are found in Indonesia; two others, *C. ilocana* Selis, 2022 and *C. williamsi* Bequaert, 1940, are from the

Philippines; while *C. etchellsii* (Cameron, 1909) is endemic to Malaysia and *C. himalayensis* (Cameron, 1904) is widely distributed from India through China to Laos and Vietnam. The last species has hitherto been the only species recorded in Vietnam.

In the present work, based on specimens deposited in the Institute of Ecology and Biological Resources, Hanoi, Vietnam (IEBR), one species of the genus *Calligaster* is described as new to science, together with its nest. In addition, the male genitalia of *C. himalayensis* are redescribed in added detail, and a key is provided to all known species in the genus.

Materials and methods

The material examined in the present study is deposited in the collections of the Institute of Ecology and Biological Resources (IEBR), Hanoi, Vietnam. Adult morphological and color characters were observed on pinned specimens with the aid of a stereomicroscope. The male terminal sterna and genitalia were dissected out, cleared in KOH, and mounted in hand-washing gel for observation and photography with a stereomicroscope. Terminology follows Bohart and Stange (1965) and Carpenter and Cumming (1985), while measurements follow Nguyen (2020); terminology for male genitalia follows that of Kojima (1999) and Nguyen et al. (2023). Measurements of body parts were made with an ocular micrometer attached to a stereomicroscope, with accuracy to 0.1 mm. Nest characters were examined after the nest had been air-dried, and the terminology of Williams (1919) was used for nest characters. Photographic images of the wasps were obtained using a Nikon SMZ 800N Digital StereoMicroscope with ILCE-5000L/WAP2 digital camera attached, using Helicon Focus 7 software for stacking; the plates were edited with Adobe Photoshop CS6.

Systematics

Genus *Calligaster* de Saussure

Calligaster de Saussure, 1852: 22. Type species: *Calligaster cyanoptera* de Saussure, 1852, by subsequent designation of Ashmead (1902: 205).

Note. A complete diagnosis of the genus has been recently provided by Nugroho et al. (2016) and is therefore not repeated here.

Calligaster inflata CQ Nguyen, Dang & Nguyen, sp. nov.

<https://zoobank.org/2B61AAEB-9084-4DCE-B009-336788716F9D>

Figs 1–10

Holotype (deposited in IEBR). VIETNAM: ♀; Vinh Phuc province, Ngoc Thanh, Me Linh; 21°23'N, 105°42'E, 50 m a.s.l.; 18 April 2013; Nest-13-ML-Eu-03; D. T. Hoa leg.

Diagnosis. This species can be distinguished from congeners by the following combination of characters: Head in frontal view with inner compound eye margins 1.1 times further apart from each other at clypeus than at vertex. Clypeus in frontal view wider than high, about 1.3 times as wide as high, apical margin produced and round medially. Propodeum deeply excavated medially, with the excavation nearly two-fifths of propodeal width and its margins marked laterally by ridges, dorsal surface largely smooth, with some sparse strong punctures near concavity, posterior and lateral surfaces bordered by blunt edge. First metasomal tergum with a median longitudinal carina and next to this on each side consisting of a few rows of quite elongate punctures, this part occupying one-third the width of the tergum, the other area on tergum with strong and sparse punctures, interspaces between punctures smooth and usually larger than their diameter; tergum II with small and sparse punctures, interspaces between punctures much larger than puncture diameter, about 3 to 4 times larger than their diameter.

Description. Holotype. Female (Fig. 9). Body length (head + mesosoma + first two metasomal segments) 20 mm; forewing length 17 mm.

Body black except two faint yellow spots on frons just above antennal toruli, dark ferruginous marks near apical margin and at base of mandible, and dark brown propodeal valvula. Wings subhyaline, veins brown.

Body covered with dense, suberect, golden setae on head, mesosoma, and metasomal segment I, and black setae on metasomal segments II–VI; setae longer on metanotum and dorsal surface of propodeum than on other body parts. Clypeus with coarse punctures, punctures in middle tend to unite and form large longitudinal punctures, with interspace strongly raised to form reticulations; frons with dense, deep, flat-bottom punctures, interspaces between punctures narrower than their diameters and raised to form reticulation; vertex less densely punctate, interspaces between punctures usually narrower than their diameter and not raised to form reticulations; punctures on gena dense, strong, well-defined, gena with a smooth band along occipital carina running from near base to near vertex. Pronotum, mesoscutum, and metapleuron with dense coarse punctures, punctures larger than punctures on frons; mesoscutum with some smooth areas between punctures medially, with deep parapsidal furrows running from apical margin to mid length, and two short and shallow longitudinal furrows laterally; punctures on mesoscutellum similar to those near apical margin of mesoscutum; metanotum with a shallow furrow medially, punctures smaller than those on mesoscutum; margins of concavity of propodeum marked laterally by ridges, propodeum with deep longitudinal fovea medially running from base to mid length of propodeum, with a short longitudinal carina running from fovea to apical margin, rugosely striated area occurring along two sides of fovea and carina; dorsal surface of propodeum largely smooth, with some sparse strong punctures near concavity; lateral surface of propodeum with strong, dense, well-defined punctures, interspaces between punctures smooth but raised to from carina apically; apical margin above valvulae round. First metasomal tergum with a median longitudinal carina bordered on each side by a few rows of quite elongate punctures, this part occupying one-third width of tergum, other area on tergum with strong sparse punctures, interspaces between punctures smooth and

usually larger than their diameter; tergum II with small sparse punctures, interspaces between punctures much larger than puncture diameter, about 3 to 4 times larger than their diameter; punctures on terga III–V larger and denser than punctures on tergum II; punctures on tergum VI sparse but larger than punctures on tergum II; punctures on sternum II larger and denser than on tergum II; punctures on sterna III–V larger and denser than on sternum II.

Head: In frontal view 1.1 times as wide as high (Fig. 1), in dorsal view 1.7 times as wide as long. Vertex well developed, strongly produced behind compound eye, without cephalic fovea (Fig. 2). Distance from posterior ocelli to apical margin of vertex about 2.3 times distance from posterior ocelli to inner compound eye margin (Fig. 2). Occipital carina incomplete, evanescent dorsally, weakly widened laterally, slightly produced at one-third length from base (Fig. 5). Inner compound eye margins in frontal view 1.1 times further apart from each other at clypeus than at vertex (Fig. 1). Clypeus in frontal view wider than high, about 1.3 times as wide as high, apical margin produced and round medially (Fig. 1); in lateral view disc of clypeus gradually and weakly convex from base to near apical margin, then depressed to apical margin. Mandible with four prominent teeth. Antennal scape about 4.7 times as long as its maximum width; flagellomere I about 1.5 times as long as its maximum width, flagellomere II as wide as long, flagellomeres III–IX wider than long, terminal flagellomere bullet-shaped, about 1.2 times as long as its basal width.

Mesosoma: About 1.1 times as wide as head and 1.1 times longer than wide in dorsal view. Pronotal carina complete, raised into low lamella, angulate at lateral corner before attaining dorsal part, reaching ventral corner of pronotum. Mesoscutum slightly convex, shorter than wide, 0.9 times as long as wide between tegulae (Fig. 3). Disc of mesoscutellum rectangular, nearly flat, with lateral margin truncate. Disc of metanotum weakly produced posteromedially. In lateral view, mesoscutellum at same level as mesoscutum (Fig. 5). Propodeum deeply excavated medially (Fig. 4), with excavation nearly two-fifths of propodeal width and its margins marked laterally by ridges, posterior and lateral surfaces bordered by blunt edge.

Metasoma: Metasomal tergum I in dorsal view strongly widened after short, basal, parallel-sided part to one-third basally, then gradually narrowly to apical margin (Fig. 6), 1.4 times as long as wide, in lateral view strongly convex from base to apical margin. Metasomal segment II petiolate at base (Figs 7, 8), tergum II in dorsal view wider than long, 1.05 times as wide as long (Fig. 8), and shorter than tergum I; sternum II in lateral view straight from base to about one-half length, then straight to apical margin (Fig. 7), and slightly produced medially. Terga I–VI not raised and without lamellae (Figs 7, 8).

Nest. (Fig. 10). One nest of this species was collected at Me Linh Station for Biodiversity of the Institute of Ecology and Biological Resources (IEBR), Vinh Phuc Province on 23 March 2013. The nest consists of four cells, each bent at the neck and enlarged at the bottom. The inner diameter of the open end of cells varied from 5 to 6 mm. The oldest cell was strongly secured to a twig of a tree, and from its underside the second cell and then those following depend. The length of cells measured 35 to 36 mm. There was a well-defined roof covering the entrance of the cells (Fig. 10). The entrance of the cell was closed up with leaf-bits. Those plugs were concave and smooth surfaced on the outer side,



Figures 1–6. *Calligaster inflata* sp. nov. **1** head, frontal view **2** head, dorsal view **3** mesosoma, dorsal view **4** propodeum, dorsal view **5** head and mesosoma, lateral view **6** metasomal tergum I, dorsal view. Scale bars: 1 mm.

rather crude on the inner surface. Three of them had a small hole on the wall of the cell and the remaining cell was intact. Three cells with a small hole on the wall were opened for examination of structural details. Unfortunately, they were empty except for their

cocoons. The cocoon was 20 to 21 mm long. They were thickest in the part facing the open end of the cells and thinner at the wall of the cells. The feces and the prey remain were always at the bottom of the cells and positioned outside the cocoon. The intact cell was preserved and a female wasp emerged from it on 18 April 2013.



Figures 7–9. *Calligaster inflata* sp. nov. **7** metasoma, lateral view **8** metasomal terga II–VI, dorsal view **9** habitus, laterodorsal view. Scale bars: 1 mm.



Figure 10. *Calligaster inflata* sp. nov. nest. Scale bar: 1 cm.

Distribution. Vietnam (northern part).

Etymology. The specific epithet is from the Latin *inflatus* (meaning swollen), and refers to the swollen metasomal segment I in this species.

Remarks. The new species is similar to *C. himalayensis* in that both have the clypeus, frons, and mesoscutum with coarse dense punctures, with interspaces between the punctures smaller than a puncture diameter and raised to form reticulation; and the lateral part of metasomal tergum I with strong sparse punctures. However, it differs from *C. himalayensis* in having metasomal tergum I about 1.4× as long as wide, with a median longitudinal carina and next to this on each side consisting of a few rows of noticeably elongate punctures, this part occupying one-third the width of the tergum (metasomal tergum I about 1.8× as long as wide, with a median longitudinal carina and next to this on each side consisting of a few longitudinal striae, this part occupying about half the width of the tergum in *C. himalayensis*); and body punctures larger and coarser than in *C. himalayensis*.

***Calligaster himalayensis* (Cameron, 1904)**

Figs 11–21

Zethus himalayensis Cameron, 1904: 13, ♀, “Sikkim” (The Natural History Museum, London).

Calligaster himalayensis; Bequaert 1928: 157 (holotype examined; possibly a valid species).

Zethus himalayensis [!]; Giordani Soika 1941: 216 (incorrect spelling of *Zethus himalayensis* Cameron; syn. of *C. cyanoptera* de Saussure).

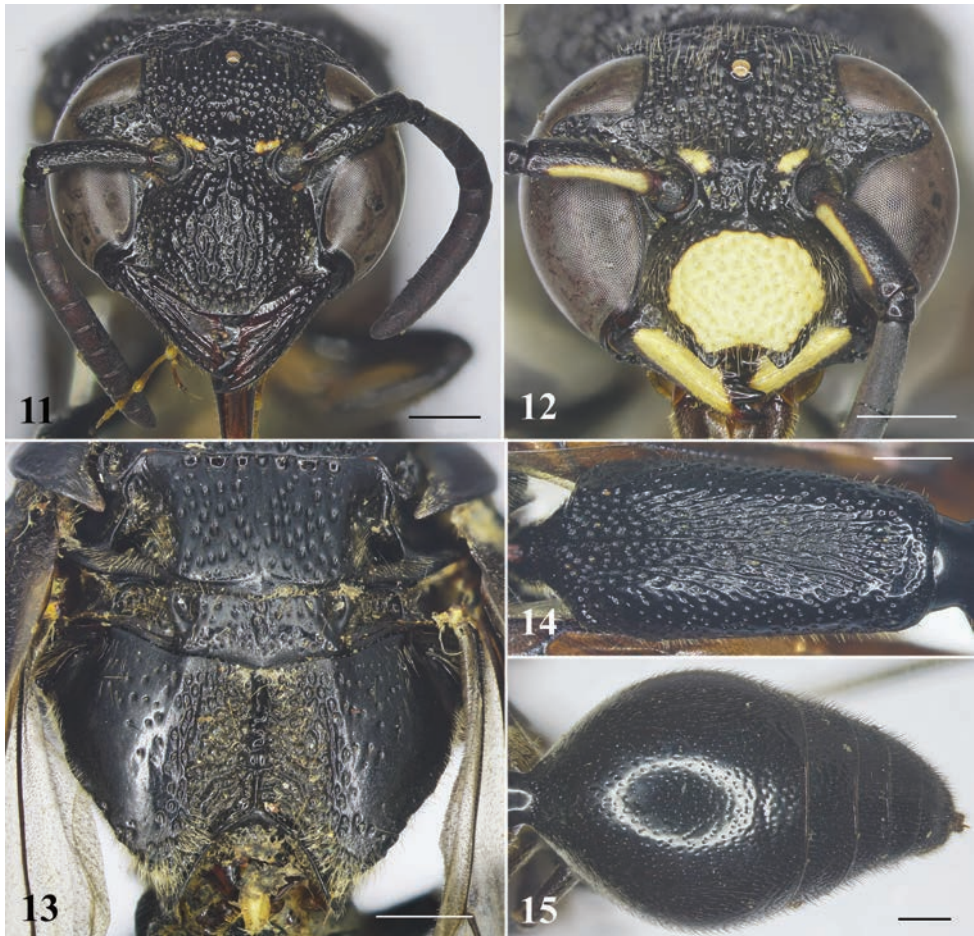
Note. This species was recorded from Vietnam by Nguyen et al. (2014) and Nugroho et al. (2016). The species occurs in the northern and central parts, as well as the Tay Nguyen highlands. Refer to Nugroho et al. (2016) for the diagnosis of this species.

Material examined. VIETNAM: 1♂, Cao Bang, Nguyen Binh, Thanh Cong, 22°32.5'N, 105°53'E, alt. 1000 m, 8 Aug. 2012, Lien Thi Phuong Nguyen et al. leg.; 1♀, Cao Bang, Tra Linh, Ho Thang Hen, 22°45'47.5"N, 106°53'35.7"E, alt. 619 m, 20 May 2023, Lien Thi Phuong Nguyen, Ngat Thi Tran, Cuong Quang Nguyen leg.; 1♀, 1♂, Tuyen Quang, Ham Yen, Phu Luu, Cham Chu NP, alt. 200 m, Jun. 2011, Lien Thi Phuong Nguyen leg.; 1♀, Son La, Moc Chau, Chieng Son, Chieng Ve, 21 Jun. 2015, Long Dang Khuat leg.; 1♀, Dien Bien, Dien Bien, Pa Thom, 20°17'50"N, 102°54'37"E, alt. 693 m, 01 Mar. 2023, Hoa Thi Dang leg.; 1♀, 1♂, Dien Bien, Tua Chua, Muong Fang, 21°50'46"N, 103°22'53"E, alt. 735 m, 04 Mar. 2023, Hoa Thi Dang leg.; 1♂, Vinh Phuc, Me Linh, Me Linh Station, 25 May 2013, Nest#ML-2013-Eum 1, Lien Thi Phuong Nguyen leg.; 1♀, Vinh Phuc, Me Linh, Me Linh Station, 2 Jun. 2018, Cuong Quang Nguyen leg.; 1♀, 1♂, Vinh Phuc, Me Linh, Me Linh Station, 01 Jul. 2020, Hoa Thi Dang leg.; 1♂, Hoa Binh, Ngo Luong, Ngoc Son NR, 20°25'13.3"N, 105°18'36"E, alt. 200 m, 27 Aug. 2020, Ngat Thi Tran leg.; 1♂, Thanh Hoa, Ba Thuoc, Thanh Son, alt. 200 m, 16–18 Jun. 2003, Huong Thi Thu Nguyen leg.; 1♀, Thanh Hoa, Thuong Xuan, Van Xuan, Hon Can, Xuan Lien NP, 19°52'27.5"N, 105°14'20.8"E, alt. 106 m, 24 Aug. 2012, Lien Thi Phuong Nguyen leg.; 1♂, Thanh Hoa, Quan Hoa, Pu Hu NP, 20°29'13.3"N, 104°57'47.2"E, alt. 408 m, 13 Jun. 2016, Lam Xuan Truong, Dac Dai Nguyen, Ngat Thi Tran, Linh Ngoc Ha leg.; 1♀, Ha Tinh, Vu Quang NP, 18°17'45"N, 105°22'29"E, alt. 78 m, 12 Jun. 2023, Cuong Quang Nguyen, Lien Thi Phuong Nguyen, Ngat Thi Tran leg.; 1♀, Quang Nam, Song Thanh, Cha Vai, alt. 400–600 m, 29 Apr. 2005, collectors from the Insect Systematic Department (IEBR) leg.; 1♀, Kom Tum, Dak Ha, Dak Mar, Dak Uy SUF, 14°33'04.6"N, 107°55'08.0"E, 19 Jun. 2012, alt. 630 m, Lien Thi Phuong Nguyen leg.; 3♂♂, Gia Lai, Chu Se, 14 Apr. 2013, Lien Thi Phuong Nguyen leg.; 1♀, Gia Lai, KBang, Kon Chu Rang NR, 14°31'10.4"N, 108°36'24.9"E, 6 Sep. 2018, Lam Xuan Truong, Tuan Viet Luong leg.; 1♀, Dak Lak, Buon Me Thuot city, Tan Hoa, 28 Jul. 2020], QH-L22-01, Bui Thi Quynh Hoa leg., 2♀♀, Dak Nong, Dak Giong, Dak Som, Ta Dung NP, 11°50'16.1"N, 107°59'16.7"E, alt. 475 m, 6 May 2016, Nest#VN-TN-2016-E-01, Lien Thi Phuong Nguyen, Dai Dac Nguyen, Ngat Thi Tran leg.

The male genitalia of this species were described by Giordani Soika (1960) but are redescribed here with added detail.

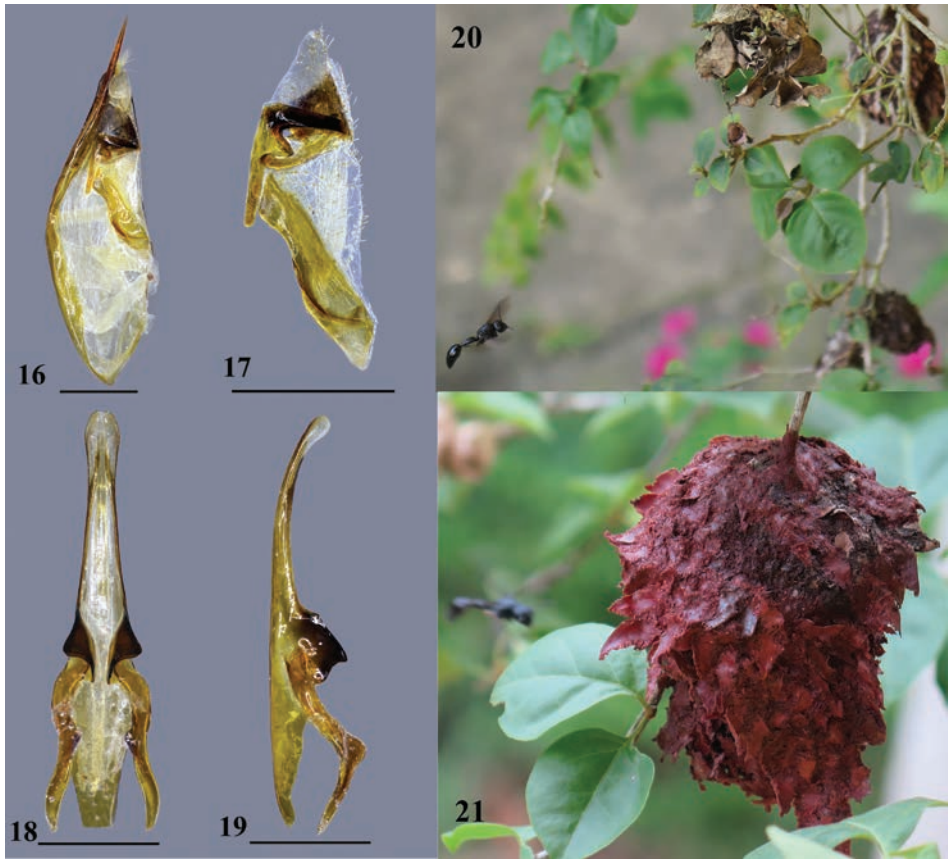
Description. Male genitalia. As in Figs 16–19. Parameral spine with setae (Fig. 16). Volsella flattened, wide on inner aspect, without setae at top (Fig. 16). Digitus gradually narrow from base to apex, with round apex, with setae on apical half (Fig. 17). Penis valve (Fig. 18), about 1.9 times as long as basal apodeme, in profile apical part strongly produced into a large pointed lobe (Fig. 19), with apical part smooth (Fig. 19), middle rod slightly shorter than basal apodeme (Figs 18, 19).

Nest. Three nests comprising 15 cells of this species were collected at Me Linh Station for Biodiversity of the Institute of Ecology and Biological Resources (IEBR), Vinh



Figures 11–15. *Calligaster himalayensis* 11, 13–15 female 12 male 11 head, frontal view 12 head, frontal view 13 mesoscutellum, metanotum, and propodeum, dorsal view 14 metasomal tergum I, dorsal view 15 metasomal terga II–VI, dorsal view. Scale bars: 1 mm.

Phuc Province on 1st July 2020. These nests were made on the branch of bougainvillea. They were not only protected by the roof like the nest of *C. inflata*, but the entire nests were covered with leaves (Fig. 21). The detailed structure of these nests was similar nest of *C. inflata*: the nests consisted of four to six cells, each bent at the neck and enlarged at the bottom; the inner diameter of open end of cells varied from 6 to 6.5 mm; the oldest cell was strongly secured to a twig of a tree, and from its underside the second cell and then those following depend; the entrance of the cell was closed up with leaf-bits; those plugs were concave and smooth surfaced on the outer side, rather crude on the inner surface. The length of the cells measured 32 to 40 mm. Among 15 cells in three nests examined, three individuals developed to the mature stage (two females and one male), other 12 cells died. Of 12 dead cells, three died at the larval stage for unknown reasons; six cells with a small hole in the wall and they were empty except for their cocoons;



Figures 16–21. *Calligaster himalayensis*. 16–19 male genitalia 16 inner aspect of paramere with volsella and digitus 17 volsella and digitus 18 aedeagus, ventral view 19 aedeagus, lateral view 20–21 adult and nest. Scale bars: 1 mm.

the other three cells containing prepupae were attacked by an eulophid species. The cocoon was 20 to 22 mm long. They were thickest in the part facing the open end of cells and thinner at the wall of the cells. The feces and the prey remain were always at the bottom of the cells and positioned outside the cocoon.

Distribution. India: Sikkim; China: Guangdong, Hong Kong; Laos; Vietnam.

Key to species of the genus *Calligaster* in the Oriental Region

This key is based on those by Nugroho et al (2016) and Selis and Femia (2022) (unless the sexes are specified, the character states given in the key can be applied to both sexes). The characters of *C. cyanoptera*, *C. etchellsii*, *C. viridipennis*, *C. williamsi*, and *C. ilocana* were taken from Bequaert (1928), Giordani Soika (1960), Nugroho et al. (2016), and Selis and Femia (2022). *Calligaster himalayensis* and *C. inflata* sp. nov. were examined based on specimens from Vietnam.

- 1 Clypeus and frons with dense coarse punctures, interspaces between punctures raised to form reticulation (Figs 1, 11). Mesoscutum with dense, strong or coarse punctures, interspaces between punctures smaller than puncture diameter and slightly or strongly raised to form reticulations (Fig. 3)..... **2**
- Clypeus and frons with strong punctures, interspaces between punctures smooth (figs 3–6 in Selis and Femia 2022). Mesoscutum with sparser and less-strong punctures, interspaces between punctures about 2–5 times puncture diameter (figs 7, 8 in Selis and Femia 2022) **4**
- 2 Metasomal tergum I less than 1.5 times as long as wide, with a median longitudinal carina and next to this on each side consisting of a few rows of noticeably elongate punctures, this part occupying one-third width of tergum (Fig. 6)..... ***C. inflata* sp. nov.**
- Metasomal tergum I about or greater than 1.8 times as long as wide, with a median longitudinal carina and next to this on each side consisting of a few longitudinal striae, this part occupying about half width of tergum (Fig. 14; figs 7, 9 in Nugroho et al. 2016) **3**
- 3 Metasomal segment I in dorsal view relatively slender, about 2.5 times as long as its maximum width (fig. 7 in Nugroho et al. 2016); tergum I hardly punctured, so that dorsal striae are more or less conspicuous. In male, proximal margin of penis valves in ventral view lobed at upper lateral margin (fig. 5 in Giordani Soika 1960), and in profile apical part strongly produced to a triangular lobe (fig. 6 in Giordani Soika, 1960) ***C. cyanoptera* de Saussure, 1852**
- Metasomal segment I in dorsal view shorter and stouter, about 1.8 times as long as its maximum width (fig. 9 in Nugroho et al. 2016); tergum I with dense distinct punctures, so that dorsal striae inconspicuous. In male, proximal margin of penis valves in ventral view without lobe at upper lateral margin (fig. 1 in Giordani Soika 1960), and in profile apical part strongly produced in to a sharply pointed lobe (Fig. 19; fig. 2 in Giordani Soika 1960) .. ***C. himalayensis* (Cameron, 1904)**
- 4 Male clypeus in frontal view about 2 times as wide as high; apical margin with a deep semi-elliptic emargination..... ***C. etchellsii* (Cameron, 1909)**
- Male clypeus in frontal view equal or less than 1.5 times as wide as high; apical margin with a shallower emargination **5**
- 5 Metasomal tergum I in lateral view strongly convex dorsally and in dorsal view strongly convex along lateral margins, with faint oblique striae. In male, proximal margin of penis valves in profile apical part weakly produced (fig. 8 in Giordani Soika 1960) ***C. viridipennis* Giordani Soika, 1960**
- Metasomal tergum I in lateral view flat dorsally and in dorsal view almost parallel along lateral margins, with a sharp longitudinal carina in the middle, flanked by a series of posteriorly diverging carinae. In male, proximal margin of penis valves in profile apical part strongly produced (figs 9, 10 in Selis and Femia 2022) **6**

- 6 Mesoscutum with parapsidal furrows shallow, with few punctures. Anterior margin of mesoscutellum with a shallow and irregular transverse furrow; mesoscutellum dull with fine punctures (fig. 8 in Selis and Femia 2022). Female clypeus more sparsely punctured on disc (fig. 6 in Selis and Femia 2022). Male clypeus regularly convex, apical emargination semicircular and as wide as deep (fig. 5 in Selis and Femia 2022). Head entirely black in both sexes ...
..... ***C. williamsi* Bequaert, 1940**
- Mesoscutum with parapsidal furrows well-defined and deep, densely punctured. Anterior margin of mesoscutellum crenate, forming six deep pits; mesoscutellum weakly shiny with big deep punctures and micropunctate interspaces (fig. 7 in in Selis and Femia 2022). Female clypeus more densely punctured on disc (fig. 4 in Selis and Femia 2022). Male clypeus with a median transverse depression, apical emargination wider than deep (fig. 3 in Selis and Femia 2022). Male with yellow lines on mandible and scape and rounded yellow spots above antennal insertions ***C. ilocana* Selis, 2022**

Discussion

Calligaster etchellsii (Cameron, 1909) was first described under the genus *Zeuthus* and was based on a single male from “Kuching, Borneo”. In the description of this species, Cameron mentioned that the, “clypeus almost as wide as long” (Cameron, 1909: 206). Bequaert (1928: 157) examined the holotype of this species and moved it to the genus *Calligaster*. He noted that, “This is quite a distinct species in the shape of the clypeus, which is unusually wide (twice as broad as high) and ends in a deep semi-elliptic emargination”. Nugroho et al. (2016) used the character of the clypeus as described by Bequaert (1928) (clypeus twice as broad as high) to separate the species from three other species. Neither Cameron (1909) nor Bequaert (1928) indicated how to measure the width of the clypeus in their studies so we could not know which measurement was correct. We visited the website of the NHML where the holotype of *C. etchellsii* was deposited, but no information on this species was found. In the study of Nugroho et al. (2016) and Selis and Femia (2022), the males of species of *Calligaster* usually have the clypeus much wider than high, about 1.4 to 1.5 times wider than high (though the proper method for measuring the height and width of the clypeus was not mentioned in their study). In our study, the width of the males of species of *Calligaster* (*C. himalayensis* and *C. inflata* sp. nov.) have the clypeus about 1.3 to 1.4 times wider than high (height of clypeus in frontal view is measured as a distance from the bottom of the dorsal emargination to the apex (medially), and width of the clypeus is measured between the extreme corners of the clypeus, at the widest point), and never “as wide as long” as mentioned by Cameron (1909). Accordingly, for the moment we tentatively use in the above key the character as mentioned in Bequaert (1928). Further extensive field sampling will be needed to obtain more specimens and study the taxonomy of this species carefully.

Acknowledgements

We are very grateful to Michael S. Engel for revising some of the English for the manuscript. We thank subject editor and both reviewers for their valuable comments on the manuscript. The present study was supported by a grant from the Vietnam Academy of Science and Technology (VAST04.07/23-24).

References

- Bequaert J (1928) A study of certain types of diplopterous wasps in the collection of the British Museum. *Annals & Magazine of Natural History* 2(10): 138–176. <https://doi.org/10.1080/00222932808672864>
- Bequaert J (1940) A new species of *Calligaster* from the Philippine Islands (Hymenoptera, Vespidae, Subfam. Zethinae). *The Pan-Pacific Entomologist* 16: 124–126.
- Bohart RM, Stange LA (1965) A revision of the genus *Zethus* Fabricius in the Western Hemisphere. *University of California Publications in Entomology* 40: 1–208.
- Cameron P (1904) Description of a new genus and some new species of east Indian Hymenoptera. *Entomologist* 37: 306–310. <https://doi.org/10.5962/bhl.part.288>
- Cameron P (1909) On a new species of *Zeuthus* (Eumenidae) from Borneo. *Entomologist* 42: 206–207. <https://doi.org/10.1002/mmnd.48019090203>
- Carpenter JM, Cumming JM (1985) A character analysis of the North American potter wasps (Hymenoptera: Vespidae; Eumeninae). *Journal of Natural History* 19: 877–916. <https://doi.org/10.1080/00222938500770551>
- Cowan DP (1991) The solitary and prosocial Vespidae. In: Ross KG, Matthews RW (Eds) *The social biology of wasps*. Cornell University Press, Ithaca, 33–73. <https://doi.org/10.7591/9781501718670-005>
- de Saussure H (1852) Études sur la Famille des Vespides 1. Monographie des Guêpes solitaires ou de la tribu des Euméniens. V. Masson, Paris and J. Kessmann, Genève, 128 pp. [pls. 2–5 + 7 + 10 + 14.]
- de Saussure H (1854–1856) Études sur la famille des Vespides 3. In: Paris MV, Kessmann J (Eds) *La Monographie des Masariens et un supplement a la Monographie des Euméniens*. Genève, 352 pp.
- Giordani Soika A (1941) Studi sui Vespidi solitari VI. Studio di alcuni tipi di vespidi solitari. *Bollettino del Museo civico di storia naturale di Venezia* 2: 212–273.
- Giordani Soika A (1960) [1958] Notulae vespilogicae. *Bollettino del Museo civico di storia naturale di Venezia* 11: 35–102. *di Storia Naturale di Genova* 21: 523–636 [pl. 1].
- Kojima J (1999) Male genitalia and antennae of an Old World paper wasp genus *Ropalidia* Guérin-Ménéville, 1831 (Insecta: Hymenoptera; Vespidae, Polistinae). *Natural History Bulletin of Ibaraki University* 3: 51–68.
- Nguyen LTP (2020) *The social wasps of Vietnam*. Publishing House for Science and Technology, Hanoi, 287 pp.

- Nguyen LTP, Dang HT, Kojima J, Carpenter JM (2014) An annotated distributional checklist of solitary wasps of the subfamily Eumeninae (Hymenoptera: Vespidae) of Vietnam. *Entomologica Americana* 120(1): 7–17. <https://doi.org/10.1664/13-RA-010.1>
- Nguyen LTP, Nguyen AD, Tran NT, Nguyen MT, Engel MS (2023) The potter wasp genus *Allorhynchium* from Vietnam, with descriptions of three new species and a new country record (Hymenoptera, Vespidae, Eumeninae). *ZooKeys* 1166: 1–32. <https://doi.org/10.3897/zookeys.1166.102674>
- Nugroho H, Ubaidillah R, Kojima J (2016) Taxonomy of the Indo-Malayan presocial potter wasp genus *Calligaster* de Saussure (Hymenoptera, Vespidae, Eumeninae). *Journal of Hymenoptera Research* 48: 19–32. <https://doi.org/10.3897/JHR.48.7045>
- Selis M, Femia A (2022) The genus *Calligaster* de Saussure (Hymenoptera: Vespidae: Zethinae) in the Philippine Islands. *Zootaxa* 5155(1): 124–132. <https://doi.org/10.11646/zootaxa.5155.1.6>
- Williams FX (1919) Philippine wasp studies. Part 2. Description of new species and life history studies. *Bulletin of the Experimental Station of the Hawaiian Sugar Plantation Association* 14: 19–187.

An integrative taxonomic study of north temperate *Cotesia* Cameron (Hymenoptera, Braconidae, Microgastrinae) that form silken cocoon balls, with the description of a new species

Vladimir Žikić¹, Milana Mitrović², Saša S. Stanković¹, José L. Fernández-Triana³,
Maja Lazarević¹, Kees van Achterberg⁴, Dawid Marczak⁵,
Marijana Ilić Milošević¹, Mark R. Shaw⁶

1 Faculty of Sciences and Mathematics, Department of Biology and Ecology, University of Niš, Niš, Serbia **2** Institute for Plant Protection and Environment, Department of Plant Pests, Banatska 33, 11000 Zemun, Serbia **3** Canadian National Collection of Insects, Arachnids and Nematodes, Agriculture and Agri-Food Canada, 960 Carling Ave., Ottawa, Ontario, K1A 0C6, Canada **4** Naturalis Biodiversity Center, P.O. 9517, 2300 RA Leiden, Netherlands **5** Faculty of Engineering and Management, University of Ecology and Management in Warsaw, 12 Olszewska Street, 00-792 Warsaw, Poland **6** Department of Natural Sciences, National Museums of Scotland, Chambers St., Edinburgh, Scotland EH1 1JF, UK

Corresponding author: Saša S. Stanković (sasasta@gmail.com)

Academic editor: J. M. Jasso-Martínez | Received 27 November 2023 | Accepted 1 March 2024 | Published 8 April 2024

<https://zoobank.org/79B242EF-19C1-4BDC-AA25-442DE3211987>

Citation: Žikić V, Mitrović M, Stanković SS, Fernández-Triana JL, Lazarević M, van Achterberg K, Marczak D, Milošević MI, Shaw MR (2024) An integrative taxonomic study of north temperate *Cotesia* Cameron (Hymenoptera, Braconidae, Microgastrinae) that form silken cocoon balls, with the description of a new species. Journal of Hymenoptera Research 97: 255–276. <https://doi.org/10.3897/jhr.97.116378>

Abstract

Using CO1 sequence analysis, we investigated the relationships of Western Palearctic and Nearctic *Cotesia* that spin aggregated cocoons in the shape of a ball, and as adults are morphologically very similar. The analysis included the conceptual taxa *C. tibialis*, *C. ofella*, *C. vanessae*, *C. ruficrus*, *C. xyliina* and *C. yakutatensis*, as well as the newly described species *C. trivaliae* **sp. nov.** The examined specimens of *C. tibialis*, *C. ofella*, *C. vanessae*, *C. ruficrus* and *C. trivaliae* **sp. nov.** were collected in several European countries, and *C. xyliina* and *C. yakutatensis* in Canada and the USA. Molecular analyses showed that *C. ruficrus* is not closely related to the other studied taxa. Based on the genetic distances as well as biology and morphology, *C. vanessae* and *C. ofella* are confirmed as solid taxa. The species *C. yakutatensis* comprises two entities. Having 8 haplotypes, *C. tibialis* also emerges as a species complex, divided into two clusters. With 26 detected haplotypes, *C. xyliina* shows the highest diversity, being composed of three segregates. The

conceptual species *C. tibialis*, *C. xyliina* and *C. yakutatensis* seem to be species complexes containing several candidates for recognition as distinct species. One from the European *C. tibialis* complex is here described as new, and the impediments to be overcome before the description of further species are outlined.

Keywords

DNA barcoding, genetic distance, hosts, species aggregates

Introduction

Cotesia Cameron, 1891 is a large genus of parasitoid wasps with about 340 species described worldwide (Fernández-Triana et al. 2020). Like other members of the subfamily Microgastrinae (Hymenoptera: Braconidae), *Cotesia* species are koinobiont parasitoids of lepidopteran larvae, mostly those known as “macrolepidoptera”. The great majority oviposit into an early larval instar, though a few species oviposit into fully-developed eggs (e.g., *C. hyphantriae* Riley, 1887). Fully grown parasitoid larvae usually erupt from a later, often final, larval instar, but never from the host pupa (Shaw and Huddleston 1991). Many species of *Cotesia* (including those discussed in the present paper) are gregarious parasitoids, but a substantial proportion are solitary (e.g., *C. vestalis* (Haliday, 1834)) (Shaw 2007; Gupta and Fernández-Triana 2014). Since *Cotesia* species attack caterpillars, some of which are serious pests in agroecosystems, several species have been used as biological control agents, e.g., *C. flavipes* Cameron, 1891 against *Busseola fusca* (Fuller, 1901) and *Sesamia calamistis* (Hampson, 1910) (Overholt et al. 1997) and several other cases (e.g., Jiang et al. 2004; van Driesche 2008; Avila et al. 2013).

Cocoon-spinning by *Cotesia* species usually takes place externally on, under, around, or near the dying caterpillar, which can live several days after the emergence of the parasitoid larvae (Shaw and Huddleston 1991). The larvae of some gregarious *Cotesia* species such as those in the *C. tibialis* (Curtis, 1830) group, and *C. vanessae* (Reinhard, 1880), make typical ball-shaped silken cocoon masses (Nixon 1974). The erupting parasitoid larvae cooperate in spinning a communal web that encloses their individual, separately spun but connected cocoons. Sometimes caterpillars are induced to additionally cover the parasitoid cocoon mass with their own silk; for example, the hosts of the unrelated *C. glomerata* (Linnaeus, 1758) (Brodeur 1992).

There is a major problem in properly understanding the host repertoires of parasitoids based on the published literature that has been uncritically compiled in sources such as Taxapad (Yu et al. 2016), because the many sources of error and accumulated misinformation (discussed by many authors, including Shaw 1994, 2023; Noyes 1994 and, in relation to Microgastrinae in particular, Fernández-Triana et al. 2020) go unrecognised and severely obscure reality. Taxapad is an extremely valuable resource, but it was not designed to give reliable host information. Here we largely ignore data from Taxapad (which, for the commonest taxon of this study, *C. tibialis*, is so bloated with unreliable data as to suggest a host repertoire of more than a hundred Lepidoptera species over as many as 17 families), but instead give only host information that we believe

to be reliable. One of the commonly collected apparent species that make cocoon masses that, to a greater or lesser extent, look like fluffy balls is *C. tibialis*. The cocoon mass is usually about 10–20 mm in diameter, depending especially on the number of parasitoid larvae that spin the cocoon (VŽ personal observation). *Cotesia tibialis* is widespread throughout the Palaearctic region and has already been considered to possibly be a complex of species, including two seasonal forms identified by Nixon (1974). This issue is discussed in detail by Lazarević et al. (2022). The colour of the cocoons is variable; they can be almost white to yellowish. Morphological variation in the adults is also considerable and may have contributed to the existence of many supposed synonyms, but it also suggests the possibility of as yet unrecognised additional species. Confirmed records refer to hosts belonging to owlet moths (Noctuidae), especially those from the major subfamily Noctuinae (*sensu lato*). The hosts (Noctuinae unless indicated) recorded several times come from caterpillars feeding in low vegetation in the following genera: *Agrotis* Ochsenheimer, 1816, *Autographa* Hübner, 1821 (Plusiinae), *Lacanobia* Billberg, 1820, *Mamestra* Ochsenheimer, 1816, *Noctua* Linnaeus, 1758, *Orthosia* Ochsenheimer, 1816, *Xestia* Hübner, 1818 and *Xylena* Ochsenheimer, 1816 (Yu et al. 2016).

Morphologically and by cocoon architecture, *Cotesia ofella* (Nixon, 1974) is very similar to *C. tibialis*. There are not many published data on the hosts for this parasitoid, but certainly its host repertoire includes noctuid species; in this case, *Acronicta aceris* (Linnaeus, 1758), *A. rumicis* (Linnaeus, 1758) (Nixon 1974; Razowski and Wiackowski 1999), *A. auricoma* (Denis & Schiffermüller, 1775) (MRS, unpublished) as well as *Simyra dentinosa* Freyer, 1838 (Karimpour et al. 2001), both genera from the subfamily Acronictinae. Beside these noctuids, Nixon (1974) noted *Spilosoma lubricipeda* (Linnaeus, 1758) (Erebidae) as a host of *C. ofella*, but this may be an error resulting from morphological similarity of that caterpillar to certain low-feeding Acronictinae larvae. The cocoon masses of *C. ofella* are mostly yellowish, sometimes intensely yellow, which may be useful in some cases for preliminary discrimination from other species, for example between *C. tibialis* and *C. ofella* (VŽ personal observation).

Another species morphologically similar to *C. tibialis* is *Cotesia berberis* (Nixon, 1974). Nothing is known about the biology of this rarely found species, recorded from just three countries (Nixon 1974; Papp 1986, 1987); although the ball-shaped cocoon mass of the type series was collected on *Berberis* sp. (Berberidaceae) (Nixon 1974) it is by no means certain that the host had fed on that plant. The outer layer of the cocoon mass is spun from yellowish silk and resembles the late summer forms of *C. tibialis*. The cocoon texture is somewhat looser than in *C. tibialis*. Due to the lack of fresh material, we are unable to consider this species further.

Unlike the previous three species, *C. vanessae* is predominantly recorded from some Nymphalidae (Nymphalini) as well as certain Noctuidae. Definite summer hosts are caterpillars of the nymphalids *Aglais urticae* (Linnaeus, 1758), *Vanessa atalanta* (Linnaeus, 1758) and *V. cardui* (Linnaeus, 1758) (Nixon 1974; Shaw et al. 2009), while winter hosts are noctuids (Nixon 1974; Hervet et al. 2014). The cocoon mass is a white ball of silk that is usually dense enough to fully conceal the individual cocoons

within. Literature data indicate that *C. vanessae* is widespread in the Palaearctic region (including North Africa), but it has also been recently recorded in the Nearctic region as a parasitoid of pest species of plusiine noctuids in greenhouses and fields in southern Ontario and Alberta, Canada (Hervet et al. 2014; Fernández-Triana et al. 2020).

Cotesia ruficrus (Haliday, 1834), a taxon with cosmopolitan distribution recorded in all regions, spins a cocoon mass that more weakly conceals the individual cocoons but overlaps with the above species in the host repertoire. In the north temperate area, this parasitoid is frequently recorded from the pest noctuids *Helicoverpa armigera* (Hübner, 1808), *Leucania loreyi* (Duponchel, 1827), *Mythimna separata* Walker, 1865 and *Spodoptera exigua* (Hübner, 1808), but it undoubtedly has a much wider host repertoire (MRS, unpublished).

In the Nearctic region, there are at least two more conceptual species that make ball-like cocoon masses, *C. xyliana* (Say, 1836) and *C. yakutatensis* (Ashmead, 1902). Hosts parasitized by *C. xyliana* include the following species of Noctuidae: *Mamestra configurata* Walker, 1856, (Wylie and Bucher 1977) *Peridroma saucia* (Hübner, 1808) (Roberts et al. 1977; Marsh 1979), *Xestia c-nigrum* (Linnaeus, 1758) (Muesebeck 1921; Marsh 1979), with records from *Epiglaea apiata* (Grote, 1874) and *Xylena nuptera* (Lintner, 1874) also probably reliable (Franklin 1950). The other Nearctic species, *C. yakutatensis* has a narrower recorded host range, including the plusiine noctuids *Autographa californica* (Speyer, 1875) (Muesebeck 1921; Clancy 1969; Marsh 1979; Miller and West 1987), *Autoplusia egena* (Guenée, 1852) (Clancy 1969; Marsh 1979), *Trichoplusia ni* (Hübner, 1803) (Miller and West 1987) and the noctuid *Xestia c-nigrum* (Linnaeus, 1758) (Marsh 1979).

Considering the morphological resemblance of these seven nominal *Cotesia* species, similar architecture of the cocoons, as well as sometimes overlapping host repertoires, it is of interest, and also importance in view of the biocontrol potential of some taxa in this group, to examine their relationships and especially their integrity.

Material and methods

Collecting and processing specimens

Samples were mostly collected from cocoon masses (Fig. 1) spun and attached to the top of stems of various low plants, often grasses. Part of the parasitoid material was obtained by rearing parasitized caterpillars that were identified, while most of the parasitoids emerged from cocoons that were collected in the field without caterpillars present. Consequently, host information is unknown in these cases. The vast majority of *Cotesia* specimens were stored in 2 ml plastic microtubes filled with 96% ethyl alcohol for later molecular analyses. Individuals included in the molecular analysis are listed in Suppl. material 1: table S1. Selected specimens of both sexes were dried and glued to cardboard, and some were dissected in a Berlese mounting medium to study details of morphological structures. Identification of the European specimens using



Figure 1. Aggregated ball-like cocoon **A** cooperative work of all parasitoid larvae in spinning the cocoon mass (*C. vanessae* ex *Aglais urticae*) **B** spun cocoon mass (*C. tibialis* ex *Mythimna conigera*).

morphological characters is mostly based on Nixon's (1974) work, whereas identification of the North American material was mostly based on Muesebeck (1921).

Photographs were taken using a Leica Flexacam C3 on a Leica M165C stereomicroscope with a magnification of 7.3 \times . For micrographs, we used a Leica DFC490 camera (Leica Microsystems, Wetzlar, Germany), adapted to a microscope Leica 2500 (Leica Microsystems, Wetzlar, Germany), at a total magnification of 5.0–20.0 \times . The equipment is in the Laboratory of Zoology at the Faculty of Sciences and Mathematics, Department of Biology and Ecology, University of Niš, Serbia.

Our material is deposited in the collections of the Faculty of Sciences and Mathematics, University of Niš, Serbia; the Naturalis Biodiversity Center, Leiden, The Netherlands; the National Museums of Scotland, Edinburgh, UK; and the Canadian National Collection of Insects, Arachnids and Nematodes, Agriculture and Agri-Food Canada, Ottawa, Ontario, Canada. Many of the specimens whose sequences were obtained from public databases are housed in depositories less accessible to us and, partly for that reason but also because many lack host data, a detailed morphological analysis of all segregates has been postponed until such a time that it can be done in conjunction with both DNA barcoding and host data.

DNA extraction, PCR amplification and sequencing

Genomic DNA was extracted from whole specimens of parasitoids using Dneasy Blood and Tissue Kit (Qiagen Inc., Valencia, CA) according to the manufacturer's instructions. For material reared from hosts, caterpillar identity was confirmed by DNA barcoding following the emergence of parasitoids. The genomic DNA used for analysis was extracted from the caterpillar head.

Taxonomic relationships among the relevant species within the genus *Cotesia* were investigated using sequence data of the barcoding region of the mitochondrial cytochrome oxidase subunit I (CO1). Standard primer pairs LCO1490/HCO2198 in combination with other primers (Table 1) were used to amplify barcoding CO1 fragments. Each PCR reaction was carried out in a volume of 20 μ l, including 1 μ l of

Table 1. The list of primers used to retrieve barcoding fragments of CO1 in *Cotesia* samples.

Primer name	5' primer sequence 3'	Primer direction	Reference
LCO1490	GGTCAACAAATCATAAAGATATTGG	Forward	Folmer et al. (1994)
HCO2198	TAAACTTCAGGCTGACCAAAAAATCA	Reverse	
LCO1490puc	TTTCAACWAATCATAAAGATATTGG	Forward	Cruaud et al. (2010)
HCO2198puc	TAAACTTCWGGRTGWCCAAARAATCA	Reverse	
LCO1490hem	TTTCAACTAAYCATAARGATATYGG	Forward	Germain et al. (2013)
HCO2198hem	TAAACYTCDGGATGBCCAAARAATCA	Reverse	
Aph2Fd	ATAATTGGWGGATTTGGWAATTG	Forward	Mitrović and Tomanović (2018)
Aph2Rd	GTWCTAATAAAAATTAATWGCWCC	Reverse	
Lys2Rd	GTWCTAATAAAAATTAATTGCHCC	Reverse	
Pr2Fd	ATAATTGGAGGRTTTGGWAATTG	Forward	

extracted DNA, 11.8 μ l H₂O, 1 μ l of each primer 0.5 μ M, 2 μ l High Yield Reaction Buffer A with 1 \times Mg, 1.8 μ l of MgCl₂ 2.25 mM, 1.2 μ l of dNTP 0.6 mM, 0.2 μ l DNA polymerase 0.05 U/ μ l. The amplification protocol included: i) initial denaturation for 5 min at 95 °C; ii) 35 cycles of 1 min at 94 °C, 1 min at 54 °C and 30 sec at 72 °C; and iii) final extension at 72 °C for 7 min. Amplified products were run on 1% agarose gel, stained with ethidium bromide, and visualized under a UV transilluminator. Barcoding CO1 fragments were sequenced using automated equipment (Macrogen Europe, Amsterdam, the Netherlands).

In addition, 63 sequences of CO1 barcoding fragments of *Cotesia* parasitoids were obtained from the public databases GenBank (<https://www.ncbi.nlm.nih.gov/genbank/>) and the Barcoding of Life Data Systems (BOLD, <http://www.boldsystems.org/>) and included in the molecular analysis (Suppl. material 1: table S1). Many of the specimens concerned (indicated by codes starting with the letters MRSJFT) are in NMS, whereas specimens with codes starting with the CNC, CNCHYM, HYM, MIC and WMIC are in the CNC. Specimens with other codes are mostly deposited in the Canadian Center for DNA Barcoding and in those cases, not all determinations could be checked.

Molecular analyses and tree constructions

Sequenced CO1 fragments were manually edited in FinchTV ver. 1.4.0 (<https://digitalworldbiology.com/FinchTV>) and aligned using the ClustalW program integrated into MEGA5 (Tamura et al. 2011). According to the obtained Akaike Information Criterion scores, the best fit model for the estimation of evolutionary divergence was the Tamura-Nei model (Tamura and Nei 1993). The Bayesian inference analysis was done by running two Markov Chain Monte Carlo searches each with one cold and three heated chains, for 3 million generations (Fig. 2 and Suppl. material 1: fig. S1) and 1,2 million generations (Fig. 3), sampling every 100 generations. The first 7,500 trees (Fig. 2 and Suppl. material 1: fig. S1) and 3,000 trees (Fig. 3) were discarded as a burn-in. The average standard deviation of split frequencies was below 0.01. The Bayesian tree was constructed using the program MrBayes 3.1.2 (Ronquist and Huelsenbeck

2003). The program FigTree 1.3.1. was used to view the consensus tree with posterior probabilities (Rambaut 2006–2009). To root the tree, we used the reference barcode sequence of *Glyptapanteles pallipes* (Reinhard, 1880) (GenBank Acc. No. KJ459198) as the outgroup within the same subfamily. For the far outgroup, which belongs to a different braconid subfamily, we used the sequence of *Aphidius sussi* Pennachio & Tremblay, 1989 (GenBank Acc. No. MT432023).

Haplotype analysis

CO1 sequences were aligned, trimmed to the same size of 501 bp (a compromise to achieve uniformity for a large number of sequences), and analysed for haplotype diversity and evolutionary distances. The haplotype data file was generated using DnaSP ver. 5.10.01 (Librado and Rozas 2009). A median-joining haplotype network (Bandelt et al. 1999) was constructed using the PopART program (<http://popart.otago.ac.nz>).

Terminology for description of the new species

Terminology of body characters follows van Achterberg (1993). For wing venation terminology follows Nixon (1965, 1974). The length of the first metasomal tergite (T1) and the length of the discoidal segments in the fore wing (1CU1 + 2CU2) are measured linearly as the shortest distances, not as total curvature length; for T1 it is the distance between the base and the apex.

Results

Preliminary morphological sorting into possible taxa is reflected in Suppl. material 1: table S1. Molecular analysis including 105 CO1 barcoding sequences of different *Cotesia* specimens segregated them into 12 distinct groups (Fig. 2, Suppl. material 1: table S1, fig. S1), which were assigned the following provisional names: ‘*tibialis* 1’; ‘*tibialis* 2’; ‘cf. *tibialis* white cocoons’; ‘*xylina* 1’; ‘*xylina* 2’; ‘*xylina* 3’; ‘*Cotesia* sp.’ (= *trivaliae* sp. nov.); ‘*ofella*’; ‘*yakutatensis* 1’; ‘*yakutatensis* 2’; ‘*vanessae*’ and ‘*ruficrus*’.

From the trimmed CO1 sequences, 56 haplotypes were determined with 108 variable sites detected (Suppl. material 1: table S1).

All three Bayesian inference trees (Figs 2, 3, Suppl. material 1: fig. S1) and the Median-joining network (Fig. 4), showed a general delineation of 12 groups of CO1 barcode haplotypes. Three sequences, determined as *C. ruficrus* originating from Serbia, were separated from the remaining *Cotesia* as a distinctive group we named ‘*ruficrus*’, supported by 100-posterior probability (Fig. 2 and Suppl. material 1: fig. S1). The two haplotypes identified within the ‘*ruficrus*’ group (H1, H2) are distant 1.5%, while they are clearly distinguished from all other groups (Table 2).

Four sequences determined as *C. vanessae* originating from Spain (3) and Canada (1) clustered together and formed the ‘*vanessae*’ group. Two haplotypes, H3 and

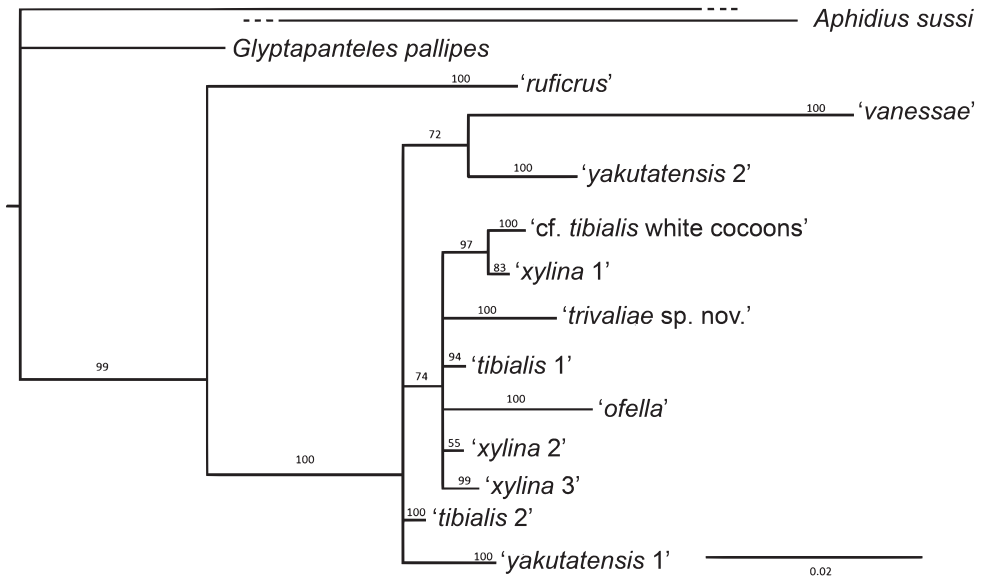


Figure 2. A condensed Bayesian tree inferred from the CO1 barcoding fragments of *Cotesia* specimens. Bayesian posterior probabilities are shown above branches; scale bar indicates substitutions per site (0.02). Potential scale reduction factors (PSRF) were all approximately equal to one. Description of *Cotesia* CO1 barcode sequences included in the analysis is given in Suppl. material 1: table S1. Outgroups: *Aphidius sussi* – Acc. No. MT432023; *Glyptapanteles pallipes* Acc. No. KJ459198.

Table 2. Average between-groups genetic distances (%) calculated using the Tamura-Nei method.

Group	[1]	[2]	[3]	[4]	[5]	[6]	[7]	[8]	[9]	[10]	[11]
[1] <i>'ruficrus'</i>											
[2] <i>'vanessae'</i>	11.5										
[3] <i>'cf. tibialis white cocoons'</i>	9.3	6.8									
[4] <i>trivaliae sp. nov.</i>	8.7	7.1	3.0								
[5] <i>'tibialis 1'</i>	8.6	6.5	1.4	2.3							
[6] <i>'tibialis 2'</i>	7.8	6.4	1.8	2.3	1.1						
[7] <i>'ofella'</i>	8.4	7.8	2.8	3.3	3.0	2.9					
[8] <i>'xylina 1'</i>	9.3	6.9	1.1	3.1	1.6	1.9	2.9				
[9] <i>'xylina 2'</i>	8.6	6.5	1.8	2.3	1.2	1.1	2.9	1.9			
[10] <i>xylina 3'</i>	8.6	6.5	1.8	2.0	1.2	1.1	2.7	1.9	1.2		
[11] <i>'yakutatensis 1'</i>	7.7	6.8	3.3	3.1	3.1	2.2	4.0	3.4	3.0	3.0	
[12] <i>'yakutatensis 2'</i>	8.5	6.9	4.3	4.4	4.1	3.2	5.1	4.4	4.0	4.0	3.4

H4 were identified, with a genetic distance of 0.4% (Fig. 3). This group undoubtedly separates from other groups, with an average distance ranging from 6.4 to 11.5% (Table 2).

Cotesia *'cf. tibialis white cocoons'* consisted of sequences extracted from three independent samples originating from Poland. Since all three sequences were identical, they appear on the tree under the same haplotype (H5). The average genetic distance of

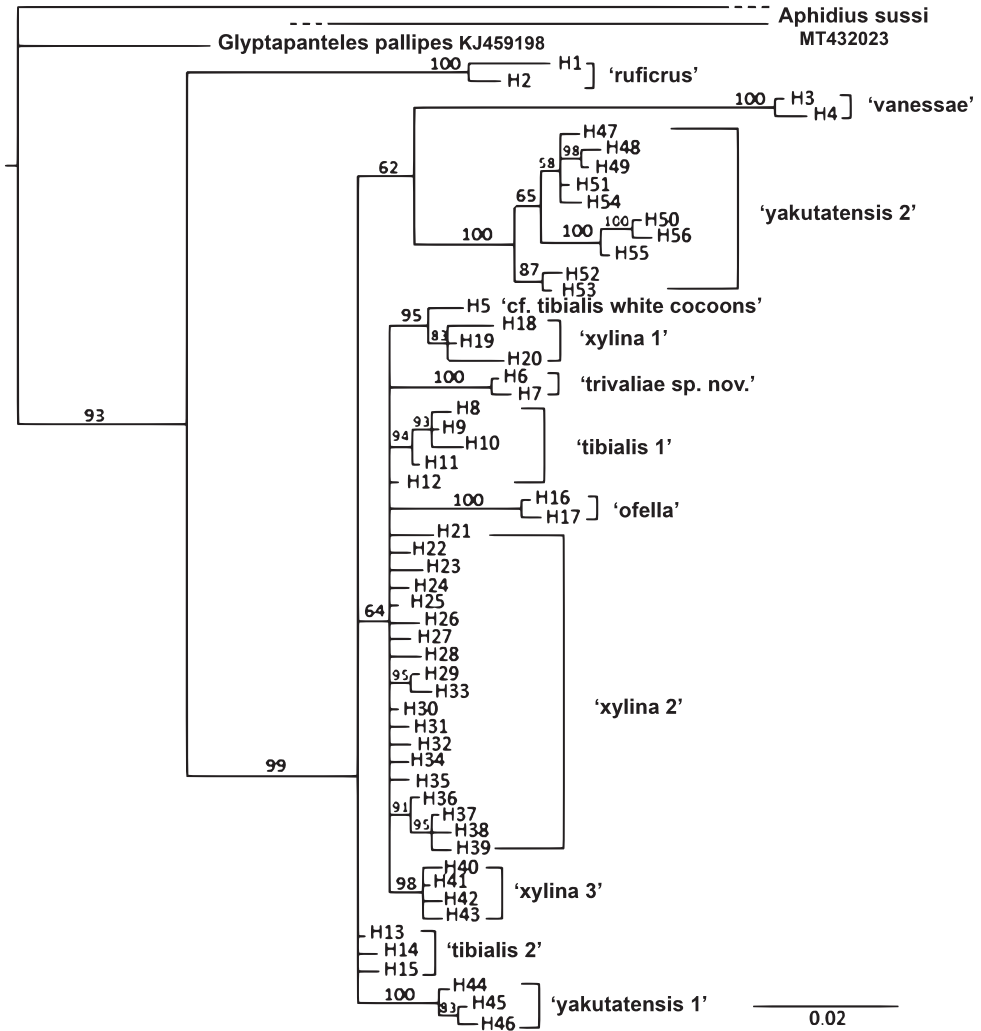


Figure 3. A Bayesian tree inferred from the *Cotesia* CO1 barcoding haplotypes. Bayesian posterior probabilities are shown above branches; scale bar indicates substitutions per site (0.02). Potential scale reduction factors (PSRF) were all approximately equal to one. Description of *Cotesia* haplotypes is given in Suppl. material 1: table S1. Outgroups: *Aphidius sussi* – Acc. No. MT432023; *Glyptapanteles pallipes* Acc. No. KJ459198.

this group from 'vanessae', 'ruficrus', '*Cotesia* sp.' (= *trivaliae* sp. nov.), 'ofella', 'yakutatensis 1' and 'yakutatensis 2' is relatively large (Table 2). However, lower distances were detected in comparison to 'tibialis 1', 'tibialis 2', 'xylina 1', 'xylina 2' and 'xylina 3'.

Sixteen CO1 sequences of specimens from Serbia (3), Austria (3), Slovenia (2), Finland (1), Germany (1) and Poland (6), initially determined as *Cotesia* cf. *tibialis* (3) or *C. tibialis* (12), were grouped within the same clade 'tibialis 1'. Five haplotypes (H8, H9, H10, H11, H12) were identified with in-group average distance of 0.4%. This

group separates from '*ruficrus*', '*vanessae*', '*ofella*', '*yakutatensis* 1' and '*yakutatensis* 2' in a range from 3.0 to 8.6% (Table 2). Lower genetic distances were detected in comparison with 'cf. *tibialis* white cocoons' and '*Cotesia* sp.', as described above, including '*tibialis* 2', '*xylina* 1', '*xylina* 2' and '*xylina* 3'.

Eight barcode CO1 sequences originating from Serbia, two from the Netherlands and one from Austria clustered within the '*tibialis* 2' group (Suppl. material 1: table S1). Three haplotypes (H13, H14, H15) were detected, with an average distance of 0.3%. The '*tibialis* 2' group can undoubtedly be discriminated from '*ruficrus*', '*vanessae*', '*ofella*' and '*yakutatensis* 2' (Table 2). On the other hand, low genetic distances were determined in comparison with '*Cotesia* sp.', 'cf. *tibialis* white cocoons', '*tibialis* 1', '*xylina* 1', '*xylina* 2', '*xylina* 3' and '*yakutatensis* 1' (Table 2).

With only one haplotype (H5), 'cf. *tibialis* white cocoons' is inserted into the '*tibialis*'/'*xylina*'/'*ofella*' part of the tree. Comparing the average genetic distances between this group and all '*tibialis*' and '*xylina*' segregates, 'cf. *tibialis* white cocoons' is closest to '*xylina* 1' with an average genetic distance of 1.1%, then to '*tibialis* 1' with an average genetic distance of 1.4%, and equally distant from the groups '*tibialis* 2', '*xylina* 2' and '*xylina* 3' with an average genetic distance of 1.8%.

Within the '*ofella*' group there are two haplotypes (H16, H17) that differ among themselves with an average distance of 0.2%. This group of haplotypes is separated from other groups with a range of 2.9 to 8.4% (Suppl. material 1: fig. S1, Table 2).

Analysis of 32 specimens initially determined as *C. xyлина*, originating from Canada (31) and the USA (1) revealed the separation of barcode sequences into three groups to which the following names were assigned: '*xylina* 1', '*xylina* 2' and '*xylina* 3' (Fig. 2 and Suppl. material 1: fig. S1). Within the group '*xylina* 1' three haplotypes were determined (H18, H19, H20) with an average distance of 0.9%. The '*xylina* 2' clade encompasses 19 haplotypes (from H21 to H39) which differ among them on average 0.7%. Four haplotypes (H40, H41, H42, H43) were recognized in the '*xylina* 3' group with an average genetic distance of 0.3%. Average distances between the three groups were as follows: '*xylina* 1' vs '*xylina* 2' 1.9%; '*xylina* 1' vs '*xylina* 3' 1.9%; '*xylina* 2' vs '*xylina* 3' 1.2%.

Barcode sequences of 16 specimens determined as *C. yakutatensis* originating from Canada (15) and the USA (1) were analysed. In total, 13 haplotypes were determined (Suppl. material 1: table S1), separated into two clades on the Bayesian tree (Fig. 3) and MJ network (Fig. 4). One branch was assigned the name '*yakutatensis* 1' which is comprised of three haplotypes (H44, H45, H46) (Suppl. material 1: table S1). The rest of the haplotypes (H47 to H56) clustered as a separate group '*yakutatensis* 2' (Suppl. material 1: table S1; Figs 3, 4). The average genetic distance between haplotypes in the '*yakutatensis* 1' group is 0.3% and in the '*yakutatensis* 2' group 1%. The average distance between the two *yakutatensis* groups was 3.4% (Table 2).

Seven sequences clustered together revealing a new taxon *Cotesia trivaliae* sp. nov., described below. This includes three sequences from Poland (host unknown) and one from Slovenia, ex *Orthosia* sp. (Suppl. material 1: table S1) from specimens that could

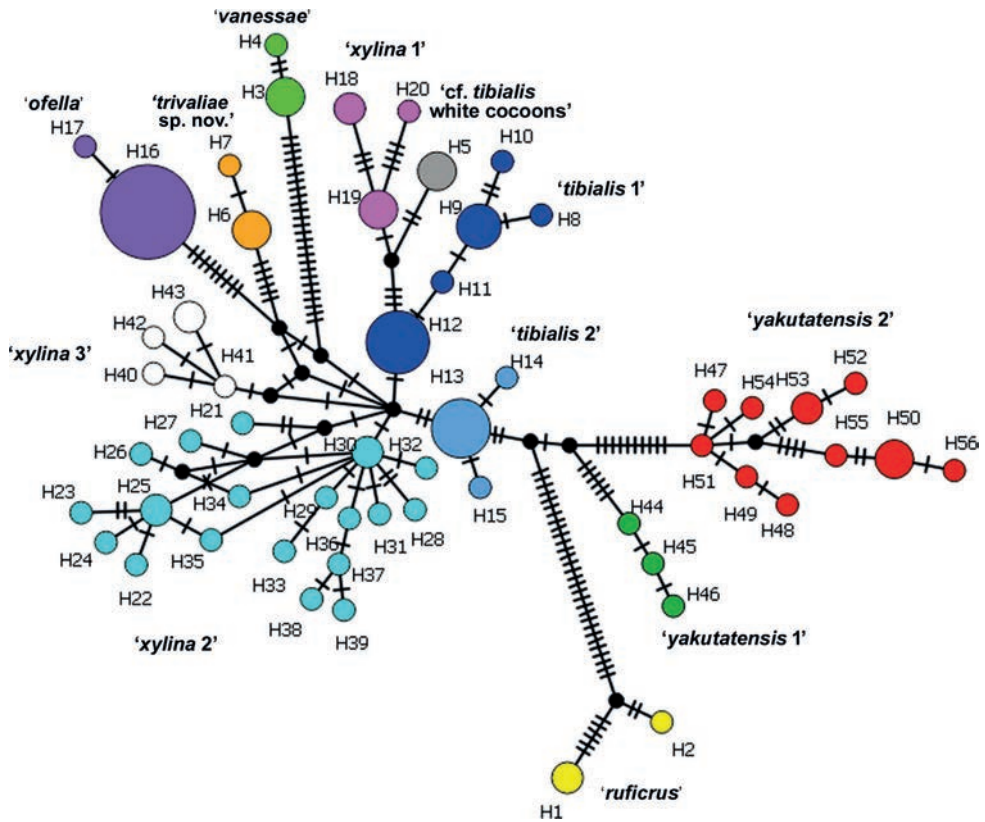


Figure 4. Median-joining network designed for 56 CO1 haplotypes of different *Cotesia* segregates. Black dots are median vectors representing the missing unsampled intermediary haplotype(s). Mutational steps are marked with short black lines. Haplotypes H1, H2 (yellow circles) = '*ruficus*'; H3, H4 (light green circles) = '*vanessae*'; H5 (grey circle) = '*cf. tibialis* white cocoons'; H6, H7 (orange circles) = '*trivaliae* sp. nov.'; H8–H12 (blue circles) = '*tibialis* 1'; H13–H15 (light blue circles) = '*tibialis* 2'; H16, H17 (purple circles) = '*ofella*'; H18–H20 (pink circles) = '*xylina* 1'; H21–H39 (turquoise circles) = '*xylina* 2'; H40–H43 (white circles) = '*xylina* 3'; H44–H46 (green circles) = '*yakutatensis* 1'; H47–H56 (red circles) = '*yakutatensis* 2'.

not initially be determined morphologically with sufficient certainty and were designated as '*Cotesia* sp.' Additionally, out of three reared series (ex *Orthosia gracilis* (Denis & Schiffermüller, 1775)) of this species from Scotland, and a non-reared series from England (Suppl. material 1: table S1), two were initially determined as *C. tibialis*, and two as *Cotesia* cf. *tibialis*. Molecular analysis clustered these specimens within the '*C. trivaliae* sp. nov.' group. Two haplotypes (H6, H7) were identified with a genetic distance of 0.2%. This particular group is distinguished from other groups with a genetic distance ranging from 2.0 to 8.7%. Lower average distances were detected in comparison with '*tibialis* 1', '*tibialis* 2', '*xylina* 2' and '*xylina* 3' (Table 2). Also, this group differs from *C. ofella* by 3.3%.

Description of the new species

Cotesia trivaliae Žikić & Shaw, sp. nov.

<https://zoobank.org/734CD2C6-46EF-4443-8427-2E52A48B5D5D>

Figs 5, 6

Diagnosis. The new species shares some morphological similarities with *C. tibialis*, including the shape of the first metasomal tergite (T1) laterally, with a medial keel near the proximal part, and the apical truncation of the hypopygium (features used by Nixon (1974) to characterise *C. tibialis*). Additionally, the coloration of the legs, particularly the presence of a dark spot on the apical part of the otherwise reddish yellow hind femora, is similar to that described by Nixon (1974) for the early summer brood of his concept of *C. tibialis*, and there is a spine (albeit extremely weak) on the fifth segment of the fore tarsus. The ovipositor sheath is as short as in *C. tibialis*, and the aedeagus is similarly shaped in the two species. However, *C. trivaliae* sp. nov. can be clearly distinguished from *C. tibialis* based on the following characteristics: male antenna is completely brown in *C. trivaliae* sp. nov., while in *C. tibialis* 4–5 apical segments are yellowish. The length index of the 1st and the 2nd part of discoides (1-CU1) / (2-CU1) of fore wings is about 0.7 in *C. trivaliae* sp. nov., relative to *C. tibialis* where this ratio is 0.8–0.9. Dorsally, (T1) length/width index ranges from 0.9 to 1.1 in *C. trivaliae* sp. nov., while it is 1.2–1.3 in *C. tibialis*. Communal cocoons in *C. trivaliae* sp. nov. are spun differently from those of *C. tibialis*, also *C. ofella*. In *C. tibialis* and *C. ofella* (Fig. 6D–F), they are fluffy to varying degrees, and individual cocoons are not visible because they are covered with very densely spun communal silk. Consequently, the structure appears as a ball mass 15–25 mm in length and about 10 mm in width. Cocoon masses of *C. trivaliae* sp. nov. are more oblong, usually 10–15 mm long and 5–6 mm wide, and much less fluffy, with at least some individual cocoons visible through sparsely spun silk. The average genetic distance revealed above between *C. trivaliae* sp. nov. and other morphologically similar taxa indicates that it is a different species. The only known host of *C. trivaliae* sp. nov. is *Orthosia gracilis*, substantially different from the known hosts of the close taxa, although it must have other as yet undiscovered hosts to enable it to complete its annual cycle.

Type material. *Holotype*: POLAND ♀; Kampinos National Park, Granica; 05.VI.2018; ex cocoon mass in grassland; V. Žikić leg.; dry mounted. Paratypes: POLAND 41 ♀ 29 ♂; Kampinos National Park, Granica; 05.VI.2018; ex same brood (3 ♀ 3 ♂ dry mounted, 3 ♀ 3 ♂ microscopic slide mounted, 1 ♀ barcoded, the rest kept 34 ♀ 23 ♂ in 96% alcohol); POLAND 40 ♂; Kampinos National Park, Granica, 05.VI.2018, (1 ♂ barcoded, 3 ♂ dry mounted, 1 ♂ microscopic slide mounted, 35 ♂ in 96% alcohol); “same data as for preceding” 15 ♀ 12 ♂ (1 ♀ barcoded, 3 ♀ 3 ♂ dry mounted, 3 ♀ 1 ♂ microscopic slide mounted, 8 ♀ 8 ♂ in 96% alcohol); “same data as for preceding” 54 ♀ 6 ♂ (1 ♀ barcoded, 3 ♀ 3 ♂ dry mounted, 3 ♀ 1 ♂ microscopic

slide mounted, the rest kept in 96% alcohol); V. Žikić leg.; SLOVENIA 1 ♀; Ljubljana; ex *Orthosia* sp.; 01.VI.2018; Š. Modic leg.; (1 ♀ barcoded, slide mounted); GREAT BRITAIN 28 ♀ 16 ♂ Scotland, Berwickshire, Foulden ex *Orthosia gracilis*, collected 10.VI.2017, (17 ♀ 5 ♂ barcoded; 8 ♀ 11 ♂ barcoded; 3 ♀ from a further brood of low emergence; VII.2017; M. R. Shaw leg.; GREAT BRITAIN 1 ♀ 1 ♂; Scotland, Fife, Fleecefauld, ex *O. gracilis* collected 14.VII.2012, emerged 04.VIII.2012 (1 ♀ 1 ♂ barcoded); M. R. Shaw leg.; GREAT BRITAIN 3 ♀; England, Kent, Swanscombe, ex cocoon mass collected on *Phragmites australis* 10.IV.2017, emerged 02.V.2017 (3 ♀ barcoded) M. Jennings leg.

Depositories. The holotype ♀ of *C. trivaliae* sp. nov., and paratypes have been deposited in the collection of the Faculty of Sciences and Mathematics, the University of Niš, Serbia. A single female from Slovenia has been deposited in the collection of the Faculty of Sciences and Mathematics, the University of Niš, Serbia. Additionally, 3 ♀ 3 ♂ from Poland, as well as all specimens from Great Britain have been deposited at the Department of Natural Sciences, National Museums of Scotland.

Etymology. The new species is named in honour of the gothic rock band Trivalia.

Distribution. The currently known distribution of the new species is Poland, Slovenia and the UK (England and Scotland).

Description. Female: (Fig. 5). Body length 2.6 mm (range 2.5–2.7 mm) (Fig. 5A).

Head: In frontal view (Fig. 5B), about 1.6 times as wide as long (from widest eye to eye), temple about 0.9 times as long as eye at first narrowing behind roundly, ocelli in moderately low triangle (Fig. 5D), diameter between anterior/posterior ocelli and between posterior ocelli 0.5. Index of intertentorial distance/tentori-ocular distance = 2.7. Face above clypeus smooth, while below antennal sockets sculptured. Stemmaticum and vertex smooth. Antennae (Fig. 5N) as long as body, 1st flagellar segment as long as 2nd, penultimate segment 2.2 times shorter than 1st, length/width of penultimate segment = 1.1, last segment 1.4 times longer than penultimate, pointed at apex.

Mesosoma: Mesoscutum in dorsal view (Fig. 5G) punctate, middle part slightly rugose, prescutellar sulcus deep, with 9 foveae. Scutellum smooth and shiny, with about thirty punctures. Propodeum (Fig. 5K) strongly rugose, median keel completely developed. Mesopleuron (Fig. 5C) in larger part shiny, marginally sculptured bearing dense setae, mid-mesoscutal line large with 24–25 deep punctures. Metapleuron rugose, small lower area smooth and shiny.

Legs: Fore leg spine on 5th tarsomere present, extremely weak; hard to see (Fig. 5L). Hind leg (Fig. 5M) with femur 3.9 times as long as wide, tibial spurs subequal, inner spur not reaching middle of hind basitarsus.

Wings: Fore wing length 2.5 mm (range 2.4–2.5 mm), and 2.5 times as long as wide at maximal distances (Fig. 5E), pterostigma 2.2 times longer than wide, metacarp (1-R1) about as long as pterostigma, 1st part of discoideus (1-CU1) about 0.7 times as long as 2nd (2-CU1), vein (cu-a) 0.4 times as short as (CU1), with posterior third bent forward. Hind wing 4.3 times as long as wide at maximal distances, vannal lobe straight without setae in mid part (Fig. 5F).

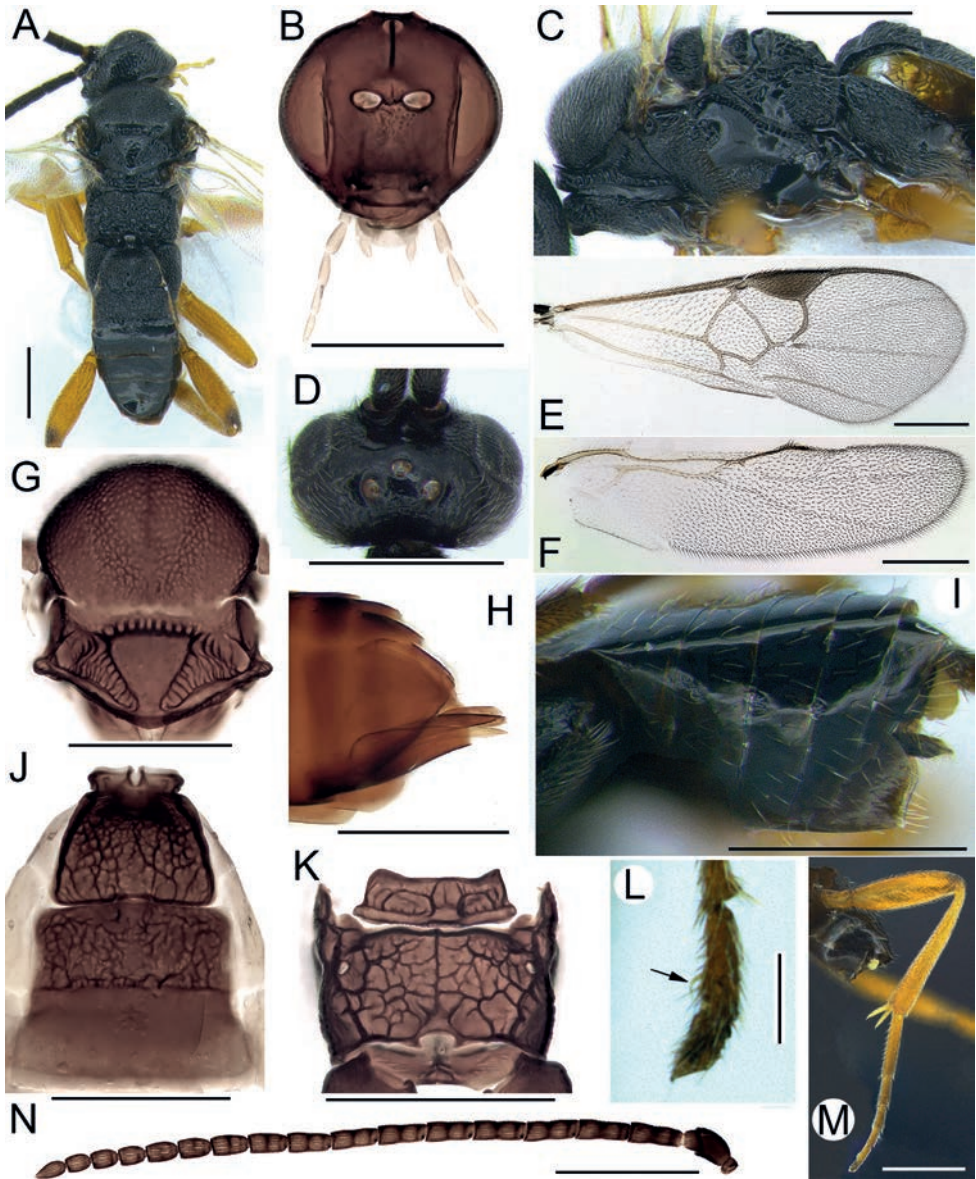


Figure 5. *Cotesia trivaliae* sp. nov. female **A** habitus **B** head frontal view **C** mesosoma and T1 lateral view **D** head dorsal view **E** fore wing **F** hind wing **G** mesoscutum dorsal view **H** ovipositor lateral view **I** metasoma lateral view **J** metasoma dorsal view (T1-T3) **K** propodeum dorsal view **L** 5th tarsomere of front leg, arrow points spine **M** hind leg outer face **N** antenna. Scale bars: 500 µm (**A–K, M, N**); 100 µm (**L**).

Metasoma: In dorsal aspect T1 heavily rugose all over, widened behind (Fig. 5J), almost as long as wide, in profile T1 bearing conspicuous short medial keel (Fig. 5C). Second tergite (T2) rectangular, 0.4–0.5 times as long as wide, sculptured, posterior margin crenulate (Fig. 5J). Third tergite (T3) almost equal to second, smooth, shiny,

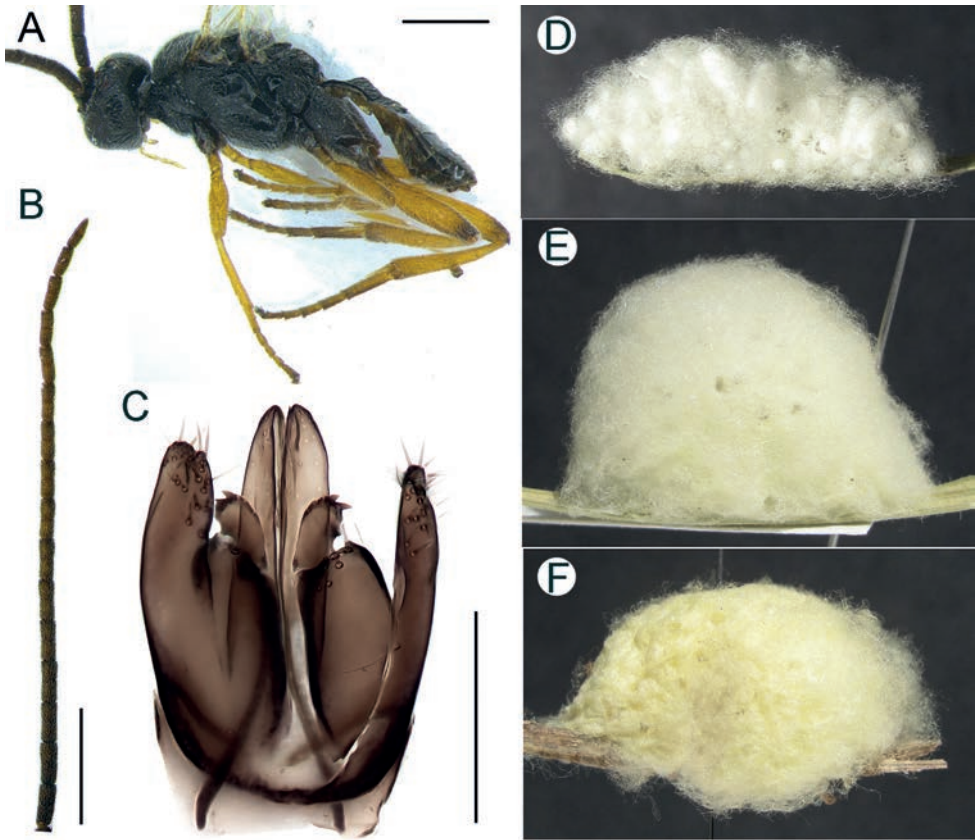


Figure 6. *Cotesia trivaliae* sp. nov., male (A–C) **A** habitus **B** antenna **C** aedeagus ventral view; cocoon masses (D–F) **D** *C. trivaliae* sp. nov. **E** *C. tibialis* **F** *C. ofella*. Scale bars: 500 μ m (A, B); 100 μ m (C).

slightly sculptured at mid base, bearing sparsely distributed hairs practically in a single row (Fig. 5J). Hypopygium in lateral view short, truncate at apex (Fig. 5I). Last tergite in line with apex of hypopygium (Fig. 5I). Ovipositor sheath short (Fig. 5H).

Colour: Head, mesosoma including tegula, all coxae and metasoma black. Trochanter brownish, rest of leg parts yellowish; hind femora apically with small dark spot. Antennae brown. Palpi yellow. Wing venation distinctly yellowish to brown, metacarp, pterostigma and radialis brown.

Male: (Fig. 6 A–C). Morphology and colouration (Fig. 6A) similar to female except for sexual characters. All antennal segments (Fig. 6B) brown, antenna about 1.2 times as long as body. Aedeagus (Fig. 6C) with two-toothed digiti at apex, teeth well developed, relatively large and sharp, digitus length/width ratio = 2.1, digitus 2.8 times as short as volsella, cuspis inconspicuous.

Cocoon mass: (Fig. 6D). Relatively small, usually elongated, 10–15 mm long, and about 5–6 mm wide, weakly fluffy, communal silk sparsely spun over individual cocoons leaving them partly visible, light-yellow coloured.

Discussion

Analysis of the barcode sequences of selected parasitoid species from the genus *Cotesia* shows clear separation of some taxa, as well as close relatedness among a significant number of others. What is common to the presently analysed species of *Cotesia* that make ball-like cocoon masses is that all of them parasitize members of the family Noctuidae, probably exclusively except for *C. vanessae* (*C. ruficrus* is considered to be outside this strict grouping, see below). The Bayesian tree (Figs 2, 3, Suppl. material 1: fig. S1) and the Median-joining network (Fig. 4) clarified somewhat a separation of 12 provisional clades to which names were assigned: ‘*ruficrus*’; ‘*vanessae*’; ‘*ofella*’; ‘cf. *tibialis* white cocoons’; ‘*Cotesia* sp (= now *trivaliae* sp. nov.)’; ‘*yakutatensis* 1’; ‘*yakutatensis* 2’; ‘*tibialis* 1’; ‘*tibialis* 2’; ‘*xylina* 1’; ‘*xylina* 2’; ‘*xylina* 3’.

Molecular analyses confirmed evident delineation as separate entities for the haplotypes of the specimens determined as *C. ruficrus*, *C. vanessae*, *C. ofella*, *C. trivaliae* sp. nov. (see below) and, for *C. yakutatensis*, two entities ‘*yakutatensis* 1’ and ‘*yakutatensis* 2’. The large genetic difference between *C. ruficrus* and the other *Cotesia* is reflected in as many as 30 mutations from the bifurcation spot, as shown in the haplotype network (Fig. 4). Too little sampling of the probably much more complex *C. ruficrus* has been done to comment on its integrity in a wider context.

All the *Cotesia* species studied here exclusively use noctuid larvae to complete their annual life cycle except *C. vanessae* which (at least in Europe) parasitises a restricted group of hosts from the Nymphalidae (Nymphalinae) during summer. These, however, do not overwinter in the larval stage, and *C. vanessae* critically depends, like the others, on overwintering as larvae inside overwintering noctuid larvae that either diapause or feed only sporadically through the winter, especially low-feeding or sub-surface resting species in the subfamilies Noctuinae and Plusiinae. It seems possible that the summer hosts of *C. vanessae* reflect an extension from its ancestral host repertoire. *Cotesia vanessae* differs from the other 11 defined groups with a genetic distance in the range of 6.4–7.8%.

In the case of *C. yakutatensis* specimens of North American origin included in this analysis, there is a clear discrimination between ‘*yakutatensis* 1’ and ‘*yakutatensis* 2’ as two separate lineages. Their within-group genetic distances are significantly lower than the between-group distance (Table 2; Figs 2–4). Considering that this parasitoid may have a narrow host repertoire (but see below), with only four species recorded (see details above in the Introduction section), this finding is potentially of interest for morphological re-examination and further investigation of possible host-associated genetic divergence patterns. This is important if *C. yakutatensis* is ever to be tested as a potential biological control agent since one of its reported hosts is *Autographa californica*, a pest of great economic importance in Canada and the USA (Vail et al. 1989). It should, however, be borne very much in mind that the rearing of parasitoids from their hosts in N. America is in its infancy in comparison with European efforts, and the apparently narrow host repertoire of *C. yakutatensis* (*sensu lato*) is quite likely an artifact due to low sampling; furthermore, none of the sequenced specimens was reared from known hosts.

DNA barcoding showed no clear discrimination between the specimens from groups 'tibialis 1', 'tibialis 2', 'cf. tibialis white cocoons', 'xylina 1', 'xylina 2' and 'xylina 3'. *Cotesia tibialis* is already considered to be a complex of species with variable morphology of the body, wings and cocoon (e.g., Nixon 1974). Considering the many synonyms related to *C. tibialis*, as well as Nixon's attempt to decipher this species complex, the results we obtained indicate that in addition to the morphological variability observed, it is indeed a genetically very variable taxon, which forms three groups in our analyses (Fig. 2 and Suppl. material 1: fig. S1). In addition, this is also confirmed by the many haplotypes detected in this group. Furthermore, these three *C. tibialis* groups were mixed with three more groups that were formed from the taxon previously identified as *C. xylina*. In this analysis, *C. xylina* was found to have even more haplotypes than *C. tibialis*, as many as 26; even though some specimens may have been misidentified, it is also likely that *xylina* comprises a complex of species. Unfortunately, none of the barcoded specimens had a known host. The DNA barcodes for *C. xylina* were taken from public databases which had been obtained from specimens sampled in Canada and the USA, from different localities, sometimes separated by significant geographical distances. In short, *C. xylina* appears to be a genetically diverse species, in a way similar to *C. tibialis*. Although these two species inhabit different geographical regions, the genetic distances between them are generally small (Table 2). The clade 'cf. tibialis white cocoons' resulting from white cocoons collected in Poland differs from 'xylina 1' (Canada) which also spins white cocoons, by only 1.1%. Such a low percentage of genetic distance often indicates merely intraspecific variability. Unfortunately, the available material was collected from already-spun cocoon masses found on grass and conclusions on the closeness of these two groups/species are troublesome without knowing their hosts.

There is a definite separation between the groups 'tibialis 1' and 'tibialis 2'. Thus 'tibialis 1' is connected with 'cf. tibialis white cocoons' and 'xylina 1', whereas 'tibialis 2' is genetically close to the segregates 'xylina 2' and 'xylina 3'. Based on the admittedly small number of identified caterpillars for the samples included in the analysis, it seems that this separation is reflected by the hosts. While 'tibialis 1' was reared from several hosts (the overwintering hosts *Noctua interposita* (Hübner, 1790) and *Xestia xanthographa* (Denis & Schiffermüller, 1775) both collected in Austria, and the summer hosts *Cucullia chamomillae* (Denis & Schiffermüller, 1775) from Finland and *Anarta myrtilli* (Linnaeus, 1761) from Germany), 'tibialis 2' was reared only from *Mythimna conigera* (Denis & Schiffermüller, 1775) collected in Serbia.

Finally, within *Cotesia tibialis* (*sensu lato*), we found a third group 'cf. tibialis white cocoons'. It stands in a common lineage with 'xylina 1' but is distant from the other 'xylina' groups and also 'tibialis 2', though still not enough to be identified as a potentially new taxon (Table 2) and we are further hampered by lacking precise data on the hosts.

Cotesia ofella could be discriminated as a separate lineage, being closest to *C. trivaliae* sp. nov. (Fig. 2 and Suppl. material 1: fig. S1). Unlike the great haplotype diversity found in *C. tibialis*, *C. xylina*, and *C. yakutatensis*, the species *C. ofella* molecular data is less variable. This narrowly oligophagous species was obtained from

several low-feeding hosts that belong to the subfamily Noctuinae (*Noctua comes* (Hübner, 1813) and *N. fimbriata* (Schreber, 1759)), and the subfamily Acronictinae (*Acronicta rumicis* and *Simyra albovenosa* (Goeze, 1781)). In addition, there are several series in the National Museums of Scotland from *Acronicta auricoma*, another low-feeding species, but these specimens have not been sequenced and so are not included in this study. However, it is clear that Acronictinae are the summer hosts and Noctuinae the overwintering ones. The analysed 20 samples were collected in several distant territories such as France, Great Britain, Hungary, Poland, Slovenia, and several spots in Serbia (Suppl. material 1: table S1). Regardless of its wide distribution and several host species from which it was reared, only two barcode haplotypes were detected differing by a single mutation (Fig. 4).

Seven specimens clustered in the separate group initially marked as ‘*Cotesia* sp.’ but described above as *C. trivaliae* sp. nov. are the only ones collected from caterpillars of the genus *Orthosia* (the single species *O. gracilis*, which is one of the few in the genus that is low-feeding rather than arboreal). Based on the general morphology of the adult body and the architecture and colour of the cocoon, they were originally identified as, or close to, *C. tibialis*. They are closely related to the *tibialis*–*xylina* groups, but genetically, morphologically, and biologically distinct enough to be described as a new species. It is crucial that we are able to describe this species as new because it differs morphologically from the concept of *C. tibialis* and synonyms as defined by their type specimens, and also because our reared material presents a consistent host repertoire that (although possibly incompletely known) is distinct. But the situation regarding the other probable new species involved in the *C. tibialis*, *C. xyлина* and *C. yakutatensis* complexes is far more problematic. In the first place, we have no molecular data for the relevant type specimens that would be needed to fix the use of available names, and neither permissions nor resources to try to obtain that. Second, biological data for the specimens analysed genetically is almost entirely lacking, so the important consideration of host repertoire differences cannot be addressed at this time. We recognise that rearing fresh material is a necessity for further progress, with next-generation techniques to obtain DNA from the old specimens in collections deemed to have reliable host data a further possibility – and we hope that this preliminary study will prompt and help to enable that. Third, a thorough morphological study of the sequenced specimens (and the relevant types, and reared specimens beyond our own) is necessary; but it is premature to conduct that until we can incorporate more reared material that still needs to be obtained. Thus, our study is held at this preliminary phase, but it is hoped that our results will promote further research that is clearly warranted.

Acknowledgements

In this extensive work, the following helped us a lot: Aleksandra Petrović, Slobodan Stevčić, Korana Kocić, Jelisaveta Čkrkić, Andjeljko Petrović, Željko Tomanović, Špela Modic. The authors thank Nigel Spring for the photo (Fig. 1A) he provided. This study

is partly founded by the Ministry of Science, Technological Development and Innovation of the Republic of Serbia (Contract No. 451-03-65/2024-03/200124, 451-03-66/2024-03/200124 and 451-03-47/2023-01/200010). Comments from reviewers Eduardo Shimbori, Mike Sharkey and Anon. greatly helped us to improve the manuscript.

References

- Achterberg C van (1993) Illustrated key to the subfamilies of the Braconidae (Hymenoptera: Ichneumonoidea). Zoologische Verhandlungen 283: 1–189. <https://repository.naturalis.nl/pub/317645/ZV1993283001.pdf>
- Avila GA, Berndt LA, Holwell GI (2013) First releases and monitoring of the biological control agent *Cotesia urabae* Austin and Allen (Hymenoptera: Braconidae). New Zealand Entomologist 36(2): 65–72. <https://doi.org/10.1080/00779962.2012.744908>
- Bandelt HJ, Forster P, Röhl A (1999) Median-joining networks for inferring intraspecific phylogenies. Molecular Biology and Evolution 16(1): 37–48. <https://doi.org/10.1093/oxford-journals.molbev.a026036>
- Brodeur J (1992) Caterpillars are more than a nutrient reservoir for parasitic wasps. Proceedings, Experimental and Applied Entomology, Netherlands Entomological Society 33: 57–61.
- Clancy DW (1969) Parasitization of cabbage and alfalfa loopers in southern California. Journal of Economic Entomology 62(5): 1078–1083. <https://doi.org/10.1093/jee/62.5.1078>
- Cruaud A, Jabbour-Zahab R, Genson G, Cruaud C, Couloux A, Kjellberg F, Noort S van, Rasplus JY (2010) Laying the foundations for a new classification of Agaonidae (Hymenoptera: Chalcidoidea), a multilocus phylogenetic approach. Cladistics 26(4): 359–387. <https://doi.org/10.1111/j.1096-0031.2009.00291.x>
- Driesche RG van (2008) Biological control of *Pieris rapae* in New England: host suppression and displacement of *Cotesia glomerata* by *Cotesia rubecula* (Hymenoptera: Braconidae). Florida Entomologist 91: 22–25. [https://doi.org/10.1653/0015-4040\(2008\)091\[0022:BCOPRI\]2.0.CO;2](https://doi.org/10.1653/0015-4040(2008)091[0022:BCOPRI]2.0.CO;2)
- Fernández-Triana J, Shaw MR, Boudreault C, Beaudin M, Broad GR (2020) Annotated and illustrated world checklist of Microgastrinae parasitoid wasps (Hymenoptera, Braconidae). ZooKeys 920: 1–1089. <https://doi.org/10.3897/zookeys.920.39128>
- Folmer O, Hoeh WR, Black MB, Vrijenhoek RC (1994) Conserved primers for PCR amplification of mitochondrial DNA from different invertebrate phyla. Molecular Marine Biology and Biotechnology 3(5): 294–299. https://www.mbari.org/wp-content/uploads/2016/01/Folmer_94MMBB.pdf
- Franklin HJ (1950) Cranberry insects in Massachusetts. Bulletin of Massachusetts Agricultural Experiment Station 445: 1–88. <https://content.wisconsinhistory.org/digital/collection/cran/id/2668>
- Germain JF, Chatot C, Meusnier I, Artige E, Rasplus JY, Cruaud A (2013) Molecular identification of *Epitrix* potato flea beetles (Coleoptera: Chrysomelidae) in Europe and North America. Bulletin of Entomological Research 103(3): 354–362. <https://doi.org/10.1017/S000748531200079X>

- Gupta A, Fernández-Triana J (2014) Diversity, host association, and cocoon variability of reared Indian Microgastrinae (Hymenoptera: Braconidae). *Zootaxa* 3800(1): 1–101. <https://doi.org/10.11646/zootaxa.3800.1.1>
- Hervet VAD, Murillo H, Fernández-Triana JL, Shaw MR, Laird RA, Floate KD (2014) First report of *Cotesia vanessae* (Hymenoptera: Braconidae) in North America. *The Canadian Entomologist* 146(5): 560–566. <https://doi.org/10.4039/tce.2014.9>
- Jiang N, Sétamou M, Ngi-Song AJ, Omwega CO (2004) Performance of *Cotesia flavipes* (Hymenoptera: Braconidae) in parasitizing *Chilo partellus* (Lepidoptera: Crambidae) as affected by temperature and host stage. *Biological Control* 31(2): 155–164. <https://doi.org/10.1016/j.biocontrol.2004.06.002>
- Karimpour Y, Fathipour Y, Talebi AA, Moharramipour S (2001) Report of two endoparasitoid wasps, *Cotesia ofella* Nixon and *Cotesia vanessae* Reinhard (Hym.: Braconidae) on larvae of *Simyra dentinosa* Freyer (Lep.: Noctuidae) from Iran. *Journal of Entomological Society of Iran* 21(2): 105–106. https://jesi.areeo.ac.ir/article_107869_f0a3160840953199f-10c8e9e58e99b62.pdf?lang=en
- Lazarević M, Stanković SS, Achterberg C van, Marczak D, Modić Š, Ilić Milošević M, Trajković A, Žikić V (2023) Morphological and genetic variability of *Cotesia tibialis* species complex (Hymenoptera: Braconidae: Microgastrinae). *Zoologischer Anzeiger* 302: 58–66. <https://doi.org/10.1016/j.jcz.2022.10.007>
- Librado P, Rozas J (2009) DnaSP v5: a software for comprehensive analysis of DNA polymorphism data. *Bioinformatics* 25(11): 1451–1452. <https://doi.org/10.1093/bioinformatics/btp187>
- Marsh PM (1979) Braconidae. Aphidiidae. Hybrizontidae. In: Krombein KV, Hurd Jr PD, Smith DR, Burks BD (Eds) *Catalog of Hymenoptera in America north of Mexico*. Smithsonian Institution Press, Washington, 144–313.
- Miller JC, West KJ (1987) Host specificity of *Cotesia yakutatensis* (Hym: Braconidae) on Lepidoptera in peppermint and alfalfa [*Autographa californica*, *Trichoplusia ni*, *Peridroma saucia*, *Mamestra configurata*, *Agrotis ipsilon*, *Dargida procineta*, *Xestia adela*]. *Entomophaga* 32(3): 227–232. <https://doi.org/10.1007/BF02373244>
- Mitrović M, Tomanović Ž (2018) New internal primers targeting short fragments of the mitochondrial CO1 region for archival specimens from the subfamily Aphidiinae (Hymenoptera, Braconidae). *Journal of Hymenoptera Research* 64: 191–210. <https://doi.org/10.3897/jhr.64.25399>
- Muesebeck CFW (1921) A revision of the North American species of ichneumon-flies belonging to the genus *Apanteles*. *Proceedings of the United States National Museum* 58: 483–576. <https://doi.org/10.5479/si.00963801.2349.483>
- Nixon GEJ (1965) A reclassification of the tribe Microgasterini (Hymenoptera: Braconidae). *Bulletin of the British Museum (Natural History) (Entomology) Supplement 2*: 1–284. <https://doi.org/10.5962/p.144036>
- Nixon GEJ (1974) A revision of the north–western European species of the *glomeratus*–group of *Apanteles* Foerster (Hymenoptera, Braconidae). *Bulletin of Entomological Research* 64: 453–524. <https://doi.org/10.1017/S0007485300031333>
- Noyes JS (1994) The reliability of published host-parasitoid records: a taxonomist's view. *Norwegian Journal of Agricultural Science* 16: 59–69. <https://nmbu.brage.unit.no/nmbu-xmlui/>

- bitstream/handle/11250/3007527/Norwegian%20Journal%20of%20Agricultural%20Sciences%20-%20Supplement%20No%2016%201994.pdf?sequence=1&isAllowed=y
- Overholt WA, Ngi-Song AJ, Omwega CO, Kimani-Njogu SW, Mbabila J, Sallam MN, Ofomata V (1997) A review of the introduction and establishment of *Cotesia flavipes* Cameron in East Africa for biological control of cereal stemborers. *International Journal of Tropical Insect Science* 17(1): 79–88. <https://doi.org/10.1017/S1742758400022190>
- Papp J (1986) A survey of the European species of *Apanteles* Först. (Hymenoptera, Braconidae: Microgastrinae), IX. The *glomeratus*-group, 1. *Annales historico-naturales Musei Nationalis Hungarici* 78: 225–247. <https://eurekamag.com/research/004/637/004637899.php>
- Papp J (1987) A survey of the European species of *Apanteles* Först. (Hymenoptera, Braconidae: Microgastrinae), X. The *glomeratus*-group 2 and the *cultellatus*-group. *Annales historico-naturales Musei Nationalis Hungarici* 79: 207–258. http://publication.nhnm.hu/pdf/annHNHM/Annals_HNHM_1987_Vol_79_207.pdf
- Rambaut A (2006–2009) FigTree – Tree Fig. Drawing Tool ver 1.3.1. Institute of Evolutionary Biology, University of Edinburgh. <http://tree.bio.ed.ac.uk/software/figtree/>
- Razowski J, Wiackowski SK (1999) Contribution to the knowledge of Braconidae (Hymenoptera), parasitoids of Lepidoptera. *Wiadomosci Entomologiczne* 18(4): 247–250. https://sparrow.up.poznan.pl/pte/we/archiw/WE18_4.pdf
- Roberts SJ, Mellors WK, Armbrust EJ (1977) Parasites of lepidopterous larvae in alfalfa and soybeans in central Illinois. *Great Lakes Entomologist* 10(3): 87–93. <https://www.cabdirect.org/cabdirect/abstract/19770549472>
- Ronquist F, Huelsenbeck JP (2003) MrBayes 3: Bayesian phylogenetic inference under mixed models. *Bioinformatics* 19(12): 1572–1574. <https://doi.org/10.1093/bioinformatics/btg180>
- Shaw MR, Huddleston T (1991) Classification and biology of braconid wasps (Hymenoptera: Braconidae). *Handbooks for the Identification of British Insects*. Royal Entomological Society of London 7(11): 1–126. https://www.royensoc.co.uk/wp-content/uploads/2022/01/Vol07_Part11.pdf
- Shaw MR (1994) Parasitoid host ranges. In: Hawkins BA, Sheehan W (Eds) *Parasitoid Community Ecology*. Oxford University Press, 111–144. <https://doi.org/10.1093/oso/9780198540588.003.0007>
- Shaw MR (2007) The species of *Cotesia* Cameron (Hymenoptera: Braconidae: Microgastrinae) parasitising Lycaenidae (Lepidoptera) in Britain. *British Journal of Entomology and Natural History* 20(4): 255–267. http://filming-varwild.com/articles/mark_shaw/231_Cotesia_Lyc.pdf
- Shaw MR, Stefanescu C, Nouhuys S van (2009) Parasitoids of European butterflies. In: Settele J, Shreeve T, Konvička M, Dyck HV (Eds) *Ecology of Butterflies of Europe*. Cambridge University Press, 130–156. <http://www.eeb.cornell.edu/saskyavndata/uploads/pdf/shaw-stefanescu-vsvn-2009.pdf>
- Shaw MR (2023) Obtaining, recording and using host data for reared parasitoid wasps (Hymenoptera). *British Journal of Entomology and Natural History* 36: 205–213.
- Tamura K, Nei M (1993) Estimation of the number of nucleotide substitutions in the control region of mitochondrial DNA in humans and chimpanzees. *Molecular Biology and Evolution* 10(3): 512–526. <https://doi.org/10.1093/oxfordjournals.molbev.a040023>

- Tamura K, Peterson D, Peterson N, Stecher G, Nei M, Kumar S (2011) MEGA5: molecular evolutionary genetics analysis using maximum likelihood, evolutionary distance, and maximum parsimony methods. *Molecular Biology and Evolution* 28(10): 2731–2739. <https://doi.org/10.1093/molbev/msr121>
- Vail PV, Pearson AC, Sevacherian V, Henneberry TJ, Reynolds HT (1989) Seasonal incidence of *Trichoplusia ni* and *Autographa californica* (Lepidoptera: Noctuidae) on alfalfa, cotton, and lettuce in the Imperial Valley of California. *Environmental Entomology* 18(5): 785–790. <https://doi.org/10.1093/ee/18.5.785>
- Wylie HG, Bucher GE (1977) The bertha armyworm, *Mamestra configurata* (Lepidoptera: Noctuidae). Mortality of immature stages on the rape crop, 1972–1975. *The Canadian Entomologist* 109(6):823–837. <https://doi.org/10.4039/Ent109823-6>
- Yu DSK, Achterberg C van, Horstmann K (2016) Taxapad 2016, Ichneumonoidea 2015. Database on flash-drive. Nepean, Ontario. <https://doi.org/10.48580/dfp3-39v>

Supplementary material I

Supplementary information

Authors: Vladimir Žikić, Milana Mitrović, Saša S. Stanković, José L. Fernández-Triana, Maja Lazarević, Kees van Achterberg, Dawid Marczak, Marijana Ilić Milošević, Mark R. Shaw

Data type: docx

Explanation note: **table S1.** The list of *Cotesia* specimens submitted to the molecular analyses. **fig. S1.** A Bayesian tree inferred from the CO1 barcoding fragments of *Cotesia* specimens.

Copyright notice: This dataset is made available under the Open Database License (<http://opendatacommons.org/licenses/odbl/1.0/>). The Open Database License (ODbL) is a license agreement intended to allow users to freely share, modify, and use this Dataset while maintaining this same freedom for others, provided that the original source and author(s) are credited.

Link: <https://doi.org/10.3897/jhr.97.116378.suppl1>

Discovery of a new *Pseudalomya* Telenga, 1930 (Hymenoptera, Ichneumonidae, Ichneumoninae) species from Taiwan and its implications for the systematic position of this genus

Hsuan-Pu Chen¹, Namiki Kikuchi^{2,3}, Shiu-Feng Shiao¹

1 Department of Entomology, National Taiwan University, No. 1, Sec. 4, Roosevelt Rd., Da'an Dist., Taipei 106, Taiwan **2** Toyohashi Museum of Natural History, 1-238 Oana, Oiwa, Toyohashi, Aichi 441-3147, Japan **3** Systematic Zoology Laboratory, Department of Biological Sciences, Graduate School of Science, Tokyo Metropolitan University, 1-1 Minamiosawa, Hachioji-shi, Tokyo, 192-0397, Japan

Corresponding author: Shiu-Feng Shiao (sfshiao@ntu.edu.tw)

Academic editor: Tamara Spasojevic | Received 25 January 2024 | Accepted 21 March 2024 | Published 9 April 2024

<https://zoobank.org/4C51A1B9-275F-448E-B940-3D544E25B1FE>

Citation: Chen H-P, Kikuchi N, Shiao S-F (2024) Discovery of a new *Pseudalomya* Telenga, 1930 (Hymenoptera, Ichneumonidae, Ichneumoninae) species from Taiwan and its implications for the systematic position of this genus. Journal of Hymenoptera Research 97: 277–296. <https://doi.org/10.3897/jhr.97.119470>

Abstract

The rare genus *Pseudalomya* Telenga comprises two species, which are found only in the Eastern Palearctic region and high mountains of the Oriental region. The phylogenetic position of *Pseudalomya* remains unclear because of its intermediate morphology between two ichneumonine tribes, Alomyini and Phaeogenini. This article reports the discovery of a new species of *Pseudalomya*: *Pseudalomya truncaticornis* **sp. nov.** Specimens were collected during a survey of insect fauna in the Dasyueshan area of Shei-Pa National Park, one of the high-altitude regions in Taiwan. The new species can be diagnosed by its body coloration, frontal horn shape, facial punctures, metasomal tergite sculpture, and wing venation. To the best of our knowledge, this is the first record of *Pseudalomya* in Taiwan. This article also presents a diagnostic key to the global species of *Pseudalomya*. In this study, molecular phylogenetic analyses were performed using one mitochondrial and two nuclear gene sequences from *P. truncaticornis* **sp. nov.** and other members of the Ichneumoniformes group. The results indicate that *Pseudalomya* should be classified within Phaeogenini, distinct from Alomyini, but more comprehensive phylogenomic studies are needed to confirm this placement.

Keywords

COI, high-altitude, molecular phylogeny, 28S, taxonomy

Introduction

Pseudalomya Telenga, 1930 is a rare genus comprising two valid species: *P. praevara* Telenga, 1930 and *P. nepalensis* Riedel, 2019. Their distribution is restricted to the Eastern Palaearctic region and high mountains of the Oriental region (Yu et al. 2016; Riedel 2019). Another previously described *Pseudalomya* species from Japan – *P. takeii* Kusigemati, 1984 – was later confirmed to be a misidentification of an oxytorine species, *Oxytorus corniger* (Momoi, 1965) (Watanabe 2016).

Because *Pseudalomya* exhibits an intermediate morphology between two ichneumonine tribes Alomyini and Phaeogenini, it has generally been placed in both tribes (Laurenne et al. 2006; Quicke et al. 2009; Tereshkin 2009; Quicke 2015; Riedel 2019). Consequently, the tribal status of *Pseudalomya* remains a topic of debate. On one hand, this genus exhibits similarity with Alomyini because of the following characters: horned frons, enlarged vertex and genae, foramen with genae meeting (or almost meeting) ventrally, oval propodeal spiracle, metasomal tergite II without thyridium, and forewing with the second abscissa of M shorter than the first. On the other hand, *Pseudalomya* also exhibits similarity with Phaeogenini because of the following characters: two-segmented trochanter, two-spurred mid tibia, and metasomal tergite I with spiracles located at apical 0.3 (Laurenne et al. 2006; Tereshkin 2009; Riedel 2019).

Phylogenetic hypotheses reconstructed based on 28S D2–D3 rDNA sequences or combined (morphology and 28S) datasets suggested the tribal placement of *Pseudalomya* within the tribe Phaeogenini (Laurenne et al. 2006; Quicke et al. 2009). Consequently, the morphological similarities between *Pseudalomya* and Alomyini were interpreted as either symplesiomorphic traits or the result of convergent evolution (Quicke 2015). However, because of the lack of sampling of this genus in subsequent comprehensive phylogenetic studies (Bennett et al. 2019; Santos et al. 2021), the phylogenetic position of *Pseudalomya* remains *incertae sedis* (Santos et al. 2021).

In this study, we analyzed three *Pseudalomya* specimens that were newly obtained from the high mountains of central Taiwan. The specimens were collected during fauna inspection for the project SP110113: A survey for the selection of insect indicator species and their microhabitat usage in the Daxueshan area of Shei-Pa National Park. After morphological examinations, these specimens were discovered to be distinct from the known species of *Pseudalomya*. On the basis of morphological evidence, the specimens were subsequently validated as a new species, *Pseudalomya truncaticornis* sp. nov. This article describes the new species and presents a key to the global species of female *Pseudalomya*. In this study, the phylogenetic position of *Pseudalomya* was reassessed through multigene phylogenetic analyses.

Materials and methods

Morphological examination

The morphological terms used in this study were identified from Broad et al. (2018). Measurements were performed with reference to Kikuchi and Konishi (2021). The following abbreviations were used in this study: **OOL**, ocello-ocular line; **POL**, postero-ocellar line; **OD**, ocellar diameter; **PSI**, propodeal spiracle index: major axis of propodeal spiracle/minor axis of propodeal spiracle; **1/M**, the first abscissa of forewing M; **2/M**, the second abscissa of forewing M; **NI**, nervellar index of hindwing: length of hindwing CU between M and cu-a/length of cu-a; **T**, metasomal tergite; **S**, metasomal sternite; and **pS**, posterior section of metasomal sternite.

The measurements in parentheses represent the measurements of the holotype. The cuticular microsculpture is described as per a study conducted by Eady (1968). The whole metasomal sternum was observed and dissected using a method developed by Kikuchi and Konishi (2021). The specimens were examined and measured using a microscope (Leica S8 APO; Leica Microsystems, Wetzlar, Germany) with a micrometer. Photographs were taken using a Leica DMC 5400 camera integrated into a Leica Z16 APO microscope equipped with the auto-stacking system Leica LAS V4.13 (all from Leica Microsystems). Line drawings were generated using Procreate (Savage Interactive, Hobart, Australia). All figures were edited and arranged into figure plates by using Adobe Illustrator CC and Photoshop CC (Adobe Systems, San Jose, CA, USA). The specimens and their photos have been deposited at the following institutes: **NMNS**, National Museum of Natural Science, Taichung, Taiwan; **NARO**, Institute for Agro-Environmental Sciences, National Agriculture and Food Research Organization, Tsukuba, Japan; and **SDEI**, Senckenberg Deutsches Entomologisches Institut, Müncheberg, Germany. The Latin term *ibidem*, meaning “same as previous except as follows,” was abbreviated as “ibid” to abridge information on the location of the materials examined.

Taxon sampling

To reassess the phylogenetic position of *Pseudalomya*, 52 operational taxonomic units (OTUs) from 38 ichneumonine genera were analyzed (Suppl. material 1). In addition, other ichneumonids belonging to the Ichneumoniformes group were included as outgroups (Suppl. material 1). These outgroups were selected from the dataset of Santos (2017) and included 24 species from 23 genera of Cryptinae, 11 species from 11 genera of Phygadeuontinae, one species from one genus of Agriotypinae (*Agriotypus armatus*), and one species from one genus of Microleptinae (*Microleptes splendidulus*). For OTUs whose sequences were obtained from an online database, species identification was double-checked using the Basic Local Alignment Search Tool (BLAST) (Altschul et al. 1990) and the position of preliminary phylogenetic reconstruction. Chimera OTUs were constructed for genera lacking available sequences of multiple markers within individual species.

Molecular data collection and analysis

Total genomic DNA was extracted from the right midleg of each specimen by using a DNeasy Blood and Tissue Kit (Qiagen, Düsseldorf, Germany). Partial sequences of the mitochondrial cytochrome c oxidase I gene (*COI*) and two nuclear genes – D2–D3 regions of 28S ribosomal RNA gene (*28S*) and 18S ribosomal RNA gene (*18S*) – served as molecular markers for phylogenetic reconstruction. The sequences were retrieved from GenBank (National Center for Biotechnology Information). Target sequences were amplified through polymerase chain reaction (PCR). The primer pairs and conditions for PCR are listed in Suppl. material 2. The reaction volume was 15 μL : 5.1 μL of sterile distilled water, 0.6 μL of each (forward/reverse) primer (10 μM), 7.5 μL of GoTaq Green Master Mix (Promega, Madison, WI, USA), and 1.2 μL of DNA template. PCR products were purified and sequenced at Tri-I Biotech (Taipei, Taiwan). Sequences were edited using CodonCode Aligner v.10.0.2 (CodonCode Corporation, Dedham, MA, USA).

MAFFT v.7 (Katoh et al. 2019) was used for automated multiple sequence alignments. The default setting was used for the alignment of *COI*. By contrast, the E-INS-I algorithm was used for the alignment of the two nuclear genes (Santos 2017); the alignments of nuclear markers were manually optimized by removing regions with variable lengths and gaps. The translated alignment of *COI* was checked for stop codons by using MEGA v.11 (Tamura et al. 2021). All newly obtained sequences were uploaded on GenBank. The numbering of positions started from the gene's first nucleotide (full-length *COI* sequences served as references for numbering: GenBank accession JX131613 [*Diadromus collaris*] and MG923483 [*Amblyjoppa* sp.]).

Molecular phylogeny

To infer the phylogenetic position of *Pseudalomya*, phylogeny was reconstructed using the following four datasets: *COI*, *28S*, *18S*, and concatenated *18S+28S+COI*. The concatenated dataset was first partitioned by gene and then, for the protein-coding *COI*, also by codon position (first plus second versus third). ModelFinder (Kalyaanamoorthy et al. 2017) with “partition merging” was used for searching the optimal partitioning scheme and substitution models under the Bayesian Information Criteria.

Maximum likelihood (ML) phylogenetic trees were reconstructed using IQ-TREE v.1.6.12 (Nguyen et al. 2015). This program was accessed through the web server W-IQ-TREE (Trifinopoulos et al. 2016), which is available at <http://iqtree.cibiv.univie.ac.at/>. Ten independent ML searches were performed for the concatenated dataset. After, the tree with the highest likelihood score was selected as the best-topology tree. Nodal support was assessed using the ultrafast bootstrap approximation (UFBoot2) method (Hoang et al. 2017) and SH-like approximate likelihood ratio test (SH-aLRT) (Guindon et al. 2010) under the default setting for the ML method. Nodes with an SH-aLRT value of $\geq 80\%$ and a UFBoot value of $\geq 95\%$ were considered to have strong support. For further interpretation of the tribal placement of *Pseudalomya*, the tribal classification system described by Santos et al. (2021) was applied herein.

Results

Taxonomy

Subfamily Ichneumoninae Latreille, 1802

Genus *Pseudalomya* Telenga, 1930

Pseudalomya Telenga, 1930: 107. Type: *Pseudalomya praevara* Telenga, 1930, by original monotypy.

Pseudalomya truncaticornis Chen & Kikuchi, sp. nov.

<https://zoobank.org/5C674A42-79DA-410C-A52C-25191684E0F6>

Figs 1–4

Diagnosis. This species can be distinguished from other congeners in having the following combination of characters: frontal horn short and apically truncated; face sparsely punctate; metasomal tergites smooth with sparse and minute punctures; forewing with 1cu-a distad to M&RS; head reddish brown; mesosoma and legs black; and metasomal tergites metallic-blue.

Material examined. Holotype. TAIWAN • 1♀; Miaoli County, Tai'an Township, Shei-Pa National Park, Mt. Huoshi; 24°22'47.78"N, 121°10'53.67"E (DMS); alt. 3160 m; 25 Aug. 2021–12 May. 2022; Jung-Chang Chen, Kuang-Yao Chen, Li-Jen Chang, Ta-Hsiang Li and Hung-Yang Shen leg.; Malaise Trap; GenBank: PP175350 (COI), PP188485 (28S), PP188484 (18S); Sample ID: SP0060; Voucher: NMNS ENT 8836-1.

Paratypes. TAIWAN • 2♀; *ibid*; GenBank: PP175351 (COI, SP0061), PP175352 (COI, SP0062); Sample ID: SP0061–SP0062; Voucher: NARO (SP0061); NMNS ENT 8836-2 (SP0062).

Description. Female. Head: 1.43–1.75 (1.75)× as wide as deep; antenna with 26–27 (27) flagellomeres; first flagellomere 1.13–1.22 (1.13)× as long as wide and 1.04–1.12 (1.04)× as long as second one; second flagellomere 1.08–1.19 (1.08)× as long as wide, remaining flagellomeres about 1.0× as long as wide; frons strongly and transversely striated; horn laterally depressed, apically truncated or slightly rounded (Figs 2A, 4A); face polished, 2.16–2.43 (2.16)× as wide as long, sparsely punctate (distance between punctures 2.0–3.0× average puncture diameter) in middle and relatively dense (distance 1.0–2.0× average puncture diameter) laterally (Figs 2B, 4C), with setae; eyes bare, frontal orbit elevated; clypeus polished, 2.25–2.88 (2.88)× as wide as long, sparsely punctate with long setae, rounded in ventral margin and flat in lateral view (Figs 2A, B, 4C, F); malar space 1.29–1.73 (1.73)× as basal width of mandible, smooth in dorsal half and densely coriaceous in ventral half (Figs 2A, B, 4C); mandible unidentate, rounded apically, broad, flat, polished and punctate with long setae at

base (Fig. 4C); gena polished and sparsely punctate (Fig. 2C), pointed and strongly narrowed ventrally, meeting under the foramen; ocellar area and vertex rugose, rugose-punctate laterally; POL/OD=1.20–1.50 (1.50), OOL/OD=2.20–2.54 (2.36) (Figs 2A, 4E); occiput smooth; occipital carina strong and complete, genal carina meeting hypostomal carina far from mandible base at ventral tip of genae in 1.40–1.73 (1.73) \times of basal width of mandible.

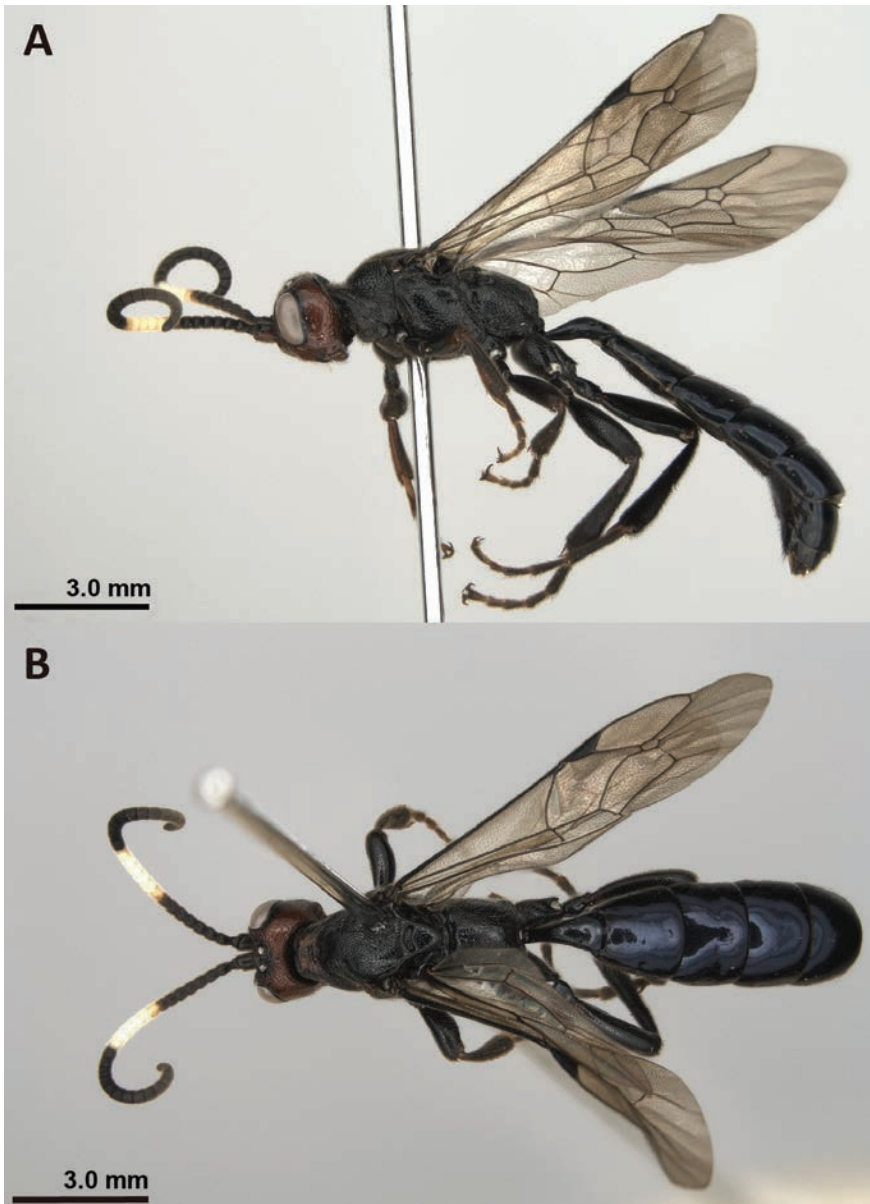


Figure 1. *Pseudalomya truncaticornis* sp. nov. holotype (NMNS ENT 8836-1) **A** lateral view of the habitus **B** dorsal view of the habitus. Photographed by Hsuan-Pu Chen.

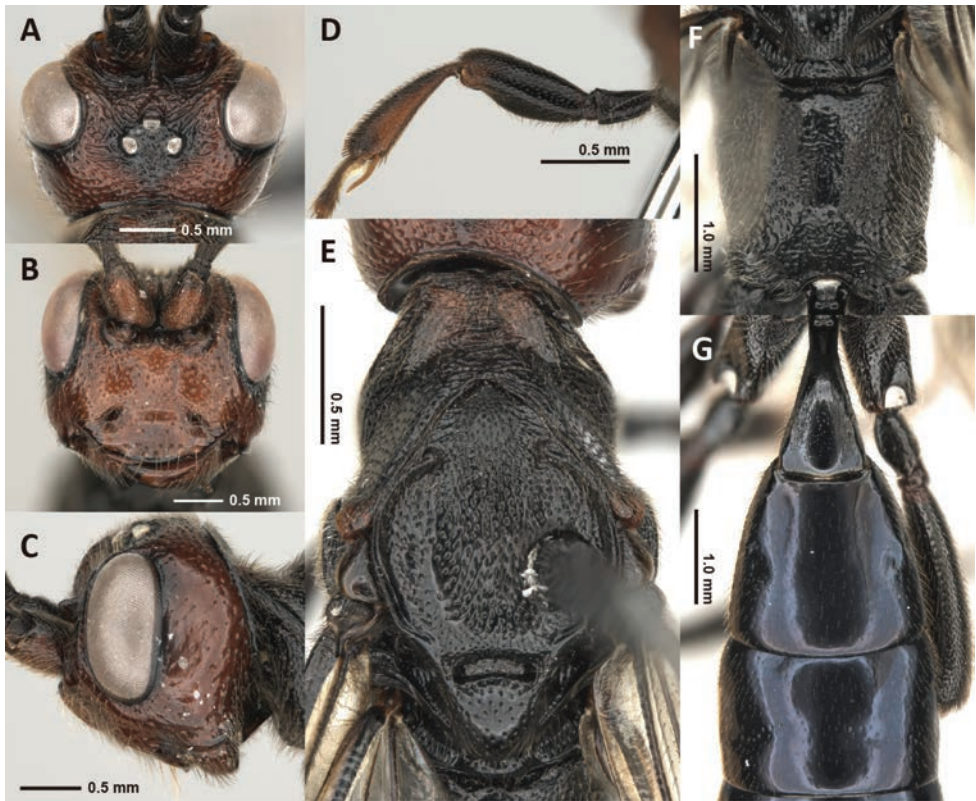


Figure 2. *Pseudalomya truncaticornis* sp. nov. holotype (NMNS ENT 8836-1) **A** dorsal view of the head **B** anterior view of the head **C** lateral view of the head **D** foreleg **E** dorsal view of the mesoscutum **F** dorsal view of the propodeum **G** dorsal view of the metasomal tergites. Photographed by Hsuan-Pu Chen.

Mesosoma: polished; pronotum with setae, transversely and strongly strigose dorsally, evenly and coarsely punctate dorsolaterally, and rugose-punctate ventrolaterally (Figs 2E, 3A); epomia present; propleuron coarsely punctate with setae; mesoscutum flat, 1.15–1.21 (1.21) \times as long as wide, with median lobe densely and coarsely punctate, lateral lobes evenly punctate but polished and sparsely punctate posteriorly, with setae (Fig. 2E); notauli present anteriorly; scutellum flat, 1.09–1.18 (1.18) \times as long as wide, sparsely punctate with setae, lateral carina absent (Fig. 2E); mesopleuron punctate, but rugose in dorso-anterior corner and middle posterior 0.5–0.8 (0.5), with mesopleural sulcus and furrow crenulate (Fig. 3A); epicnemial carina complete, extend to whole height of mesopleuron; sternaulus present in anterior 0.4 of mesopleuron; mesepisternum smooth; metapleuron evenly and coarsely punctate with setae in upper division and dorsal half, strongly and transversely strigose in ventral half; propodeal spiracle oval, 1.43–1.57 (1.43) \times as long as wide; posterior transverse carina of mesosternum interrupted anterior to mid-coxa; propodeum evenly and coarsely punctate with setae, with area basalis smooth, area superomedia and area petiolaris rugose-punctate, and area postero-externa rugose-foveolate (Fig. 2F); juxtacoxal carina present in

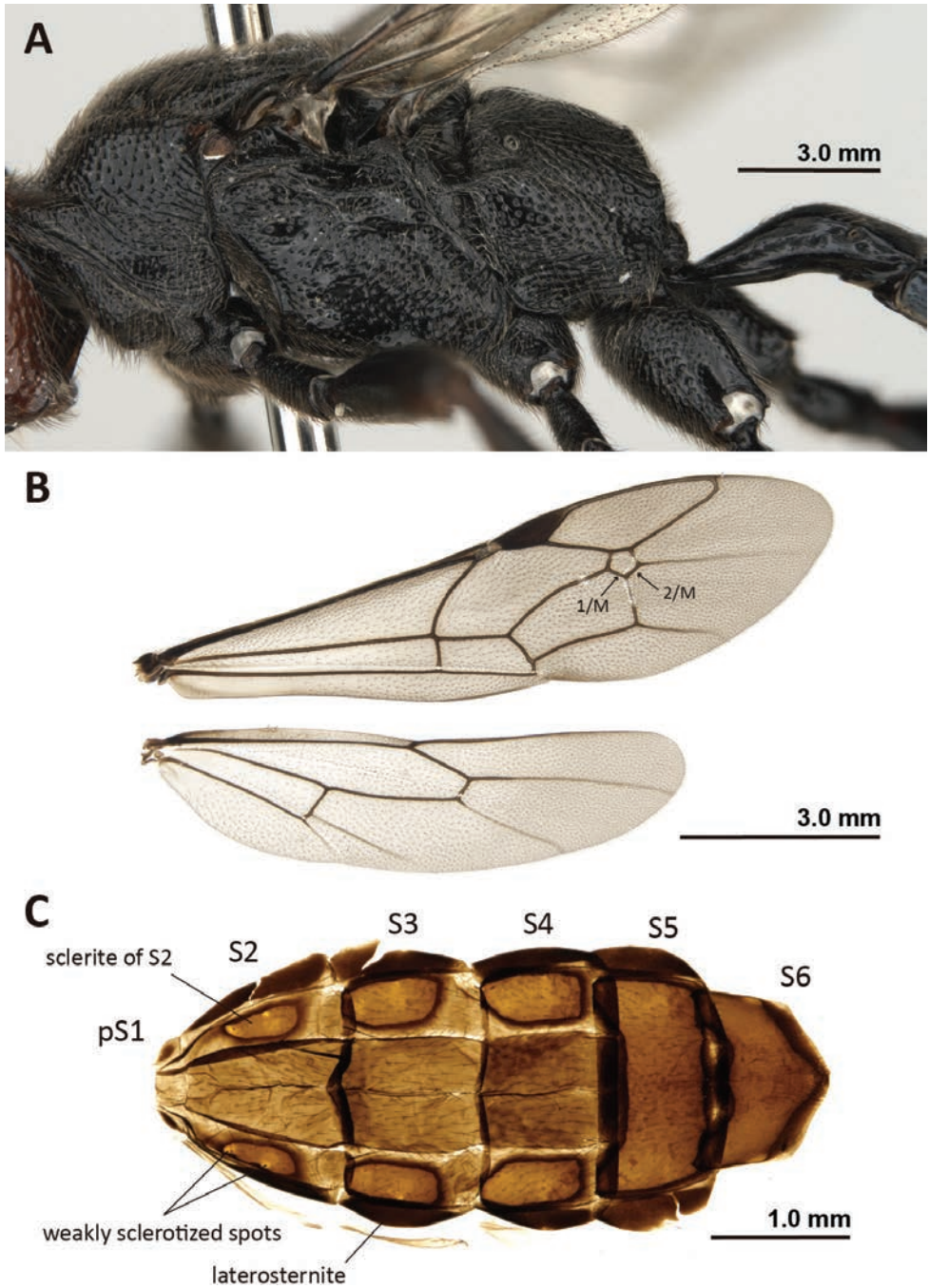


Figure 3. *Pseudalomya truncaticornis* sp. nov., NMNS ENT 8836-1 (A), NMNS ENT 8836-2 (B), and NARO (C) A lateral view of the mesosoma B wings C metasomal sternites. Photographed by Hsuan-Pu Chen (A, B) and Namiki Kikuchi (C).

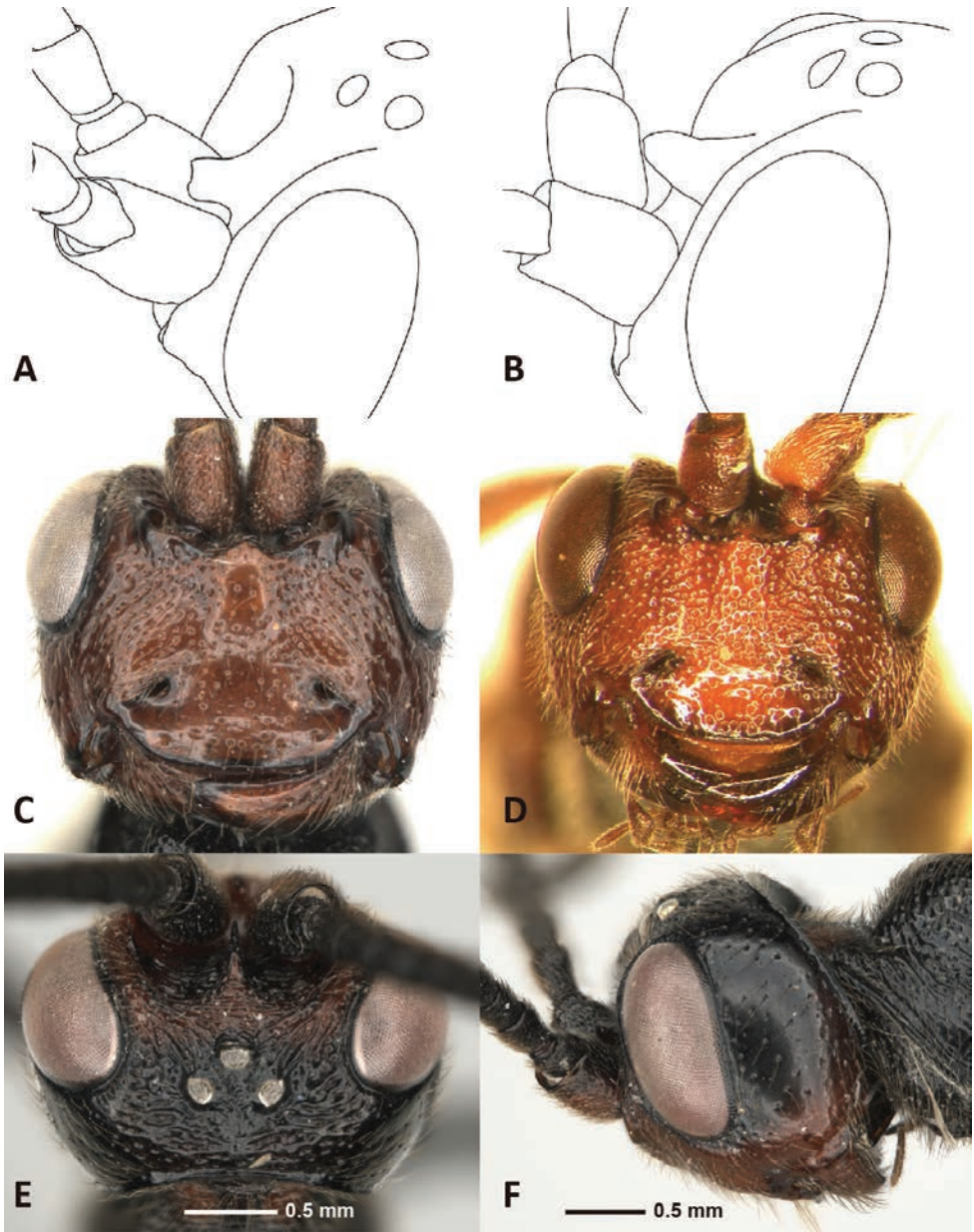


Figure 4. Characters of two *Pseudalomya* species. Frontal horns: **A** *Pseudalomya truncaticornis* sp. nov. (holotype, NMNS ENT 8836-1) **B** *Pseudalomya nepalensis* (holotype, SDEI). Faces: **C** *P. truncaticornis* sp. nov. (holotype, NMNS ENT 8836-1) **D** *P. nepalensis* (holotype, SDEI) **E** darker specimen of *P. truncaticornis* sp. nov. (paratype, NMNS ENT 8836-2), dorsal view of the head **F** darker specimen of *P. truncaticornis* sp. nov. (paratype, NMNS ENT 8836-2), lateral view of the head. Illustrated and photographed by Hsuan-Pu Chen (**A–C, E, F**) and Matthias Riedel (**D**).

basal 0.6; pleural and submetapleural carina present basally; lateromedian longitudinal carina weak; lateral longitudinal carina, anterior transverse carina, and propodeal apophysis absent; posterior transverse carina present, but weak medially.

Legs: evenly punctate with setae; coxa smooth dorso-apically; fore femur 2.63–2.84 (2.74)× as long as wide; hind femur 3.23–3.34 (3.34)× as long as wide, 0.21–0.24 (0.21)× as long as hind tibia; hind first tarsomere 1.75–1.92 (1.92)× as long as second tarsomere, and 0.45–0.49 (0.45)× as long as hind tibia; tibial spurs 2; tarsal claws normal.

Wings: forewings narrowed, 3.80–4.22 (4.12)× as long as wide, and length 8.01–8.45 (8.45) mm (Fig. 3B); forewing 1cu-a postfurcal, distad M & RS 0.23–0.33 (0.33)× by its length; areolet pentagonal, truncate anteriorly, with 2rs-m 1.10–1.26 (1.16)× as long as 3rs-m, and 1/M 1.05–1.14× as long as 2/M; 2 m-cu with two bulla; hindwing hamuli 7–9 (9), NI = 3.52–4.29 (4.29), CU and AA after cu-a weak.

Metasoma: polished; T1 2.00–2.68 (2.01)× as long as its apical width, smooth, postpetiole sparsely and minutely punctate (Fig. 2G); spiracles of T1 located at about 0.7 of length of tergite (Fig. 3A); T2 0.91–0.95 (0.91)× as long as its apical width, with gastrocoeli and thyridium absent (Fig. 2G); T3 0.63–0.72 (0.63)× as long as its apical width; tergites after T1 smooth with sparse and minute puncture (Fig. 2G); pS1 and S2 separated by weak crease (Fig. 3C); laterosternites strongly sclerotized in S1–5, separately from median sternites by crease; median sternites strongly sclerotized, with weakly sclerotized median area in S2–4 and separated by creases; sclerites of S2 0.5× as long as S2, not touched its posterior margin, with two weakly sclerotized spots; median sternites of S5 and S6 complete; metasomal apex amblypygous (Fig. 1A), with apical margin of hypopygium pointed (Fig. 3C); ovipositor sheath 0.16–0.20 (0.17)× as long as hind tibia, smooth with setae; ovipositor with upper valve slightly longer than lower valve, and lower valve with fine teeth.

Coloration: head mainly reddish brown, except central area of frons, horn, orbits, ventral margin of gena and clypeus, face below antennal sockets and around tentorial pits, ocellar area, apical half of mandible, occiput except its dorsal margin, and occipital carina black (Fig. 2A–C); antenna mainly black except flagellomeres 8 (or 9)–13 ivory and ventral surface of scape reddish brown (Fig. 1A, B); mesosoma mainly black, except two stripes at dorsal surface of pronotum, posterior corner of pronotum, and postspiracular sclerite before tegula reddish brown (Figs 1A, B, 2E, 3A); metasomal tergites metallic dark blue (Fig. 2G), with sternites black tinged with reddish brown; ovipositor sheaths black and ovipositor reddish brown; legs mainly black except apical fore femur, ventral side of fore tibia, basal and apical basitarsus, apical tarsomeres reddish brown (Fig. 1A); wings tinged with infusate, with veins and pterostigma black (Fig. 3B). One specimen (NMNS ENT 8836-2; SP0062) with temple above eyes, whole occiput, and all legs black (Fig. 4E, F).

Male. Unknown.

Etymology. The specific name “*truncaticornis*” is derived from the Latin “*truncati-*” (meaning “maimed” or “having appendages cut off”) plus “*cornis*” (meaning “horned”). It refers to the truncated apex of the horn on the frons in this species. Name is an adjective.

Distribution. Taiwan.

Bionomics. Host and phenology unknown. The specimens were collected from Taiwan Hemlock (*Tsuga chinensis*) (Pinaceae) forest in the high-altitude area (alt. 3160 m) of central Taiwan, with *Yushania niitakayamensis* (Bambusoideae, Poaceae), *Rhododendron* species (Ericaceae), and moss as ground-cover plants (Fig. 5).

Remarks. Comparisons of the photos of holotypes and descriptions of congener species revealed the highest level of similarity between *P. truncaticornis* sp. nov. and *P. nepalensis* Riedel, 2019. However, unlike *P. nepalensis*, the new species had the black coloration in mesosoma and legs (reddish brown in *P. nepalensis*), the middle of face with sparse punctures with distance between punctures 2.0–3.0× their diameter (dense in *P. nepalensis*, distance less than 1.0× their diameter), and a short and apically truncated frontal horn (long and apically rounded in *P. nepalensis*). While variation in the color of the head was observed within *P. truncaticornis* sp. nov., given the disjunct geographical distributions between *P. truncaticornis* sp. nov. and *P. nepalensis* (Taiwan and the Himalaya, respectively) and the presence of morphological differences beyond mere coloration, *P. truncaticornis* sp. nov. is considered a distinct species. To the best of our knowledge, this is the first record of *Pseudalomya* in Taiwan.



Figure 5. Habitat of *Pseudalomya truncaticornis* sp. nov. in Mount Huoshi (24°22'47.78"N, 121°10'53.67"E DMS), Shei-Pa National Park. Photographed by Ta-Hsiang Lee.

Key to world species of female *Pseudalomya* Telenga, 1930

- 1 Metasomal tergites not smooth, with postpetiole of T1 rugose, and T2 coriaceous; Forewing 1cu-a interstitial, opposite to M&RS; metasomal tergites not metallic-blue..... ***P. praevara* Telenga, 1930**
- Metasomal tergites smooth (Figs 1B, 2G); Forewing 1cu-a postfurcal, distad to M&RS (Fig. 3B); tergites metallic-blue (Figs 1B, 2G) **2**
- 2 Frontal horn long, rounded apically (Fig. 4B); punctures separated by less than 1.0× their diameter in middle of face (Fig. 4D); mesosoma and legs almost reddish brown..... ***P. nepalensis* Riedel, 2019**
- Frontal horn short, truncated apically (Fig. 4A); punctures separated by 2.0–3.0× their diameter in middle of face (Figs 2B, 4C); mesosoma and legs black (Fig. 1A, B)..... ***P. truncaticornis* sp. nov.**

Molecular dataset

The dataset for molecular phylogeny comprised six newly obtained sequences: three *COI* sequences from the ichneumonine species *Quandrus pepsoides* (Smith, 1852), *Callajoppa exaltatoria* (Panzer, 1804), and *Holcojoppa bicolor* (Radoszkowski, 1887) and one sequence each of *COI*, *28S*, and *18S* from *P. truncaticornis* sp. nov.. In addition, the dataset included 250 sequences – 83 *COI*, 88 *28S*, and 79 *18S* sequences – from GenBank (Suppl. material 1).

No pseudogene, identifiable by the occurrence of stop codons in translated (amino acid) sequences, was detected in the protein-coding gene dataset. However, one *18S* sequence from *Pseudoplatylabus apicalis* (GenBank accession KU753140) was eliminated because of its abnormal genetic distance in the *18S* gene tree pretest. Table 1 presents the basic details of each aligned dataset. The information presented in this table includes the average length of unaligned sequences, length of aligned sequences, number of variable and parsimony-informative sites, and percentage of GC content. The datasets for the concatenated and individual markers are presented in Suppl. material 3.

Molecular phylogeny

Figs 6, 7 depict the ML phylogenetic trees reconstructed using the concatenated *18S+28S+COI* dataset and the *COI* and *28S* datasets, respectively. The *18S* gene tree

Table 1. Summary of each aligned and trimmed molecular dataset. The table presents information on the average length of unaligned sequences, length of aligned sequences, number of variable and parsimony-informative (Pars-Inf) sites, and percentage of GC content.

	Number of sequences	Average length	Aligned length	Variable sites	Pars-Inf sites	GC (%)
<i>COI</i>	87	638.8	648	414	351	27.7
<i>28S</i>	89	613.3	625	283	169	59.7
<i>18S</i>	79	890.9	1302	70	31	49.5
<i>18S+28S+COI</i>	89	2028.6	2575	767	551	45.9

could not satisfactorily resolve the phylogenetic relationships in the Ichneumoniformes group (see Suppl. material 4: fig. S3). All trees were rerooted using the outgroup *Agriotypus armatus* (Agriotypinae). The complete phylogenetic trees resulting from all datasets are presented in Suppl. material 4.

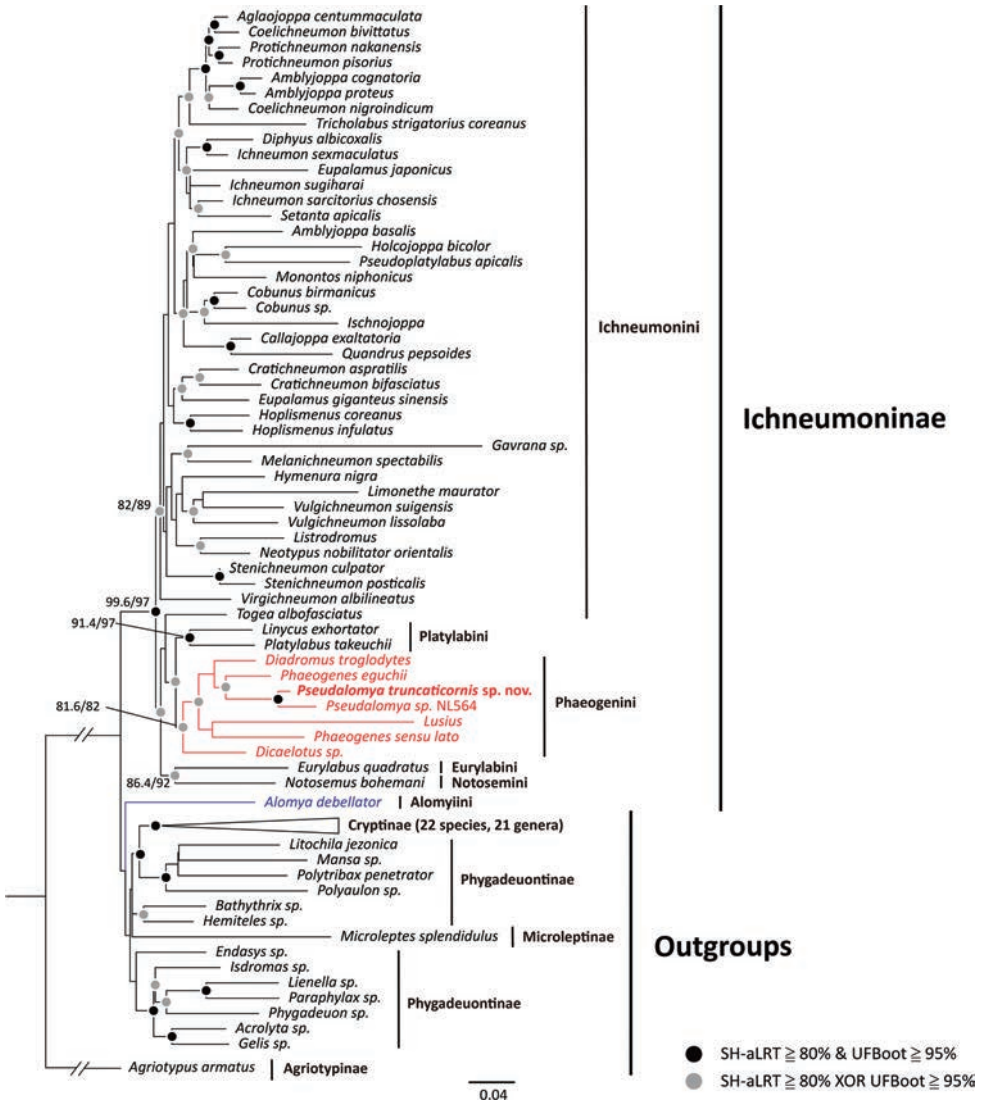


Figure 6. Maximum likelihood phylogenetic tree of Ichneumoninae reconstructed using the concatenated *18S+28S+COI* dataset (2575 bp; *18S*: 1302 bp; *28S*: 625 bp; *COI*: 648 bp; SYM+I+G4 [1–1302, 1303–1927, 1928–2575\3, and 1929–2575\3 bp]; HKY+F+I+G4 [1930–2575\3 bp]). The red and blue colors indicate Phaeogenini and Alomyiini, respectively. Branch lengths of the phylogenetic tree are proportional to the infer number of nucleotide substitutions per site, except for the branch of the outgroup *Agriotypus armatus*. Circles on the nodes indicate different SH-aLRT/UFBoot values. Nodal support with an SH-aLRT value of <80% and a UFBoot value of <95% is not shown. Abbreviations: SH-aLRT, SH-like approximate likelihood ratio test; UFBoot, ultrafast bootstrap approximation; XOR, one or the other but not both.

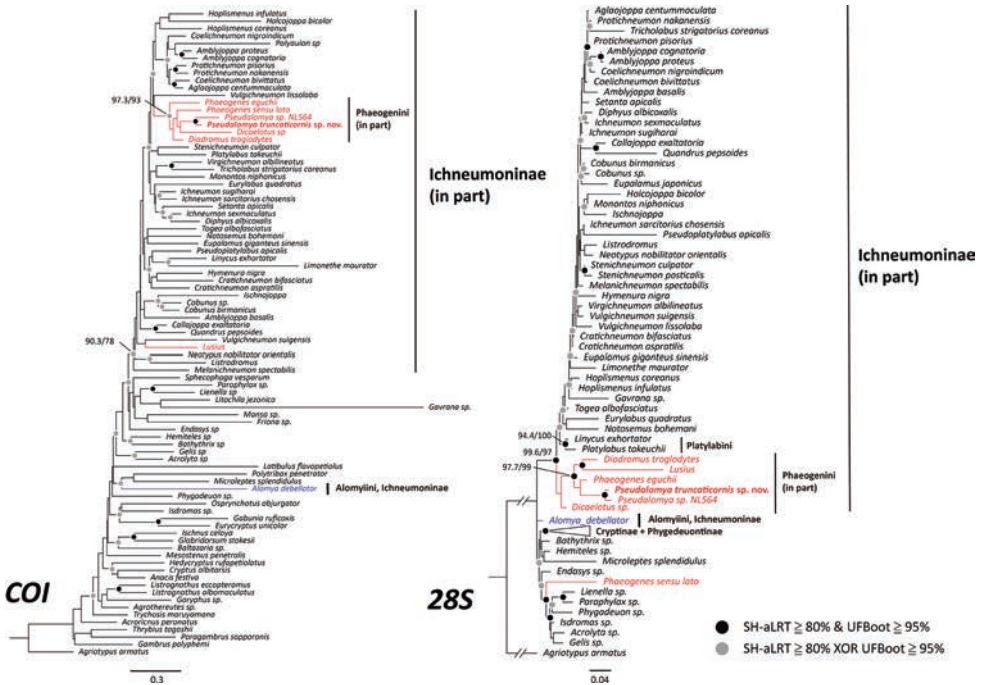


Figure 7. Maximum likelihood phylogenetic trees of Ichneumoninae reconstructed using the *COI* and *28S* datasets (*COI*: 648 bp; GTR+F+I+G4 [1–648\3 and 2–648\3 bp]; HKY+F+I+G4 [3–648\3 bp]; *28S*: 625 bp; GTR+F+I+G4 [1–625 bp]). The red and blue colors indicate Phaeogenini and Alomyiini, respectively. Branch lengths of the phylogenetic trees are proportional to the infer number of nucleotide substitutions per site, except for the branch of the outgroup *Agriotypus armatus*. Circles on the nodes indicate different SH-aLRT/UFBoot values. Nodal support with an SH-aLRT value of <80% and a UF-Boot value of <95% is not shown. Abbreviations: SH-aLRT, SH-like approximate likelihood ratio test; UFBoot, ultrafast bootstrap approximation; XOR, one or the other but not both.

In the tree reconstructed using the concatenated dataset, the subfamily Ichneumoninae excluding *Alomya debellator* (tribe: Alomyiini), is recovered as a strongly supported clade (SH-aLRT/UFBoot = 99.6/97) and sister to the clade including Alomyiini, Microleptinae, Cryptinae, and Phygadeuontinae (Fig. 6). *A. debellator* is sister to the clade including Microleptinae, Cryptinae, and Phygadeuontinae (low nodal support; SH-aLRT/UFBoot = 70.1/78) but was not a member of the Ichneumoninae. The ichneumonine tribes proposed by Santos et al. (2021) are recovered as monophyletic groups, with the exception of Ichneumonini; *Togea albofasciatus* was nested within the clade including Notosemini, Eurylabini, Platylabini, and Phaeogenini. However, with the exception of Platylabini (SH-aLRT/UFBoot = 91.4/97), none of the sampled tribes were strongly supported (SH-aLRT/UFBoot = 81.6/82 in Phaeogenini and 86.4/92 in the clade including Notosemini and Eurylabini). Finally, *Pseudalomya* is recovered as a member of Phaeogenini, distinct from Alomyiini (Fig. 6); however, the sister relationship of the new species with *Phaeogenes eguchii* was not strongly supported (SH-aLRT/UFBoot = 52.2/95).

In the gene tree reconstructed using *COI*, *Pseudalomya* is recovered in the phaeogenine clade excluding *Lusius* (SH-aLRT/UFBoot = 97.3/93); in the tree reconstructed using *28S*, *Pseudalomya* is recovered in the strongly supported phaeogenine clade excluding *Phaeogenes sensu lato* and *Dicaelotus* sp. (SH-aLRT/UFBoot = 97.7/99; Fig. 7). Notably, neither tree indicates *A. debellator* as a member of the Ichneumoninae. Neither Ichneumoninae nor ichneumonine tribes are recovered as strongly supported monophyletic groups in either tree. However, Platylabini is recovered as a strongly supported monophyletic group in the *28S* tree (SH-aLRT/UFBoot = 94.4/100; Fig. 7).

Discussion

The genus *Pseudalomya* has been sampled in previous phylogenies reconstructed by *28S* data (Laurenne et al. 2006) or combined (*28S* + morphology) data (Quicke et al. 2009). Both hypotheses supported the placement of *Pseudalomya* within Phaeogenini. To the best of our knowledge, our study is the first to present *COI*-based and multigene molecular phylogeny that includes *Pseudalomya*. The results support the placement of *Pseudalomya* within Phaeogenini. However, the precise relationship of *Pseudalomya* with other members of Phaeogenini as reported in the literature and the present study differs because of between-study differences in taxon sampling and methodology. *Pseudalomya* was shown sister to *Tycherus* in the study of Laurenne et al. (2006), to an unidentified phaeogenine genus in the study of Quicke et al. (2009), to *Dicaelotus* sp. in our *COI*-based phylogenetic analysis (Fig. 7), and to *Phaeogenes eguchii* in our *28S*-based and concatenated multigene phylogenetic analyses (Figs 6, 7). The aforementioned relationships are not highly supported, with the exception of that reported in Laurenne et al. (2006).

In our study, the Alomyini (*Alomya debellator*) is not recovered as a member of Ichneumoninae; this finding is congruent with the *28S*-based hypothesis proposed by Laurenne et al. (2006) but incongruent with phylogenetic hypotheses reconstructed using morphological data (Gokhman 1992, 1995), combined morphological and multigene data (Quick et al. 2009; Bennett et al. 2019), or genomic data (Santos et al. 2021).

Our findings, which were derived from phylogenetic analyses performed using universal genetic markers via Sanger sequencing, unveiled incongruent phylogenetic relationships within Ichneumoninae (Figs 6, 7). The tree reconstructed using the *18S* dataset even failed to reveal subfamily-level relationships, likely because of to the conservativeness of this marker (see Suppl. material 4: fig. S3). These results imply probable constraints in phylogenetic inference using a restricted set of Sanger-based genetic markers or involving incomprehensive taxon sampling. However, our results do distinctly demonstrate the position of *Pseudalomya* as not belonging to Alomyini and clustered within Phaeogenini. Additionally, the alignment of *COI* sequences revealed that *Pseudalomya* lacked a unique insertion sequence (nucleotides 403–408) specific to *Alomya* (see Suppl. material 3: pseudalomya_ichneumoniformes_coi_withreference.fas), providing an additional character for differentiating between *Pseudalomya* and Alomyi-

ni (at least *Alomya*). Considering the discrepancies between the literature and our study regarding the limitations of Sanger-based phylogenetic analyses, we refrained from the tribal reclassification of *Pseudalomya*. Comprehensive phylogenetic analyses based on genomic data are required to accurately determine the tribal status of *Pseudalomya*.

Lastly, this study indicates that the distribution of *Pseudalomya* extends from the Eastern Palaearctic region (Russia, Korea) and the Himalayas (Nepal) to Taiwan. The oriental species of *Pseudalomya* – *P. nepalensis* and *P. truncaticornis* sp. nov. – exhibit disjunct distributions between the Himalayas and Taiwan. This unique distribution pattern is also observed in vascular plants, vertebrates, and insects (e.g., Hsu and Yen 1997; Päckert et al. 2012; Niu et al. 2018). This pattern may be explained by long-distance dispersal, postglacial contraction, limited faunistic studies in the high-altitude intermediate regions, or the lack of material examined (Yen et al. 2000; Wang et al. 2013; Niu et al. 2018). Thus, further studies are required to comprehensively clarify the distribution of *Pseudalomya*.

Funding

This study was funded by Taiwan's National Science and Technology Council [grant to the corresponding author: 111-2621-B-002-002] and Bureau of Animal and Plant Health Inspection and Quarantine [grants to the corresponding author: 111AS-5.3.3-BQ-B2(2), 112AS-5.3.3-BQ-B2(2), and 112-RA-BQ-01(Z)].

Competing interests

The authors have declared that no competing interests exist.

Acknowledgments

We would like to express our sincere thanks to Matthias Riedel (Zoologische Staatssammlung München, Bad Fallingb., Germany) for providing the holotype photos of *Pseudalomya nepalensis*; Yun Hsiao (Institute of Ecology and Evolutionary Biology, National Taiwan University, Taipei, Taiwan) for assisting in phylogenetic analyses; Yu-Feng Hsu, Yu-Ming Hsu, and Kuang-Yao Chen (Department of Life Science, National Taiwan Normal University, Taipei, Taiwan), and Jung-Chang Chen, Li-Jen Chang, Ta-Hsiang Li, and Hung-Yang Shen for providing the specimens and collecting under the project SP110113 (“A survey for selection of insect indicator species and their microhabitat usage in the Daxueshan area of Shei-Pa National Park”); and two reviewers, Brandon Claridge (Utah State University, Logan, USA) and Davide Dal Pos (Department of Biology, University of Central Florida, Orlando, USA), for providing constructive feedback that improved the quality of our manuscript.

References

- Altschul SF, Gish W, Miller W, Myers EW, Lipman DJ (1990) Basic local alignment search tool. *Journal of Molecular Biology* 215: 403–410. [https://doi.org/10.1016/S0022-2836\(05\)80360-2](https://doi.org/10.1016/S0022-2836(05)80360-2)
- Bennett AM, Cardinal S, Gauld ID, Wahl DB (2019) Phylogeny of the subfamilies of Ichneumonidae (Hymenoptera). *Journal of Hymenoptera Research* 71: 1–156. <https://doi.org/10.3897/jhr.71.32375>
- Broad GR, Shaw MR, Fitton MG (2018) Ichneumonid Wasps (Hymenoptera: Ichneumonidae): their classification and biology. *Handbooks for the identification of the British insects* 7(12): 1–418.
- Eady RD (1968) Some illustrations of microsculpture in the Hymenoptera. *Proceedings of the Royal Entomological Society of London* 43: 66–72. <https://doi.org/10.1111/j.1365-3032.1968.tb01029.x>
- Gokhman VE (1992) On the origin of endoparasitism in the subfamily Ichneumoninae (Hym., Ichneumonidae). *Zhurnal Obshchei Biologii* 53: 600–608.
- Gokhman VE (1995) Trends of biological evolution in the subfamily Ichneumoninae and related groups (Hymenoptera, Ichneumonidae): an attempt of phylogenetic reconstruction. *Russian Entomological Journal* 4: 91–103.
- Guindon S, Dufayard J-F, Lefort V, Anisimova M, Hordijk W, Gascuel O (2010) New algorithms and methods to estimate maximum-likelihood phylogenies: Assessing the performance of PhyML 3.0. *Systematic Biology* 59(3): 307–321. <https://doi.org/10.1093/sysbio/syq010>
- Hoang DT, Chernomor O, von Haeseler A, Minh BQ, Vinh LS (2017) UFboot2: Improving the Ultrafast Bootstrap Approximation. *Molecular Biology and Evolution* 35 (2): 518–522. <https://doi.org/10.1093/molbev/msx281>
- Hsu YF, Yen SH (1997) Notes on *Boloria pales yangi*, ssp. nov., a remarkable disjunction in butterfly biogeography (Lepidoptera: Nymphalidae). *Journal of Research on the Lepidoptera* 34: 142–146. <https://doi.org/10.5962/p.266565>
- Kalyaanamoorthy S, Minh BQ, Wong TKF, von Haeseler A, Jermini LS (2017) Modelfinder: Fast model selection for accurate phylogenetic estimates. *Nature Methods* 14: 587–589. <https://doi.org/10.1038/nmeth.4285>
- Katoh K, Rozewicki J, Yamada KD (2019) MAFFT online service: Multiple sequence alignment, interactive sequence choice and visualization. *Briefings in Bioinformatics* 20 (4): 1160–1166. <https://doi.org/10.1093/bib/bbx108>
- Kikuchi N, Konishi K (2021) A taxonomic revision of the genus *Linyctus* Cameron, 1903 from Japan. *Zootaxa* 4948(4): 546–558. <https://doi.org/10.11646/zootaxa.4948.4.3>
- Laurenne NM, Broad G, Quicke DLJ (2006) Direct optimization and multiple alignment of 28S D2–D3 rDNA sequences: problems with indels on the way to a molecular phylogeny of the cryptine ichneumon wasps (Insecta: Hymenoptera). *Cladistics* 22: 442–473. <https://doi.org/10.1111/j.1096-0031.2006.00112.x>
- Nguyen LT, Schmidt HA, von Haeseler A, Minh BQ (2015) IQ-TREE: a fast and effective stochastic algorithm for estimating maximum-likelihood phylogenies. *Molecular Biology and Evolution* 32(1): 268–274. <https://doi.org/10.1093/molbev/msu300>

- Niu Y-T, Ye J-F, Zhang J-L, Wan J-Z, Yang T, Wei X-X, Lu L-M, Li J-H, Chen Z-D (2018) Long-distance dispersal or postglacial contraction? Insights into disjunction between Himalaya–Hengduan Mountains and Taiwan in a cold-adapted herbaceous genus, *Triplostegia*. *Ecology and Evolution* 8: 1131–1146. <https://doi.org/10.1002/ece3.3719>
- Päckert M, Martens J, Sun YH, Severinghaus LL, Nazarenko AA, Ting J, Töpfer T, Tietze DT (2012) Horizontal and elevational phylogeographic patterns of Himalayan and Southeast Asian forest passerines (Aves: Passeriformes). *Journal of Biogeography* 39: 556–573. <https://doi.org/10.1111/j.1365-2699.2011.02606.x>
- Quicke DLJ (2015) The braconid and ichneumonid parasitoid wasps: biology, systematics, evolution and ecology. John Wiley & Sons (West Sussex), 704 pp. <https://doi.org/10.1002/9781118907085>
- Quicke DLJ, Laurence NM, Fitton MG, Broad GR (2009) A thousand and one wasps: a 28S rDNA and morphological phylogeny of the Ichneumonidae (Insecta: Hymenoptera) with an investigation into alignment parameter space and elision. *Journal of Natural History* 43 (23–24): 1305–1421. <https://doi.org/10.1080/00222930902807783>
- Riedel M (2019) Contribution to the Ichneumoninae (Hymenoptera, Ichneumonidae) of Nepal. *Linzer Biologische Beiträge* 51: 1119–1162.
- Santos BF (2017) Phylogeny and reclassification of Cryptini (Hymenoptera, Ichneumonidae, Cryptinae), with implications for ichneumonid higher-level classification. *Systematic Entomology* 42: 650–676. <https://doi.org/10.1111/syen.12238>
- Santos BF, Wahl DB, Rousse P, Bennett AMR, Kula R, Brady SG (2021) Phylogenomics of Ichneumoninae (Hymenoptera, Ichneumonidae) reveals pervasive morphological convergence and the shortcomings of previous classifications. *Systematic Entomology* 46: 704–724. <https://doi.org/10.1111/syen.12484>
- Tamura K, Stecher G, Kumar S (2021) MEGA11: Molecular Evolutionary Genetics Analysis Version 11. *Molecular Biology and Evolution* 38 (7): 3022–3027. <https://doi.org/10.1093/molbev/msab120>
- Telenga NA (1930) Einige neue Ichneumoniden-Arten aus USSR. *Revue Russe d'Entom* 24: 104–108.
- Tereshkin AM (2009) Illustrated key to the tribes of subfamilia Ichneumoninae and genera of the tribe Platylabini of world fauna (Hymenoptera, Ichneumonidae). *Linzer Biologische Beiträge* 41(2): 1317–1608.
- Trifinopoulos J, Nguyen LT, von Haeseler A, Minh BQ (2016) W-IQ-TREE: a fast online phylogenetic tool for maximum likelihood analysis. *Nucleic Acids Research* 44(W1): W232–W235. <https://doi.org/10.1093/nar/gkw256>
- Wang WJ, McKay BD, Dai CY, Zhao N, Zhang RY, Qu YH, Song G, Li SH, Liang W, Yang XJ, Pasquet E, Lei FM (2013) Glacial expansion and diversification of an East Asian montane bird, the green-backed tit (*Parus monticolus*). *Journal of Biogeography* 40: 1156–1169. <https://doi.org/10.1111/jbi.12055>
- Watanabe K (2016) Taxonomic Position of *Pseudalomya takeii* Kusigemati, 1984 (Hymenoptera: Ichneumonidae), with a New Synonym. *Japanese Journal of Systematic Entomology* 22(1): 35–36.

- Yen SH, Nässig WA, Naumann S, Brechlin R (2000) A new species of the *miranda*-group of the genus *Loepa* from Taiwan (Lepidoptera: Saturniidae). *Nachrichten des Entomologischen Vereins Apollo* 21: 153–162.
- Yu DSK, van Achterberg C, Horstmann K (2012) *Taxapad 2012, Ichneumonoidea 2011*. Ottawa, Ontario. <http://www.taxapad.com> [database on flash-drive]

Supplementary material 1

Sequences used in this study

Authors: Hsuan-Pu Chen, Namiki Kikuchi

Data type: xlsx

Explanation note: The cells in blue with bold font indicate the newly obtained sequences in this study.

Copyright notice: This dataset is made available under the Open Database License (<http://opendatacommons.org/licenses/odbl/1.0/>). The Open Database License (ODbL) is a license agreement intended to allow users to freely share, modify, and use this Dataset while maintaining this same freedom for others, provided that the original source and author(s) are credited.

Link: <https://doi.org/10.3897/jhr.97.119470.suppl1>

Supplementary material 2

PCR primers and conditions used in this study

Author: Hsuan-Pu Chen

Data type: pdf

Explanation note: Regarding PCR conditions, 35 cycles were run for *COI* and *18S*, whereas 30 cycles were run for *28S*. Abbreviations: PCR, polymerase chain reaction.

Copyright notice: This dataset is made available under the Open Database License (<http://opendatacommons.org/licenses/odbl/1.0/>). The Open Database License (ODbL) is a license agreement intended to allow users to freely share, modify, and use this Dataset while maintaining this same freedom for others, provided that the original source and author(s) are credited.

Link: <https://doi.org/10.3897/jhr.97.119470.suppl2>

Supplementary material 3

Fasta and Nexus files for the analysis in this study

Authors: Hsuan-Pu Chen, Namiki Kikuchi

Data type: zip

Explanation note: Fasta files containing alignments of all markers analyzed in this study, along with the Nexus file specifically for the optimal partition scheme identified based on the *COI* and concatenated *18S+28S+COI* datasets for the analysis

Copyright notice: This dataset is made available under the Open Database License (<http://opendatacommons.org/licenses/odbl/1.0/>). The Open Database License (ODbL) is a license agreement intended to allow users to freely share, modify, and use this Dataset while maintaining this same freedom for others, provided that the original source and author(s) are credited.

Link: <https://doi.org/10.3897/jhr.97.119470.suppl3>

Supplementary material 4

Complete maximum likelihood trees reconstructed using the *COI*, *28S*, *18S*, and concatenated *18S+28S+COI* datasets

Author: Hsuan-Pu Chen

Data type: pdf

Explanation note: All trees were rerooted using the outgroup *Agriotypus armatus*. The red and blue colors indicate Phaeogenini and Alomyini, respectively. Branch lengths of the phylogenetic trees are proportional to the inferred number of nucleotide substitutions per site, except for the branch of the outgroup *Agriotypus armatus*. Circles on the nodes indicate different SH-aLRT/UFBboot values. Nodal support with an SH-aLRT value of <80% and a UFBboot value of <95% is not shown. Abbreviations: SH-aLRT, SH-like approximate likelihood ratio test; UFBboot, ultrafast bootstrap approximation; XOR, one or the other but not both.

Copyright notice: This dataset is made available under the Open Database License (<http://opendatacommons.org/licenses/odbl/1.0/>). The Open Database License (ODbL) is a license agreement intended to allow users to freely share, modify, and use this Dataset while maintaining this same freedom for others, provided that the original source and author(s) are credited.

Link: <https://doi.org/10.3897/jhr.97.119470.suppl4>

Justin Schmidt's originality

Christopher K. Starr¹, Robert S. Jacobson², William L. Overal³

1 *Dep't of Life Sciences, University of the West Indies, St Augustine, Trinidad and Tobago* **2** *10572 Tanagerhills Dr, Cincinnati, Ohio 45249, USA* **3** *Museu Paraense "Emílio Goeldi", Belém, Pará 66.000, Brazil*

Corresponding author: Christopher K. Starr (ckstarr@gmail.com)

Academic editor: Michael Ohl | Received 21 February 2024 | Accepted 1 March 2024 | Published 24 April 2024

<https://zoobank.org/32B1883B-45AB-435A-AEDB-C627FDABF13D>

Citation: Starr CK, Jacobson RS, Overal WL (2024) Justin Schmidt's originality. *Journal of Hymenoptera Research* 97: 297–306. <https://doi.org/10.3897/jhr.97.121387>

Abstract

The research career of Justin O. Schmidt (1947–2023) is reviewed and assessed. The pioneering nature of his research lay in treating the defensive means and tactics of aculeate hymenoptera and some arachnids as features of their overall anti-predator strategies. He devised methods for comparing the effects of hymenopteran venoms and stings that challenged the assumed correlation between venom potency and the pain that it induces.

Keywords

Dasympulilla, defensive tactics, honey bee, Hymenoptera, *Pogonomyrmex*, sting, venom

Introduction

Justin Orvel Schmidt (1947–2023) was an American entomologist, the main focus of whose long and fruitful life in science was stinging insects (Hymenoptera: Aculeata) and how venom figured in their lives. He was born in Wisconsin, USA into a middle-class family. During most of his life he lived in the USA, while traveling widely and studying stinging insects in the field in all habitable continents. Our purpose here is to characterize Schmidt's research program and how it stands apart from all others. In this we have relied on some of his writings (especially his 2016 book "The Sting of the Wild" and an unpublished 2020 autobiographical essay), some of what others have written about him (Binford et al. 2023; Cane et al. 2023) and our long personal association with him.

Becoming a Chemical Ecologist

Schmidt (Fig. 1) was born on 23 March 1947 and spent his formative years in Pennsylvania, USA. Like many children, he was drawn to natural history from a very early age. Unlike most, he persisted throughout his life in a powerful fascination with nature and its creatures and a desire to make sense of their workings.

He was first introduced to stinging insects as a child when he accepted a challenge from other boys to throw a stone at a nest of the large social wasp *Dolichovespula maculata*. For this he was punished by the wasps. During his primary and secondary schooling he showed a keen interest in many fields of natural science, of which chemistry came to take precedence. He received his BS in Chemistry in 1969 at Pennsylvania State University and then enrolled in a PhD program in the same area at the University of British Columbia. However, as a student at UBC two factors prompted a major change in direction. First, the working environment of a professional chemist -- white lab coats in a room smelling of solvents -- was distasteful to him. Second, he had a long-standing affinity with insects and the outdoor activities of natural history. The critical point may have come when his wife, Deborah, remarked to him one day that by temperament he was a biologist, not a chemist. Accordingly, he downgraded his Chemistry degree to an MSc (1972). This presented a dilemma, as Debbie had yet to complete her degree. Justin made use of the interval by enrolling in the College of Education to obtain his teaching certificate for high school science. While he never taught high school, he considered the training worthwhile in developing the skills in making public presentations that were later to become a large part of his activity.

Upon completion of their degrees at UBC, the Schmidts moved across the continent for graduate study at the University of Georgia (UGa). It was a natural development for Justin to combine his expertise in chemistry with his developing strength in natural history to focus on chemical ecology. His major professor, Murray S. Blum (1929–2015) (Fig. 2), was a pioneering figure in the chemical interactions of insects with their environment and with each other. Also advantageous was the presence in UGa's Department of Entomology of Robert S. Matthews, a specialist in insect behavior, and Henry R. Hermann, the leading expert on the hymenopteran venom apparatus. As outlined below, it was as a student at UGa that Schmidt framed the research program in arthropod venoms and envenomation that would be his main occupation for the rest of his life. It should be noted that during this period Debbie succumbed to a rare and very aggressive form of cancer.

Schmidt met his second wife, Patricia, in Arizona. In some ways they were a very good match, as she shared many of his scientific interests and collaborated well with him in field work. However, a stable, harmonious marriage requires more than that, and after some years they parted company. A few years later he recruited a promising student from China, Shen Li, to study in the USA and aid in his research. It is a well-known rule that “nothing propinks like propinquity”, and in time she became his third wife, remaining with him to the end of his life.



Figure 1. Justin O. Schmidt early in his post-doctoral career. Source: Archive of the International Union for the Study of Social Insects.

An innovative research program

Stings and venom were a matter of comment already in classical antiquity. In the 2nd century BC, for example, Nicander of Colophon (1953) presented an extensive list of stings and their remedies. Similarly, two centuries later Pliny the Elder (1855) listed many supposed antidotes to various stings. However, this remained the extent of writings on the topic until much later. Later centuries saw an increasingly exact understanding of such aspects as the composition of venoms and their effects on human health (e.g. Piek 1986). In addition, there gradually emerged more or less isolated studies of various biological aspects of venoms.

Accordingly, there was already a substantial literature on the venoms of Hymenoptera and other arthropods when Schmidt entered the field in the mid-1970s, although with a predominant medical/pharmacological focus. Almost entirely missing from the literature was research from the animal's point of view, and the few studies taking such a biological viewpoint can best be described as scattered or isolated. The larger question remained "What roles do venom play in the lives of those who synthesize and deploy them?"

Justin Schmidt's originality lies precisely in addressing this question with respect to a wide array of creatures, especially aculeate Hymenoptera. As he later expressed it with respect to his experience in Georgia (Schmidt 2020), "I had finally found



Figure 2. Murray S. Blum and associates circa 1980. Left to right: Post-doc David J.C. Fletcher, Blum, Schmidt, Mrs Pauline Fletcher, Post-doc Clive G. Jones. Source: Archive of the International Union for the Study of Social Insects.

what I wanted to do in life. That was, study defensive behaviors and venoms of ants, wasps, and bees, and how they enabled the evolution of sociality in the Hymenoptera.”

We can depict the components of Schmidt’s research program in a two-dimensional graph, in which each dimension represents a group of thematically-associated problems (Fig. 3). On the x-axis are some of the main means by which arthropods defend themselves and – in the case of social insects – their colonies against predators and other natural enemies. On the y-axis are aspects of venom studies. While the whole of Schmidt’s research ranged over much of this graph, its core lies at the interface between the two axes, the effects of stinging on the adversary.

The two dimensions are already apparent in Schmidt’s (1977) PhD thesis. Titled “Defensive strategies of wasps and ants: *Dasymutilla occidentalis* and *Pogonomyrmex badius*”, it comprised three chapters. The first analyzed the full repertoire of physical and behavioral defensive features of the solitary wasp *D. occidentalis* that make it all but invulnerable to most classes of potential predators, although not to all of them. The other two treated the biochemical, pharmacological and toxicological features of the venom of the harvester ant *P. badius*, all within the context of the life of the colony. While working on *P. badius*, he also collected and studied several other members of the genus toward understanding how and why their venoms varied. This arose from the question of why their stings were so painful and the venom so very toxic. It was a natural progression from there to extend attention to a broad array of aculeate Hymenoptera, with some attention to arachnids.

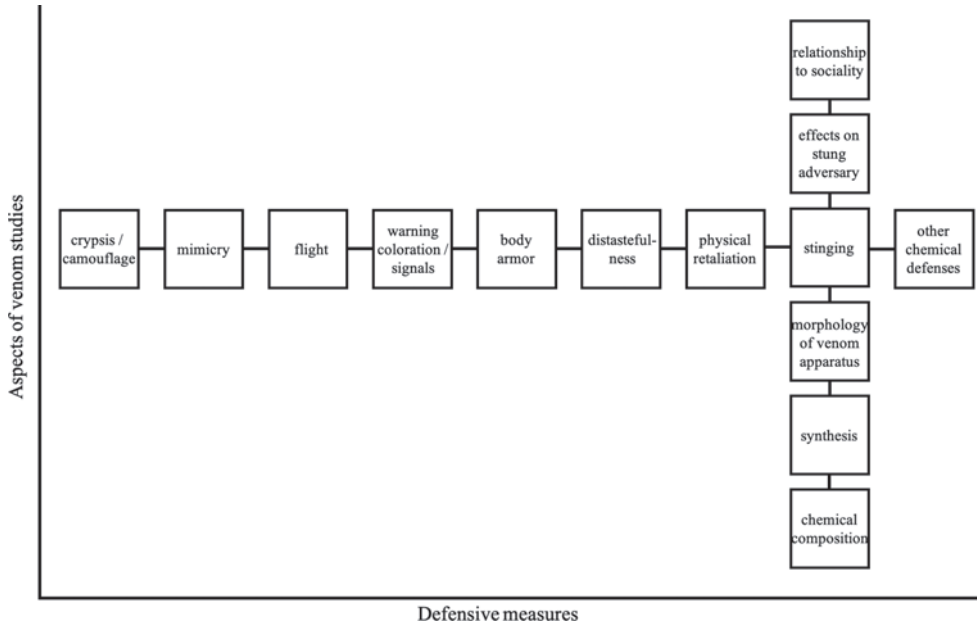


Figure 3. Diagrammatic representation of the scope of J.O Schmidt's research program. Further explanation in text. Graph by Nova Y. Starr.

His decades of investigations of a great many additional species and the nature of their venoms has opened a new era in the biological understanding of stinging insects. He devised and implemented new ways of extracting venom, analyzing its chemical composition and comparing venom toxicity, and documented the relative pain of their stings to humans. Once again, let us emphasize that the focus of this latter was not how we humans feel about this or that sting but on what it means in the lives of those who sting. Over the decades one of us (CKS) has recorded stings (and a few sting-like bites) from more than 60 species of Hymenoptera. That is quite respectable, but Schmidt (2016: Appendix) tops it with his own list of effects from 77 species, which appears not to comprise his entire experience.

No one before had addressed the question of what tissue damage from stings has to do with the pain that they cause. Perhaps the most striking result of Schmidt's comparative studies across taxa was the conclusion that there is no particular correlation between these two aspects, all within the context of their significance in the life of the insect (Schmidt 2016, 2019). He found, for example, that they very painful stings of spider wasps (Pompilidae) have very low toxicity.

One occasionally encounters the notion of Schmidt as a strange guy who liked to be stung. This is nonsense. He very seldom deliberately induced a sting, and then only when he had no other way to find out how much it hurt and its other effects. It was all in the interest of science, and of course when he did get stung by chance he was not going to let it go to waste but took careful note of the effects.

Before Schmidt, the roles of venoms in the lives of stinging animals had seldom been treated in any but a perfunctory manner, and the effects of venom on the stung

had remained a pharmacological question. Part of Schmidt's radical departure was to separate three kinds of sting effects in the affected animal -- pain, tissue damage, and immobilization, especially the first two – and to ask how and why these should vary among venomous animals. His most striking result was that there is at most a very weak correlation among the different effects. While some insects (e.g. harvester ants, *Pogonomyrmex* spp.) have very painful stings that are at once highly toxic, some others (e.g. spider wasps, Pompilidae) deliver very painful stings that quickly immobilize their prey but are of only slight toxicity. This led to the conception of stings as a deception or false alarm, and selection pressure on some predators (e.g. skunks on soil-nesting social wasps and bees) to disregard the pain.

Taking this separation of effects a step further, a part of his biochemical research consisted in identifying venom components that cause pain and those that cause tissue damage (Schmidt 2016: Ch. 5).

In trying to understand why harvester-ant stings, for example, are so painful to humans (and presumably to most other vertebrates), Schmidt directed his attention to both proximate and ultimate causation. That is, he addressed both the question “What is it about the venom or its delivery that makes it hurt so much?” and “How is it in the ants' interest for their stings to hurt so much, or is it?”

The Amateur Scientist

Some comment on Schmidt's employment history is in order. Aside from a brief post-doctoral position in Blum's lab not long after completing his PhD, he was hardly at all employed to do the research that we describe here. Most notably, his one long-term job (1980–2005) was as a bee nutritionist at the Carl Hayden Bee Research Center of the US Department of Agriculture (USDA) in Tucson, Arizona. It bears mention that he had no experience in beekeeping aside from a very limited project in a youth group long before.

As the African honey bee, *Apis mellifera scutellata*, moved north through Central America toward the southern USA in the 1980s, his official duties came to include some attention to monitoring and managing “killer bees”, while he was still paid mainly to work on such questions as characteristics of various pollens that make them attractive to the bees. Accordingly, as a venom researcher Schmidt was an amateur in the narrow sense of one who does it out of avocation, rather than gainful employment.

The conditions of his employment are very much relevant to this factor. Unlike the considerable freedom of research in academia, government labs tend to be quite restrictive in the problems that scientists may pursue. He later commented (Schmidt 2020) that “The change from an academic and intellectual environment in Georgia to a USDA environment in Tucson was an earthquake-sized cultural shock.” To him, the USDA lab was little better than an intellectual wasteland and one beset by bureaucratic obstacles to serious research. These latter extended to suspicion of independent research outside of working hours. He gained some relief as an adjunct member of the

graduate faculty in Entomology at the local University of Arizona. As another major work-around, he established a substantial home lab as the Southwestern Biological Institute, in which he kept a broad array of experimental animals. In addition, he lived and worked in a spectacular part of the country, the Sonoran Desert, with a grand abundance of creatures of interest. The result of these factors is in abundant evidence in his research output. If anything, this increased in intensity after his retirement from the USDA in 2005.

It should not be supposed that Schmidt neglected the job for which he was paid. As seen in his list of publications, he was productive in projects relating to beekeeping, even if these may not figure prominently in his legacy.

The final push

After receiving a number of hints over the years that all was not well in his physical makeup, in 2013 Schmidt was unequivocally diagnosed with a relatively severe form of Parkinson's Syndrome. It affected his mental acuity hardly at all, but it gradually came to impose severe physical limitations. It was plain that he could not expect to live a great many more years. Facing the situation, he determined to give greater attention to completing his research projects, with emphasis on those already at a fairly mature stage. At the same time, he also accepted some invitations to prepare papers that could be completed relatively quickly (e.g. Schmidt and Overal 2021). As seen in the bibliography (Suppl. material 1), the last 10 years of this life saw the publication of 55 papers and "The Sting of the Wild".

The Public Intellectual

Many scientists and others with advanced degrees are quite incapable of communicating their subjects to the general public (if it even occurs to them that they should try). Schmidt was very far from being in this mold. There was a keen public interest in stinging insects and arachnids, and he was the very rare individual adept at satisfying it. He knew the subject in greater depth than anyone else, communicated well to individuals and groups in all sectors of society, projected well on television, and he was glad to go public.

Schmidt had always been a sought-after speaker at scientific gatherings, interviewed several times by the news media, and in 2015 a recipient of the prestigious Ig Nobel Prize (https://en.wikipedia.org/wiki/List_of_Ig_Nobel_Prize_winners). With the success of "The Sting of the Wild", he became yet more of a public figure and in greater demand for interviews. Most prominently, he was a featured guest on the "Jimmy Kimmel Live" television show <https://spaces.hightail.com/space/rFcTAWIG1a>. "The Sting of the Wild" probably did as much as all of his media appearances to promote the biological view of venoms and stinging. It is presented in an unrelenting spirit of

curiosity, even of fun, with many episodes of trial-and-error learning recounted. One virtue of the book is its frequent mention of unanswered questions. Although he never held an academic position, Schmidt was very much a teacher, as the many younger individuals that he mentored can testify (e.g. Binford et al. 2023). In pointing to areas of ignorance, he was plainly hoping to stimulate and guide others to provide answers through research.

Acknowledgements

Thanks to the journal's reviewers (R.M. Crewe and J.W. Wenzel) for critical comment.

References

- Binford GJ, Robinson SD, Klotz SA (2023) Justin O. Schmidt – His extraordinary impact on toxinology and arthropod biodiversity science. *Toxicon* 234: 107287. <https://doi.org/10.1016/j.toxicon.2023.107287>
- Cane JH, Singer TL, Pernal SF (2023) Stung by insatiable curiosity. *American Entomologist Summer 2023*: 54–55. <https://doi.org/10.1093/ae/tmad038>
- Nicander of Colophon (1953) *Theriaca*. www.attalus.org/poetry/theriaca.html
- Piek T (Ed.) (1986) *Venoms of the Hymenoptera: Biochemistry, Pharmacology, and Behavioural Aspects*. Academic Press (London), 1–570. <https://doi.org/10.1016/C2013-0-11309-8>
- Pliny the Elder (1855) *The Natural History of Pliny*. Vol. 1. London: Henry G. Bohn, 496 pp. <https://doi.org/10.5962/bhl.title.56616>
- Robinson SD, Deuis JR, Touchard A, Keramidas A, Mueller A, Schroeder CI, Barassé V, Walker AA, Brinkwirth N, Jami S, Bonnafé E, Treilhou M, Undheim EAB, Schmidt JO, King GF, Vette I (2023) Ant venoms contain vertebrate-selective pain-causing sodium channel toxins. *Nature Communications* 14: 2977. <https://doi.org/10.1038/s41467-023-38839-1>
- Schmidt JO (1977) *Defensive strategies of wasps and ants: Dasymutilla occidentalis and Pogonomyrmex badius*. PhD thesis, University of Georgia, Athens.
- Schmidt JO (1978) Ant venoms: A study of venom diversity. In: Shankland DL, Hollingworth RM, Smyth T (Eds) *Pesticide and Venom Neurotoxicity*. Plenum (New York), 247–263.* https://doi.org/10.1007/978-1-4615-8834-4_20
- Schmidt JO (1982) Biochemistry of insect venoms. *Annual Review of Entomology* 27: 339–368.* <https://doi.org/10.1146/annurev.en.27.010182.002011>
- Schmidt JO (1986) Chemistry, pharmacology, and chemical ecology of ant venoms. In: Piek T (Ed.) *Venoms of the Hymenoptera: Biochemical, Pharmacological and Behavioural Aspects*. Academic Press (London), 425–508.* <https://doi.org/10.1016/B978-0-12-554770-3.50013-9>

* Asterisks mark a selection of Schmidt's papers that we consider most significant (whether cited in this paper or not). For a complete list of his research publications, see the Suppl. material 1.

- Schmidt PJ, Schmidt JO (1989) Harvester ants and horned lizards: Predator-prey interactions. In: Schmidt JO (Ed.) Special Biotic Relationships in the Arid Southwest. Univ. of New Mexico Press (Albuquerque), 25–51.*
- Schmidt JO (1990) Hymenopteran venoms: striving toward the ultimate defense against vertebrates. In: Evans DL, Schmidt JO (Eds) Insect Defenses: Adaptive Mechanisms and Strategies of Prey and Predators. State Univ. of New York Press (Stony Brook), 387–419.*
- Schmidt JO (1995) Toxinology of venoms from the honeybee genus *Apis*. *Toxicon* 33: 917–927.* [https://doi.org/10.1016/0041-0101\(95\)00011-A](https://doi.org/10.1016/0041-0101(95)00011-A)
- Schmidt JO (1998) Mass action in honey bees: Alarm, swarming and the role of releaser pheromones. In: VanderMeer RK, Breed MD, Espelie KE, Winston ML (Eds) Pheromone Communication in Social Insects. Westview (Boulder), 257–290.* <https://doi.org/10.1201/9780429301575-11>
- Schmidt JO (2004) Venom and the good life in tarantula hawks (Hymenoptera: Pompilidae): How to eat, not be eaten, and live long. *Journal of the Kansas Entomological Society* 77: 402–413.* <https://doi.org/10.2317/E-39.1>
- Schmidt JO (2015) Allergy to venomous insects. In: Graham JM (Ed.) *The Hive and the Honey Bee* (new rev. ed.). Dadant (Hamilton, Illinois), 907–952.*
- Schmidt JO (2016) *The Sting of the Wild*. Johns Hopkins Univ. Press (Baltimore), 1–280.*
- Schmidt JO (2018) Arthropod toxins and venoms. In: Mullen GR, Durden LA (Eds) *Medical and Veterinary Entomology*. Academic Press (London), 23–31.* <https://doi.org/10.1016/B978-0-12-814043-7.00003-0>
- Schmidt JO (2019) Pain and lethality induced by insect stings: an exploratory and correlational study. *Toxins* 11: 427. <https://doi.org/10.3390/toxins11070427>
- Schmidt JO (2020a) March 23 (unpublished autobiographical essay). Archive of the International Union for the Study of Social Insects, Copenhagen.
- Schmidt JO (2020b) Decision making in honeybees: a time to live, a time to die? *Insectes Sociaux* 67: 337–344.* <https://doi.org/10.1007/s00040-020-00759-4>
- Schmidt JO, Blum MS (1978) A harvester ant venom: chemistry and pharmacology. *Science* 200 (4345): 1064–1066.* <https://doi.org/10.1126/science.653354>
- Schmidt JO, Blum MS (1977) Adaptations and responses of *Dasymutilla occidentalis* to predators. *Entomologia Experimentata et Applicata* 21: 99–111.* <https://doi.org/10.1111/j.1570-7458.1977.tb02663.x>
- Schmidt JO, Blum MS, Overall WL (1980) Comparative lethality of venoms from stinging hymenoptera. *Toxicon* 18: 469–474.* [https://doi.org/10.1016/0041-0101\(80\)90054-9](https://doi.org/10.1016/0041-0101(80)90054-9)
- Schmidt JO, Blum MS, Overall WL (1984) Hemolytic activities of stinging insect venoms. *Archives of Insect Biochemistry and Physiology* 1: 155–160.* <https://doi.org/10.1002/arch.940010205>
- Schmidt JO, Schmidt LS, Schmidt DK (2021) The paradox of the velvet-ant (Hymenoptera, Mutillidae). *Journal of Hymenoptera Research* 84: 327–337.* <https://doi.org/10.3897/jhr.84.68795>
- Schmidt JO, Schmidt LS (2022) Vinegaroons (Uropygi: *Mastigoproctus tohono*) in a multi-predator/multi-prey system: Prey, predators, and cannibalism. *Journal of Arachnology* 50: 267–276.* <https://doi.org/10.1636/JoA-S-21-005>

Schmidt JO, Yamane Sô, Matsuura M, Starr CK (1986) Hornet venoms: Lethalities and lethal capacities. *Toxicon* 24: 950–954.* [https://doi.org/10.1016/0041-0101\(86\)90096-6](https://doi.org/10.1016/0041-0101(86)90096-6)

Schmidt JO, Overal WL (2021) Giant Amazonian ants (*Dinoponera*). In: Starr CK (Ed.) *Encyclopedia of Social Insects*. Springer (Cham, Switzerland), 434–439. https://doi.org/10.1007/978-3-030-28102-1_50

Schoeters E, Schmidt JO, Billen J (1997) Venom gland morphology in *Pepsis pallidolimbata pallidolimbata* and biological use and activity of *Pepsis* venom. *Canadian Journal of Zoology* 75: 1014–1019.* <https://doi.org/10.1139/z97-122>

Supplementary material I

Publications of Justin O. Schmidt

Authors: Christopher K. Starr, Robert S. Jacobson, William L. Overal

Data type: docx

Copyright notice: This dataset is made available under the Open Database License (<http://opendatacommons.org/licenses/odbl/1.0/>). The Open Database License (ODbL) is a license agreement intended to allow users to freely share, modify, and use this Dataset while maintaining this same freedom for others, provided that the original source and author(s) are credited.

Link: <https://doi.org/10.3897/jhr.97.121387.suppl1>

A review of *Trypoxylon* Latreille, 1796 (Hymenoptera, Crabronidae) of Southwest China with descriptions of two new species

Yan Fu¹, Nawaz Haider Bashir^{1,2}, Qiang Li¹, Li Ma¹

1 Department of Entomology, College of Plant Protection, Yunnan Agricultural University, Kunming, Yunnan, 650201, China **2** College of Biological Resource and Food Engineering, Qujing Normal University, Qujing, Yunnan, 655011, China

Corresponding authors: Qiang Li (liqiangkm@126.com); Li Ma (maliwasps@aliyun.com)

Academic editor: Editor | Received 20 February 2024 | Accepted 14 April 2024 | Published 29 April 2024

<https://zoobank.org/A4411DB8-035B-4BB6-A2C6-8E3B40AD0C85>

Citation: Fu Y, Bashir NH, Li Q, Ma L (2024) A review of *Trypoxylon* Latreille, 1796 (Hymenoptera, Crabronidae) of Southwest China with descriptions of two new species. Journal of Hymenoptera Research 97: 307–347. <https://doi.org/10.3897/jhr.97.121279>

Abstract

Two new species of the genus *Trypoxylon* (Hymenoptera: Crabronidae: Crabroninae: Trypoxylini) from Yunnan Province, China: *T. abelothoracicus* Fu & Li, **sp. nov.** and *T. ferrugineipes* Fu & Li, **sp. nov.** are described and illustrated. The female of *T. infoveatum* Li & Li, 2007 is described for the first time. In addition, ten species of *Trypoxylon* are newly recorded from China: *T. buddha* Cameron, 1889, *T. flavipes* Tsuneki, 1979, *T. fulvocollare* Cameron, 1904, *T. gampahae* Tsuneki, 1981, *T. imayoshii* Yasumatsu, 1938, *T. kandyianum* Tsuneki, 1979, *T. khasiae* Cameron, 1904, *T. nasale* Tsuneki, 1979, *T. pahangense* Tsuneki, 1979, and *T. pendleburyi* Tsuneki, 1979. An updated key to *Trypoxylon* of Southwest China is provided.

Keywords

Crabronidae, Identification key, new records, taxonomy

Introduction

Southwest China, belonging to the main bioregions of Southeast Asia (Indochina), is recognized as one of the world's 36 biodiversity hotspots and one of the regions with the richest and most threatened fauna worldwide. It's located at the intersection of the

Oriental and Palearctic regions, spanning subtropics and tropics and including plateau climate, tropical rainforest climate, and subtropical monsoon climate (CEPF 2020; Myers et al. 2000; Liu et al. 2022; Liu et al. 2023; Meng et al. 2023).

Southwest China, with an area of 2.5 million square kilometers, includes Yunnan Province, Guizhou Province, Sichuan Province, Chongqing Municipality, and Tibet Autonomous Region and is divided into three terrain units (Qinghai-Tibet Plateau, Yunnan-Guizhou Plateau, and Sichuan Basin), with the Hengduan Mountains, Yunnan-Guizhou Plateau, and Wushan Mountains regarded as the ‘Sky Islands of China’ and is a refuge for a wide range of flora and fauna, with an obvious vertical distribution of species (He and Jiang 2014; Yi et al. 2021; Wang et al. 2023). The species found in the southern and western regions have distinct Oriental characteristics, while those inhabiting the high mountain areas are related Palearctic species; hence, the insect fauna is diversified and abundant (Kryzhanovskiy 1956).

Trypoxylon Latreille, 1796, has the widest distribution and most species (633 species and 84 subspecies) among the seven genera of Trypoxylini (Hymenoptera: Crabronidae: Crabroninae) (Pulawski 2024). They usually build their nests in the wood or plant stalks and prey on spiders (Barth 1910; Kazenas 2001). Its members have a slender body 5.5–22.0 mm long; the inner eye orbits are notched; the antennal socket is far away from the frontoclypeal suture; the forewing has only one submarginal cell; and the petiole is long, stick-shaped, or flask-shaped (Bohart and Menke 1976).

Many authors studied the taxonomy of *Trypoxylon*. Richards (1934) revised the New World species, recognizing several species groups, and Tsuneki (1956a, b, 1972, 1973, 1974, 1976, 1977, 1978a, b, 1979a, b, c, 1980a, b, 1981a, b, c, d, e, f, 1986) studied the species of the Oriental and Australian Regions, including certain species of Northeast Asia and Europe. Bohart and Menke (1976) reviewed the genus on the worldwide basis, and Antropov (1984, 1985, 1986, 1987, 1988, 1989a, b, c, 2011, 2016) examined the species of the Palearctic and Oriental Regions. As of 2024, 633 species are known (Pulawski 2024).

In China, 55 species and nine subspecies of this genus are currently known, with 37 species and one subspecies found in southwest China (Strand 1922; Tsuneki 1966–1981; Wu and Zhou 1996; Li and Li 2007, 2010). Despite the extensive taxonomic studies conducted there over the past few decades, new species are continuously being discovered in various regions of Southwest China, especially in the tropical rainforests of Yunnan Province. In this study, two new species from Xishuangbanna, Yunnan, China, are described and illustrated; the female of *T. infoveatum* Li & Li, 2007 is described for the first time; ten species are recorded for the first time from China; and a key to the genus *Trypoxylon* of southwest China is provided.

Material and methods

The specimens examined are deposited in the Insect Collection of Yunnan Agricultural University, Kunming, China (YNAU). The specimens were observed and illustrated using an Olympus stereomicroscope (SZ Series) with an ocular micrometer.

The photographs were taken with the VHX-5000 digital microscopic system and edited with Adobe Photoshop® 8.0. The descriptive terminology of morphological structures follows Bohart and Menke (1976) and Tsuneki (1979a). The abbreviations are as follows:

AW	apical width of the first flagellomere;
BW	basal width of the apical flagellomere in male;
CV1, CV2	abscissa I of cubital vein, abscissa II of cubital vein;
F I, F II, F III, etc.	the first, second and third flagellomere, etc.;
GL/ W	ratio of gastral petiole length to apical width (dorsal view);
HL	head length (frontal view);
HW	head width (frontal view);
IOD	interocular distance;
IODc	minimum IOD at base of clypeus (frontal view);
IODv	minimum IOD at vertex (dorsal view);
IODs	ratio of IODv to IODc;
OOD	ocellocular distance;
Od	posterior ocellus diameter;
PD	puncture diameter;
PIS	puncture interspace;
POD	postocellar distance;
RI	apical part of forewing vein RI beyond the meeting point with Rs;
TCV	transverse cubital vein.

The frontal shield in some species has lateral bifurcation directed towards the eye incision; the upper area of the frontal shield is the area from the top to the base of the lateral bifurcation, and the lower area is from the base of the lateral bifurcation to the junction of the lateral carina in the frontal end.

Key to the species of *Trypoxylon* from Southwest China

Females

- 1 Frons with shield-shaped enclosure; fore-wings with CV2 and TCV usually forming acute angle; dorsal and posterior area of propodeum with several conspicuous, transverse carinae **2**
- Frons without shield-shaped enclosure; fore-wings with CV2 and TCV usually forming right or obtuse angle; dorsal and posterior area of propodeum without transverse carinae **4**
- 2 Frontal shield discontinued, upper lateral carina broadly interrupted but dorsal carina clearly defined..... *Trypoxylon interruptum* Tsuneki, 1978
- Frontal shield complete, upper lateral carina and dorsal carina continued **3**
- 3 Frontal shield with upper area subequal in length to lower area, at most 1.5 × as long as lower area, lateral carina of upper area curved; lateral surface of propo-

- deum coriaceous, conspicuously obliquely rugose
 *Trypoxylon schmiedeknechtii* Kohl, 1906
- Frontal shield with upper area more than 1.5 × as long as lower area, lateral carina of upper area almost parallel; lateral surface of propodeum smooth medially and posteriorly, with inconspicuous oblique rugae anteriorly
 *Trypoxylon thaianum* Tsunek, 1961
- 4 Gastral terga I–III with apical fovea; pronotal collar narrow, with median tubercle 5
- Gastral terga I–III without apical fovea; pronotal collar broad, without median tubercle 8
- 5 Frons and mesoscutum with large punctures, PIS ≤ 0.5 × PD, PIS shiny; lateral surface of propodeum dull, with conspicuous oblique rugae; free margin of clypeus markedly concave laterally, with short and wide protrusion medially
 *Trypoxylon buddha* Cameron, 1889
- Frons and mesoscutum with fine punctures, PIS ≈ PD, PIS microscopically coriaceous; lateral surface of propodeum smooth, without rugae; free margin of clypeus straight or slightly convex laterally 6
- 6 Gastral tergum I without apicomedian fovea; legs black, at most partly brown....
 *Trypoxylon bifoveatum* Tsuneki, 1979
- Gastral tergum I with apicomedian fovea; legs broadly yellow, only partly brown or black 7
- 7 Supraantennal tubercle with transverse subquadrate edge anteriorly; R1 equal to TCV, not reaching wing apex; gaster wholly black
 *Trypoxylon maculipes* Tsuneki, 1979
- Supraantennal tubercle rounded, without anterior transverse edge; R1 longer than TCV, almost reaching wing apex; gastral terga II–IV, base of gastral sternum III, gastral sternum IV ferruginous *Trypoxylon flavipes* Tsuneki, 1979
- 8 Gastral petiole clavate, gradually widening apically, as long as, or shorter than following two segments combined 9
- Gastral petiole flask-shaped, apical swelling rather abrupt, with parallel-sided stalk, longer than following two segments combined 22
- 9 Mandible thick, bidentate on inner margin near apex; head in frontal view quadrate, in dorsal view thick; median and lower frons roundly swollen
 *Trypoxylon gampahae* Tsuneki, 1981
- Mandible slender, without denticle on inner margin; head wider than long; median and lower frons not roundly swollen 10
- 10 Frontal furrow deeply impressed; legs slender and long (hind tibia about 1.25 × as long as HW, midtarsomere I longer than half HW), hind coxa more than three × apical width; propodeal dorsum long, more than 3.5 × as long as scutellum
 *Trypoxylon ferrugineipes* Fu & Li, sp. nov.
- Frontal furrow very fine, inconspicuously impressed; legs thick and short (hind tibia about 0.93 × as long as HW, midtarsomere I shorter than half HW), hind coxa as long as, or shorter than twice apical width; propodeal dorsum short, shorter than 3.5 × as long as scutellum 11

- 11 Supraantennal tubercle with deep, longitudinal groove 12
- Supraantennal tubercle without deep, longitudinal groove 13
- 12 Sides of supraantennal tubercle with few rugae; gaster wholly black; IODs = 2:1
..... *Trypoxylon koreanum* Tsuneki, 1956
- Sides of supraantennal tubercle without rugae; gastral sterna II–III ferruginous brown, and apex of gastral petiole to sternum V yellow; IODs = 5:2.....
..... *Trypoxylon okinawanum* Tsuneki, 1966
- 13 Propodeal enclosure not delimited by boundary groove, densely covered with irregular, reticulate carinae; pronotal collar with black posterior band..... 14
- Propodeal enclosure delimited by more or less distinct U-shaped groove, surface smooth or covered with several transverse carinae medially; pronotal collar with light brown, translucent posterior band..... 15
- 14 Supraantennal tubercle conspicuously nasiform, with thick, longitudinal carina; clypeus with dense tiny punctures, free margin with small, rectangular protrusion medially, protruding area shallowly incised mesally
..... *Trypoxylon fronticorne obliquum* Tsuneki, 1981
- Supraantennal tubercle low, with thin, longitudinal carina; clypeus with sparse large punctures, free margin with large, rectangular protrusion medially
..... *Trypoxylon figulus* (Linnaeus, 1758)
- 15 Supraantennal tubercle low, medial longitudinal carina thin 16
- Supraantennal tubercle highly nasiform, medial longitudinal carina thick..... 20
- 16 Gaster black, most of gastral sterna brownish 17
- Gaster more or less ferruginous 18
- 17 Free margin of clypeus with nearly triangular protrusion, bidentate mesally; side of propodeum with distinct lateral carina..... *Trypoxylon shimoyamai* Tsuneki, 1958
- Free margin of clypeus with inverted trapezoid protrusion medially; side of propodeum without lateral carina *Trypoxylon aphelothoracicus* Fu & Li, sp. nov.
- 18 Free margin of clypeus rounded, without protrusion medially; U-shaped boundary groove on propodeal enclosure almost invisible and medial furrow shallow, surface smooth and shiny, without punctures or rugae
..... *Trypoxylon truncatum* Tsuneki, 1979
- Free margin of clypeus with distinct protrusion medially; U-shaped boundary groove on propodeal enclosure and medial furrow clear and distinct, surface with conspicuous and dense rugae..... 19
- 19 Free margin of clypeus with distinct obtuse protrusion; supraclypeal area slightly narrow and long; gaster wholly ferruginous..... *Trypoxylon pahangense* Tsuneki, 1979
- Free margin of clypeus medially with distinctly inverted trapezoidal protrusion; supraclypeal area broad and short; gaster ferruginous from apex of petiole to apical gastral segment *Trypoxylon ferrugiabdominale* Li & Li, 2007
- 20 Free margin of clypeus conspicuously produced, with large semi-elliptic protrusion medially, as long as Od; gastral petiole and segments IV–VI black; legs wholly black *Trypoxylon clypeisinuatum* Li & Li, 2010
- Free margin of clypeus slightly produced medially, protrusion small, shorter than Od; gastral terga IV–VI ferruginous or with black maculae; legs partly ferruginous..... 21

- 21 Free margin of clypeus ferruginous, with semicircular protrusion, produced area shallowly incised mesally; gastral petiole broad and short, $GL/W = 2.7-3.0$; gaster wholly ferruginous; all trochanters amber yellow.....
..... *Trypoxylon nasale* Tsuneki, 1979
- Free margin of clypeus black, with two barely separated and round teeth medially; gastral petiole much slender, $GL/W = 3.5-3.9$; gaster ferruginous from apex of petiole to apical segment; all trochanters black.....
..... *Trypoxylon pendleburyi* Tsuneki, 1979
- 22 Gaster wholly or from apex of petiole to apical segment ferruginous..... 23
- Gaster black or middle part (from apex of petiole to segment III or IV or base of segments II–III) ferruginous 25
- 23 Gaster wholly ferruginous, petiole with black macula; supraantennal furrow absent; supraantennal tubercle low, with anterior transverse carina connected to antennal socket rim..... *Trypoxylon kandyanum* Tsuneki, 1979
- Gaster from apex of petiole to apical segment ferruginous; supraantennal furrow well developed; supraantennal tubercle without anterior transverse carina..... 24
- 24 Supraantennal tubercle attenuate apically, apex of supraantennal tubercle obliquely inclined, forming smooth and shiny area with large median hollow; margin of clypeus sinuate; antenna and legs mostly ferruginous; body length 11.9–12.5 mm..... *Trypoxylon kbasiae* Cameron, 1904
- Supraantennal tubercle broaden apically, without anterior oblique flattened area; free margin of clypeus rounded; antenna and legs mostly black; body length 22.0 mm..... *Trypoxylon szechuen* Tsuneki, 1981
- 25 Mesoscutum microscopically coriaceous, with fine, dense punctures, $PIS \leq PD$ 26
- Mesoscutum smooth and shiny, with fine, scattered punctures, $PIS > PD$ 28
- 26 Supraantennal tubercle without median carina, instead impressed line separated apex of supraantennal tubercle; pronotal collar thick.....
..... *Trypoxylon bilobatum* Tsuneki, 1961
- Supraantennal tubercle with median carina; pronotal collar thin..... 27
- 27 Supraantennal tubercle low tuberiform; propodeal enclosure with clear U-shaped boundary groove and medial furrow; base of gastral segments II–IV and legs mostly ferruginous *Trypoxylon imayoshii* Yasumatsu, 1938
- Supraantennal tubercle highly nasiform, with deep groove medially; propodeal enclosure with vague U-shaped boundary groove, without medial furrow; gaster wholly and legs black *Trypoxylon infoveatum* Li & Li, 2007
- 28 Supraantennal furrow shallow; antennal socket rim anteriorly expanded into two separate cylinders; gaster wholly black..... *Trypoxylon takasago* Tsuneki, 1966
- Supraantennal furrow deep; antennal socket rim not expanded; gaster ferruginous medially 29
- 29 Setae on head and thorax golden; pronotal collar posteriorly and base of gastral segments II–III ferruginous; body length 22.2 mm.....
..... *Trypoxylon fulvocollare* Cameron, 1904
- Setae on head and thorax silvery; pronotal collar black posteriorly, gaster ferruginous from apex of petiole to segment III or IV; body length 18.0–20.0 mm.... 30

- 30 Free margin of clypeus transversely produced mesally, slightly incised; gaster ferruginous from apex of petiole to segment III, darkly marked dorsally and ventrally; legs black; IODs = 1:1..... *Trypoxylon orientale* Cameron, 1904
- Free margin of clypeus rounded mesally, not produced and incised; gaster ferruginous from apex of petiole to base of segment IV; legs black, with ferruginous spots; IODs varied 31
- 31 Side of propodeum with distinct lateral carina; all trochanters amber yellow; IODs = 1.5:1 *Trypoxylon errans* Saussure, 1867
- Side of propodeum without lateral carina; all trochanters amber black..... 32
- 32 Lateral tubercles of pronotum toothed; vertex conspicuously depressed; F I = 2.8–3.3 × AW; antenna mostly ferruginous beneath; body length 14.0–19.0 mm
..... *Trypoxylon bicolor* Smith, 1856
- Lateral tubercles of pronotum triangular; vertex undepressed; F I = 2.0–2.5 × AW; antenna brown beneath; body length 10.0–19.0 mm
..... *Trypoxylon petiolatum* Smith, 1858

Males

- 1 Frons with shield-shaped enclosure; fore-wings with CV2 and TCV usually forming acute angle; dorsal and posterior area of propodeum with several conspicuous, transverse carinae 2
- Frons without shield-shaped enclosure; fore-wings with CV2 and TCV usually forming right or obtuse angle; dorsal and posterior area of propodeum without transverse carinae 4
- 2 Frontal shield discontinued, upper lateral carina broadly interrupted but dorsal carina clearly defined; flagellomere III beneath with linear tyloids, flagellomere IV excavate beneath at base (apical flagellomere longer than two but shorter than three preceding articles combined)
..... *Trypoxylon interruptum* Tsuneki, 1978
- Frontal shield complete, upper lateral carina and dorsal carina continued; flagellomeres not modified 3
- 3 Frontal shield with upper area as long as lower area, upper lateral carina curved; apical flagellomere longer than three but shorter than four preceding articles combined *Trypoxylon schmiedeknechtii* Kohl, 1906
- Frontal shield with upper area longer than lower area; apical flagellomere as long as three preceding articles combined.....
..... *Trypoxylon thaianum* Tsunek, 1961
- 4 Gastral terga I–III with apical fovea; pronotal collar narrow, with median tubercle 5
- Gastral terga I–III without apical fovea; pronotal collar broad, without median tubercle 8
- 5 Frons and mesoscutum with large punctures, PIS ≤ 0.5 × PD, PIS shiny; lateral surface of propodeum dull, with conspicuous oblique rugae; lateral margin of clypeus slightly concave, with short, wide protrusion medially (penis valve sub-

- apically with narrow, curved hook on each side).....
- *Trypoxylon buddha* Cameron, 1889
- Frons and mesoscutum with fine punctures, PIS ≈ PD, PIS microscopically coriaceous; lateral surface of propodeum smooth, without rugae; lateral margin of clypeus straight or slightly convex 6
- 6 Gastral tergum I without fovea; flagellomeres II–VI beneath with tyloids, flagellomeres VII–VIII excavate at base *Trypoxylon bifoveatum* Tsuneki, 1979
- Gastral tergum I with fovea; flagellomeres II–VI beneath without tyloids, flagellomeres V–VI excavate at base..... 7
- 7 Supraantennal tubercle subquadrate, surface nearly flat, including supraantennal furrow; R1 equal to TCV, not reaching wing apex; penis valve simple at apex
- *Trypoxylon maculipes* Tsuneki, 1979
- Supraantennal tubercle low, broad, roundly tuberiform, apical edge curved, not including supraantennal furrow; R1 longer than TCV, almost reaching apex of wing; penis valve subapically with narrow, curved hook on each side
- *Trypoxylon flavipes* Tsuneki, 1979
- 8 Gastral petiole clavate, as long as or shorter than segments II–III combined 9
- Gastral petiole flask-shaped, longer than segments II–III combined..... 20
- 9 Supraantennal tubercle with deep longitudinal groove
- *Trypoxylon koreanum* Tsuneki, 1956
- Supraantennal tubercle without deep longitudinal groove..... 10
- 10 Propodeal enclosure not delimited by boundary groove, densely covered with irregular, reticulate carinae; pronotal collar with black posterior band; penis valve with more or less pronounced preapical enlargement 11
- Propodeal enclosure delimited by more or less distinct U-shaped groove, surface smooth or covered with several transverse carinae medially; pronotal collar with light brown, translucent posterior band; penis valve without preapical enlargement 12
- 11 Supraantennal tubercle highly nasiform, with thick mid-longitudinal carina; flagellomeres without tyloids *Trypoxylon fronticorne obliquum* Tsuneki, 1981
- Supraantennal tubercle low, longitudinal carina thin; flagellomeres III–VIII beneath with tyloids *Trypoxylon figulus* (Linnaeus, 1758)
- 12 Median and lower frons flat, without apical transverse carina and medial carina (flagellomeres I–XI beneath with tyloids, flagellomere IV excavate at base beneath)
- *Trypoxylon planifrons* Tsuneki, 1977
- Median and lower frons raised, with apical transverse carina or medial carina . 13
- 13 Supraantennal tubercle highly nasiform, medial longitudinal carina thick..... 14
- Supraantennal tubercle low, medial longitudinal carina narrow..... 17
- 14 Antenna without tyloids..... 15
- Antenna with tyloids..... 16
- 15 Apical flagellomere as long as three preceding articles combined; gaster ferruginous, with vaguely outlined, black, regular-shaped band on gastral terga I–IV
- *Trypoxylon fenchibuense* Tsuneki, 1967
- Apical flagellomere as long as four preceding articles combined; gaster brown to black
- *Trypoxylon similichingi* Li & Li, 2010

- 16 Flagellomeres II–IV beneath with linear tyloids, apical flagellomere as long as, or shorter than five preceding articles combined.....
 *Trypoxylon chypeisinuatum* Li & Li, 2010
- Flagellomeres III–IV beneath with linear tyloids, apical flagellomere as long as four preceding articles combined..... *Trypoxylon pacificum* Gussakovskij, 1932
- 17 Apical flagellomere curved, conspicuously hollowed beneath (as long as three preceding articles combined); U-shaped boundary groove on propodeal enclosure almost invisible and medial furrow shallow, surface smooth and shiny, without punctures or rugae *Trypoxylon truncatum* Tsuneki, 1979
- Apical flagellomere not curved; U-shaped boundary groove on propodeal enclosure and medial furrow clear, distinct, surface with conspicuous dense rugae ..18
- 18 Flagellomeres without tyloids and not excavate beneath (apical flagellomere as long as four preceding articles combined).....
 *Trypoxylon ferrugiabdominale* Li & Li, 2007
- Flagellomeres with tyloids 19
- 19 Flagellomeres V–VI stoutly dentate beneath, apical flagellomere as long as two preceding articles combined *Trypoxylon shimoyamai* Tsuneki, 1958
- Flagellomeres not dentate beneath, flagellomeres III–VIII beneath with linear tyloids, apical flagellomere as long as three preceding articles combined.....
 *Trypoxylon kansitakum* Tsuneki, 1971
- 20 Apical flagellomere as long as or longer than four preceding articles combined21
- Apical flagellomere shorter than four preceding articles combined23
- 21 Flagellomere VIII excavate beneath at base, distinctly incrassate toward apex; supraantennal tubercle highly nasiform, with deep longitudinal groove at base.....
 *Trypoxylon infoveatum* Li & Li, 2007
- Flagellomeres unmodified; supraantennal tubercle tuberiform, without groove...
 22
- 22 Apical flagellomere longer than five preceding articles combined; setae on head and thorax silvery; gastral segments II–III ferruginous
 *Trypoxylon errans* Saussure, 1867
- Apical flagellomere as long as four preceding articles combined; setae on head and thorax golden; apex of gastral segments II–III ferruginous
 *Trypoxylon fulvocollare* Cameron, 1904
- 23 Mesoscutum distinctly microscopically coriaceous, superimposed with punctures, PIS \approx PD, PIS coarse (apical flagellomere longer than two preceding articles combined; base of gastral segments II–IV ferruginous).....
 *Trypoxylon imayoshii* Yasumatsu, 1938
- Mesoscutum without microsculpture, simply punctated, PIS > PD, PIS smooth and shiny 24
- 24 Supraantennal furrow shallow, antennal socket rim anteriorly expanded (supraantennal tubercle round, without transverse carina or band-like expansion at anterior margin; apical flagellomere longer than three preceding articles combined)..
 *Trypoxylon takasago* Tsuneki, 1966
- Supraantennal furrow deep, antennal socket rim not expanded.....25

- 25 Supraantennal tubercle attenuate apically, apex of supraantennal tubercle obliquely inclined, forming smooth and shiny area with large hollow mesally (apical flagellomere longer than two preceding articles combined and shorter than three preceding articles combined)..... *Trypoxylon khasiae* Cameron, 1904
 – Supraantennal tubercle broaden apically, without anterior oblique flattened area 26
- 26 Side of propodeum with distinct lateral carina; clypeus conspicuously protruded medioapically; gaster from apex of petiole to segment III ferruginous laterodorsally, dark dorsally and ventrally *Trypoxylon orientale* Cameron, 1904
 – Side of propodeum without lateral carina; clypeus round medioapically; gaster ferruginous from apex of petiole to base of gastral segment IV 27
- 27 Lateral tubercles of pronotum dentate; vertex conspicuously depressed; apical flagellomere in lateral view distinctly tapering..... *Trypoxylon bicolor* Smith, 1856
 – Lateral tubercles of pronotum triangular; vertex undepressed; apical flagellomere in lateral view not tapering, slightly curved medially
 *Trypoxylon petiolatum* Smith, 1858

***Trypoxylon aphelothoracicus* Fu & Li, sp. nov.**

<https://zoobank.org/23AF9F03-3F22-419E-832F-E62658160F28>

Fig. 1

Type material. *Holotype*: ♀: CHINA, Yunnan Province, Jinghong City, Menghai County, Bulang Mountain, 21°37'35"N, 100°24'23"E, 1438 m., 20.VI–20.VII.2018, Li Ma project team (YNAU). *Paratypes*: 29♀♀: same locality as for holotype except: 20.VI–20.VII.2018 (10♀♀), 20.VII–15.VIII.2018 (3♀♀), 17.V–21.VI.2018 (2♀♀), 25.IV–17.V.2018 (3♀♀), 28.V–28.VI.2019 (10♀♀), 15.IV–27.V.2021 (1♀); 1♀, CHINA, Yunnan, Jinghong City, Menghai County, Guanggang Village, Ancient tea forest, 21°49'15"N, 100°29'44"E, 1526 m, 20.VIII–16.IX.2018, coll. Li Ma project team (YNAU).

Diagnosis. The species resembles *T. minutum* Tsuneki, 1979 and *T. undatum* Tsuneki, 1979 in lacking the lateral carina on the propodeum. It differs from both by the supraantennal tubercle with small U-shaped carina, transverse carina on both sides of apex, and with short, longitudinal carina mesally (in *T. minutum* the supraantennal tubercle is triangular, without transverse carina anteriorly and without middle carina; in *T. undatum* the supraantennal tubercle is low, with conspicuous, transverse carina anteriorly and thick, longitudinal carina mesally), free margin of clypeus with an inverted trapezoid projection (in *T. minutum* the free margin of clypeus is triangularly produced; in *T. undatum* the clypeal margin is wavy, without projection), gastral sterna II–IV black, gastral terga II–IV brown to black (in *T. minutum* gastral sterna II–IV are dark red, gastral terga II–IV are ferruginous; in *T. undatum* gastral sterna and terga II–IV are ferruginous, gastral terga II–III each with broad brown mark).

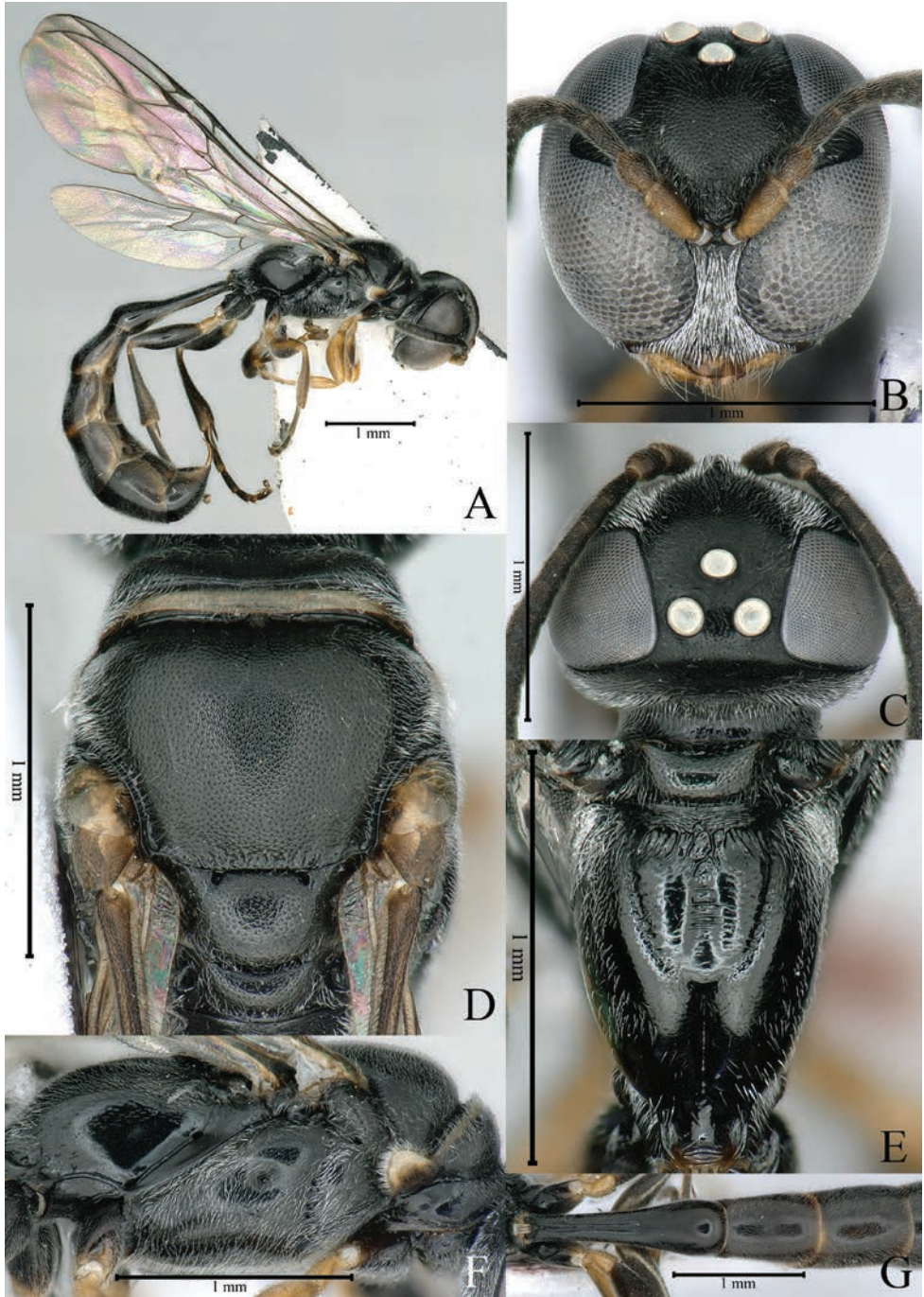


Figure 1. *Trypoxylon aphelothoracicus* sp. nov. holotype ♀ **A** habitus (lateral view) **B** head (frontal view) **C** head (dorsal view) **D** thorax (dorsal view) **E** propodeum (dorsal view) **F** thorax (lateral view) **G** gastral segments I–III (dorsal view).

Description. Female: Body length, 6.9–7.2 mm (Fig. 1A). Body black; labial palpi, maxillary palpi and pronotal lobe apically ivory; yellowish brown are: most of mandible, clypeal apex, scape beneath, foretrochanter, forefemur except with brown stripe on inner surface, foretibia, apex of midcoxa, mid- and hindtrochanters; brown are: mandible apically, pedicel beneath, tegula, midfemur except yellow stripe on outer surface, midtibia and fore- and midtarsi; wings hyaline, veins and pterostigma brown. The following body parts covered with short, dense, silvery pubescence (length of setae less than Od): most of clypeus, supraclypeal area, lower inner orbit, gena, pronotum, metapleuron, side of propodeal dorsum and posterior part of propodeum.

Head: Head quadrate in frontal view (Fig. 1B), HW: HL = 10: 10, thick in dorsal view (Fig. 1C). Mandible simple, without denticle on inner margin. Clypeus nearly flat, with fine, dense punctures; lateral margin of clypeus more concave; free margin of clypeus with inverted trapezoid protrusion that is slightly concave in middle (Fig. 1B). Supraclypeal area narrow, long, length greater than its maximum apical width. Supraantennal tubercle low, its anterior margin with small U-shaped carina, with anterior transverse carina connected to antennal socket rim, and short longitudinal carina mesally (Fig. 1B). Supraantennal furrow lacking. F I = 2.0 × AW, F I: F II: F III = 7: 5: 4. Frons slightly convex medially, microscopically coriaceous, with fine, dense punctures (PIS ≈ PD) and hardly visible medial furrow. Inner eye orbits convergent below, broadly, shallowly notched (IODs = 10:4.5). Vertex slightly convex, ocellar triangle flattened (OOD: Od: POD = 2: 9: 5) (Fig. 1C). Gena narrow, evenly convex.

Thorax: Pronotum with deep, transverse furrow anteriorly, convex laterally, flattened anteriorly, pronotal collar narrow medially, enlarged towards side, without median tubercle, with distinct, translucent, posterior border; pronotal lobes rounded. Mesoscutum (Fig. 1D) microscopically coriaceous, with fine, dense punctures (PIS ≈ PD); admedial line inconspicuously impressed, only extended to 1/4 of scutum length; prescutal sutures absent; parapsidal line distinct. Scutellum and metanotum microscopically coriaceous, with fine and dense punctures (PIS ≈ PD). Metapleuron impunctate (Fig. 1F). Propodeal enclosure with deep U-shaped groove (Fig. 1E), basally with short oblique rugae, with narrow, deep mid furrow and short transverse rugae within furrow, side of groove smooth, impunctate. Posterior part of propodeum with deep mid groove, except apically. Side of propodeum without lateral carina; lateral surface shiny, impunctate (Fig. 1F). In forewing, R1 equal to TCV, CV1 = CV2 × 2.8, TCV < CV2. Hind coxa without small tubercle ventrally.

Gaster: Gastral petiole (Fig. 1G) clavate, about 3.40 × as long as apical width in dorsal view, shorter than segments II–III combined.

Male. Unknown.

Distribution. China (Yunnan).

Etymology. The specific name is derived from two Greek words: *apheles* - (=smooth) and *-thoracicus* (= Latinized form of thorax), referring to the mesopleuron, metapleuron, and propodeal lateral surface smooth, and the side of propodeum without lateral carina in the female.

***Trypoxylon ferrugineipes* Fu & Li, sp. nov.**

<https://zoobank.org/9AE3DBB3-47D1-4DE6-A468-EE7F9EAE5DB9>

Fig. 2

Type material. *Holotype*: ♀: CHINA, Yunnan Province, Jinghong City, Menghai County, Bulang Mountain, 21°37'35"N, 100°24'23"E, ca 1438 m, 21.VI–20.VII.2018, Li Ma project team (YNAU). *Paratype*: 3♀♀: same date as holotype except: 28.V–28.VI.2019 (2♀♀), 13.VIII–15.IX.2020 (1♀).

Diagnosis. The species resembles *T. longipes* Tsuneki, 1979 in having the legs markedly slender and elongate (hind tibia about $1.25 \times$ as long as HW, midtarsomere I longer than half HW), free margin of clypeus wavy, supraantennal tubercle low and supraantennal furrow shallow. It differs by the IODs = 10:7 (in *T. longipes* the IODs = 10:4), gastral petiole slightly flask-shaped, GL/ W = 4.1 (in *T. longipes* gastral petiole distinctly flask-shaped, GL/ W = 5.6), gaster wholly ferruginous (in *T. longipes* gastral tergum V blackish). The species also resembles *T. ambiguum* Tsuneki, 1956 in the shape of the clypeal free margin and pronotal collar, but has a shallow supraantennal furrow (in *T. ambiguum* the supraantennal furrow is absent), IODs = 10:7 (in *T. ambiguum* IODs = 10:9), gastral petiole slightly clavate (in *T. ambiguum* gastral petiole flask-shaped), GL/ W = 4.1 (in *T. ambiguum* GL/ W = 5.0).

Description. Female: Body length, 7.7–8.0 mm (Fig. 2A). Body black; labial palpi, maxillary palpi and most of pronotal lobe ivory; yellow are: most of mandible, clypeal apex, scape and pedicel beneath, foreleg except base of forecoxa, midleg from apex of midcoxa to midtarsomere I; yellowish brown are: mandible apically, midtarsomere II–IV, hindcoxa on inner surface, hindtrochanter and inner surface of hindfemur; gaster wholly ferruginous; wings hyaline, veins and pterostigma brown. The following body parts covered with short, dense, silvery pubescence (length of setae less than Od): most of clypeus, supraclypeal area, lower inner orbit, gena, pronotum, side of propodeal dorsum and posterior part of propodeum.

Head: Head rounded in frontal view (Fig. 2B), HW: HL = 10: 9, thin in dorsal view (Fig. 2C). Mandible simple, without denticle on inner margin. Clypeus nearly flat, with fine, dense punctures; lateral margin of clypeus slightly concave; margin of clypeus sinuate, slightly concave medially (Fig. 2B). Supraclypeal area narrow and long, length greater than its maximum apical width. Supraantennal tubercle low, without anterior transverse carina, with short longitudinal carina mesally (Fig. 2B); supraantennal furrow shallow in dorsal view. F I = $3.0 \times$ AW, F I: F II: F III = 3: 2: 2. Frons microscopically coriaceous, with fine, dense punctures (PIS \approx PD), frontal furrow deeply impressed. Inner eye orbits convergent below, with broad, shallow notch (IODs = 10:7). Vertex slightly convex, ocellar triangle flattened (OOD: Od: POD = 1: 7: 5) (Fig. 2C). Gena narrow, evenly convex.

Thorax: Pronotum with deep transverse furrow anteriorly, convex laterally, flattened anteriorly, pronotal collar narrow medially and enlarged towards side, with minute median tubercle, with distinct, translucent, posterior border; pronotal lobe round-

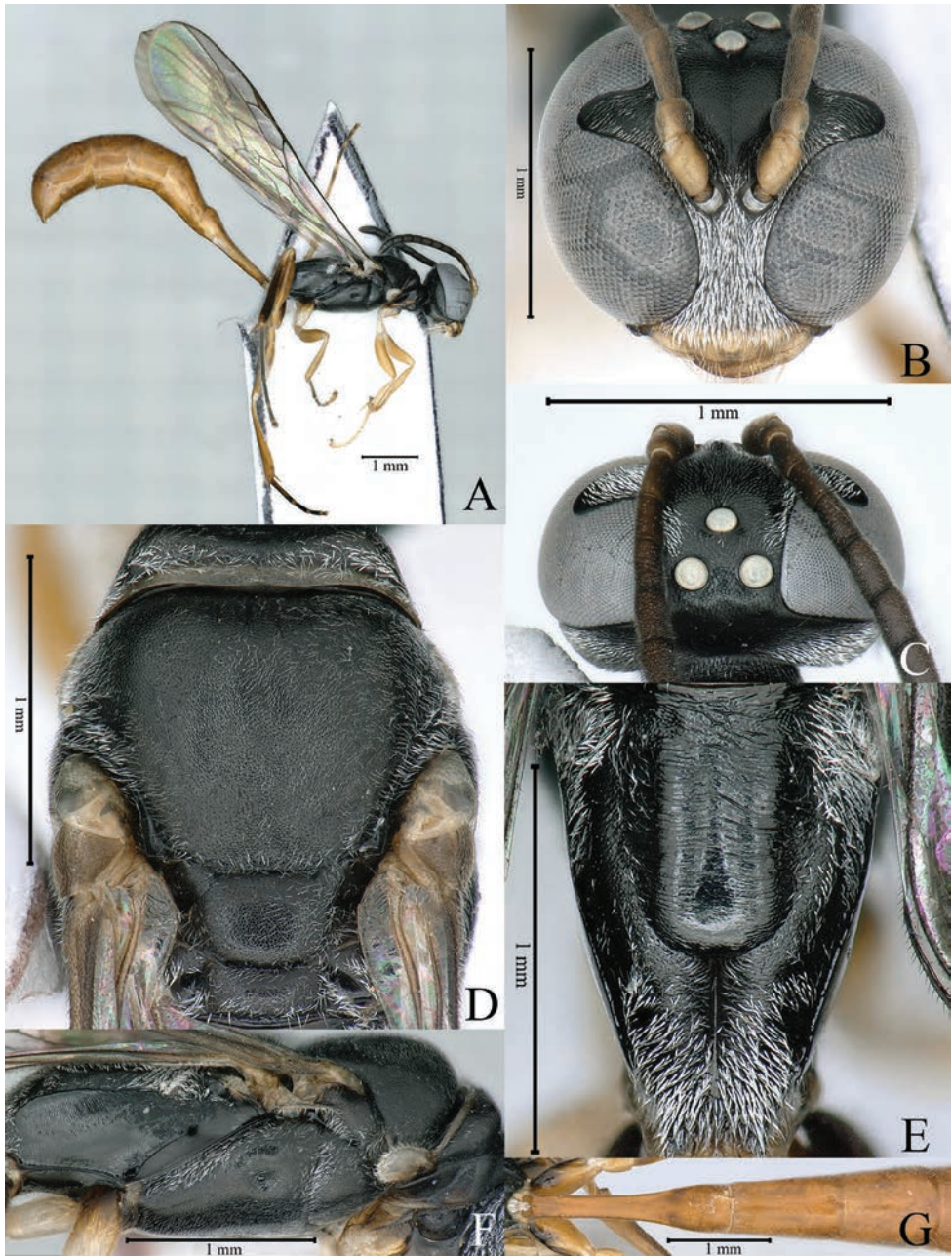


Figure 2. *Trypoxylon ferrugineipes* sp. nov. holotype ♀ **A** habitus (lateral view) **B** head (frontal view) **C** head (dorsal view) **D** thorax (dorsal view) **E** propodeum (dorsal view) **F** thorax (lateral view) **G** gastral segments I–III (dorsal view).

ed. Mesoscutum (Fig. 2D) microscopically coriaceous, with fine, dense punctures (PIS \approx PD); admedial line inconspicuously impressed, only extending to 1/5 of scutum; prescutal suture absent; parapsidal line distinct. Scutellum and metanotum microscop-

ically coriaceous, with fine, dense punctures (PIS \approx PD). Metapleuron microscopically coriaceous, impunctate (Fig. 2F). Propodeal enclosure with deep U-shaped groove (Fig. 2E), with few, short and oblique rugae basomedially, with broad, deep mid furrow, long and transverse rugae within furrow, sides of furrow smooth, scattered with fine punctures. Posterior part of propodeum with deep medial groove, except for apical portion. Propodeal lateral carina well-developed (Fig. 2F); propodeal lateral surface dull, microscopically coriaceous, with inconspicuous rugae anteriorly. In fore wing, R1 longer than TCV, almost reaching wing apex, CV1 = CV2 \times 3.1, TCV = CV2. Legs very slender, elongate, hindtibia about 1.25 \times as long as HW, midtarsomere I longer than half HW and hindcoxa longer than three \times apical width; hindcoxa without small ventral tubercle.

Gaster: Gastral petiole (Fig. 2G) slightly clavate, about 4.10 \times as long as apical width in dorsal view, shorter than segments II–III combined.

Male. Unknown.

Distribution. China (Yunnan).

Etymology. The specific name is derived from two Latin words: *ferrugineus* - (= ferruginous) + *-pes* (= leg), referring to the legs partly ferrugineous in female.

Trypoxylon infoveatum Li & Li, 2007

Fig. 3

Trypoxylon infoveatum Li & Li, 2007: 6.

Material examined. 6♀♀: CHINA, Yunnan Province, Jinghong City, Menghai County, Bulang Mountain, 21°37'35"N, 100°24'23"E, ca 1438 m, 21.VI–20.VII.2018 (1♀), 25.IV–17.V.2018 (1♀), 19.IV–28.V.2019 (2♀♀), 28.V–28.VI.2019 (2♀♀), Li Ma project team (YNAU); 15♂♂: same data as for preceding: 25.IV–17.V.2018 (1♂), 17.V–21.VI.2018 (1♂), 21.VI–20.VII.2018 (1♂), 20.VII–15.VIII.2018 (1♂), 15.IX–16.X.2018 (2♂♂), 16.X–17.XI.2018 (2♂♂), 26.II–22.III.2019 (1♂), 22.III–19.IV.2019 (1♂), 28.VI–19.VII.2019 (3♂♂), 13.VIII–15.IX.2020 (1♂), 27.V–15.VI.2021 (1♂).

Diagnosis. The species resembles *T. koreanum* Tsuneki, 1956 and *T. koikense* Tsuneki, 1956 in having the supraantennal tubercle highly nasiform, with deep groove medially. It differs from both by gastral petiole flask-shaped, longer than following two segments combined, GL/ W = 5.25 (in *T. koreanum* and *T. koikense* the gastral petiole is clavate, shorter than following two segments combined, GL/ W = 2.0–2.7), propodeal dorsum without mid furrow, obliquely carinae (in *T. koreanum* and *T. koikense* the propodeal dorsum with mid furrow, without oblique carinae), flagellomere VIII excavate beneath at base and distinctly incrassate toward apex in male (in *T. koreanum* flagellomeres unmodified in male; in *T. koikense* flagellomere VIII unmodified but flagellomere IV excavate beneath at base in male).

Description. Female (first description of female): Body length, 7.5 mm (Fig. 3A). Black; yellowish brown are: labial and maxillary palpi, most of mandible, tegula, apex of foretibia, foretarsus and midtarsomere I; brown are: wings hyaline, veins and pter-

ostigma. The following body parts covered with long, dense, silvery pubescence (length of setae greater than Od): most of clypeus, supraclypeal area, lower inner orbit, gena, pronotum, metapleuron, side of propodeal dorsum and posterior part of propodeum.

Head: Head rounded in frontal view (Fig. 3D), HW: HL = 10: 8.8, thin in dorsal view. Mandible simple, without denticle on inner margin. Clypeus nearly flat, with fine, dense punctures; lateral margin of clypeus slightly concave; free margin of clypeus with short rectangular protrusion, protrusion shallowly incised mesally (Fig. 3D). Supraclypeal area broad, short, shorter than its maximum apical width. Supraantennal tubercle highly nasiform, with deep longitudinal groove at base (Fig. 3D). F I = 2.5 × AW, F I: F II: F III = 1: 1: 1. Frons slightly (mainly mesally) convex, microscopically coriaceous, with fine, dense punctures, and hardly visible medial furrow. Inner eye orbits convergent below, broadly and shallowly notched (IODs = 10:10). Vertex slightly convex, ocellar triangle flattened (OOD: Od: POD = 2: 6: 5). Gena narrow, evenly convex.

Thorax: Pronotum with deep transverse furrow anteriorly, convex laterally, flattened anteriorly, pronotal collar narrow medially, enlarged towards side, with minute median tubercle, with distinct black posterior border; pronotal lobe rounded. Mesoscutum microscopically coriaceous (Fig. 3G), with fine, dense punctures (PIS ≈ PD); admedial line inconspicuously impressed, only extended to 1/4 of scutum; prescutal suture absent; parapsidal line distinct. Scutellum and metanotum microscopically coriaceous, with fine, dense punctures (PIS ≈ PD). Metapleuron microscopically coriaceous, dull. Propodeal enclosure with shallow U-shaped groove, without mid furrow, oblique striation covering almost entire propodeal enclosure surface (Fig. 3F). Posterior part of propodeum with deep medial groove, except for apical portion. Lateral carina of propodeum well-developed (Fig. 3J), propodeal lateral surface dull, with inconspicuous rugae anteriorly. In fore wing, R1 equal to TCV, CV1 = CV2 × 2.5, TCV = CV2.

Gaster: Gastral petiole (Fig. 3L) flask-shaped, about 5.25 × as long as apical width in dorsal view, longer than segments II–III combined.

Male: Sculpture, setae, and body coloration (Fig. 3E, H, I, K, M) as in female except as follows: body length 7.3 mm (Fig. 3B); clypeal free margin not obviously produced (Fig. 3E); IODs = 10:8; OOD: Od: POD = 3.5: 2.5: 2.5; F I: F II: F III = 9: 3: 5; flagellomere VIII excavate beneath at base and distinctly incrassate toward apex (Fig. 3C); F XI = 3.5 × BW, flagellomere XI as long as four preceding articles combined; male sternum VIII (Fig. 3N); and male genitalia (Fig. 3O, P).

Distribution. China (Yunnan).

Trypoxylon buddha Cameron, 1889

Fig. 4

Trypoxylon buddha Cameron, 1889: 118, 119; Bingham 1897: 225; Richards 1934: 338; R. Bohart and Menke 1976: 345; Tsuneki 1978b: 33, 76, 1979a: 3, 19, 1979b: 3, 8, 1980b: 4, 16, 21, 1981d: 18, 22, 1981f: 41.

Trypoxylon monstrosus Tsuneki, 1974: 633, synonymized with *Trypoxylon buddha* by Tsuneki 1978b: 36; R. Bohart and Menke 1976: 630.

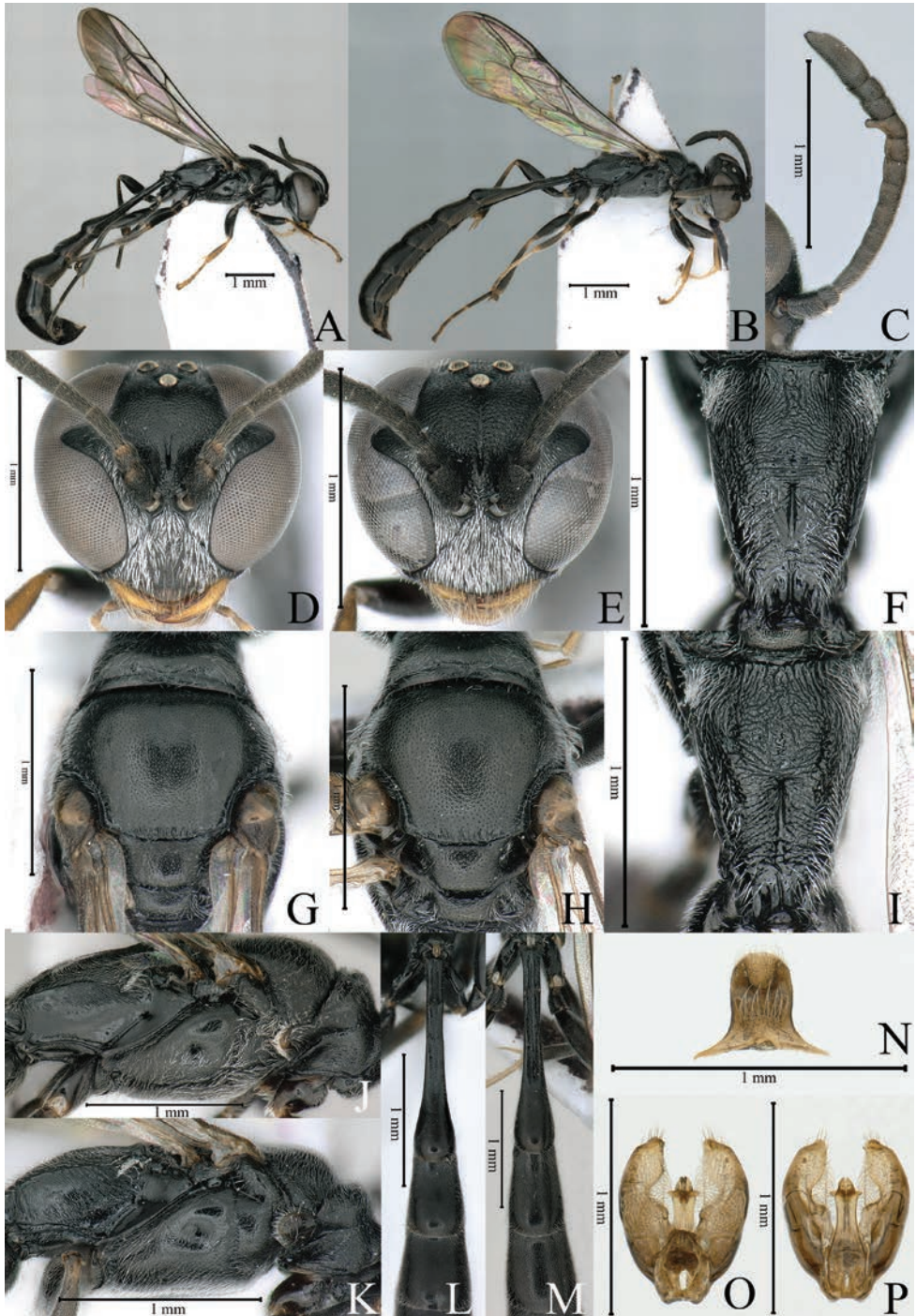


Figure 3. *Trypoxylon infoveatum* Li & Li, 2007. ♀ (A, D, F, G, J, L); ♂ (B, C, E, H, I, K, M, N, O, P) A, B habitus (lateral view) C male antenna (lateral view) D, E head (frontal view) G, H thorax (dorsal view) F, I propodeum (dorsal view) J, K thorax (lateral view) L, M gastral segments I–III (dorsal view) N male sternum VIII O, P genitalia.

Trypoxylon buddhae tarawakanum Tsuneki, 1976: 92, synonymized with *Trypoxylon buddha* by Tsuneki 1978b: 36.

Material examined. 1♀: CHINA, Yunnan Province, Jinghong City, Mengla County, Longmen Village, 21°16'46"N, 101°32'19"E, ca 923 m, 10.IV.2010, Rui Zhang (YNAU).

Diagnosis. *T. buddha* resembles *T. brevipenne* de Saussure, 1867 in having large punctures on the frons and mesoscutum, metapleural keel conspicuously curved and hind coxae with tubercle in female. It differs by the apex of gastral terga I–III each with apicomedian fovea (in *T. brevipenne* the gastral terga I–III without fovea), free margin of clypeus with short, wide protrusion medially (in *T. brevipenne* free margin of clypeus with semicircular protrusion medially). The species also resembles *T. maculipes* Tsuneki, 1979 in sharing the apex of gastral terga I–III each with apicomedian fovea and in body colour, but the punctures on frons and mesoscutum are large (in *T. maculipes* punctures on the frons and mesoscutum are small), supraantennal tubercle with middle carina and anterior transverse carina (in *T. maculipes* supraantennal tubercle without middle carina and anterior transverse carina inconspicuous), free margin of clypeus with short, wide protrusion medially (in *T. maculipes* free margin of clypeus with bidentate protrusion medially).

Description. Female (first record from China): Body length 9.5 mm (Fig. 4A). Body black; head and thorax with dense, short silvery setae (length of setae less than Od). Head sub-quadrangle in frontal view (Fig. 4B), almost equal in width and height; lateral margin of clypeus markedly concave, with short, wide protrusion medially; supraclypeal area broad, short; supraantennal tubercle highly nasiform, with conspicuous middle carina, and anterior transverse carina connected to antennal socket rim; frons with large, irregular punctures (PIS < PD), PIS smooth, shiny, frontal furrow deeply impressed. Pronotal collar flat, without median tubercle; mesoscutum, scutellum and metanotum with large, scattered punctures (PIS < PD), PIS smooth, shiny (Fig. 4C); propodeal enclosure with distinct U-shaped groove (Fig. 4D), with wide mid furrow and transverse wrinkles in furrow; gastral petiole slightly flask-shaped (Fig. 4E), shorter than following two segments combined, apex of gastral terga I–III each with apicomedian fovea. Side of propodeum with distinct lateral carina (Fig. 4F), propodeal lateral surface dull, with conspicuous oblique rugae. HW: HL = 10: 10. IODs = 10:6. OOD: Od: POD = 2: 7: 8; F I = 3.2 × AW, F I: F II: F III = 7: 8: 6. R1 longer than TCV, almost reaching wing apex, CV1 = CV2 × 2, CV2 = 1/2 TCV. GL/ W = 4.2.

Distribution. China (Yunnan); India; Philippines; Sri Lanka.

Trypoxylon flavipes Tsuneki, 1979

Fig. 5

Trypoxylon flavipes Tsuneki, 1979a: 3, 24, 1979b: 3, 8, 1980a: 4, 17, 1981a: 4, 13, 1981b: 100, 103, 1981d: 18, 1981f: 43.

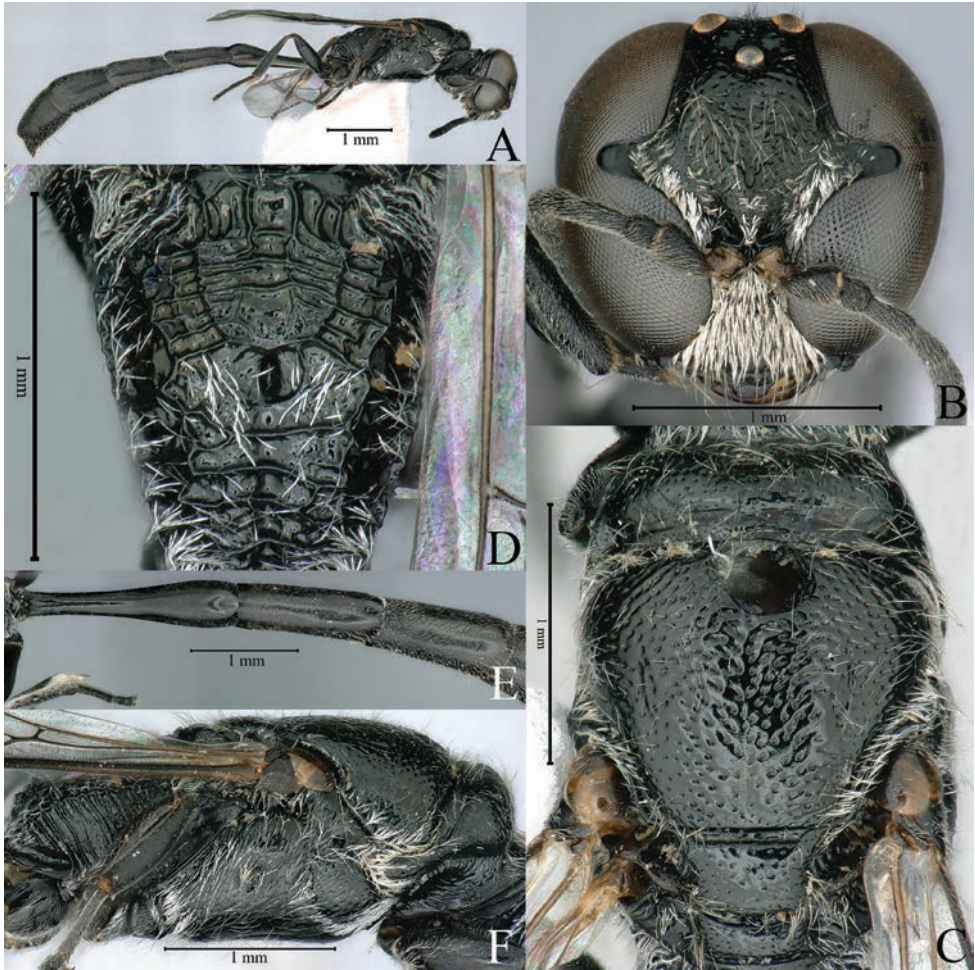


Figure 4. *Trypoxylon buddha* Cameron, 1889 ♀ **A** habitus (lateral view) **B** head (frontal view) **C** thorax (dorsal view) **D** propodeum (dorsal view) **E** gastral segments I–III (dorsal view) **F** thorax (lateral view).

Material examined. 2♀♀: CHINA, Yunnan Province, Jinghong City, Mengla County, Xishuangbanna Tropical Botanical Garden, Rainforest, 21°91'37"N, 101°27'07"E, ca 606 m, 24.IV–31.V.2019, Yongsheng Pu (YNAU).

Diagnosis. *T. flavipes* resembles *T. buddha* Cameron, 1889 and *T. maculipes* Tsuneki, 1979 in having the apex of gastral terga I–III each with apicomedian fovea and head sub-quadrated in frontal view. It differs from both by the anterior edge of supraantennal tubercle rounded (in *T. buddha* supraantennal tubercle with conspicuous transverse carina anteriorly; in *T. maculipes* the anterior edge of supraantennal tubercle transverse), the gaster and legs more or less ferruginous (in *T. buddha* and *T. maculipes* the gaster and legs wholly black), punctures on the frons and mesoscutum are small (in *T. buddha* punctures on the frons and mesoscutum are large), free margin of clypeus with bidentate protrusion medially (in *T. buddha* free margin of clypeus with short,

wide protrusion medially), the penis valve subapically with narrow, curved hook on each side (in *T. maculipes* the penis valve is simple at apex).

Description. Female (first record from China): Body length 7.7–7.8 mm (Fig. 5A). Body black; yellow are: mandible basally, scape and pedicel beneath, pronotal lobe, tegula, fore legs, midleg except midtarsomere II–V, hindtrochanter and apex of hindtibia; ferruginous are: apex of mandible, clypeus, base of gastral terga II–IV, base of gastral sternum III, gastral sternum IV. Head and thorax with dense, short silvery setae (length of setae less than Od). Head sub-quadrated in frontal view (Fig. 5B), almost equal in width and height; clypeus with bidentate protrusion; supraclypeal area narrow and long; supraantennal tubercle low, with conspicuous middle carina, anterior carina rounded; frons microscopically coriaceous, with fine, dense punctures (PIS \approx PD), frontal furrow deeply impressed. Pronotal collar with median tubercle; mesoscutum, scutellum and metanotum with fine, dense punctures (PIS \approx PD), PIS microscopically coriaceous (Fig. 5C); propodeal enclosure with distinct U-shaped groove (Fig. 5D), with wide mid furrow, and transverse wrinkles in furrow; gastral petiole slightly flask-shaped (Fig. 5E), shorter than following two segments combined, apex of gastral terga I–III each with fovea medially. Side of propodeum with distinct lateral carina (Fig. 5F), propodeal lateral surface shiny. HW: HL = 10: 10. IODs = 10:4. OOD: Od: POD = 1: 3: 4. F I = 3.0 \times AW, F I: F II: F III = 10: 9: 8. R1 longer than TCV, almost reaching wing apex, CV1 = CV2 \times 4, CV2 = TCV. GL/ W = 5.8.

Distribution. Australia; Borneo; China (Yunnan); India; Laos; Moluccas; New Guinea; Pacific Islands; Philippines; Sri Lanka; Sulawesi.

Trypoxylon fulvocollare Cameron, 1904

Fig. 6

Trypoxylon fulvocollare Cameron, 1904: 217; Tsuneki 1978b: 52, 78, 1979a: 12, 101, 1979c: 8, 1980a: 7, 55, 1980b: 8, 70, 1981f: 70.

Material examined. 1 ♀: CHINA, Yunnan Province, Jinghong City, Mengla County, Xishuangbanna Tropical Botanical Garden, Rainforest, 21°91'37"N, 101°27'07"E, ca 606 m, 19.VI–13.VII.2021, Yongsheng Pu (YNAU).

Diagnosis. *T. fulvocollare* resembles *T. taiwanum* Tsuneki, 1967 and *T. atricorne* Tsuneki, 1979 in having the supraantennal tubercle low, with thin mid-longitudinal carina, without anterior carina, the antennal socket rim tricarinate, the shape of pronotal collar and punctures on the frons and mesoscutum fine and sparse. It differs from both by the body covered with golden setae (in *T. taiwanum* and *T. atricorne* the setae are silvery), the flagellomeres I–II beneath and pronotal collar posteriorly yellow (in *T. taiwanum* the pronotal collar posteriorly black to light brown; in *T. atricorne* the flagellomeres I–II black and pronotal collar posteriorly are black to light brown), the base of gastral segments II–III are ferruginous (in *T. taiwanum* and *T. atricorne* the

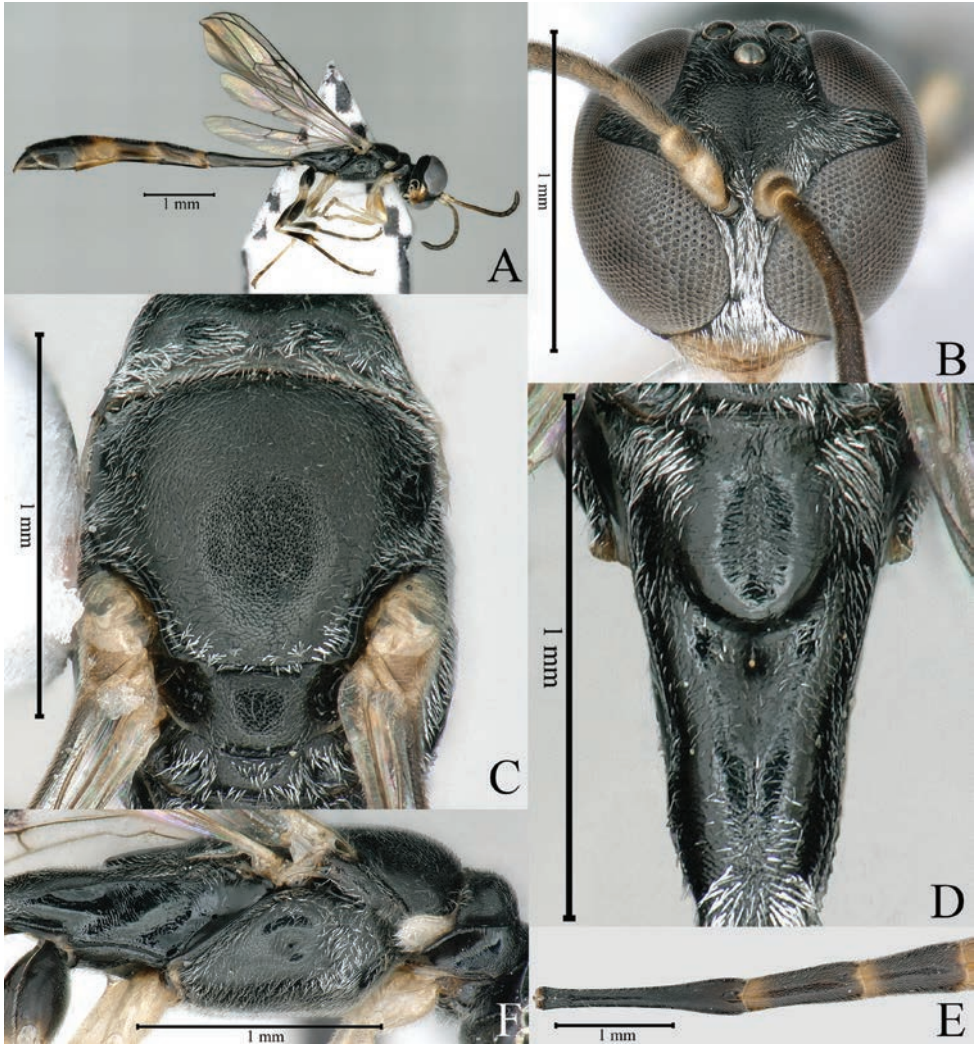


Figure 5. *Trypoxylon flavipes* Tsuneki, 1979. ♀ **A** habitus (lateral view) **B** head (frontal view) **C** thorax (dorsal view) **D** propodeum (dorsal view) **E** gastral segments I–III (dorsal view) **F** thorax (lateral view).

gaster is ferruginous from apex of petiole to segment III or IV), OOD: POD = 2: 3 (in *T. taiwanum* OOD: POD = 1: 3 and in *T. atricorne* OOD: POD = 1: 2), free margin of clypeus rounded (in *T. taiwanum* free margin of clypeus is conspicuously rounded; in *T. atricorne* free margin of clypeus is rounded and shallowly incised mesally).

Description. Female (first record from China): Body length 21.2 mm (Fig. 6A). Body black; yellow are: mandible, clypeal apex, scape, pedicel, flagellomeres I–II beneath, pronotal collar posteriorly, pronotal lobe, tegula, fore- and midlegs except base of coxa, apex of hindtibia; base of gastral segments II–III ferruginous. Head and thorax with dense, long golden setae (length of setae greater than Od). Head rounded in fron-

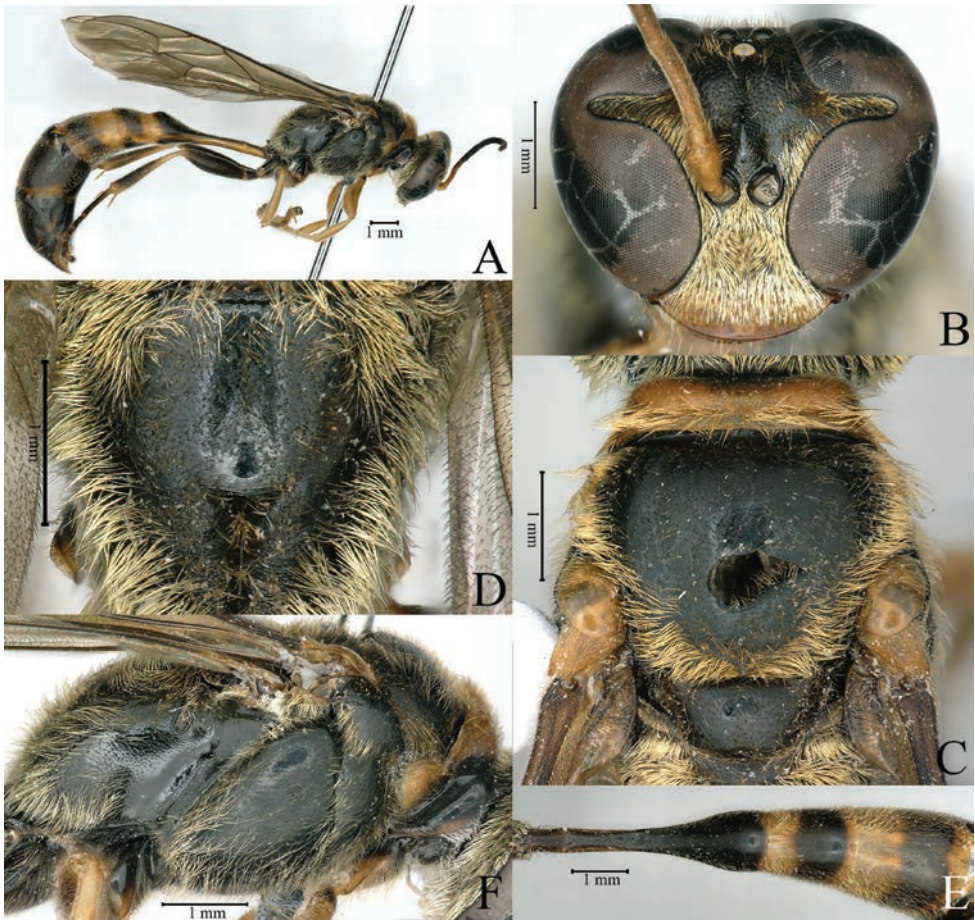


Figure 6. *Trypoxylon fulvocollare* Cameron, 1904. ♀ **A** habitus (lateral view) **B** head (frontal view) **C** thorax (dorsal view) **D** propodeum (dorsal view) **E** gastral segments I–III (dorsal view) **F** thorax (lateral view).

tal view (Fig. 6B); free margin of clypeus rounded, without protrusion; supraclypeal area broad and short; supraantennal tubercle low, with thin mid-longitudinal carina, without anterior transverse carina; frons microscopically coriaceous, with midsize to large and dense punctures ($PIS \approx PD$), frontal furrow deeply impressed. Pronotal collar flat, without tubercle mesally; mesoscutum, scutellum and metanotum with fine, scattered punctures ($PIS > PD$), PIS smooth, shiny (Fig. 6C); propodeal enclosure with inconspicuous U-shaped groove (Fig. 6D), with wide mid furrow, without transverse carinae; gastral petiole flask-shaped (Fig. 6E), longer than following two segments combined. Side of propodeum with distinct lateral carina (Fig. 6F), propodeal lateral surface shiny. HW: HL = 10: 8.2. IODs = 10:10. OOD: Od: POD = 2: 3: 3. F I = 5.7 \times AW, F I: F II: F III = 10: 7: 7. R1 short, R1 = 1/2 TCV, CV1 = CV2 \times 7, CV2 = 1/2 TCV. GL/ W = 4.5.

Distribution. Borneo; China (Yunnan); Indonesia; Java; Lesser Sunda Islands; Malaysia; Moluccas; Philippines; Sulawesi; Sumatra.

***Trypoxylon gampahae* Tsuneki, 1981**

Fig. 7

Trypoxylon gampahae Tsuneki, 1981d: 5, 19.

Material examined. 1♀: CHINA, Yunnan Province, Jinghong City, Menghai County, Bulang Mountain, 21°37'35"N, 100°24'23"E, ca 1438 m, 27.V–15.VI.2021, Yongsheng Pu (YNAU).

Diagnosis. *T. gampahae* resembles *T. mandibulatum* Richards, 1933 and *T. pygmaeum* Cameron, 1900 in having the mandible bidentate on inner margin near apex, median and lower frons roundly swollen and head sub-quadrangle in frontal view. It differs from both by punctures on the frons and mesoscutum are fine and sparse (in *T. mandibulatum* punctures on the frons and mesoscutum somewhat are large and conspicuous), the frons in lateral view is highly raised and inclined to antennal socket rim anteriorly (in *T. pygmaeum* the frons in lateral view is inconspicuously raised and almost flat anteriorly), the free margin of clypeus is conspicuously produced and with bidentate protrusion medially (in *T. mandibulatum* the clypeal free margin is inconspicuously produced and with truncate protrusion medially; in *T. pygmaeum* the free margin of clypeus is inconspicuously produced and slightly wavyed).

Description. Female (first record from China): Body length 7.5 mm (Fig. 7A). Body black; head and thorax with dense, short silvery setae (length of setae less than Od). Head sub-quadrangle in frontal view (Fig. 7B); mandible thick, bidentate on inner margin near apex; free margin of clypeus gently raised, inconspicuously incised medially; supraclypeal area broad, short; median and lower frons roundly swollen, without anterior transverse carina; frons microscopically coriaceous, with fine, dense punctures (PIS ≈ PD), frontal furrow shallow. Pronotal collar flat, without median tubercle; mesoscutum, scutellum and metanotum with fine, dense punctures (PIS ≈ PD), PIS microscopically coriaceous (Fig. 7C); propodeal enclosure with shallow but distinct U-shaped groove (Fig. 7D), without mid furrow, oblique striation covering almost entire propodeal enclosure surface; gastral petiole clavate (Fig. 7E), shorter than following two segments combined. Side of propodeum with distinct lateral carina (Fig. 7F), propodeal lateral surface dull, with inconspicuous rugae anteriorly. HW: HL = 10: 10. IODs = 10:7. OOD: Od: POD = 2: 5: 8. F I = 2.0 × AW, F I: F II: F III = 10: 7: 7. R1 equal to TCV, CV1 = CV2 × 2.3, CV2 = TCV. GL/ W = 3.3.

Distribution. China (Yunnan); Sri Lanka.

***Trypoxylon imayoshii* Yasumatsu, 1938**

Fig. 8

Trypoxylon imayoshii Yasumatsu, 1938: 451, 453; Tsuneki 1956a: 120, 122, 1956b: 4, 8, 19, 1972: 8, 1973: 32, 36, 1981e: 6, 1981f: 36; Antropov 1988: 87; 416; Terayama and Nambu 2009: 7, 26; Jeong and J.-K. Kim 2020: 246, 248.

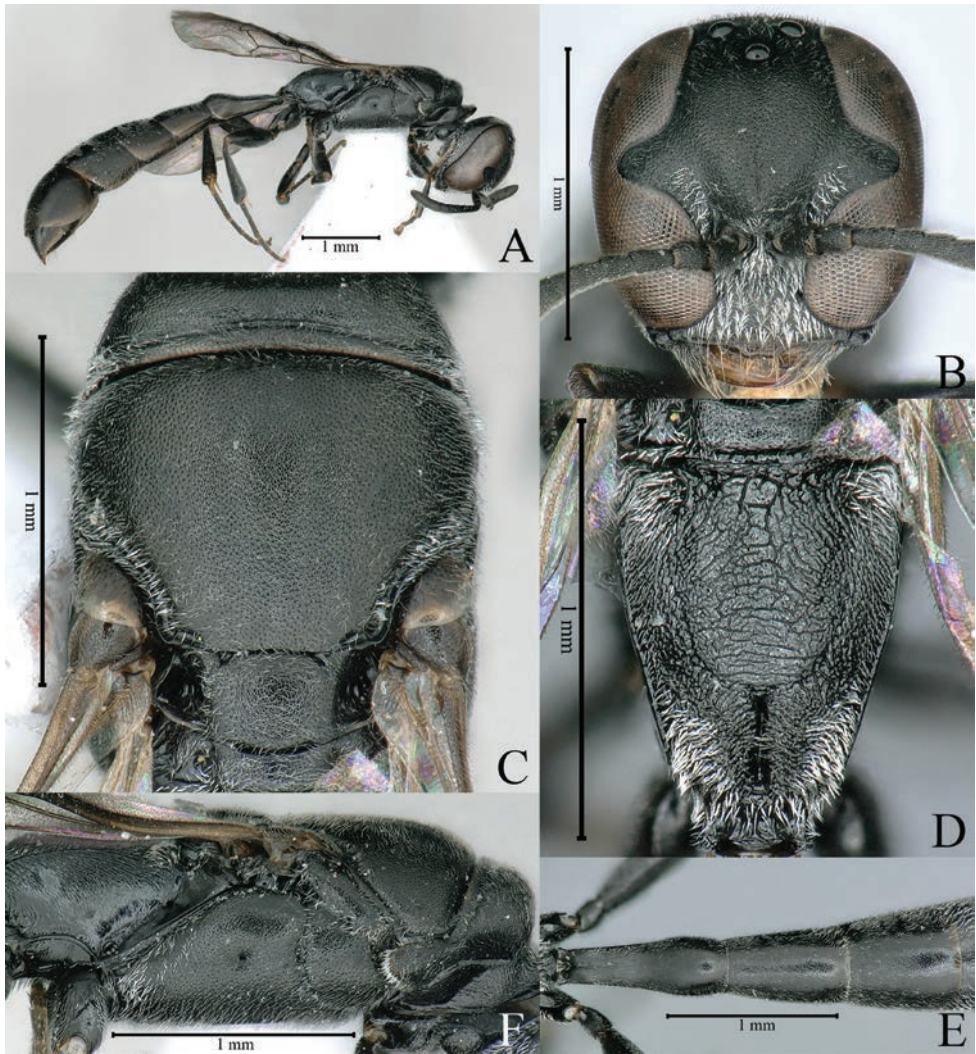


Figure 7. *Trypoxylon gampahae* Tsuneki, 1981 ♀ **A** habitus (lateral view) **B** head (frontal view) **C** thorax (dorsal view) **D** propodeum (dorsal view) **E** gastral segments I–III (dorsal view) **F** thorax (lateral view).

Material examined. 1♀1♂: CHINA, Guizhou Province, Zunyi City, Leigong Mountain, 27°52'06"N, 106°56'53"E, 1184 m, 19.VII.2019 (1♀), 15.VII.2019 (1♂), Yan Zhang (YNAU). 2♀♀3♂♂: CHINA, Guizhou Province, Zunyi City, Dabanshui Forest Park, 27°42'18"N, 106°51'15"E, ca 1001 m, 10. VII. 2011, Feng Dongdong (YNAU).

Diagnosis. *T. imayoshii* resembles *T. ambiguum* Tsuneki, 1956 in having a similar shape of the supraantennal tubercle, the pronotal collar and gastral petiole, punctures on the frons and mesoscutum are fine and sparse. It differs by the free margin of clypeus is conspicuously produced and with slightly bidentate protrusion medially (in *T. ambiguum* the margin of clypeus is inconspicuously produced and slightly waved), the frontal furrow is conspicuously impressed, the surface gently inclined towards middle

(in *T. ambiguum* the frontal furrow is inconspicuous, only conspicuous before anterior ocellus), the flagellomere XI longer than two preceding articles combined in male (in *T. ambiguum* the flagellomere XI shorter than two preceding articles), the apex of sternum VIII rounded in male (in *T. ambiguum* the apex of sternum VIII incised mesally in male). The species also resembles *T. infoveatum* Li & Li, 2007 in having the shape of pronotal collar and gastral petiole, punctures on the frons and mesoscutum are fine and sparse, but the supraantennal tubercle is low (in *T. infoveatum* the supraantennal tubercle is highly nasiform), the gaster is more or less ferruginous (in *T. infoveatum* the gaster is wholly black), the flagellomeres are unmodified in male (in *T. infoveatum* the flagellomere VIII excavate beneath at base and markedly incrassate toward apex).

Description. Female (first record from China): Body length 8.0–9.7 mm (Fig. 8A). Body black; yellowish brown are: mandible, clypeal apex, pronotal lobe, tegula, foreleg except base of forecoxa, midleg except midtarsomere II–IV, apex of hindcoxa, hindtrochanter and base of hindtibia; base of gastral segments II–IV ferruginous. Head and thorax with dense, long silvery setae (length of setae greater than Od). Head rounded in frontal view (Fig. 8D); free margin of clypeus with reversed trapezoidal protrusion, produced area shallowly incised mesally; supraclypeal area broad and short; supraantennal tubercle low, without anterior transverse carina; frons microscopically coriaceous, with fine, dense punctures, frontal furrow shallow. Pronotal collar trituberculate, with median tubercle; mesoscutum, scutellum and metanotum with fine, dense punctures, PIS microscopically coriaceous (Fig. 8G); propodeal enclosure with distinct U-shaped groove (Fig. 8F), with wide mid furrow, and transverse rugae in furrow; gastral petiole flask-shaped (Fig. 8L), longer than following two segments combined. Side of propodeum with distinct lateral carina (Fig. 8J), propodeal lateral surface shiny. HW: HL = 10: 8.2. IODs = 10:9. OOD: Od: POD = 1: 5: 3. F I = 3.6 × AW, F I: F II: F III = 12: 9: 9. R1 equal to TCV, CV1 = CV2 × 2.9, CV2 = TCV. GL/ W = 4.9.

Male. Body length 7.0–9.6 mm (Fig. 8B). Sculpture, setae, and coloration (gaster sometimes wholly brown) (Fig. 8E, H, I, K, M) as in female except as follows: clypeal free margin roundly produced (Fig. 8E); IODs = 10:8. OOD: Od: POD = 3: 4: 3; F I: F II: F III = 9: 8: 8; F XI = 2.4 × BW, flagellomere XI longer than two preceding articles combined, but shorter than three preceding articles combined (Fig. 8C). Male sternum VIII (Fig. 8N). Male genitalia (Fig. 8O, P).

Distribution. China (Fujian, Guangdong, Guangxi, Shandong, Yunnan, Zhejiang); Japan; Korea; Russia.

Trypoxylon kandyianum Tsuneki, 1979

Fig. 9

Trypoxylon kandyianum Tsuneki, 1979b: 4, 17, 1981d: 19.

Material examined. 1♀: CHINA, Yunnan Province, Jinghong City, Mengla County, Xishuangbanna Tropical Botanical Garden, Rainforest, 21°91'37"N, 101°27'07"E, ca 606 m, 24.IV–31.V.2019, Yongsheng Pu (YNAU); 1♀: CHINA, Yunnan Province, Jin-

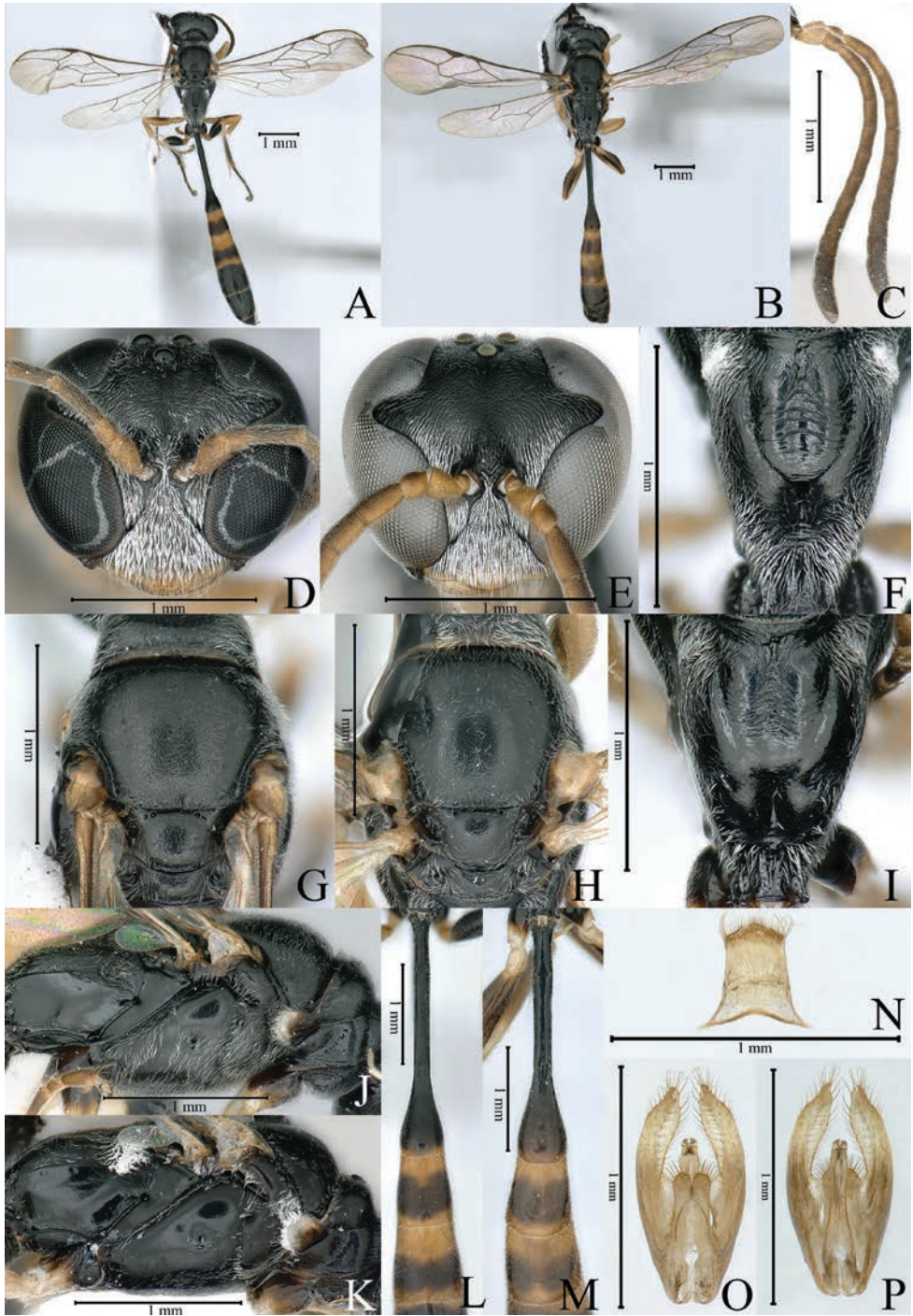


Figure 8. *Trypoxylon imayoshii* Yasumatsu, 1938. ♀ (A, D, F, G, J, L); ♂ (B, C, E, H, I, K, M, N, O, P) A, B habitus (lateral view) C male antenna (lateral view) D, E head (frontal view) G, H thorax (dorsal view) F, I propodeum (dorsal view) J, K thorax (lateral view) L, M gastral segments I–III (dorsal view) N male sternum VIII O, P genitalia.

ghong City, Mengla County, Xishuangbanna Tropical Botanical Garden, Sandalwood and pomelo mixed forest, 27°90'04"N, 106°27'21"E, ca 508 m, 25.IX–25.X.2019, Yongsheng Pu (YNAU).

Diagnosis. The species resembles *T. formosicola* Strand, 1922 in having the supraantennal tubercle is low, but differs by rounded free margin of clypeus (in *T. formosicola* free margin of clypeus have short, wide protrusion), the scape and pedicel beneath and gaster are wholly ferruginous (in *T. formosicola* the scape and pedicel beneath and gaster are wholly black). The species also resembles *T. gracilescens* F. Smith, 1860 in having the free margin of clypeus rounded. It differs by the supraantennal furrow is absent (in *T. gracilescens* the supraantennal furrow is deep), the side of the propodeum have conspicuous lateral carina (in *T. gracilescens* the lateral carina is inconspicuous, almost lacking), the supraantennal tubercle is low, with anterior transverse carina connected to antennal socket rim (in *T. gracilescens* the medio-apical area of supraantennal tubercle is obliquely flattened into smooth, shiny and round area, not connected to the antennal socket rim).

Description. Female (first record from China): Body length 11.9–12.5 mm (Fig. 9A). Body black; yellow are: mandible, clypeal apex, scape and pedicel beneath and flagellomere I, pronotal lobe, tegula, fore- and midlegs except coxa and trochanter, hindtibia and hindtarsus; gaster ferruginous from apex of petiole to apical gastral segment. Head and thorax with dense, long silvery setae (length of setae greater than Od). Head rounded in frontal view (Fig. 9B); free margin of clypeus rounded, without protrusion; supraclypeal area broad and short; supraantennal tubercle low, with anterior transverse carina connected to antennal socket rim; frons microscopically coriaceous, with medium-large, dense punctures (PIS = PD), frontal furrow deeply impressed. Pronotal collar flat, without median tubercle; mesoscutum, scutellum and metanotum with fine, scattered punctures (PIS > PD), PIS smooth and shiny (Fig. 9C); propodeal enclosure with inconspicuous U-shaped groove (Fig. 9D), mid furrow shallow, transversely rugose; gastral petiole flask-shaped (Fig. 9E), longer than following two segments combined. Side of propodeum with distinct lateral carina (Fig. 9F), propodeal lateral surface shiny. HW: HL = 10: 8. IODs = 11:9. OOD: Od: POD = 1: 3: 2. F I = 4.0 × AW, F I: F II: F III = 10: 7: 6. R1 equal to TCV, CV1 = CV2 × 7, CV2 = 1/2 TCV. GL/ W = 5.1.

Distribution. China (Yunnan); Sri Lanka.

Trypoxylon khasiae Cameron, 1904

Fig. 10

Trypoxylon khasiae Cameron, 1904d: 218; Tsuneki 1978b: 54, 80, 1979a: 11, 12, 84, nec 1979c: 7, 8, 9, 36 (= *Trypoxylon varipilosum*), 1981f: 58.

Material examined. 3♀♀: CHINA, Yunnan Province, Honghe Prefecture, Hekou County, Nanxi Town, 22°37'32"N, 103°56'53"E, ca 121 m, 6.VIII.2016 (2♀♀), 28.X.2016 (1♀), Hesheng Wang (YNAU); 3♀♀: CHINA, Yunnan Province, Jin-

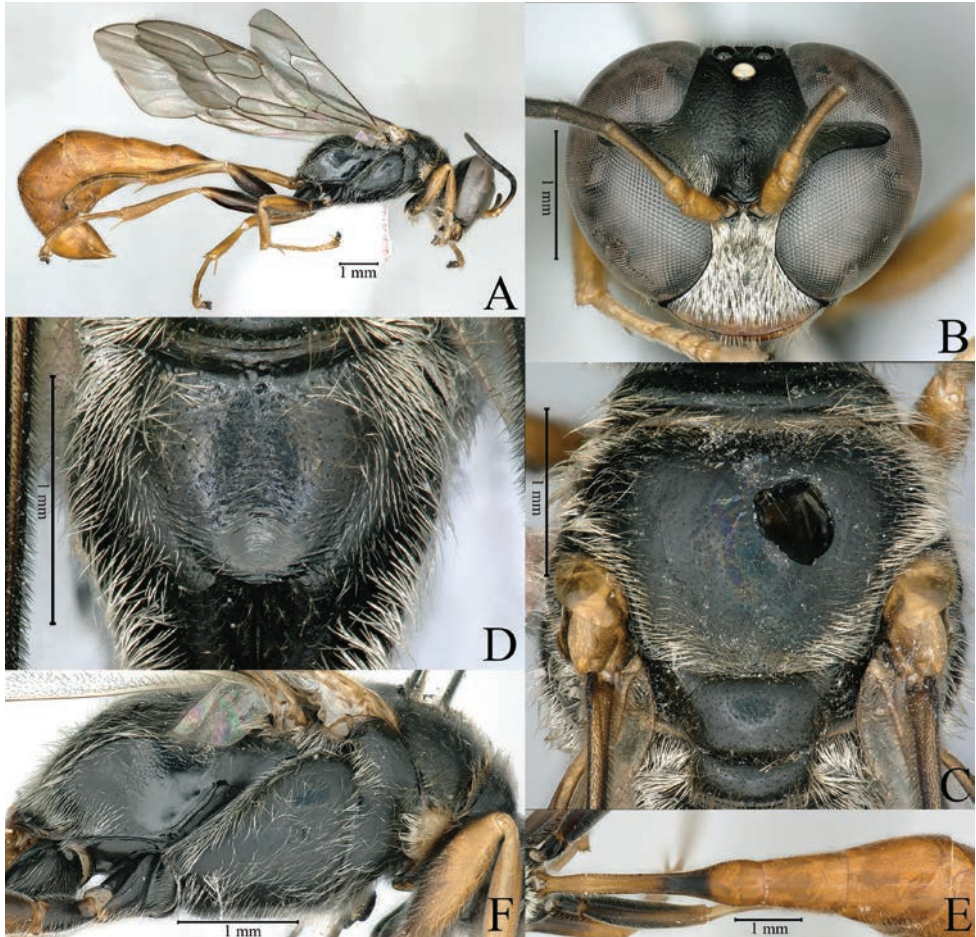


Figure 9. *Trypoxylon kandyianum* Tsuneki, 1979 ♀ **A** habitus (lateral view) **B** head (frontal view) **C** thorax (dorsal view) **D** propodeum (dorsal view) **E** gastral segments I–III (dorsal view) **F** thorax (lateral view).

ghong City, Mengla County, Xishuangbanna Tropical Botanical Garden, Rubber forest, 21°92'26"N, 101°26'50"E, ca 543 m, 20.VIII–18.IX.2018, Li Ma project team (YNAU); 1♀: CHINA, Yunnan Province, Jinghong City, Mengla County, Xishuangbanna Tropical Botanical Garden, Rainforest, 21°91'37"N, 101°27'07"E, ca 606 m, 20.VIII–18.IX.2018, Li Ma project team (YNAU); 1♀: CHINA, Yunnan Province, Jinghong City, Mengla County, Xishuangbanna Tropical Botanical Garden, Sandalwood and pomelo mixed forest, 27°90'04"N, 106°27'21"E, ca 508 m, 26.VIII–26.IX.2019, Li Ma project team (YNAU).

Diagnosis. *T. khasiae* resembles *T. varipilosum* Cameron, 1901 and *T. hyperorientale* Strand, 1922 in having the medio-apical area of supraantennal tubercle obliquely flattened into smooth, shiny and round area, the shape of pronotal collar, and a smooth mesoscutum. It differs from both by the body with silvery setae (in *T. varipilosum* the setae brassy), oblique area of supraantennal tubercle carrying fovea on it (in *T. var-*

ipilosum oblique area is flat), IODs = 10:5.6 (in *T. varipilosum* IODs = 10:9.0), the free margin of clypeus is rounded out, with two notches medially (in *T. hyperorientale* the margin of clypeus is rounded, slightly incised mesally), flagellomeres beneath and gaster from apex of petiole to apical gastral segment are ferruginous (in *T. hyperorientale* the flagellomeres and gaster are wholly black).

Description. Female (first record from China): Body length 11.9–12.5 mm (Fig. 10A). Body black; yellow are: mandible, clypeal apex, scape and pedicel beneath and all flagellomeres beneath, pronotal lobe, tegula, fore- and midfemora and all tibiae and tarsi; gaster ferruginous from apex of petiole to apical gastral segment. Head and thorax with dense and long silvery setae (length of setae greater than Od). Head rounded in frontal view (Fig. 10B); free margin of clypeus rounded out, with two notches medially; supraclypeal area broad, short; supraantennal tubercle nasiform, without anterior transverse carina, medio-apical area of supraantennal tubercle obliquely flattened into smooth, shiny, round area, with distinct fovea on it; frons with deep medial groove, punctures fine (PIS = PD). Pronotal collar flat, without median tubercle; mesoscutum, scutellum and metanotum with fine, scattered punctures (PIS > PD), PIS smooth and shiny (Fig. 10C); propodeal enclosure with inconspicuous U-shaped groove (Fig. 10D), with wide, transversely rugose middle furrow; gastral petiole flask-shaped (Fig. 10E), longer than following two segments combined. Side of propodeum with distinct lateral carina (Fig. 10F), propodeal lateral surface shiny. HW: HL = 10:8.5. IODs = 10:5.6. OOD: Od: POD = 2: 7: 4. F I = 4.0 × AW, F I: F II: F III = 27: 18: 16. R1 equal to TCV, CV1 = CV2 × 4.1, CV2 = 1/2 TCV. GL/ W = 4.7.

Distribution. China (Yunnan); India; Indonesia; Laos; Thailand.

Trypoxylon nasale Tsuneki, 1979

Fig. 11

Trypoxylon nasutum Tsuneki, 1979a: 5, 37.

Trypoxylon nasale Tsuneki, 1980a: 2. Substitute name for *Trypoxylon nasutum* Tsuneki, 1979.

Trypoxylon minahime Tsuneki, 1992: 54. Unnecessary substitute name for *Trypoxylon nasutum* Tsuneki, 1979.

Material examined. 3♀♀: CHINA, Yunnan Province, Jinghong City, Mengla County, Xishuangbanna Tropical Botanical Garden, Rainforest, 21°91'37"N, 101°27'07"E, ca 606 m, 24.IV–31.V.2019, Yongsheng Pu (YNAU); 3♀♀: CHINA, Yunnan Province, Jinghong City, Mengla County, Xishuangbanna Tropical Botanical Garden, Rubber forest, 21°92'26"N, 101°26'50"E, ca 543 m, 15.V–18.VI.2018, Lin Zhao (YNAU).

Diagnosis. *T. nasale* resembles *T. sauteri* Tsuneki, 1981 and *T. clypeisinuatum* T. Li and Q. Li, 2010 in having the supraantennal tubercle is high nasiform, with anterior transverse carina connected to antennal socket rim. It differs from both by IODs = 10:8 (in *T. sauteri* IODs = 10:3.4), the fore- and midlegs except base of coxa and gaster

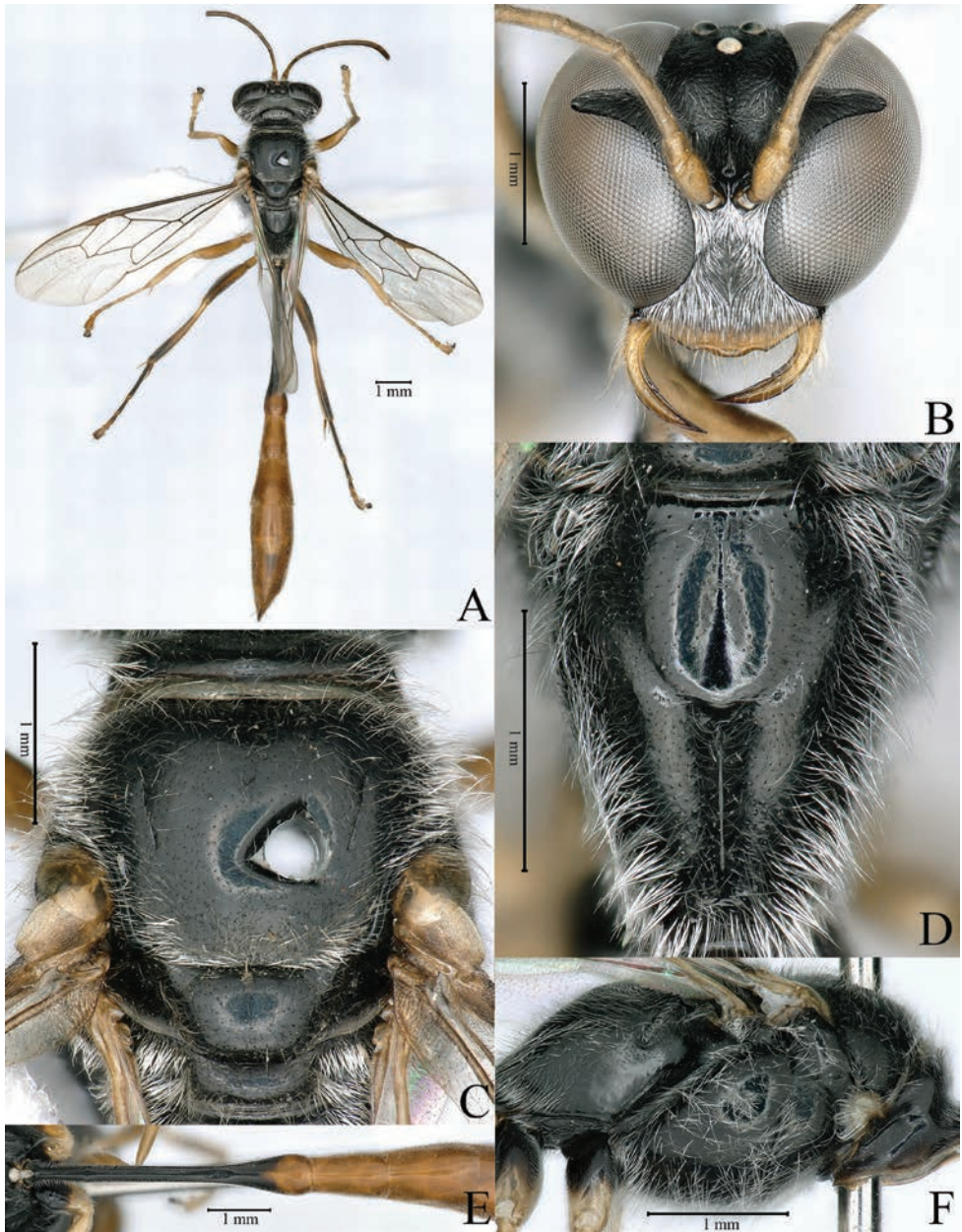


Figure 10. *Trypoxylon khasiae* Cameron, 1904 ♀ **A** habitus (lateral view) **B** head (frontal view) **C** thorax (dorsal view) **D** propodeum (dorsal view) **E** gastral segments I–III (dorsal view) **F** thorax (lateral view).

are ferruginous (in *T. sauteri* the gastral segment I, V and VI are black; in *T. clypeisinuatum* the legs are wholly black, the gastral segment I, V and VI are black), free margin of clypeus have semicircular protrusion, the protrusion is shallowly incised mesally (in *T. sauteri* the margin of clypeus is slightly semicircularly produced; in *T. clypeisinuatum* the margin of clypeus is conspicuously semicircularly produced).

Description. Female (first record from China): Body length 8.7–9.2 mm (Fig. 11A). Body black; ferruginous are: mandible basally, clypeal apex, scape and pedicel beneath and flagellomere I, pronotal lobe, tegula, fore- and midlegs except base of coxa, apex of hindcoxa, hindtrochanter, apex of hindtibia, hindtarsus and gaster. Head and thorax with dense, short silvery setae (length of setae less than Od). Head rounded in frontal view (Fig. 11B); free margin of clypeus with semicircular protrusion, produced area shallowly incised mesally; supraclypeal area broad and short; supraantennal tubercle high nasiform, with anterior transverse carina connected to antennal socket rim; frons microscopically coriaceous, with fine, dense punctures (PIS \approx PD), frontal furrow shallow. Pronotal collar flat, without median tubercle; mesoscutum, scutellum and metanotum with fine, dense punctures (PIS \approx PD), PIS microscopically coriaceous (Fig. 11C); propodeal enclosure with distinct U-shaped groove (Fig. 11D), with wide, transversely rugose middle furrow; gastral petiole clavate (Fig. 11E), shorter than following two segments combined. Side of propodeum with distinct lateral carina (Fig. 11F), propodeal lateral surface shiny. HW: HL = 10: 9. IODs = 10:8. OOD: Od: POD = 2: 9: 6. F I = $3.7 \times$ AW, F I: F II: F III = 10: 7: 6. R1 equal to TCV, CV1 = CV2 \times 2.8, CV2 = TCV. GL/ W = 2.7–3.0.

Distribution. China (Yunnan); Malaysia.

Trypoxylon pahangense Tsuneki, 1979

Fig. 12

Trypoxylon pahangense Tsuneki, 1979a: 6, 51, 1981d: 26, 38.

Material examined. 1♀: CHINA, Yunnan, Jinghong City, Menghai County, Guang-gang Village, Ancient tea forest, 21°49'15"N, 100°29'44"E, ca 1526 m, 20.VIII–16. IX.2018, coll. Li Ma project team (YNAU); 1♀: CHINA, Yunnan Province, Jinghong City, Menghai County, Bulang Mountain, 21°37'35"N, 100°24'23"E, ca 1438 m, 17.V–20.VI.2018, Li Ma project team (YNAU); 13♀♀: same data as for preceding: 20.VI–20.VII.2018 (2♀♀), 20.VII–16.VIII.2018 (3♀♀), 16.VIII–14.IX.2018 (3♀♀), 28.V–28.VI.2019 (1♀), 28.VI–19.VII.2019 (1♀), 19.VII–21.VIII.2019 (1♀), 21.VIII–20.IX.2019 (1♀), 10.VII–13.VIII.2020 (1♀).

Diagnosis. *T. pahangense* resembles *T. truncatum* Tsuneki, 1979 and *T. brunnei-maculatum* T. Li and Q. Li, 2007 in having the supraantennal tubercle is low, with anterior transverse carina connected to antennal socket rim. It differs from both by the free margin of clypeus have conspicuously obtuse-shaped protrusion (in *T. truncatum* the margin of clypeus is rounded, without projection; in *T. brunneimaculatum* the clypeal free margin is slightly semicircularly produced), the gaster is wholly ferruginous (in *T. truncatum* the gastral petiole is black; in *T. brunneimaculatum* the gastral segment I, V and VI are black).

Description. Female (first record from China): Body length 7.7–10.1 mm (Fig. 12A). Body black; yellow are: mandible, clypeal apex, pronotal lobe, tegula, fore- and midlegs except base of coxa, apex of hindcoxa, hindtrochanter, hindtibia and hind-

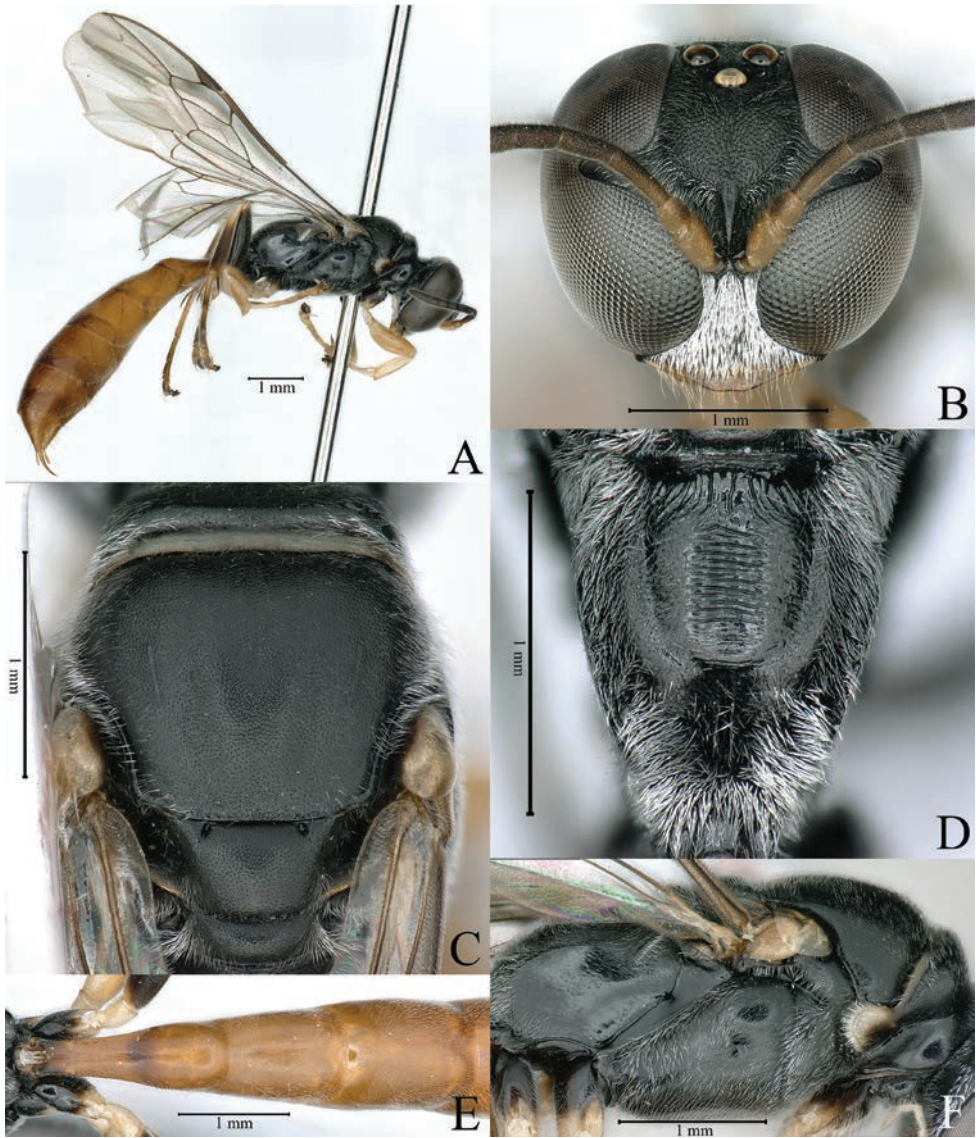


Figure 11. *Trypoxylon nasale* Tsuneki, 1979 ♀ **A** habitus (lateral view) **B** head (frontal view) **C** thorax (dorsal view) **D** propodeum (dorsal view) **E** gastral segments I–III (dorsal view) **F** thorax (lateral view).

tarsomere I; gaster ferruginous. Head and thorax with dense and short silvery setae (length of setae less than Od). Head rounded (Fig. 12B); free margin of clypeus with distinctly obtuse-shaped protrusion; supraclypeal area broad, short; supraantennal tubercle low, with anterior transverse carina; frons microscopically coriaceous, with fine, dense punctures ($PIS \approx PD$), frontal furrow shallow. Pronotal collar flat, without median tubercle; mesoscutum, scutellum and metanotum with fine, dense punctures ($PIS \approx PD$), PIS microscopically coriaceous (Fig. 12C); propodeal enclosure with distinct U-shaped groove (Fig. 12D), with wide, transversely rugose middle furrow; gastral petiole

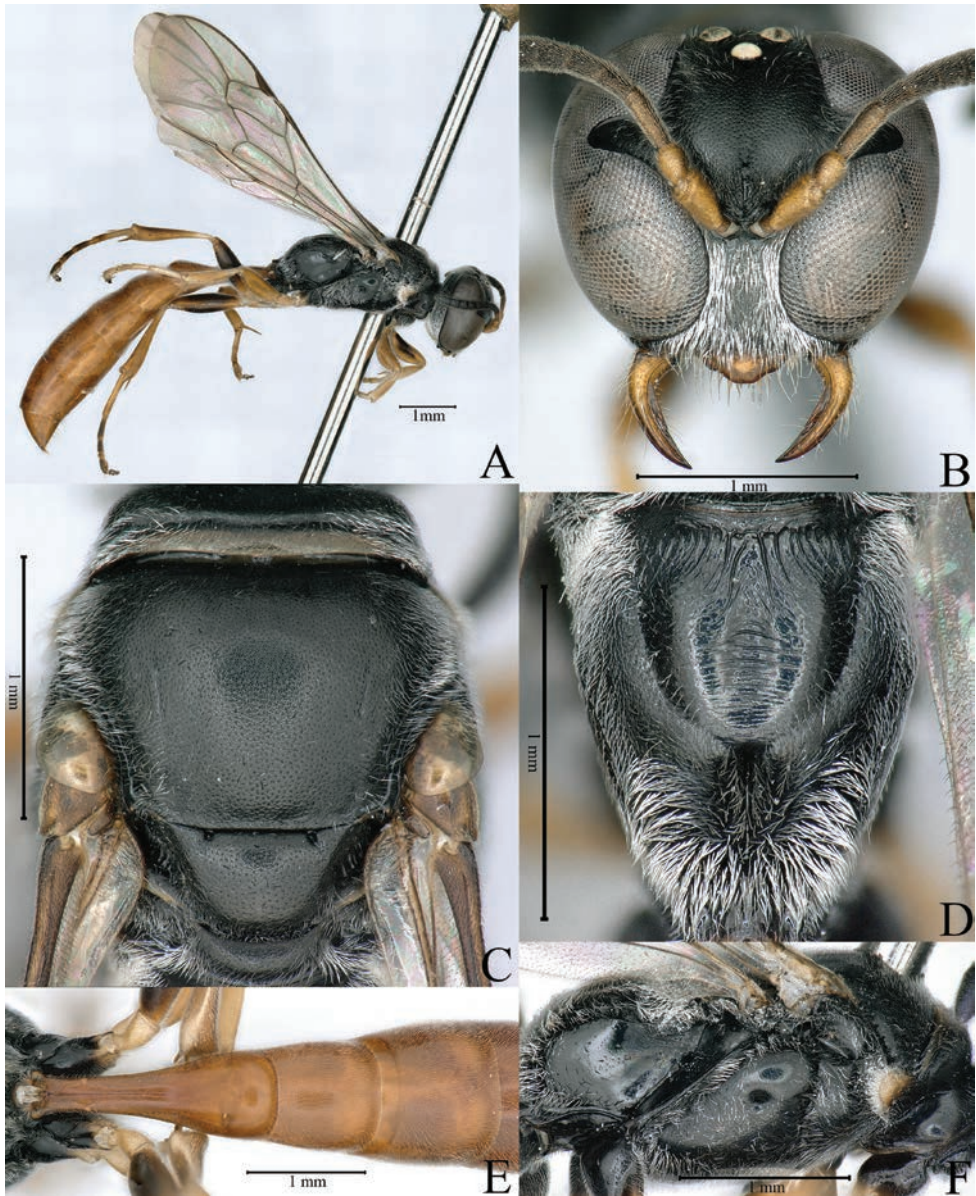


Figure 12. *Trypoxylon pahangense* Tsuneki, 1979 ♀ **A** habitus (lateral view) **B** head (frontal view) **C** thorax (dorsal view) **D** propodeum (dorsal view) **E** gastral segments I–III (dorsal view) **F** thorax (lateral view).

clavate (Fig. 12E), shorter than following two segments combined. Side of propodeum with distinct lateral carina (Fig. 12F), propodeal lateral surface shiny. HW: HL = 10: 9. IODs = 10:5. OOD: Od: POD = 1: 3: 2. F I = 3.5 × AW, F I: F II: F III = 10: 6: 6. R1 equal to TCV, CV1 = CV2 × 3.2, CV2 = TCV. GL/ W = 2.7–3.0.

Distribution. China (Yunnan); Malaysia.

***Trypoxylon pendleburyi* Tsuneki, 1979**

Fig. 13

Trypoxylon pendleburyi Tsuneki, 1979a: 5, 36.

Material examined. 1♀, CHINA, Yunnan, Jinghong City, Menghai County, Guanggang Village, farmland, 21°49'50"N, 100°28'20"E, ca 1229 m, 16.IX–19.X.2018, coll. Li Ma project team (YNAU); 9♀♀: same data as for preceding: 28.V–28.VI.2019 (1♀), 20.VII–23.VIII.2019 (2♀♀), 23.X–24.XI.2019 (2♀♀), 13.I–15.II.2021 (4♀♀).

Diagnosis. *T. pendleburyi* resembles *T. nasale* Tsuneki, 1979 and *T. clypeisinuatum* T. Li and Q. Li, 2010 in having the supraantennal tubercle is highly nasiform, with anterior transverse carina connected to antennal socket rim. It differs from both by free margin of clypeus have two barely separated and round teeth medially (in *T. nasale* the margin of clypeus have semicircular protrusion, the protrusion is shallowly incised mesally; in *T. clypeisinuatum* the margin of clypeus is conspicuously produced and with semicircular protrusion), the all trochanter are black, the gaster from apex of petiole to end is ferruginous (in *T. nasale* the all trochanter and gaster are wholly ferruginous; in *T. clypeisinuatum* the gastral segment I, V and VI are black), the gastral petiole is much slender (in *T. nasale* the gastral petiole is broad and short).

Description. Female (first record from China): Body length 7.5–9.2 mm (Fig. 13A). Body black; yellow are: base of mandible, clypeus, pronotal lobe, tegula, foretibia and foretarsus, base of midtibia, midtarsomere I and base of hindtibia; gaster ferruginous from apex of petiole to segment VI, sometimes gastral segment V with black mark. Head and thorax with dense and short silvery setae (length of setae less than Od). Head rounded in frontal view (Fig. 13B); free margin of clypeus with two barely separated and round teeth medially; supraclypeal area broad, short; supraantennal tubercle high nasiform, with anterior transverse carina connected to antennal socket rim; frons microscopically coriaceous, with fine, dense punctures (PIS ≈ PD), frontal furrow shallow. Pronotal collar flat, without median tubercle; mesoscutum, scutellum and metanotum with fine, dense punctures (PIS ≈ PD), PIS microscopically coriaceous (Fig. 13C); propodeal enclosure with distinct U-shaped groove (Fig. 13D), with wide mid furrow, and transverse rugae in furrow; gastral petiole clavate (Fig. 13E), shorter than following two segments combined. Side of propodeum with distinct lateral carina (Fig. 13F), propodeal lateral surface shiny. HW: HL = 10: 8.4. IODs = 10:5. OOD: Od: POD = 2: 5: 6. F I = 3.5 × AW, F I: F II: F III = 10: 7: 6. R1 equal to TCV, CV1 = CV2 × 2.7, CV2 = TCV. GL/ W = 3.5–3.9.

Distribution. Australia; Borneo; China (Yunnan); India; Laos; Moluccas; New Guinea; Pacific Islands; Sri Lanka; Sulawesi.

Discussion

Species from southwest China are found in both the Oriental and Palearctic regions, highlighting the richness and uniqueness of the region's biodiversity and reflecting the complexity and diversity of the region's natural environment. This study lays the foun-

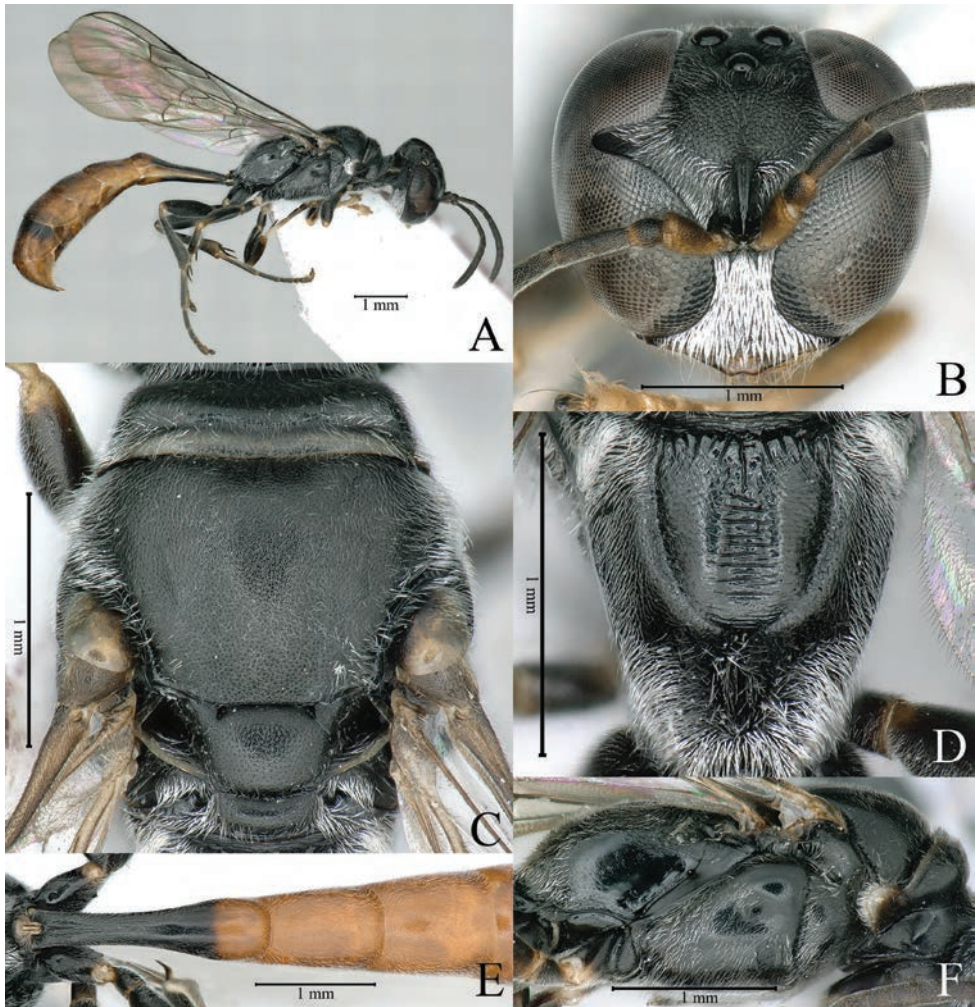


Figure 13. *Trypoxylon pendleburyi* Tsuneki, 1979 ♀ **A** habitus (lateral view) **B** head (frontal view) **C** thorax (dorsal view) **D** propodeum (dorsal view) **E** gastral segments I–III (dorsal view) **F** thorax (lateral view).

dation for further research on the relationship between climate change, environmental heterogeneity, and the diversity of sphecid wasps in southwest China.

Southeast Asia has the greatest diversity of the genus *Trypoxylon*, with Indonesia and Malaysia harboring the highest species diversity (Pulawski 2024). The research and supplementation of *Trypoxylon* species in Southeast Asia have mainly benefited from the contributions of Tsuneki (1956–1986). The ecological diversity of Southeast Asia is remarkable, encompassing tropical rainforests, monsoon forests, mountain forests, swamps, and other ecosystems (Sodhi et al. 2004; Buerki et al. 2014; Jiang et al. 2017; Tan et al. 2020; Meng et al. 2023). Southwest China, covering an area of 2.5 million square kilometers, features complex landforms and diverse climate types. Serving as a main ecological environment in Southeast Asia, it hosts a large number of plant and

animal species along with various ecosystem types (Zhang et al. 2014; Cao et al. 2011; Zhang et al. 2011). This region offers not only different ecological environments and habitat options but also abundant food resources, which may be the main reason why the genus *Trypoxylon* is concentrated in southwest China.

The endemic and newly recorded species of China are mainly distributed in southern China, which is part of the Indochina bioregions. The discovery of new species and the revision of existing ones in this region will provide new insights into the biodiversity and biogeographic distribution of Indochina. Additionally, it will provide a basis for further research on the origin, diffusion paths, and historical evolution processes of biological species across various bioregions.

Prospect. On the basis of morphological classification studies and the analysis of insect gene sequences by molecular biology methods, insect species can be identified and classified more accurately, thereby solving the problem of some species being very similar in morphology and difficult to distinguish (Liu et al. 2021). It is also possible to jointly construct phylogenetic trees of insects to reveal their relationships and evolutionary history (Ilyasov et al. 2018). Furthermore, combining geographical and ecological environment analysis can help us explore the patterns and mechanisms of biological evolution, as well as the causes and processes of biodiversity formation in the region.

Acknowledgments

We would like to thank the editor and two reviewers for suggestions that helped improve this article. We express our heartfelt thanks to Wojciech J. Pulawski (California Academy of Sciences, California) for providing us with many valuable references. We are also grateful to Dr. Jing-xian Liu (South China Agricultural University, Guangzhou, China), Yong-sheng Pu, Yu Tao, and Ling Zhao (Yunnan Agriculture University, Kunming, China) for helping us collect specimens. This work was supported by the National Natural Science Foundation of China under Grant number 32270485, the Agricultural Basic Research joint project of Yunnan Province under Grant number 202101BD070001-004 and the Yunnan Provincial Department of Science and Technology “Yunnan Talent Program” plan (202303AM140032).

References

- Antropov AV (1984) A new species of digger wasps of the genus *Trypoxylon* (Hymenoptera, Sphecidae) from Adzhariya. *Zoologicheskii Zhurnal* 63: 626–628.
- Antropov AV (1985) New species of digger wasps of the genus *Trypoxylon* (Hymenoptera, Sphecidae) from Transcaucasia. *Zoologicheskii zhurnal* 64: 630–633.
- Antropov AV (1986) Digger wasps of the genus *Trypoxylon* (Hymenoptera, Sphecidae) from the Palearctic fauna. *Zoologicheskii Zhurnal* 65: 624–628.

- Antropov AV (1987) A contribution to the sphecid wasps genus *Trypoxylon* of the eastern Palearctic. *Novye dannye po sistematike nasekomykh Dal'nego Vostoka*. BPI DVNTS AN SSSR Vladivostok 57–61.
- Antropov AV (1988) A contribution to the fauna of Trypoxylini (Hymenoptera, Sphecidae) of the Soviet Far East. *Taksonomiya nasekomykh Sibirii i Dal'nego Vostoka SSR*. BPI DVNTS AN SSSR, Vladivostok 85–88.
- Antropov AV (1989a) To the knowledge of the digger wasps of the tribe Trypoxylini (Hymenoptera, Sphecidae, Larrinae) of the Palearctic fauna. *Bulletin de la Societe des Naturalistes de Moscow. Section biologique* 94: 55–58.
- Antropov AV (1989b) A new species of digger wasps of the genus *Trypoxylon* (Hymenoptera, Sphecidae) from the Transcaucasus. *Zoologicheskii Zhurnal* 67(2): 309–311.
- Antropov AV (1989c) The new digger wasps of the genus *Trypoxylon* (Hymenoptera, Sphecidae) from south-western Palearctic. *Byulleten' Moskovskogo Obshchestva Ispytateley Prirody. Otdel Biologicheskii* 94(5): 63–67.
- Antropov AV (1994) Four new species of the digger wasps genus *Trypoxylon* Latreille (Hymenoptera, Sphecidae) of the Palaearctic and Oriental Regions, with taxonomic notes on some others previously described. *Russian Entomological Journal* 3(1–2): 123–133.
- Antropov AV (2011) Order Hymenoptera, family Crabronidae. Genera *Trypoxylon*, *Pseudomicroides* and *Belomicroides*. *Arthropod Fauna of the UAE* 4: 609–629.
- Antropov AV, Mokrousov MV (2016) New data on distribution of four species of the genus *Trypoxylon* (Hymenoptera: Crabronidae: Trypoxylini) in European Russia. *Russian Entomol Journal* 25(3): 265–269. <https://doi.org/10.15298/RUSENTJ.25.3.07>.
- Barth GP (1910) Some observations on solitary wasps about Milwaukee. *Bulletin of the Wisconsin Natural History Society (New Series)* 8: 118–121.
- Bingham CT (1897) The fauna of British India, including Ceylon and Burma, Hymenoptera, I. wasps and bees. Taylor and Francis, London, [xxix +] 222–228. <https://doi.org/10.5962/bhl.title.100738>
- Bohart RM, Menke AS (1976) Sphecid wasps of the world. A generic revision. Univ of California Press 327–349. <https://doi.org/10.1525/9780520309548>
- Buerki S, Forest F, Alvarez N (2014) Proto-South-East Asia as a trigger of early angiosperm diversification. *Botanical Journal of the Linnean Society* 174(3): 326–333. <https://doi.org/10.1111/boj.12129>
- Cameron P (1889) Hymenoptera Orientalis: or contributions to knowledge of the Hymenoptera of the Oriental Zoological Region. Manchester Literary and Philosophical Society, 118–119. <https://doi.org/10.5962/bhl.title.8802>
- Cameron P (1904) Descriptions of new species of aculeate and parasitic Hymenoptera from northern India. *Journal of Natural History* 13(75): 216–219. <https://doi.org/10.1080/00222930408678900>
- Cao WC, Tao HP, KB, Liu BT, Sun YL (2011) Research on Automatic Identification of Landform in Southwest China Based on DEM Data Segmentation. *Soil and Water Conservation in China* 3: 38–41.
- CEPF [Critical Ecosystem Partnership Fund] (2023) The biodiversity hotspots. <https://www.cepf.net/our-work/biodiversity-hotspots/hotspots-defined>

- He K, Jiang X (2014) Sky islands of Southwest China. I. An overview of phylogeographic patterns. *Chinese Science Bulletin* 59(7): 585–597. <https://doi.org/10.1007/s11434-013-0089-1>
- Ilyasov RA, Park J, Takahashi J, Kwon HW (2018) Phylogenetic Uniqueness of Honeybee *Apis Cerana* from the Korean Peninsula Inferred from The Mitochondrial, Nuclear, and Morphological Data. *Journal of Apicultural Science* 62(2): 189–214. <https://doi.org/10.2478/jas-2018-0018>
- Jeong E, Kim JK (2020) The genus *Trypoxylon* Latreille (Hymenoptera: Crabronidae) in Korea: a revision of the species with flask-shaped metasomal segment 1. *Journal of Asia-Pacific Biodiversity* 13(2): 245–254. <https://doi.org/10.1016/j.japb.2020.01.007>
- Jiang C, Tan K, Ren MX (2017) Effects of monsoon on distribution patterns of tropical plants in Asia. *Chinese Journal of Plant Ecology* 41(10): 1103–1112. <https://doi.org/10.17521/cjpe.2017.0070>
- Kazenas VL (2001) Fauna and biology of sphecid wasps (Hymenoptera, Sphecidae) of Kazakhstan and Central Asia. Kazgos INTI, Almaty 173 pp.
- Kryzhanovskiy OL, Guangzhou Ma (1956) Some characteristics of insect fauna in southwestern China and the tasks of future research. *Acta Entomologica Sinica* 6(3): 361–369.
- Li TJ, Li Q (2007) Four new species and nine new species records of the subgenus *Trypoxylon* (*Trypoxylon*) Latreille (Hymenoptera: Crabronidae) from China. *The Pan-Pacific Entomologist* 83(1): 1–12. <https://doi.org/10.3956/0031-0603-83.1.1>
- Li TJ, Li Q (2010) The *Trypoxylon* Latreille (Hymenoptera: Crabronidae) of southwest China with descriptions of two new species. *Journal of the Kansas Entomological Society* 83(3): 240–247. <https://doi.org/10.2317/JKES0912.05.1>
- Liu T, Liu HY, Tong JB, Yang YX (2022) Habitat suitability of neotenic net-winged beetles (Coleoptera: Lycidae) in China using combined ecological models, with implications for biological conservation. *Diversity and Distributions* 28(12): 2806–2823. <https://doi.org/10.1111/ddi.13545>
- Liu T, Liu HY, Wang YN, Xi HC, Yang YX (2022) Assessing the diversity and distribution pattern of the speciose genus *Lycocerus* (Coleoptera: Cantharidae) by the global-scale data. *Frontiers in Ecology and Evolution* 10: 797450. <https://doi.org/10.3389/fevo.2022.794750>
- Liu T, Liu HY, Yang YX (2023) Uncovering the determinants of biodiversity hotspots in China: Evidence from the drivers of multiple diversity metrics on insect assemblages and implications for conservation. *Science of the Total Environment* 880: 163287. <https://doi.org/10.1016/j.scitotenv.2023.163287>
- Liu Z, Yang SJ, Wang YY, Peng YQ, Chen HY, Luo SX (2021) Tackling the Taxonomic Challenges in the Family Scoliidae (Insecta, Hymenoptera) Using an Integrative Approach: A Case Study from Southern China. *Insects* 12(10): 892. <https://doi.org/10.3390/insects12100892>
- Meng HH, Song YG (2023) Biogeographic patterns in Southeast Asia: Retrospectives and perspectives. *Biodiversity Science* 31(12): 23261. <https://doi.org/10.17520/biods.2023261>
- Myers N, Mittermeier RA, Mittermeier CG, da Fonseca GAB, Kent J (2000) Biodiversity hotspots for conservation priorities. *Nature* 403: 853–858. <https://doi.org/10.1038/35002501>

- Pulawski WJ (2024) *Trypoxylon*. https://researcharchive.calacademy.org/research/entomology/entomology_resources/hymenoptera/sphecidae/genera/Trypoxylon.pdf [Accessed 14 April 2024]
- Richards OW (1934) The American species of the genus *Trypoxylon* (Hymenopt., Sphecoidea). Transactions of the Royal Entomological Society of London 82: 173–362. <https://doi.org/10.1111/j.1365-2311.1934.tb00033.x>
- Sodhi NS, Koh LP, Brook BW, Ng PK (2004) Southeast Asian biodiversity: an impending disaster. Trends in ecology & evolution 19(12): 654–660. <https://doi.org/10.1016/j.tree.2004.09.006>
- Strand EH (1922) Sauter's Formosa-Ausbeute. Crabronidae und Scoliidae. IV. (Die Gattungen *Trypoxylon*, *Bembex* und *Oxybelus*). Internationale Entomologische Zeitschrift 16: 163–164.
- Tan K, Malabrigo PL, Ren MX (2020) Origin and evolution of biodiversity hotspots in Southeast Asia. Acta Ecologica Sinica 40: 3866–3877. <http://dx.doi.org/10.5846/stxb201904160762>
- Terayama M, Nambu T (2009) Taxonomic guide to the Japanese Aculeate wasps. 10. Family Crabronidae, subfamily Larrinae, tribe Trypoxyloninae. Tsunekibachi 16: 1–40.
- Tsuneki K (1956a) Classification of the Japanese species of *Trypoxylon* (Hymen., Sphecidae), with notes on some problem [sic] of their ecology. The Insect Ecology 5: 119–128.
- Tsuneki K (1956b) Die *Trypoxylonen* der nordöstlichen Gebiete Asiens (Hymenoptera, Sphecidae, Trypoxyloninae). Memoirs of the Faculty of Liberal Arts and Education, Ser II, Natural Science 6: 1–42.
- Tsuneki K (1966) Taxonomic notes on *Trypoxylon* of Formosa and the Ryukyus with descriptions of new species and subspecies (Hymenoptera, Sphecidae). Etizenia 13: 1–19.
- Tsuneki K (1967) Studies on the Formosan Sphecidae (II). The subfamily Trypoxyloninae (Hymenoptera). Etizenia 22: 1–21.
- Tsuneki K (1971) Studies on the Formosan Sphecidae (X). Revision of and supplement to the subfamily Trypoxyloninae (Hymenoptera). Etizenia 54: 1–19.
- Tsuneki K (1972) On some species of the Japanese Sphecidae (Hym.). Notes and descriptions. Etizenia 59: 1–20.
- Tsuneki K (1973) A guide to the study of the Japanese Hymenoptera (31). The genus *Trypoxylon* Latreille. The Life Study (Fukui) 17: 31–38.
- Tsuneki K (1974) A contribution to the knowledge of Sphecidae occurring in southeast Asia (Hym.). Polskie Pismo Entomologiczne 44: 585–660.
- Tsuneki K (1976) Sphecoidea taken by the Noona Dan expedition in the Philippine Islands (Insecta, Hymenoptera). Steenstrupia 4: 33–120.
- Tsuneki K (1977) Some *Trypoxylon* species from the southwestern Pacific (Hymenoptera, Sphecidae, Larrinae). Special Publications of the Japan Hymenopterists Association 6: 1–20.
- Tsuneki K (1978a) Studies on the genus *Trypoxylon* Latreille of the Oriental and Australian Regions (Hymenoptera, Sphecidae). I. Group of *Trypoxylon scutatatum* Chevrier, with some species from Madagascar and the adjacent islands. Special Publications of the Japan Hymenopterists Association 7: 1–87.

- Tsuneki K (1978b) Studies on the genus *Trypoxylon* Latreille of the Oriental and Australian Regions (Hymenoptera, Sphecidae). II. Revision of the type series of the species described by F. Smith, P. Cameron, C.G. Nurse, W. H. Ashmead, R.E. Turner and O.W. Richards. Special Publications of the Japan Hymenopterists Association 8: 1–84.
- Tsuneki K (1979a) Studies on the genus *Trypoxylon* Latreille of the Oriental and Australian Regions (Hymenoptera, Sphecidae). III. Species from the Indian subcontinent including southeast Asia. Special Publications of the Japan Hymenopterists Association 9: 1–178.
- Tsuneki K (1979b) Studies on the genus *Trypoxylon* Latreille of the Oriental and Australian Regions (Hymenoptera, Sphecidae). IV. Species from Sri Lanka. Special Publications of the Japan Hymenopterists Association 10: 1–20.
- Tsuneki K (1979c) Studies on the genus *Trypoxylon* Latreille of the Oriental and Australian Regions (Hymenoptera, Sphecidae). V. Species from Sumatra, Java, and the Lesser Sunda Islands. Special Publications of the Japan Hymenopterists Association 11: 1–68.
- Tsuneki K (1980a) Studies on the genus *Trypoxylon* Latreille of the Oriental and Australian Regions (Hymenoptera, Sphecidae). VI. Species from Borneo, Celebes and Moluccas. Special Publications of the Japan Hymenopterists Association 12: 1–118.
- Tsuneki K (1980b) Studies on the genus *Trypoxylon* Latreille of the Oriental and Australian Regions (Hymenoptera, Sphecidae). VII. Species from the Philippines. Special Publications of the Japan Hymenopterists Association 13: 1–130.
- Tsuneki K (1981a) Studies on the genus *Trypoxylon* Latreille of the Oriental and Australian Regions (Hymenoptera, Sphecidae). VIII. Species from New Guinea and South Pacific Islands. Special Publications of the Japan Hymenopterists Association 14: 1–98.
- Tsuneki K (1981b) Studies on the genus *Trypoxylon* Latreille of the Oriental and Australian Regions (Hymenoptera, Sphecidae). IX. Species from Australia. Special Publications of the Japan Hymenopterists Association 14: 99–105.
- Tsuneki K (1981c) Studies on the genus *Trypoxylon* Latreille of the Oriental and Australian Regions (Hymenoptera, Sphecidae). X. Revision of the Formosan species. Special Publications of the Japan Hymenopterists Association 15: 1–56.
- Tsuneki K (1981d) Studies on the genus *Trypoxylon* Latreille of the Oriental and Australian Regions (Hymenoptera, Sphecidae). XI. Additional species from various parts of the Regions, with an appendix on some species from other Regions. Special Publications of the Japan Hymenopterists Association 16: 1–90.
- Tsuneki K (1981e) Revision of the *Trypoxylon* species of Japan and northeastern part of Asiatic continent, with comments on some species of Europe (Hymenoptera, Sphecidae). Special Publications of the Japan Hymenopterists Association 17: 1–92.
- Tsuneki K (1981f) Tentative grouping of the *Trypoxylon* species based upon the structure of the male genital organs with appendix of the distribution table (Hymenoptera, Sphecidae). Special Publications of the Japan Hymenopterists Association 18: 1–100.
- Tsuneki K (1986) New species and subspecies of the aculeate Hymenoptera from East Asia, with some synonyms, specific remarks and distributional data. Special Publications of the Japan Hymenopterists Association 32: 28–31.
- Tsuneki K (1992) Corrigenda. Special Publications of the Japan Hymenopterists Association 38: 54.

- Wang YM, Fan SX, Zhang WW, Hu YF, Cui P, Luo X (2023) Seasonal Variation and Vertical Distribution of Bird Diversity in Wenshan, Yunnan Province. *Journal of Ecology and Rural Environment* 39(3): 369–377. <https://doi.org/10.19741/j.issn.1673-4831.2022.0644>
- Wu YR, Zhou Q (1996) *Economic Entomology of China*. Vol. 52, Hymenoptera Scleroididae. Science Press 96–104.
- Yasumatsu K (1938) Two unrecorded species of the genus *Trypoxylon* from Nippon (Hymenoptera, Trypoxylonidae). *Dobutsugaku Zasshi* (= Zoological Magazine) 50: 451–455.
- Yi L, Dong YK, Miao BG, Peng YQ (2021) Diversity of butterfly communities in Gaoligong region of Yunnan. *Biodiversity Science* 29(7): 950–959. <https://doi.org/10.17520/biods.2020486>
- Zhang Q, Li Y (2014) Climatic Variation of Rainfall and Rain Day in Southwest China for Last 48 Years. *Plateau Meteorology* 33(2): 372–383.
- Zhang YD, Zhang XH, Liu SR (2011) Correlation analysis on normalized difference vegetation index (NDVI) of different vegetations and climatic factors in Southwest China. *Chinese Journal of Applied Ecology* 22(2): 323–330.

A new European species of *Mesocrina* (Hymenoptera, Braconidae, Alysiiinae, Alysiini) with notes on the biology and systematics of the genus

H. Charles J. Godfray¹, Cornelis van Achterberg²

1 Department of Biology, University of Oxford, South Parks Road, Oxford OX1 3PS, UK **2** Naturalis Biodiversity Center, P.O. 9517, 2300 RA Leiden, Netherlands

Corresponding author: H. Charles J. Godfray (charles.godfray@biology.ox.ac.uk)

Academic editor: Jovana M. Jasso-Martínez | Received 29 March 2024 | Accepted 22 April 2024 | Published 30 April 2024

<https://zoobank.org/5893CA68-2DB5-4D61-8FD3-3D54424D55D8>

Citation: Godfray HCJ, van Achterberg C (2024) A new European species of *Mesocrina* (Hymenoptera, Braconidae, Alysiiinae, Alysiini) with notes on the biology and systematics of the genus. *Journal of Hymenoptera Research* 97: 349–361. <https://doi.org/10.3897/jhr.97.124215>

Abstract

Mesocrina chandleri Godfray & van Achterberg, **sp. nov.**, is described in the small Holarctic genus *Mesocrina* Foerster, 1863, the second European species. The holotype was collected in England and further specimens are recorded from Finland, France and the Netherlands. A key is provided to the Palaearctic *Mesocrina* species. DNA sequence from the CO1 barcode locus was obtained and the new species is 10% divergent from *M. indagatrix* (the other European species) and 5% divergent from an undetermined North American species. We provide evidence that *Mesocrina* spp. parasitise cyclorrhaphan Diptera in fungi (and that previous host records from phytophagous insects are incorrect) and that the taxon is not part of the *Dapsilarthra* genus-group as often previously assumed.

Keywords

DNA barcode, Europe, hosts, *Mesocrina chandleri*, Palaearctic key

Introduction

The genus *Mesocrina* Foerster, 1863 was erected for *M. indagatrix* Foerster, 1863, which for a long time was the sole member of the genus as understood today. In the last quarter of the 20th century four further species were described from the Eastern Palaearctic and India (van Achterberg 1983; Belokobylskij 1998) and two from

North America (Wharton 1980). Females of the genus are distinctive as they have a laterally compressed metasoma with dorsal carina on the third and distal tergites, but both sexes can be identified to genus relatively easily in standard keys to the Alysiini (Fischer 1971; Tobias 1986; Wharton 1997; Belokobylskij and Tobias 1998; Zhu et al. 2017).

Mesocrina indagatrix, hitherto the only species known from Europe (Königsmann 1959; van Achterberg 1983, 2014), is a widespread but uncommon species with relatively few specimens in major collections. An examination of the four *Mesocrina* in the collection of the National Museum of Scotland found that in addition to three *M. indagatrix*, there is a single female specimen that differs from *M. indagatrix* in several aspects, notably it is larger in size and has a longer ovipositor. DNA sequence from the CO1 barcode locus was obtained from both *M. indagatrix* and the aberrant specimen and were clearly distinct (10% divergence). The BOLD database contained a specimen from Finland with identical sequence to the new taxon which was borrowed and found to be a male. Four further specimens were then discovered in recent collections from the Netherlands and France. The wasps differ from the species known from the East Palaearctic and North America and here are described as belonging to a new species.

Methods

Details of the holotype and five paratypes are given below in the type designation. The holotype is deposited in the National Museum of Scotland, Edinburgh, the male paratype in the Zoological Collections of the Finnish Museum of Natural History, University of Helsinki, Finland, and the remaining paratypes in the entomological collection of the Naturalis Biodiversity Center, Leiden.

The specimen of *Mesocrina indagatrix* from which DNA sequence was obtained has the data: ♀, Savernake Forest, Wiltshire, England, United Kingdom (51.402N, 1.694E; UK Grid Reference SU214671); Malaise trap, 22 August – 25 September 1991; (collector not recorded); (Sample ID: NR1040; BOLD process ID: BRAAL476-19).

Photographs were taken through a Leica M125C microscope with focus stacking using the Leica Application Suite X (LAS X) image analysis software with final processing in Photoshop. Ratio measurements were also made using the LAS X system. Morphology terminology follows Wharton et al. (1997).

CO1 sequencing was carried out by the Biodiversity Institute of Ontario at the University of Guelph with initial Sanger sequencing supplemented in the case of the *M. indagatrix* specimen by “next generation” short read sequencing (Prosser et al. 2016). Our sequence data are publicly available at <http://v4.boldsystems.org/> which also provides full details of primers. Sequence analysis was carried out on the BOLD platform and using the programme MEGA11 (Molecular Evolutionary Genetics Analysis version 11, Tamura et al. (2021)).

Systematics

Mesocrina chandleri Godfray & van Achterberg, sp. nov.

<https://zoobank.org/F38D6FA7-860D-4378-9150-23D8E1CF53C3>

Figs 1, 2

Type material. *Holotype*, ♀, south side of Haugh Wood, Herefordshire, England, **United Kingdom** (52.021°N, 2.600°W; UK Grid Reference SO589360); 10 October 1998; swept, P.J. Chandler; National Museum of Scotland (Sample ID: NR980; BOLD process ID: BRAAL477-19).

Paratype, ♂, near Nurmijärvi, Uusimaa, **Finland** (60.523°N, 24.842°E; Finnish Grid Reference 6711:381); 8 September 1994; Malaise Trap, M. Koponen; Finnish Museum of Natural History (MZH) (Sample ID, MZH_GQ.22; BOLD process ID: LEFIJ28469-22).

Paratype, ♀, Lac de Remoray, Doubs, **France** (46.785°N, 6.254°E; French [Lambert 93] Grid reference 948242, 6634560); 27 October 2021; Malaise Trap, H. Gens, (RMNH'23") Naturalis Biodiversity Center.

Paratypes 2 ♀, Veluvia-Hamelakkers, Wageningen, Gelderland, **The Netherlands** (51.969°N, 5.681°E); 25–29th October 2022; caught at a skylight, D. Belgers, RMNH'23"; Naturalis Biodiversity Center.

Paratype, ♀, Wassenaar, Zuid-Holland, **The Netherlands** (52.142°N, 4.379°E; Dutch [RDS] Grid reference 86.60, 462.12); 20 October 2023; on underside of *Armillaria mellea* (honey fungus), P.H. Hoekstra, RMNH'23"; Naturalis Biodiversity Center.

Name. The new species is named for Peter J. Chandler, the eminent Diptera entomologist who collected the first specimen in 1998.

Description of female holotype. *Holotype*, ♀, length of body 3.8 mm, of fore wing 4.7 mm (Fig. 1).

Head. Antenna with 36 segments, 1.1 times length of fore wing and 1.5 times body, densely clothed with anteriorly directed setae projecting at an angle of 30°; length of third segment 0.7 times fourth segment, lengths of third, fourth and penultimate segments 3.9, 2.7 and 2.4 times their widths, respectively; maxillary and labial palps with 6 and 4 segments, respectively; length of maxillary palp ~ 2.6 times height of eye; OOL 2.3 times greater than POL, POL 1.4 times posterior ocellus diameter; in dorsal view head 2.0 times wider than maximum length, margin of temples posterior to eye slightly convex; vertex shiny with scattered anteriorly-directed setae especially near occiput and margin of eye, a weak furrow runs from between posterior ocelli to occiput; frons largely smooth and glabrous with small areas of rugosity and a small number of setae; dorsal length of eyes 0.6 times maximum length of head, glabrous; face 1.8 times wider than high medially, 0.6 times as wide as head, largely smooth with some slight rugosity medially, with moderately dense setae apart from a narrow medial glabrous band, the setae dorsally directed except at sides where they point laterally and latero-ventrally; clypeus glabrous with sparse punctures, ventral margin very slightly convex, epistomal suture distinct; malar space 0.15 times basal width of mandible; mandibles

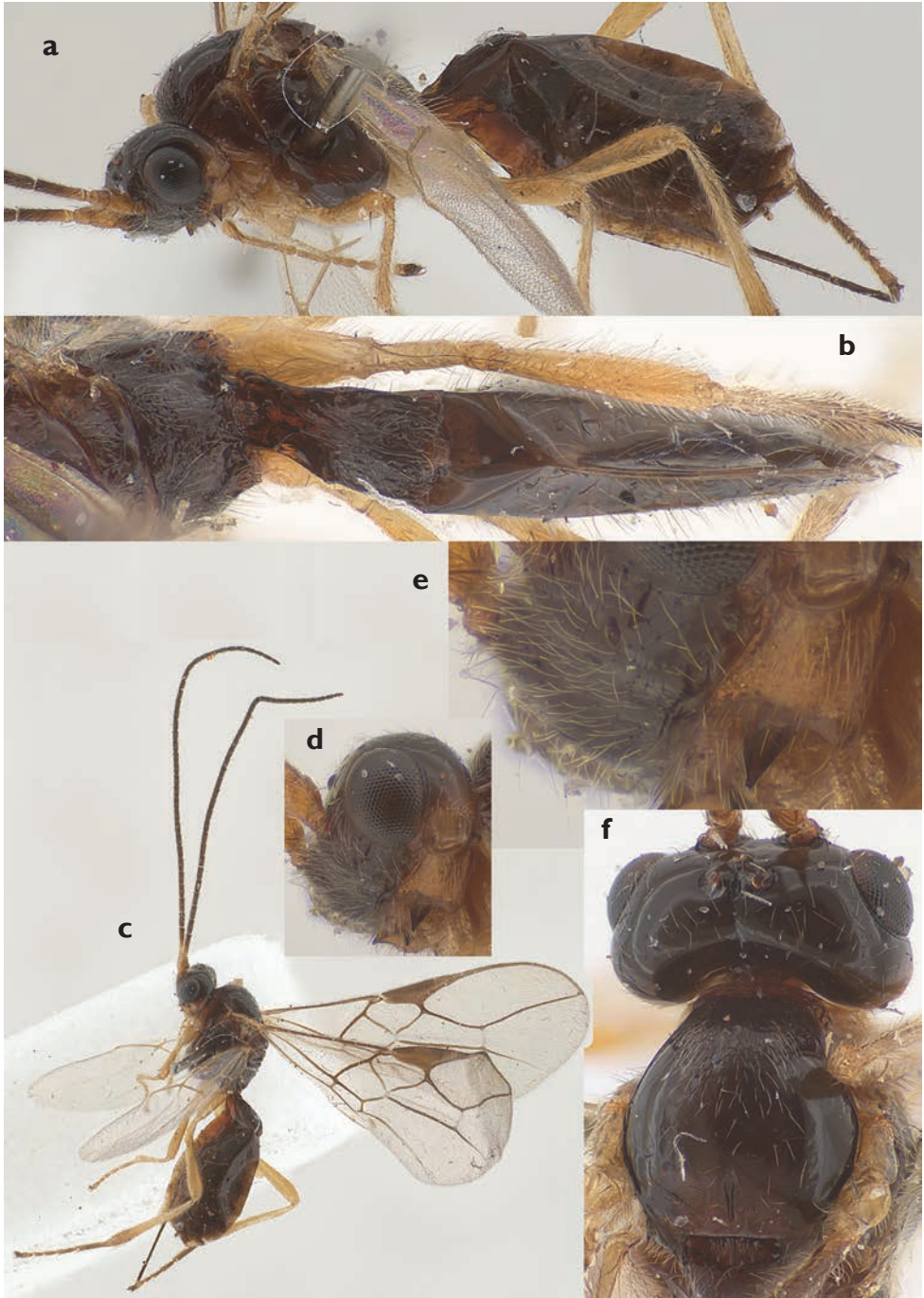


Figure 1. Montage of photographs of the female holotype (Sample ID NR890) of *M. chandleri* **a** lateral view **b** dorsal metasoma **c** whole insect **d** lateroventral head **e** face and mandible **f** dorsal head and mesosoma. The length of the body (excluding antennae and ovipositor) is 3.8 mm.

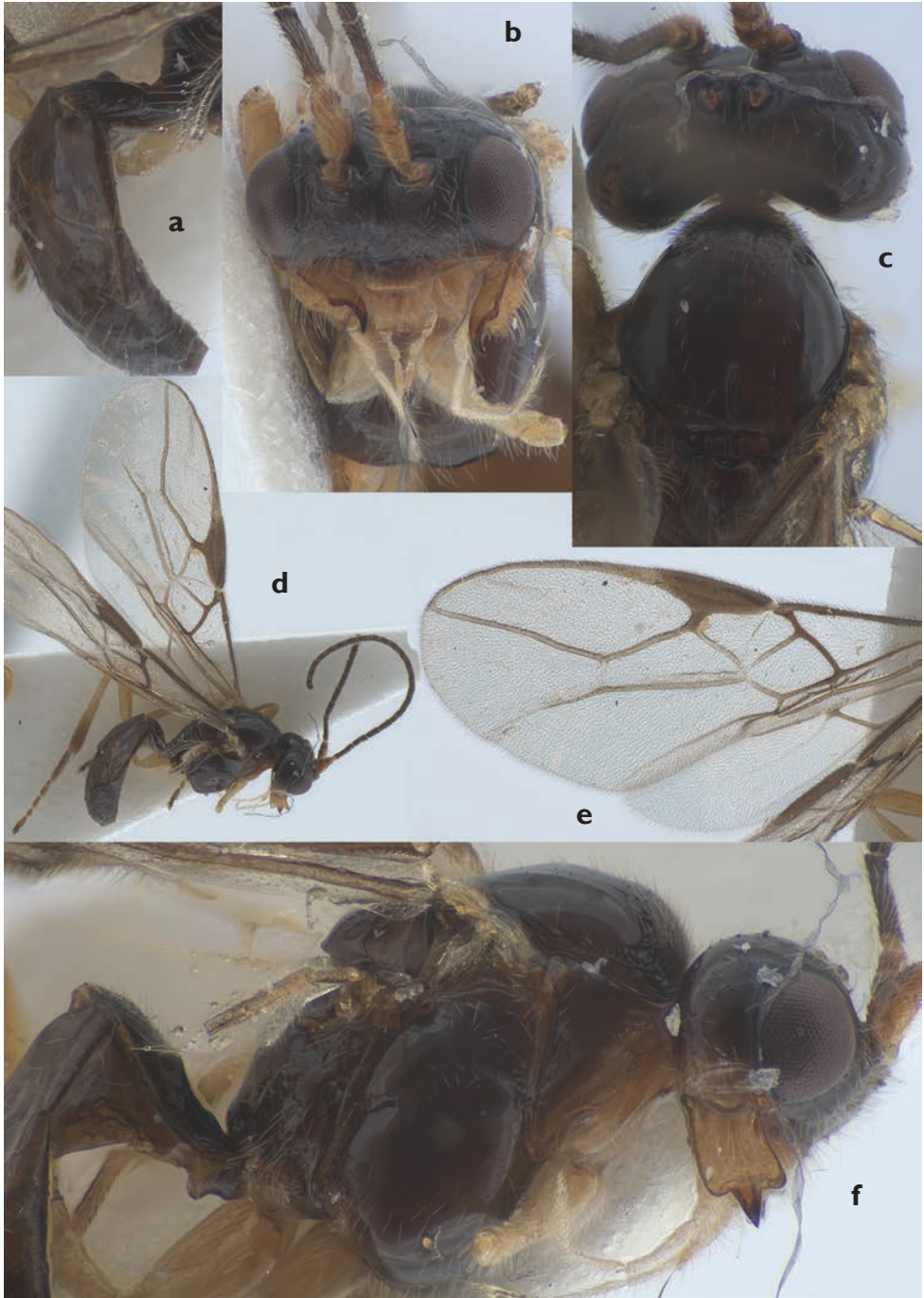


Figure 2. Montage of photographs of the male paratype (Sample ID MZH_GQ.22) of *M. chandleri* **a** lateral metasoma **b** face **c** dorsal head and mesosoma **d** whole insect **e** wing **f** lateral head and mesosoma. The length of the body (excluding antennae) is 3.3 mm.

1.6 times longer than maximum width which is 1.3 times basal width, finely rugulose and setose; three teeth with the central pointed and 0.3 times mandible length, the others obtuse and slightly reflexed relative to the axis of the mandible, no sharp incisions between teeth; head 1.3 times as wide as mesoscutum.

Mesosoma. Length of mesosoma 1.25 times its height; pronope absent; side of pronotum glabrous and largely smooth with some crenulation antero-medially and ventrally; mesopleuron smooth with scattered setae, mesopleural sulcus finely crenulate, precoxal sulcus completely absent; mesosternum with moderately dense posteriorly directed setae and a narrow punctate sulcus; metapleuron shallowly rugulose with sparse setae; mesoscutum with a triangular area of dense setae and punctuation on its anterior surface extending somewhat dorso-medially, but dorsal surface largely shiny with sparse setae, notauli punctate anteriorly but absent from dorsal surface, a medio-posterior groove runs from $2/3$ to posterior edge, margin adjoining pronotum with longitudinal striae; scutellar sulcus 3.0 times as wide as long, with a strong medial carinae and two pairs of weaker lateral carinae; scutellum smooth with a few setae; axillar depression well developed and weakly crenulate; metanotum rugose with an indistinct antero-medial carina that bifurcates posteriorly, not protruding in lateral view; propodeum rugulose anteriorly, medially and laterally, with a relatively smooth area latero-medially, posterior region adjacent to insertion of first metasomal tergite incised and raised with horizontal striae, lateral posterior margin with small protuberance, surface with scattered sparse setae.

Wings. Fore wing: closed marginal, three submarginal, discal and subdiscal cells; pterostigma sub-elliptical, about 4.5 times as long as maximally wide, r inserted at about 0.4 times the length of the pterostigma, anterior ventral margin of pterostigma before insertion convex, beyond insertion it narrows and merges gradually with $1-R1$; length of r 0.6 times the width of pterostigma, approximately orthogonal to anterior wing margin; ratio of r : $3-SR$: SRI = 1: 5.2: 9.3, SRI slightly sinuate ending near wing apex; second submarginal cell narrows distally, 5-sided (i.e. $m-cu$ postfurcal), ratio $2-SR$: $3-SR$: $r-m$: $2-M$ = 1: 1.45: 0.46: 2.16, angle subtended by $2-SR$ and $3-SR$ 125° , $2-SR$ slightly sinuate; $1-CU1$ very short; $3-CU1a$ 1.3 times longer than $CUIb$; $CUIa$ concave down and extends nearly to wing margin. Hind wing: closed basal cell; $cu-a$ and $2-M$ present.

Legs. Hind coxa smooth; hind femur ~ 5 times longer than maximally wide, densely clothed with short setae dorsally projecting at an angle of 30° , ventrally approximately half the width of the femur and projecting at 60° ; hind tibia slender, densely clothed with setae (projecting at 30°), 1.15 times longer than tarsi; apical tibial spur inconspicuous, less than 0.2 times length of basitarsus; tarsi with similar setae to tibia, tarsal segment length ratios 1 (basitarsus): 0.53: 0.42: 0.31: 0.38; tarsal claws and arolium well developed and 0.75 times length of fifth tarsal segment; structure of fore and mid legs similar though femur more slender and legs shorter, ratio of hind: mid: fore femur 1: 0.90: 0.81.

Metasoma. Length of first tergite 1.7 times its apical width, the latter 1.7 times its narrowest width near its base, a pair of dorsal carinae arise basally from the lat-

eral carinae and reach the dorsum at about $\frac{1}{4}$ and run close together in parallel to about $\frac{1}{2}$ where they lose their distinctiveness, posterior dorsal surface with longitudinal sculpturing and sparsely scattered setae, a distinct dorsope present; metasoma beyond first tergite strongly lateral compressed with a strong dorsal medial carina extending from the third tergite to the end; second tergite smooth; scattered setae on second and posterior tergites; ovipositor straight and projecting, its exposed setose part 0.7 times the length of the hind tibia; ovipositor sheath with posterior directed setae projecting at an angle of 60–80°, their length up to twice the width of sheath; hypopygium slightly postero-ventrally produced, terminating at level of the cerci.

Colour. Head, mesosoma and metasoma dark brown except for yellow brown parts: scape, pedicel, base of the third antennal segment, mandibles (apart from tooth tips) and ventral part of gena, latero-ventral prothorax, tegulum, medio-ventral region of the laterally-compressed metasoma; precoxal area of mesopleuron slightly lighter than the remainder of the surface; palps and legs yellow, the mid and hind tarsi slightly darker, areola contrastingly dark brown; wing venation and pterostigma dark brown, wing membrane hyaline.

Variation amongst females. The French and Netherland female specimens generally match the holotype. The number of antennal segments were 34 and 37 (two specimens without complete antenna); extent of setation on dorsal surface of mesoscutum varies from comparatively well developed as shown in holotype (Fig. 1) to largely restricted to a few remote setae as figured in the male paratype (Fig. 2). In addition, the medio-longitudinal carina of propodeum is weakly developed in some specimens.

Description of male. Paratype, ♂, length of body 3.3 mm, of fore wing 4.1 mm (Fig. 2).

This specimen is somewhat damaged with both antennae truncated and some legs missing. Similar to the female but differing in the following features.

Head. Posterior ocelli slightly closer together (OOL 3.4 times POL); face somewhat less setose.

Wings. Veins thicker than in female; second submarginal cell slightly shorter – ratio of $r: 3-SR: SRI = 1: 4.3: 8.3$, ratio $2-SR: 3-SR: r-m: 2-M = 1: 1.37: 0.38: 2.06$.

Legs. Hind leg first tarsal segment slightly longer – tarsal segment length ratios = 1 (basitarsus): 0.50: 0.36: 0.26: 0.34.

Mesosoma. Anterior surface of mesonotum setose but setae extending less onto the dorsal surface than in the female holotype; propodeum smoother.

Metasoma. The metasoma is not laterally compressed and does not have longitudinal carinae on the posterior tergites; thus, having a “normal” Alysiiini appearance.

Colour. Ventral margin of clypeus yellow; metasoma more uniformly brown.

Molecular analysis. Sequence data from the mitochondrial CO1 gene (the standard barcode locus) were obtained from the *M. chandleri* holotype (607 base pairs) and a British specimen of *M. indagatrix* (550 b.p.). A male Finnish specimen with identical gene sequence to the holotype was found in the BOLD database. No further Old World sequences were present in BOLD, but it did contain seven closely-related

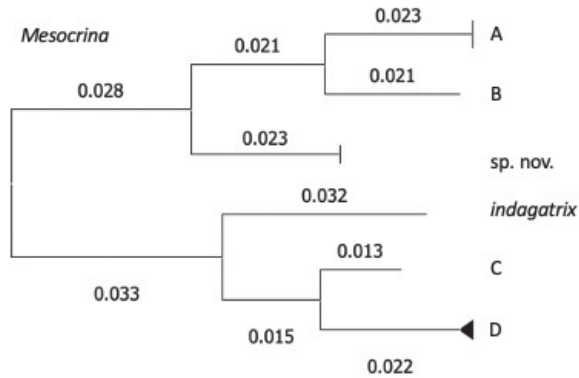


Figure 3. Maximum-likelihood tree (CO1 gene, Tamura-Nei model) with branch lengths of the 10 *Mesocrina* sequences in the BOLD database. The height of the terminal triangular wedges represents sample number and their horizontal width the genetic variation within the species (where no variation the wedge is a vertical line). Letters represent putative and undetermined Canadian (**A**, **B**, **D**) or Californian (**C**) species of *Mesocrina*.

North American sequences, some identified as *Mesocrina* and others that appeared from images in BOLD to belong to the genus. A maximum likelihood phylogenetic tree (CO1 gene, Tamura-Nei model; default MEGA settings) of the 10 sequences was created (Fig. 3), and they segregated into six putative species or BINs (Barcode Index Numbers; BIN codes as of February 2024).

Mesocrina chandleri (BIN: BOLD:ADX0117) shows a 6.5% divergence from its nearest relative, a Californian BIN (BOLD: AFO2946) represented by a single specimen. The two together with a Canadian BIN (3 specimens, BOLD:ACD3275) form a clade separated by 6.1% from a clade containing *M. indagatrix* (BOLD:AED2809) and two Canadian BINs (BOLD:AAU8494 & ACL6319). *M. indagatrix* shows a 11.6% separation from *M. chandleri* and 6.0% from the nearest Canadian BIN. The genetic data thus strongly supports the distinctiveness of the new species.

Discussion

The Palaearctic species of *Mesocrina* Foerster can be distinguished by the following key which is based on Belokobylskij’s (1998) key (in Russian).

- 1 Precoxal sulcus distinctly crenulate; posterior surface of propodeum sloping vertically; first metasomal tergite about as long as its apical width; mesoscutum, pronotum and mesosternum brownish yellow; propleuron brownish; [vein r of fore wing much longer than wide; vein 1-SR short]; India, N. China (Jilin, Fujian, Hainan, Yunnan) ***M. dalhousiensis* Sharma, 1978**
- Precoxal sulcus smooth or absent; propodeum gradually sloping posteriorly; first metasomal tergite 1.2–2.0 times as long as its apical width; at most the pronotum ventrally, and the propleuron, brownish yellow **2**

- 2 Setose part of ovipositor sheath about as long as first tergite, 0.3–0.5 times as long as hind tibia (and shorter than apical height of metasoma and 0.13–0.14 times as long as fore wing); anterior half of middle lobe of mesoscutum largely glabrous and without distinct punctures; Palaearctic & NE Oriental; Fig. 4 ***M. indagatrix* Foerster, 1863**
- Setose part of ovipositor sheath 1.5–2.0 times as long as first tergite, 0.7–0.9 times as long as hind tibia (and about equal to apical height of metasoma and about 0.2 times as long as fore wing); anterior half of middle lobe of mesoscutum more or less setose and with some punctures..... **3**
- 3 Third antennal segment about 1.2 times longer than fourth segment; third tooth of mandible much smaller than first tooth; pterostigma robust and strongly sclerotised, about 5.0 times wider than length of vein r; [clypeus blackish]; East Palaearctic..... ***M. lesovik* Belokobylskij, 1998**
- Third antennal segment 1.5–1.7 times longer than fourth segment; third tooth of mandible similar to first tooth or larger; pterostigma more slender and less sclerotised, about twice times wider than length of vein r..... **4**
- 4 Mandible less robust, with first tooth of mandible not protruding and similar to third tooth; vein 2-SR of fore wing distinctly sinuate; antenna with 31–32 segments; propodeum without sculpture medially; East Palaearctic.....
..... ***M. licho* Belokobylskij, 1998**
- Mandible more robust, with first tooth of mandible rather protruding and sometimes larger than third tooth; vein 2-SR of fore wing straight or slightly sinuate; antenna with 34–40 segments; propodeum more rugulose or with carina medially..... **5**
- 5 Vein r of fore wing 0.8 times maximum width of pterostigma and narrow; first metasomal tergite 1.1 times as long as apically wide, twice as wide posteriorly as minimum width; propodeum with distinctly developed medio-longitudinal carina; clypeus largely yellow; second submarginal cell of fore wing robust and vein SR1 about 2.2 times as long as vein 3-SR; [middle lobe of mesoscutum only anteriorly setose (confined to anterior edge)]; East Palaearctic..... ***M. lesii* Belokobylskij, 1998**
- Vein r of fore wing thickened and 0.3–0.6 times maximum width of pterostigma; first metasomal tergite 1.7 times as long as apically wide, 1.7 times as wide posteriorly as minimum width; propodeum at most with weakly developed medio-longitudinal carina; clypeus dark brown or yellowish near ventral rim; second submarginal cell of fore wing less robust and vein SR1 1.7–2.0 times as long as vein 3-SR; [linear medio-posterior depression deep and comparatively long; females with 34–37 antennal segments; setose area of middle lobe of mesoscutum variable]; West Palaearctic; Figs 1, 2..... ***M. chandleri* sp. nov.**

In Europe only *M. indagatrix* (Fig. 4) and the new species are currently known. Females of *M. chandleri* are easily distinguished by their longer ovipositor. Males are harder to tell apart, but *M. indagatrix* is somewhat smaller and the anterior of the mesoscutum middle-lobe is smoother and bears fewer setae.

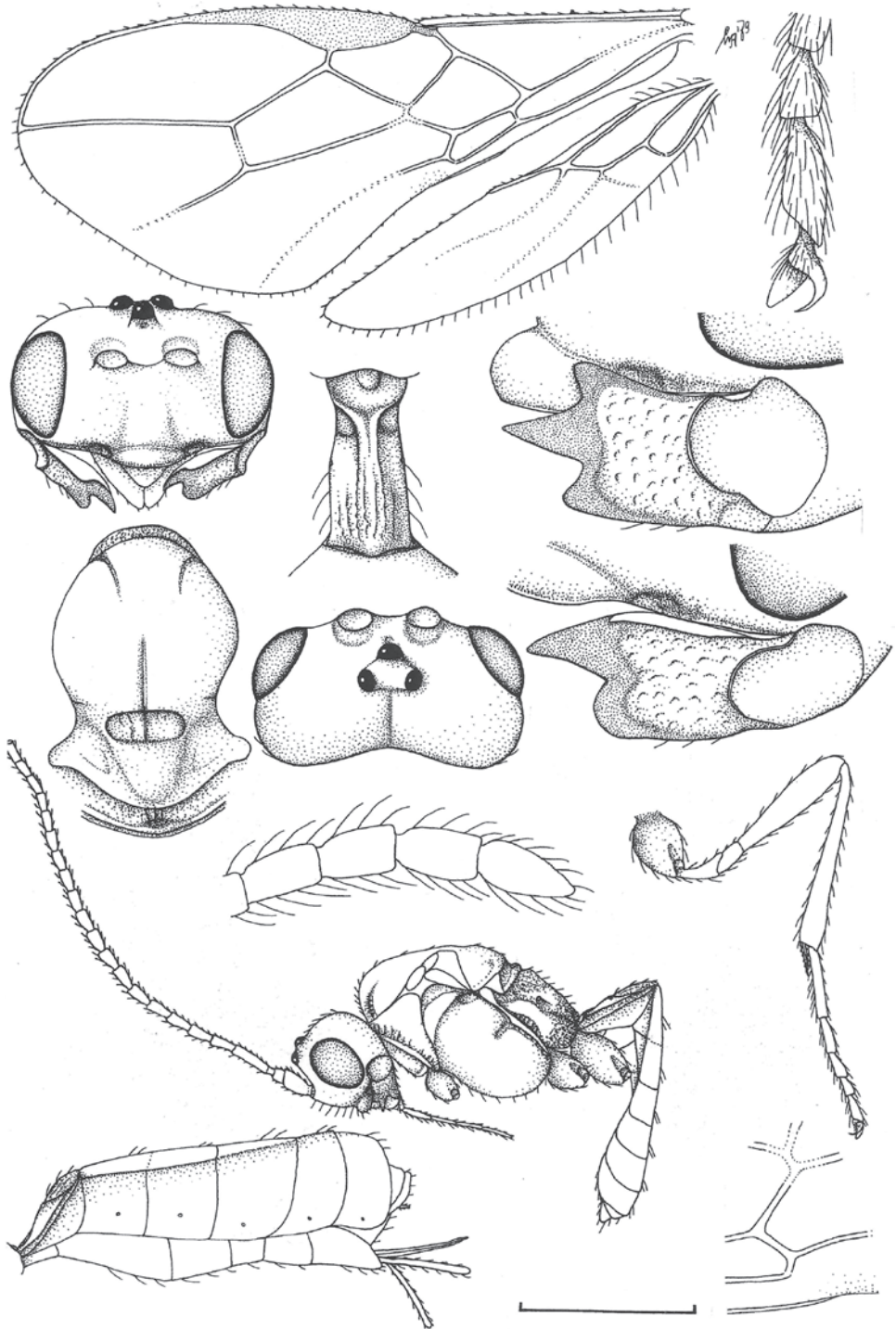


Figure 4. Montage of drawings (by C.v.A. using a camera lucida) of male and female *Mesocrina indagatrix*. Scale bar: 1.0 mm.

Females of both European species of *Mesocrina* and an American species (Wharton 1980) have been captured on gilled fungi, and it has been hypothesised that the laterally flattened female metasoma allows it to be inserted between closely packed fungal gills (Wharton 1980). We are unaware of any substantiated host rearing records but as all Alysini attack Diptera we presume *Mesocrina* spp. parasitise fly larvae feeding in fungal fruiting bodies.

Königsmann (1959) quotes two non-fungi-associated host records for *M. indagatrix* which he referred to as *Pseudomesocrina venatrix* Marshall, later synonymised by van Achterberg (1983). The first a male from a *Pegomya* sp. (Anthomyiidae) leaf mining *Rumex* sp. in the UK (Morley 1933). The first author and his students have reared 1880 parasitoid specimens from *Pegomya* spp. feeding on *Rumex* in the UK of which the only Alysini were *Adeluroloa florimela* Haliday which made up 35% of the rearings. As males lack the distinctive compressed metasoma, and as Morley says the male only differs from the female in antennal segment number (which would be a curious observation to make about a highly sexually dimorphic *Mesocrina*), we suspect Morley's record is a misidentification, possibly of *A. florimela*. The second is *Nanna* (= *Amaurosoma*) *armillata* and/or *Nanna flavipes* (Scathophagidae) in developing flower heads of grasses, *Phleum* spp. (Poaceae), in Sweden (Borg 1959). We suspect this is a misidentification of *Synelix semirugosa* Haliday (Braconidae, Alysini) which attacks these hosts (King et al. 1935; Telenga 1935) and also has a laterally compressed metasoma. Our working hypothesis thus remains that *Mesocrina* spp. are parasitoids of Diptera in fungi.

The UK, Netherland and French specimens of the new species were all captured in October while the more northerly record from Finland is from September. The three specimens of *M. indagatrix* in the NMS collection were also collected in the autumn. The abundance of fungal fruiting bodies peaks at this time of year, and so the phenology and putative biology are consistent. *Mesocrina chandleri* is a relatively large and distinctive species (for an Alysini) and given how widespread it is we are surprised it has not been noted before, especially as some of the recent records come from sites that have been regularly surveyed for Braconidae. We speculate that the species may be undergoing a current expansion of range and/or abundance.

There are currently eight described species of *Mesocrina*, six from the Palaearctic and two from the Nearctic (Wharton 1980; van Achterberg 1983; Belokobylskij 1998). However, DNA CO1 sequences of the two European species cluster closely with four North American taxa that we believe are *Mesocrina* (that may or may not include the two described by Wharton) suggesting greater diversity in the Nearctic than currently recognised.

The genus *Mesocrina* was described by Foerster (1863 [1862]) though van Achterberg (1983) treated it as a subgenus of *Dapsilarthra*. Later Papp (1991 [1990]) raised it to genus level which was followed by other authors (van Achterberg 2014). Other *Dapsilarthra* genus-group braconids attack phytophagous cyclorrhaphan Diptera and they are thought to be the sister group of the Dacusini which have the same biology (Griffiths 1964). Van Achterberg (1983) noted that the association of *Mesocrina* spp. with fungi was atypical for the genus group, and Wharton (1980) suggested an

affinity with *Alysia* which is supported by our (relatively limited) DNA sequence data. Stronger evidence comes from a recent phylogenomic study of the Braconidae that included single species of *Alysia*, *Mesocrina* and *Dapsilarthra*: the first two genera are closely associated, while *Dapsilarthra* is distantly related and is indeed placed near the root of the Dacnusiini (Jasso-Martinez et al. 2022).

Acknowledgements

We are grateful to Sergey Belokobylskij for supplying photographs of the holotype of *Mesocrina leshii*, to Mark Shaw for access to the National Museum of Scotland's collection, to Marko Mutanen and Juho Paukkunen for loan of the male paratype, and to Paul Hebert & Jayme Sones (University of Guelph) for DNA sequencing and information from the BOLD database.

References

- Belokobylskij SA (1998) *Mesocrina*. In: Tobias VI (Ed.) Key to the insects of Russian Far East Vol 4 Neuropteroidea, Mecoptera, Hymenoptera Pt 3 (general editor: PA Ler). Dal'nauka, Vladivostok, 191–195, 200.
- Belokobylskij SA, Tobias VI (1998) Alysiinae. In: Ler PA (Ed.) Key to the insects of Russian Far East Vol 4 Neuropteroidea, Mecoptera, Hymenoptera Pt 3 (in Russian). Dal'nauka, Vladivostok, 162–411.
- Borg A (1959) Investigations on the biology and control of timothy grass flies *Amaurosoma armillatum* Zett. and *A. flavipes* Fall. (Dipt. Cordyluridae). Statens Växtskyddsanstalt, Meddelanden 75: 297–372.
- Fischer M (1971) Untersuchungen über die europäischen Alysiini mit besonderer Berücksichtigung der Fauna Niederösterreichs (Hymenoptera, Braconidae, Alysiinae). Polskie Pismo Entomologiczne 41: 19–160.
- Foerster A (1863) [1862] Synopsis der Familien der Gattung der Braconen. Verhandlungen des naturhistorischen Vereines der preussischen Rheinlande 19: 225–288.
- Griffiths GCD (1964) The Alysiinae (Hym. Braconidae) parasites of the Agromyzidae (Diptera). I. General questions of taxonomy, biology and evolution. Beiträge zur Entomologie 14: 823–914. <https://doi.org/10.21248/contrib.entomol.14.7-8.823-914>
- Jasso-Martinez JM, Santos BF, Zaldivar-Riveron A, Fernandez-Triana JL, Sharanowski BJ, Richter R, Dettman JR, Blaimer BB, Brady SG, Kula RR (2022) Phylogenomics of braconid wasps (Hymenoptera, Braconidae) sheds light on classification and the evolution of parasitoid life history traits. Molecular Phylogenetics and Evolution 173: 107452. <https://doi.org/10.1016/j.ympev.2022.107452>
- King LAL, Meikle AA, Broadfoot A (1935) Observations on the Timothy Grass Fly (*Amaurosoma armillatum* Zett). Annals of Applied Biology 22: 267–278. <https://doi.org/10.1111/j.1744-7348.1935.tb07162.x>

- Königsmann E (1959) Revision der paläarktischen Arten der Gattung *Mesocrina*. Beiträge zur Entomologie 9: 609–619.
- Morley C (1933) Notes on Braconidae: XIV - Alysiides. The Entomologist 66: 183–185.
- Papp J (1991) [1990] Second survey of the braconid wasps in the Bátorliget Nature Conservation Areas, Hungary (Hymenoptera: Braconidae). Studia Naturalia, Magyar Természettudományi Múzeum, Budapest 1: 639–674.
- Prosser SWJ, deWaard JR, Miller SE, Hebert PDN (2016) DNA barcodes from century-old type specimens using next-generation sequencing. Molecular Ecology Resources 16: 487–497. <https://doi.org/10.1111/1755-0998.12474>
- Tamura K, Stecher G, Kumar S (2021) MEGA11: Molecular Evolutionary Genetics Analysis version 11. Molecular Biology and Evolution 38: 3022–3027. <https://doi.org/10.1093/molbev/msab120>
- Telenga NA (1935) Uebersicht de aus U.S.S.R. bekannten Arten der Unterfamilie Dacnusiinae (Braconidae, Hymenoptera). Vereinsschrift der Gesellschaft Luxemburger Naturfreunde (1934) 12: 107–125.
- Tobias VI (1986) Subfamily Alysiinae. In: Medvedev GS (Ed.) Opredelitel nasekomykh Evropeiskoi chasti SSSR [Key to insects of the European part of the USSR] 3(5). Nauka [Translation: Science Publishers Inc.], Leningrad [Translation: Lebanon NH, USA.], 156–386.
- van Achterberg C (1983) Revisionary notes on the genera *Dapsilarthra* auct. and *Mesocrina* Foerster (Hymenoptera, Braconidae, Alysiinae). Tijdschrift voor Entomologie 126: 1–24.
- van Achterberg C (2014) Notes on the checklist of Braconidae (Hymenoptera) from Switzerland. 87: 191–213. Mitteilungen der Schweizerischen Entomologischen Gesellschaft 87: 191–213. <https://doi.org/10.5169/seals-403088>
- Wharton RA (1980) Review of the Nearctic Alysiini (Hymenoptera, Braconidae) with discussion of generic relationships within the tribe. University of California Publications in Entomology 88: 1–112.
- Wharton RA (1997) Subfamily Alysiinae. In: Wharton RA, Marsh PM, Sharkey MJ (Eds) Manual of the New World Genera of Braconidae (Hymenoptera). Special Publication of the International Society of Hymenopterists. Vol. 1, 1–439.
- Wharton RA, Marsh PM, Sharkey MJ (1997) Manual of the New World Genera of the Family Braconidae (Hymenoptera). [Special Publication of the International Society of Hymenopterists Number 1.]. International Society of Hymenopterists.
- Zhu J-C, van Achterberg C, Chen X-X (2017) An illustrated key to the genera and subgenera of the Alysiini (Hymenoptera, Braconidae, Alysiinae), with three genera new for China. ZooKeys 722: 37–79. <https://doi.org/10.3897/zookeys.722.14799>

Six in one: cryptic species and a new host record for *Olixon* Cameron (Rhopalosomatidae, Hymenoptera) revealed by DNA barcoding

Allaina L. Armstrong¹, Jayme E. Sones², Volker Lohrmann^{3,4},
Paul D. N. Hebert², Dan H. Janzen⁵, Winnie Hallwachs⁵, Jeremy D. Blaschke¹

1 Union University, Jackson, USA **2** University of Guelph, Guelph, Canada **3** Übersee-Museum Bremen, Bremen, Germany **4** Museum für Naturkunde, Leibniz-Institut für Evolutions- und Biodiversitätsforschung, Berlin, Germany **5** Department of Biology, University of Pennsylvania, Philadelphia, USA

Corresponding author: Jeremy D. Blaschke (jblaschke@uu.edu)

Academic editor: Michael Ohl | Received 1 December 2023 | Accepted 14 April 2024 | Published 7 May 2024

<https://zoobank.org/3AED773F-6420-47CF-A898-78340D375416>

Citation: Armstrong AL, Sones JE, Lohrmann V, Hebert PDN, Janzen DH, Hallwachs W, Blaschke JD (2024) Six in one: cryptic species and a new host record for *Olixon* Cameron (Rhopalosomatidae, Hymenoptera) revealed by DNA barcoding. Journal of Hymenoptera Research 97: 363–378. <https://doi.org/10.3897/jhr.97.116726>

Abstract

Olixon testaceum is a widely distributed species of brachypterous parasitoid wasp (Vespoidea: Rhopalosomatidae) occurring in Meso- and South America, but little is known of its biology. Here, the first known host of *O. ?testaceum* is identified as the cricket *Anaxipha* sp. (Grylloidea: Trigonidiidae) through DNA barcoding of six *Olixon* larvae and their hosts. Barcoding results also indicated substantial genetic diversity within nominal *O. testaceum* specimens. The number of species and statistical significance of these groups were tested using Maximum Likelihood phylogenies, distance-based cluster analyses, and coalescence models. All analyses revealed at least six distinct lineages, which suggests six or more cryptic species within *O. ?testaceum*. Combined with what is currently known about *Rhopalosoma* host use, these results indicate that rhopalosomatids may be generalist rather than specialist parasitoids, and further confirm the benefits of open global collaboration and DNA barcoding in advancing taxonomic knowledge.

Keywords

Cricket-assassin wasp, integrative taxonomy

Introduction

In recent decades, new discoveries have greatly increased our knowledge of the diversity, systematics, and behavior of *Olixon* Cameron, 1887—an historically understudied genus of cricket-assassin wasps (Vespoidea: Rhopalosomatidae) (Townes 1977) (Fig. 1). These unusual brachypterous wasps are rarely seen alive but are now being collected in substantial numbers in pitfall and Malaise traps around the world (Mayhew and Dytham 2008; Lohrmann et al. 2012). These specimens have led to new species descriptions (e.g., Lohrmann and Ohl 2007; Krogmann 2009; Lohrmann et al. 2012; Bulbol et al. 2023), new distributional records (e.g., Ramsdell and Taylor 2006; Wood and Maupin 2007), and behavioral notes (Lohrmann et al. 2014), as well as discussions of *Olixon* biogeography and diversification (Krogmann 2009). However, knowledge of their biology remains limited. Here, we report the cricket *Anaxipha* sp. (Grylloidea: Trigonidiidae) as the first confirmed host of *O. ?testaceum* and discuss evidence that six cryptic species are included within the nominal species *O. testaceum* in Meso- and South America.

Of the 74 currently described species of extant Rhopalosomatidae (Lohrmann et al. 2020; Bulbol et al. 2021; Bulbol et al. 2023), only three have confirmed hosts. *Rhopalosoma nearcticum* Brues, 1943 are ectoparasitoids of two cricket genera—*Anaxipha* Saussure, 1874 and *Hapithus* Uhler, 1864 (Grylloidea) (Hood 1913; Gurney 1953; Miller et al. 2019), while a single specimen of *O. australiae* (Perkins) has been reared from a cricket identified only to the subfamily Trigonidiinae (Grylloidea: Trigonidiidae) (Perkins 1908). Based upon the examination of museum specimens, Townes (1977), it has been speculated, based on the size of the larvae found attached to hosts, that *O. banksii* (Brues, 1922) may parasitize nemobiine crickets while the scaly cricket, *Cycloptilum trigonipalpus* (Rehn & Hebard, 1912) (Mogoplistidae), may be host for *O. testaceum* Cameron. The observation of its female attacking a nemobiine cricket (Lohrmann et al. 2014) added the first direct evidence for Townes' speculation regarding the host of *O. banksii*.

Despite their brachypterous wings which would seem to limit long-range dispersal, *Olixon testaceum*, as currently understood, is among the most widespread of all rhopalosomatids, occurring throughout Meso- and South America, from Argentina to Arizona (Lohrmann et al. 2012). Specimens are most often collected in Malaise traps and can be found in diverse habitats including rain forests, dry forests, prairies, and cultivated landscapes. The broad distribution of *O. testaceum* coupled with the recent discovery of sympatric cryptic species of *Rhopalosoma nearcticum* in the USA (Miller et al. 2019) made *O. testaceum* an excellent candidate for a species delimitation study using sequence records from the Barcode of Life Database (BOLD; www.boldsystems.org).

An initial search of publicly available rhopalosomatid records revealed 221 sequences from specimens identified as *O. cf. testaceum* using the key to species in Lohrmann et al. (2012). Remarkably, four sequences from unidentified rhopalosomatid larvae were also included among these records (Fig. 2). Most of the *O. cf. testaceum* and all the larvae originated from the ongoing BioAlfa inventory of the Area de Conservación Guanacaste (ACG) in northwestern Costa Rica in Sector Santa Rosa (Janzen 1986; Janzen and Hallwachs 2016; Janzen et al. 2009). Given the biological significance of new host



Figure 1. **A** An adult *Olixon* cf. *testaceum* (photo: Paul Bertner) and **B** an *Olixon* cf. *testaceum* 6 larva (BIOUG55891-B08_parasite) attached to its cricket host (BIOUG55891-B08) (photo: CBG Photography Group).



Figure 2. Representative *Olixon* cf. *testaceum* larvae used in this study. BOLD sample IDs **A** BIOUG59151-H08 **B** BIOUG55891-B08_parasite **C** BIOUG63752-H08 **D** BIOUG58943-C02 (photos: CBG Photography Group).

records for Rhopalosomatidae, our objectives were to 1) identify the unknown larvae to species by placing them within a phylogeny of Rhopalosomatidae, 2) identify their host species by searching for associated specimens within BOLD and by generating new barcode sequences as needed, and 3) explore the genetic diversity of *O. testaceum* for evidence of cryptic species.

Methods

Specimens from each sequence cluster in this study were identified to genus using Townes' (1977) key to rhopalosomatid genera and the specimen photos available through BOLD. The subsequent assignment of *Olixon* specimens to the nominal taxon *O. testaceum* was based on the presence of the following combination of characters that distinguishes this species: a more or less uniform testaceous to pale brown coloration with the exception of a dark marking on metasomal segment II, the presence of a malar sulcus, a short temple, and a strong and complete carina between the posterolateral processes of the propodeum (Lohrmann et al. 2012).

The publicly available records (n = 221) were combined with additional private sequences of rhopalosomatids made available by JS, PH, DJ, and WH to ensure maximum coverage, including another two larvae (for a total of six). Specimens were predominantly collected via weekly Malaise trap samples (n = 398) between 2012 and 2020. All but 10 specimens (sourced from GenBank) were sequenced at the Centre for Biodiversity Genomics, and most sequences (n = 309) were generated by a Sequel (Pacific Biosciences) high-throughput sequencer, while 95 were analyzed using Sanger sequencing (<https://ccdb.ca/resources/>). All sequences, specimen images, and collection data are available in the dataset “DS-RHOP” on BOLD.

An initial Maximum Likelihood (ML) phylogeny of Rhopalosomatidae was created using RAxML (v.8.2.12) (Stamatakis 2014) through the CIPRES Science Gateway (Miller et al. 2010). Alignments were partitioned by codon position and analyzed using the GTRCAT model of nucleotide substitution. Statistical significance was analyzed using 1000 bootstrap (BS) pseudoreplicates. This tree (not shown) included 424 specimens, of which 221 represented *O. testaceum* and six were larvae. All six larvae were located within clades of nominal *O. testaceum*, five in one clade and one in another. In total, the specimens of *O. testaceum* formed six distinct clades, one of which contained 206 of the 221 specimens. As this group contained very little genetic diversity (average genetic distance = 0.0099), subsequent analyses reduced the number of specimens for this clade was reduced from 206 to five representatives.

To narrow the focus to only larvae and potential cryptic species of *O. testaceum*, a new ML phylogeny was created using all six larvae, specimens from each apparent *O. testaceum* clade, all other *Olixon* specimens available (five in total), and four outgroup specimens (two each for *Liosphex* Townes, 1977 and *Rhopalosoma* Cresson, 1865). Sequences were aligned using MAFFT v.7.450 (Katoh et al. 2002; Katoh and Standley 2013) in Geneious Prime® 2020.0.2 (Biomatters, Auckland, NZ). The presence of pseudogenes in the alignment was checked via translation to amino acids. No stop codons were present. The ML phylogeny was reconstructed as described above. Specimen IDs, collection information, and tentative species groups are found in Table 1. Intra- and interspecific genetic distances (K2P) were calculated in MEGA 11 (Tamura et al. 2021).

Table 1. Specimens used in phylogenetic and statistical analyses. Process and Voucher IDs from BOLD: www.boldsystems.org.

Species	Location	Date Collected	Elevation (M)	Stage	Process ID	Sample ID	BIN
<i>O. ?testaceum</i> 1	Cortes, HND	7/2/2014	1219	Adult	GMHJK402-15	BIOUG18597-F10	BOLD:ACE2345
<i>O. ?testaceum</i> 1	Cortes, HND	7/27/2012	1219	Adult	GMHDO003-13	BIOUG04583-G09	BOLD:ACE2345
<i>O. ?testaceum</i> 1	Cortes, HND	6/18/2015	1219	Adult	GMHMQ600-15	BIOUG26862-E11	BOLD:ACE2345
<i>O. ?testaceum</i> 1	Cortes, HND	7/24/2014	1196	Adult	GMHKP138-15	BIOUG19409-D02	BOLD:ACE2345
<i>O. ?testaceum</i> 1	Cortes, HND	7/16/2015	1219	Adult	GMHMU283-16	BIOUG28324-G04	BOLD:ACE2345
<i>O. ?testaceum</i> 2	ACG, CRI	5/25/2020	1366	Adult	CRALC14238-21	BIOUG72979-B05	BOLD:AEO2513
<i>O. ?testaceum</i> 3	ACG, CRI	3/13/2014	853	Adult	JICFX017-16	BIOUG29019-H01	BOLD:ACZ7577
<i>O. ?testaceum</i> 3	ACG, CRI	1/9/2014	831	Adult	PLEA1182-19	BIOUG48962-D09	BOLD:ACZ7577
<i>O. ?testaceum</i> 3	ACG, CRI	5/12/2014	575	Adult	GMAAT178-16	BIOUG27868-D08	BOLD:ACZ7577
<i>O. ?testaceum</i> 3	ACG, CRI	8/10/2015	575	Adult	GMADY103-16	BIOUG28200-H03	BOLD:ACZ7577
<i>O. ?testaceum</i> 3	ACG, CRI	4/14/2014	575	Adult	GMAAR037-16	BIOUG28246-C12	BOLD:ACZ7577
<i>O. ?testaceum</i> 3	ACG, CRI	1/26/2017	828	Adult	PLVAK389-20	BIOUG55894-F08	BOLD:ACZ7577
<i>O. ?testaceum</i> 4	ACG, CRI	1/28/2020	15	Adult	CROAC13695-21	BIOUG68837-C03	BOLD:AEM2374
<i>O. ?testaceum</i> 4	ACG, CRI	3/3/2022	62	Adult	CROCA33528-21	BIOUG68316-G10	BOLD:AEM2374
<i>O. ?testaceum</i> 5	Paramaribo, SUR	10/2/2017	n/a	Larva	GMSPA14567-21	BIOUG70270-H11	BOLD:AEK9228
<i>O. ?testaceum</i> 6	ACG, CRI	8/5/2012	300	Adult	GMCRRH028-13	BIOUG05414-E09	BOLD:ACG4885
<i>O. ?testaceum</i> 6	ACG, CRI	1/18/2018	828	Adult	PLBCJ264-20	BIOUG57554-G01	BOLD:ACG4885
<i>O. ?testaceum</i> 6	ACG, CRI	8/30/2018	811	Adult	PLEFA082-21	BIOUG64629-H07	BOLD:ACG4885
<i>O. ?testaceum</i> 6	ACG, CRI	5/26/2020	15	Adult	CROAD12739-22	BIOUG80688-H11	BOLD:ACG4885
<i>O. ?testaceum</i> 6	ACG, CRI	6/16/2020	15	Adult	CROAD18508-22	BIOUG81047-E07	BOLD:ACG4885
<i>O. ?testaceum</i> 6	ACG, CRI	1/19/2017	828	Larva	PLVAJ397-22	BIOUG55891-B08_	BOLD:ACG4885
						parasite	
<i>O. ?testaceum</i> 6	ACG, CRI	8/20/2020	791	Larva	PLDFN085-21	BIOUG63752-H08	BOLD:ACG4885
<i>O. ?testaceum</i> 6	ACG, CRI	8/27/2020	811	Larva	PLEFO304-21	BIOUG59841-H04	BOLD:ACG4885
<i>O. ?testaceum</i> 6	ACG, CRI	1/18/2018	809	Larva	PLKCJ206-20	BIOUG59151-H08	BOLD:ACG4885
<i>O. ?testaceum</i> 6	ACG, CRI	8/30/2018	809	Larva	PLKDP220-20	BIOUG58943-C02	BOLD:ACG4885
<i>O. banksii</i>	IO, USA	22/8/2009	–	Larva	Olixon_Larva_IO	–	
<i>O. banksii</i>	TX, USA	7/6/2011	81	Adult	BBHYA2946-12	BIOUG02644-C10	BOLD:ACA7258
<i>O. banksii</i>	VA, USA	9/28/1993	–	Adult	SICOD002-19	CCDB-34061-A02	BOLD:AEA2163
<i>O. banksii</i>	OK, USA	6/19/2011	–	Adult	BBHYA2958-12	BIOUG02644-D10	BOLD:ACA7139
<i>Olixon</i> sp.	WA, AUS	11/21/2014	–	Adult	GMCWM011-15	BIOUG23860-E06	BOLD:ACZ3980
<i>Liosphex</i> sp.	ACG, CRI	4/28/2014	575	Adult	GMAAS028-16	BIOUG28345-C04	BOLD:ADA1369
<i>Liosphex</i> sp.	ACG, CRI	6/11/2015	1220	Adult	GMCCI021-17	BIOUG36436-H10	BOLD:ADL6377
<i>Rhopalosoma</i> sp.	ACG, CRI	7/12/2018	809	Adult	PLKDI021-20	BIOUG58153-D12	BOLD:ADC7061
<i>Rhopalosoma</i> sp.	ACG, CRI	5/14/2012	300	Adult	GMCGG056-14	BIOUG17755-D09	BOLD:ACG8319

To test for potential cryptic species diversity within *O. testaceum*, both distance-based cluster analyses and phylogenetically informed tests of species delimitation were employed. Assemble Species by Automatic Partitioning (ASAP) (Puillandre et al. 2021) is a distance-based method that tests various species hypotheses using the intra- and inter-genetic distance scores for putative species to calculate a custom ASAP score for each hypothesis (lower scores = more statistical robustness). The online version of ASAP (<https://bioinfo.mnhn.fr/abi/public/asap>, last accessed Dec. 12, 2022) was used under default settings with genetic distances calculated using the K2P model of molecular evolution.

Additional distance-based cluster analyses were carried out in R (Paradis et al. 2005; R Core Team 2017; Paradis and Schliep 2018). The “dist.DNA” function with model = “TN93” was used to calculate a corrected distance matrix from the imported nucleotide alignment. TN93 was used as it most closely approximates the more complex GTR

model used in the ML analyses which is unavailable using dist.DNA. Hierarchical clustering, which iteratively combines taxa with minimal dissimilarity to create a dendrogram of potentially statistically significant clusters, was performed within the function “parPvclust” using the correlation method and average linkage agglomeration (Suzuki and Shimodaira 2006). The statistical significance of the clusters was confirmed by 1000 bootstrap replicates and the calculation of Approximately Unbiased p-values (AU) and Bootstrap Probability (BP) values as suggested by Suzuki and Shimodaira (2006). The distance matrix was also analyzed using partitioning around medoids, which creates and scores clusters by collapsing the distance of intra-cluster points to a hypothetical centroid. Statistical significance is inferred from average silhouette width of clusters (>0.5 is considered significant) (Kaufman and Rousseeuw 1987). (The “pam” function (Schubert and Rousseeuw 2019) and variable k values ranging from 2 to 8 were used. Results were visualized using “fviz_silhouette” (Kassambara and Mundt 2020).

Phylogenetically informed species delimitation methods were also used. The Multi-rate Poisson Tree Process (mPTP) introduced by Kapli et al. (2017) uses maximum likelihood and is based on a single-locus coalescent-based method. The online version of mPTP (<https://mptp.h-its.org/#/tree>, last accessed Dec. 12, 2022) was used with default parameters. For a Bayesian analysis, the Bayesian Poisson Tree Process (bPTP) program of Zhang et al. (2013) (<https://species.h-its.org/ptp/>, last accessed Dec. 12, 2022) was used. The rooted phylogeny was uploaded and analyzed for 250,000 MCMC generations, thinning was set to 150, and the first 25% were discarded as burn-in. Within the program, a simple heuristic search determined the most likely number of species represented on the tree according to the most supported partition. Convergence was verified by visually checking the likelihood plot.

High throughput sequencing (HTS) has the advantage of generating sequences of biota associated with the target specimen. This property enables the identification of potential host-parasitoid interactions, predator-prey relationships, pathogen infections, etc. If a specimen yields more than one sequence contig, the additional contig(s) can be examined for biologically relevant associations. To identify the host for each larva, we compared any additional sequence information generated by the HTS to BOLD and generated a new barcode record when a potential orthopteran host sequence was found.

Results

Thirty-four sequences were used to generate the ML tree (Fig. 3). All sequences are publicly available in BOLD (dataset “DS-RHOP”) and identification codes are listed in Table 1. Within *Olixon*, two major lineages were recovered, one including 25 specimens of *O. testaceum* and the other primarily composed of *O. banksii* specimens from the USA. The single specimen of *Olixon* from Australia was recovered as sister to *O. banksii*. Six clades were well-resolved (BS = 100) within *O. testaceum* (informal species IDs are included in Table 1). All rhopalosomatid larvae from Costa Rica were recovered as members of the group “*O. ?testaceum* sp. 6”, thus confirming *Anaxipha*

Table 2. All novel host associations of *Olixon*. Sample IDs from BOLD: www.boldsystems.org.

Species	BIN	Location	Larva Sample ID	Host Sample ID	Host Species	Host BIN	Status
<i>O. ?testaceum</i> 5	BOLD:AEK9228	Paramaribo, SUR	BIOUG70270-H11	—	—	—	—
<i>O. ?testaceum</i> 6	BOLD:ACG4885	ACG, CRI	BIOUG55891-B08_parasite	BIOUG55891-B08	<i>Anaxipha</i> sp.	BOLD:ACO0556	Known
<i>O. ?testaceum</i> 6	BOLD:ACG4885	ACG, CRI	BIOUG63752-H08	BIOUG63752-H08.NTS	<i>Anaxipha</i> sp.	BOLD:ACO0556	Known
<i>O. ?testaceum</i> 6	BOLD:ACG4885	ACG, CRI	BIOUG59841-H04	BIOUG59841-H05	Trigonidiidae	BOLD:ACG0099	Associated?
<i>O. ?testaceum</i> 6	BOLD:ACG4885	ACG, CRI	BIOUG59151-H08	BIOUG59151-H08.NTS	<i>Anaxipha</i> sp.	BOLD:ACO0556	Associated?
<i>O. ?testaceum</i> 6	BOLD:ACG4885	ACG, CRI	BIOUG58943-C02	BIOUG58943-C02.NTS	Trigonidiidae	—	Associated?

Table 3. Mean pairwise intra- and interspecific genetic distances (K2P) between sampled *Olixon testaceum* specimens. Bold values = intraspecific genetic distance. “n/a” = not applicable due to single taxon.

<i>O. ?testaceum</i> 1	0.000						
<i>O. ?testaceum</i> 2	0.138	n/a					
<i>O. ?testaceum</i> 3	0.149	0.072	0.003				
<i>O. ?testaceum</i> 4	0.144	0.071	0.074	0.010			
<i>O. ?testaceum</i> 5	0.159	0.107	0.113	0.104	n/a		
<i>O. ?testaceum</i> 6	0.149	0.079	0.063	0.061	0.103	0.006	

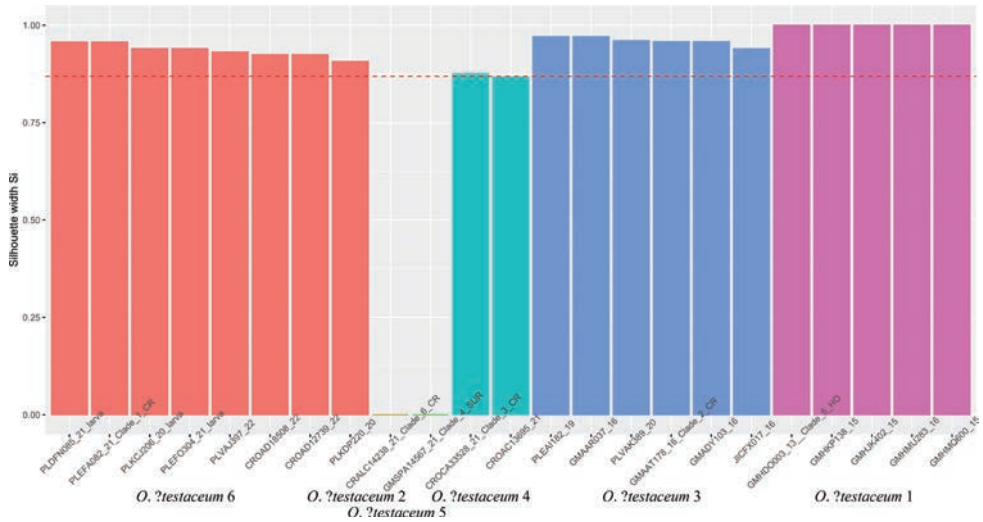


Figure 4. Partitioning Around Medoids analysis of *Olixon* ?*testaceum*. Average silhouette width = 0.87. Statistically significant clusters of *O. ?testaceum* are labeled in correlation to ML phylogeny.

partition assuming six hypothetical species (ASAP-score = 1.0; threshold distance = 3.2%). The mPTP suggested six unique lineages, while the bPTP results supported at least six, and possibly up to nine species within *O. testaceum*, although species 7–9 were recovered with very low support. Genetic distances between and within species (Table 3) show very little intraspecific variation per clade (average = .005) and substantial interspecific variation (average = .106).

Discussion

Our analyses indicate several genetic lineages fall within the morphological variation of “*Olixon testaceum*.” However, since the holotype has not been barcoded, we are unable to link any particular genetic lineage with the “real” *O. testaceum*. To indicate this uncertainty and acknowledge that future morphological work is needed to formally describe these cryptic species, we refer to the species group collectively as “*O. ?testaceum*.”

Although *O. ?testaceum* is one of the most widespread morphospecies of Rhopalosomatidae, very little is known about its biology (Lohrmann et al. 2012). Here, we have confirmed one new host record for the genus *Olixon* and added several new associated host records for the *O. ?testaceum* species group. At the family level, a new host record for *O. ?testaceum* adds a fourth confirmed host for rhopalosomatid species (Lohrmann et al. 2014; Miller et al. 2019).

Olixon is now known to parasitize species within two subfamilies of crickets: Trigonidiinae (herein, Perkins 1908) and Nemobiinae (*O. banksii*, Lohrmann et al. 2014). Similarly, the only other rhopalosomatid with known hosts, *Rhopalosoma ?nearcticum*, parasitizes both Trigonidiinae and Podoscirtinae crickets (Miller et al. 2019).

The finding of two different subfamilies of crickets as hosts each for *Olixon* and *Rhopalosoma* supports the hypothesis that rhopalosomatids, at least at the genus level, are generalist rather than specialist parasitoids.

Furthermore, the identification of *Anaxipha* as a host of *O. ?testaceum* is quite remarkable as *Anaxipha* are also among the known hosts of the distantly related *R. ?nearcticum* (Miller et al. 2019). *Olixon* is hypothesized to be the basal branch of Rhopalosomatidae and sister to a clade comprising all recent macropterous forms (Guidotti 1999; Lohrmann et al. 2020) (Fig. 5). The basal position of *Olixon* coupled with the fact that these two rhopalosomatid genera (*Olixon* and *Rhopalosoma*) are not sister taxa but utilize species of the same genus of crickets as hosts may suggest Trigonidiinae as the ancestral host for Rhopalosomatidae. However, other groups of crickets (i.e., Nemobiinae and Podoscirtinae) are also used as hosts by rhopalosomatids and we still know relatively little about host use throughout the family. It is possible the shared trigonidiine host of *Olixon* and *Rhopalosoma* is an example of convergent evolution rather than a plesiomorphy. Unfortunately, hosts for *Paniscomima* Enderlein, 1904 and *Liosphex* are still unknown, but as seen here, large-scale Malaise trap sampling programs are excellent sources for rhopalosomatid adults, larvae, and hosts that may soon fill the gaps in our knowledge of rhopalosomatid biology and evolution of host use.

While a new host record and discovery of cryptic species is significant, there is still much work to be done. Future efforts relating to *O. ?testaceum* should investigate morphological or ecological differences that might further distinguish clades from one another. A previous study in the ACG (Hebert et al. 2004), discovered that the target species *Telegonus* (previously *Astraptus*) *fulgerator* (Walch, 1775) contained at least ten cryptic species with defining variation in morphology and host plant preference. Future efforts should investigate whether *O. ?testaceum* displays similar variation, especially considering its widespread range. Brief comparison of the six clades revealed by this study showed that *O. ?testaceum* sp. 1 from Honduras is easily characterized by its distinct wings which seem, in terms of the grade of their reduction, intermediate between *O. melinsula* Lohmann et al., 2012 and *O. ?testaceum* (Fig. 6). Formal species descriptions of these genetic clades should employ an integrative taxonomy approach (e.g. Padial et al. 2010)—adding morphological, behavioral, and host data to the genetic data presented here.

Such integrative taxonomic research may reveal more cryptic species within *O. testaceum* beyond those discovered here. In their revision of the New World *Olixon*, Lohrmann et al. (2012) investigated several hundred specimens assigned to *O. testaceum* originating from the southern United States (Arizona) to northern Argentina. The cryptic diversity of *O. testaceum* reported here is certainly an underestimation of this clade's true diversity since all but one of the specimens analyzed were from Honduras and Costa Rica. The holotype of *Olixon testaceum* was collected in Bugaba, Panama (Cameron 1887), but it is not clear whether its barcode would match any of the clades examined in this study. Furthermore, the slightly different color pattern of *Saphobethylus pallidus* Kieffer, 1911 from Teapa in Mexico, currently treated as a synonym of *O. testaceum* (e.g., Turner and Waterston 1917; Townes 1977; Lohrmann et al. 2012), supports the hypothesis that it too represents a distinct species.

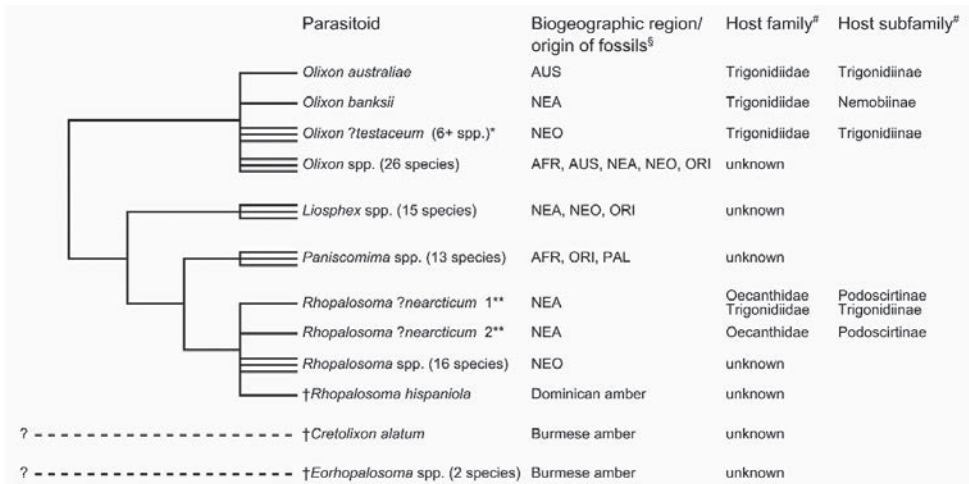


Figure 5. Generalized phylogeny of Rhopalosomatidae showing currently confirmed host associations. The tree topology is based on Brothers (1999), Guidotti (1999), and unpublished molecular data (Blaschke et al., unpublished results). The information on the parasitoid-host-associations are based on Hood (1913), Gurney (1953), and Miller et al. (2019) for *Rhopalosoma* cf. *nearcticum*, Townes (1977) and Lohrmann et al. (2014) for *O. banksii*, Perkins (1908) for *O. australiae*, and the herein presented data for *O. cf. testaceum*. Townes (1977) mentioned *Cycloptilum trigonipalpus* (Mogoplistidae) as the potential host of *O. testaceum*, however, this association is not included here since the association is based only on the size of the wasp larva and the fact that no other *Olixon* species was known from Honduras at that time. Symbols: § Information on the biogeographic regions of the parasitoids are based on Lohrmann et al. (2020; table 1) and Bulbol et al. (2021) for *Liosphex*, Krogmann et al. (2009), Lohrmann et al. (2012), Lohrmann et al. (2020), and Bulbol et al. (2023) for *Olixon*, Lohrmann (2011) and Lohrmann et al. (2020; table 1) for *Paniscomima*, Townes (1977), Miller et al. (2019), and Lohrmann et al. (2019) for *Rhopalosoma*, and Lohrmann et al. (2020) for *Cretolixon* and *Eorhopalosoma*. # The classification of the hosts follows Cigliano et al. (2023). * The herein published data suggests at least six species in the *O. testaceum* species group. **Miller et al. (2019) discovered that the nearctic species *R. nearcticum* actually consists of at least two distinct genetic lineages, i.e., *R. ?nearcticum* 1 and *R. ?nearcticum* 2.



Figure 6. *Olixon* spp., female, variations in fore wing morphology **A** *O. cf. testaceum* (Costa Rica) **B** *O. ?testaceum* 1 (Honduras) **C** *O. melinsula*, paratype (Florida) (photos: Volker Lohrmann).

Rhopalosomatidae appears to be a hotspot for cryptic species diversity. Our ML tree included four specimens of nominal *O. banksii* specimens from Iowa, Texas, Virginia, and Oklahoma. Three specimens from IO, TX, and VA showed low intra-group variation (patristic distance = 0.032), while the average nearest-neighbor distance be-

tween these three and a specimen from OK was significantly higher (patristic distance = 0.234). Another closely related species, *O. melinsula*, is currently known only from Texas to Florida (along the Gulf of Mexico) and southern Paraguay. This distribution pattern may well represent “two sibling species, so similar as to be indistinguishable at the moment” (Lohrmann et al. 2012). Both *O. banksii* and *O. melinsula* are promising groups for future investigations of cryptic species diversity among the cricket-assassin wasps.

The utility of DNA barcoding to identify and reveal cryptic species complexes is well established across a wide range of taxa and biomes (e.g., Hebert et al. 2003; Janzen et al. 2005; Sáez and Lozano 2005; Bickford et al. 2007). Many of the early case studies that applied barcoding to discover cryptic diversity exposed many undescribed species (e.g., Hebert et al. 2004; Smith et al. 2006; Smith et al. 2008). DNA barcoding offers solutions to many of the limitations of a morphologically dependent taxonomic system. Traditional methods for classification require much time and expertise (Stoeckle and Hebert 2008). As barcoding gains wide adoption by both taxonomists and ecologists (Valentini et al. 2009), open collaboration and accessibility to sequences are essential. In order to aid access, BOLD has consolidated this information into a public database with over 15 million specimen records for over 330,000 named species and more than a million putative species.

The taxonomic impediment is a significant and well-known problem in entomology (e.g., Agnarsson and Kunter 2007; Engel et al. 2021) and the results of our study highlight the importance of BOLD’s open access policies and friendly collaboration among researchers for the future of insect systematics. In this case, exploring BOLD as part of an undergraduate class revealed unexpected and interesting discoveries in rhopalosomatid host use. New collaborators enthusiastically joined the project, freely sharing specimens, photographs, and their expertise in rhopalosomatid systematics and morphology, DNA barcoding, and species delimitation. We hope future researchers will be similarly generous and collaborative across disciplines and skill levels, allowing for a deeper scientific understanding of the diversity of life and inspiring the next generation of insect taxonomists.

Acknowledgements

This research was funded in part by an undergraduate research grant from Union University (Jackson, TN) received by AA and JDB. A special thanks to the taxonomists and parataxonomists in Costa Rica for collecting specimens, to the Centre for Biodiversity Genomics (CBG) for sequencing specimens, to BioAlfa for providing images of specimens, to the government of Costa Rica for allowing use of the data, and to Barcode of Life Data Systems for informatics support and metadata. All ACG specimens were collected, exported and DNA barcoded under Costa Rican government permits issued to BioAlfa (Janzen and Hallwachs 2019) (R-054-2022-OT-CONAGEBIO; R-019-2019-CONAGEBIO; National Published Decree #41767), JICA-SAPI #0328497 (2014) and DHJ and WH (ACG-PI-036-2013; R-SINAC-ACG-PI-061-2021; Resolución N°001-2004 SINAC; PI-028-2021). Awards from the Walder Foundation, the Canada Foundation for Innovation, the New Frontiers in

Research Fund, and Genome Canada through Ontario Genomics to PDNH aided the CBG's capacity to gather sequence data and sustain BOLD. We thank Paul Bertner for his permission to use his photo of *Olixon* (Fig. 1).

References

- Agnarsson I, Kuntner M (2007) Taxonomy in a changing world: seeking solutions for a science in crisis. *Systematic Biology* 56(3): 531–539. <https://doi.org/10.1080/10635150701424546>
- Bickford D, Lohman D, Sodhi N, Peter KL, Meier R, Winker K, Ingram K, Das I (2007) Cryptic species as a window on diversity and conservation. *Trends in Ecology and Evolution* 22(3): 148–155. <https://doi.org/10.1016/j.tree.2006.11.004>
- Brothers DJ (1999) Phylogeny and evolution of wasps, ants and bees (Hymenoptera, Chrysoidea, Vespoidea and Apoidea). *Zoologica Scripta* 28(1–2): 233–250. <https://doi.org/10.1046/j.1463-6409.1999.00003.x>
- Bulbol MM, Bartholomay PR, de Oliveira, ML, Somavilla A (2023) A new species of *Olixon* Cameron, 1887 (Hymenoptera: Rhopalosomatidae) and new records for the genus in Brazil. *Zootaxa* 5277(3): 573–580. <https://doi.org/10.11646/zootaxa.5277.3.9>
- Bulbol MM, Somavilla A, Fernandes DRR, Bartholomay PR (2021) A new species of *Liosphex* Townes, 1977 (Hymenoptera: Rhopalosomatidae) from the Amazon forest and new records for the genus in Brazil. *Neotropical Entomology* 50(3): 444–452. <https://doi.org/10.1007/s13744-021-00862-6>
- Cigliano MM, Braun H, Eades DC, Otte D (2023) *Orthoptera Species File*. Version 5.0/5.0. [30.05.2023]. <http://Orthoptera.SpeciesFile.org>
- Engel MS, Ceríaco LMP, Daniel GM, Dellapé PM, Löbl I, Marinov M, Reis RE, Young MT, Dubois A, Agarwal I, Lehmann A P, Alvarado M, Alvarez N, Andreone F, Araujo-Vieira K, Ascher JS, Baêta D, Baldo D, Bandeira SA, Barden P, Barrasso DA, Bendifallah L, Bockmann FA, Böhme W, Borkent A, Brandão CRF, Busack SD, Bybee SM, Channing A, Chatzimanolis S, Christenhusz MJM, Crisci JV, D'elía G, Da Costa LM, Davis SR, De Lucena CAS, Deuve T, Elizalde SF, Faivovich J, Farooq H, Ferguson AW, Gippoliti S, Gonçalves FMP, Gonzalez VH, Greenbaum E, Hinojosa-Díaz IA, Ineich I, Jiang J, Kahono S, Kury AB, Lucinda PHF, Lynch JD, Malécot V, Marques MP, Marris JWM, Mckellar RC, Mendes LF, Nihei SS, Nishikawa K, Ohler A, Orrico VGD, Ota H, Paiva J, Parrinha D, Pauwels OSG, Pereyra MO, Pestana LB, Pinheiro PDP, Prendini L, Prokop J, Rasmussen C, Rödel M-O, Rodrigues MT, Rodríguez SM, Salatnaya H, Sampaio Í, Sánchez-García A, Shebl MA, Santos BS, Solórzano-Kraemer MM, Sousa ACA, Stoev P, Teta P, Trape J-F, Dos Santos CVD, Vasudevan K, Vink CJ, Vogel G, Wagner P, Wappler T, Ware JL, Wedmann S, Zacharie CK (2021) The taxonomic impediment: a shortage of taxonomists, not the lack of technical approaches. *Zoological Journal of the Linnean Society* 193, 381–387. <https://doi.org/10.1093/zoolinnean/zlab072>
- Guidotti AE (1999) Systematics of little known parasitic wasps of the family Rhopalosomatidae (Hymenoptera: Vespoidea). MSc. Thesis, University of Toronto, Toronto.
- Gurney AB (1893) Notes on the biology and immature stages of a cricket parasite of the genus *Rhopalosoma*. *Proceedings of the United States National Museum* 103(3313): 19–34. <https://doi.org/10.5479/si.00963801.103-3313.19>

- Hebert PDN, Penton E, Burns J (2004) Ten species in one: DNA barcoding reveals cryptic species in the neotropical skipper butterfly *Astraptes fulgerator*. PNAS 101(41): 14812–14817. <https://doi.org/10.1073/pnas.0406166101>
- Hebert PDN, Cywinska A, Ball SL, deWaard JR (2003) Biological identifications through DNA barcodes. Proceedings: Biological Sciences 270(1512): 313–321. <https://doi.org/10.1098/rspb.2002.2218>
- Hood JD (1913) Notes on the life history of *Rhopalosoma poeyi* Cresson. Proceedings of the Entomological Society of Washington 15: 145–147.
- Janzen DH (1986) Guanacaste National Park: tropical ecological and cultural restoration. In Rehabilitating Damaged Ecosystems 2: 143–192. <https://copa.acguanacaste.ac.cr/handle/11606/338>
- Janzen DH, Hallwachs W (2016) DNA barcoding the Lepidoptera inventory of a large complex tropical conserved wildland, Area de Conservacion Guanacaste, northwestern Costa Rica. Genome 59: 641–660. <https://doi.org/10.1139/gen-2016-0005>
- Janzen DH, Hajibabaei M, Burns J, Hallwachs, W, Remigo E, Hebert PDN (2005) Wedding biodiversity inventory of a large and complex Lepidoptera fauna with DNA barcoding. Philosophical Transactions of the Royal Society 360: 1835–1845. <https://doi.org/10.1098/rstb.2005.1715>
- Janzen DH, Hallwachs W, Blandin P, Burns JM, Cadiou J, Chacon I, Dapkey T, Deans AR, Epstein ME, Espinoza B, Franclemont JG, Haber WA, Hajibabaei M, Hall JP, Hebert PD, Gauld ID, Harvey DJ, Hausmann A, Kitching IJ, Lafontaine D, Landry JF, Lemaire C, Miller JY, Miller JS, Miller L, Miller SE, Montero J, Munroe E, Green SR, Ratnasingham S, Rawlins JE, Robbins RK, Rodriguez JJ, Rougerie R, Sharkey MJ, Smith MA, Solis MA, Sullivan JB, Thiaucourt P, Wahl DB, Weller SJ, Whitfield JB, Willmott KR, Wood DM, Woodley NE, Wilson JJ (2009) Integration of DNA barcoding into an ongoing inventory of complex tropical diversity. Molecular Ecology Resources 9: 1–26. <https://doi.org/10.1111/j.1755-0998.2009.02628.x>
- Kapli P, Lutteropp S, Zhang J, Kobert K, Pavlidis P, Stamatakis A, Flouri T (2017) Multi-rate Poisson tree processes for single-locus species delimitation under maximum likelihood and Markov chain Monte Carlo. Bioinformatics 33(11): 1630–1638. <https://doi.org/10.1093/bioinformatics/btx025>
- Kassambara A, Mundt F (2020) Factoextra: Extract and visualize the results of multivariate data analyses. R Package Version 1.0.7. <https://CRAN.R-project.org/package=factoextra>
- Katoh K, Misawa K, Kuma K, Miyata T (2002) MAFFT: a novel method for rapid multiple sequence alignment based on fast Fourier transform. Nucleic Acids Research 30(14): 3059–66. <https://doi.org/10.1093/nar/gkf436>
- Katoh K, Standley D (2013) MAFFT multiple sequence alignment software version 7: improvements in performance and usability. Molecular Biology and Evolution 30(4): 772–780. <https://doi.org/10.1093/molbev/mst010>
- Kaufman L, Rousseeuw P (1987) Clustering by means of medoids. Statistical Data Analysis Based on the L1-Norm and Related Methods, 405–416. <https://wis.kuleuven.be/stat/robust/papers/publications-1987/kaufmanrousseeuw-clusteringbymedoids-l1norm-1987.pdf>
- Krogmann L, Austin A, Nauman I (2009) Systematic and biogeography of Australian Rhopalosomatid wasps (Hymenoptera: Rhopalosomatidae) with a global synopsis of the enigmatic

- genus *Olixon* Cameron. Systematic Entomology 34: 222–251. <https://doi.org/10.1111/j.1365-3113.2008.00460.x>
- Lohrmann V (2011) A revision of the *Paniscomima* of the African subregion with the description of two new species from Malawi and Tanzania (Hymenoptera: Rhopalosomatidae). Zoosystematics and Evolution 87: 371–378. <https://doi.org/10.1002/zoos.201100014>
- Lohrmann V, Fox M, Solis M, Krogmann L (2012) Systematic revision of the New World *Olixon* Cameron with descriptions of *O. melinsula* sp. n. and the hitherto unknown female of *O. bicolor* (Hymenoptera: Rhopalosomatidae). Deutsche Entomologische Zeitschrift 59: 259–275.
- Lohrmann V, Falin ZH, Bennet DJ, Engel MS (2014) Recent findings of *Olixon banksii* in the Nearctic with notes on its biology (Hymenoptera: Rhopalosomatidae). Journal of the Kansas Entomological Studies 85: 258–260. <https://doi.org/10.2317/JKES130820.1>
- Lohrmann V, Ohl M (2007) The wasp genus *Olixon* Cameron in Madagascar: first record and description of two new species (Hymenoptera: Rhopalosomatidae). Zootaxa 1465: 39–46. <https://doi.org/10.11646/zootaxa.1465.1.4>
- Lohrmann V, Ohl M, Michalik P, Pitts JP, Jeanneau L, Perrichot V (2019) Notes on rhopalosomatid wasps of Dominican and Mexican amber (Hymenoptera: Rhopalosomatidae) with a description of the first fossil species of *Rhopalosoma* Cresson, 1865. Fossil Record 22: 31–44. <https://doi.org/10.5194/fr-22-31-2019>
- Lohrmann V, Zhang Q, Michalik P, Blaschke J, Müller P, Jeanneau L, Perrichot V (2020) *Cretolixon*—a remarkable new genus of rhopalosomatid wasps (Hymenoptera: Vespoidea: Rhopalosomatidae) from chemically tested, mid-Cretaceous Burmese (Kachin) amber supports the monophyly of Rhopalosomatidae. Fossil Record 23: 215–236. <https://doi.org/10.5194/fr-23-215-2020>
- Mayhew P, Dytham C (2008) The effectiveness and optimal use of Malaise traps for monitoring parasitoid wasps. Insect Conservation and Diversity 1: 22–31. <https://doi.org/10.1111/j.1752-4598.2007.00003.x>
- Miller MA, Pfeiffer W, Schwartz T (2010) “Creating the CIPRES Science Gateway for inference of large phylogenetic trees” in Proceedings of the Gateway Computing Environments Workshop (GCE), 14 Nov. 2010, New Orleans, LA, 1–8. <https://doi.org/10.1109/GCE.2010.5676129>
- Miller LA, Benefield TD, Lounsbury SA, Lohrmann V, Blaschke JD (2019) DNA barcoding of rhopalosomatid larvae reveals a new host record and genetic evidence of a second species of *Rhopalosoma* Cresson (Hymenoptera: Rhopalosomatidae) in America north of Mexico. Journal of Hymenopteran Research 74: 35–46. <https://doi.org/10.3897/jhr.74.38276>
- Padial, JM, Miralles A, De la Riva I, Vences M (2010) The integrative future of taxonomy. Frontiers in Zoology 7(1): 1–14. <https://doi.org/10.1186/1742-9994-7-16>
- Paradis E, Schliep K (2018) Ape 5.0: An environment for modern phylogenetics and evolutionary analyses in R. Bioinformatics 35(3): 526–528. <https://doi.org/10.1093/bioinformatics/bty633>
- Paradis E, Claude J, Strimmer K (2005) APE: Analyses of phylogenetics and evolution in R language. Bioinformatics 20(2): 289–290. <https://doi.org/10.1093/bioinformatics/btg412>
- Perkins RCL (1908) Some remarkable Australian Hymenoptera. Proceedings of the Hawaiian Entomological Society 2: 27–35. <http://biostor.org/reference/58184>
- Puillandre N, Brouillet S, Achaz G (2021) ASAP: assemble species by automatic partitioning. Molecular Ecology Resources 21(2): 609–620. <https://doi.org/10.1111/1755-0998.13281>

- Ramsdell KMM, Taylor SJ (2006) A new state record for *Olixon Banksii* Brues (Hymenoptera: Rhopalosomatidae) in Indiana, USA. *Entomological News* 17(3): 351–352. [https://doi.org/10.3157/0013-872X\(2006\)117\[351:ANSRFO\]2.0.CO;2](https://doi.org/10.3157/0013-872X(2006)117[351:ANSRFO]2.0.CO;2)
- Ratnasingham S, Hebert PDN (2013) A DNA-based registry for all animal species: the Barcode Index Number (BIN) system. *PLoS ONE* 8(7): e66213. <https://doi.org/10.1371/journal.pone.0066213>
- R Core Team (2017) R: A language and environment for statistical computing. R Foundation for Statistical Computing, Vienna, Austria. <https://www.R-project.org/>
- Sáez A, Lozano E (2005) Body doubles. *Nature* 433: 111. <https://doi.org/10.1038/433111a>
- Schubert E, Rousseeuw P (2019) Faster k-Medoids Clustering: Improving the PAM, CLARA, and CLARANS Algorithms. *SISAP 2020* 171–187. https://doi.org/10.1007/978-3-030-32047-8_16
- Smith MA, Woodley NE, Janzen DH, Hebert PDN (2006) DNA barcodes reveal cryptic host-specificity within the presumed polyphagous members of a genus of parasitoid flies (Diptera: Tachinidae). *PNAS* 103(10): 3657–3662. <https://doi.org/10.1073/pnas.0511318103>
- Smith MA, Rodriguez JJ, Whitfield JB, Deans AR, Hanzen DH, Hallwachs W, Hebert PDN (2008) Extreme diversity of tropical parasitoid wasps exposed by interactive integration of natural history, DNA barcoding, morphology, and collections. *PNAS* 105(34): 12359–12364. <https://doi.org/10.1073/pnas.080531910>
- Stamatakis A (2014) RaxML version 8: a tool for phylogenetic analysis and post-analysis of large phylogenies. *Bioinformatics* 30(9): 1312–1313. <https://doi.org/10.1093/bioinformatics/btu033>
- Stoeckle M, Hebert PDN (2008) Barcode of life. *Scientific American* 299(4): 82–88. <https://doi.org/10.1038/scientificamerican1008-82>
- Suzuki R, Shimodaira H (2006) Pvcust: An R Package for assessing the uncertainty in hierarchical clustering. *Bioinformatics* 22(12): 1540–1542. <https://doi.org/10.1093/bioinformatics/btl117>
- Tamura K, Stecher G, Kumar S (2021) MEGA11: molecular evolutionary genetics analysis version 11. *Molecular Biology and Evolution* 38: 3022–3027. <https://doi.org/10.1093/molbev/msab120>
- Townes H (1977) A revision of the Rhopalosomatidae (Hymenoptera). *Contributions of the American Entomological Institute* 58: 173–321. <https://agris.fao.org/agris-search/search.do?recordID=US19810690678>
- Turner RE, Waterston J (1917) Notes on the hymenopterous families Bethyridae and Rhopalosomatidae. *Annals and Magazine of Natural History* 8(20): 101–108. <https://doi.org/10.1080/00222931709486976>
- Valentini A, Pompanon F, Taberlet P (2009) DNA barcoding for ecologists. *Trends in Ecology and Evolution* 24(2): 110–117. <https://doi.org/10.1016/j.tree.2008.09.011>
- Wood DL, Maupin MA (2007) A new state record for *Olixon banksii* (Hymenoptera: Rhopalosomatidae) in Missouri. *The Great Lakes Entomologist* 40(1–2): 101–102. <https://doi.org/10.22543/0090-0222.2181>
- Zhang J, Kapli P, Pavlidis P, Stamatakis A (2013) A general species delimitation method with applications to phylogenetic placements. *Bioinformatics* 29 (22): 2869–2876. <https://doi.org/10.1093/bioinformatics/btt499>

Review of the ant genus *Manica* (Hymenoptera, Formicidae), with a new record of the genus in China and description of a new species

Yuqing He^{1,2}, Zhilin Chen^{1,2}, Congcong Du^{1,2}

1 Key Laboratory of Ecology of Rare and Endangered Species and Environmental Protection (Guangxi Normal University), Ministry of Education, Guilin 541006, China **2** Guangxi Key Laboratory of Rare and Endangered Animal Ecology, Guangxi Normal University, Guilin 541006, China

Corresponding author: Congcong Du (cleverduwang@gmail.com)

Academic editor: Francisco Hita Garcia | Received 24 August 2023 | Accepted 22 April 2024 | Published 8 May 2024

<https://zoobank.org/D1B9A375-7F1A-4737-B165-8D19C60EC4BD>

Citation: He Y, Chen Z, Du C (2024) Review of the ant genus *Manica* (Hymenoptera, Formicidae), with a new record of the genus in China and description of a new species. Journal of Hymenoptera Research 97: 379–398. <https://doi.org/10.3897/jhr.97.111418>

Abstract

Seven known extant species of *Manica* have been identified worldwide: *M. bradleyi* (Wheeler, 1909), *M. hunteri* (Wheeler, 1914), *M. invidia* Bolton, 1995, *M. parasitica* (Creighton, 1934), *M. rubida* (Latreille, 1802), *M. shanyii* **sp. nov.**, and *M. yessensis* Azuma, 1955. The discovery of the new species is documented from Sichuan Province, China, marking the first recorded instance of the genus *Manica* in China. Additionally, an identification key for distinguishing the known species within the genus *Manica* is provided.

Keywords

Distribution map, *Manica shanyii* sp. nov., Myrmicinae, Myrmicini, taxonomy

Introduction

The genus *Manica*, first described by Jurine in 1807, traces its origins to at least the Eocene epoch (Zharkov et al. 2023). Presently, *Manica* stands out as a rare genus in ants, classified within the tribe Myrmicini of the subfamily Myrmicinae. However, the morphological definition of the tribe Myrmicini has been challenging due to a lack of distinctive characteristics (Jansen and Savolainen 2010). Initially, Myrmicini was defined based on several morphological features, many of which were not exclusive to

Myrmicini, encompassing seven genera (Bolton 2003). Recent molecular studies have suggested that the tribe may not be monophyletic (Brady et al. 2006; Moreau et al. 2006), although there were discrepancies regarding the genera included in the tribe. It was only later, with the work conducted by Ward et al. (2015), that the membership of Myrmicini was restricted to two genera, *Manica* and *Myrmica*, establishing its position as sister to all other members of the subfamily.

Currently, only six extant species and two fossil species of *Manica* are recognized in the Holarctic region. Among these, *M. rubida* (Latreille, 1802) is distributed in Europe (Borowiec 2014); while four species, namely, *M. bradleyi* (Wheeler, 1909), *M. hunteri* (Wheeler, 1914), *M. invidia* Bolton, 1995 and *M. parasitica* (Creighton, 1934), are found in western North America. *Manica yessensis* Azuma, 1955 is endemic to Japan, representing the sole recorded species of *Manica* in Asia so far. Despite extensive surveys in the region, no additional species of this genus have been discovered in the past 70 years. However, given the extant distribution of this genus in Japan and southern Europe, with China's vast expanse offering numerous habitats suitable for *Manica*, it is plausible that cryptic, undiscovered species of *Manica* may exist in China.

In this study, while examining ants from the Emei and Gongga Mountains in Sichuan Province, China, we identified a new species of the genus *Manica*, marking the first documented occurrence of the genus and a new species in China. Here, we describe this new species and recognize the six known extant species, providing an identification key to *Manica* species based on the worker caste.

Materials and methods

The specimens of *Manica shanyii* sp. nov. were collected alive during field expeditions to Emei and Gongga Mountains in Sichuan, China (Fig. 1) by hand. Subsequently, they were preserved in a vial containing absolute ethyl alcohol. The specimens were then pin-mounted and examined using a Leica M205A stereomicroscope. High-quality multifocused montage images were generated with a KEYENCE (VHX-6000) digital imaging system.

The images of the *Manica* species, accessible on AntWeb (<https://www.antweb.org>), were meticulously examined and compared. The general terminology for *Manica* workers adheres to Bolton (1975). All measurements are given in millimeters. The abbreviations employed for the measurements and indices are as follows:

- CI** Cephalic Index = $HW \times 100 / HL$.
- DPI** Dorsal Petiole Index = $DPW \times 100 / PL$.
- DPW** Dorsal Petiole Width, maximum width of petiole in dorsal view.
- ED** Eye Diameter, maximum diameter of eye.
- HL** Head Length, straight-line length of head in full-face view, measured from midpoint of anterior clypeal margin to midpoint of posterior

margin, or terminal horizontal line in some species with a concave posterior margin.

- HW** Head Width, maximum width of head in full-face view, excluding eyes.
LPI Lateral Petiole Index = $PH \times 100 / PL$.
MSL Mesosoma Length, diagonal length of mesosoma in lateral view, measured from point at which pronotum meets cervical shield to posterior basal angle of metapleuron.
PH Petiole Height, height of petiole measured in lateral view from apex of ventral (subpetiolar) process vertically to a line intersecting dorsal most point of node.
PL Petiole Length, length of petiole measured in lateral view from anterior process to posterior most point of tergite, where it surrounds gastral articulation.
PW Pronotal Width, maximum width of pronotum measured in dorsal view.
SI Scape Index = $SL \times 100 / HW$.
SL Scape Length, straight-line length of antennal scape, excluding basal constriction or neck.
TL Total Length, total outstretched length of individual, from mandibular (occlusion) apex to gastral apex (not including the sting).

The holotype and paratypes specimens have been or will be deposited in the following institutions:

- GXNU** Insect Collection, Guangxi Normal University, Guilin, Guangxi, China.
IZCAS Institute of Zoology, Chinese Academy of Sciences, Beijing, China.



Figure 1. Global map showing the type localities of †*M. andrannae*, *M. bradleyi*, *M. hunteri*, *M. invidia*, †*M. iviei*, *M. parasitica*, *M. rubida*, *M. shanyii* sp. nov. and *M. yessensis* (Source: Esri, Maxar, GeoEye, Earthstar geographics, CNES/Airbus DS, USDA, USGS, AeroGRID, IGN, and the GIS User Community).

Results

Synopsis of *Manica* species

†*M. andrannae* Zharkov & Dubovikoff, 2023 [Baltic Amber]

M. bradleyi (Wheeler, 1909) [United States]

M. hunteri (Wheeler, 1914) [Canada, United States]

M. invidia Bolton, 1995 [Canada, United States]

M. parasitica (Creighton, 1934) [United States]

M. rubida (Latreille, 1802) [Andorra, Armenia, Austria, Belgium, Bulgaria, Croatia, Czech Republic, France (type locality), Georgia, Germany, Greece, Hungary, Italy, Montenegro, Poland, North Macedonia, Romania, Slovakia, Slovenia, Switzerland, Turkey]

†*M. iviei* LaPolla, 2023 [United States]

M. shanyii sp. nov. [China]

M. yessensis Azuma, 1955 [Japan]

Key to *Manica* based on worker castes

- 1 Posterior portion of the head and dorsum of mesosoma smooth and shining, (Fig. 5) [United States]..... ***M. parasitica* (Creighton, 1934)**
- Posterior portion of the head and dorsum of mesosoma more or less striate or punctate (Figs 2, 4) **2**
- 2 Body uniformly colored, ranging from brownish yellow, reddish brown to blackish (Figs 3, 4, 7) **3**
- Body bicolored, head and gaster black with mesosoma, petiole and postpetiole reddish brown (Figs 2, 8), or gaster blackish brown with head, mesosoma, petiole and postpetiole yellowish brown (Fig. 6)..... **5**
- 3 Dorsum of pronotum and mesonotum abundantly transversely striate (Fig. 7B) [China] ***M. shanyii* sp. nov.**
- Dorsum of pronotum and mesonotum longitudinally rugose (Figs 3C, 6C, 8C) **4**
- 4 In lateral view, lateral face of mesosoma, petiole, and postpetiole mainly punctate, appearing dull and not shining (Fig. 4D); in lateral view, postpetiole as long as high (Fig. 4D) [Canada, United States]..... ***M. invidia* Bolton, 1995**
- In lateral view, lateral face of mesosoma longitudinally striate and without punctae, petiole and postpetiole smooth and shining (Fig. 3D); in lateral view, postpetiole compressed anteroposteriorly, distinctly higher than long (Fig. 3D) [Canada, United States]..... ***M. hunteri* (Wheeler, 1914)**
- 5 Head reddish brown (Fig. 6A); dorsum of pronotum only with indistinctly, finely longitudinal striation, extremely shining (Fig. 6C); in lateral view, the

- posterior face of postpetiole straight and steep (Fig. 6D) [Western Europe] .
 *M. rubida* (Latreille, 1802)
- Head black (Figs 2A, 8A); dorsum of pronotum with prominent rugae and not shining (Figs 2C, 8C); in lateral view, the posterior face of postpetiole unobscured (Fig. 2D) or sloping forward (Fig. 8D)..... **6**
- 6 In lateral view, anteroventral corner of postpetiole distinctly conically protuberant (Fig. 2D); dorsal face of postpetiole evenly and slightly convex (Fig. 2D); petiole and postpetiole smooth and shining (Fig. 2C, D) [United States] *M. bradleyi* (Wheeler, 1909)
- In lateral view, anteroventral corner of postpetiole distinctly angular (Fig. 8D); dorsal face of postpetiole strongly convex (Fig. 8D); petiole and lateral face of postpetiole rugose-punctate (Fig. 8C, D) [Japan] *M. yessensis* Azuma, 1955

Taxonomic accounts of *Manica*

Manica bradleyi (Wheeler, 1909)

Fig. 2

Myrmica bradleyi Wheeler, 1909: 77 (w.) U.S.A. (California). Combination in *Myrmica* (*Oreomyrma*) by Wheeler 1914: 120; in *Myrmica* (*Neomyrma*) by Emery 1915: 69 (footnote); Forel 1915: 364; in *Myrmica* (*Manica*) by Emery 1921: 43; in *Manica* by Weber 1947: 440.

Aphaenogaster (*Neomyrma*) *calderoni* Forel, 1914: 275 (w.) U.S.A. (Nevada). Synonymized by Wheeler 1915: 50.

Type material. Unexamined, but high-resolution images of syntype worker (CASENT0907664, imaged by Alexandra Westrich) were reviewed.

Diagnosis. Head and gaster blackish brown to black, while mesosoma yellow. In lateral view, postpetiole as broad as its long, with an evenly convex anterior margin and a unobscured posterior margin; ventral surface flat, lacking any pointed protuberance. Petiole and postpetiole smooth and shining.

Recognition. *M. bradleyi* (Wheeler, 1909) and *M. yessensis* Azuma, 1955, are easily distinguishable from all other species of *Manica* due to their distinctive characteristics. They both feature a black or dark brown head and gaster, contrasted with a light brown to reddish yellow mesosoma. Furthermore, *M. bradleyi* can be easily identified from *M. yessensis* by its postpetiole, which is as long as its high in lateral view, with a distinctly conically protuberant anteroventral corner; the dorsal face of the postpetiole is evenly and slightly convex, while both the petiole and postpetiole exhibit a smooth and shining appearance (Fig. 2C, D).

Distribution. In the Sierra Nevada Mountains of California, western Nevada, and the Transverse Ranges in southern California, with a single record from the Cascade Range of Oregon.

***Manica hunteri* (Wheeler, 1914)**

Fig. 3

Myrmica (*Oreomyrma*) *hunteri* Wheeler, 1914: 121, fig. 1c (w.) U.S.A. (Montana).

Combination in *Myrmica* (*Neomyrma*) by Wheeler 1917: 507; in *Myrmica* (*Manica*) by Emery 1921: 43; in *Manica* by Weber 1947: 440.

Myrmica (*Oreomyrma*) *aldrichi* Wheeler, 1914: 120, fig. 1b (w.) U.S.A. (Idaho).
Synonymized by Cole 1956: 262.

Type material. Unexamined, but high-resolution images of worker specimen were reviewed from AntWeb (CASENT0922741, imaged by Wade Lee, label's photo by Michele Esposito).

Diagnosis. Body uniformly brownish yellow. In lateral view, dorsum feebly convex, with posterolateral corner of propodeum obtusely angular. Additionally, in lateral view, postpetiole compressed anteroposteriorly, distinctly higher than long. The lateral face of mesosoma longitudinal striae without puncta, while petiole and postpetiole smooth and not shining.

Recognition. *M. hunteri* (Wheeler, 1914) and *M. invidia* Bolton, 1995 can be easily distinguished from the congeners of this genus by their uniformly brownish yellow, or reddish brown to blackish. While *M. hunteri* may initially resemble an immature *M. invidia*, closer examination reveals distinct characteristics that differentiate them. In lateral view, the postpetiole of *M. hunteri* compressed anteroposteriorly, distinctly higher than long. Additionally, the lateral face of mesosoma exhibits longitudinal striae without puncta, and both petiole and postpetiole are smooth and shining (Fig. 3D).

Distribution. From northern Utah and northern Nevada to central California, extending northwards into southern Canada. The northernmost is Edmonton, Alberta, while the easternmost range extends to Sundance, Wyoming.

***Manica invidia* Bolton, 1995**

Fig. 4

Myrmica mutica Emery, 1895: 311 (w.) U.S.A. (Colorado). Combination in *Myrmica* (*Oreomyrma*) by Wheeler 1914: 119; in *Myrmica* (*Neomyrma*) by Emery 1915: 69 (footnote); Forel 1915: 364; in *Myrmica* (*Manica*) by Emery 1921: 43; in *Manica* by Wheeler, G.C. & Wheeler, E.W. 1944: 244.

Manica invidia Bolton, 1995: 249. Replacement name for *Myrmica mutica* Emery, 1895: 311 (junior primary homonym of *Myrmica mutica* Nylander, 1849: 39).

Type material. Unexamined, but high-resolution images of syntype worker (CASENT0904061, imaged by Alexandra Westrich) were reviewed.

Diagnosis. Body dully yellow or nearly orange. In lateral view, posterolateral corner of propodeum broadly rounded. Furthermore, in lateral view, postpetiole as long as

high. The lateral face of mesosoma, petiole, and postpetiole mainly punctate, appeared dull and not shining.

Recognition. *M. invidia* Bolton, 1995 bears resemblance to *M. hunteri* (Wheeler, 1914), yet it can be distinguished by the following characteristics: in lateral view, the

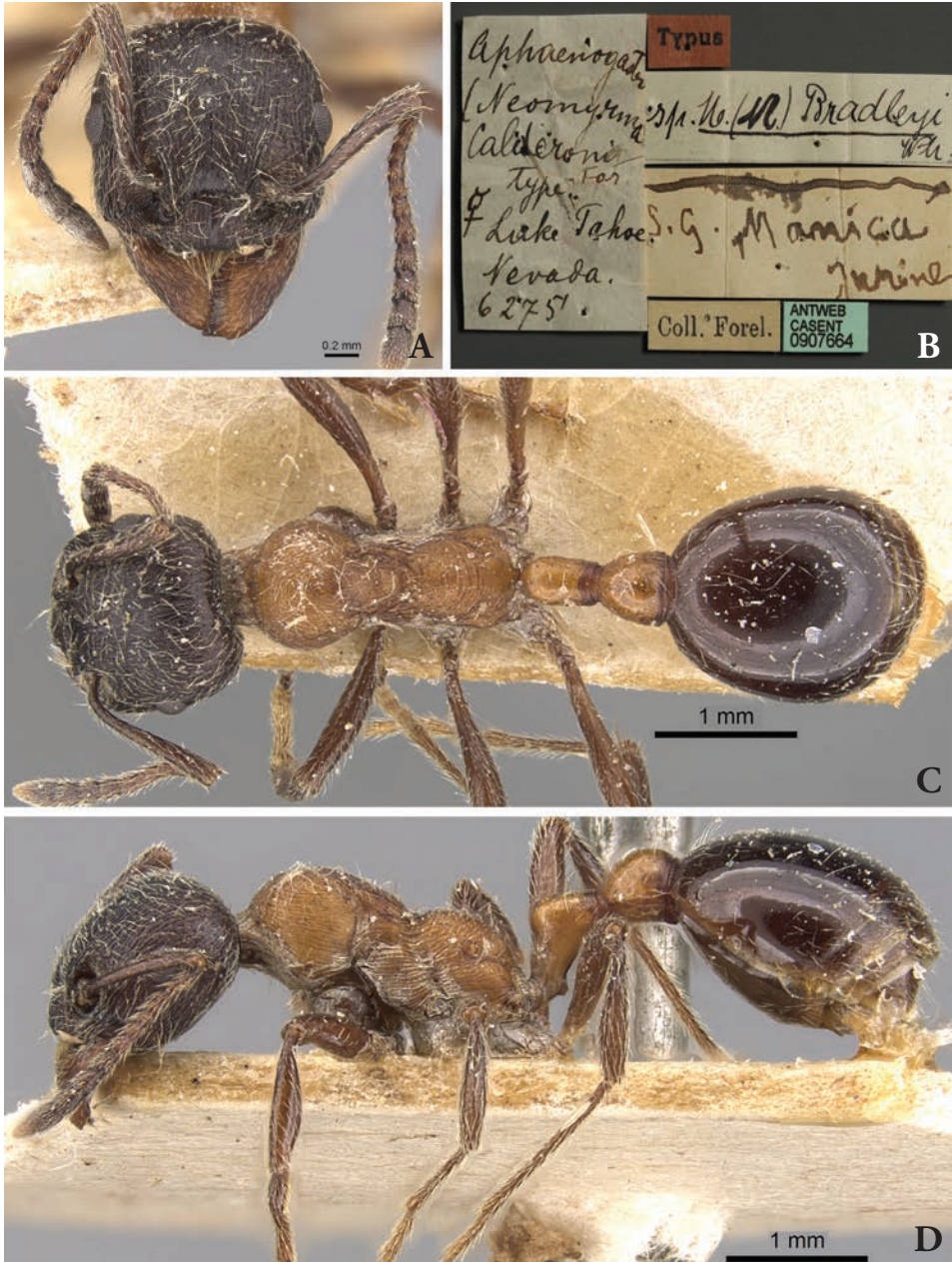


Figure 2. *Manica bradleyi* worker (Syntype, images cited from <https://www.antweb.org/>, CASENT0907664, imaged by Alexandra Westrich) **A** head in full-face view **B** label **C** body in dorsal view **D** body in lateral view.



Figure 3. *Manica hunteri* worker (Non-type, images cited from <https://www.antweb.org/>, CASENT0922741, specimen's photos by Wade Lee, label's photo by Michele Esposito) **A** head in full-face view **B** label **C** body in dorsal view **D** body in lateral view.



Figure 4. *Manica invidia* worker (Syntype, images cited from <https://www.antweb.org/>, CASENT0904061, imaged by Alexandra Westrich) **A** head in full-face view **B** label **C** body in dorsal view **D** body in lateral view.

mesosoma, petiole, and postpetiole are predominantly punctate, resulting in a dull and non-shining appearance (Fig. 4D); the posterolateral corner of propodeum in lateral view broadly rounded; and the postpetiole is as long as its high.

Distribution. From the eastern slopes of the Sierra Nevada and the Cascade Range in California, eastward to northeastern New Mexico, Colorado, Wyoming, the Black Hills of South Dakota and southwestern North Dakota, northwestward into British Columbia and Alberta, with one record from Alaska.

Manica parasitica (Creighton, 1934)

Fig. 5

Myrmica (*Manica*) *parasitica* Creighton, 1934: 185 (w.) U.S.A. (California). Combination in *Manica* by Weber, 1947: 440.

Type material. Unexamined, but high-resolution images of syntype worker (CASENT0005974, imaged by April Nobile) were reviewed.

Diagnosis. Body almost uniformly light blackish brown. Head smooth and shining, except for the frontal area and cheek with longitudinal stripes. Similarly, mesosoma and metasoma smooth and shining, except for katapisternum and the lower part of lateral face of propodeum with finely punctate-striate patterns.

Recognition. *M. parasitica* (Creighton, 1934) can be easily distinguished from the congeners of this genus by the characteristics mentioned in the “Diagnosis” of this species.

Distribution. This species is only known from a few records in the Sierra Nevada Mountains in California.

Manica rubida (Latreille, 1802)

Fig. 6

Formica rubida Latreille, 1802: 267, pl. 10, fig. 65 (q.) FRANCE. Combination in *Manica* by Jurine, 1807: 279; in *Myrmica* by Schenck, 1852: 132; in *Myrmica* (*Oreomyrma*) by Wheeler 1914: 118; in *Myrmica* (*Neomyrma*) by Emery, 1915: 69 (footnote), Forel, 1915: 364; in *Neomyrma* by Bondroit, 1918: 97; in *Myrmica* (*Manica*) by Emery, 1921: 43; in *Manica* by Weber, 1947: 440.

Myrmica leonina Losana, 1834: 332, pl. 36, fig. 7 (w.) ITALY. Synonymized by Roger, 1859: 252.

Myrmica montana Labram & Imhoff, 1838, pl. 36, figs 1–3 (w.q.m.) SWITZERLAND. Synonymized by Roger, 1859: 252.

Type material. Unexamined, non-type worker, but high-resolution images of worker specimen were reviewed from AntWeb (CASENT0173135, specimen’s photos by April Nobile, label’s photo by Michele Esposito).



Figure 5. *Manica parasitica* worker (Syntype, imaged cited from <https://www.antweb.org/>, CASENT0005974, imaged by April Nobile) **A** head in full-face view **B** label **C** body in dorsal view **D** body in lateral view.

Diagnosis. Body reddish brown with gaster blackish brown. In lateral view, with posterolateral corner of propodeum obtusely angular. Petiole node in lateral view with an almost vertical posterior face. Postpetiolar node in lateral view with a vertical posterior face; postpetiolar sternite anteroventrally produced as an acute angle directed forward.



Figure 6. *Manica rubida* worker (Non-type, imaged cited from <https://www.antweb.org/>, CASENT0173135, specimen's photos by April Nobile, label's photo by Michele Esposit) **A** head in full-face view **B** label **C** body in dorsal view **D** body in lateral view.

Recognition. *M. rubida* (Latreille, 1802) can be easily distinguished from the congeners of this genus by the following characteristics: the body is reddish-brown with a gaster that is distinctly darker than the reddish-brown head. Additionally, in lateral view, the petiolar node is erect, exhibiting distinct anterior and posterior margins along

with a well-defined dorsal margin. Similarly, the postpetiolar node, when viewed laterally, displays a vertical posterior face.

Distribution. This species is found in the mountainous regions of Central and Southern Europe (excluding the Iberian Peninsula), Ukraine (including Crimea), Turkey, and the Caucasus.

***Manica shanyii* sp. nov.**

<https://zoobank.org/F7ECF81C-86B9-4F92-8BA2-CE8186F6FFBC>

Fig. 7

Type material. *Holotype* worker, CHINA, Sichuan, Leshan City, Lei Dongping of Emei Mountain, 29.5252°N, 102.3320°E, 2900 m, 2. Aug. 2011, leg. Ruigang Yang, No. GXNU110273; 3 paratype workers, CHINA, Sichuan, Garze Tibetan Autonomous Prefecture, Moxi Town, Hailuoguo in the Gongga Mountain National Nature Reserve, 29.5845°N, 102.0289°E, 2740 m, 28. May. 2022, leg. Yanping Wu, No. GXNU220539. [Holotype worker and two paratype worker are deposited in the Insect Collection of Guangxi Normal University, Guilin, Guangxi, China (GXNU), one paratype worker are deposited in Institute of Zoology, Chinese Academy of Sciences, Beijing, China (IZCAS)].

Diagnosis. Body brownish black. In full-face view, head longer than broad, with broadly rounded posterior corners; the anterior margin of clypeus narrowly rounded, without prominent botches medially; the antennal scapes slightly surpass the posterior corners of the head. In lateral view, the dorsum of propodeum roughly straight, with obtusely angular posterolateral corners. Petiole in lateral view slightly longer than high, with a slightly concave anterior margin and a dorsal outline more or less narrowly rounded; the subpetiolar process in lateral view acutely toothed anteroventrally. Similarly, the postpetiole in lateral view as broad as long, with a convex anterior margin and steep posterior margin; the sternite slightly convex, with rounded anteroinferior corners.

Holotype worker. TL 6.32, HL 1.64, HW 1.45, CI 87.96, SL 1.31, SI 90.46, ED 0.34, PW 0.99, MSL 2.241, PL 0.61, PH 0.46, DPW 0.39, LPI 75.21, DPI 64.20.

Description. *Head.* In full-face view, the head longer than broad, with slightly convex lateral margins and broadly rounded posterior corners, while the posterior margin nearly straight (Fig. 7A). Mandibles slightly convex and armed with one large apical tooth, one secondary tooth, and followed by five smaller teeth. The anterior margin of clypeus relatively narrowly rounded, with a prominent upward edge in the middle. Frontal carinae curved outwards to merge with the rugae surrounding the antennal sockets, but they not reaching to middle of head (Fig. 7A). Frons wide, frontal lobes not extended. Antennae 12-segmented, featuring with a distinct 5-segmented club; scape relatively long, slightly surpassing the posterior corners of the head, and gradually curved at the base, without any trace of lobe or carina (Fig. 7A). Ocelli absent. Eyes relatively large, located slightly before the mid-point of the lateral sides of the head (Fig. 7A). *Mesosoma.* In lateral view, promesonotum evenly convex; metanotal groove strongly depressed; propodeum roughly straight, passing through a distinct, but obtuse

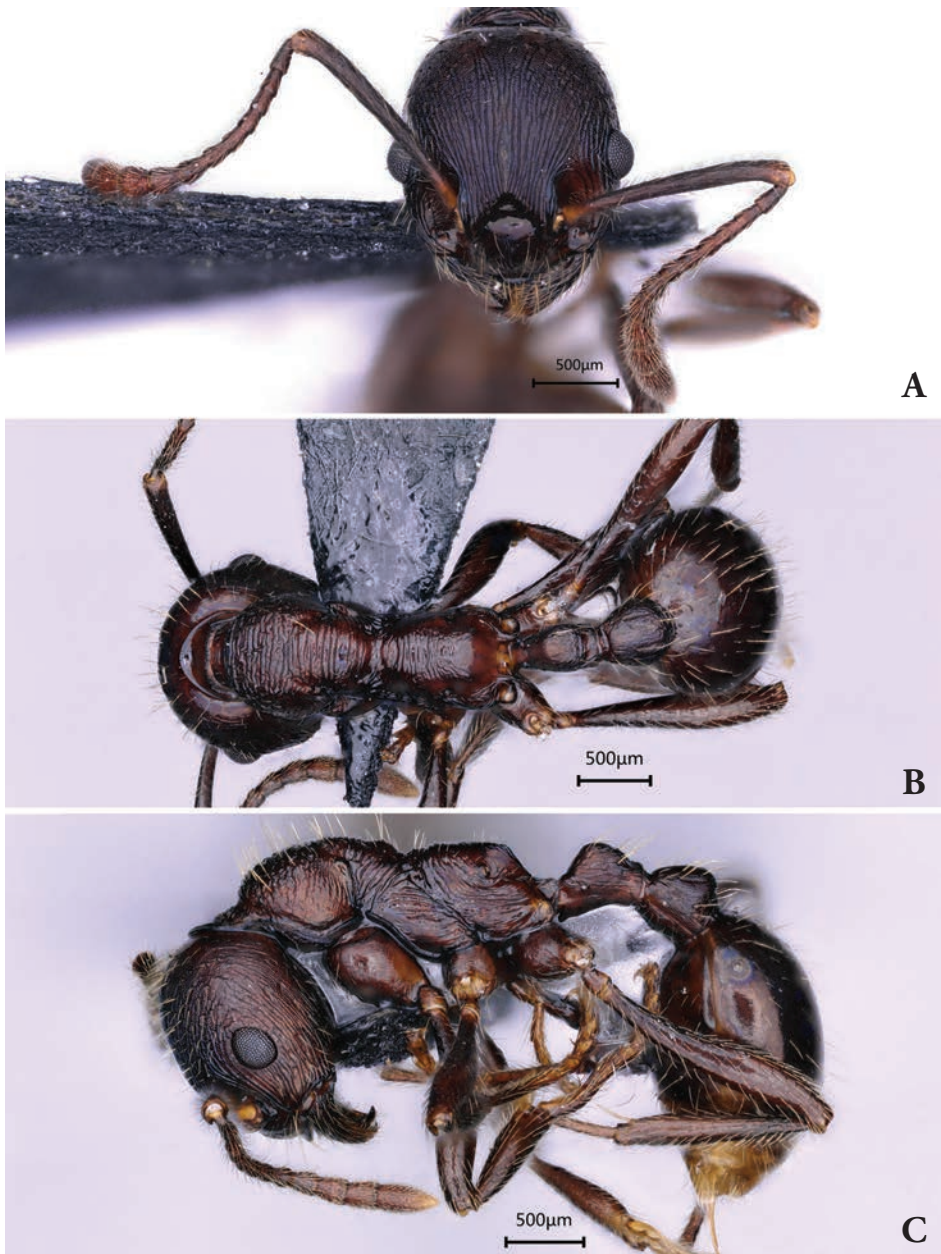


Figure 7. *Manica shanyii* sp. nov. worker (Holotype, imaged by Yuqing He) **A** head in full-face view **B** body in dorsal view **C** body in lateral view.

angle or obtuse roundness into the somewhat straight and sloping declivity (Fig. 7C). In dorsal view, rather robust, with a faint but visible promesonotal suture; lateral margins slightly convex, anterior margin convex, and posterior margin slightly concave (Fig. 7B). **Metasoma.** Petiole in lateral view with a very short peduncle, slightly longer than high, with a slightly concave anterior margin and a dorsum of node that more

or less narrowly rounded, while posterior margin slightly convex (Fig. 7C); in dorsal view subcampanulate, longer than broad, with a relatively narrow anterior margin and slightly convex lateral margins. Subpetiolar process in lateral view acute toothed anteroventrally (Fig. 7C). Postpetiole in lateral view as long as high, anterior margin rising in a gentle slope towards the posterior margin and then abruptly descending (Fig. 7C); in dorsal view clearly larger than petiole, roughly pyriform, with a relatively narrow anterior margin and slightly convex lateral margins (Fig. 7B); postpetiolar sternite in lateral view slightly convex, with rounded anteroinferior corners (Fig. 7B). Gaster in lateral view elliptical (Fig. 7C). **Sculpture.** Mandibles longitudinally striate (Fig. 7A). Clypeus smooth and shining, antennal scape finely punctate. The posterior portion of the head longitudinally striate, with densely punctate spaces between them (Fig. 7A). Promesonotal rugae extend laterally, the lower part of mesopleuron and metapleuron longitudinally striate (Fig. 7C). Pronotum with finely transverse rugae, mesonotum densely transversely striate, and anterodorsal propodeum sparsely transversely striate, with shining declivity (Fig. 7B). Dorsum of petiole sparsely rugose and punctate (Fig. 7C). Gaster smooth and shining. **Pilosity.** Body entirely covered erect to suberect and yellowish hairs. Antennal scape with subdecumbent hairs. **Coloration.** Body reddish brown to blackish brown (Fig. 7).

Paratype workers. TL 5.99–6.34, HL 1.64–1.74, HW 1.37–1.48, CI 83.08–87.96, SL 1.31–1.46, SI 90.46–103.80, ED 0.32–0.35, PW 0.92–0.99, MSL 2.15–2.43, PL 0.61–0.71, PH 0.45–0.46, DPW 0.39–0.40, LPI 64.32–75.21, DPI 55.29–64.31 (n = 3).

Recognition. *Manica shanyii* sp. nov. can be easily distinguished from its congeners by the following characteristics: the entire dorsum of mesosoma exhibits transverse striation and punctae, and masticatory margin of mandibles only with seven teeth, comprising one large apical tooth, one secondary tooth, and followed by five smaller teeth.

Distribution. Emei and Gongga Mountains in Sichuan, China.

Habitat. The nest of *Manica shanyii* sp. nov. was discovered in the Gongga Mountain National Nature Reserve and Emei Mountain National Nature Reserve, Sichuan, China. The sampled sites are positioned within a mixed coniferous broad-leaved forest, where the ants were found inhabiting dead wood on the forest floor covered with brown forest soil.

Etymology. This species is named after Professor Zhou Shanyi from Guangxi Normal University, China, in recognition of his significant contributions to the field of ant taxonomy in China.

Manica yessensis Azuma, 1955

Fig. 8

Manica yessensis Azuma, 1955: 80 (footnote) (w.) JAPAN.

Type material. Unexamined, but high-resolution images of paratype worker (CASENT0900372, imaged by Ryan Perry) were reviewed.



Figure 8. *Manica yessensis* worker (Paratype, images cited from <https://www.antweb.org/>, CASENT0900372, imaged by Ryan Perry) **A** head in full-face view **B** label **C** body in dorsal view **D** body in lateral view.

Diagnosis. Head and gaster black, while other parts reddish brown. In lateral view, posterodorsal corner of propodeum obtusely angular. Petiole in lateral view longer than high, with a distinct dorsum, anterior margin of node concave and posterior slopes convex; subpetiolar process in lateral view acutely angled anteroventrally. Postpetiole

in lateral view higher than long; sternite of postpetiole anteroventrally produced as a blunt angle directed forward. Petiole and lateral face of postpetiole rugose-punctate.

Recognition. *M. yessensis* Azuma, 1955 is closely related to *M. bradleyi* (Wheeler, 1909), but it can be separated from the latter by the following characteristics: the posterodorsal corner of propodeum in lateral view is obtusely angular; the postpetiole in lateral view is higher than long; the sternite of postpetiole is anteroventrally produced as a blunt angle directed forward; and both the petiole and the lateral face of postpetiole exhibit rugose-punctate patterns.

Distribution. This species is found exclusively in the northern and central regions of Japan.

Discussion

Zharkov et al. (2023) described a Baltic amber – *Manica andrannae*, which from the Kaliningrad region of Russia (formerly part of the Palearctic Region). This newly described taxon is the first fossil species of the genus *Manica*, serving as an important link in understanding the origin and evolution of this genus. Among the known nine species of the genus *Manica*, four extant species (*M. bradleyi*, *M. hunteri*, *M. invidia*, *M. parasitica*) and one extinct species (†*M. iviei*) are predominantly distributed in the western part of the Nearctic Region, two species (†*M. andrannae*, *M. rubida*) are concentrated in the western part of the Palearctic Region, one species (*M. yessensis*) is found in Japan in the eastern part of the Palearctic Region, and the newly discovered species (*M. shanyii*) is distributed in the southernmost part of the Palearctic Region. Based on the current distribution, North America evidently serves as the center of species diversity for the genus *Manica* (Fig. 1). Zharkov et al. (2023) hypothesized that the genus *Manica* may have originated in the Nearctic Region and later dispersed to the Palearctic Region. However, based on the “Diversification rate hypothesis” (Wiens and Dykhuizen 2011), regions with high species diversity do not necessarily indicate older taxa in that area. Therefore, inferring the Nearctic Region as the center of origin for the genus *Manica* solely based on species distribution, although plausible, remains contentious. However, the discovery sites and formation times of fossils can provide valuable insights into the origin of species. Despite fossil distribution in both the Nearctic Region and the Palearctic Region, fossil species of †*M. andrannae* in the Palearctic Region was formed during the Middle to Late Eocene, while the †*M. iviei* in the Nearctic Region was formed during the Oligocene. Consequently, the fossil species in the Palearctic Region are older, hinting that the earliest *Manica* might have been distributed in the Palearctic Region, particularly in Europe, during the Eocene. Based on this, we hypothesize that *Manica* possibly originated in the mid-Eocene, with its center of origin in Europe within the Palearctic Region, before dispersing to the Nearctic Region over long distances. As for species in East Asia, they might have originated from species in the Nearctic Region through the Bering Land Bridge or from European species dispersing to East Asia over long distances. Discovering new species or records of this genus in Central Asia

in the future could somewhat support the latter hypothesis. Of course, for a systematic elucidation of the origin and dispersal of *Manica*, future biogeographical studies based on phylogenetic relationships could be conducted.

Acknowledgments

We are grateful to the California Academy of Sciences (San Francisco) for permitting us to use images of *Manica* Jurine, 1807 on the AntWeb. This study was supported by the National Natural Science Foundation of China (No. 32100345), Natural Science Foundation of Guangxi (2021AC19142), National Animal Collection Resource Center of China, Key Laboratory of Ecology of Rare and Endangered Species and Environmental Protection (Guangxi Normal University), Ministry of Education and Guangxi Key Laboratory of Rare and Endangered Animal Ecology (Guangxi Normal University).

References

- AntWeb (2023) Version 8.75.3. California Academy of Science. [online at] <https://www.antweb.org> [Accessed 17 Mar. 2023]
- Azuma M (1955) A list of ants (Formicidae) from Hokkaido Is. [In Japanese.]. Hyogo Biology 3: 79–80.
- Bolton B (1975) A revision of the ant genus *Leptogenys* Roger (Hymenoptera: Formicidae) in the Ethiopian region with a review of the Malagasy species. Bulletin of the British Museum (Natural History). Entomology 31: 235–305. <https://doi.org/10.5962/bhl.part.29487>
- Bolton B (1995) A new general catalogue of the ants of the world. Mass.: Harvard University Press, Cambridge, 504 pp.
- Bolton B (2003) Synopsis and classification of Formicidae. Memoirs of the American Entomological Institute 71: 1–370.
- Bondroit J (1918) Les fourmis de France et de Belgique. Annales de la Société Entomologique de France 87: 1–174.
- Borowiec L (2014) Catalogue of ants of Europe, the Mediterranean Basin and adjacent regions (Hymenoptera: Formicidae). Genus (Wroclaw) 25(1–2): 1–340.
- Brady SG, Schultz TR, Fisher BL, Ward PS (2006) Evaluating alternative hypotheses for the early evolution and diversification of ants. Proceedings of the National Academy of Sciences of the United States of America 103: 18172–18177. <https://doi.org/10.1073/pnas.0605858103>
- Cole Jr AC (1956) New synonymy in the genus *Manica* Jurine (Hymenoptera: Formicidae). Journal of the Tennessee Academy of Science 31: 260–262.
- Creighton WS (1934) Descriptions of three new North American ants with certain ecological observations on previously described forms. Psyche (Cambridge) 41: 185–200. <https://doi.org/10.1155/1934/26532>

- Emery C (1895) Beiträge zur Kenntniss der nordamerikanischen Ameisenfauna. (Schluss). Zoologische Jahrbücher. Abteilung für Systematik, Geographie und Biologie der Tiere 8: 257–360.
- Emery C (1915) Definizione del genere *Aphaenogaster* e partizione di esso in sottogeneri. *Paraphidole* e *Novomessor* nn. gg. Rendiconti delle Sessioni della Reale Accademia delle Scienze dell'Istituto di Bologna. Classe di Scienze Fisiche (n.s.) 19: 67–75.
- Emery C (1921) Hymenoptera. Fam. Formicidae. Subfam. Myrmicinae. [part]. Genera Insectorum 174A: 1–94 [+ 7 plates].
- Forel A (1914) Le genre *Camponotus* Mayr et les genres voisins. Revue Suisse de Zoologie 22: 257–276. <https://doi.org/10.5962/bhl.part.36672>
- Forel A (1915) Formicides d'Afrique et d'Amérique nouveaux ou peu connus. IIe partie. Bulletin de la Société Vaudoise des Sciences Naturelles 50: 335–364.
- Jansen G, Savolainen R (2010) Molecular phylogeny of the ant tribe Myrmicini (Hymenoptera: Formicidae). Zoological Journal of the Linnean Society 160: 482–495. <https://doi.org/10.1111/j.1096-3642.2009.00604.x>
- Jurine L (1807) Nouvelle méthode de classer les Hyménoptères et les Diptères. Hyménoptères. Vol. 1. Genève: Paschoud, 319 pp. <https://doi.org/10.5962/bhl.title.60886>
- Labram JD, Imhoff L (1838) Insekten der Schweiz. 2. Basel: published by the authors (in commission of C. J. Spittler), 84 pls., 84 pp.
- LaPolla JS (2023) Fossil ants (Hymenoptera: Formicidae) of the early Oligocene Canyon Ferry Reservoir deposit. Palaeoentomology 6(4): 385–397. <https://doi.org/10.11646/palaeoentomology.6.4.10>
- Latreille PA (1802) Histoire naturelle des fourmis, et recueil de mémoires et d'observations sur les abeilles, les araignées, les faucheurs, et autres insectes. Paris: Impr. Crapelet (chez T. Barrois), [xvi +] 445 pp. <https://doi.org/10.5962/bhl.title.11138>
- Losana M (1834) Saggio sopra le formiche indigene del Piemonte. Memorie della Reale Accademia delle Scienze di Torino 37: 307–333.
- Moreau CS, Bell CD, Vila R, Archibald SB, Pierce NE (2006) Phylogeny of the ants: diversification in the age of angiosperms. Science (Washington, D. C.) 312: 101–104. <https://doi.org/10.1126/science.1124891>
- Nylander W (1849) Additamentum alterum adnotationum in monographiam formicarum borealium. Acta Societatis Scientiarum Fennicae 3: 25–48.
- Roger J (1859) Beiträge zur Kenntniss der Ameisenfauna der Mittelmeerländer. I. Berliner Entomologische Zeitschrift 3: 225–259. <https://doi.org/10.1002/mmnd.18590030209>
- Schenck CF (1852) Beschreibung nassauischer Ameisenarten. Jahrbuch des Vereins für Naturkunde im Herzogthum Nassau. Wiesbaden 8: 1–149.
- Ward PS, Brady SG, Fisher BL, Schultz TR (2015) The evolution of Myrmicine ants: phylogeny and biogeography of a hyperdiverse ant clade (Hymenoptera: Formicidae). Systematic Entomology 40: 61–81. <https://doi.org/10.1111/syen.12090>
- Weber NA (1947) A revision of the North American ants of the genus *Myrmica* Latreille with a synopsis of the Palearctic species. I. Annals of the Entomological Society of America 40: 437–474. <https://doi.org/10.1093/aesa/40.3.437>

- Wheeler GC, Wheeler J (1970) The natural history of *Manica* (Hymenoptera: Formicidae). Journal of the Kansas Entomological Society 43: 129–162.
- Wheeler GC, Wheeler J (1986) The ants of Nevada. Los Angeles: Natural History Museum of Los Angeles County, [vii +] 138 pp.
- Wheeler WM (1909) A decade of North American Formicidae. Journal of the New York Entomological Society 17: 77–90.
- Wheeler WM (1914) The American species of *Myrmica* allied to *M. rubida* Latreille. Psyche (Cambridge) 21: 118–122. <https://doi.org/10.1155/1914/75241>
- Wheeler WM (1915) *Neomyrma* versus *Oreomyrma*. A correction. Psyche (Cambridge) 22: 50. <https://doi.org/10.1155/1915/71842>
- Wheeler WM (1917) The mountain ants of western North America. Proceedings of the American Academy of Arts and Sciences 52: 457–569. <https://doi.org/10.2307/20025695>
- Wheeler GC, Wheeler EW (1944) The ants of North Dakota. North Dakota Historical Quarterly 11: 231–271.
- Wiens JJ, Dykhuizen D (2011) The causes of species richness patterns across space, time, and clades and the role of “ecological limits”. The Quarterly review of biology 86(2): 75–96. <https://doi.org/10.1086/659883>
- Zharkov D, Dubovikoff D, Abakumov E (2023) The first fossil record of the genus *Manica* Jurine, 1807 from Late Eocene Baltic amber and discussion of the early evolution of Myrmicini (Hymenoptera: Formicidae: Myrmicinae). Insects 14(1): 21. [10 pp] <https://doi.org/10.3390/insects14010021>

Cryptic or underworked? Taxonomic revision of the *Antistrophus rufus* species complex (Cynipoidea, Aulacideini)

Louis F. Nastasi¹, John F. Tooker¹, Charles K. Davis¹, Cecil N. Smith¹,
Timothy S. Frey², M. J. Hatfield³, Tara M. Presnall⁴,
Heather M. Hines^{1,5}, Andrew R. Deans¹

1 Department of Entomology, The Pennsylvania State University, 501 Agricultural Science and Industries Building, University Park, PA, 16802, Pennsylvania, USA **2** Department of Plant Pathology, The Ohio State University, 1680 Madison Ave, Wooster, OH, 44691, USA **3** 3079 Coldwater Creek Road, Cresco, IA, 52136, USA **4** Department of Mechanical Engineering, The Pennsylvania State University, 137 Reber Building, University Park, PA, 16802, Pennsylvania, USA **5** Department of Biology, The Pennsylvania State University, 208 Mueller Labs, University Park, PA 16802, Pennsylvania, USA

Corresponding author: Louis F. Nastasi (lfnastasi@gmail.com)

Academic editor: Miles Zhang | Received 1 March 2024 | Accepted 29 April 2024 | Published 21 May 2024

<https://zoobank.org/9675CE30-77A6-458A-A3EE-56E032633E9C>

Citation: Nastasi LF, Tooker JF, Davis CK, Smith CN, Frey TS, Hatfield MJ, Presnall TM, Hines HM, Deans AR (2024) Cryptic or underworked? Taxonomic revision of the *Antistrophus rufus* species complex (Cynipoidea, Aulacideini). Journal of Hymenoptera Research 97: 399–439. <https://doi.org/10.3897/jhr.97.121918>

Abstract

Cryptic species present challenges across many subdisciplines of biology. Not all “cryptic” species, however, are truly cryptic; many are simply underexplored morphologically. We examined this idea for the *Antistrophus rufus* species complex, which previously contained three species thought to be morphologically cryptic. To determine whether the *A. rufus* complex are truly cryptic species, we assessed species boundaries of members of the *A. rufus* species complex using morphological, ecological, and DNA barcode data, and tested whether a set of 50 morphological characters could adequately diagnose these species. We revealed that this complex includes five species, and that there are useful phenotypic diagnostic characters for all members of this species complex. This enabled redescription of four species and the description of *Antistrophus laurenae* Nastasi, **sp. nov.**, which induces externally inconspicuous galls in stems of *Silphium integrifolium* Michx., a host not associated with other members of the complex. We use these new diagnostic characters to construct a key to the five species of the *rufus* complex. We conclude that the *A. rufus* complex was not a true case of cryptic species. Our Bayesian analysis of DNA barcode data suggests possible cospeciation of members of the *rufus* complex and their *Silphium* host plants, but further study is necessary to better understand the evolution of host use in the lineage.

Keywords

Cryptic species, gall wasp, morphology, *Silphium*, superficial description impediment

Introduction

Cryptic species are those that cannot readily be distinguished on the basis of phenotypic variation alone (Struck et al. 2018); they have created challenges in myriad areas of the life sciences, especially in agro-economic systems (Andrews et al. 2020; Hansen et al. 2021; MacLeod et al. 2021). One such system of emerging significance is that of the genus *Silphium* L., a genus of composite herbs in the sunflower tribe (Asteraceae: Heliantheae) that is currently being investigated for use as biofuels, oilseeds, and additional economic purposes (Kowalski et al. 2013; Jasinskas et al. 2014; Peni et al. 2020; Vilela et al. 2020; von Cossel et al. 2020; Țîței et al. 2021). Despite recent interest in cultivating and domesticating various *Silphium* species, as well as their prominence in threatened tallgrass prairie habitats, their associated arthropod fauna remains poorly studied (Henderson and Sauer 2010; Buffington et al. 2017). A major component of *Silphium* communities is herb gall wasps of the genus *Antistrophus* Walsh, 1869 (Fig. 1), which includes a known case of cryptic species (Tooker et al. 2004).

Six described species of *Antistrophus* induce galls in the disc flowers and stems of four *Silphium* species (Nastasi and Deans 2021). Perhaps the most intriguing *Silphium* gall wasps are three cryptic species composing the *rufus* species complex (*A. jeanae* Tooker and Hanks, *A. meganae* Tooker and Hanks, and *A. rufus* Gillette). These species are not only thought to be morphologically cryptic, but also induce galls that are inconspicuous and do not externally deform the host plant's tissues (often referred to as "cryptic galls" in the literature; e.g., Ronquist and Liljeblad 2001); each species induces these galls within stems of their respective host species of the genus *Silphium* (Tooker et al. 2004; Nastasi and Deans 2021). The complex was described by Tooker et al. (2004), who found each species to be distinct based on allozyme and ecological data, including use of host plant species (Tooker et al. 2004); *A. jeanae* is associated with *S. perfoliatum* L., *A. meganae* is associated with *S. terebinthinaceum* Jacq., and *A. rufus* is associated with *S. laciniatum* L. These species would be considered cryptic, or functionally so, based on the diagnostic morphological criteria which included averages of precise ratios of antennomere dimensions, lengths of dissected ovipositors, depths of galls within host stems, and masses of mature larvae (Tooker et al. 2004). These metrics are hard to replicate and do not fully diagnose the species, thus the original diagnoses are arguably insufficient to reliably arrive at a species identification without host plant data. While these are the only morphological diagnostic characters given by Tooker et al. (2004), the descriptions of these species, including Gillette's 1891 description of *A. rufus*, are fairly limited in the number of morphological characters examined. Due to the brief original descriptions of species composing the *A. rufus* complex, it seems



Figure 1. Examples of *Silphium*-galling *Antistrophus* wasps and their galls **A** adult female *A. jeanae* Tooker & Hanks, 2004 **B** galls and larvae of *A. jeanae* in stem pith of *S. perfoliatum* L. **C** adult female *A. silphii* Gillette, 1891 **D** galls of *A. silphii* on terminal stem of *S. integrifolium* Michx **E** adult female *A. laciniatus* Gillette, 1891 **F** galls of *A. laciniatus* in disc flower of *S. laciniatum* L. adult gall wasps photographed by Antoine Guiguet. Galls photographed by Andrew R. Deans.

likely that this is a case of the so-called “superficial description impediment”, a taxonomic phenomenon in which species are not readily identifiable based on characterization in existing literature (Meier et al. 2021), rather than a true case of cryptic species.

The potential for a superficial description impediment in the *A. rufus* complex is supported by the minimal history of taxonomic investigation of herb gall wasps in North America; among the early diverging lineages of gall wasps are several tribes of non-oak herbaceous galls (Aylacini sensu lato), but these remain more poorly understood than the species-rich oak galls (Cynipini). While the herb gall wasp fauna of the Western Palearctic has been comparatively well studied (e.g., Nieves-Aldrey 1994; Nieves-Aldrey et al. 2008; Nieves-Aldrey 2012; Nieves-Aldrey 2022), those in North America remain poorly investigated. Eighteen valid native species are known (Nastasi and Deans 2021; Nastasi et al. 2024); only 14 published papers explore genus- or species-level taxonomy of these taxa, and many of these papers treat only a single species (Table 1). Of these works, only two (Nieves-Aldrey 1994; Tooker et al. 2004) have been published in the last 100 years. When combined with the known diagnostic characters for the *rufus* complex, the paucity of taxonomic work on this group further increases the likelihood of a taxonomic impediment rather than a true case of the cryptic species phenomenon.

In our analysis of the *Antistrophus rufus* complex, we included *A. jeanae* (gall inducer on *S. perfoliatum*), *A. meganae* (gall inducer on *S. terebinthinaceum*), and *A. rufus* (gall inducer on *S. laciniatum*) by sampling individuals reared from stems of these three *Silphium* host species. In the process we reveal in the stems of *S. integrifolium* the presence of an additional species that we newly describe, *Antistrophus laurennae* Nastasi sp. nov.; *S. integrifolium* is a new host plant for the *rufus* complex. We include in this analysis *A. minor* Gillette, 1891; we treat this species in the *rufus* complex based on its adherence to the diagnostic criteria for the *rufus* complex

Table 1. Taxonomic treatments of North American herb gall wasps, 1869–present. Names later transferred to other genera marked with (*). Names later synonymized marked with (◊). Species that are non-native to North America (or questionably so) are excluded.

Author and year	Description of taxonomic work
Riley and Walsh 1869	Described <i>Antistrophus pisum</i>
Ashmead 1887	Described <i>Aylax harringtoni</i> *
Bassett 1890	Described <i>Aylax tumidus</i> * and <i>Aylax podagrae</i> *
Gillette 1891	Described <i>Aylax bicolor</i> *◊ and five species of <i>Antistrophus</i>
Brodie 1892	Described <i>Aylax nabali</i> *
Ashmead 1896	Described <i>Aylax ambrosiaecola</i> *, <i>A. cavicola</i> *◊, <i>A. mulgediicola</i> *◊, and <i>A. sonchicola</i> *◊
Ashmead 1897	Described the genus <i>Aulacidea</i> for some species placed in <i>Aylax</i>
Beutenmüller 1908	Described <i>Aylax chrysothamni</i> *
Beutenmüller 1910a	Reviewed North American species of <i>Aylax sensu lato</i>
Beutenmüller 1910b	Reviewed North American species of <i>Aulacidea</i>
Kinsey 1920	Described <i>Aulacidea abdita</i> and <i>A. annulata</i>
McCracken and Egbert 1922	Described <i>Aylax microseris</i> *
Nieves-Aldrey 1994	Revised genera of “Aylacini” including those in North America
Tooker et al. 2004	Described <i>Antistrophus rufus</i> species complex including <i>A. jeanae</i> and <i>A. meganae</i>

we propose here along with that of Tooker et al. (2004). *Antistrophus minor* induces inconspicuous, externally imperceptible galls like those of *A. rufus* in the same host plant species (*S. laciniatum*). While some authors have discussed these species as potential synonyms (e.g., Beutenmüller 1910a), no nomenclatural actions have been published. *Antistrophus minor* was excluded from Tooker et al.'s (2004) description of the *A. rufus* complex, but because its status as a valid species remained unclear, we opted to treat *A. minor* here.

Methods

Gall collection and rearing

In late autumn and winter of 2020, 2021, and 2022, we collected entire, senesced stems of *Silphium integrifolium*, *S. laciniatum*, *S. perfoliatum*, and *S. terebinthinaceum* from sites in Illinois, Indiana, Iowa, and Ohio (details below). We identified plants in the field based on external morphology, as the *Silphium* species we studied are easily diagnosable in our sampling region by characters of the leaves and stems that are observable even in senescent plants (e.g., Brock and Weakley 2020). At each site, we confirmed via stem dissection that externally inconspicuous stem galls were present in each host plant species. We then collected additional stems, cut them into evenly sized pieces, labeled them, and stored them in plastic zip bags, which we aerated by poking holes in them using insect pins. We returned stems to lab facilities at The Pennsylvania State University (University Park, Pennsylvania, USA), where we stored bagged stem samples in a barn (without climate controls) to expose occupants to natural environmental conditions. From April through September, we checked stems every two to three days for emerging insects, which we collected into vials containing ethanol and stored at -20 °C. For morphological study, we air-dried and mounted selected individuals. Nastasi (2023) provides further recommendations for rearing cynipid galls on herbaceous plants.

Museum collection material

We examined specimens from the following collections:

- AMNH** American Museum of Natural History, New York, NY, USA
- INHS** Illinois Natural History Survey, University of Illinois, Champaign, IL, USA
- PSUC** Frost Entomological Museum, The Pennsylvania State University, University Park, PA, USA
- USNM** National Museum of Natural History, Washington, DC, USA
- WIRC** Wisconsin Insect Research Collection, University of Wisconsin, Madison, WI, USA

Using Darwin Core biodiversity data standards (Wieczorek et al. 2012), we digitized label data of all specimens that we examined. Digitized specimen data for all individuals we examined, including plant sample numbers and exact emergence dates for newly reared material, are available in Suppl. material 1: table 1.

Morphological character selection, description, and examination

To assess morphological boundaries of species belonging to the *rufus* complex, we selected 50 morphological characters (Suppl. material 1: table 2) from contemporary works on taxonomy of herb gall wasps (i.e., Nieves-Aldrey 1994; Tooker et al. 2004; Melika 2006; Ronquist et al. 2015; Azmaz and Katilmiş 2020; Buffington et al. 2020; Nieves-Aldrey 2022; Tavakoli et al. 2022). We selected characters based on perceived potential for species-level diagnosis as well as ubiquity across the taxonomic treatments that we considered. We matched anatomical terms for adult wasps to concepts in the Hymenoptera Anatomy Ontology (Yoder et al. 2010) and provide a URI table (see Seltmann et al. 2012) outlining morphological terminology (Suppl. material 1: table 3). Our terminology relating to cuticular surface sculpture follows Harris (1979). We used the following additional abbreviation that is absent from the Hymenoptera Anatomy Ontology:

- **DLO** (diameter of lateral ocellus) for the largest possible diameter of either lateral ocellus.

We evaluated each character for five females and five males of each species (“primary morphological exemplars;” Suppl. material 1: table 1); we putatively identified these individuals based on the associated host plant species and characters presented in the original descriptions and scored the primary type and some secondary types for each species. We selected specimens based on geographic origin and used material from various counties across four states to ensure that we accounted for different populations and intraspecies variability. In addition to “target” specimens that we used in the primary morphological analysis, we examined an additional 20 females and 20 males of each species (“secondary morphological exemplars;” Suppl. material 1: table 1) to confirm the characters given in descriptions and obtain replicate measurements of body length for each species. We provide raw morphological data (Suppl. material 1: table 4), and a summary of characters, states, and corresponding diagnostic utility (Suppl. material 1: table 5). We report morphological characters in taxon treatments as character-state pairs matching the findings of the morphological “test”.

We performed morphological observations and measurements of mounted specimens with an Olympus SZX16 stereo microscope (Olympus Life Science, Tokyo, Japan) fitted with an optical micrometer. We measured antennae at a resolution of 0.005 (1/200) millimeters using 10× magnification in combination with the 2× objective. Other measurements were taken at an appropriate magnification using the 1× objective. We used a gooseneck illuminator fitted with mylar strips to diffuse light, which

was especially helpful for discerning minute patterns involving sculpture and other aspects of the cuticular surface.

Terms relating to gall phenotypes follow Deans et al. (2023).

Imaging and drawings

We took images of point-mounted adult wasps using a Macroscopic Solutions ‘micro-kit’ (Tolland, CT) imaging system. Additional images were captured from mounted wasps using Olympus SZX16 microscope (Olympus Life Science, Tokyo, Japan). We stacked images using Zerene Stacker LLC (Richland, WA), edited them using Adobe Photoshop (Adobe Inc.), and prepared plates using Adobe Illustrator (Adobe Inc.).

Nomenclature of host plants

For taxonomy of *Silphium* host plants we follow Brock and Weakley (2020). While taxonomy of *Silphium* is widely considered unsettled, the four species considered here (*Silphium integrifolium*, *S. laciniatum*, *S. perfoliatum*, and *S. terebinthinaceum*) are robust in the geographic area that we considered (M. Brock, in litt.).

Distribution of gall wasps and host plants

We generated maps showing confirmed and potential distribution of each gall wasp species using MapChart (figures are licensed via CC BY-SA 4.0). We defined potential distribution of each gall wasp species as the known native range of its host plant; distribution of *Silphium* species follows Kartesz (2015).

Molecular phylogenetics

We sequenced and analyzed the *cytochrome c oxidase subunit I* (COI) gene to test the species concepts suggested by our morphological analysis and host plant data. We sequenced the COI gene of three individuals of each species of the *Antistrophus rufus* complex. We also sequenced single specimens of three additional *Antistrophus* species: *A. silphii* Gillette, 1891 reared from a terminal stem gall on *Silphium integrifolium* Michx. (Fig. 1D), *A. laciniatus* Gillette, 1891 reared from a flower gall on *Silphium laciniatum* (Fig. 1F), and *A. microseris* (McCracken & Egbert, 1922) reared from a stem gall on *Microseris douglasii* (DC.) Sch.Bip. We also included a single sequence of *Isocolus leuzeae* Nieves-Aldrey, 2003 from GenBank (DQ012643) to serve as outgroups to the *A. rufus* complex.

We performed DNA extraction using an E.Z.N.A. Microelute Genomic DNA Kit (Omega Biotek Inc., Norcross, Georgia, USA) following kit protocols and eluting in 30 µL of buffer (15 µL eluted in two steps). We extracted DNA from wasps either entirely destructively, by grinding the entire body, or minimally destructively, by incubating the entire insect. We amplified the COI gene using primer pairs LEPR

and LEPF (Hebert et al. 2004) or LCO1490 and HCO2198 (Folmer et al. 1994), following Hebert et al.'s PCR conditions for LEP primers and following those of Pang et al. (2020) for Folmer primers. Sequencing of PCR products was performed using The Huck Institute's Genomics Core Facility (The Pennsylvania State University, University Park, PA). We edited and aligned sequence data using Geneious (Biomatters Ltd., Auckland, New Zealand, <http://www.geneious.com/>) using the Geneious alignment function. Aligned sequence ends were trimmed to exclude primer sequences. We calculated genetic distances in Geneious using the Tamura-Nei distance model and 1,000 bootstrap replications. We determined the number of variable and parsimony informative sites in our alignment using AMAS v1.0 (Borowiec, 2016).

We estimated phylogenetic relationships using MrBayes v3.2.7a (Ronquist et al. 2012) using the following parameters: ngen=1500000; samplefreq=1000; nchains=4; nrns=3. We used two partitions for the first+second and third codon positions, respectively, and selected nucleotide substitution models for the two partitions using PartitionFinder 2 (Lanfear et al. 2017) using a greedy search (Lanfear et al. 2012) and specifying for models available in MrBayes; PartitionFinder 2 recommended GTR+G for the first+second positions and HKY+G for the third position. We specified *I. leuzeae* as the outgroup and used a burnin value of 3750000 corresponding to 25% of samples. We visualized our consensus tree using FigTree v1.4.4 (<https://tree.bio.ed.ac.uk/software/figtree/>).

All new sequences generated for this study were deposited in GenBank, accessions PP739172–PP739189. We provide collection data for sequenced specimens (Suppl. material 1: table 6) and DNA barcode divergence data (Suppl. material 1: table 7). We deposited DNA vouchers and additional material from gall samples and/or rearing events at PSUC.

Identification of additional museum material

After developing diagnostic characters for each studied species of *Antistrophus*, we identified additional material of the *A. rufus* species complex from collections we referenced, with the goal of checking previous determinations of identified specimens and identifying undetermined specimens for the first time.

Results

Morphological evaluation

Of the 50 characters that we assessed, 13 had utility as diagnostic characters for at least one species of the *rufus* complex. Two of the diagnostic characters, both of which concerned dimensions of the first two flagellomeres, were used previously by Tooker et al. (2004) in their treatment of the complex; our observations of those characters were generally consistent with those of Tooker et al. (2004).

While the specimens that we reared from *S. laciniatum*, *S. perfoliatum*, and *S. terebinthinaceum* all matched existing species concepts, the wasps associated with *S. integrifolium* appeared to compose an independent species, and our morphological observations suggest significant differences between these individuals and those of the described members of the *rufus* complex. Based on these differences, and the results of our molecular phylogenetic analysis, we describe below the species associated with *S. integrifolium* as *Antistrophus laurenae* Nastasi, sp. nov.

Molecular phylogenetics

Our trimmed alignment was 623 bp in length and contained 216 variable sites and 187 parsimony informative sites. Our Bayesian phylogenetic analysis of the 19 sequences (Fig. 2) provided clear evidence of distinct species matching those found by our morphological data, as each of the species had very short branch lengths within species (maximum COI divergence of 1.4% in *A. meganae*) and very long branch lengths between them. COI species divergences between the closest species pair (*A. meganae* and *A. minor*) averaged 10.6% (Suppl. material 1: table 7), well beyond the often contested 2% ‘suggestion’ for distinguishing species. Each species was supported by a posterior

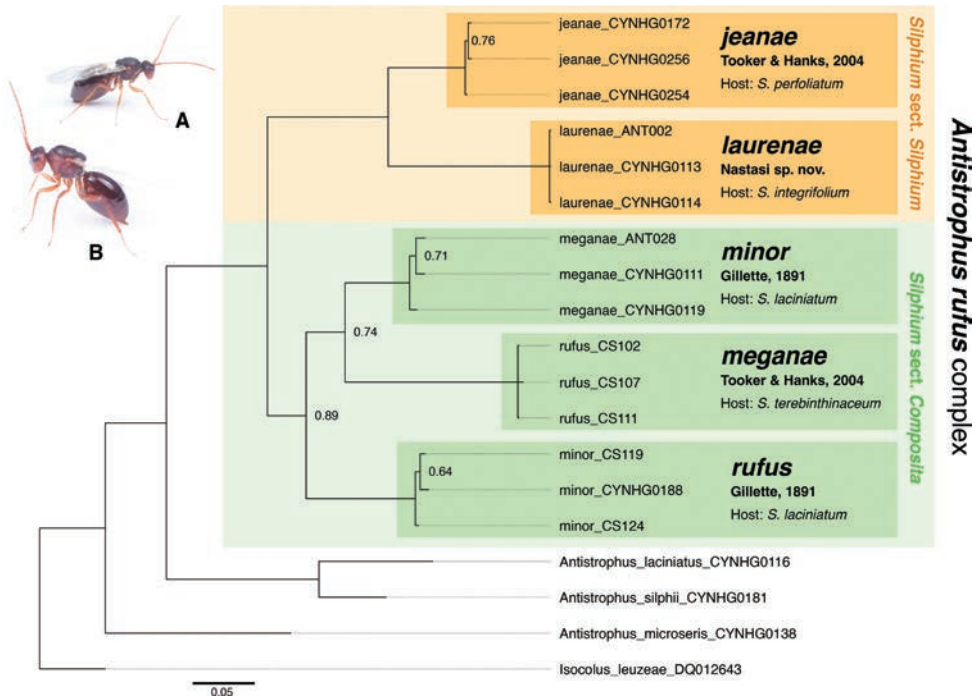


Figure 2. Bayesian phylogenetic tree of DNA barcodes for the *Antistrophus rufus* complex. Support values shown only for nodes with posterior probability <1. Host plant clade associations are indicated by colored boxes (*Silphium* sect. *Silphium* in orange and *S.* sect. *Composita* in green) **A** adult female *Antistrophus jeanae* Tooker & Hanks, 2004 **B** adult female *Antistrophus rufus* Gillette, 1891.

probability of 1, and *A. laurenae* and *A. jeanae* were strongly supported as sister species, but the remainder of the between-species relationships are less robust. Each recognized species has a distinct host plant except for *A. rufus* and *A. minor*, which are both associated with *Silphium laciniatum* but were not supported as sister species. Our analysis also retrieved the *Antistrophus rufus* complex as monophyletic within the sampled species of *Antistrophus* with a posterior probability of 1.

Taxonomy of the *Antistrophus rufus* species complex

Antistrophus rufus species complex

Diagnosis. Overall, the *A. rufus* complex is best diagnosed by the following combination of characters: head and mesosoma mostly reddish-brown in color (Figs 3A–D); facial radiating striae complete (Fig. 3A); compound eye longer than malar space in anterior view (Fig. 3A); F2 much longer than F1 (e.g., Fig. 4B); mesopleuron sculpture reticulate with fine intermediate striae (Fig. 3B); notauli incomplete, indistinct in anterior third of mesoscutum (Fig. 3C); female fore wing without apparent marginal setae (Fig. 3D); galls inconspicuous, induced in stems of *Silphium* species (e.g., Fig. 4F). Comparative diagnostic characters for the *Antistrophus rufus* species complex relative to other *Antistrophus* are presented in Fig. 3 and Table 2 below.

Table 2. Diagnostic characters of the *Antistrophus rufus* complex. Morphological data for species outside the *A. rufus* complex are from ongoing revisionary work on Aulacideini (Nastasi et al., unpublished data). Biological data are from Nastasi and Deans (2021). * = Gall and host unconfirmed for *A. bicolor* Gillette, 1891; see Nastasi and Deans (2021). † = Coloration of fresh material unknown; based on description by Beutenmüller (1908).

<i>Antistrophus</i> species	Head and mesosoma coloration	Facial radiating striae	Malar space: eye	F2:F1 length	Mesopleuron sculpture	Notauli	Fore wing marginal setae (♀)	Gall morphotype and host plant
<i>rufus</i> complex (<i>jeanae</i> , <i>laurenae</i> , <i>meganae</i> , <i>minor</i> , & <i>rufus</i>)	Mostly reddish-brown	Complete, reaching eye (Fig. 3A)	Eye longer (Fig. 3A)	F2 much longer (e.g., Fig. 4B)	Reticulate with fine intermediate striae (Fig. 3B)	Incomplete, indistinct in anterior third (Fig. 3C)	Absent (Fig. 3D)	Inconspicuous, in stems of <i>Silphium</i> (e.g., Fig. 4F)
<i>bicolor</i> , <i>laciniatus</i> , & <i>silphii</i>	Entirely black	Complete	Eye longer	F2 subequal to F1	Reticulate with fine intermediate striae	Complete, distinct across mesoscutum length	Absent	Conspicuous, on stems or flowers of <i>Silphium</i> *
<i>chrysothamni</i>	Black to reddish-brown†	Absent	Eye longer	F2 much longer	Strongly striate with interspaces reticulate	Incomplete, distinct only in posterior third	Absent	Conspicuous, apparently on <i>Chrysothamnus</i>
<i>microseris</i>	Entirely black	Complete	Eye longer	F2 much longer	Reticulate with fine intermediate striae	Incomplete, distinct only in posterior third	Present	Conspicuous, on stems of <i>Microseris</i>
<i>pisum</i>	Mostly reddish-brown	Incomplete, reaching halfway to eye	Malar space longer	F2 much longer	Entirely reticulate	Incomplete, distinct only in posterior third	Absent	Conspicuous, on stems of <i>Lygodesmia</i>

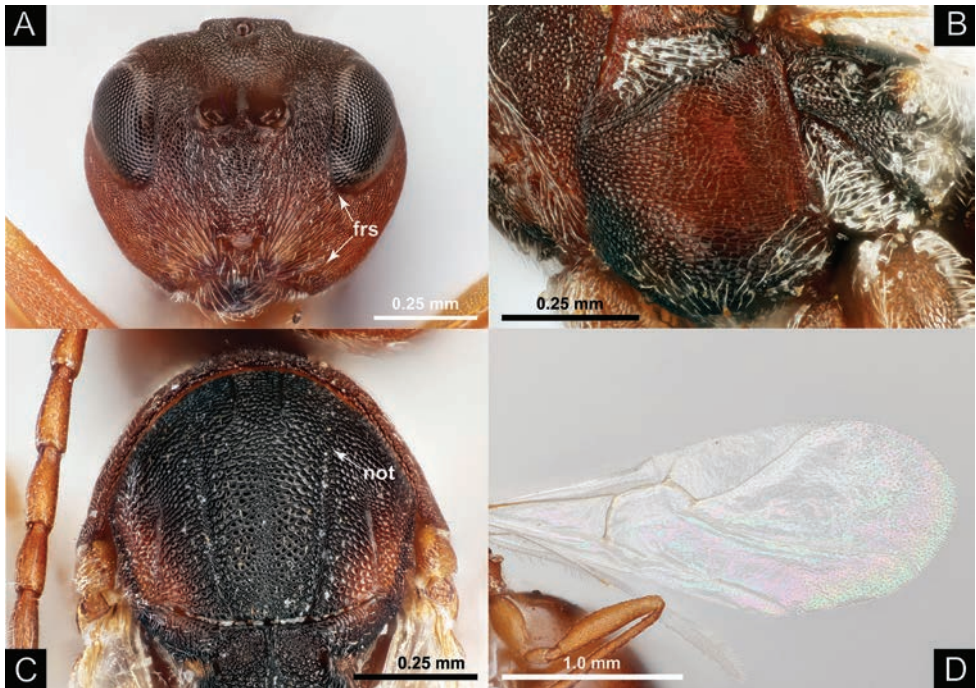


Figure 3. Diagnostic characters of the *Antistrophus rufus* complex **A** head, anterior view, *A. meganae* female (PSUC_FEM_247320); frs = facial radiating striae **B** mesopleuron, lateral view, *A. laurenae* female (PSUC_FEM_248174) **C** mesoscutum, dorsal view, *A. rufus* female (PSUC_FEM_253129); not = notauli; arrow indicates end of distinct portion **D** fore wing, *A. minor* female (PSUC_FEM_253176).

Remarks. The *Antistrophus rufus* complex includes all species of *Antistrophus* known to induce inconspicuous galls in stems of *Silphium* species. While other species of *Antistrophus* induce galls on *Silphium*, they induce perceptible galls on the apical stems or in the flowerheads (Gillette 1891; Nastasi and Deans 2021) and are generally distinct morphologically (Table 2). Other species of *Antistrophus* induce galls on different host genera. A complete revision of *Antistrophus* and other North American Aulacideini is being undertaken by the authors (Nastasi et al., unpublished data).

Antistrophus jeanae Tooker & Hanks, 2004

Fig. 4

Antistrophus jeanae Tooker & Hanks, 2004 in Tooker et al. 2004: 132. ♀, ♂ (type locality: Buckley Railroad Prairie, Iroquois Co., Illinois, USA).

Material examined. *Holotype* (deposited at INHS). USA • ♀; Illinois, Iroquois County, Buckley Railroad Prairie; 40°34.88'N, 88°02.70'W; J. Tooker leg.; reared from stem of *Silphium perfoliatum* in June 2000; INHS Insect Collection 25845.

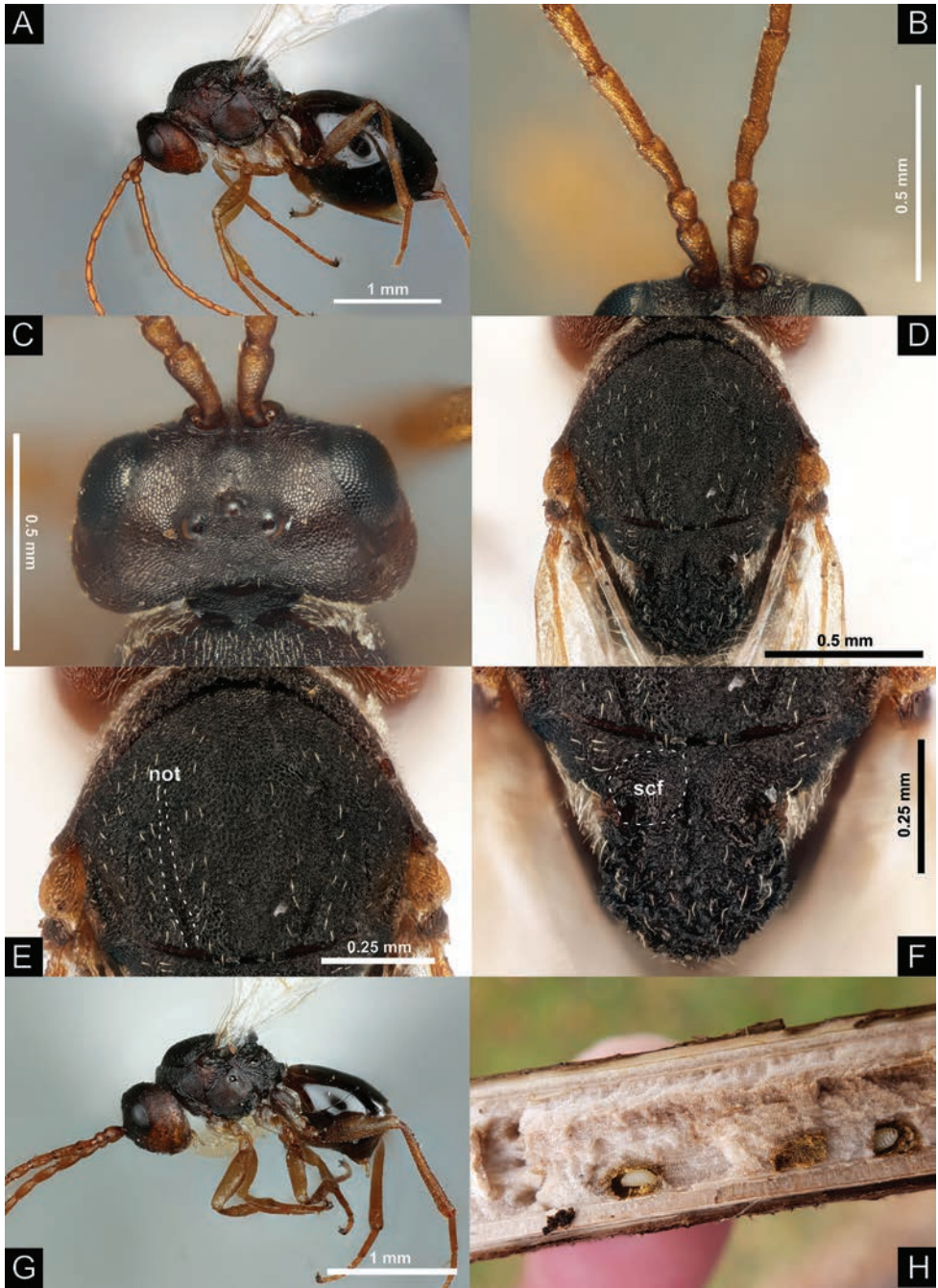


Figure 4. *Antistrophus jeanae* Tooker & Hanks, 2004 **A** female lateral habitus (PSUC_FEM_248169) **B** female proximal antennomeres (PSUC_FEM_248395) **C** female dorsal head (PSUC_FEM_247240) **D** female dorsal mesosoma (PSUC_FEM_247240) **E** female mesoscutum (PSUC_FEM_247240); not = notaulus **F** female dorsal scutellum (PSUC_FEM_247240); scf = mesoscutellar fovea **G** male lateral habitus (PSUC_FEM_248416) **H** galls and larvae of *A. jeanae* in a stem of *Silphium perfoliatum* L.

Paratypes (14 ♀ and 8 ♂). Deposited at INHS: USA • 5 ♀ and 2 ♂; same data as for holotype; INHS Insect Collection 52846–52852 • 4 ♀ and 3 ♂; Illinois, Ford County, Paxton Railroad Prairie; 40°26.17'N, 88°06.36'W; J. Tooker leg.; reared from stems of *Silphium perfoliatum*, emerging in June 2000; INHS Insect Collection 52853–52859.

Deposited at USNM: USA • 2 ♀ and 1 ♂; same data as for holotype; USNMENT 01790168–01790170 • 3 ♀ and 2 ♂; Illinois, Ford County, Paxton Railroad Prairie; 40°26.17'N, 88°06.36'W; J. Tooker leg.; reared from stems of *Silphium perfoliatum*, emerging in June 2000; USNMENT 00961127; 01790165–01790167; 01790171.

Other material (10 ♀ and 17 ♂). Deposited at PSUC: USA • 3 ♀ and 1 ♂; Illinois, Champaign County, Mahomet, Buffalo Trace Prairie; 40.208, -88.411; galled plant material collected 11 Nov 2020; JF Tooker and AR Deans leg.; reared from stems of *Silphium perfoliatum*, emerging in May or June 2021; PSUC_FEM_248395; 248398; 248413; 248423 • 4 ♀ and 3 ♂; Indiana, Parke County; 39.661, -87.371; galled plant material collected 12 Nov 2020; JF Tooker and AR Deans leg.; reared from stems of *Silphium perfoliatum*, emerging in May or June 2021; PSUC_FEM_248169–248170; 248396–248397; 248401–248403 • 2 ♀ and 3 ♂; Iowa, Winneshiek County, Plymouth Rock Prairie; 43.437, -92.005; galled plant material collected 19 Nov 2020; MJ Hatfield leg.; reared from stems of *Silphium perfoliatum*, emerging in May 2021; PSUC_FEM_248406; 248416; 248418; 248420; 248422.

Deposited at WIRC: 4 ♂; Wisconsin, Dane County, Anthony Branch F.A.; 42.896072, -89.340018; galled plant material collected 4 Apr 2012; DNR Study SSGB leg.; reared from stems of *Silphium perfoliatum*, emerging in Apr 2012; WIRC 00171031–00171032; 00171035–00171036 • 2 ♂; Wisconsin, Dane County, Badger Pr. Park - North; galled plant material collected 3 Apr 2012; DNR Study SSGB leg.; reared from stems of *Silphium perfoliatum*, emerging in Apr 2012; WIRC 00171041; 00171043 • 1 ♂; Wisconsin, Dane County, E-way at Mooreland; galled plant material collected 4 Apr 2012; DNR Study SSGB leg.; reared from stems of *Silphium perfoliatum*, emerging in Apr 2012; WIRC 00171047 • 1 ♀; Wisconsin, Iowa County, Noll Valley; galled plant material collected 4 Apr 2012; DNR Study SSGB leg.; reared from stems of *Silphium perfoliatum*, emerging in Apr 2012; WIRC 00170518 • 3 ♂; Wisconsin, Iowa County, Pr. Grove Rd at stream; galled plant material collected 5 Apr 2012; DNR Study SSGB leg.; reared from stems of *Silphium perfoliatum*, emerging in Apr 2012; WIRC 00171027–00171029.

Diagnosis. *A. jeanae* is most similar to *A. laurenae* sp. nov. but is best distinguished by the dimensions of F2 in females, which in *A. jeanae* is 3.8× as long as wide (Fig. 4B) but 3.3× as long as wide in *A. laurenae* (Fig. 5B). The sculpture of the mesoscutellar disc (Fig. 4F) is also useful; the mesoscutellar disc is more or less rugose-reticulate throughout in *A. jeanae* but only has rugose-reticulate sculpture toward the outer margins in *A. laurenae*.

Description. Female (Fig. 4A)—**Body length:** 1.9–3.2 mm (\bar{x} = 2.7 mm; n = 25; holotype = 2.6 mm). **Color:** Antenna color: red brown throughout, at most slightly darker distally than proximally. Head color: vertex and occiput dark red brown, mandi-

bles red brown basally to darker red brown apically, rest of head red brown throughout. Mesosoma color: pronotum and propodeum red brown laterally to dark red brown medially, mesoscutum dark red brown, scutellum dark red brown, and mesopleuron dark red brown dorsally and ventrally but red brown medially. Wing membrane color: hyaline throughout. Wing vein color: light brown. Leg color: red brown throughout, except for apical tarsomere which is conspicuously darker. Metasoma color: red brown to dark red brown. **Antennae** (Fig. 4B): Antennomere count: 13. F1 length: $2.4\times$ as long as wide. F2 length: $3.8\times$ as long as wide. F2:F1 length ratio: 1.5. Placodeal sensilla on F2: absent; sensilla present only on F3 and following antennomeres. **Head** (Fig. 4C): Upper frons sculpture: reticulate. Gena posterolateral projection in anterior view: distinctly projecting past compound eyes. Facial radiating striae: distinct and complete, reaching compound eyes. Supraclypeal area sculpture: reticulate. Supraclypeal area projection: slightly projecting. OOL vs POL: OOL distinctly longer. OOL vs LOL: OOL greater than twice LOL. POL vs LOL: POL greater than twice LOL. LOL vs DLO: LOL longer. Vertex sculpture: reticulate throughout. Clypeus sculpture: reticulate. **Mesosoma** (Figs 4D–F): Pronotum pilosity: densely pilose along anterior margin and with only sparse setae elsewhere. Pronotum excluding pronotal plate sculpture: reticulate. Pronotal plate sculpture: reticulate. Mesopleuron excluding speculum sculpture: reticulate with fine intermediate striae. Speculum sculpture: reticulate. Mesopleuron pilosity: ventral margin and mesopleural triangle densely pilose and bare elsewhere. Mesoscutum pilosity: sparsely pilose. Mesoscutum sculpture: reticulate. Apparent length of anterior parallel lines: reaching one third across mesoscutum. Morphology of anterior parallel lines: narrow, distinct throughout perceptible length. Apparent length of parapsidal grooves: reaching halfway across mesoscutum. Morphology of parapsidal grooves: narrow, distinct throughout perceptible length. Morphology of median mesoscutal impression: apparent as a shallow impression extending across most of mesoscutum. Notauli completeness: incomplete, distinct posteriorly to indistinct in anterior third. Morphology of notauli: appearing as wide indentations with sloping edges throughout distinct portions. Metapleural sulcus: meeting posterior mesopleuron at about one third of its height. Lateral propodeal carinae: distinct and subparallel. Metapleuron sculpture: reticulate. Mesoscutellar foveae distinction: distinct, relatively deep anteriorly to shallower and inconspicuously delimited posteriorly. Mesoscutellar foveae sculpture: reticulate. Mesoscutellar disc sculpture: usually rugose-reticulate throughout; primarily reticulate, but usually with distinct rugose sculpture apparent throughout most of mesoscutellar disc. Mesoscutellar foveae length: reaching about one third across mesoscutellar disc. Mesoscutellar foveae shape: subquadrate, about as wide as long, separated by a narrow linear carina. Mesoscutellar disc shape: subcircular, about as wide as long. **Wings**: Marginal cell length: $3.2\times$ as long as wide. Fore wing distal fringe of marginal setae: absent. **Metasoma**: Punctuation of metasomal terga: T3 punctate only in posterior third and with T4 and following punctate throughout.

Male (Fig. 4G)—Same as female except for the following: **Body length**: 1.8–2.6 mm ($\bar{x} = 2.1$ mm; $n = 25$). **Antennae**: Antennomere count: 14. F1 length: $2.4\times$ as long as wide. F2 length: $2.9\times$ as long as wide. F2:F1 length ratio: 1.4. Placodeal sensilla

on F2: present. **Wings:** Fore wing distal fringe of marginal setae: present. **Metasoma:** Metasoma size: conspicuously smaller than in female.

Biology. *A. jeanae* induces inconspicuous, externally imperceptible galls in stems of *Silphium perfoliatum* (Fig. 4H) (Tooker et al. 2004; Nastasi and Deans 2021).

Distribution. Tooker et al. (2004) reported this species only from several prairie sites in Illinois (USA). Nastasi and Deans (2021) did not report additional localities. However, specimens we examined revealed records from three additional state records: Indiana, Iowa, and Wisconsin. A verifiable iNaturalist observation (<https://www.inaturalist.org/observations/114414672>) also records this species from Ohio; we have since examined adult gall wasps reared from the plant material from the same site, which confirmed their suspected identity (in litt.). Lastly, a specimen identified during this study (USNMNT 01822302; see complete specimen data in Suppl. material 1: table 1) confirms the occurrence of this species in Missouri (Columbia, Boone County) (see discussion). Known and potential distribution are summarized in Fig. 9.

***Antistrophus laurenae* Nastasi, sp. nov.**

<https://zoobank.org/3EA96644-BC93-4B03-908C-C62BEAABDCDF>

Fig. 5

Material examined. Holotype (deposited at PSUC). USA • ♀; Illinois, Ford and Iroquois Counties, Paxton Railroad Prairie; 40.359, -88.106; galled plant material collected 11 November 2020; JF Tooker and AR Deans leg.; reared from stems of *Silphium integrifolium*, emerging in May or June 2021; PSUC_FEM_248174.

Paratypes (24 ♀ and 25 ♂). Deposited at PSUC: USA • 2 ♂; same data as for holotype; PSUC_FEM_248338–248339 • 1 ♀ and 4 ♂; Illinois, Iroquois County, Loda Cemetery Prairie; 40.528, -88.074; galled plant material collected 10 November 2020; JF Tooker and AR Deans leg.; reared from stems of *Silphium integrifolium*, emerging in May or June 2021; PSUC_FEM_248173 • 5 ♀ and 4 ♂; Illinois, McLean County, Weston Cemetery Prairie; 40.725, -88.606; galled plant material collected 11 November 2020; JF Tooker and AR Deans leg.; reared from stems of *Silphium integrifolium*, emerging in May or June 2021; PSUC_FEM_248178; 248325–248327; 248329–248330; 248333; 248336 • 2 ♀ and 2 ♂; Iowa, Story County, Grant, intersection of I-35 and E 13th St. prairie restoration; galled plant material collected 28 November 2020; MJ Hatfield leg.; reared from stems of *Silphium integrifolium*, emerging in June 2021; PSUC_FEM_248176; 248331; 248334; 248337.

Deposited at USNM: USA • 1 ♀; Illinois, McLean County, Weston Cemetery Prairie; 40.725, -88.606; galled plant material collected 11 November 2020; JF Tooker and AR Deans leg.; reared from stems of *Silphium integrifolium*, emerging in May or June 2021; PSUC_FEM_248332 • 1 ♀ and 2 ♂; same data as for holotype; PSUC_FEM_248175; 248335; 248340.

Deposited at WIRC: 2 ♀ and 1 ♂; Iowa, Delaware County, Dyersville West; 42.48564, -91.15425; galled plant material collected 2 May 2009; DNR Study SSGB

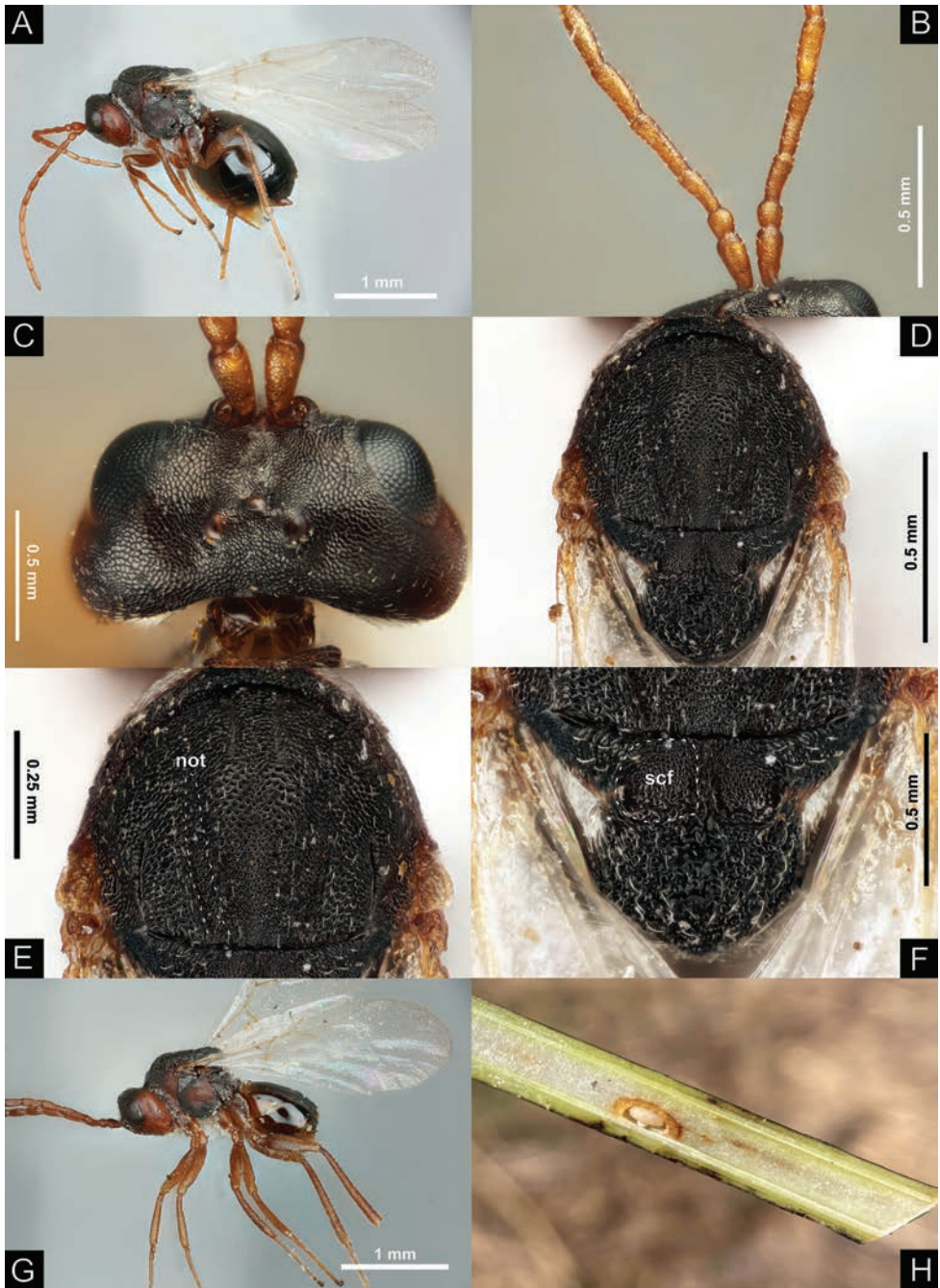


Figure 5. *Antistrophus laurenuae* Nastasi, sp. nov. **A** paratype female lateral habitus (PSUC_FEM_248173) **B** holotype female proximal antennomeres (PSUC_FEM_248174) **C** holotype female dorsal head (PSUC_FEM_248174) **D** holotype female dorsal mesosoma **E** holotype female dorsal mesoscutum; not = notaulus **G** holotype female dorsal scutellum; scf = mesoscutellar fovea. Paratype male lateral habitus (PSUC_FEM_248334) **H** galls and larva of *A. laurenuae* in a stem of *Silphium integrifolium* Michx.

leg.; reared from stems of *Silphium integrifolium*, emerging in May 2009; WIRC 00171299–00171301 • 2 ♀ and 1 ♂; Iowa, Delaware County, Dyersville West Prairie; 42.47330, -91.138372; galled plant material collected 2 May 2009; DNR Study SSGB leg.; reared from stems of *Silphium integrifolium*, emerging in May 2009; WIRC 00171267–00171268; 00171283 • 1 ♀ and 2 ♂; Iowa, Marshall County, Twinkle Hill Restoration; 42.064396, -92.854943; galled plant material collected 2 May 2009; DNR Study SSGB leg.; reared from stems of *Silphium integrifolium*, emerging in May 2009; WIRC 00171284; 00171306–00171307 • 1 ♀; Wisconsin, Columbia County, Goose Pond Jill's Pr.; galled plant material collected 3 Apr 2012; DNR Study SSGB leg.; reared from stems of *Silphium integrifolium*, emerging in Apr 2012; WIRC 00171314 • 1 ♂; Wisconsin, Dane County, Anthony Branch F.A.; 42.896072, -89.340018; galled plant material collected 4 Apr 2012; DNR Study SSGB leg.; reared from stems of *Silphium integrifolium*, emerging in Apr 2012; WIRC 00171322 • 2 ♀ and 2 ♂; Wisconsin, Dane County, Badger Pr. Park - North; 42.896072, -89.340018; galled plant material collected 3 Apr 2012; DNR Study SSGB leg.; reared from stems of *Silphium integrifolium*, emerging in Apr 2012; WIRC 00170523; 00170837; 00171315; 00171331 • 1 ♀; Wisconsin, Dane County, Black Earth Prairie; 43.140146, -89.773011; galled plant material collected 5 Apr 2012; DNR Study SSGB leg.; reared from stems of *Silphium integrifolium*, emerging in Apr 2012; WIRC 00170838 • 1 ♀ and 1 ♂; Wisconsin, Dane County, E-way at Mooreland; 43.030588, -89.349114; galled plant material collected 4 Apr 2012; DNR Study SSGB leg.; reared from stems of *Silphium integrifolium*, emerging in Apr 2012; WIRC 00170524; 00171329 • 1 ♀ and 1 ♂; Wisconsin, Dane County, Festge Roadside; 43.118267, -89.683665; galled plant material collected 18 Apr 2009; DNR Study SSGB leg.; reared from stems of *Silphium integrifolium*, emerging in May 2009; WIRC 00171227; 00171289 • 1 ♂; Wisconsin, Dane County, Garfoot Road; galled plant material collected 5 Apr 2012; DNR Study SSGB leg.; reared from stems of *Silphium integrifolium*, emerging in Apr 2012; WIRC 00171337 • 2 ♀ and 2 ♂; Wisconsin, Dane County, Gov Nelson 1997; 43.137321, -89.437257; galled plant material collected 3 Apr 2012; DNR Study SSGB leg.; reared from stems of *Silphium integrifolium*, emerging in Apr 2012; WIRC 00170839; 00171303; 00171330; 00171341 • 2 ♀ and 1 ♂; Wisconsin, Dane County, TNC Waubesa Wetland; galled plant material collected 22 Nov 2008; DNR Study SSGB leg.; reared from stems of *Silphium integrifolium*, emerging in May 2009; WIRC 00171271; 00171274; 00171286 • 1 ♂; Wisconsin, Iowa County, TNC/Lease; 42.97357, -89.88900; galled plant material collected 17 Apr 2009; DNR Study SSGB leg.; reared from stems of *Silphium integrifolium*, emerging in May 2009; WIRC 00171287 • 1 ♂; Wisconsin, Iowa County, Underwood Prairie; galled plant material collected 9 May 2009; DNR Study SSGB leg.; reared from stems of *Silphium integrifolium*, emerging in May 2009; WIRC 00171298.

Diagnosis. See diagnosis to *Antistrophus jeanae* Tooker & Hanks, 2004.

Description. Female (Fig. 5A)—**Body length:** 1.8–2.6 mm (\bar{x} = 2.2 mm; n = 25; holotype = 2.6 mm). **Color:** Antenna color: red brown throughout, at most slightly darker distally than proximally. Head color: vertex and occiput dark red brown, mandi-

bles red brown basally to darker red brown apically, rest of head red brown throughout. Mesosoma color: pronotum and propodeum red brown laterally to dark red brown medially, mesoscutum dark red brown, scutellum dark red brown, and mesopleuron dark red brown dorsally and ventrally but red brown medially. Wing membrane color: hyaline throughout. Wing vein color: light brown. Leg color: red brown throughout, except for apical tarsomere which is conspicuously darker. Metasoma color: red brown to dark red brown. **Antennae** (Fig. 5B): Antennomere count: 13. F1 length: $2.2\times$ as long as wide. F2 length: $3.3\times$ as long as wide. F2:F1 length ratio: 1.4. Placodeal sensilla on F2: absent; sensilla present only on F3 and following antennomeres. **Head** (Fig. 5C): Upper frons sculpture: reticulate. Gena posterolateral projection in anterior view: distinctly projecting past compound eyes. Facial radiating striae: distinct and complete, reaching compound eyes. Supraclypeal area sculpture: reticulate. Supraclypeal area projection: slightly projecting. OOL vs POL: OOL distinctly longer. OOL vs LOL: OOL greater than twice LOL. POL vs LOL: POL greater than twice LOL. LOL vs DLO: LOL longer. Vertex sculpture: reticulate throughout. Clypeus sculpture: reticulate. **Mesosoma** (Figs 5D–F): Pronotum pilosity: densely pilose along anterior margin and with only sparse setae elsewhere. Pronotum excluding pronotal plate sculpture: reticulate. Pronotal plate sculpture: reticulate. Mesopleuron excluding speculum sculpture: reticulate with fine intermediate striae. Speculum sculpture: reticulate. Mesopleuron pilosity: ventral margin and mesopleural triangle densely pilose and bare elsewhere. Mesoscutum pilosity: sparsely pilose. Mesoscutum sculpture: reticulate. Apparent length of anterior parallel lines: reaching one third across mesoscutum. Morphology of anterior parallel lines: narrow, distinct throughout perceptible length. Apparent length of parapsidal grooves: reaching halfway across mesoscutum. Morphology of parapsidal grooves: narrow, distinct throughout perceptible length. Morphology of median mesoscutal impression: apparent as a shallow impression extending across most of mesoscutum. Notauli completeness: incomplete, distinct posteriorly to indistinct in anterior third. Morphology of notauli: appearing as wide indentations with sloping edges throughout distinct portions. Metapleural sulcus: meeting posterior mesopleuron at about one third of its height. Lateral propodeal carinae: distinct and subparallel. Metapleuron sculpture: reticulate. Mesoscutellar foveae distinction: distinct, relatively deep anteriorly to shallower and inconspicuously delimited posteriorly. Mesoscutellar foveae sculpture: reticulate. Mesoscutellar disc sculpture: rugose-reticulate, primarily reticulate, but with distinct rugose-reticulate sculpture seemingly restricted to outer margins. Mesoscutellar foveae length: long, reaching about one third across mesoscutellar disc. Mesoscutellar foveae shape: subquadrate, about as wide as long, separated by a narrow linear carina. Mesoscutellar disc shape: subcircular, about as wide as long. **Wings**: Marginal cell length: $3.1\times$ as long as wide. Fore wing distal fringe of marginal setae: absent. **Metasoma**: Punctuation of metasomal terga: T3 punctate only in posterior third and with T4 and following punctate throughout.

Male (Fig. 5G)—Same as female except for the following: **Body length**: 1.3–2.1 mm ($\bar{x} = 1.8$; $n = 25$). **Antennae**: Antennomere count: 14. F1 length: $2.3\times$ as long as wide. F2 length: $3.2\times$ as long as wide. F2:F1 length ratio: 1.5. Placodeal sensilla

on F2: present. **Wings:** Fore wing distal fringe of marginal setae: present. **Metasoma:** Metasoma size: conspicuously smaller than in female.

Etymology. Named for Lauren Ahlert, a biology teacher at Wayne Valley High School in Wayne, New Jersey, USA, who has served as a tremendous source of inspiration and passion for the author of this species.

Biology. *Antistrophus laurenae* induces inconspicuous, externally imperceptible galls in stems of *Silphium integrifolium* (Fig. 5H).

Distribution. Material examined in this study reveals that this species occurs in Illinois, Iowa, and Wisconsin (USA; see Suppl. material 1: table 1). A verified iNaturalist record (<https://www.inaturalist.org/observations/136446787>) also suggests that this species occurs in Mississippi. Known and potential distribution are summarized in Fig. 9.

Antistrophus meganae Tooker & Hanks, 2004

Fig. 6

Antistrophus meganae Tooker & Hanks, 2004 in Tooker et al. 2004: 132. ♀, ♂ (type locality: East St. Joseph Railroad Prairie, Iroquois Co., Illinois, USA).

Material examined. Holotype (deposited at INHS). USA • ♀; Illinois, Champaign County, St. Joseph, roadside prairie; J. Tooker leg.; reared from stem of *Silphium terebinthinaceum*, emerging in June 2000; INHS Insect Collection 52830.

Paratypes (14 ♀ and 8 ♂). Deposited at INHS: USA • 8 ♀ and 4 ♂; same data as for holotype; INHS Insect Collection 52831–52837 • 4 ♀ and 3 ♂; Illinois, Ford County, Paxton, Paxton Railroad Prairie; J. Tooker leg.; reared from stem of *Silphium terebinthinaceum*, emerging in June 2000; INHS Insect Collection 52838–52844.

Deposited at USNM: USA • 2 ♀ and 1 ♂; Illinois, Ford County, Paxton, Paxton Railroad Prairie; J. Tooker leg.; reared from stem of *Silphium terebinthinaceum*, emerging in June 2000; USNMENT 01790188–01790190.

Other material (10 ♀ and 17 ♂). Deposited at PSUC: USA • 1 ♀; Illinois, Champaign County, St. Joseph, roadside prairie; JF Tooker and AR Deans leg.; 40.113, -88.064; galled plant material collected 10 Nov 2020; reared from stem of *Silphium terebinthinaceum*, emerging in June 2021; PSUC_FEM_248429 • 1 ♀ and 1 ♂; Illinois, McLean County, Chenoa, Weston Cemetery Prairie; 40.725, -88.606; galled plant material collected 11 Nov 2020; reared from stem of *Silphium terebinthinaceum*, emerging in June 2021; PSUC_FEM_248165–248166.

Deposited at WIRC: USA • 2 ♀; Wisconsin, Columbia County, Mass Rd.; galled plant material collected Fall 2008; reared from stem of *Silphium terebinthinaceum*, emerging in June 2009; WIRC 00171156; 00171166 • 2 ♀ and 2 ♂; Wisconsin, Dane County, Co A and Oak Ridge (Anthony Branch F.A.); 42.892454, -89.320011; galled plant material collected 15 Apr 2009; reared from stem of *Silphium terebinthinaceum*, emerging in June 2009; WIRC 00170514; 00171140; 00171154–00171155 • 1 ♂;

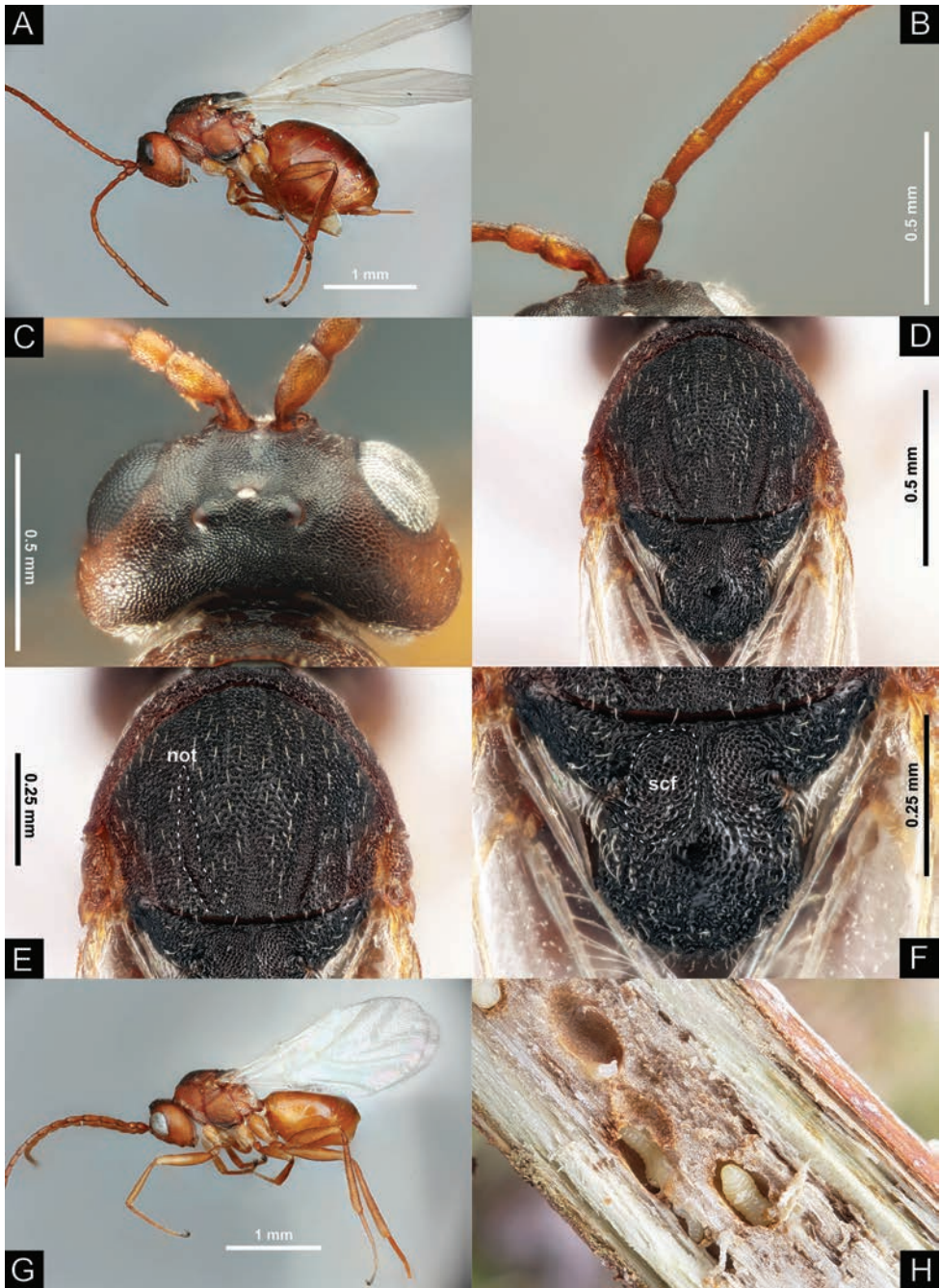


Figure 6. *Antistrophus meganae* Tooker & Hanks, 2004 **A** female lateral habitus (PSUC_FEM_248165) **B** female proximal antennomeres (PSUC_FEM_247325) **C** female dorsal head (PSUC_FEM_247325) **D** female dorsal mesosoma (PSUC_FEM_247230) **E** female dorsal mesoscutum (PSUC_FEM_247230); not = notaulus **F** female dorsal scutellum (PSUC_FEM_247230); scf = mesoscutellar fovea **G** male lateral habitus (PSUC_FEM_248498) **H** galls and larvae of *A. meganae* in a stem of *Silphium terebinthinaceum* Jacq.

Wisconsin, Dane County, Kelly Road and RR, roadside; galled plant material collected Fall 2008; reared from stem of *Silphium terebinthinaceum*, emerging in July 2009; WIRC 00170513 • 1 ♂; Wisconsin, Dane County, Malone Road; galled plant material collected 17 Apr 2009; reared from stem of *Silphium terebinthinaceum*, emerging in June 2009; WIRC 00171112 • 1 ♂; Wisconsin, Dane County, Noll Valley; galled plant material collected 5 Apr 2012; reared from stem of *Silphium terebinthinaceum*, emerging in June 2012; WIRC 00171114 • 1 ♂; Wisconsin, Dane County, Prairie Ridge City Park; galled plant material collected 3 Apr 2012; reared from stem of *Silphium terebinthinaceum*, emerging in May 2012; WIRC 00171124 • 1 ♀ and 1 ♂; Wisconsin, Dane County, Sugar Ridge Savanna; galled plant material collected 20 Mar 2012; reared from stem of *Silphium terebinthinaceum*, emerging in May 2012; WIRC 00171122; 00171134 • 1 ♂; Wisconsin, Dane County, TNC Waubesa Wetland; galled plant material collected 22 Nov 2008; reared from stem of *Silphium terebinthinaceum*, emerging in May 2009; WIRC 00170515 • 1 ♂; Wisconsin, Jefferson County, Bluejoint Prairie; 43.163398, -88.938815; galled plant material collected 16 Apr 2009; reared from stem of *Silphium terebinthinaceum*, emerging in July 2009; WIRC 00170517 • 1 ♂; Wisconsin, Jefferson County, Bluejoint Prairie; 43.163398, -88.938815; galled plant material collected 16 Apr 2009; reared from stem of *Silphium terebinthinaceum*, emerging in May 2009; WIRC 00170512 • 1 ♀ and 2 ♂; Wisconsin, Jefferson County, Cold Spring Prairie; 42.872556, -88.770194; galled plant material collected 15 Apr 2009; reared from stem of *Silphium terebinthinaceum*, emerging in June 2009; WIRC 00171109; 00171137; 00171141 • 3 ♂; Wisconsin, Walworth County, Skoponong Prairie; 42.829155, -88.620586; galled plant material collected 4 Oct 2011; reared from stem of *Silphium terebinthinaceum*, emerging in May or June 2012; WIRC 00170749; 00171113; 00171120 • 1 ♀; Wisconsin, Walworth County, Young Pr. East Annex; 42.839419, -88.63002; galled plant material collected 16 Apr 2009; reared from stem of *Silphium terebinthinaceum*, emerging in June 2009; WIRC 00170750 • 1 ♀ and 2 ♂; Wisconsin, Winnebago County, Oshkosh-Larsen Trl mid (B); 44.13912, -88.624272; galled plant material collected 10 Oct 2011; reared from stem of *Silphium terebinthinaceum*, emerging in June 2012; WIRC 00171115–00171116; 00171118.

Diagnosis. *A. meganae* is the only species of the *rufus* complex in which the mesoscutellar foveae (Fig. 6F) are long and ovate, reaching nearly halfway across the mesoscutellar disc. *A. meganae* also differs from most other members of the *rufus* complex by the POL (Fig. 6C), which is longer than the OOL in *A. meganae* and *A. minor* but shorter than the OOL in the other species.

Description. Female (Fig. 6A)—**Body length:** 1.8–3.2 mm (\bar{x} = 2.5 mm; n = 25; holotype = 2.3 mm). **Color:** Antenna color: red brown throughout, at most slightly darker distally than proximally. Head color: vertex and occiput dark red brown, mandibles red brown basally to darker red brown apically, rest of head red brown throughout. Mesosoma color: pronotum and propodeum red brown laterally to dark red brown medially, mesoscutum dark red brown with distinct posterolateral red brown spots, scutellum dark red brown, and mesopleuron dark red brown dorsally

and ventrally but red brown medially. Wing membrane color: hyaline throughout. Wing vein color: light brown. Leg color: red brown throughout, except for apical tarsomere which is conspicuously darker. Metasoma color: red brown to dark red brown. **Antennae** (Fig. 6B): Antennomere count: 13. F1 length: 2.6× as long as wide. F2 length: 3.6× as long as wide. F2:F1 length ratio: 1.4. Placodeal sensilla on F2: absent; sensilla present only on F3 and following antennomeres. **Head** (Fig. 6C): Upper frons sculpture: reticulate. Gena posterolateral projection in anterior view: distinctly projecting past compound eyes. Facial radiating striae: distinct and complete, reaching compound eyes. Supraclypeal area sculpture: reticulate. Supraclypeal area projection: slightly projecting. OOL vs POL: POL distinctly longer. OOL vs LOL: OOL less than twice LOL. POL vs LOL: POL twice LOL. LOL vs DLO: LOL longer. Vertex sculpture: reticulate throughout. Clypeus sculpture: reticulate. **Mesosoma** (Figs 6D–F): Pronotum pilosity: densely pilose along anterior margin and with only sparse setae elsewhere. Pronotum excluding pronotal plate sculpture: reticulate. Pronotal plate sculpture: reticulate. Mesopleuron excluding speculum sculpture: reticulate with fine intermediate striae. Speculum sculpture: reticulate. Mesopleuron pilosity: ventral margin and mesopleural triangle densely pilose and bare elsewhere. Mesoscutum pilosity: sparsely pilose. Mesoscutum sculpture: reticulate. Apparent length of anterior parallel lines: reaching one third across mesoscutum. Morphology of anterior parallel lines: narrow, distinct throughout perceptible length. Apparent length of parapsidal grooves: reaching halfway across mesoscutum. Morphology of parapsidal grooves: narrow, distinct throughout perceptible length. Morphology of median mesoscutal impression: apparent as a shallow impression extending across most of mesoscutum. Notauli completeness: incomplete, distinct posteriorly to indistinct in anterior third. Morphology of notauli: appearing as wide indentations with sloping edges throughout distinct portions. Metapleural sulcus: meeting posterior mesopleuron at about one third of its height. Lateral propodeal carinae: distinct and subparallel. Metapleuron sculpture: reticulate. Mesoscutellar foveae distinction: distinct, relatively deep anteriorly to shallower and inconspicuously delimited posteriorly. Mesoscutellar foveae sculpture: reticulate. Mesoscutellar disc sculpture: rugose-reticulate, primarily reticulate, but with distinct rugose-reticulate sculpture seemingly restricted to outer margins. Mesoscutellar foveae length: long, reaching nearly halfway across mesoscutellar disc. Mesoscutellar foveae shape: ovate, slightly longer than wide, separated by a subtriangular carina slightly wider posteriorly than anteriorly. Mesoscutellar disc shape: subcircular, about as wide as long. **Wings**: Marginal cell length: 3.3× as long as wide. Fore wing distal fringe of marginal setae: absent. **Metasoma**: Punctuation of metasomal terga: T3 punctate only in posterior third and with T4 and following punctate throughout.

Male (Fig. 6G)—Same as female except for the following: **Body length**: 1.3–2.5 mm (\bar{x} = 2.1 mm; n = 25). **Antennae**: Antennomere count: 14. F1 length: 2.5× as long as wide. F2 length: 3.0× as long as wide. F2:F1 length ratio: 1.4 (as in female). Placodeal sensilla on F2: present. **Wings**: Fore wing distal fringe of marginal setae: present. **Metasoma**: Metasoma size: conspicuously smaller than in female.

Biology. *Antistrophus meganae* induces inconspicuous, externally imperceptible galls in stems of *Silphium terebinthinaceum* (Fig. 6H) (Tooker et al. 2004; Nastasi and Deans 2021).

Distribution. Tooker et al. (2004) reported this species only from several prairie sites in Illinois (USA). Nastasi and Deans (2021) did not report additional localities; however, the specimens we examined revealed novel records from Wisconsin (Suppl. material 1: table 1). We also sequenced DNA barcodes for individuals from Ohio (Suppl. material 1: table 6), and a series of specimens identified using the key represents a new state record from Michigan (see Discussion; Suppl. material 1: table 1). Known and potential distribution are summarized in Fig. 9.

Antistrophus minor Gillette, 1891

Fig. 7

Antistrophus minor Gillette, 1891: 195. ♀, ♂ (type locality: unknown location in Illinois, USA).

Aulax gillettei (Gillette, 1891); Kieffer 1902: 93.

Material examined. Lectotype (deposited at INHS; designated by Frison [1927]). USA • ♀; Illinois; reared from stem of *Silphium laciniatum*; record number 5500; INHS Insect Collection 212949.

Lectoallotype (deposited at INHS; designated by Frison [1927]). USA • ♂; same data as lectotype; INHS Insect Collection 212950.

Other material (24 ♀ and 24 ♂). Deposited at PSUC: USA • 3 ♀; Illinois, Champaign County, Gifford, Shortline Railroad Prairie; 40.305, -87.999; JF Tooker and AR Deans leg.; galled plant material collected 10–11 Nov 2020; reared from stem of *Silphium laciniatum*, emerging in May or June 2021; PSUC_FEM_248257; 253063; 253067 • 2 ♀; Illinois, Iroquois County, Loda, Loda Cemetery Prairie; 40.528, -88.074; JF Tooker and AR Deans leg.; galled plant material collected 10 Nov 2020; reared from stem of *Silphium laciniatum*, emerging in June 2021; PSUC_FEM_248273; 253060 • 2 ♀ and 1 ♂; Illinois, McLean County, Chenoa, Weston Cemetery Prairie; 40.725, -88.606; JF Tooker and AR Deans leg.; galled plant material collected 11 Nov 2020; reared from stem of *Silphium laciniatum*, emerging in May or June 2021; PSUC_FEM_248278; 248283; 248288; 248303 • 3 ♀ and 3 ♂; Illinois, McLean County, Chenoa, Weston Cemetery Prairie; 40.725, -88.606; LF Nastasi and AR Casadei leg.; galled plant material collected 16 Oct 2021; reared from stem of *Silphium laciniatum*, emerging in June 2022; PSUC_FEM_253166–253168; 253170; 253180; 253192 • 1 ♀ and 2 ♂; Iowa, Story County, Grant, Interstate 35 and E 13th St prairie restoration; MJ Hatfield leg.; galled plant material collected 30 Nov 2020; reared from stem of *Silphium laciniatum*, emerging in May or June 2021; PSUC_FEM_248265; 248291; 248295 • 1 ♂; Iowa, Winneshiek County, Decorah Community Prairie; MJ Hatfield leg.; galled plant material collected 18 Apr 2022; reared from

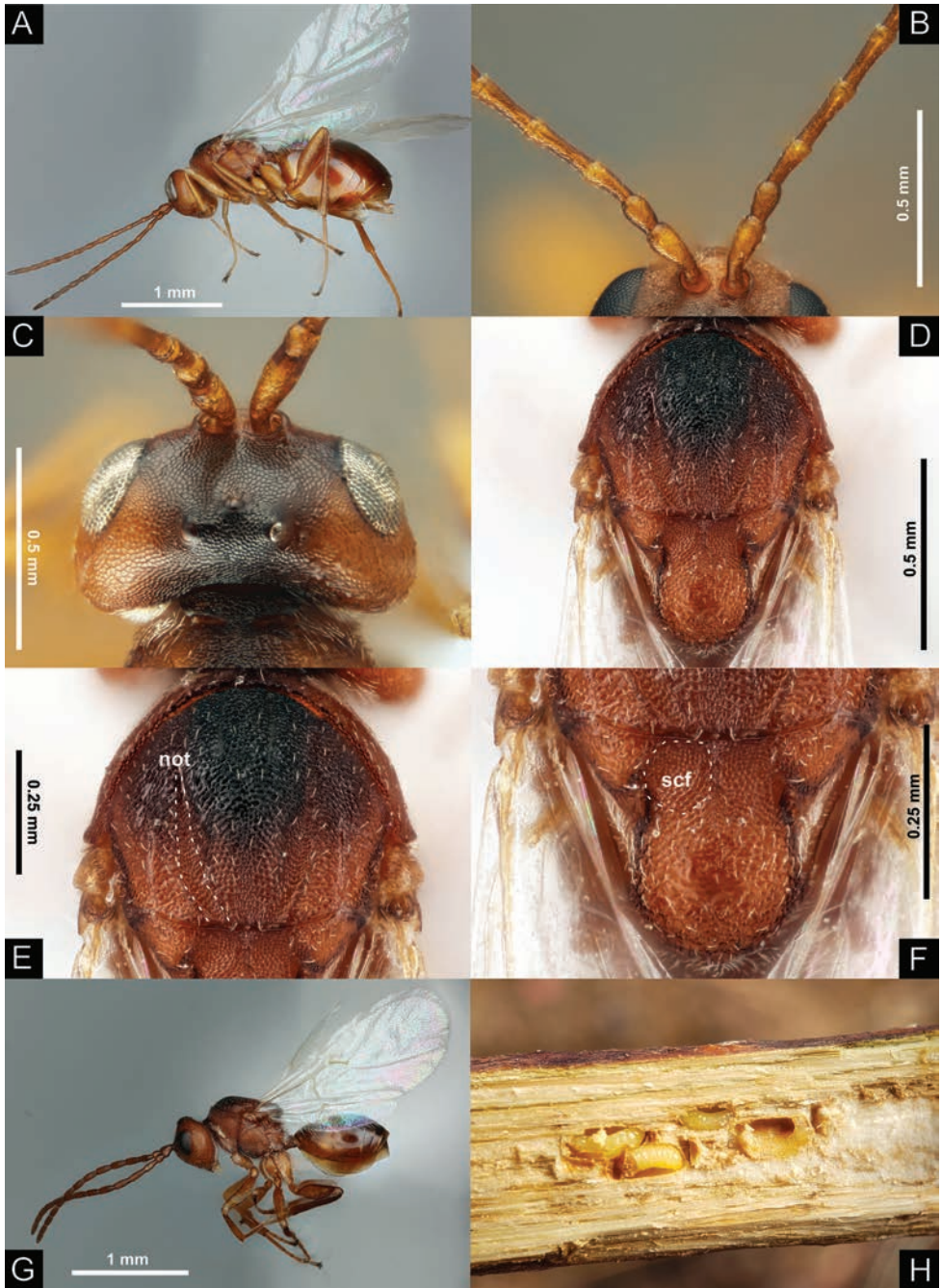


Figure 7. *Antistrophus minor* Gillette, 1891 **A** female lateral habitus (PSUC_FEM_248273) **B** female proximal antennomeres (PSUC_FEM_253176) **C** female dorsal head (PSUC_FEM_253091) **D** female dorsal mesosoma (PSUC_FEM_248257) **E** female dorsal mesoscutum (PSUC_FEM_248257); not = notaulus **F** female dorsal scutellum (PSUC_FEM_248257); scf = mesoscutellar fovea **G** male lateral habitus (PSUC_FEM_253191) **H** gallus and larvae of *A. minor* or *A. rufus* in a stem of *Silphium laciniatum* L.

stem of *Silphium laciniatum*, emerging in May or June 2022; PSUC_FEM_253229 • 3 ♀ and 2 ♂; Iowa, Winneshiek County, Plymouth Rock Prairie; 43.438, -92.006; MJ Hatfield leg.; galled plant material collected 17 Apr 2016; reared from stem of *Silphium laciniatum*, emerging in May 2016; PSUC_FEM_253085; 253088; 253089; 253090; 253094.

Deposited at USNM: USA • 1 ♀; Illinois, McLean County, Chenoa, Weston Cemetery Prairie; 40.725, -88.606; JF Tooker and AR Deans leg.; galled plant material collected 11 Nov 2020; reared from stem of *Silphium laciniatum*, emerging in May or June 2021; PSUC_FEM_248286 • 1 ♀; Illinois, McLean County, Chenoa, Weston Cemetery Prairie; 40.725, -88.606; JF Tooker and AR Deans leg.; galled plant material collected 11 Nov 2020; reared from stem of *Silphium laciniatum*, emerging in May or June 2021; PSUC_FEM_248303 • 3 ♂; Illinois, McLean County, Chenoa, Weston Cemetery Prairie; 40.725, -88.606; LF Nastasi and AR Casadei leg.; galled plant material collected 16 Oct 2021; reared from stem of *Silphium laciniatum*, emerging in June 2022; PSUC_FEM_253190; 253191; 253194 • 1 ♀; Illinois, McLean County, Chenoa, Weston Cemetery Prairie; 40.725, -88.606; LF Nastasi and AR Casadei leg.; galled plant material collected 16 Oct 2021; reared from stem of *Silphium laciniatum*, emerging in June 2022; PSUC_FEM_253165.

Deposited at WIRC: USA • 1 ♀; Iowa, Blackhawk County, Hudson Railroad Prairie; 42.436349, -92.427034; DNR Study SSGB leg.; galled plant material collected 2 May 2009; reared from stem of *Silphium laciniatum*, emerging in June 2009; WIRC 00170819 • 1 ♀; Iowa, Linn County, Walford 2; 41.883014, -91.825962; DNR Study SSGB leg.; galled plant material collected 3 May 2009; reared from stem of *Silphium laciniatum*, emerging in June 2009; WIRC 00170772 • 1 ♂; Wisconsin, Columbia County, Goose Pd. Sue Ames; DNR Study SSGB leg.; galled plant material collected Fall 2008; reared from stem of *Silphium laciniatum*, emerging in July 2009; WIRC 00170816 • 1 ♀; Wisconsin, Columbia County, Hopkins Restoration; DNR Study SSGB leg.; galled plant material collected Fall 2008; reared from stem of *Silphium laciniatum*, emerging in July 2009; WIRC 00170661 • 1 ♂; Wisconsin, Dane County, Badger Pr. Park North; DNR Study SSGB leg.; galled plant material collected 3 Apr 2012; reared from stem of *Silphium laciniatum*, emerging in May 2012; WIRC 00170757 • 1 ♂; Wisconsin, Dane County, E-way @ Mooreland; DNR Study SSGB leg.; galled plant material collected 4 Apr 2012; reared from stem of *Silphium laciniatum*, emerging in Apr 2012; WIRC 00170683 • 2 ♀; Wisconsin, Dane County, Smith Drumlin; 42.98988, -89.06097; DNR Study SSGB leg.; galled plant material collected 15 Apr 2009; reared from stem of *Silphium laciniatum*, emerging in May 2009; WIRC 00170786; 00170788 • 2 ♂; Wisconsin, Dane County, Waubesa Wetlands; WDNR Misc/SB Sauer leg.; galled plant material collected Apr 2007; reared from stem of *Silphium laciniatum*, emerging before 19 May 2007; WIRC 00170805; 00170807 • 2 ♂; Wisconsin, Grant County, Dewey Heights Prairie; 42.734647, -91.020306; DNR Study SSGB leg.; galled plant material collected 14 Oct 2011; reared from stem of *Silphium laciniatum*, emerging in May 2012; WIRC 00170664; 00171400 • 2 ♀; Wisconsin, Green County, Green Cemetery Prairie; DNR Study

SSGB leg.; galled plant material collected 4 Apr 2012; reared from stem of *Silphium laciniatum*, emerging in May 2012; WIRC 00170663; 00170758 • 1 ♂; Wisconsin, Green County, Muralt - South; 42.695505, -89.49367; DNR Study SSGB leg.; galled plant material collected 4 Apr 2012; reared from stem of *Silphium laciniatum*, emerging in May 2012; WIRC 00170754 • 1 ♂; Wisconsin, Iowa County, Hollandale Seed Orchard; DNR Study SSGB leg.; galled plant material collected 5 Apr 2012; reared from stem of *Silphium laciniatum*, emerging in May 2012; WIRC 00170756 • 1 ♂; Wisconsin, Iowa County, TNC/Lease; 42.97357, -89.88900; DNR Study SSGB leg.; galled plant material collected 17 Apr 2009; reared from stem of *Silphium laciniatum*, emerging in May 2009; WIRC 00170678 • 1 ♂; Wisconsin, Kenosha County, Bain Station; 42.556352, -87.893763; DNR Study SSGB leg.; galled plant material collected 30 Sep 2011; reared from stem of *Silphium laciniatum*, emerging in May 2012; WIRC 00170778 • 1 ♀; Wisconsin, Waukesha County, Scuppernong Prairie State Natural Area; 42.89947, -88.50180; DNR Study SSGB leg.; galled plant material collected 15 Apr 2009; reared from stem of *Silphium laciniatum*, emerging in June 2009; WIRC 00170637.

Diagnosis. *A. minor* is the only described species of *Antistrophus* in which the mesoscutellar disc is strongly ovate and distinctly wider than long (Fig. 7F). Additionally, *A. minor* is easily separable from *A. rufus* (which also induces inconspicuous galls in stems of the *S. laciniatum*) and *A. meganae* by the shape and length of the mesoscutellar foveae; in *A. minor*, the mesoscutellar foveae are subquadrate and reach about one third across the mesoscutellar disc (Fig. 7F) but are shorter and subrectangular in *A. rufus* (Fig. 8F) and longer and ovate in *A. meganae* (Fig. 6F). *A. minor* and *A. meganae* are also the only species of the *rufus* complex in which the POL is longer than the OOL. See additional comments in the diagnosis to *A. rufus*.

Description. Female (Fig. 7A)—**Body length:** 1.4–2.4 mm (\bar{x} = 2.0 mm; n = 25; lectotype = 2.3). **Color:** Antenna color: red brown throughout, at most slightly darker distally than proximally. Head color: vertex and occiput dark red brown, mandibles red brown basally to darker red brown apically, rest of head red brown throughout. Color: pronotum and propodeum mostly red brown, with some dark red brown coloration medially, mesoscutum dark red brown with at least distinct red brown spots posterolaterally, scutellum red brown to dark red brown, and mesopleuron dark red brown to red brown. Wing membrane color: hyaline throughout. Wing vein color: light brown. Leg color: red brown throughout, except for apical tarsomere which is conspicuously darker. Metasoma color: red brown to dark red brown. **Antennae** (Fig. 7B): Antennomere count: 13. F1 length: 2.6× as long as wide. F2 length: 3.6× as long as wide. F2:F1 length ratio: 1.4. Placodeal sensilla on F2: absent; sensilla present only on F3 and following antennomeres. **Head** (Fig. 7C): Upper frons sculpture: reticulate. Gena posterolateral projection in anterior view: distinctly projecting past compound eyes. Facial radiating striae: distinct and complete, reaching compound eyes. Supraclypeal area sculpture: reticulate. Supraclypeal area projection: slightly projecting. OOL vs POL: POL distinctly longer. OOL vs LOL: OOL twice LOL. POL vs LOL: POL greater than twice LOL. LOL vs DLO: LOL longer. Vertex sculpture:

reticulate throughout. Clypeus sculpture: reticulate. **Mesosoma** (Figs 7D–F): Pronotum pilosity: densely pilose along anterior margin and with only sparse setae elsewhere. Pronotum excluding pronotal plate sculpture: reticulate. Pronotal plate sculpture: reticulate. Mesopleuron excluding speculum sculpture: reticulate with fine intermediate striae. Speculum sculpture: reticulate. Mesopleuron pilosity: ventral margin and mesopleural triangle densely pilose and bare elsewhere. Mesoscutum pilosity: sparsely pilose. Mesoscutum sculpture: reticulate. Apparent length of anterior parallel lines: reaching one third across mesoscutum. Morphology of anterior parallel lines: narrow, distinct throughout perceptible length. Apparent length of parapsidal grooves: reaching halfway across mesoscutum. Morphology of parapsidal grooves: narrow, distinct throughout perceptible length. Morphology of median mesoscutal impression: apparent as a shallow impression extending across most of mesoscutum. Notauli completeness: incomplete, distinct posteriorly to indistinct in anterior third. Morphology of notauli: appearing as wide indentations with sloping edges throughout distinct portions. Metapleural sulcus: meeting posterior mesopleuron at about one third of its height. Lateral propodeal carinae: distinct and subparallel. Metapleuron sculpture: reticulate. Mesoscutellar foveae distinction: distinct, relatively deep anteriorly to shallower and inconspicuously delimited posteriorly. Mesoscutellar foveae sculpture: reticulate. Mesoscutellar disc sculpture: rugose-reticulate, primarily reticulate, but with distinct rugose-reticulate sculpture seemingly restricted to outer margins. Mesoscutellar foveae length: long, reaching about one third across mesoscutellar disc. Mesoscutellar foveae shape: subovate, slightly longer than wide, separated by a narrow linear carina. Mesoscutellar disc shape: ovate, distinctly longer than wide. **Wings**: Marginal cell length: 3.1× as long as wide. Fore wing distal fringe of marginal setae: absent. **Metasoma**: Punctuation of metasomal terga: T3 punctate only in posterior third and with T4 and following punctate throughout.

Male (Fig. 7G)—Same as female except for the following: **Body length**: 1.1–2.0 mm (\bar{x} = 1.6; n = 25). **Antennae**: Antennomere count: 14. F1 length: 2.3× as long as wide. F2 length: 2.9× as long as wide. F2:F1 length ratio: 1.3. Placodeal sensilla on F2: present. **Wings**: Fore wing distal fringe of marginal setae: present. **Metasoma**: Metasoma size: conspicuously smaller than in female.

Biology. *Antistrophus minor* induces inconspicuous, externally imperceptible galls in stems of *Silphium laciniatum* (Fig. 7H) (Tooker et al. 2004; Nastasi and Deans 2021). Weld (1926) reported *A. minor* from *Silphium terebinthinaceum*, but Weld's specimens from this host plant truly represent *Antistrophus meganae*.

Distribution. *Antistrophus minor* was described from adults reared alongside *A. rufus* in Illinois. We examined specimens providing new state records from Iowa and Wisconsin. Known and potential distribution are summarized in Fig. 9. It appears that *A. minor* is likely sympatric with *A. rufus* throughout the distribution of *S. laciniatum*, although further rearing of *Silphium* species will be needed to better understand the role of geography in the distribution of *Antistrophus*, especially regarding these two species.

Remarks. See remarks under *Antistrophus rufus* for notes on generic nomenclature and distinction of *A. minor* from *A. rufus*.

***Antistrophus rufus* Gillette, 1891**

Fig. 8

Antistrophus rufus Gillette, 1891: 195. ♀, ♂ (type locality: unknown location in Illinois, USA).

Aulax rufa (Gillette, 1891): Kieffer 1902: 93.

Material examined. Lectotype (deposited at INHS; designated by Frison [1927]). USA • ♀; Illinois; reared from stem of *Silphium laciniatum*; record number 5500; INHS Insect Collection 52812.

Lectoallotype (deposited at INHS; designated by Frison [1927]). USA • ♂; same data as lectotype; INHS Insect Collection 52813.

Paralectotypes. Deposited at AMNH: USA • 1 ♀; same data as lectotype; AMNH_IJC 00393875.

Deposited at INHS: USA • 3 ♀ and 1 ♂; same data as lectotype; INHS Insect Collection 294742–294745.

Deposited at USNM: USA • 4 ♀ and 2 ♂; same data as lectotype; USNMMENT 00961146; 01822098–01822102.

Other material (16 ♀ and 21 ♂). Deposited at INHS: • 5 ♀ and 1 ♂; Illinois, Iroquois County, Buckley Railroad Prairie; J. Tooker leg.; reared from stem of *Silphium laciniatum*, emerging in June 2000; INHS Insect Collection 52815–52818; 52820–52821 • 1 ♀ and 1 ♂; Illinois, McLean County, Chenoa, Weston Cemetery Prairie; J. Tooker leg.; reared from stem of *Silphium laciniatum*, emerging in June 2000; INHS Insect Collection 18238–18239.

Deposited at PSUC: USA • 3 ♀ and 4 ♂; Illinois, Champaign County, Gifford, Shortline Railroad Prairie; 40.305, -87.999; JF Tooker and AR Deans leg.; galled plant material collected 10 Nov 2020; reared from stem of *Silphium laciniatum*, emerging in May or June 2021; PSUC_FEM_248301; 248307; 248310; 248315–248317 • 1 ♀ and 1 ♂; Illinois, McLean County, Chenoa, Weston Cemetery Prairie; 40.725, -88.606; JF Tooker and AR Deans leg.; galled plant material collected 11 Nov 2020; reared from stem of *Silphium laciniatum*, emerging in May or June 2021; PSUC_FEM_248293; 248296 • 1 ♀ and 7 ♂; Iowa, Story County, Grant, Interstate 35 and E 13th St. Prairie Restoration; MJ Hatfield leg.; galled plant material collected 30 Nov 2020; reared from stem of *Silphium laciniatum*, emerging in May or June 2021; PSUC_FEM_248163; 248308; 248311–248313; 248318–248320.

Deposited at USNM: USA • 1 ♀ and 2 ♂; Illinois, Ford County, Gifford, Ludlow Railroad Prairie; J. Tooker leg.; reared from stem of *Silphium laciniatum*, emerging in June 2000; USNMMENT 01822106; 01822109–01822110 • 2 ♀ and 1 ♂; Illinois, Iroquois County, Buckley Railroad Prairie; J. Tooker leg.; reared from stem of *Silphium laciniatum*, emerging in June 2000; USNMMENT 01822104; 01822107–01822108 • 7 ♀ and 2 ♂; Illinois, Vermillion County, Fithian Railroad Prairie; J. Tooker leg.; reared from stem of *Silphium laciniatum*, emerging in June 2000; INHS Insect Collection 52822–52828; UNSMMENT 01822103; 01822105 • 1 ♂; Illinois, Evanston; reared; UNSMMENT 01822112.

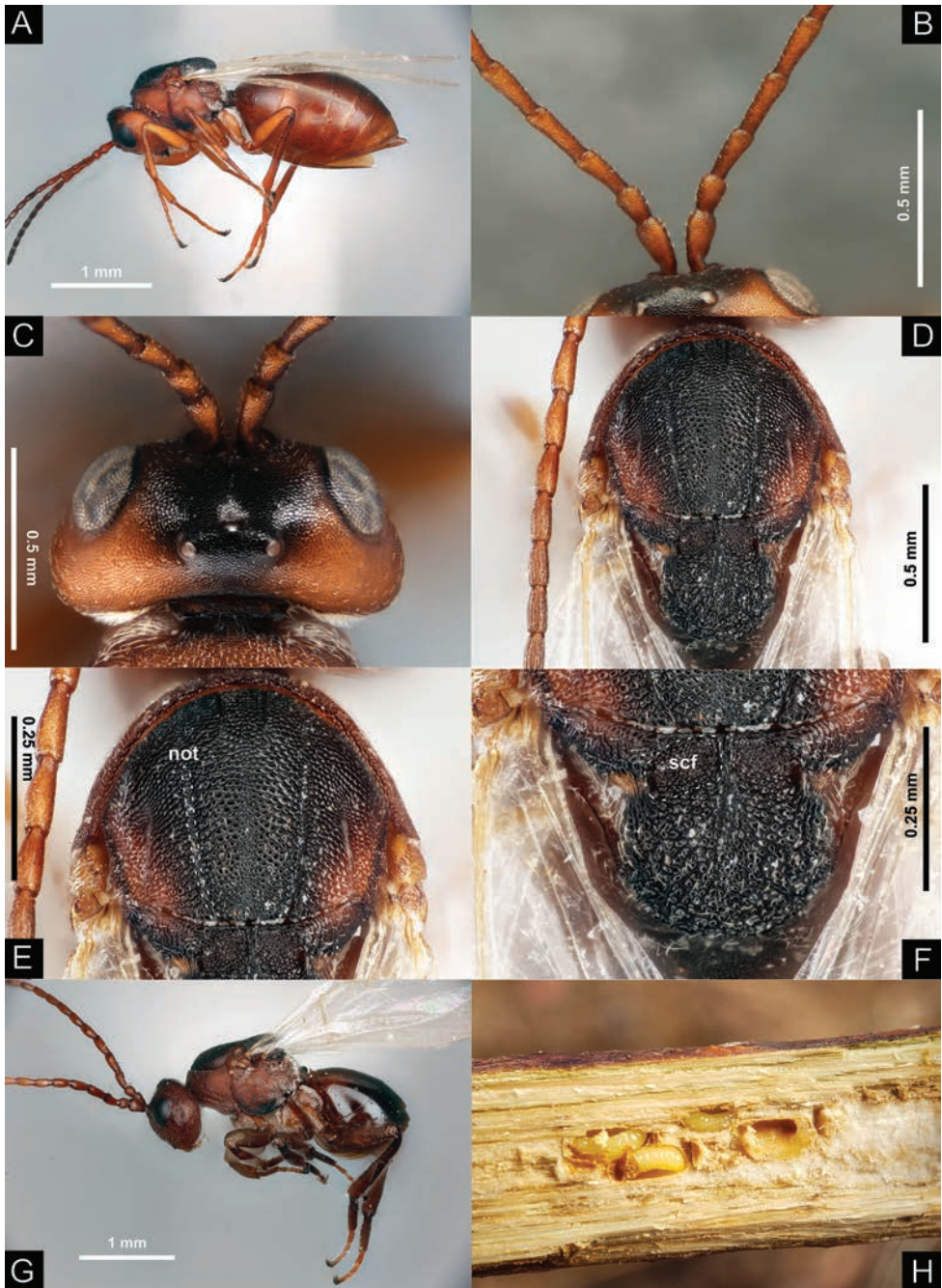


Figure 8. *Antistrophus rufus* Gillette, 1891 **A** female lateral habitus (PSUC_FEM_248316) **B** female proximal antennomeres (PSUC_FEM_246062) **C** female dorsal head (PSUC_FEM_246062) **D** female dorsal mesosoma (PSUC_FEM_253129) **E** female dorsal mesoscutum (PSUC_FEM_253129); not = notaulus **F** female dorsal scutellum (PSUC_FEM_253129); scf = mesoscutellar fovea **G** male lateral habitus (PSUC_FEM_248308) **H** galls and larvae of *A. minor* or *A. rufus* in a stem of *Silphium laciniatum* L.

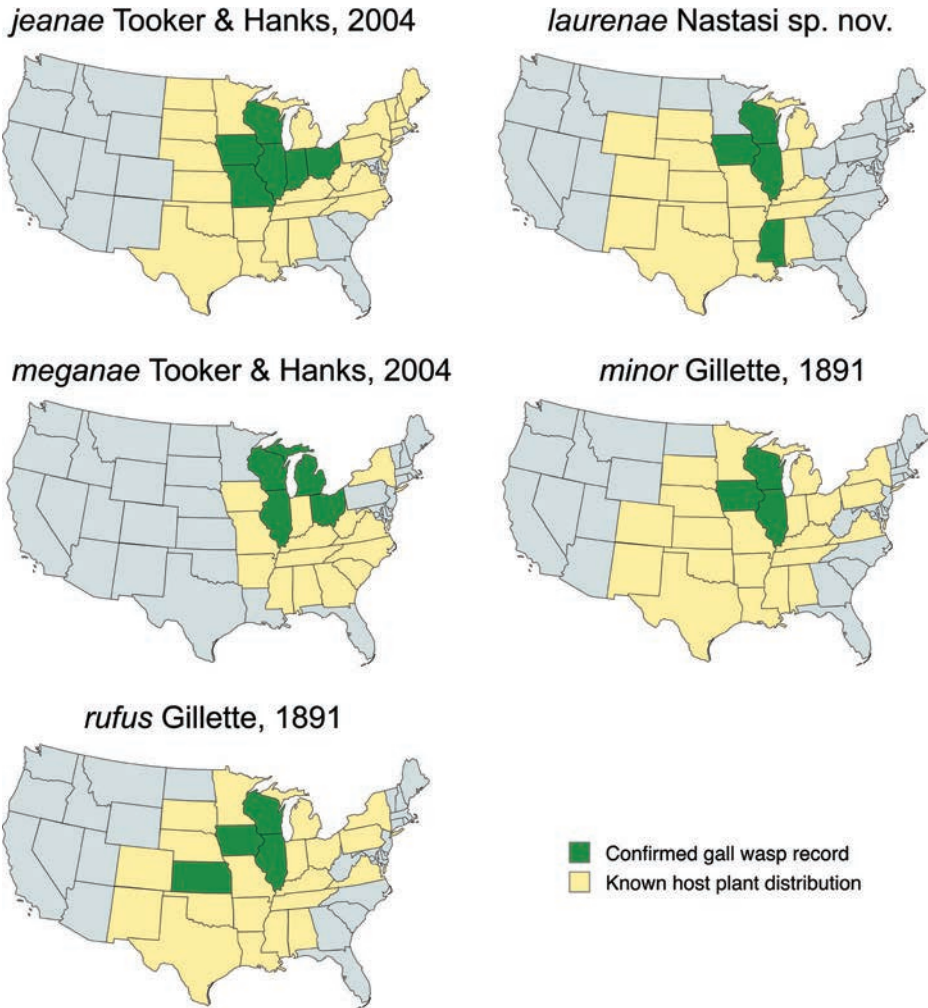


Figure 9. Known and potential distributions for species of the *Antistrophus rufus* complex. Host plant distribution follows Kartesz (2015). States in green reflect established distribution, while states in yellow reflect potential distribution based on records of the host plant.

Deposited at WIRC: USA • 1 ♀; Wisconsin, Columbia County, Goose Pd. Bicentennial; DNR Study SSGB leg.; galled plant material collected Fall 2008; reared from stem of *Silphium laciniatum*, emerging in July 2009; WIRC 00170506 • 1 ♀; Wisconsin, Dane County, Thousands Rock Pt. Pr.; 42.99064, -89.8303; DNR Study SSGB leg.; galled plant material collected 17 Apr 2009; reared from stem of *Silphium laciniatum*, emerging in May 2009; WIRC 00170687 • 1 ♂; Wisconsin, Waukesha County, Scuppernong Prairie State Natural Area; 42.89947, -88.5018; DNR Study SSGB leg.; galled plant material collected 15 Apr 2009; reared from stem of *Silphium laciniatum*, emerging in Apr 2009; WIRC 00170643.

Diagnosis. *A. rufus* is easily recognized amongst members of the *rufus* complex by the shape and dimensions of the mesoscutellar foveae (Fig. 8F), which are short and

subrectangular in *A. rufus* but longer and subquadrate or ovate in the other species. The narrow, well-defined notauli (Fig. 8E) are also characteristic, as the other species all have wider and less-defined notauli. The smallest *A. rufus* specimens may exhibit slightly wider notauli, but the short, rectangular scutellar foveae are always apparent and readily distinguish this species from others. *A. rufus* also has the shortest F2 relative to its width in females (2.8× as long as wide; Fig. 8B)).

A. rufus are commonly reared alongside *A. minor* from inconspicuous, externally imperceptible galls in stems of *Silphium laciniatum* L.; these species are separated by the characters given above and those in the diagnosis of *A. minor*.

Description. Female (Fig. 8A)—**Body length**: 2.3–3.6 mm (\bar{x} = 2.9 mm; n = 25; lectotype = 2.8 mm). **Color**: Antenna color: red brown throughout, at most slightly darker distally than proximally. Head color: vertex and occiput dark red brown, mandibles red brown basally to darker red brown apically, rest of head red brown throughout. Mesosoma color: pronotum and propodeum red brown laterally to dark red brown medially, mesoscutum dark red brown with distinct posterolateral red brown spots, scutellum dark red brown, and mesopleuron dark red brown dorsally and ventrally but red brown medially. Wing membrane color: hyaline throughout. Wing vein color: light brown. Leg color: red brown throughout, except for apical tarsomere which is conspicuously darker. Metasoma color: red brown to dark red brown. **Antennae** (Fig. 8B): Antennomere count: 13. F1 length: 2.4× as long as wide. F2 length: 2.8× as long as wide. F2:F1 length ratio: 1.2. Placodeal sensilla on F2: absent; sensilla present only on F3 and following antennomeres. **Head** (Fig. 8C): Upper frons sculpture: reticulate. Gena posterolateral projection in anterior view: distinctly projecting past compound eyes. Facial radiating striae: distinct and complete, reaching compound eyes. Supraclypeal area sculpture: reticulate. Supraclypeal area projection: slightly projecting. OOL vs POL: OOL distinctly longer. OOL vs LOL: OOL greater than twice LOL. POL vs LOL: POL twice LOL. LOL vs DLO: LOL longer. Vertex sculpture: reticulate throughout. Clypeus sculpture: reticulate. **Mesosoma** (Figs 8D–F): Pronotum pilosity: densely pilose along anterior margin and with only sparse setae elsewhere. Pronotum excluding pronotal plate sculpture: reticulate. Pronotal plate sculpture: reticulate. Mesopleuron excluding speculum sculpture: reticulate with fine intermediate striae. Speculum sculpture: reticulate. Mesopleuron pilosity: ventral margin and mesopleural triangle densely pilose and bare elsewhere. Mesoscutum pilosity: sparsely pilose. Mesoscutum sculpture: reticulate. Apparent length of anterior parallel lines: reaching one third across mesoscutum. Morphology of anterior parallel lines: narrow, distinct throughout perceptible length. Apparent length of parapsidal grooves: reaching halfway across mesoscutum. Morphology of parapsidal grooves: narrow, distinct throughout perceptible length. Morphology of median mesoscutal impression: apparent as a shallow impression extending across most of mesoscutum. Notauli completeness: incomplete, distinct posteriorly to indistinct in anterior third. Morphology of notauli: appearing as narrow, well-delimited indentations throughout distinct portions. Metapleural sulcus: meeting posterior mesopleuron at about one third of its height. Lateral propodeal carinae: distinct and subparallel. Metapleuron sculpture: reticulate. Mesoscutellar foveae distinction: distinct, relatively deep anteriorly to shallower and inconspicuously delimited posteriorly. Mesoscutellar foveae sculpture: reticulate. Mesoscutellar disc sculpture: rugose-

reticulate, primarily reticulate, but with distinct rugose-reticulate sculpture seemingly restricted to outer margins. Mesoscutellar foveae length: short, occupying only anterior quarter of mesoscutellar disc. Mesoscutellar foveae shape: subrectangular, distinctly wider than long, and separated by a broad, elevated linear carina. Mesoscutellar disc shape: subcircular, about as wide as long. **Wings:** Marginal cell length: $2.7\times$ as long as wide. Fore wing distal fringe of marginal setae: absent. **Metasoma:** Punctuation of metasomal terga: T3 punctate only in posterior third and with T4 and following punctate throughout.

Male (Fig. 8G)—Same as female except for the following: **Body length:** 1.9–3.5 mm ($\bar{x} = 2.5$ mm; $n = 25$). **Antennae:** Antennomere count: 14. F1 length: $2.1\times$ as long as wide. F2 length: $2.5\times$ as long as wide. F2:F1 length ratio: 1.3. Placodeal sensilla on F2: present. **Wings:** Fore wing distal fringe of marginal setae: present. **Metasoma:** Metasoma size: conspicuously smaller than in female.

Biology. *Antistrophus rufus* induces inconspicuous, externally imperceptible galls in stems of *Silphium laciniatum* (Fig. 8H) (Tooker et al. 2004; Nastasi and Deans 2021). Records associating *A. rufus* with other host plants most likely represent distinct species including the other species addressed in the present work.

Distribution. *Antistrophus rufus* was described from material collected in Illinois (USA) and has since been reported from Kansas (Tooker et al. 2004; Nastasi and Deans 2021). Additional material that we examined revealed additional records from Iowa and Wisconsin, and reiterated occurrence of this species in Kansas (Suppl. material 1: table 1). Known and potential distribution are summarized in Fig. 9.

Remarks. Kieffer (1902) synonymized *Antistrophus* with *Aylax* (= *Aulax*) Hartig, 1840. Some authors (e.g., Beutenmüller 1910) follow Kieffer's synonymy, but others appear to have rejected or otherwise omitted this change from many works treating the group (e.g., Weld 1951; Nieves-Aldrey 1994). This generic synonymy and the resulting species synonyms were accidentally omitted from Nastasi and Deans' (2021) catalogue, and we are unable to locate a nomenclatural act reinstating *Antistrophus* as a valid genus. The genus *Aylax* has now long been regarded to include only two species of gall wasps inducing galls on *Papaver* (Papaveraceae) (Nieves-Aldrey 1994; Ronquist et al. 2015). Additionally, the two genera are now placed in different tribes: *Aylax* is now placed in the tribe Aylacini, while *Antistrophus* is placed in the Aulacideini. We regard here *Antistrophus* as a valid genus independent of *Aylax*, although *Antistrophus* represents a heterogeneous assemblage as currently defined based on preliminary data from an ongoing revisionary study (Nastasi et al., unpublished data).

Lastly, two specimens labeled as paralectotypes in the USNM collection (USNM-ENT 01823001; 01823000) do not appear to be *Antistrophus rufus* and more closely resemble *A. minor*. They are both in relatively poor condition; at this time, their species identities cannot be substantiated due to damage to multiple body parts.

Key to the species of the *Antistrophus rufus* complex

Our assessment of diagnostic characters allowed for development of a key to the species of the *rufus* complex. A key to all species of *Antistrophus* is beyond the scope of this work but will be prepared as part of ongoing revisionary studies of North

American herb gall wasps (Nastasi et al., unpublished data). For best results using this key, we recommend using light diffusion in combination with high magnification (see Methods).

Before running a specimen through the below key, one should confirm that it is indeed an *Antistrophus* species using the keys in Nastasi et al. (2024) and/or Buffington et al. (2020) where appropriate, and then confirming that the specimen belongs to the *A. rufus* complex using the diagnostic criteria given in the diagnosis to the *A. rufus* complex and in Table 2.

- 1 Mesoscutellar disc (Fig. 7F) elongate and ovate, about 1.3× as long as wide. Galls in stems of *Silphium laciniatum*.....***A. minor***
- Mesoscutellar disc subcircular, about 1.1× as long as widest width (Figs 4F, 5F, 6F, 8F). Galls in stems of various *Silphium* including *S. laciniatum***2**
- 2 Mesoscutellar foveae (Fig. 8F) subrectangular, distinctly wider than long, and relatively short, only about one fourth as long as mesoscutellar disc. Notauli (Fig. 8E) usually apparent as narrower, well-defined lines throughout distinct portion. F2 of female about 2.8× as long as wide (Fig. 8B). Galls in stems of *Silphium laciniatum****A. rufus***
- Mesoscutellar foveae subquadrate or ovate, at least as long as wide, and relatively longer, at least one third as long as mesoscutellar disc (Figs 4F, 5F, 6F). Notauli apparent as wider, sloping indentations throughout distinct portion (Figs 4E, 5E, 6E). F2 of female longer, at least 3.3× as long as wide. Galls in stems of other hosts**3**
- 3 Mesoscutellar foveae (Fig. 6F) ovate, longer than wide, and reaching nearly halfway across mesoscutellar disc. POL longer than OOL (Fig. 6C). Galls in stems of *Silphium terebinthinaceum* ***A. megalae***
- Mesoscutellar foveae subquadrate, occupying anterior third of mesoscutellar disc (Figs 5F, 6F). POL shorter than OOL (Figs 5C, 6C). Galls in stems of other hosts **4**
- 4 F2 of female about 3.8× as long as wide (Fig. 4B). Mesoscutellar disc (Fig. 4F) usually with coarser sculpture, with sculpture mostly rugose-reticulate, especially medially. Galls in stems of *Silphium perfoliatum****A. jeanae***
- F2 of female about 3.3× as long as wide (Fig. 5B). Mesoscutellar disc (Fig. 5F) mostly reticulate, with rugose sculpture restricted to outer margins. Galls in stems of *Silphium integrifolium* ***A. laurenae***

Discussion

Our findings suggest that the species belonging to the *A. rufus* complex are not truly cryptic, and are readily identifiable with appropriate diagnostic characters. Other species complexes of herb gall wasps might benefit from a similar investigation of morphological species boundaries, especially species of *Aulacidea* Ashmead inducing galls on *Lactuca* L. or other *Antistrophus* inducing externally perceptible galls on terminal

stems and in flowers of *Silphium*. Such analyses would supplement the original descriptions and would help determine whether true cryptic species occur in Aulacideini.

While the taxonomic impediment impacts a tremendous number of species across all taxa, especially in groups such as “little brown beetles,” microlepidoptera, and many groups of parasitic wasps, our study of the *A. rufus* complex demonstrates that such issues can be disentangled with dedicated revisionary approaches. While no number of characters can ensure discovery of novel diagnostic characters, attempts to evaluate larger numbers of characters, as attempted here, may help decipher boundaries of cryptic species that would otherwise require molecular characters or additional methods. Examining 50 characters proved sufficient for the *rufus* complex, but for other taxa, it could be useful to apply a “brute force” approach involving a much greater number of candidate morphological characters. In such a scenario, different groups of characters could be tested iteratively until robust species diagnoses are achieved.

After developing the key to the *rufus* complex that we present above, we keyed and identified over 50 additional specimens belonging to the *rufus* complex from the INHS and USNM collections (Suppl. material 1: table 1), including both already determined and previously unidentified material. One series of specimens deposited at USNM represents a new state record of *A. meganae* from Michigan; these specimens’ labels suggesting they were collected off “elecampane” (presumably referring to *Inula helenium* L.), but this likely constitutes a misidentification of the proper host plant *Silphium terebinthinaceum* which is rather similar visually. We found a single specimen of *A. jeanae* amongst unsorted material in the USNM collection (USNMENT 01822302); this specimen was collected in Missouri and represents a new state record (see also remarks for *A. jeanae*).

Our examination indicates that *A. minor* is truly a species distinct from *A. rufus* despite previous suggestion that they may be synonymous. In various cynipid taxa, including Aulacideini, a single host plant species is galled by several distinct species of gall wasps (Nieves-Aldrey et al. 2004; Melika 2006; Nastasi and Deans 2021; Nastasi et al. 2024). However, few (if any) gall wasps share the same host plant while inhabiting the same plant organ and the same portion of gall phenospace (i.e., host plant organ combined with gall phenotype). While most of the *A. rufus* complex species each occupy a unique host plant species, the *Antistrophus rufus* complex appears to be somewhat unique among gall wasps, as two species both induce inconspicuous galls within the stems of the same host plant *S. laciniatum*. This suggests speciation mechanisms may be involved (e.g., geographic isolation or host switching) that may not follow the typically observed speciation in gall wasps, which normally is associated with shifts between host plants or gall morphotypes, at least in oak gall wasps (Cynipini) or their inquilines (Synergini *sensu lato*) (e.g., Ward et al. 2020, 2022, 2024).

Regarding evolution of host plant associations, the topology of our Bayesian analysis provides suggestion of cospeciation of *A. rufus* complex species with their host plants, as there was sorting of *A. rufus* complex species by host plant lineage (Fig. 2). Clevinger and Panero’s (2000) phylogenetic analysis of ETS and ITS markers suggested two major clades of *Silphium*; the *rufus* complex includes species associated with both

sections. Their sect. *Composita* includes species with deep taproots and prominent basal rosettes, including *S. laciniatum* and *S. terebinthinaceum*, while their sect. *Silphium* is composed mostly of species with more fibrous roots and without prominent basal rosettes, including *S. integrifolium* and *S. perfoliatum*. In our phylogenetic analysis, species galling sect. *Silphium* (*A. jeanae* and *A. laurennae*) formed a well-supported clade sister to the three species galling sect. *Composita* (*A. meganae*, *A. minor*, and *A. rufus*), although the latter clade was less strongly supported (posterior probability = 0.89).

More generally, our data show that each studied *Silphium* species has distinct species of *Antistrophus* occupying their stems. While the present study focused on the “big four” species of *Silphium* ubiquitous in prairies in the Midwestern U.S., a recent taxonomic treatment (Brock and Weakley 2020) suggests there are as many as 23 *Silphium* species; it is likely that more species of the *rufus* complex or other *Antistrophus* will be revealed in these other species. The deep divergences in DNA barcodes among these gall wasps suggest a long history of isolation and may indicate that additional species of the *A. rufus* complex await discovery and description. While interspecific divergences in our DNA barcode data are much higher than the supposed 2% “barcode gap” between animal species, other studies of diverse insect groups often find divergence in excess of 10% between congeneric species (Pentisaari et al. 2014; Lin et al. 2015; Song et al. 2018). Locating additional undescribed members of the *rufus* complex could aid in resolving relationships amongst the known species, and future research on host plant affinity and co-phylogeny between *Silphium* and their gall wasps will help inform understanding of these processes.

Acknowledgments

We thank many individuals for their contributions to this manuscript: R. Luke Kresslein co-proposed the symposium for the 2022 Entomological Society of America annual meeting that inspired this study. Matt Buffington assisted us in imaging specimens at USNM, as well as providing valuable advice in cynipid taxonomy. Mason Brock provided valuable commentary on systematics of *Silphium*. Jim Nardi allowed us to collect on his property. The Grand Prairie Friends and the Illinois Nature Preserves Commission provided permits for field collection in Illinois. José-Luis Nieves-Aldrey provided commentary on taxonomy of Aulacideini. Richard Henderson, Jay Watson, and Zhiwei Liu provided material and commentary on the *Silphium* gall wasp system. Katherine Myers transcribed some gall wasp label data for material referenced in this study. Antoine Guiguet assisted in rearing gall wasps and allowed us to use his phenomenal photographs of adult gall wasps. Antonio Casadei assisted with field collections. Laura Porturas and Codey Mathis provided much-needed encouragement and support to the Frost Entomological Museum team during the course of this study. Jimmie Thompson and many others provided many specimens that we have been referencing in our ongoing studies of herb gall wasp systems.

We are also indebted to the following individuals for making their respective collections accessible to us for this study: Jim Carpenter, Christine LeBeau, and Melody

Doering (AMNH); Tommy McElrath, Chris Dietrich, and Michelle Kohler (INHS); Craig Brabant and Dan Young (WIRC); and Matt Buffington and Cecilia Escobar (USNM).

Lastly, Matt Buffington, José Luis Nieves-Aldrey, and Y. Miles Zhang contributed excellent reviews that greatly improved the quality of our manuscript.

The first author was generously supported by two awards from the Society of Systematic Biologists: Mini-ARTS and the Graduate Student Research Award.

This material is based, in part, upon work supported by the National Science Foundation under Grant Nos. DEB-1856626 and DEB-2338008. Any opinions, findings, and conclusions or recommendations expressed in this material are those of the authors and do not necessarily reflect the views of the National Science Foundation.

References

- Andrews KR, Gerritsen A, Rashed A, Crowder DW, Rondon SI, van Herk WG, Vernon R, Wanner KW, Wilson CM, New DD, Fagnan MW, Hohenlohe PA, Hunter SS (2020) Wireworm (Coleoptera: Elateridae) genomic analysis reveals putative cryptic species, population structure, and adaptation to pest control. *Communications Biology* 3: 489. <https://doi.org/10.1038/s42003-020-01169-9>
- Ashmead WH (1887) On the cynipidous galls of Florida, with descriptions of new species and synopses of the described species of North America. *Transactions of the American Entomological Society* 14: 125–158. <https://doi.org/10.2307/25076487>
- Ashmead WH (1896) Descriptions of new cynipidous galls and gall-wasps in the United States National Museum. *Proceedings of the United States National Museum* 19(1102): 113–136. <https://doi.org/10.5479/si.00963801.19-1102.113>
- Ashmead, WH (1897) Description of some new genera in the family Cynipidae. *Psyche* 8(253): 67–69. <https://doi.org/10.1155/1897/60546>
- Azmaz M, Katılmış Y (2020) A new species of herb gall wasp (Cynipidae, Aulacideini, Aulacidea) from Turkey. *Zootaxa* 4747(2): 378–390. <https://doi.org/10.11646/zootaxa.4747.2.9>
- Bassett HF (1890) New species of North American Cynipidae. *Transactions of the American Entomological Society* 17(1): 59–92.
- Beutenmüller W (1908) A new cynipid from Arizona. *Journal of the New York Entomological Society* 16: 45.
- Beutenmüller W (1910a) The North American species of *Aylax* and their galls. *Bulletin of the American Museum of Natural History* 28: 137–144.
- Beutenmüller W (1910b) The North American species of *Aulacidea* and their galls. *Bulletin of the American Museum of Natural History* 28: 253–258.
- Borowiec ML (2016) AMAS: a fast tool for alignment manipulation and computing of summary statistics. *PeerJ* 4:e1660. <https://doi.org/10.7717/peerj.1660>
- Brock M, Weakley AS (2020) *Silphium* Linnaeus 1753 (Rosinweed) In: Weakley AS (Ed.) *Flora of the Southeastern United States*. University of North Carolina at Chapel Hill Herbarium (Chapel Hill, North Carolina), 1563–1566.

- Brodie WM (1892) Canadian galls and their occupants—*Aulax nabali*, N. S. The Canadian Entomologist 24(1): 12–14. <https://doi.org/10.4039/ent2412-1>
- Buffington ML, Forshage M, Liljeblad J, Tang CT, van Noort S (2020) World Cynipoidea (Hymenoptera): a key to higher-level groups. Insect Systematics and Diversity 4(4): 1. <https://doi.org/10.1093/isd/ixaa003>
- Buffington ML, Prasifka JR, Gates MW, Kula RR, Peterson K (2017) New host plant and distribution records for *Antistrophus laciniatus* Gillette, 1891 (Hymenoptera: Cynipidae), an herb gall wasp on *Silphium integrifolium* Michx.(Asteraceae), with notes on other *S. integrifolium*-associated wasps. Proceedings of the Entomological Society of Washington 119(4): 660–666. <https://doi.org/10.4289/0013-8797.119.4.660>
- Clevinger JA, Panero JL (2000) Phylogenetic analysis of *Silphium* and subtribe Engelmanniinae (Asteraceae: Heliantheae) based on ITS and ETS sequence data. American Journal of Botany 87(4): 565–572. <https://doi.org/10.2307/2656600>
- von Cossel M, Amarysti C, Wilhelm H, Priya N, Winkler B, Hoerner L (2020) The replacement of maize (*Zea mays* L.) by cup plant (*Silphium perfoliatum* L.) as biogas substrate and its implications for the energy and material flows of a large biogas plant. Biofuels, Bioproducts and Biorefining 14(2): 152–179. <https://doi.org/10.1002/bbb.2084>
- Deans AR, Nastasi LF, Montelongo DC (2023) Glossary of gall terms. V7. <https://doi.org/10.26207/22e9-ck06> [Accessed 16 March 2023]
- Folmer O, Black M, Hoeh W, Lutz R, Vrijenhoek R (1994) DNA primers for amplification of mitochondrial cytochrome c oxidase subunit I from diverse metazoan invertebrates. Molecular Marine Biology and Biotechnology 3(5): 294–299.
- Frison TH (1927) A list of the insect types in the collections of the Illinois State Natural History Survey and the University of Illinois. Illinois Natural History Survey Bulletin 16(04): 1–7. <https://doi.org/10.21900/j.inhs.v16.295>
- Gillette CP (1891) Descriptions of new Cynipidae in the collection of the Illinois State Laboratory of Natural History. Illinois Natural History Survey Bulletin 3(11): 191–206. <http://hdl.handle.net/2142/55691>
- Hansen S, Addison P, Benoit L, Haran JM (2021) Barcoding pest species in a biodiversity hotspot: the South African polyphagous broad-nosed weevils (Coleoptera, Curculionidae, Entiminae). Biodiversity Data Journal 9: e66452. <https://doi.org/10.3897/2FBDJ.9.e66452>
- Harris RA (1979) A glossary of surface sculpturing. Occasional Papers in Entomology 28: 1–31.
- Hartig T (1843) Zweiter nachtrag zur naturgeschichte der Gallwespen. Zeitschrift für Entomologie 4: 395–422.
- Hebert PD, Penton EH, Burns JM, Janzen DH, Hallwachs W (2004) Ten species in one: DNA barcoding reveals cryptic species in the neotropical skipper butterfly *Astraptes fulgerator*. Proceedings of the National Academy of Sciences 101(41): 14812–14817. <https://doi.org/10.1073/pnas.0406166101>
- Henderson R, Sauer SB (2010) *Silphium* gall wasps: little-known prairie specialists. In 22nd North American Prairie Conference. Cedar Falls, Iowa, 116–121.
- Jasinskas A, Simonavičiūtė R, Šiaudinis G, Liaudanskienė I, Antanaitis Š, Arak M, Olt J (2014) The assessment of common mugwort (*Artemisia vulgaris* L.) and cup plant (*Silphium per-*

- foliatum* L.) productivity and technological preparation for solid biofuel. *Zemdirbyste-Agriculture* 101(1): 19–25. <https://doi.org/10.13080/z-a.2014.101.003>
- Kartesz JT (2015) The Biota of North America Program (BONAP). North American Plant Atlas. Chapel Hill, N.C. <http://bonap.net/napa> [accessed 15 April 2024]
- Kinsey AC (1920) New species and synonymy of American Cynipidae. *Bulletin of the American Museum of Natural History* 42: 293–317.
- Kowalski R, Wierciński J (2004) Evaluation of chemical composition of some *Silphium* L. species seeds as alternative foodstuff raw materials. *Polish Journal of Food and Nutrition Sciences* 13(4): 349–354. <https://doi.org/10.3390/agriculture10040132>
- Lanfear R, Calcott B, Ho SY, Guindon S (2012) PartitionFinder: combined selection of partitioning schemes and substitution models for phylogenetic analyses. *Molecular Biology and Evolution* 29(6): 1695–1701. <https://doi.org/10.1093/molbev/mss020>
- Lanfear R, Frandsen PB, Wright AM, Senfeld T, Calcott B (2017) PartitionFinder 2: New Methods for Selecting Partitioned Models of Evolution for Molecular and Morphological Phylogenetic Analyses. *Molecular Biology and Evolution* 34(3):772–773. <https://doi.org/10.1093/molbev/msw260>
- Lin X, Stur E, Ekrem T (2015) Exploring Genetic Divergence in a Species-Rich Insect Genus Using 2790 DNA Barcodes. *PLoS ONE* 10(9): e0138993. <https://doi.org/10.1371/journal.pone.0138993>
- MacLeod N, Canty RJ, Polaszek A (2022) Morphology-based identification of *Bemisia tabaci* cryptic species puparia via embedded group-contrast convolution neural network analysis. *Systematic Biology* 71(5): 1095–1109. <https://doi.org/10.1093/sysbio/syab098>
- McCracken MI, Egbert DB (1922) California gall-making Cynipidae: With descriptions of new species. Stanford University Press (Stanford, California), 70 pp.
- Meier R, Blaimer BB, Buenaventura E, Hartop E, von Rintelen T, Srivathsan A, Yeo D (2021) A re-analysis of the data in Sharkey et al.'s (2021) minimalist revision reveals that BINs do not deserve names, but BOLD Systems needs a stronger commitment to open science. *Cladistics* 38(2): 264–275. <https://doi.org/10.1111/cl.12489>
- Melika G (2006) Gall wasps of Ukraine, Vol. 1. *Vestnik zoologii*, The Schmalhausen Institute of Zoology, National Academy of Sciences of Ukraine (Kiev, Ukraine), 300 pp.
- Nastasi LF, Buffington ML, Davis CK, Deans AR (2024) Key to the North American tribes and genera of herb, rose, bramble, and inquiline gall wasps (Hymenoptera, Cynipoidea, Cynipidae sensu lato). *Zookeys* 1196: 177–207. <https://doi.org/10.3897/zookeys.1196.118460>
- Nastasi LF, Deans AR (2021) Catalogue of Rose Gall, Herb Gall, and Inquiline Gall Wasps (Hymenoptera: Cynipidae) of the United States, Canada and Mexico. *Biodiversity Data Journal* 9: e68558. <https://doi.org/10.3897/BDJ.9.e68558>
- Nastasi LF (2023) SOP LFN-01: Collecting and Rearing Cynipid Wasp Galls on Herbaceous Plants. ScholarSphere, The Pennsylvania State University. <https://doi.org/10.26207/b4p8-zn49>
- Nieves-Aldrey JL (1994) Revision of West-European Genera of the Tribe Aylacini Ashmead (Hymenoptera, Cynipidae). *Journal of Hymenoptera Research* 3: 175–206.
- Nieves-Aldrey JL (2012) Two new herb gall wasps from Spain, including the description of a new species of *Aulacidea* Ashmead, 1897 (Hymenoptera, Cynipidae, "Aylacini") inducing

- galls on *Serratula nudicaulis* L. DC (Asteraceae). Graellsia 68(2): 325–339. <https://doi.org/10.3989/graellsia.2012.v68.077>
- Nieves-Aldrey JL (2022) Description of *Fumariphilus* Nieves-Aldrey, gen. nov., a new genus of herb gall wasps, with a key to genera of the tribe Aulacideini (Hymenoptera: Cynipidae). Zootaxa 5155(3): 393–413. <https://doi.org/10.11646/zootaxa.5155.3.5>
- Nieves-Aldrey JL, Gómez JF, Hernández Nieves M (2004) Nuevos datos sobre *Aulacidea freesei* y *Phanacis zwowlferi* (Hymenoptera, Cynipidae, Aylacini), inductores de agallas en *Silybum marimum* (Asteraceae), en la Península ibérica, incluyendo la descripción y comparación de sus larvas terminales y sus agallas. Boletín de la Sociedad Entomológica Aragonesa 34: 85–93.
- Nieves-Aldrey JL, Sánchez I, Massa B, Gómez JF (2008) Cynipid wasps inducing galls on plants of the genus *Picris* (Asteraceae) in Europe, with a description of a new species of *Phanacis* Foerster (Hymenoptera: Cynipidae) from the Iberian Peninsula. Annales de la Société Entomologique de France 44(3): 257–269. <https://doi.org/10.1080/00379271.2008.10697561>
- Pang Y, Liu Z, Su CY, Zhu DH (2020) A new species of *Periclistus* Foerster, 1869 from China and review of the tribe Diastrophini (Hymenoptera, Cynipoidea, Cynipidae). Zookeys 964: 109–126. <https://doi.org/10.3897/zookeys.964.47441>
- Peni D, Stolarski MJ, Bordican A, Krzyżaniak M, Dębowski M. (2020) *Silphium perfoliatum*—A herbaceous crop with increased interest in recent years for multi-purpose use. Agriculture 10(12): 640. <https://doi.org/10.3390/agriculture10120640>
- Pentinsaari M, Hebert PDN, Mutanen M (2014) Barcoding beetles: A regional survey of 1872 species reveals high identification success and unusually deep interspecific divergences. PLoS ONE 9(9): e108651. <https://doi.org/10.1371/journal.pone.0108651>
- Riley CV, Walsh B (1869) The *Lygodesmia* pea gall. American Entomologist 2: 73–74. <https://www.biodiversitylibrary.org/page/32620520>
- Ronquist F, Liljeblad J (2001) Evolution of the gall wasp-host plant association. Evolution 55(12): 2503–2522. <https://doi.org/10.1111/j.0014-3820.2001.tb00765.x>
- Ronquist F, Teslenko M, van der Mark P, Ayres DL, Darling A, Höhna S, Larget B, Liu L, Suchard MA, Huelsenbeck JP (2012) MrBayes 3.2: Efficient Bayesian Phylogenetic Inference and Model Choice Across a Large Model Space. Systematic Biology (61)3: 539–542. <https://doi.org/10.1093/sysbio/sys029>
- Ronquist F, Nieves-Aldrey JL, Buffington ML, Liu Z, Liljeblad J, Nylander JA (2015) Phylogeny, evolution and classification of gall wasps: the plot thickens. PLoS ONE 10(5): e0123301. <https://doi.org/10.1371/journal.pone.0123301>
- Seltmann KC, Yoder MJ, Mikó I, Forshage M, Bertone MA, Agosti D, Austin AD, Balhoff JP, Borowiec ML, Brady SG, Broad GR, Brothers DJ, Burks RA, Buffington ML, Campbell HM, Dew KJ, Ernst AF, Fernández-Triana JL, Gates MW, Gibson GAP, Jennings JT, Johnson NF, Karlsson D, Kawada R, Krogmann L, Kula RR, Mullins PL, Ohl M, Rasmussen C, Ronquist F, Schulmeister S, Sharkey MJ, Talamas E, Tucker E, Vilhelmsen L, Ward PS, Wharton RA, Deans AR (2012) A hymenopterists' guide to the Hymenoptera Anatomy Ontology: utility, clarification, and future directions. Journal of Hymenoptera Research 27: 67–88. <https://doi.org/10.3897/jhr.27.2961>

- Song C, Lin XL, Wang Q, Wang XH (2018) DNA barcodes successfully delimit morphospecies in a superdiverse insect genus. *Zoological Scripta* 47(3): 311–324. <https://doi.org/10.1111/zsc.12284>
- Struck TH, Feder JL, Bendiksbj M, Birkeland S, Cerca J, Gusarov VI, Kistenich S, Larsson KH, Liow LH, Nowak MD, Stedje B, Bachmann L, Dimitrov, D (2018) Finding evolutionary processes hidden in cryptic species. *Trends in Ecology & Evolution* 33(3): 153–163. <https://doi.org/10.1016/j.tree.2017.11.007>
- Tavakoli M, Stone GN, Pujade-Villar J, Melika G (2022) New herb gall wasps from Iran (Hymenoptera: Cynipidae). *Zootaxa* 5155(3): 301–333. <https://doi.org/10.11646/zootaxa.5155.3.1>
- Țiței V, Cîrlig N, Guțu A (2020) Some biological peculiarities and economic value of the cultivation of cup plant, *Silphium perfoliatum* L. *Studia Universitatis Moldaviae (Seria Științe Reale și ale Naturii)* 136(6): 79–82. <https://doi.org/10.5281/zenodo.4431626>
- Tooker JF, Deans AR, Hanks LM (2004) Description of the *Antistrophus rufus* (Hymenoptera: Cynipidae) species complex, including two new species. *Journal of Hymenoptera Research* 13: 125–133.
- Vilela AE, González-Paleo L, Ravetta DA, Murrell EG, Van Tassel DL (2020) Balancing forage production, seed yield, and pest management in the perennial sunflower *Silphium integrifolium* (Asteraceae). *Agronomy* 10(10): 1471. <https://doi.org/10.3390/agronomy10101471>
- Ward AKG, Sheikh SI, Forbes AA (2020) Diversity, host ranges, and potential drivers of speciation among the inquiline enemies of oak gall wasps (Hymenoptera: Cynipidae). *Insect Systematics and Diversity* 4(6): 3. <https://doi.org/10.1093/isd/ixaa017>
- Ward AK, Bagley RK, Egan SP, Hood GR, Ott JR, Prior KM, Shiekh SI, Weinersmith KL, Zhang L, Zhang YM, Forbes AA (2022) Speciation in Nearctic oak gall wasps is frequently correlated with changes in host plant, host organ, or both. *Evolution* 76(8): 1849–1867. <https://doi.org/10.1111/evo.14562>
- Ward AKG, Zhang YM, Brown GE, Hippie AC, Prior KM, Rollins S, Sierra N, Sheikh SI, Tribull CM, Forbes AA (2024) Speciation in kleptoparasites of oak gall wasps often correlates with shifts into new tree habitats, tree organs, or gall morphospace. *Evolution* 78(1): 174–187. <https://doi.org/10.1093/evolut/qqad202>
- Weld LH (1926) Field notes on gall-inhabiting cynipid wasps with descriptions of new species. *Proceedings of the United States National Museum* 68(2611): 1–131. <https://doi.org/10.5479/si.00963801.68-2611.1>
- Weld LH (1951) Superfamily Cynipoidea. In: Muesebeck CFW, Krombein KV, Townes HK (Eds) *Hymenoptera of America north of Mexico: Synoptic catalog* (No. 2). US Department of Agriculture, 594–654.
- Wieczorek J, Bloom D, Guralnick R, Blum S, Döring M, Giovanni R, Robertson T, Vieglais D (2012) Darwin Core: an evolving community-developed biodiversity data standard. *PLoS ONE* 7(1): e29715. <https://doi.org/10.1371/journal.pone.0029715>
- Yoder MJ, Mikó I, Seltmann KC, Bertone MA, Deans AR (2010) A gross anatomy ontology for Hymenoptera. *PLoS ONE* 5(12): e15991. <https://doi.org/10.1371/journal.pone.0015991>

Supplementary material I

Supplementary information

Authors: Louis F. Nastasi, John F. Tooker, Charles K. Davis, Cecil N. Smith, Timothy S. Frey, M. J. Hatfield, Tara M. Presnall, Heather M. Hines, Andrew R. Deans

Data type: (measurement/occurrence/multimedia/etc.)

Explanation note: **table 1.** Digitized complete specimen data for all material examined **table 2.** Morphological characters examined **table 3.** Hymenoptera Anatomy Ontology URI table listing morphological terminology **table 4.** Raw morphological data **table 5.** Overview of diagnostic utility of examined characters **table 6.** Specimen data for sequenced material.

Copyright notice: This dataset is made available under the Open Database License (<http://opendatacommons.org/licenses/odbl/1.0/>). The Open Database License (ODbL) is a license agreement intended to allow users to freely share, modify, and use this Dataset while maintaining this same freedom for others, provided that the original source and author(s) are credited.

Link: <https://doi.org/10.3897/jhr.97.121918.suppl1>

Circumscription of the *Ganaspis brasiliensis* (Ihering, 1905) species complex (Hymenoptera, Figitidae), and the description of two new species parasitizing the spotted wing drosophila, *Drosophila suzukii* Matsumura, 1931 (Diptera, Drosophilidae)

Jeffrey Sosa-Calvo¹, Mattias Forshage², Matthew L. Buffington³

1 Department of Entomology, Smithsonian NMNH, 10th and Constitution Ave NW, Washington DC 20013, USA **2** Naturhistoriska riksmuseet, Department of Zoology, Box 50007, SE-104 05 Stockholm, Sweden **3** Systematic Entomology Laboratory, USDA, c/o Smithsonian NMNH, 10th and Constitution Ave NW, Washington DC 20013, USA

Corresponding authors: Jeffrey Sosa-Calvo (sossajef@si.edu); Matthew L. Buffington (matt.buffington@usda.gov)

Academic editor: Miles Zhang | Received 11 January 2024 | Accepted 11 April 2024 | Published 29 May 2024

<https://zoobank.org/D7F62554-5C6E-4A64-98B2-628F2D94972B>

Citation: Sosa-Calvo J, Forshage M, Buffington ML (2024) Circumscription of the *Ganaspis brasiliensis* (Ihering, 1905) species complex (Hymenoptera, Figitidae), and the description of two new species parasitizing the spotted wing drosophila, *Drosophila suzukii* Matsumura, 1931 (Diptera, Drosophilidae). Journal of Hymenoptera Research 97: 441–470. <https://doi.org/10.3897/jhr.97.118567>

Abstract

Based on host specificity and distribution data, it has been hypothesized that *Ganaspis brasiliensis* (Ihering, 1905), a natural enemy of the horticultural pest spotted-wing drosophila, *Drosophila suzukii* Matsumura, 1931 (SWD), was composed of multiple, cryptic species. Parasitoid wasps assigned to the species name *Ganaspis brasiliensis* and *Ganaspis* cf. *brasiliensis* were investigated using a molecular dataset of ultra-conserved elements (UCEs) and morphology. We report strong evidence for the presence of cryptic species based on the combination of UCE data (1,379 UCE loci), host specificity, ovipositor morphology, and distribution data. We describe these new cryptic species as: *Ganaspis lupini* **sp. nov.**, and *Ganaspis kimorum* **sp. nov.** *Ganaspis lupini* was formerly recognized as *Ganaspis brasiliensis* G3, and *Ganaspis kimorum* as *Ganaspis brasiliensis* G1. These two new species appear to be restricted to the temperate climates, whereas *Ganaspis brasiliensis* (formerly recognized as *Ganaspis brasiliensis* G5) has a more pan-tropical distribution. We investigated the characterization of the ovipositor clip of these species, and hypothesize that *G. kimorum*, which has a reduced ovipositor clip, has an advantage in ovipositing into fresh fruit, still on the host

plant, while attacking SWD; as a corollary, *G. brasiliensis* and *G. lupini*, which both have a larger ovipositor clip, are better adapted to attacking hosts in softer, rotting fruit on the ground. As *Ganaspis kimorum* was authorized for release as a biological control agent against SWD under the name *Ganaspis brasiliensis* G1, the results here have direct impact on the field of biological control.

Keywords

Biological control, cryptic species, pest fly, soft fruit, taxonomy

Introduction

Species that have not yet manifested morphological differences can often be separated based on molecular sequence data as well as behavioral data (Struck et al., 2018). These ‘cryptic’ species are a reality in modern systematics, and there are numerous examples recently published in Hymenoptera, including ants (Prebus 2021; Branstetter and Longino 2022; Schar et al. 2022), encyrtid wasps (Wang et al. 2016), eulophid wasps (Hansson and Hambäck 2013), aphelinid wasps (Heraty et al. 2007), microgastriine braconids (Alex Smith et al. 2013) and parasitoids of cynipid wasps (Zhang et al. 2022), to mention some. Within biological control research, cryptic species can present a major challenge in finding the safest, most reliable, natural enemy (Rosen 1986).

Ganaspis brasiliensis (Ihering, 1905) (Hymenoptera: Figitidae: Eucilinae) has been hypothesized to be a cryptic species complex (Nomano et al. 2017; Hopper et al. 2024). While a great deal of international exploration has been conducted in pursuit of natural enemies of the spotted-wing drosophila (SWD), *Drosophila suzukii* Matsumura, 1931 (Diptera: Drosophilidae) (Nomano et al. 2017; Giorgino et al. 2018; Abram et al. 2022), much work has also been conducted on which wasp populations attack this pest with the most specificity. *Ganaspis brasiliensis* was, early on, recognized as a common natural enemy of SWD, and was redescribed (Buffington and Forshage 2016). Since then, additional field and lab studies (summarized by Seehausen et al. 2020) have suggested *G. brasiliensis* could in fact be a cryptic species complex, composed of as many as five species (Nomano et al. 2017). The study by Nomano et al. (2017) reported five lineages of *G. brasiliensis*, namely G1–G5. Since that study, G1 has been recognized as the most host-specific population of *G. brasiliensis* (Giorgini et al. 2018; Abram et al. 2022) and has even been cleared for release in the United States by USDA-APHIS; G3, also a natural enemy of SWD, has a slightly broader host range, and where it co-occurs with G1, a slightly less effective natural enemy of SWD; and G5 appears to be pan-tropical and not able to exploit SWD at all; other *Drosophila* species are hosts for G2 and G4 (Nomano et al. 2017). Altogether, these data led Seehausen et al. (2020) to set the stage for these populations of *G. brasiliensis* G1, G3, and G5, to be recognized as distinct species (G2 and G4 lacked sufficient sample data). Hopper et al. (2024) presented whole genome datasets that suggest G1 and G3 are in fact separate species (although G5 was not included, as it has not been recorded attacking SWD).

We utilize an integrative approach, including novel ultra-conserved element (UCE) molecular data, morphological data (based on ovipositor and scutellar characters), published host specificity studies, published crossing experiments, and distribution data to distinguish at least three lineages within the formerly recognized *Ganaspis brasiliensis*. As such, we herewith describe two new species: *Ganaspis kimorum*, new species, and *Ganaspis lupini*, new species. In light of these new data, *Ganaspis brasiliensis* is redescribed and the circumscription of this species updated.

Materials and methods

Specimen acquisition

The source for all specimens in this study resulted from the combined rearing efforts of collaborators from around the world, as well as researchers with established *Ganaspis* spp. laboratory colonies for genetic research; these collaborators are listed in Suppl. material 1: table S1 as well as in the acknowledgments. As specimens were reared in the field or the lab, a subset of specimens was sent to one of us (MLB) for morphological determination and vouchering in the National Museum of Natural History, Smithsonian Institution (USNM); these were typically dry mounted and labeled, but some were retained in 95% ethanol. In some cases, large numbers of specimens were sent and kept in 95% ethanol. Outgroups included were *Ganaspis hookeri* (Crawford, 1913) (from a laboratory colony), two other undescribed, but morphologically distinct, species of *Ganaspis*, that were bred true from a laboratory colony, and specimens identified as belonging to the eucoiline genus *Leptopilina* Föster.

Specimen illustration and observation

Representative specimens were imaged using the Macropod[™] multiple-focus imaging system to illustrate diagnostic characters; single montage images were produced from image stacks with the program Zerene Stacker[™]. Scanning electron micrographs were generated using a Hitachi[™] TM3000 desktop scanning electron microscope; specimens were coated in 25–30 nm gold-palladium alloy (Cressington[™] 108 auto sputtercoater), using ‘analysis’ voltage, running in ‘compo’ mode. Diagnoses focus on easily recognized gross morphologies, and species/genera that can be confused with *G. brasiliensis* are diagnosed. Terminology for all descriptive characters, as well as phylogenetic characters, follow Buffington and Forshage (2016).

DNA extraction

DNA was extracted using the Qiagen DNeasy[®] Blood and Tissue Kit (Qiagen, Valencia, CA, U.S.A.). DNA extractions were performed by either placing an entire individual (male or female) or their metasoma, in a 2 mL tube with 0.5 mm diameter glass

lysis beads (BioSpec Products, Bartlesville, OK, U.S.A.). The samples were placed in a -20°C freezer for ~ 10 minutes and then placed in a TissueLyser II (Qiagen Inc., USA) for 30 s at 30 Hz to disrupt the tissue and facilitate the lysis process. Cell lysis was performed overnight with $20\ \mu\text{L}$ of Proteinase K in a dry bath shaker at 56°C and at 500 rpm. The recommendations of the manufacturer were followed for the extraction process except that the cleaned, extracted DNA from the spin-collection columns was eluted with two (rather than one) washes, each consisting of $55\ \mu\text{L}$ of nuclease-free water, differing from the manufacturer's recommendation of $200\ \mu\text{L}$ of AE buffer. DNA extractions were quantified using $2\ \mu\text{L}$ of DNA template in a Qubit 4 Fluorometer and with the 1X dsDNA High Sensitivity (HS) assay Kit (Thermo Fisher Scientific, Inc.). DNA extraction concentration ranged from $0.001\text{--}7.20\ \text{ng}/\mu\text{L}$ (mean = $0.943\ \text{ng}/\mu\text{L}$).

Generation of UCE data: Library preparation

Prior to library preparation, $1\text{--}50\ \text{ng}$ of DNA template was sheared to an average fragment length of $300\text{--}600\ \text{bp}$ using a Qsonica Q800R2 Sonicator (Qsonica LLC, Newton, CT, U.S.A.) for 60 s with amplitude set at 25 and the pulse set at 10. Libraries were prepared on 96-well plates on a DynaMagTM-96 side magnet (Invitrogen, Thermo Fischer Scientific, Waltham, MA, U.S.A.) and using the Kapa Hyper Prep Library Kit (Roche Diagnostics Corporation, Indianapolis, IN, U.S.A.) as described in Faircloth et al. (2015) with the iTru Adapter protocol. We implemented all magnetic bead clean-up steps (Fisher et al. 2011) as described in Faircloth et al. (2015) and used dual-indexing TruSeq adapters (Faircloth and Glenn 2012, Glenn et al. 2019) for ligation. The ligation step was followed by PCR-amplification of $15\ \mu\text{L}$ of the library product using $25\ \mu\text{L}$ of KAPA HiFi ReadyMix (Roche Diagnostics Corporation, Indianapolis, IN, U.S.A.), $2.5\ \mu\text{L}$ of each of Illumina TruSeq (i5 and i7) primers, and $5\ \mu\text{L}$ nuclease-free ddH_2O . The following thermal cycler program was executed: 98°C for 45 s; 13 cycles of 98°C for 15 s, 60°C for 30 s, 72°C for 60 s; and final extension at 72°C for 5 m. Following PCR, we purified DNA products using $1.1\times$ Kapa Pure beads and rehydrated the purified product in $22\ \mu\text{L}$ of Elution Buffer (pH = 8). Individual libraries were quantified using $2\ \mu\text{L}$ of library product in a Qubit 4 Fluorometer using the 1X dsDNA Broad Range (BR) assay Kit (Thermo Fisher Scientific, Inc.). Post-PCR libraries have concentrations ranging from $3.05\text{--}114.9\ \text{ng}/\mu\text{L}$.

Library pooling and target enrichment of libraries

Post-PCR libraries were pooled at equimolar concentrations into 25 pools, each containing 6–12 libraries. Pool concentration was adjusted to $\sim 71.5\ \text{ng}/\mu\text{L}$ by drying the sample in a vacuum centrifuge for 45–60 min or until all liquid was evaporated at 60°C , and then by re-suspending the pool in nuclease-free water at the estimated volume. We then used $2\ \mu\text{L}$ of the resuspended product to measure the pool final concentration in a Qubit 4 Fluorometer with the 1X dsDNA BR assay Kit. The final concentration of the pre-enrichment pools was $63.6\text{--}91.4\ \text{ng}/\mu\text{L}$. The pool was enriched by

using the myBaits (Arbor Biosciences, Ann Harbor, MI, U.S.A.) UCE Hymenoptera bait set (“Hymenoptera 2.5Kv2P”) targeting 2590 conserved loci in Hymenoptera (Branstetter et al. 2017) at an incubation temperature of 65 °C for 24 h in a thermal cycler. Enrichment, bead-cleaning, and PCR reaction procedures partially followed the Arbor Biosciences v5.0.1 (<https://arborbiosci.com/mybaits-manual/>) protocol and Branstetter et al. (2021) and Hanisch et al. (2022). The resulting reaction was purified using 1.0X Kapa Pure beads (Roche Diagnostics Corporation, Indianapolis, IN, U.S.A.) and the enriched pool was then rehydrated in 22 µL elution buffer. The final two enriched pools were submitted to Admera Health Biopharma Services (NJ, U.S.A.) for quality control and sequencing of two lanes on an Illumina HiSeq2500 instrument. A summary of the raw data, contigs, UCE loci recovered, and other assembly statistics for each sample is presented in Suppl. material 1: table S2. Most extractions and UCE laboratory work were conducted in the Laboratories of Analytical Biology (LAB) facilities of the National Museum of Natural History, Smithsonian Institution. New raw sequences generated as part of this study are deposited in the NCBI Sequence Read Archive (SRA) under BioProject number PRJNA1088885 and under accession No. SAMN40504884–SAMN40505120.

Molecular phylogenetics: Processing of UCE sequence data

We trimmed the demultiplexed FASTQ output files for adapter contamination and low-quality bases using Illumiprocessor v.2.0.6 (Faircloth 2013, modified by R. Dikow and P. Frandsen to use trim_galore v0.4.1 (Krueger 2015)). We used SPAdes v.3.14 (Bankvich et al. 2012, Nurk et al. 2013) to assemble the clean reads into contigs. We used a series of scripts available in the PHYLUCE package (Faircloth 2016) to further process our data and we followed the methods used in Barrera et al. (2022), Hanisch et al. (2022), Blaimer et al. (2023). We aligned each UCE locus using MAFFT v7.407 (Katoh and Standley 2013) using the default algorithm. The alignment step was repeated using the L-INS-I algorithm in MAFFT, which tends to generate more accurate alignments (Katoh et al. 2005, Katoh and Standley 2014). We trimmed poorly aligned regions in each UCE locus with GBLOCKS (Castresana 2000, Talavera and Castresana 2007) using relaxed settings ($b1 = 0.5$, $b2 = 0.5$, $b3 = 12$, $b4 = 7$). Initial alignments were generated by first aligning individual UCE loci with different percentage of taxon representation, thus 50% (119 taxa, 1,477 loci), 60% (143 taxa, 1,379 loci) and 70% (166 taxa, 1,211 loci) using the PHYLUCE script *phyluce_align_get_only_loci_with_min_taxa*. We then concatenated those loci into a data matrix using the PHYLUCE script *phyluce_align_format_nexus_files_for_raxml*, named Ganasbra237t_50p, Ganasbra237t_60p, and Ganasbra237t_70p, respectively, for exploratory and downstream analyses.

UCE phylogenetic analyses

Initial analyses were conducted on the unpartitioned three alignments generated (Ganasbra237t at 50%, 60%, and 70%, respectively) using IQ-TREE multicore v.2.1.3

(Minh et al. 2020), the GTR+F+G4 model of evolution (as selected by IQ-TREE), the default number of unsuccessful iterations to stop (-nstop 100), and an initial neighbor-joining tree (-t BIONJ). Node support was estimated by conducting 1,000 ultrafast bootstraps (UFBoot) (Hoang et al. 2018).

To identify and remove outlier or poorly aligned sequence fragments we used the Python tool SPRUCEUP (Borowiec 2019) on the Ganasbra237t_60p alignment. Parameters in the configuration file were set up to the uncorrected p-distance for computing the distances, window size = 20 bp and overlap = 15 bp, a lognormal distribution to identify outlier distances, and a global cutoff of 0.997. As a result, SPRUCEUP removed 56,045 (0.02%) outlier nucleotide-site state assignments (i.e., matrix cell values (Suppl. material 1: table S3). We then used the resulting SPRUCEUP-trimmed alignment and repeated the unpartitioned analysis using the same parameters as above, including 1,000 replicates of the SH-like approximation likelihood-ratio test (-alrt 1000) (Guindon et al. 2010). Upon inspection of the resulting tree and the png files generated by SPRUCEUP, additional, manual cutoffs were performed for 23 taxa (see Suppl. material 1: table S3 for cutoff values).

We partitioned the resulting trimmed alignment using the Sliding Window Site Characteristics based in Entropy method (SWSC-EN; Tagliacollo and Lanfear 2018), in which each UCE locus is divided into three regions (a core and two flanking regions). The SWSC-EN algorithm identified 4,137 subsets. We then identified the best partitioning scheme by merging the resulting subsets using ModelFinder (Kalyaanamoorthy et al. 2017) as implemented in IQ-TREE (Minh et al. 2020). For the merging step, we used the *-m MF+MERGE* command, the fast relaxed *-rclusterf* algorithm (set to 10; Lanfear et al. 2017) and compared the top 10% of the resulting partitioning schemes using the corrected Akaike information criterion (AICc), restricting the evaluated models to those implemented in RAxML by using the command *-mset raxml*. The best-fit partitioning scheme (0.997_lognorm_man_Ganasbra237t_60p_SWSCEN) consisted of 1,629 partitions.

We tested for model violation based on assumptions of stationarity and homogeneity by performing a test of symmetry (Naser-Khdour et al. 2019) as implemented in IQ-TREE 2.1.3 (Chernomor et al. 2016; Minh et al. 2020) on the partitioned dataset above. We removed bad partitions by using the *-symtest-remove-bad* option with a *P*-value cutoff set as the default (*P* = 0.05). The test of symmetry identified and removed 536 out of the 4,137 subsets generated by SWSC-EN. The resulting best-fit partitioning scheme (0.997_lognorms_cutoff_man_Ganaspis237-60p_partitions.nex.good_SYMTEST) consisted of 1,422 partitions.

We performed further maximum-likelihood (ML) analyses on the trimmed alignment with the different partitioning schemes using IQ-TREE multicore v.2.1.3 (Chernomor et al. 2016; Minh et al. 2020), estimating branch support with the ultrafast bootstrap (Hoang et al. 2018) and the SH-like approximation likelihood ratio test (Guindon et al. 2010) set at 1,000 replicates, with other settings set at default values on the 0.997_lognorms_cutoff_man_Ganaspis237-60p_partitions.nex.good_SYMTEST alignment. Statistics for all the data matrices generated for this study are summarized

in Suppl. material 1: table S4 and all trees generated for this study are in supplementary information (<https://figshare.com/s/93d692506c0fe68a7ddd>).

We employed the *species delimitation* plugin v.1.4.5 (Masters et al. 2011) in Geneious Prime (www.biomatters.com) to summarize the average pairwise tree distance (using the tree in Fig. 6) among members of a clade (Intra Dist) and the average pairwise tree distance among a clade and its closest clade (Inter Dist). Results are summarized in Table 1 and Suppl. material 1: table S5.

Generation of DNA Barcoding (COI)

Employing the Phyluce script *phyluce_assembly_match_contigs_to_barcode* and a COI sequence as reference ('*Ganaspis brasiliensis*' downloaded from GenBank accession No. MN013168.1), we extracted from the UCE data bycatch (Ströher et al. 2017) the *cytochrome oxidase I* (COI) gene fragment for a subset of samples, including from a non-type specimen of the original description of *Ganaspis brasiliensis* not included in the UCE data analyses above. The *contig.slice* files were then inspected in Geneious Prime v.2024.0.4 (www.biomatters.com) and mapped to the reference sequence (MN013168.1) using the BBMap v.1.0 (Bushnell 2014) plugin. COI sequences, of some specimens, are given at the end of the description of each species, and they have also been deposited in GenBank under accession No. PP599368–PP599375 (see Suppl. material 1: table S6).

Results

UCE sequencing and matrix assembly

In average, we recovered 1,369 UCE loci (range: 672–1,670) with a mean length of 878 bp (range: 341–1,801 bp). The final alignment included 237 terminals, 1,379 UCE loci, and 1,221,982 bp of sequence data, of which 523,179 were parsimony-informative sites. The alignment was composed mostly of samples in the genus *Ganaspis* and two samples belonging to the genus *Leptopilina* Förster, 1862, as a distant outgroup. The test of symmetry conducted in IQTREE 2.1.3 (Chernomor et al. 2016; Minh et al. 2020) identified and removed 536 and 565 bad partitions depending on the SPRUCEUP manual cut-off employed (Suppl. material 1: table S3). The resulting 'good' alignments consisted of 964,889 and 960,213 bp of sequence data and 427,640 and 427,499, respectively. For additional assembly and additional statistics, see Suppl. material 1: table S4. All trees generated in this study are deposited in supplemental information (<https://figshare.com/s/93d692506c0fe68a7ddd>).

Morphological study

Morphological examination of the scutellum and ovipositor revealed subtle but consistent differences among specimens examined (Fig. 3). For the scutellum, the lateral

Table 1. Summary of differences among species in the *Ganaspis brasiliensis* species complex.

Species	Host	Distribution	scutellum	Ovipositor clip	Intra-species genetic distance	Inter species genetic distance
<i>Ganaspis brasiliensis</i>	<i>D. melanogaster</i> <i>D. simulans</i> other <i>Drosophila</i>	Pan tropical: Neotropical, Afrotropical, Hawaiian	sides with carinae/ grooves	Present, large	0.041	0.076
<i>Ganaspis lupini</i>	SWD and other <i>Drosophila</i>	Paleartic: China, Japan, Korea	sides smooth	Present, large	0.05	0.067
<i>Ganaspis kimorum</i>	SWD	Paleartic: China, Japan, Korea, Nearctic: USA, Canada	sides smooth	Present, small to indistinguishable	0.021	0.075

aspects were carinate/striate in tropical specimens (*G. brasiliensis*), but totally smooth in more temperate specimens (*G. kimorum*, *G. lupini*). Further, members of *G. kimorum* were discovered to have a reduced ovipositor clip (Fig. 4). Research on the genome (Hopper et al. 2024), host specificity (Girod et al. 2018b; Wang et al. 2018; Seehausen et al. 2020; Daane et al. 2021), reproductive isolation (Seehausen et al. 2020; Hopper et al. 2024), and DNA barcode region (Nomano et al. 2017) are consistent with the morphological characters and UCE phylogenomic data shown here (Fig. 6). Together these data support the description of *G. kimorum* and *G. lupini* as species new to science. Fig. 6 shows the phylogram of these species; major sources of specimens are highlighted. Table 1 summarizes the various lines of study for species delimitation.

Ganaspis brasiliensis species group

Included species. *Ganaspis brasiliensis* (Ihering, 1905); *Ganaspis kimorum* sp. nov.; *Ganaspis lupini* sp. nov.

Diagnosis. Scutellum large, terminating anterior to the end of the scutellum; convex in lateral view, bulging slightly. Marginal cell closed in forewing. Posterior edge of metapleuron uninterrupted. Segments of female antennal clava very moderately enlarged and concolorous with other flagellomeres (Buffington and Forshage 2016). In the *Ganaspis brasiliensis* species group, the plate covers at least half of the scutellum, when viewed dorsally; in lateral view, the scutellar plate is clearly convex, even bulging, anterior to the glandular release pit. In other *Ganaspis* species, the scutellar plate may be as large or smaller, covering less than half of the scutellum when viewed dorsally; the plate, in lateral view, is flat or gently convex, and if large, not bulging. The marginal cell and claval characters are quite variable in other *Ganaspis* species.

Description. Coloration with head, mesosoma, and metasoma black to dark brown; legs uniformly light brown. Sculpture on vertex, lateral surface of pronotum, mesosoma, and metasoma absent, surface entirely smooth (Fig. 1). Length 1.5–1.75 mm.

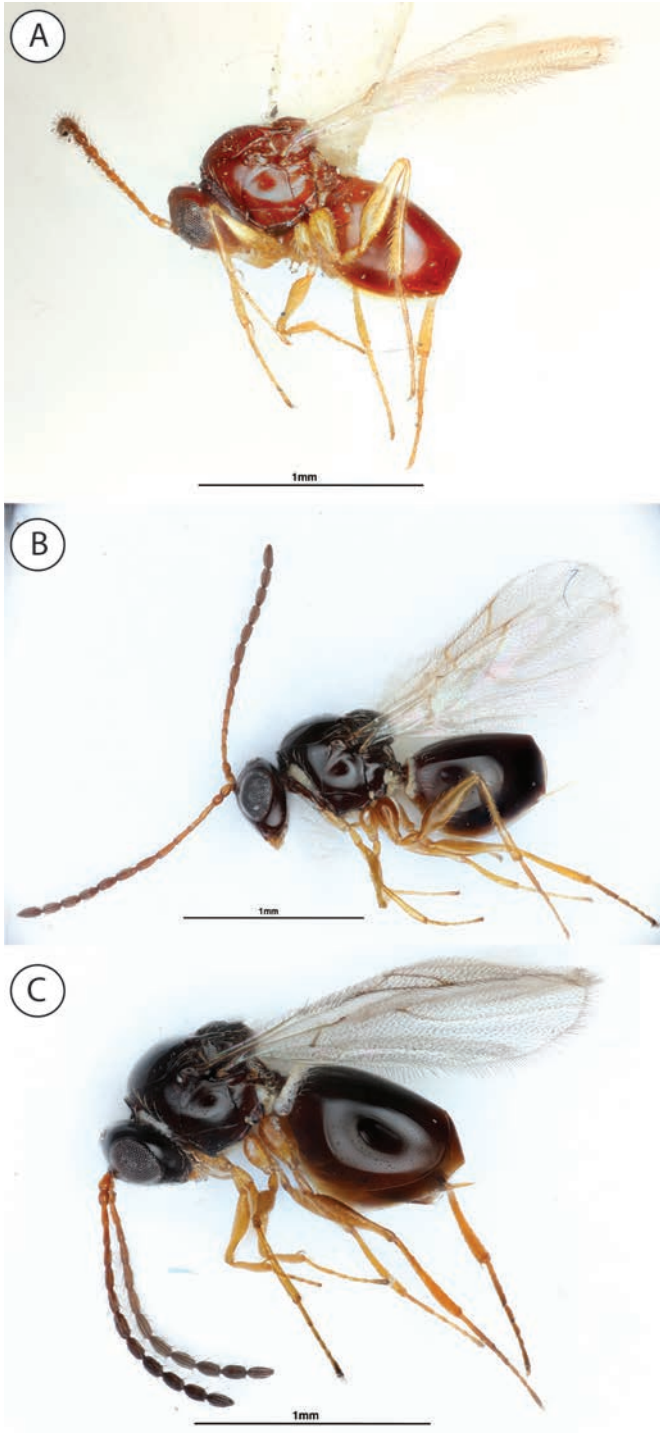


Figure 1. Type-specimens of the species belonging to the *G. brasiliensis* species complex **A** *brasiliensis*, lectotype **B** *kimorum*, holotype **C** *lupini*, holotype.

Head. In anterior view, rounded, approximately as high as broad; in lateral view, more transverse, not protruding. Pubescence on head sparse, nearly glabrous. Sculpture along lateral margin of occiput absent (Fig. 2A). Gena (measured from compound eye to posterolateral margin of head) short, ratio of length of gena to length of compound eye in dorsal view <0.3 mm. Sculpture of gena absent, smooth. Lateral margin of occiput evenly rounded, not well defined (Fig. 2A). Occiput (except extreme lateral margin) smooth. Carina issuing from lateral margin of postocciput absent. Ocelli small, ratio of maximum diameter of a lateral ocellus to shortest distance between lateral ocelli $0.2\text{--}0.4$ mm. Anterior ocellus far from posterior ocelli, clearly anterior to anterior margins of posterior ocelli. Relative position of antennal sockets close to ocelli, ratio of vertical distance between inner margin of antennal foramen and ventral margin of clypeus to vertical distance between anterior ocellus and antennal rim <2.0 . Median keel of face absent. Vertical carina adjacent to ventral margin of antennal socket absent. Facial sculpture absent, surface smooth. Facial impression absent, face flat. Antennal scrobe absent. Anterior tentorial pits small. Longitudinal axis of posterior tentorial pits oblique. Vertical delineations on lower face absent. Ventral clypeal margin laterally, close to anterior mandibular articulation, straight. Ventral clypeal margin medially straight, not projecting. Clypeus smooth, evenly rounded. Malar space adjacent to anterior articulation of mandible evenly rounded, smooth. Malar sulcus present. Eye close to ocelli, ratio of distance between compound eye and posterior mandibular articulation to distance between posterior ocellus and compound eye >1.2 mm. Compound eyes, in dorsal view, distinctly protruding from the surface of the head, particularly laterally. Pubescence on compound eyes absent. Orbital furrows absent. Lateral frontal carina of face absent. Dorsal aspect of vertex smooth. Posterior aspect of vertex smooth. Hair punctures on lateral aspect of vertex absent. Posterior surface of head deeply impressed around post-occiput.

Labial-maxillary complex. Apical segment of maxillary palp with pubescence, consisting only of erect setae. First segment of labial palp shorter than apical segment. Labial palp composed of two segments. Apical seta on apical segment of maxillary palp longer than twice length of second longest apical seta. Erect setae medially on apical segment of maxillary palp absent. Maxillary palp composed of four segments. Last two segments of maxillary palp (in normal repose) curved inwards. Distal margin of subapical segment of maxillary palp slanting inwards, apical segment bending inwards. Apical segment of maxillary palp more than $1.5\times$ as long as preceding segment.

Antenna. Articulation between flagellomeres in antenna moniliform, segments distinctly separated by narrow neck-like articulation (Fig. 2C). Female antenna composed of 11 flagellomeres (Fig. 2C). Male antenna composed of 13 flagellomeres. Female F1 longer than F2. Flagellomeres of female antenna cylindrical, gently widened towards apex, slightly clavate (Fig. 2C). Placoidal sensilla present on F6-11 (Fig. 2C). Second flagellomere of male antenna cylindrical. Length of second flagellomere of male antenna equal to length of first flagellomere. Last antennal flagellomeres of female antenna not conspicuously enlarged compared to adjacent flagellomeres (Fig. 2C).

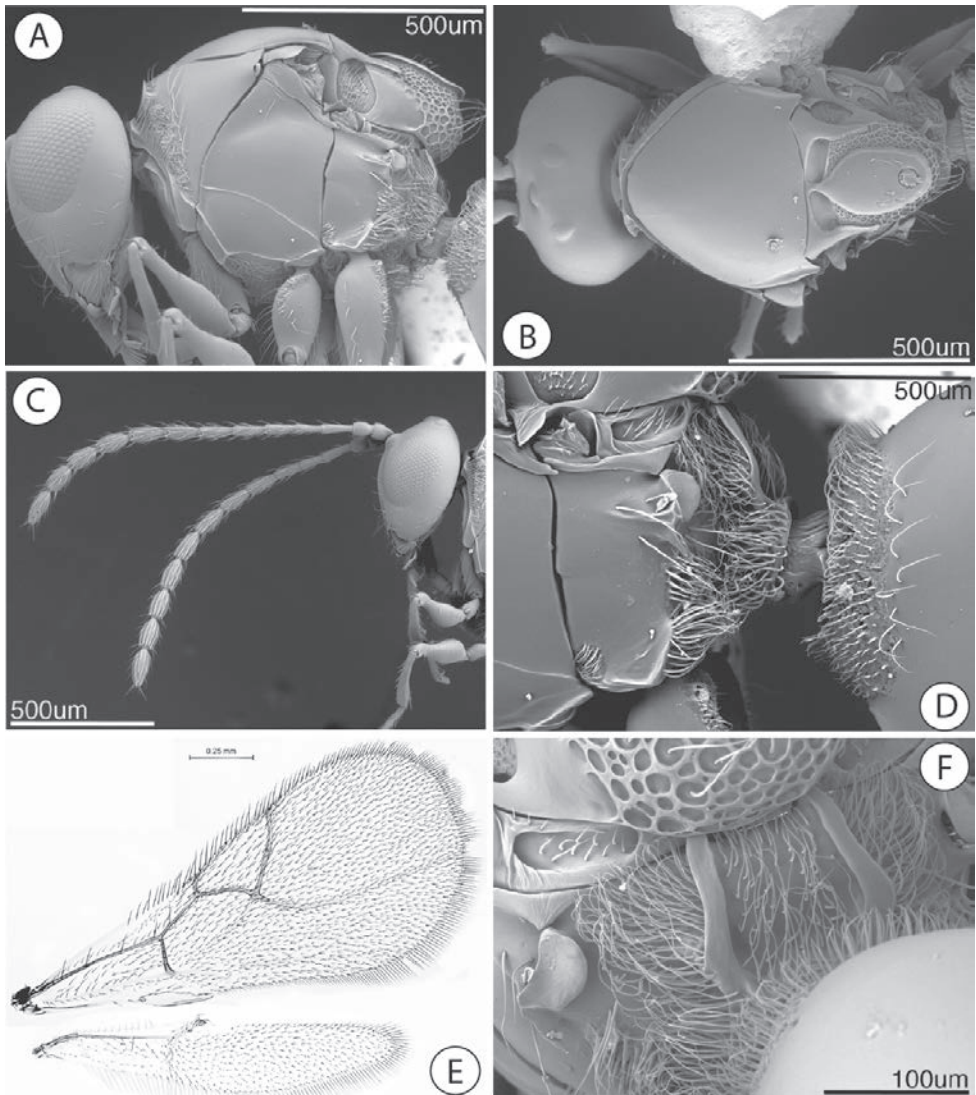


Figure 2. External anatomy of *Ganaspis kimorum*, a member of the *Ganaspis brasiliensis* species complex **A** head and mesosoma, lateral view **B** head and mesosoma, dorsal view **C** female antennae **D** metapectal-propodeal complex, lateral view **E** fore- and hindwings, female **F** propodeum, dorso-lateral view.

Mesosoma. Macrosculpture on lateral surface of pronotum absent (Fig. 2A). Anteroventral inflection of pronotum narrow. Pubescence on lateral surface of pronotum present, sparse, consisting of few short hairs posterior to setal trench (Fig. 2A). Anterior flange of pronotal plate subvertical, protruding, transversely strigate. Ridges extending posteriorly from lateral margin of pronotal plate absent (Fig. 2A). Lateral pronotal carina absent. Crest of pronotal plate absent. Dorsal margin of pronotal plate (in anterior

view) straight; rounded. Submedian pronotal depressions open laterally, deep. Lateral margin of pronotal plate defined all the way to the dorsal margin of the pronotum. Width of pronotal plate narrow, not nearly as wide as head (Fig. 2B). Mesoscutal surface convex, evenly curved (Fig. 2A). Sculpture on mesoscutum absent, entire surface smooth, shiny (Fig. 2B). Notauli absent. Median mesoscutal carina absent. Anterior admedial lines absent. Median mesoscutal impression absent. Parascutal carina nearly straight anteriorly, posteriorly curved mesally. Mesopleuron entirely smooth (Fig. 2A). Subpleuron entirely smooth, glabrous (Fig. 2A). Lower pleuron entirely smooth, glabrous. Epicnemial carina absent. Lateroventral mesopleural carina present, marking abrupt change of slope of mesopectus (Fig. 2A). Mesopleural triangle present, slightly impressed without distinct ventral border (Fig. 2A). Subalar pit absent, subalar groove indistinct. Speculum absent. Mesopleural carina present, complete, composed of one complete, uninterrupted carina (Fig. 2A). Anterior end of mesopleural carina inserting above notch in anterior margin of mesopleuron. Dorsal surface of scutellum foveate-areolate (Figs 2B, 3). Circumscutellar carina absent (Fig. 3). Posterior margin of axillula marked by distinct ledge, axillula distinctly impressed adjacent to ledge (Fig. 3 A, C, E). Latero-ventral margin of scutellum posterior to auricula entirely smooth (Fig. 3A, C, E). Dorsoposterior part of scutellum rounded (Fig. 3A, C, E). Transverse median carina on scutellar plate absent. Dorsal part of scutellum entirely foveate. Scutellar plate large, widest in anterior half, covering most of scutellum; dorsally smooth, polished; glandular release pit at posterior end (Fig. 3B, D, F); in lateral view, often with an anterior hump, sunken around release pit, slightly upturned along posterior margin (Fig. 3A, C, E). Scutellar fovea present, two, distinctly margined posteriorly (Fig. 3B, D, F). Single longitudinal carina separating scutellar foveae present, short, ending at posterior margin of foveae (Fig. 3B, D, F). Longitudinal scutellar carinae absent. Postero-lateral margin of scutellum rounded. Lateral bar weakly strigate, narrow.

Metapectal-propodeal complex. Metapectal cavity anterodorsal to metacoxal base present, well-defined (Fig. 2D). Anterior margin of metapectal-propodeal complex meeting mesopleuron at same level at point corresponding to anterior end of meta-pleural carina. Posteroventral corner of metapleuron (in lateral view) rounded, not drawn out posteriorly (Fig. 2D). Anterior impression of metepimeron absent. Posterior margin of metepimeron distinct, with median part slightly depressed, not forming circular incision, separating metepimeron from propodeum (Fig. 2D). Subalar area slightly broadened anteriorly, with distinct laterally protruding lobe ventrally. Prespiracular process present, blunt, lobe-like, polished (Fig. 2D). Dorsellum present, smooth, glabrous. Anterior impression of metepisternum, immediately beneath anterior end of meta-pleural carina, absent. Pubescence not extremely dense on posterior part of metapectal-propodeal complex (Fig. 2D). Propodeal spurs absent (Fig. 2D). Lateral propodeal carinae present, elongate, projecting beyond metanotum to reach scutellum (Fig. 2D). Ventral end of lateral propodeal carina reaching nucha, carinae separated from each other. Inter propodeal carinae space lightly setose, smooth. Petiolar rim of uniform width along entire circumference. Petiolar foramen removed from metacoxae, directed posteriorly. Horizontal carina running anteriorly from lateral propodeal carina

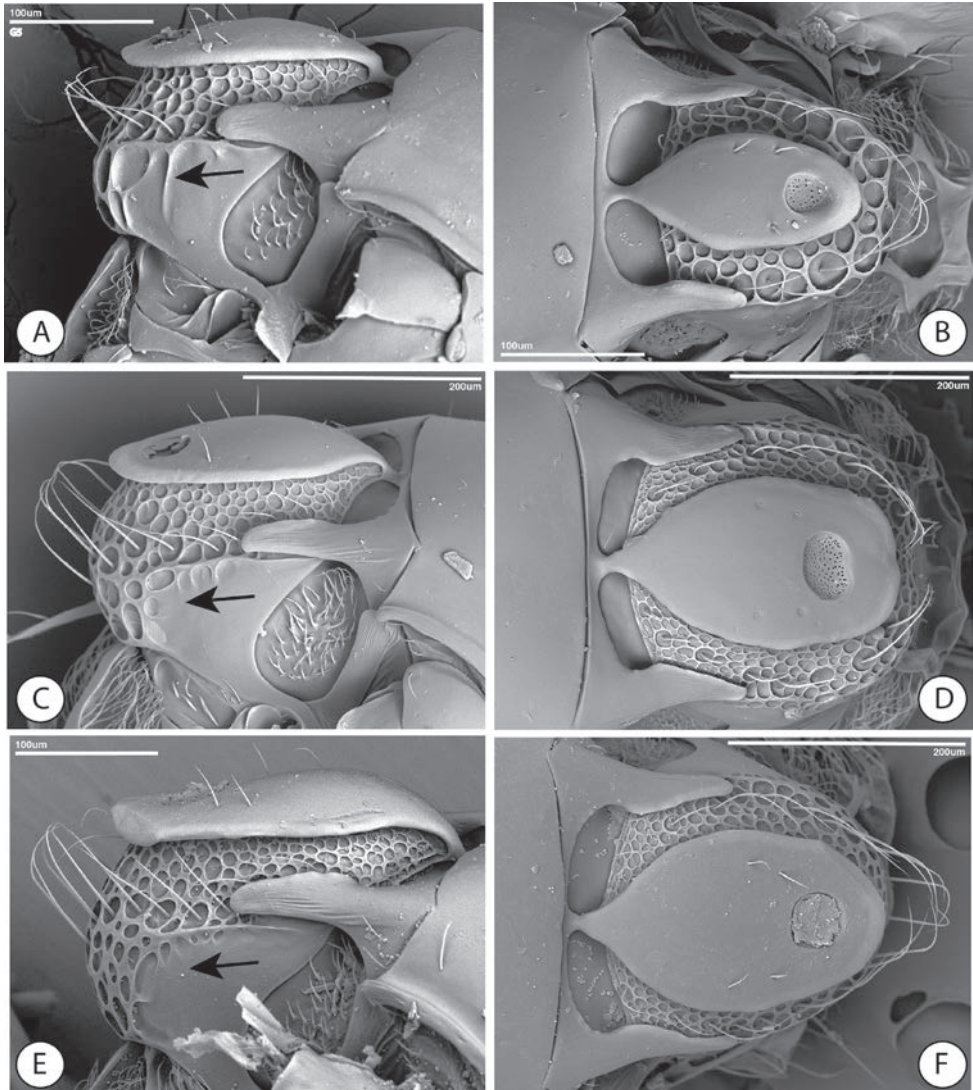


Figure 3. Comparison of the scutellar morphology between *G. brasiliensis* (A, B), *G. lupini* (C, D) and *G. kimorum* (E, F). Black arrows indicate sculptured (A) and smooth (C, E) lateral aspect of scutellum.

present. Lateral propodeal carina uniformly curved inward. Calyptra, in lateral view, rounded. Propodeum relatively short, not drawn out posteriorly (Fig. 2D). Calyptra, in posterior view, rounded.

Legs. Pubescence posterolaterally on metacoxa with a confined, elongate, dense hair patch, other pubescence lacking. Microsculpture on hind coxa absent (Fig. 2A). Longitudinal ridge on the posterior surface of metatibia absent. Metafemoral tooth absent. Distal mesotibial spurs shorter than medial spurs. Distal metatibial spurs shorter than medial spurs. Ratio of first metatarsal segment to remaining 4 segments <1.0.

Pubescence on outer surface of metatarsal claw sparse, consisting of few setae. Outer surface of metatarsal claw almost entirely smooth. Base of metatarsal claw lammellate, with translucent cuticular flange.

Wings. Pubescence of fore wing present, long, dense on most of surface (Fig. 2E). Apical margin of female fore wing rounded. R_{s+M} of forewing completely defined (Fig. 2E). Vein R1 tubular along at least basal part of anterior margin of marginal cell. Mesal end of R_{s+M} vein situated closer to posterior margin of wing, directed towards posterior end of basalis (Fig. 2E). Basal abscissa of R1 (the abscissa between 2r and the wing margin) of fore wing as broad as adjacent wing veins. Coloration of wing absent, entire wing hyaline (Fig. 2E). Marginal cell of fore wing membranous. Areolet absent. Hair fringe along apical margin of fore wing present, very short.

Metasoma. Petiole about as long as wide. Surface of petiole dorsally striate, laterally shagreen. Posterior part of female petiole not abruptly widened. Ventral flange of annulus of female petiole absent. Ventral and lateral parts of petiolar rim narrow. Setal band (hairy ring) at base of tergum 3 present, complete dorsally, extending ventrally to ventral margin of tergum, beneath petiole. Tergum 3 indistinct, fused with syntergum. Posterior margin of tergum 3 indistinct, fused with tergum 4 in syntergum. Posterior margin of tergum 4 evenly rounded. Sternum 3 encompassed by syntergum. Sculpture on metasomal terga absent. Syntergum present with terga 3 to 5 fused, ventral margin rounded. Annulus present as continuous ring. Peglike setae on T6–T7 absent. Postero-ventral cavities of female metasoma T7 absent. Female postero-ventral margin of T6–T7 straight, parallel, with distinct postero-ventral setal tuft. Terebrum and hypopygium (in lateral view) straight, pointing posteriorly. Ovipositor clip present.

***Ganaspis brasiliensis* (Ihering, 1905)**

Figs 1A, 3A, B, 4A

Diagnosis. Separated from *G. kimorum* and *G. lupini* by the sculpturing on the side of the scutellum. In *G. brasiliensis*, this area has distinct dorso-ventral carinae enclosing one or a few cells (Fig. 3A). In *G. kimorum* and *G. lupini*, this area is totally smooth (arrows, Fig. 3C, E). Further separated from *G. kimorum* by the well-developed ovipositor clip that is expanded across more the half the width of the ovipositor valve (Fig. 4A).

Redescription. As in the description for the *G. brasiliensis* species complex, but lateral aspect of pronotum with distinct ridge with associated fovea; ovipositor clip large, extending beyond the halfway point across the fused ovipositor valve. Previous studies referencing ‘Gb G5’ or ‘G5’, refer to this species (Nomano et al. 2017).

Material examined. Lectotype (female): Collection Ashmead [first label]; Ipiranga, Brazil [second label]; No 2066 from a peach [third label]; S.S. Paulo Museum 190 [third label]; Lectotype [fourth label, red, Weld’s hand]; Ipiranga, S.S. Paulo Museum 190, No. 4066a, on peach [folded hand-written label]; EUCOILIDAE, *Pseudeucoila* (*Hexamerocera*) *brasiliensis* Ashmead [white computer generated label]; USNM0119750. Deposited in USNM. Paralectotype (male): Collection Ash-

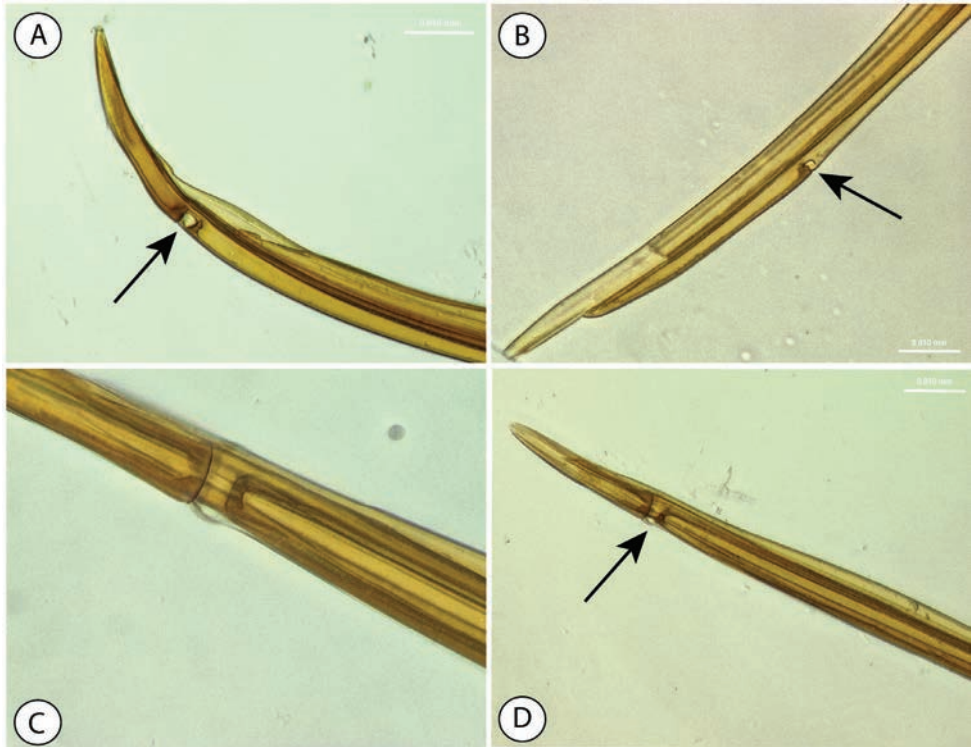


Figure 4. Comparison of the ovipositor clip between *G. lupini* (**A, C**) and *G. kimorum* (**B, D**). **A** *G. lupini* ovipositor tip, lateral view **B** *G. kimorum*, ovipositor tip, lateral view **C** *G. lupini* ventral of ovipositor showing ovipositor clip and membrane **D** *G. kimorum* ventral of ovipositor showing ovipositor clip and membrane. Black arrows indicate the location of the ovipositor clip.

mead [first label]; *Hexamerocera brasiliensis* male/female symbol Ashm (over) [front side, second label] ex *Drosophila punctata* fruitfly [back side, second label]; Paratype [third label, red]; *Eucoila (Hexamerocera) brasiliensis* Ihering [fourth label, in Weld's hand]; *Pseudeucoila brasiliensis* (R.v. Ihr.) [fifth label, Weld's hand]; EUCOILIDAE *Eucoila brasiliensis* [white computer generated label]; USNMMENT01119745. Deposited in USNM.

Other material examined. PANAMA: Monte Oscuro, June-July '95 [1895] Z-5203, USNMMENT01119746 (male); USNMMENT01119747 (female); Panama City, Z-3661 [no date]; 2 male specimens/ pin: USNMMENT01119748–USNMMENT01119749, USNMMENT01119740–USNMMENT01119742; Canal Zone, Balboa, VI.10.1936, J Zetek, collector, P.R. no. 1803; 4 females: USNMMENT01119645–USNMMENT01119648; 3 males: USNMMENT01119649, USNMMENT01119743, USNMMENT01119744; Monte Oscuro, Panama City, Z-3666 [no date]; 1 female: USNMMENT01119650; Monte Oscuro, Panama City, Z-3665 [no date]; 1 female: USNMMENT01119651; Monte Oscuro, Panama City, Z-3665, ex *Anastrepha acidusa*, emerge 2–3 weeks after last fly out–25 days after pupation [no date]; 1 female:

USNMENT01119652; Ancon, Canal Zone, Z-2748, Ex *Anastrepha fratercula* or *Drosophila striata*, July 1927, I. Molino, collector; 2 females: USNMENT01119653 and USNMENT01119654; Taboga Island, Sept. 30, 1926, I. Molino, collector, Z-2727; 11 females: USNMENT01119656–USNMENT01119665, 1 male: USNMENT01119666; Panama City, Z-3222, Ex *Anastrepha serpentina* in nispero, May 1930, J Zetek, collector; 2 males: USNMENT01119667, USNMENT01119668; Ancon, Canal Zone, Z-2715, Oct. 12, 1926, bred by Molina, ex fruit of *Spondias lutea*, parasite of diptera Z-2716; 1 female: USNMENT01119669. **GUADELOUPE:** *Ganaspis* G. 302.1, Y. Carton; 3 females: USNMENT01119670–USNMENT01119672; 3 males USNMENT01119673–USNMENT01119675.

Cytochrome c oxidase subunit I (COI) Barcode region.

> Pseudoeucoila_brasiliensis_AP7BC36 (USNMENT01119647)

NNNNNNNNNNNNNNNNNNNNNNNNNNNAATTTGATCAGGAATAATTGGATCAAGTTTAAGAATAATTATTCGTCTAGAATTAGGCACCCCTTCACAATTAATTAATAATGATCAAATTTATAATACAATTGTTACCACTCATGCATTTGTAATAATTTTTTTTATAGTAATACCAATTATAGTAGGAGGATTTGGAAATTACTTAATTCCTTAATATTATCTGCCCTGATATATCATTTCTCGTCTTAATAATATAAGATTCTGATTATTAATTCCTTCTTTAATTTTAATAATTTCAAGTATATTTATTTGATGAAGGATCTGGAACCGGATGAACCATTTATCCTCCTTTATCATTAATAAAATCACATCCAGGAATTTCAACTGATTTAGTAATTTTCTCCCTTCATCTTAGAGGAATTTCTTCAATTTTAGGATCAATTAATTTTATTACAACCTATTTTAAATATACGACCTAATTTTATAAGTATAGATAAAATTTCTTTATTTACTTGATCCATTTTCTTACTACCATTTTATTATTATCTTTACCAGTATTAGCAGGCGGAATCACTATATATTATTTGACCGAAACATTAATACATCTTTTATGACCCAATAGGAGGAGGTGATCCTATTC

>Ganaspis_brasiliensis_2966

TATATTATATTTTATTTTTTGGAAATTTGATCAGGAATAATTGGATCAAGTTTAAGAATAATTATTCGACTAGAATTAGGCACCCCTTCACAATTAATTAATAATGATCAAATTTATAATACAATTGTTACCACTCATGCATTTGTAATAATTTTTTTTATAGTAATACCAATTATAGTAGGAGGATTTGGAAATTACTTAATTCCTTTAATATTATCTGCCCTGATATATCATTTCTCGTCTTAATAATATAAGATTCTGATTATTAATCCCTTCTTTAATTTTAATAATTTCAAGTATATTTATTTGATGAAGGATCTGGAACAGGATGAACAGTTTATCCTCCTTTATCATTAATAAAATCACATCCAGGAATTTCAACTGATTTAGTAATTTTCTCCCTTCATCTTAGAGGAATCTCTTCAATTTCTAGGATCAATTAATTTTATTACAACCTATTTTAAATATACGACCTAATTTTATAAGTATAGATAAAATTTCTTTATTTACTTGATCTATTTTTCTTACTACCATTTTACTATTATTATCTTTACCAGTATTAGCAGGTGGAATCACTATATTACTGTTTGATCGAAACATTAATACATCTTTTATGATCCAATAGGAGGAGGTGACCCTATTCTATACCAACATTTATTC

>Ganaspis_brasiliensis_2919

TATATTATATTTTATTTTGGGAATTTGATCAGGAATAATTGGATCAA-
GTTTAAGAATAATTATTTCGACTAGAATTAGGCACCCCTTCACAAT-
TAATTAATAATGATCAAATTTATAATACAATTGTTACCACTCATGCATTT-
GTAATAATTTTTTTTATAGTAATACCAATTATAGTAGGAGGATTTG-
GAAATTACTTAATTCCTTTAATATTATCTGCCCTGATATATCATTTTC-
CTCGTCTTAATAATATAAGATTCTGATTATTAATCCCTTCTTTAATTT-
TAATAATTTCAAGTATATTTATTGATGAAGGATCTGGAACAGGATGAA-
CAGTTTATCCTCCTTTATCATTAATAAATCACATCCAGGAATTTCAACT-
GATTTAGTAATTTTCTCCCTTCATCTTAGAGGAATCTCTTCAATTCTAG-
GATCAATTAATTTTATTACAACATTTTAAATATACGACCTAATTTTATAA-
GTATAGATAAAAATTTCTTTATTTACTTGATCTATTTTCTTACTAC-
CATTTTACTATTATTATCTTTACCAGTATTAGCAGGTGGAATCACTATAT-
TACTGTTTGATCGAAACATTAATACATCTTTTATGATCCAATAGGAG-
GAGGTGACCCTATTCTATACCAACATTTATTC

Biology. Kionobiont endoparasitoid of *Drosophila melanogaster*, *D. simulans*, and other *Drosophila* in decaying fruit. Original description and some label data suggesting *Anastrepha* (Tephritidae) as a host are most likely to represent erroneous associations (cf. Buffington and Forshage 2016).

***Ganaspis lupini* Buffington, sp. nov.**

<https://zoobank.org/9CD88092-9D40-4C1D-BEBD-C15AAA722B39>

Figs 1B, 3C, D, 4C, F

Diagnosis. Separated from *G. brasiliensis* by the completely smooth lateral aspect of the scutellum (Fig. 3C). Separated from *G. kimorum* by a well-developed ovipositor clip that is expanded across more than half the width of the ovipositor valve (Fig. 4C); in *G. kimorum*, the clip is smaller and does not extend past the midwidth of the ovipositor valve (Fig. 4E, F).

Description. As in description for *G. brasiliensis* species complex, but with the lateral aspect of the scutellum completely smooth; ovipositor clip large, extending beyond the halfway point across the fused ovipositor valve. Previous studies referencing ‘Gb G3’ or ‘G3’ refer to this species (Nomano et al. 2017; Giorgini et al. 2018; Abram et al. 2022).

Material examined. Holotype. **JAPAN:** Nagano, Yamanouchi, Shiga Kogen Hasuike Ski Resort 36.7189°N, 138.4935°E ex *D. suzukii*, *D. subpulchrella* on *Vaccinium* spp. 17 Aug 2017 Kenis, collector G3_Nagano, USNMENT01867461. Deposited in USNM. Paratypes. **JAPAN:** Nagano, Yamanouchi, Shiga Kogen Hasuike Ski Resort 36.7189°N, 138.4935°E ex *D. suzukii*, *D. subpulchrella* on *Vaccinium* spp. 17 Aug 2017 Kenis, collector G3_Nagano: USNMENT01867461, USNMENT01867462;

Tokyo Kimura Lab, field collected *G. xanthopoda* 'lutescens type' Received USNM July 2015 From culture in lab; USNMENT00877742, USNMENT00877792, USNMENT00877779; Tokyo, Hachioji Naganuma Park 35.6368°N, 139.3647°E, INRA GO fruit on ground 16 Jun 2017 Girod, collector; USNMENT01734716, USNMENT01734717, USNMENT01734719, USNMENT01734696, USNMENT01025529, USNMENT01734695. **CHINA:** Yunnan, Kunming Multiple sites in suburbs 25.0986°N, 102.8350°E ex *D. suzukii*, *D. pulchrella* on *Rubus foliosus*, *Fragraria moupinensis* *Sambucus adnate*; 16 Jul 2017; Daane, Hoelmer, Wang, collectors; ARS Colony, Newark voucher G3_Yunnan; USNMENT01867450–USNMENT01867453; Yunnan, Kunming, Chang Chong Shan, Wu Hua District, 25.132223°N 102.706662°E, 2207m, ex *D. suzukii* on *Rubus foliosus*; collected 12.VII.2016, Giorgino and Guerreiri DSZ187; USNMENT01025535; Yunnan, Kunming, Dong Da Cun, Pan Long District, 25.098602°N 102.835000°E, 2239m, ex *D. suzukii* on *Sambucus adnata*; collected 25.VII.2016, emerged 24.VIII.2016 Giorgino and Guerreiri DSZ130 (USNMENT01025534); Yunnan, Shiping, ex *D. suzukii*/*Myrica rubra*; 15 Jun 2017 Kenis, collector CABI colony voucher G3_Shiping; USNMENT01867471, USNMENT01867470. Paratypes deposited in USNM.

Etymology. This species is named in honor of the manga character "*Lupin the Third*" (MonkeyPunch 1967). The name reflects the 'G3' naming convention of this species, as well as Lupin the Third's personality as professional thief that sometimes tries to do good. We think *G. lupini* is certainly proficient in attacking SWD, but does not attack the most destructive stage of this pest fly.

Cytochrome c oxidase subunit I (COI) Barcode region.

>Ganaspis_lupini_GB86

TATATATATTTATTTTGGAAATTTGATCAGGAATAATTGGATCAA-
GTTTAAGAATAATTATTCGACTAGAATTAGGTACCCCTTCACAAT-
TAATTAATAATGATCAAATTTATAATACAATTGTAACCACTCATGCATTT-
GTAATAATTTTTTTTATAGTAATACCAATTATAGTAGGAGGATTTG-
GAAATTATTTAATTCCTTAATATATCTACCCCTGATATATCATTTTC-
CTCGTCTCAATAATATAAGATTCTGATTATTAATTCCTTCTTTAATTT-
TAATAATTTCAAGTATATTTATTGATGAAGGATCTGGAACCGGATGAA-
CAGTTTATCCTCCTTTATCATTAATAAATCACACCCAGGAATTTCAACT-
GATTTAGTAATTTCTCCCTTCATCTTAGAGGAATTTCTTCAATTCTAG-
GATCAATTAATTTTATTACAATTTTAAATATACGACCTAATTTTATAA-
GTATAGATAAAATTTCTTTATTTACTTGATCTATTTTCTTACTAC-
CATTTTATTATTATTATCTTTACCAGTATTAGCAGGTGGAATTACTATAT-
TACTATTTGACCGAAACATTAATACATCTTTTATGACCCAATAGGAG-
GAGGTGACCCTATTCTATACCAACATTTATTC

>Ganaspis_lupini_BBP860

TATATATATTTATTTTGGAAATTTGATCAGGAATAATTGGATCAA-
GTTTAAGAATAATTATTCGACTAGAATTAGGTACCCCTTCACAAT-
TAATTAATAATGATCAAATTTATAATACAATTGTAACCACTCATGCATTT-

GTAATAATTTTTTTTATAGTAATACCAATTATAGTAGGAGGATTTG-
 GAAATTATTTAATTCCTTAATATATCTACCCCTGATATATCATTTC-
 CTCGTCTCAATAATATAAGATTCTGATTATTAATTCCTTCTTTAATTT-
 TAATAATTTCAAGTATATTTATTGATGAAGGATCTGGAACCGGATGAA-
 CAGTTTATCCTCCTTTATCATTAAATAAATCACACCCAGGAATTTCAACT-
 GATTTAGTAATTTCTCCCTTCATCTTAGAGGAATTTCTTCAATTCTAG-
 GATCAATTAATTTTATTACAACATTTTAAATATACGACCTAATTTTATAA-
 GTATAGATAAAAATTTCTTTATTTACTTGATCTATTTTTCTTACTAC-
 CATTTTATTATTATTATCTTTACCAGTATTAGCAGGTGGAATTACTATAT-
 TACTATTTGACCGAAACATTAATACATCTTTTTTATGACCCAATAGGAG-
 GAGGTGACCCTATTCTATACCAACATTTATTC

Biology. Koinobiont endoparasitoid of *Drosophila lutescens*, *D. rufa*, and *D. biau-
 raria* (Mitsui and Kimura 2010). Nomano et al. (2017) indicate this species does not
 oviposit into *D. suzukii*, but Seehausen et al. (2020) recorded successful parasitism of *D.*
suzukii by '*Ganaspis cf. brasiliensis*' G3, and we consider this a trustworthy host record.

***Ganaspis kimorum* Buffington, sp. nov.**

<https://zoobank.org/330D215F-8FEA-4D7B-8D80-C409DC2C4199>

Figs 1C, 2, 3E, F, 4B, D, E

Material examined. Holotype. **JAPAN:** Tokyo Kimura Lab, field collected *G. xan-
 thopoda* '*suzukii* type' Collected June 2010 Received USNM July 2015; female, USN-
 MENT00877810. Deposited in USNM. Paratypes: **JAPAN:** Tokyo Kimura Lab, field col-
 lected *G. xanthopoda* '*suzukii* type' Collected June 2010 Received USNM July 2015;
 USNMENT00877811, USNMENT00877772, USNMENT00877823; Kanto Prov-
 ince, Tokyo district, Hachioji, Naganuma Park 35°38'12"N, 139°21'54"E Ex larva of
Drosophila suzukii Coll. 3.VI.2015, Leg. N. Ris & P. Girod; USNMENT 01025537–
 USNMENT01025541; Tokyo, Hachioji Naganuma Park 35.6368°N, 139.3647°E,
 ex *D. suzukii* on *Prunus serrulata* 16 Jun 2017; Girod, collector CABI colony voucher
 G1_Tokyo; USNMENT01867459, USNMENT01867458, USNMENT01025536.
CHINA: Yunnan Province, Kunming district, Kunming, Yunnan Agricultural University,
 25°07'41"N, 102°44'50"E, Ex larva of *Drosophila suzukii* Coll. 3.VI.2015, Leg. M. Kenis;
 USNMENT01025542–USNMENT01025546; Yunnan Province, Honghe district,
 Shiping 23°41'15"N, 102°32'53"E Ex larva of *Drosophila suzukii* Coll. 6.VI.2015, Leg.
 M. Kenis; USNMENT01025547–USNMENT01025551; Yunnan Province, Kunming
 district, Kunming, Yunnan Agricultural University 25°07'41"N, 102°44'50"E Ex larva
 of *Drosophila suzukii* Coll. 3.VI.2015, Leg. M. Kenis; USNMENT01025552, USN-
 MENT01025553; USNMENT01734709; Yunnan, Kunming Xining Temple 25.1072°N,
 102.7167°E, ex *D. suzukii*/ *D. pulchrella*; on *Prunus* sp.; 17 May 2017 Kenis, collector
 CABI colony voucher G1_Yunnan; USNMENT01867468, USNMENT01867467,
 USNMENT01867454–USNMENT01867457, USNMENT01025528. Yunnan Prov-

ince, Honghe district, Shiping 23°41'15"N, 102°32'53"E Ex larva of *Drosophila suzukii* Coll. 6.VI.2015, Leg. M. Kenis; USNMENT01734706, USNMENT01734705, USNMENT01025530, USNMENT01734714. Yunnan, Kunming, Dong Da Cun, Pan Long District, 25.098602°N 102.835000°E, 2239m, ex *D. suzukii* on *Sambucus adnata*; collected 25.VII.2016, emerged 24.VIII.2016 Giorgino and Guerreiri DSZ118, DSZ137, DSZ188; USNMENT01025531–USNMENT01025533; Yunnan, Dali, ex *D. suzukii*/*Sambucus williamsii*; 16 Jun 2017 Kenis, collector CABI colony voucher G1_Dali; USNMENT01867465, USNMENT01867466. Paratypes deposited in USNM.

Diagnosis. Separated from *G. brasiliensis* by the completely smooth lateral aspect of the scutellum (Fig. 3E). Separated from *G. lupini* by the less-developed ovipositor clip that does not extend past the midwidth of the ovipositor valve (Fig. 4B, E). In *G. lupini* the ovipositor clip expands across more than half the width of the ovipositor valve (Fig. 4C).

Description. As in description for *G. brasiliensis* species complex, but with the lateral aspect of scutellum completely smooth; ovipositor clip reduced, not extending beyond the halfway point across the fused ovipositor valve. Previous studies referencing ‘Gb G1’ or ‘G1’ refer to this species (Nomano et al. 2017; Giorgini et al. 2018; Abram et al. 2022).

Etymology. Named in honor of Prof. Kimura (Hokkaido University, retired) and Dr Kim Hoelmer (USDA-ARS, retired). The name is a combination of Kimura and Kim Hoelmer.

Cytochrome c oxidase subunit I (COI) Barcode region.

>Ganaspis_kimorum_BBP857

```
NATATTATATTTTATTTTTGGTATTTGATCAGGAATAATTGGATCAA-
GTTTAAGAATAATTATTCGATTAGAATTAGGAACCCCTTCACAAT-
TAATTAATAATGATCAAATTTATAATACAATTGTTACTACTCATGCATTT-
GTAATAATTTTTTTTATAGTTATACCAATTATAGTTGGAGGATTTG-
GAAATTACTTAATTCCTTTAATATATCTGCTCCTGATATATCATTC-
CTCGTCTTAATAATATAAGATTTTGATTATTAATCCCTTCTTTAATTT-
TAATAATTTCAAGTATATTTATTGATGAAGGGTCTGGAAGTGGATGAACA-
GTTTATCCTCCTTTATCACTAAATAAGTCCCACCCAGGAATCTCAACT-
GACTTAGTAATTTTTTCTCTTCATCTTAGAGGAATTTCTTCAATTTTAG-
GATCAATTAATTTTATTACAACCTATTCTAAATATACGACCAAATTTAATAA-
GTATAGATAAAAATTTCTTTATTTACTTGATCCATTTTTCTTACCAC-
TATTTTATTATATTATCTTTACCAGTATTAGCAGGTGGAATCACTATAT-
TACTTTTTGACCGAAATATTAATACATCTTTTTATGACCCAATAGGAG-
GAGGAGACCCAATTTCTATACCAACACTTATTT
```

>Ganaspis_kimorum_233137974_E02 (partial sequence, 592 bp)

```
ATTAGAATTAGGAACCCCTTCACAATTAATTAATAATGATCAAATTT-
TATAATACAATTGTTACTACTCATGCATTTGTAATAATTTTTTTTATAGT-
TATACCAATTATAGTTGGAGGATTTGGAAATTAATTCCCTTTAATAT-
TATCTGCTCCTGATATATCATTCCTCGTCTTAATAATATAAGATTTTGAT-
TATTAATCCCTTCTTTAATTTAATAATTTCAAGTATATTTATTGATGAA-
GGGTCTGGAAGTGGATGAACAGTTTATCCTCCTTTATCACTAAATAA-
```

GTCCCACCCAGGAATCTCAACTGACTTAGTAATTTTTTCTCTTCATCT-
TAGAGGAATTTCTTCAATTTTAGGATCAATTAATTTTATTACAAC-
TATTCTAAATATACGACCAAATTTAATAAGTATAGATAAAATTTCTT-
TATTTACTTGATCCATTTTCTTACCACTATTTTATTATTATTATCTT-
TACCAGTATTAGCAGGTGGAATCACTATATTACTTTTTTGACCGAAATAT-
TAATACATCTTTTTTATGACCCAATAGGAGGAGGAGACCCAATTTCTATAC-
CAACACTTATTT

>Ganaspis_kimorum_233137957_F06

NATATTATATTTTATTTTTTGGTATTTGATCAGGAATAATTGGATCAA-
GTTTAAGAATAATTATTCGATTAGAATTAGGAACCCCTTCACAAT-
TAATTAATAATGATCAAATTTATAATACAATTGTTACTACTCATGCATTT-
GTAATAATTTTTTTTATAGTTATACCAATTATAGTTGGAGGATTTG-
GACATTACTTAATTCCTTTAATATTATCTGCTCCTGATATATCATTC-
CTCGTCTTAATAATATAAGATTTTGATTATTAATCCCTTCTTTAATTT-
TAACAATTTCAAGTATATTTATTGATGAAGGATCTGGAACCGGATGAACA-
GTTTATCCTCCTTTATCACTAAATAAGTCCCACCCAGGAATCTCAACT-
GACTTAGTAATTTTTTCTCTTCATCTTAGAGGAATTTCTTCAATTTTAG-
GATCAATTAATTTTATTACAACCTATTCTAAATATACGACCAAATTTAATAA-
GTATAGATAAAATTTCTTTATTTACTTGATCCATTTTTCTTACCAC-
TATTTTATTATTATTATCTTTACCAGTATTAGCAGGTGGAATCACTATAT-
TACTTTTTTGACCGAAATATTAATACATCTTTTTTATGACCCAATAGGAG-
GAGGAGACCCAATTTCTATACCAACACTTATTT

Biology. Koinobiont endoparasitoid of *Drosophila suzukii* (Nomano et al. 2017; Girod et al. 2018b; Wang et al. 2018; Seehausen et al. 2020; Daane et al. 2021). Seehausen et al. (2020) found ‘*Ganaspis* cf. *brasiliensis*’ G1 could successfully parasitize *D. melanogaster* in lab culture.

Discussion

The logic behind this comprehensive phylogenetic species delimitation study is based on observations that COI can sometimes be error-prone in species discrimination in Eucolilinae, as well as other insect groups (Brower 2006; Lohse 2009; Goldstein and LaSalle 2011; Collins and Cruickshank 2012), sometimes mediated by the presence of *Wolbachia* (Jiggins 2003; Klopstein et al. 2016; Cariou et al. 2017). When we compared our trees with the basic topology of Nomano et al. (2017), which relied on COI and ITS2 for discriminating the ‘G-species’, we find some disagreement with respect to phylogeny. The former G3 (now *G. lupini*) is recovered as the sister-group to *G. brasiliensis*, and G1 (now *G. kimorum*) is recovered as sister-group to the clade containing *G. brasiliensis*+*G. lupini*. As our dataset is more comprehensive than that of Nomano et al. (2017), both in terms of taxon sampling and number of loci, we suggest the tree pre-

sented here is a more accurate interpretation of the evolution of this group. While the use of UCE markers coupled with nex-gen sequencing technology has made generating larger amounts of data much easier and more affordable, there is still a place for mitochondrial ‘barcode’ data with respect to determining these cryptic species. We *strongly* encourage newly generated barcode data to be only compared to barcode data here in this paper, as well as barcode data in the *Drosophila* parasitoid database DROP (Lue et al. 2021) where sequences are backed by authoritatively identified voucher specimens.

The dataset here has yielded more nuanced results concerning in-group relationships than previous studies of these taxa. For instance, *Ganaspis lupini* has three distinct subclades within the species; we have decided to retain these three clades as members of the same species. Within *Ganaspis brasiliensis*, even more subclades can be discerned, some of which may eventually be split out into additional species. The ratio of the intra vs inter pairwise tree distances (Table 1 and Suppl. material 1: table S5) suggests that members of both *G. brasiliensis* and *G. lupini* seem to be more diverse compared to members within of *G. kimorum*. However, unlike the situation between *G. brasiliensis*, *G. lupini* and *G. kimorum*, where morphological differences were noted, though difficult to observe, there are no such morphological differences among the clades of *G. brasiliensis*. Hence, for the present time, we are considering all these subclades to be members of *G. brasiliensis*. It would have been very interesting to consider UCE data from types of *G. brasiliensis*, but unfortunately, attempts at amplifying extracts from the type series yield low-quality UCE data.

Biogeographically, *G. brasiliensis* appears to be a pan-tropical species, and seemingly no specimens of this species have been collected outside the subtropics (with Hawai’i being the most ‘temperate’ locality), while *Ganaspis lupini* and *G. kimorum* appear to be temperate species.

This appears to be the first study to utilize the ovipositor clip for species-level discrimination. Prior to this study, the clip was formally described (van Lenteren et al. 1998), followed by Buffington (2007) where the presence/absence of the clip across Figitidae was examined. Buffington (2007) hypothesized that the absence of the clip in Aspicerinae and Anacharitinae was linked to a ‘quick-strike’ oviposition strategy, as the hosts they attacked (Syrphidae and Hemerobiidae, respectively) are themselves aggressive hosts to be attacking. Further, the Charipinae are hyperparasitoids of aphidophagous braconids and chalcidoids, where there is no need for host restraint. Finally, the leaf-miner specialists, among the eucoiline Zaeucoilini and Diglyphosematini, also lack the clip as their host is a ‘captive audience’ that cannot readily escape parasitization. Together, these data suggest the ovipositor clip, in the appropriate circumstance, is an asset; in other circumstances, a liability.

The pattern observed in the *Ganaspis brasiliensis* species complex can be interpreted along the same lines. In the case of both *G. brasiliensis* and *G. lupini*, the ovipositor clip has retained its typical size, spanning the width and depth of the fused valve of the ovipositor (Figs 4, 5). By contrast, *G. kimorum* has a much-reduced ovipositor clip, so much reduced that the last author had to mount some 40 ovipositors before the nature of the reduced clip could actually be observed (in some cases, there appeared to be no

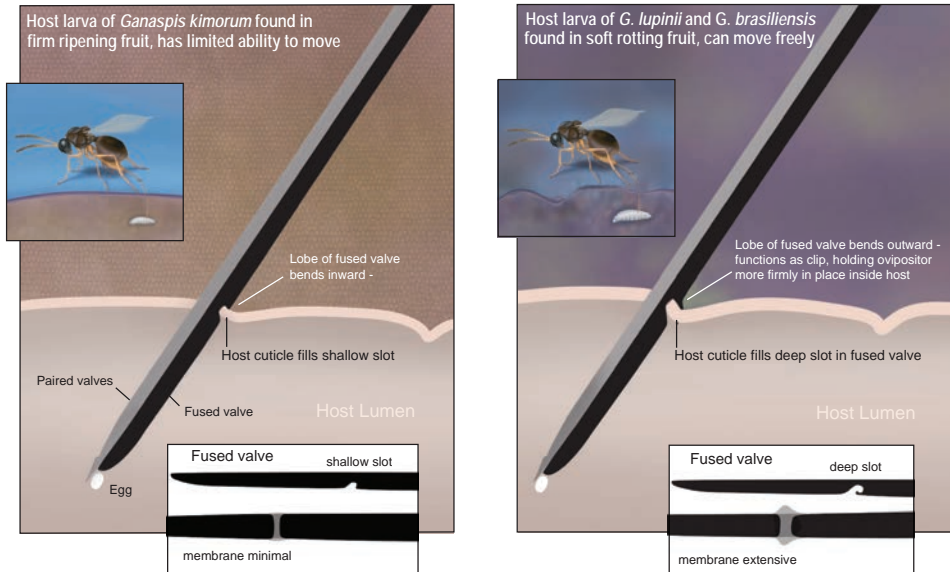


Figure 5. Functional morphology of the ovipositor clip.

ovipositor clip present) (Fig. 4). Both *G. brasiliensis* and *G. lupini* are attacking hosts within an already decomposing substrate, allowing the would-be host ample room for escape. Further, the skin of the fruit, if still intact, would be very soft, and the clip itself would not be engaged by it. In the case of *G. kimorum*, which attacks its host in ripe fruit, the host larvae would have much less space for escape. Further, as the skin of the fruit is still intact, this more rigid barrier may in fact cause complications for the insertion of the ovipositor, as the clip itself may in fact snag on the fruit skin during insertion. The reduction of the clip into a much more streamlined silhouette, we hypothesize, helps the ovipositor insert into the fruit more effectively and not engage the fruit skin. And, as the host larvae has a reduced chance of escape inside of fresh fruit, this shallower ovipositor clip remains effective at securing the host (Fig. 5).

What is the future of species delimitation using UCE data? We have demonstrated here that these data are quite effective at discriminating among morphologically virtually identical but biologically distinct species. We may very well be observing the immediate after-effects of speciation, where morphological characters have not yet manifested themselves to be observed, but clearly, biological and genetic characters distinguishing these species are present. And if this is the case, the much larger amount of sequence data per specimen that UCE methodology provides is rather critical. As the cost of this technique continues to decline, we predict this technique will certainly be considered more closely in the future.

Perhaps a more difficult question to consider is: what is the future of *Ganaspis* taxonomy? *Ganaspis* currently has only 49 nominal species, of which 17 actually belong in other genera and are awaiting new combinations, while 8 are *nomina inquirenda*, the types of which have never been studied by modern researchers, leaving 24 described

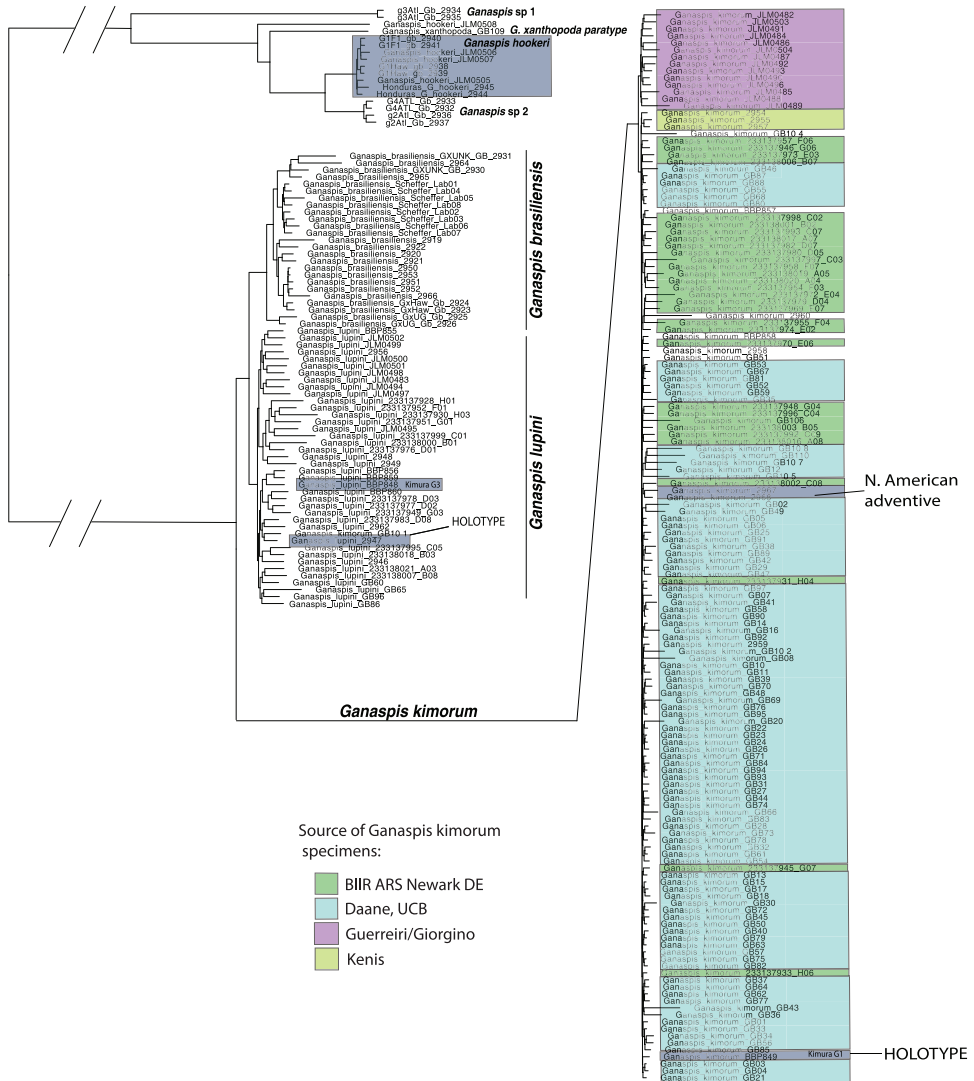


Figure 6. Phylogeny of the *Ganaspis brasiliensis* species complex based on the SYMTEST analysis. Specific populations, mentioned in previous studies, are highlighted by arrows, as well as where the holotypes of the two new species are located. The adventive population in British Columbia is also noted.

Ganaspis species. But then there are an additional 46 *Ganaspis* species that are currently classified in other genera and await new combinations in *Ganaspis* (unpublished data). On top of this there are numerous undescribed species, including a remarkable number of ‘BINs’ in BOLD (Sosa-Calvo and Buffington, pers. obs.) But these considerations are all based on current circumscription where it seems very likely that *Ganaspis* is at least a paraphyletic assemblage of all the “typical Ganaspini” without certain striking apomorphies which define related genera such as *Areaspis* Lin, 1988, *Didyctium* Riley, 1879, *Discaspis* Lin, 1988, *Endecameres* Yoshimoto, 1963, *Gastraspis* Lin, 1988 and

Hexacola Förster, 1869 (cf. the keys in van Noort et al. 2014; Buffington and Forshage 2015). But there is also a possibility that this represents a morphology that several lineages have been converging into based on similar life histories (the similarity between different *Ganaspis* and *Leptopilina* species attacking similar drosophilid hosts is rather striking, considering that *Leptopilina* belongs to an entirely different group within Eucolidae (the tribe Eucolini)). Indeed, in all published phylogenetic analyses where it has been tested, *Ganaspis* has come out non-monophyletic (Fontal-Cazalla et al. 2002; Buffington et al. 2007; Blaimer et al. 2020). Whether the genus is indeed a paraphyletic grouping of the more plesiomorphic crown-group Ganaspini, or rather a polyphyletic assemblage of wasps having converged on a similar morphology, is very difficult to say, and is perhaps not even a very meaningful question to ask before a more rigid circumscription of the genus has been attained. A global review of the genus is desperately needed to give it a meaningful circumscription and to identify monophyletic species groups which can be properly revised. Perhaps the new UCE methodology can assist, especially since UCE can be generated effectively from older museum specimens.

In conclusion, working out the limits of these three species of *Ganaspis*, like in other cases of cryptic species complexes, has required a great deal of behavioral study, genetic study, and morphological study, and benefitted from the reciprocal illumination they have offered. This has also involved researchers from around the world, conducting very careful work documenting these species, as well as the centralization of voucher specimens such that various lines of evidence can be directly, and quickly, compared. Thus, this work represents a celebration of international collaboration between research groups in different countries with different specializations for an integrated solution to independently noted problems.

Acknowledgements

Collectively we would like to thank the following people and groups for providing the specimens, and data, needed to complete this project: members of the ARS-BIIR group in Newark, DE; the Daane Lab, UC Berkeley; Abram Lab, Agassiz Research and Development Centre, Agassiz, British Columbia, Canada; M. Giorgino and E. Guerrieri, Institute for Sustainable Plant Protection, National Research Council of Italy, via Università 133, 80055 Portici, Italy; and the Kimura Lab, Hokkaido University, Sapporo, Japan. Jim Woolley (retired, Texas A&M), Fredrik Ronquist (Naturhistoriska riksmuseet, Stockholm, Sweden) and combined SI-USDA Hymenoptera Unit at NMNH helped flesh out ideas and concepts presented here. JSC was financially supported by the National Science Foundation grants DEB 1754242 and DEB 1927161, and would like to thank Sean Brady and Ted Schultz (Department of Entomology, NMNH). The editor, Miles Zhang, and the two reviewers, Mar Ferrer-Suay and Simon van Noort, helped improve this manuscript. Mention of trade names or commercial products in this publication is solely for the purpose of providing specific information and does not imply recommendation or endorsement by the USDA. USDA is an equal opportunity provider and employer.

References

- Abram PK, McPherson AE, Kula R, Hueppelsheuser T, Thiessen J, Perlman SJ, Curtis CI, Fraser JL, Tam J, Carrillo J, Gates M, Scheffer S, Lewis M, Buffington M (2020) New records of *Leptopilina*, *Ganaspis*, and *Asobara* species associated with *Drosophila suzukii* in North America, including detections of *L. japonica* and *G. brasiliensis*. *Journal of Hymenoptera Research* 78: 1–17. <https://doi.org/10.3897/jhr.78.55026>
- Abram PK, Wang X, Hueppelsheuser T, Franklin MT, Daane KM Lee JC, Lue CH, Girod P, Carrillo J, Wong WHL, Kula RR, Gates MW, Hogg B, Moffat CE, Hoelmer KA, Sial AA, Buffington ML (2022) A Coordinated Sampling and Identification Methodology for Larval Parasitoids of Spotted-Wing *Drosophila*. *Journal of Economic Entomology* 115: 922–942. <https://doi.org/10.1093/jee/toab237>
- Alex Smith M, Fernández-Triana JL, Eveleigh E, Gómez J, Guclu C, Hallwachs W, Hebert PD, Hrcek J, Huber JT, Janzen D, Mason PG, Miller S, Quicke DL, Rodriguez JJ, Rougerie R, Shaw MR, Várkonyi G, Ward DF, Whitfield JB, Zaldívar-Riverón A (2013) DNA barcoding and the taxonomy of Microgastrinae wasps (Hymenoptera, Braconidae): impacts after 8 years and nearly 20 000 sequences. *Molecular Ecology Resources* 13: 168–176. <https://doi.org/10.1111/1755-0998.12038>
- Bankevich A, Nurk S, Antipov D, Gurevich AA, Dvorkin M, Kulikov AS, Lesin V, Nikolenko S, Pham S, Pribelski A, Pyshkin A, Sirotkin A, Vyahhi N, Tesler G, Alekseyev M, Pevzner P (2012) SPAdes: A new genome assembly algorithm and its applications to single-cell sequencing. *Journal of Computational Biology* 19(5): 455–477. <https://doi.org/10.1089/cmb.2012.0021>
- Barrera CA, Sosa-Calvo J, Schultz TR, Rabeling C, Bacci Jr M (2022) Phylogenomic reconstruction reveals new insights into the evolution and biogeography of *Atta* leaf-cutting ants (Hymenoptera: Formicidae). *Systematic Entomology* 47: 13–35. <https://doi.org/10.1111/syen.12513>
- Blaimer BB, Santos BF, Cruaud A, Gates MW, Kula RR, Mikó I, Rasplus JY, Smith D, Talamas E, Brady S, Buffington M (2023) Key innovations and the diversification of Hymenoptera. *Nature Communications* 14: 1212. <https://doi.org/10.1038/s41467-023-36868-4>
- Blaimer BB, Gotzek D, Brady S, Buffington ML (2020) Comprehensive phylogenomic analyses re-write the evolution of parasitism within cynipoid wasps. *BMC Evolutionary Biology* 20: 1–22. <https://doi.org/10.1186/s12862-020-01716-2>
- Borowiec ML (2019) Spruceup: fast and flexible identification, visualization, and removal of outliers from large multiple sequence alignments. *Journal of Open Source Software* 4: 1635. <https://doi.org/10.21105/joss.01635>
- Branstetter MG, Danforth BN, Pitts JP, Faircloth BC, Ward PS, Buffington ML, Gates MW, Kula RR, Brady SG (2017) Phylogenomic Insights into the Evolution of Stinging Wasps and the Origins of Ants and Bees. *Current Biology* 27: 1019–1025. <https://doi.org/10.1016/j.cub.2017.03.027>
- Branstetter MG, Muller A, Griswold TL, Orr MC, Zhu CD (2021) Ultraconserved element phylogenomics and biogeography of the agriculturally important mason bee subgenus *Osmia* (*Osmia*). *Systematic Entomology* 46: 453–472. <https://doi.org/10.1111/syen.12470>
- Branstetter MG, Longino JT (2022) UCE phylogenomics of new world *Cryptopone* (Hymenoptera: Formicidae) elucidates genus boundaries, species boundaries, and the vicariant

- history of a temperate–tropical disjunction. *Insect Systematics and Diversity* 6: 1–23. <https://doi.org/10.1093/isd/ixab031>
- Brower AVZ (2006) Problems with DNA barcodes for species delimitation: ‘ten species’ of *Astraptus fuligator* reassessed (Lepidoptera: Hesperidae). *Systematics and Biodiversity* 4: 127–132. <https://doi.org/10.1017/S147720000500191X>
- Buffington M (2007) The occurrence and phylogenetic implications of the ovipositor clip within the Figitidae (Insecta: Hymenoptera: Cynipoidea). *Journal of Natural History* 41: 2267–2282. <https://doi.org/10.1080/00222930701579732>
- Buffington ML, Forshage M (2016) Redescription of *Ganaspis brasiliensis* (Hering, 1905), new combination (Hymenoptera: Figitidae), a natural enemy of the invasive *Drosophila suzukii* (Matsumura, 1931) (Diptera: Drosophilidae). *Proceedings of the Entomological Society of Washington* 118: 1–13. <https://doi.org/10.4289/0013-8797.118.1.1>
- Buffington ML, Nylander JAA, Heraty JM (2007) The phylogeny and evolution of Figitidae (Hymenoptera: Cynipoidea). *Cladistics* 23: 403–431. <https://doi.org/10.1111/j.1096-0031.2007.00153.x>
- Bushnell Brian (2014) BBMap: A fast, accurate, splice-aware aligner, United States. <https://www.osti.gov/services/purl/1241166>
- Cariou M, Duret L, Charlat S (2017) The global impact of *Wolbachia* on mitochondrial diversity and evolution. *Journal of Evolutionary Biology* 30: 2204–2210. <https://doi.org/10.1111/jeb.13186>
- Castresana J (2000) Selection of conserved blocks from multiple alignments for their use in phylogenetic analysis. *Molecular Biology and Evolution* 17: 540–552. <https://doi.org/10.1093/oxfordjournals.molbev.a026334>
- Chernomor O, von Haeseler A, Minh BQ (2016) Terrace aware data structure for phylogenomic inference from supermatrices. *Systematic Biology* 65: 997–1008. <https://doi.org/10.1093/sysbio/syw037>
- Collins RA, Cruickshank RH (2012) The seven deadly sins of DNA barcoding. *Molecular Ecology Resources* 13: 969–975. <https://doi.org/10.1111/1755-0998.12046>
- Faircloth BC, Branstetter MG, White ND, Brady SG (2015) Target enrichment of ultraconserved elements from arthropods provides a genomic perspective on relationships among Hymenoptera. *Molecular Ecology Resources* 15: 489–501. <https://doi.org/10.1111/1755-0998.12328>
- Faircloth BC, Glenn TC (2012) Not All Sequence Tags Are Created Equal: Designing and Validating Sequence Identification Tags Robust to Indels. *PLoS ONE* 7(8): e42543. <https://doi.org/10.1371/journal.pone.0042543>
- Fontal-Cazalla FM, Buffington M, Nordlander G, Liljeblad J, Ros-Farre’ P, Nieves-Aldrey JL, Pujade-Villar J, Ronquist F (2002) Phylogeny of the Eucilinae (Hymenoptera: Cynipoidea: Figitidae). *Cladistics* 18:154–199. <https://doi.org/10.1111/j.1096-0031.2002.tb00147.x>
- Giorgini M, Wang XG, Wang Y, Chen FS, Hougardy E, Zhang HM, Chen ZQ, Chen HY, Liu CX, Cascone P, Formisan G, Carvalho GA, Biondi A, Buffington ML, Daane KM, Hoelmer KA, Guerrieri E (2019) Exploration for native parasitoids of *Drosophila suzukii* in China reveals a diversity of parasitoid species and narrow host range of the dominant parasitoid. *Journal of Pest Science* 92: 509–522. <https://doi.org/10.1007/s10340-018-01068-3>
- Glenn TC, Pierson TW, Bayona-Vasquez NJ, Kieran TJ, Hoffberg SL, Thomas JC, Lefever DE, Finger JW, Gao B, Bian X, Louha S, Kolli RT, Bentley KE, Rushmore J, Wong K, Shaw TI, Ro-

- throck Jr MJ, McKee AM, Guo TL, Mauricio R, Molina M, Cummings BS, Lash LH, Lu K, Gilbert GS, Hubbell SP, Faircloth BC (2019) Adapterama II: universal amplicon sequencing on Illumina platforms (TaggiMatrix). *PeerJ*. 7: e7786. <https://doi.org/10.7717/peerj.7786>
- Goldstein P, DeSalle R (2011) Integrating DNA barcode data and taxonomic practice: determination, discovery, and description. *BioEssays: news and reviews in molecular, cellular and developmental biology* 33: 135–147. <https://doi.org/10.1002/bies.201000036>
- Guindon S, Dufayard J-F, Lefort V, Anisimova M, Hordijk W, Gascuel O (2010) New algorithms and methods to estimate Maximum-Likelihood phylogenies: Assessing the performance of PhyML 3.0. *Systematic Biology* 59: 307–321. <https://doi.org/10.1093/sysbio/syq010>
- Hanisch PE, Sosa-Calvo J, Schultz TR (2022) The last piece of the puzzle: Phylogenetic position and natural history of the monotypic fungus-farming ant genus *Paramycetophylax* (Formicidae: Attini). *Insect Systematics and Diversity* 6: 1–17. <https://doi.org/10.1093/isd/ixab029>
- Hansson C, Hambäck P (2013) Three cryptic species in *Asecodes* (Förster) (Hymenoptera, Eulophidae) parasitizing larvae of *Galerucella* spp. (Coleoptera, Chrysomelidae), including a new species. *Journal of Hymenoptera Research* 30: 51–64. <https://doi.org/10.3897/jhr.30.4279>
- Heraty JM, Woolley JB, Hopper K, Hawks D, Kim JW, Buffington ML (2007) Molecular phylogenetics and reproductive incompatibility in a complex of cryptic species of aphid parasitoids. *Molecular Phylogenetics and Evolution* 45: 480–493. <https://doi.org/10.1016/j.ympev.2007.06.021>
- Hoang DT, Chernomor O, von Haeseler A, Minh BQ, Vinh LS (2018) UFBoot2: Improving the Ultrafast Bootstrap Approximation. *Molecular Biology And Evolution* 35: 518–522. <https://doi.org/10.1093/molbev/msx281>
- Hopper KR, Wang X, Kenis M, Seehausen ML, Abram PK, Daane KM, Buffington ML, Hoelmer KA, Kingham BF, Shevchenko O, Bernberg E (2024) Genome divergence and reproductive incompatibility among populations of *Ganaspis* near *brasiliensis*. *G3: Genes, Genomes, Genetics*: jkae090. <https://doi.org/10.1093/g3journal/jkae090>
- Jiggins F (2003) Male-killing *Wolbachia* and mitochondrial DNA: Selective sweeps, hybrid introgression and parasite population dynamics. *Genetics* 164: 5–12. <https://doi.org/10.1093/genetics/164.1.5>
- Kalyaanamoorthy S, Minh BQ, Wong TK, von Haeseler A, Jermini LS (2017) ModelFinder: fast model selection for accurate phylogenetic estimates. *Nature Methods* 14: 587–589. <https://doi.org/10.1038/nmeth.4285>
- Katoh K, Standley DM (2013) MAFFT multiple sequence alignment software version 7: Improvements in performance and usability. *Molecular Biology And Evolution* 30: 772–780. <https://doi.org/10.1093/molbev/mst010>
- Katoh K, Kuma K-I, Toh H, Miyata T (2005) MAFFT version 5: Improvement in accuracy of multiple sequence alignment. *Nucleic Acids Research* 33: 511–518. <https://doi.org/10.1093/nar/gki198>
- Katoh K, Standley DM (2014) MAFFT: iterative refinement and additional methods. *Multiple Sequence Alignment Methods*: 131–146. https://doi.org/10.1007/978-1-62703-646-7_8
- Klopfstein S, Kropf C, Baur H (2016) *Wolbachia* endosymbionts distort DNA barcoding in the parasitoid wasp genus *Diplazon* (Hymenoptera: Ichneumonidae). *Zoological Journal of the Linnean Society* 177: 541–557. <https://doi.org/10.1111/zoj.12380>

- Krueger F (2015) Trim Galore!: A wrapper around Cutadapt and FastQC to consistently apply adapter and quality trimming to FastQ files, with extra functionality for RRBS data. Babraham Institute. https://www.bioinformatics.babraham.ac.uk/projects/trim_galore/
- Lue CH, Buffington ML, Scheffer S, Lewis M, Elliott TA, Lindsey AR, Driskell A, Jandova A, Kimura MT, Carton Y (2021) DROP: Molecular voucher database for identification of *Drosophila* parasitoids. *Molecular Ecology Resources* 21: 2437–2454. <https://doi.org/10.1111/1755-0998.13435>
- Lohse K (2009) Can mtDNA barcodes be used to delimit species: A response to Pons et al. (2006). *Systematic Biology* 58: 439–442. <https://doi.org/10.1093/sysbio/syp039>
- Masters BC, Fan V, Ross HA (2011) Species Delimitation – a Geneious plugin for the exploration of species boundaries. *Molecular Ecology Resources* 11: 154–157. <https://doi.org/10.1111/j.1755-0998.2010.02896.x>
- Minh BQ, Schmidt HA, Chernomor O, Schrempf D, Woodhams MD, von Haeseler A, Lanfear R (2020) IQ-TREE 2: New Models and Efficient Methods for Phylogenetic Inference in the Genomic Era. *Molecular Biology And Evolution* 37: 1530–1534. <https://doi.org/10.1093/molbev/msaa015>
- Naser-Khdour S, Minh BQ, Zhang W, Stone EA, Lanfear R. (2019) The prevalence and impact of model violations in phylogenetic analysis. *Genome Biology and Evolution* 11: 3341–3352. <https://doi.org/10.1093/gbe/evz193>
- Nomano FY, Kasuya N, Matsuura A, Suwito A, Mitsui H, Buffington ML, Kimura MT (2017) Genetic differentiation of *Ganaspis brasiliensis* (Hymenoptera: Figitidae) from East and Southeast Asia. *Applied Entomology and Zoology* 52: 429–437. <https://doi.org/10.1007/s13355-017-0493-0>
- Nurk S, Bankevich A, Antipov D, Gurevich AA, Korobeynikov A, Lapidus A, Prjibelski AD, Pyshkin A, Sirotkin A, Sirotkin Y, Stepanauskas R, Clingenpeel SR, Woyke T, McLean JS, Lasken R, Tesler G, Alekseyev MA, Pevzner PA (2013) Assembling single-cell genomes and mini-metagenomes from chimeric MDA products. *Journal of Computational Biology* 20(10): 714–737. <https://doi.org/10.1089/cmb.2013.0084>
- Prebus MM (2021) Phylogenomic species delimitation in the ants of the *Temnothorax salvini* group (Hymenoptera: Formicidae): an integrative approach. *Systematic Entomology* 46: 307–326. <https://doi.org/10.1111/syen.12463>
- Rosen D (1986) The role of taxonomy in effective biological control programs. *Agriculture, Ecosystems and Environment* 15: 121–129. [https://doi.org/10.1016/0167-8809\(86\)90085-X](https://doi.org/10.1016/0167-8809(86)90085-X)
- Schär ST, Rana G, Espadaler J, Cover X, Shattuck S, Roger S (2022) Integrative taxonomy reveals cryptic diversity in North American *Lasius* ants, and an overlooked introduced species. *Scientific Reports* 12: 5970. <https://doi.org/10.1038/s41598-022-10047-9>
- Seehausen ML, Ris N, Driss L, Racca A, Girod P, Warot S, Borowiec N, Toševski I, Kenis M (2020) Evidence for a cryptic parasitoid species reveals its suitability as a biological control agent. *Scientific Reports* 10: 19096. <https://doi.org/10.1038/s41598-020-76180-5>
- Ströher PR, Zarza E, Tsai W, McCormack J, Feitosa R, Pie M (2017) The mitochondrial genome of *Octostruma stenognatha* and its phylogenetic implications. *Insectes Society* 64: 149–154. <https://doi.org/10.1007/s00040-016-0525-8>
- Struck TH, Feder JL, Bendiksbj M, Birkeland S, Cerca J, Gusarov VI, Kistenich S, Larsson KH, Liow LH, Nowak MD, Stedje B, Bachmann L, Dimitrov D (2018) Finding Evolu-

- tionary Processes Hidden in Cryptic Species. *Trends Ecology and Evolution* 33:153–163. <https://doi.org/10.1016/j.tree.2017.11.007>
- Tagliacollo VA, Lanfear R (2018) Estimating improved partitioning schemes for ultraconserved elements. *Molecular Biology and Evolution* 35: 1798–1811. <https://doi.org/10.1093/molbev/msy069>
- Talavera G, Castresana J (2007) Improvement of phylogenies after removing divergent and ambiguously aligned blocks from protein sequence alignments. *Systematic Biology* 56: 564–577. <https://doi.org/10.1080/10635150701472164>
- van Lenteren JC, Isidoro N, Bin F (1998) Functional anatomy of the ovipositor clip in the parasitoid *Leptopilina heterotoma* (Thompson) (Hymenoptera: Eucoilidae), a structure to grip escaping larvae. *International Journal of Insect Morphology and Embryology* 27: 263–268. [https://doi.org/10.1016/S0020-7322\(98\)00019-1](https://doi.org/10.1016/S0020-7322(98)00019-1)
- van Noort S, Buffington ML, Forshage M (2015) Afrotropical Cynipoidea (Hymenoptera). *ZooKeys* 493: 1–176. <https://doi.org/10.3897/zookeys.493.6353>
- Wang Y, Zhou QS, Qiao HJ, Zhang AB, Yu F, Wang X, Zhu CD, Zhang YZ (2016) Formal nomenclature and description of cryptic species of the *Encyrtus sasakii* complex (Hymenoptera: Encyrtidae). *Scientific Reports* 6: 34372. <https://doi.org/10.1038/srep34372>
- Zhang YM, Sheikh SI, Ward AKG, Forbes AA, Prior KM, Stone GM, Gates MW, Egan SP, Zhang L, Davis C, Weinersmith KL, Melika G, Lucky A (2022) Delimiting the cryptic diversity and host preferences of *Sycophila* parasitoid wasps associated with oak galls using phylogenomic data. *Molecular Ecology* 31: 4417–4433. <https://doi.org/10.1111/mec.16582>

Supplementary material I

Supplementary data

Authors: Jeffrey Sosa-Calvo, Mattias Forshage, Matthew L. Buffington

Data type: xlsx

Explanation note: **table S1.** Voucher specimen data (FIMS) and SRA accession numbers for the *Ganaspis* samples used in this study; **table S2.** Assembly statistics for all the samples included in this study; **table S3.** SPRUCEUP manual cut-off employed in this study; **table S4.** Alignment statistics and summary of alignments and partitions generated in this study; **table S5.** Summaries of *intra* and *inter* tree distances for the three major clades identified in this study: *Ganaspis brasiliensis*, *G. lupini* sp.nov., and *G. kimorum* sp. nov.; **table S6.** Voucher specimen data and GenBank accession number for the *Ganaspis* samples for which COI sequences were generated.

Copyright notice: This dataset is made available under the Open Database License (<http://opendatacommons.org/licenses/odbl/1.0/>). The Open Database License (ODbL) is a license agreement intended to allow users to freely share, modify, and use this Dataset while maintaining this same freedom for others, provided that the original source and author(s) are credited.

Link: <https://doi.org/10.3897/jhr.97.118567.suppl1>